

# Kent Academic Repository

## Full text document (pdf)

### Citation for published version

Selnø, Anette Teo Hansen (2021) Biochemical Regulation of the Tim-3-Galectin-9 Immunosuppressive Pathway under Normal Conditions and upon Cell Malignant Transformation. Doctor of Philosophy (PhD) thesis, University of Kent, University of Greenwich.

### DOI

### Link to record in KAR

<https://kar.kent.ac.uk/90836/>

### Document Version

UNSPECIFIED

#### Copyright & reuse

Content in the Kent Academic Repository is made available for research purposes. Unless otherwise stated all content is protected by copyright and in the absence of an open licence (eg Creative Commons), permissions for further reuse of content should be sought from the publisher, author or other copyright holder.

#### Versions of research

The version in the Kent Academic Repository may differ from the final published version.

Users are advised to check <http://kar.kent.ac.uk> for the status of the paper. **Users should always cite the published version of record.**

#### Enquiries

For any further enquiries regarding the licence status of this document, please contact:

[researchsupport@kent.ac.uk](mailto:researchsupport@kent.ac.uk)

If you believe this document infringes copyright then please contact the KAR admin team with the take-down information provided at <http://kar.kent.ac.uk/contact.html>

Biochemical Regulation of the  
Tim-3-Galectin-9  
Immunosuppressive Pathway  
under Normal Conditions and  
upon Cell Malignant  
Transformation

Thesis by

Anette Teo Hansen Selnø

A thesis submitted in partial fulfilment of the requirements of the  
University of Kent and the University of Greenwich for the Degree of  
Doctor of Philosophy

March 2021

## DECLARATION

"I certify that this work has not been accepted in substance for any degree and is not concurrently being submitted for any degree other than that of Doctor of Philosophy being studied at the Universities of Greenwich and Kent. I also declare that this work is the result of my own investigations except where otherwise identified by references and that I have not plagiarised the work of others."

The Candidate

\_\_\_\_\_ Date \_\_\_\_\_

The Supervisor

\_\_\_\_\_ Date \_\_\_\_\_

## ACKOWEDLEDMENTS

I would like to start thanking all the collaborators that made this project possible.

Many thanks to Dr Inna Yasinska, Dr Svetlana Sakhnevych and Stephanie Schlichtner for permission to include some of their results in my thesis. Their participation allowed me to put together this puzzle.

Thanks to Louise Hansen, which as a dyslexia specialist has help me with language and gramma corrections.

I would like to give a special thanks to Dr Bernhard Gibbs for his guidance during my PhD

I would like to express my deepest appreciation and gratitude to Dr Vadim Sumbayev for the guidance and support in completing this PhD project. It is with his supervision that it was possible to complete this PhD.

Finally, I would like to thank my family, for supporting me in all the ways they could during this stage of my life.

A big and sincere thanks to all of you!

## ABSTRACT

Cancer is a group of diseases involving abnormal cell proliferation with a high potential to spread or invade into other parts of the body and is currently considered as one of the leading causes of death worldwide. Cancer cells can be recognised and killed by cytotoxic immune cells of lymphoid lineage. However, malignant cells are capable of suppressing the host's cytotoxic immune responses using a variety of biochemical mechanisms. One of the critical and poorly understood mechanisms of immune evasion is the Tim-3 (T cell immunoglobulin and mucin domain-containing protein 3)-galectin-9 immunosuppressive pathway. Galectin-9, a protein highly conserved through evolution, is used to suppress anti-cancer activities of cytotoxic lymphoid cells. It has recently been reported that acute myeloid leukaemia (AML) cells are able to promote galectin-9 and Tim-3 translation and secretion through stimulation induced by fibronectin leucine-rich transmembrane protein 3 (FLRT3), which activates transmembrane receptor latrophilin-1 (LPHN1). LPHN1 mediates activation of Tim-3 and galectin-9 translation and facilitates their exocytosis. However, the molecular mechanisms underlying biochemical regulation of galectin-9 expression and control of the pathway activity remain unknown. Thus, uncovering this crucial biochemical machinery was the aim of this PhD programme.

First of all, our group discovered that the Tim-3-galectin-9 pathway is active in a variety of human solid tumours and is also used to suppress the activities of cytotoxic lymphoid cells. We found that transforming growth factor beta 1 (TGF- $\beta$ ) is crucial for upregulation of galectin-9 expression in human cancer but not in non-malignant human cells. The transcription factors hypoxia-inducible factor 1 (HIF-1) and activator protein 1 (AP-1) were found to upregulate TGF- $\beta$  expression, leading to activation of the transcription factor Smad3 through autocrine action. Smad3 was found to be responsible for TGF- $\beta$ -mediated upregulation of galectin-9 expression. As a follow-up, we have discovered that high-mobility group box 1 (HMGB1, a nuclear protein secreted by stressed, damaged or dying cells and thus highly present in the tumour microenvironment) upregulates TGF- $\beta$  production through the innate immune receptor called Toll-like receptor 4 (TLR4). Thus, HMGB1 can lead to induction of galectin-9 expression in cancer cells directly (if they express functional TLR4) or indirectly through TLR4 expressing myeloid cells present in the tumour microenvironment. Collectively, our results suggest that Tim-3-galectin-9 and TGF- $\beta$ -dependent signalling pathways are potential targets for the immunotherapy of a large number of human cancers.

# CONTENTS

DECLARATION .....	i
ACKNOWLEDGMENTS.....	ii
ABSTRACT.....	iii
FIGURES.....	viii
TABLES.....	xxiv
ABBREVIATIONS.....	xxv
1 INTRODUCTION .....	1
1.1 The Immune System .....	2
1.2 Immune Tolerance.....	4
1.2.1 Central Tolerance Is Programmed During T Cell Development.....	5
1.2.2 Mechanisms of Peripheral Tolerance Influence T Cell Response .....	6
1.3. Biochemical Pathways Operated by Cancer Cells to Escape Host Immune Surveillance .....	11
1.3.1 The Cancer-Immune Cycle.....	13
1.4 Biochemical Regulation of Activities of Immune Checkpoint Proteins Used as Potential Targets for Immunotherapy of Cancer and other Disorders.....	21
1.4.1 Cytotoxic T-lymphocyte-associated Protein 4 (CTLA-4)-mediated Signalling Pathways.....	24
1.4.2 Programmed Cell Death Protein 1 (PD-1) Signalling Pathways .....	36
1.4.3 T-Cell Immunoglobulin and Mucin Domain 3 (Tim-3) and Galectin-9 Pathway ..	49
1.5 Background (in short) and Rationale for Studying Galectin-9 .....	70
1.6 Looking for Regulators of Galectin-9 .....	71
1.6.1 Transforming Growth Factor-beta (TGF- $\beta$ ).....	72
1.6.2 Immunogenic Cell Death (ICD).....	82
2 AIMS AND OBJECTIVES .....	95
3 MATERIALS AND METHODS .....	96
3.1 Materials.....	96
3.2 Cell Lines, Primary Cells, and Primary Tissue.....	97
3.2.1 Cell Lines .....	97
3.2.2 Primary Cells.....	97
3.2.3 Primary Tissue .....	98
3.3 DOTAP Transfection .....	98

3.3.1 Plasmid Transfection with Dominant-negative ASK1 or Constitutive Active TLR4 .....	100
3.3.2 Gene Knockdown .....	100
3.4 Protein Quantification .....	101
3.5 Western Blot Analysis.....	102
3.5.1 Sample Preparation.....	105
3.5.2 SDS-PAGE.....	106
3.5.3 Transfer.....	107
3.5.4 Blocking, Detection and Imaging .....	108
3.5.5 WB Analysis .....	109
3.6 On-Cell Western Assay (OCA) .....	109
3.6.1 OCA on Suspension Cells.....	109
3.6.2 OCA on Adherent Cells .....	110
3.7 Enzyme-linked immunoSorbent Assay (ELISA).....	111
3.7.1 Quantification of Galectin-9, Tim-3, IL-2, IFN $\gamma$ , and TNF $\alpha$ Concentrations in Cell Lysates and Culture Medium.....	112
3.7.2 Quantification of TGF $\beta$ Concentrations in Cell Lysates and Culture Medium...	113
3.8 DNA Protein Interaction (DPI)-ELISA - DNA Binding Activity Assay.....	113
3.9 Granzyme B and Caspase-3 Activity Assay .....	115
3.9.1 Sample Preparation.....	115
3.9.2 Granzyme B Activity Assay .....	116
3.9.3 Caspase-3 Activity Assay .....	116
3.11 Xanthine Oxidase (XOD) Activity Assay .....	117
3.12 NADPH oxidase (Nox) activity assay.....	117
3.13 Thiobarbiturate Reactive Substance (TBRS) Assay .....	118
3.14 Statistical Analysis.....	119
<b>4 RESULTS AND DISCUSSIONS .....</b>	<b>119</b>
4.1 The FLRT3-LPHN and Galectin-9-Tim-3 Signalling Pathways – a Possible Common Mechanism in Different Types of Cancer to Mediate Immune Escape .....	120
4.1.1 Breast Tumour Cells Have Elevated Levels of Expression of LPHN, FLRT3, Tim-3 and galectin-9.....	121
4.1.2 Breast Tumour Cells Have Increased Activity of PLC and PKC $\alpha$ , not mTOR Activity.....	123
4.1.3 Breast Tumour Cells Express Tim-3 and galectin-9 as a Complex .....	124
4.1.4 MCF-7 Express Similar Components of the FLRT3-LPHN-galectin-9-Tim-3 Pathway and Act as a Model for Breast Cancer.....	126

4.1.5 The FLRT3-LPHN Pathway Induces Translocation of Galectin-9 onto the Surface of MCF-7 Breast Cancer Cells .....	127
4.1.6 Galectin-9 Protects Breast Cancer Cells Against Cytotoxic Immune Attack.....	129
4.1.7 The Majority of Solid and Liquid Tumours Expresses Key Components of the FLRT3-LPHN-Galectin-9-Tim-3 Pathway .....	136
4.1.8 Discussion .....	138
4.2 Transforming Growth Factor-beta Type 1 (TGF- $\beta$ ) and Hypoxia-inducible Factor 1 (HIF-1) Transcription Complex as Master Regulators of the Immunosuppressive Protein Galectin-9 Expression in Human Cancer Cells.....	142
4.2.1 Oxidative Stress, HIF-1, TGF- $\beta$ , Smad3 and Galectin-9 are Upregulated in Primary Human Cancers .....	144
4.2.2 Redox-dependent Mechanisms Contribute to TGF- $\beta$ and Galectin-9 Expression in Models of Human Cancers .....	150
4.2.3 The HIF-1 Transcription Complex Triggers Galectin-9 Expression by Inducing TGF- $\beta$ Production; Smad3 is Involved in both TGF- $\beta$ and Galectin-9 Expression.....	156
4.2.4 TGF- $\beta$ Induces Galectin-9 Expression in Human Cancer.....	163
4.2.5 Discussion .....	166
4.3 HMGB1 Derived From Dying Tumour Cells Can Promote Immune Escape Inducing TGF- $\beta$ in TLR4 Dependent Mechanism, which Signalling Upregulate Galectin-9 .....	174
4.3.1 HMGB1 Promote Increased TGF- $\beta$ Production and Secretion and Its Autocrine Signalling Augment Galectin-9 Secretion in THP-1 cells.....	175
4.3.2 HMGB1 Do not Increase Galectin-9 Expression in Adherent Cells .....	178
4.3.3 HMGB1 Mediated Effects on Galectin-9 is Dependent on TLR4 expression....	183
4.3.4 Stressed/dying Cancer Cells Promote the Release of HMGB1, which Can Induce TGF- $\beta$ -mediated Galectin-9 Production.....	187
4.3.5 Discussion .....	191
5 CONCLUSIONS.....	196
6 BIBLIOGRAPHY .....	198
7 APPENDIX.....	a
7.1 The FLRT3-LPHN and Galectin-9-TIM-3 Signalling Pathways – a Common Mechanism Among Different Types of Cancer to Mediate Immune Escape.....	a
7.2 Human TGF- $\beta$ 1 Promoter Region and AP-1, HIF-1 and Smad3 Binding Sites.....	f
7.3 LGALS9 Promoter Region and Smad3 Response Element.....	h
7.4 Transforming Growth Factor Beta Type 1 (TGF- $\beta$ ) and Hypoxia-inducible Factor 1 (HIF-1) Transcription Complex as Master Regulators of the Immunosuppressive Protein Galectin-9 Expression in Human Cancer.....	i
7.5 HMGB1 Derived from Dying Tumour Cells Can Promote Immune Escape by Upregulating Galectin-9 in TLR4 Expressing Cancer Cells .....	k



7.6 Buffers, Gel-solutions and Antibodies for Western Blot .....	l
7.6.1 Prepare Buffers .....	l
7.6.2 Gel Solutions .....	m
7.6.3 Antibody List.....	n
7.7 List of Publications.....	p

## FIGURES

**Figure 1: Simple overview of the innate and adaptive immune system.** The innate immune response occurs rapidly upon encounter with a pathogen. The dendritic cells (DCs) are innate cells but are crucial for the activation of the adaptive immune response, thus acting as a bridge between the innate and adaptive immune system. Once activated, the naïve lymphocytes, T and B cells undergo clonal expansion and differentiation to become effector cells and memory cells (not depicted), this process takes a few days. Naïve CD8<sup>+</sup> and CD4<sup>+</sup> T cells become cytotoxic T cells (T<sub>c</sub> or CTL) and T helper cells (T<sub>h</sub>), respectively, which further can differentiate into different subgroups of phenotypes. In addition, the immune system also encompasses other types of immune cells, such as Innate-like lymphocytes, regulatory B cells,  $\gamma\delta$  T cells and natural killer T (NKT) cells, and other newer subset of T helper cells, not shown here.....3

**Figure 2: A simple overview of the most common types of immune responses and how they in general relate to different diseases such as cancer, autoimmune disease and atopic conditions.** (A) The immune response mounted to fend off cancer, such as breast cancer, is a Th1 immune response where the major contributors are cytotoxic T lymphocytes (CTLs), natural killers (NK) cells, Th1 cells and macrophages. Although, the cancer cells can recruit and co-opt some immune cells such as T regulatory cells (Tregs), myeloid-derived suppressor cells (MDSCs) and tumour-associated macrophages (TAMs), which are M2-like macrophages to help them escape immune destruction. (B) On the other hand, a Th17 immune response is most common in autoimmune diseases, such as psoriasis, where CTLs and Th17 cells are the main players and to some extent also Th1 cells. (C) Finally, atopic disease, such as allergy, is characterized by a Th2 response where the predominating immune cells are mast cells, basophils, Th2 cells and eosinophils, and IgE-producing plasma cells.....4

**Figure 3: T cell receptor complex with co-receptor and antigen presentation** (adapted from (1)). The T cell receptor complex (TCR) consists of the TCR $\alpha$  and TCR $\beta$  chain, and CD3 protein ( $\gamma$ ,  $\delta$ ,  $\epsilon$  and  $\zeta$ ), which is required for TCR surface expression and intracellular signalling with immunoreceptor tyrosine-based activator motif (ITAM). However, the TCR receptor complex does not have any intrinsic kinase ability. Thus, upon binding of an antigen-MHC complex, the co-receptor (either CD4 or CD8) partners with the TCR complex to facilitate TCR-mediated signalling as these co-receptors are constitutively associated with the non-receptor tyrosine kinase Lck (a Src family kinase). Upon TCR engagement Lck becomes activated. Lck is the kinase responsible for the phosphorylation of ITAMs, which allows the recruitment of other kinases and binding of adaptor/scaffold proteins that mediates downstream signalling (1, 19). (A) CD8 T cells are presented with antigen on MHC class I, which is expressed on any nucleated cell. (B) CD4 T cells are presented with antigen on MHC class II, which is expressed by APCs or by thymic epithelial cells during development. ....6

**Figure 4: Differentiation of naïve CD4 T cells** (adapted from Naïve CD4 T cells require three signals to be activated and undergo clonal expansion and differentiation. Signal 1 and signal 2 is provided by APCs through cell-cell interaction. Signal 1 is the recognition of antigen-peptide presented on MHC II protein, which induces signal through TCR receptor complex. Signal 2 is binding of B7 co-stimulatory molecules (B7-1/CD80 or B7-2/CD86) on the CD28 receptor, which aids the TCR signal in the generation of IL-2, which is required for proliferation and survival of activated T cells. Finally, signal 3 is a cytokine signal, where local cytokine milieu often provided by the APCs drives the expression of different

lineage-specific transcription factors (such as T-box expressed in T cell (T-bet), GATA3, (RAR-related orphan receptor gamma) ROR $\gamma$ T and (Forkhead box p3) Foxp3) that promote the differentiation into distinct classes of T helper cells, e.g. Th1, Th2, Th17 cells and Tregs, other types are not depicted (1, 19). The required cytokines for Th1 differentiation are IL-12 and/or IFN $\gamma$  (1, 26), for Th2 it is IL-4 (1), for Th17 cells, it is IL-6, TGF- $\beta$  and/or IL-1 $\beta$  (1, 27), and for Tregs, it is TGF- $\beta$  (1, 26). These T helper subsets are characterized by secretion of different cytokines, which assist in distinct function, such as activation of macrophages and CD8 T cells, B cell isotype switching, and suppression of the immune system (1). .....7

**Figure 5: Differentiation of naïve CD8 T cells** (adapted from (1)). As the naïve CD4 T cells, Naïve CD8 T cells require three signals to become activated and undergo clonal expansion and differentiation (28). Here is shown differentiation of a Tc1/CTL cell, which amongst others is involved in viral and cancer clearing. As CD4 T cells, signal 1 (the antigen-specific signal) and signal 2 (co-stimulatory signal) are provided by cell-cell interaction by the APC, although the antigen is required to be presented on MHC class I protein. These two signals are enough for activation and proliferation for a few rounds; however, the cell becomes tolerant rather than gaining its cytolytic function. To obtain cytolytic function, a third cytokine signal from either IL-12 or type I interferons is required (29, 30). Most probably due to the damage that the cytolytic function can cause, the CD8 T cells require more positive co-stimulation to become activated. This is achieved in a 3-way dialogue between the naïve CD8 T cells, an APC (with low intrinsic co-stimulatory activity), and Th1 cells (which provide help by promoting more co-stimulatory signals and IL-2) (1). (A) In the T helper cells, signalling from TCR, CD28 and IL-12R induces production of IL-2 and expression of other co-stimulatory proteins, such as CD40L, which binds to the CD40 receptor on DCs. (B) The CD40L delivers a positive signal that enhances the surface expression of co-stimulatory proteins, such as B7s and 4-1BBL (CD137L) on DCs. These signals provide strong co-stimulatory signal required for activation of naïve CD8 T cells and induce induction of IL-2 and together with IL-12 or type 1 interferon they drive the proliferation and differentiation into effector cytotoxic T cells.....8

**Figure 6: Multiple co-stimulatory and co-inhibitory interactions regulate T cell responses** (adapted from (31)). Depicted are some ligands typically expressed by APCs (and/or tumours) and their cognitive receptor present on T cells. These interactions regulate the T cell response by providing either co-stimulatory or co-inhibitory signals when the T cells already have recognized its specific antigen-peptide bound on an MHC molecule. Not all receptors and ligands are constitutively present, some are present in resting state, and some are upregulated upon activation. In most cases, co-inhibitory receptors are upregulated upon activation.....10

**Figure 7: TME and Hallmarks of cancers** (adapted from (39)). The TME consists of many cells, not only tumour cells. Inside the circle, the different cells of the TME are depicted, which consist of endothelial cells, pericytes, cancer-associated fibroblast, local and bone marrow-derived stromal stem cells and progenitor cells, cancer stem cells, cancer cells, both pro-tumour and anti-tumour immune cells, and invasive cancer cells. Collectively, they influence each other and are “corrupted” by the cancer cells to enable tumour growth and progression. The outer ring illustrates the specific traits or hallmarks, which reflect tumour intrinsic and extrinsic barriers, which must be overcome for malignant transformation.....12

**Figure 8 – The cancer immunoediting process – the three Es of cancer** (adapted from (40)). Equilibrium phase, the immune system has not been able to destroy all the tumour

cells and surviving cancer cells try to proliferate while being under constant attack from the immune cells, which try to control and contain progression. C) Escape phase, at every stage the tumour increases its genetic instability and heterogeneity. This is caused by the immune pressure - “Darwinian” selection of tumour cells with new capabilities, such as reduced immunogenicity, and are able to promote an immunosuppressive TME and functional exhaustion of anti-tumour immune cells, which eventually result in escape from the immune system and tumour progression. In the elimination and equilibrium phase, the immune cells are sometimes successful, and the tissue returns to normal (white arrows).

..... 13  
**Figure 9: The three stages of the Cancer-immune cycle** (adapted from (13, 42, 43)). 14

**Figure 10: CTLA-4 structure and binding to B7 molecules** (adapted from (110)). (A) full length (fl)CTLA-4 consists of 4 exons: exon 1 is the signal peptide, exon 2 the IgV-like domain including the MYPPV binding motive to B7 molecules, exon 3 is the transmembrane (TM) domain, which also contains a cysteine required for dimerization, and exon 4 is the cytoplasmic tail. There are no functional signalling domains, however, in its cytoplasmic tail, there are a lysine-rich motif and two tyrosine motives YVKM and YFLIP, which can recruit different proteins that mediate its immunosuppressive function. Soluble (s)CTLA-4 lacks exon 3 and thus the cysteine required for dimerization. Membrane-associated CTLA-4 is thus a dimer with two IgV-like domains and can interact with B7 molecules consisting of an IgV and IgC-like domain. (B) CD28 and CTLA-4 are quite similar and both have the MYPPV binding motive to bind CD80 (B7-1) and CD86 (B7-2), however, they have different affinities for each ligand, which is attributed to their distinct way of engaging with the ligands. Bivalent CTLA-4 dimer bridges with bivalent CD80 dimer, whereas CD28 interacts monovalent with the B7 molecules.....25

**Figure 11: Some proposed CTLA-4 cell-intrinsic and extrinsic suppressive mechanisms.** CTLA-4 surface presence is tightly regulated by AP1 and AP2 adaptor proteins (not shown) and cycles between surface and endosome/lysosome, its surface expression becomes stable upon phosphorylation of the YVKM motif and engagement of ligand. CTLA-4 can activate PP2A, which inhibits AKT. Furthermore, CTLA-4 can indirectly mediate activation of SHP-2, which dephosphorylates TCR proximal signalling proteins and activates Cbl and Itch, which target their substrate for proteolytical degradation. This results in inhibition of the PI3K-AKT, PLC $\gamma$ -PKC $\theta$  and the MEK-ERK MAPK pathways and consequently also attenuation of the transcription factors, such as NFAT, AP-1 and NF $\kappa$ B, but enhanced Smad3 activity, which promotes TGF- $\beta$  production. It is thought that some of the CTLA-4-mediated immunosuppressive effects are via CTLA-4-induced TGF- $\beta$ -mediated suppression. Another proposed mechanism is that CTLA-4 can reverse signal into APCs and induce IDO expression and activity, which also is immunosuppressive. Recently, CTLA-4 has been proposed to mediate trans-endocytosis and thus removing B7 ligands from the surface of APCs. ....36

**Figure 12: PD-1 and PD-L1 structure and binding** (adapted from (179)). PD-1 consists of 5 exons: exon 1 is the signal peptide, exon 2 encodes the IgV-like binding domain, exon 3 the TM, and exon 4 and exon 5 encode the cytoplasmic tail, which have two signalling motives, the ITIM and the ITSM. (B) PD-1 and PD-L1 binding. PD-1 is upregulated upon activation of T cells as a negative feedback mechanism to attenuate response and can engage with PD-L1 or PD-L2 expressed APCs or cancer cells. PD-L1 and PD-L2 have other binding partners. PD-L1 can interact with CD80 in cis (meaning that they need to be expressed by the same cell. ....40

**Figure 13: PD-1 signalling pathway** (adapted from (206)). Upon activation, T cells upregulates PD-1 as a negative feedback mechanism. PD-1 can be phosphorylated at both ITIM and ITSM, although the latter has been shown to be the major contributor to its immunosuppressive activity. SHP-2 is recruited to PD-1 that has both phosphorylated ITIM and ITSM or to two PD-1 with phosphorylated on ITSM creating a form of dimer. Activated SHP-2 dephosphorylates TCR proximal signalling components, such as CD3 $\zeta$ , ZAP70 and CD28. By ligation of PD-1, SHP-2 is sequestered, and therefore it cannot prevent Csk recruitment and inactivation of Lck. PD-1 signalling also inhibits CK2, possibly through SHP-2. These effects result in inhibition of the PI3K-AKT, PLC $\gamma$ -PKC $\theta$  and the MEK-ERK MAPK pathways, and consequently attenuation of the transcription factors, such as NFAT, AP-1 and NF $\kappa$ B, but enhanced Smad3 activity. SHP-1 has also been associated to PD-1, however, its role is unclear in the PD-1 setting, but in other settings has been reported in dephosphorylating Cbl and thus prevent its degradation. Active Cbl, is involved in the down-modulation of the TCR expression and/or its phosphorylation status. PD-1 signalling is also involved in the upregulation of BATF transcription factor, which promotes T cell exhaustion by impairing T cell proliferation and cytokine secretion. ....46

**Figure 14: CTLA-4 and PD-1 suppressive function includes alteration of cellular metabolism** (adapted from (213)). Changes in cellular metabolism influence the fate of the T cell. Naive T cells use oxidative phosphorylation (OXPHOS) for ATP production. A metabolic switch to fatty-acid  $\beta$ -oxidation (FAO) promotes conversion to Treg or memory T cell. When naive T cells are activated, there is a metabolic switch to glycolysis (Gly), which is mediated by activation of the PI3K-AKT-mTOR-HIF-1 pathway. Upon T cell activation, immunosuppressive receptors PD-1 and CTLA-4 are upregulated as a negative feedback mechanism to attenuate immune response; however, upon exhaustion of T cells, there are sustained expression of these immune checkpoints. Both CTLA-4 and PD-1 can inhibit Gly by suppressing the PI3K-AKT pathway, although through different targets. In addition, PD-1 can induce the conversion to iTreg by promoting a metabolic switch to FAO. This occurs by PD-1-induced AMPK increased expression of CPT1A. AMPK also inhibit mTORC1, which is required for Th1 and Th17 differentiation. ....49

**Figure 15: Tim-3 and galectin-9 structure and some of their respective binding partners** (adapted from (215, 216)). (A) Structure of Tim-3 and galectin-9. Tim-3 consists of a signal peptide and an IgV-like binding domain, a mucin domain, TM and a cytoplasmic tail with six conserved tyrosine residues (Y), which are important for downstream signalling. Human Tim-3 has two N-linked glycosylation in the IgV domain and one O-glycosylation in the mucin domain. Galectin-9 consists of two non-homologues carbohydrate recognition domains (CRD) and a variable linker region. It does not have a signal sequence and thus requires a trafficker to be externalized and secreted. (B) Tim-3 and galectin-9 binding partners. Both Tim-3 and galectin-9 can interact with multiple binding partners. As galectin-9 binds to sugar groups, it has been reported to interact with many different proteins, of which only some is portrayed here, such as IgE, CD40, CD44, CD137 and Tim-3. However, not all effects of galectin-9 can be blocked by lactose (which diminished the carbohydrate binding interaction), suggesting that it in some circumstances may bind to other non-glycosylate proteins. Tim-3 has been reported to interact with PtdSer presented on apoptotic cells, HMGB1, Ceacam-1 and galectin-9. Furthermore, MMPs, such as ADAM10 and ADAM 17, have been shown to cleave Tim-3 either alone or in complex with galectin-9, secreting soluble (s)Tim-3 and galectin-9. ....61

**Figure 16: Tim-3-galectin-9 signalling pathway** (adapted from (348)). (A) T cell activation promotes T cell proliferation, survival and a metabolic switch to glycolysis, which

is triggered by the activation of the PI3K-AKT, MAPK (ERK) and PLC $\gamma$  pathways. These pathways signal downstream to activate transcription factors, such as AP-1, NF $\kappa$ B and NFAT, which is required of cytokine production such IL-2 and IFN $\gamma$ . T cell activation also results in the upregulation of Tim-3, albeit without engagement of ligand, it functions to enhance TCR signalling. Active Lck (in a phosphorylation-independent manner) can interact with Bat3, which is associated to Tim-3 and this mediated phosphorylation of Tim-3 cytoplasmic tail that allows for recruitment and activation of proteins, such as ERK, PI3K and PLC $\gamma$ , and thus enhanced production of cytokines is observed. (B) When Tim-3 is engaged by galectin-9, this mediates phosphorylation of the region where Bat3 interacts with Tim-3 and releases Bat3. Bat3 can interact with p300 and translocate to the nucleus where it mediates transcription of CDK inhibitor p21 and thus inhibits cell cycle progression. Bat3 can also interact with AIFs and this promotes PtdSer exposure, which is involved in the uptake of apoptotic cells. Furthermore, galectin-9 has two binding regions, which allows the possibility of recruitment of other proteins to the vicinity of the TCR receptors, such as receptor phosphatase, CD45. CD45 can then inactivate Lck, (which is main initiator of TCR signalling), and thus the abrogation of TCR signalling pathway and TCR-mediated cytokine production is observed. ....69

**Figure 17: TGF- $\beta$  structure** (adapted from (357, 358)). TGF- $\beta$  is synthesized as precursor protein consisting of a signal peptide, a pro-domain also known as latency-associated peptide (LAP), and the growth factor domain (mature polypeptide). The pro-peptide is processed by proteolytical cleavage, thus separating the pro-domain from the mature polypeptide, although it remains non-covalently associated, this complex is known as small latent TGF- $\beta$  complex (SLC). The mature polypeptide form disulfide-linked dimerization. SLC can associate with latent TGF- $\beta$  binding protein (LTBP) and forms the large latent complex (LLC), which is then secreted and associated with the extracellular matrix (ECM) components. Proteolytic degradation of ECM proteins by e.g. MMPs is thought to activate TGF- $\beta$ 1 by releasing it from LTBP and LAP, and consequently it becomes bioactive and able to bind to its receptors. ....73

**Figure 18: TGF- $\beta$  mediated Smad dependent signalling** (adapted from (357, 358)). (A) bioactive TGF- $\beta$  binds to T $\beta$ RII possibly facilitated by T $\beta$ RIII (not shown). (B) T $\beta$ RI then associated with T $\beta$ RII and binds TGF- $\beta$ , which induces conformational change and stable association as well as the release of Smad7 and FKBP12, which inhibit T $\beta$ RI. (C) When TGF- $\beta$  binds, it creates a hetero-tetrameric complex of two T $\beta$ RI and two T $\beta$ RII receptors. With the release of inhibitors and the cytoplasmic tails of the two receptors in proximity, T $\beta$ RII activates T $\beta$ RI by phosphorylation. (D) Activation of T $\beta$ RI allows recruitment of R-Smad, such as Smad2 and Smad3, which becomes phosphorylated. (E) Phosphorylated R-Smad dissociates from the T $\beta$ Rs. (F) Activated R-Smad forms a trimeric complex with Smad4 (or possibly TIF1 $\gamma$ ), which allows for translocation to the nucleus where it with other transcription factors (TR) and co-regulators mediates activation (or repression) of target genes. Activation of Smad3 can induce more TGF- $\beta$ . ....77

**Figure 19: TGF- $\beta$  mediated non-Smad signalling** (adapted from (357)). Although the TGF $\beta$  receptors are mainly classified as serine/threonine kinases, they possess the ability to phosphorylate tyrosine as well, and are thus considered as dual-specificity kinases. Therefore, engagement of T $\beta$ Rs can also result in tyrosine phosphorylation, which allows for recruitment of ShcA and Grb2 adaptor proteins, which form complex with the guanine exchange factor SOS to activate the GTPase Ras. Ras activates the MAPK pathway Raf-MEK-ERK. TGF- $\beta$  ligation also induces association with the RING domain E3 ubiquitin ligases TRAF6, which undergo polyubiquitination that allows recruitment and activation of

TAK1, which can activate both MKK4 and MKK3/MKK6, resulting in JNK and p38 activation, respectively. All of the MAPK pathways can lead to AP-1 activation, which has been reported to be involved in TGF- $\beta$  production. TAK1 also leads to activation of the I $\kappa$ B (IKK) complex, which mediates release and activation of NF $\kappa$ B. Crosslinking TGF- $\beta$  receptors can also activate the PI3K-AKT-mTOR pathway either through direct association with the p85 (the regulatory unit of PI3K) or with p38 and JNK through association with TRAF6. Activation of the PI3K-AKT-mTOR pathway can lead to translation of HIF-1 $\alpha$ , which is involved in TGF- $\beta$  production .....78

**Figure 20: TGF- $\beta$ -mediated apoptosis by Bim regulation** (adapted from (365)). (A) When the cell receives survival signal, Bim (a pro-apoptotic factor) is released from its binding partner Bcl-XI (an anti-apoptotic factor), and Bim is targeted for proteolytical degradation by phosphorylation-dependent ubiquitination, mediated by the activation of the Raf-MEK-ERK MAPK pathway. TGF- $\beta$  regulates Bim both at transcriptional and translational level. At translational level, TGF- $\beta$ -mediated Smad3 activation induces Runx1 and MKP2. MKP2 dephosphorylates ERK1/2 and thus inactivates it, which prevents proteolytical degradation of Bim. Prolonged TGF- $\beta$  treatment induces a sustained induction of Bim. Bim mediates intrinsic pathway to apoptosis by sequestering Bcl-XL, and thus allows pro-apoptotic effector proteins, such as Bax and Bak, to oligomerize and mediate mitochondrial outer membrane permeabilization, which releases cytochrome C and induces the intrinsic apoptosis programme. (B) Cancer escapes from TGF- $\beta$ -mediated apoptosis. Cancer cells frequently have mutations that result in overexpression or constitutively active RAS, PI3K and CDKs. ERK is downstream of RAS and alone or together with Cdk2/4 can phosphorylate Smad3 and target it for ubiquitination-mediated proteolytical degradation. AKT is downstream of PI3K and it mediates inhibitory phosphorylation of Foxo3. In both cases, there is no transcription of Bim, and whatever Bim there is, is targeted for degradation. ....80

**Figure 21: Immunogenic cell death** (directly from (374)). Therapy-induced ICD promotes exposure of CRT at the surface of dying cells at a pre-apoptotic stage, induces secretion of ATP during apoptosis and release HMGB1 during secondary necrosis (when their membranes become permeabilized). CRT, ATP and HMGB1 bind to their respective receptors on DC, which are CD91, P2RXY and TLR4. ATP acts as a find me signal facilitating the recruitment of DC into the tumour bed. Here, it engulfs dying tumour cells showing CRT on the surface (eat me signal) and with the exposure to HMGB1, they obtained the capacity for processing and presentation of the tumour antigens as well as maturation, and thus optimally activates T cells. This results in IL-1 $\beta$  and IL-17-dependent and IFN $\gamma$ -mediated anti-tumour immune response involving both  $\gamma\delta$  T cells and CTLs, which have been suggested to eliminate residual chemotherapy resistant tumour cells. ...86

**Figure 22: HMGB1 structure** (adapted from (384)). HMGB1 structure illustrating two functional DNA binding domains designated A box and B box, and a C-terminal acidic tail, which is flexible allowing modularly ability. HMGB1 is a multi-binding protein, which interacts with both intracellular and extracellular partners and surface receptors. Intracellular HMGB1 is able to interact with Beclin-1 and p53, regulating autophagy and apoptosis. Extracellular HMGB1 can interact with partners, such as LPS, heparin, ITA, C1q, IL-1 $\beta$ , CXCL12, ssDNA and nucleosomes. Finally, HMGB1 is able to engage different receptors, including receptor for advanced glycation endproducts (RAGE), TLR2, TLR4, TLR9 and CD24-Siglec10. ....88

**Figure 23: HMGB1 redox status mediates different biological effects by interacting with different receptors** (adapted from (384, 388)). HMGB1 can be passively released by

necrotic or apoptotic cells or actively secreted from activated immune cells or stressed cancer cells. Dependent of its redox state, HMGB1 mediated different functional effects. Some of the most important receptors and their simplified signalling pathways are illustrated here. Al-thiol (reduced) HMGB1 can interact with CXCL12 and engage CXCR4 to promote **chemotaxis and recruitment of inflammatory cells**. Al-thiol form of HMGB1 can directly engage the RAGE receptor to induce **autophagy and pro-inflammatory cytokines**. Disulfied (semi oxidised) HMGB1 can directly bind to TLR4 to promote production of **pro-inflammatory cytokines**. HMGB1 has also been shown to bind to TLR2, TLR9 and Tim-3, although the redox form of HMGB1 upon interaction with these receptors has not been identified. Like with RAGE and TLR4, engagement of TLR2 and TLR9 activates NFκB, which induces **production of inflammatory cytokines**. When HMGB1 interacts with Tim-3, it has been shown to prevent binding of nucleotide and thus inhibiting **nucleic acid-mediated immune response as well as inducing production of VEGF, promoting angiogenesis**. Apoptosis promotes mitochondrial ROS and release of oxidized HMGB1. Fully oxidized (sulfonate cysteines) HMGB1 is immunological inert and thus mediates **immune tolerance**. HMGB1 can undergo post-translational modification, such as acetylation and oxidation, which increases its cytoplasmic accumulation and extracellular secretion. ....89

**Figure 24: Density gradient centrifugation.** Lymphoprep and Ficoll-Paque-Plus have a density of 1.077 g/mL. A density gradient centrifugation will result in three layers, a bottom layer of erythrocytes and granulocytes, an intermediate layer of PBMCs and an upper layer of plasma (420, 421). ....98

**Figure 25: Lipofection** (adapted from (422)). (A) Chemical structure of the cationic-lipid transfection reagent 1,2-dioleoyl-3-trimethylammoniumpropyl chloride (DOTAP) (423). (B) Schematic illustration of Lipoplex-mediated transfection and endocytosis (422). The lipoplex complex structure (consisting of liposomes and DNA) fuse with the cell membrane where it is internalised by endocytosis, resulting in the formation of a double-layer inverted micellar vesicle. During the maturation of the endosome into a lysosome, the endosomal wall might rupture, releasing the contained DNA into the cytoplasm and potentially towards the nucleus. DNA imported into the nucleus might result in gene expression. Alternatively, DNA might be degraded within the lysosome (422). In this study, siRNA is transfected instead of DNA and this is accumulated in the cytosol where it causes gene silencing when interacting with the RNA-inducing silencing complex (RISC). The chemical structure was drawn in ChemSpider. ....99

**Figure 26: Schematic illustration of gene knockdown with RNAi.** Transfected siRNA is loaded on to Ago-2 in the RISC. Once loaded the passenger-strand is discarded and the remaining strand is used as the guide-strand to find and cleave mRNA with complementary sequence (424, 426)..... 100

**Figure 27: Chemical structure and spectrum of Coomassie Brilliant Blue G-250** (adapted from (430)). (A) Chemical structure of Coomassie Brilliant Blue G-250. (B) The spectrum from unbound (red line) and protein-bound (green line) Coomassie Brilliant Blue. After binding the absorbance maximum of the dye shifts from 465 nm to 595 nm (430). (C) An example of BSA standard curve, which is used to calculate the protein concentration from an unknown sample. The chemical structure was drawn in ChemSpider ..... 102

**Figure 28: The sequential stage of the western blot process** (adapted from (431)). 1) Sample preparation, 2) SDS-PAGE, 3) transfer, 4) blocking, 5) detection and imaging, and 6) quantitative analysis. Here is shown enhance chemiluminescent detection (ECL) with horseradish peroxidase (HRP), however, in this study, fluorescent detection was used. 104



<b>Figure 29: Principle of SDS-PAGE</b> (adapted from (433)). In this study, DTT was used as a reducing agent instead of $\beta$ -mercaptoethanol.....	106
<b>Figure 30: Schematic representation of the sandwich assembly in (A) semidry and (B) wet transfer.</b> For semi-dry transfer, the sandwich is placed directly in the transfer machine, whereas in wet transfer, the sandwich is assembled in the blotting module, which is positioned in the gel tank and then immersed with transfer buffer. ....	107
<b>Figure 31: Multiplex detection using a near-infrared (NIR) fluorescent WB</b> (adapted from LI-Cor's webpage). Secondary antibodies IRDy680RD = red, and IRDye800CW = green detect the fluorescent signal at 700 nm and 800 nm, respectively. Yellow depicts overlapping signal between the green and red channel (434). ....	108
<b>Figure 32: On-Cell Western assay (OCA).</b> The illustration is an example of detection of Tim-3 on the surface of Jurkat T cells. Cultured cells with or without treatment are exposed to primary antibody (which in this case anti-Tim-3) followed by incubation with secondary antibody conjugated to a fluorophore (in this case the green fluorophore IRDye 800CW was used as the secondary antibody).....	110
<b>Figure 33: Schematic illustration of the HRP reaction.</b> o-phenylenediamine (OPD) oxidation catalysed by HRP leads to the formation of 2,3-diaminophenazine (DAP), which can absorb at three different wavelengths, depending on pH and its protonated structure. The structure can have a neutral charge, be mono-cation or di-cation and the absorbance for these are respectively, 418 nm, 430-450 nm and 490 nm (439-441). Structures were drawn in ChemSpider. ....	111
<b>Figure 34: Schematic illustration of indirect sandwich ELISA.</b> Well from a 96-well poly-D-lysine (PDL) plate coated with capture antibody and blocked with BSA. Antigen (Ag) from the samples binds to the captured antibody and detection antibody conjugated to biotin (B) binds to the antigen creating a sandwich with antigen in the middle. Streptavidin, which is conjugated to horseradish peroxidase (HRP), has a high affinity to B. HRP together with H <sub>2</sub> O <sub>2</sub> catalyse the conversion of o-phenylenediamine (OPD) to 2,3-diaminophenazine (DAP). The signal is measured at 492 nm in a plate-reader. ....	112
<b>Figure 35: Schematic illustration of DPI-ELISA for detection of DNA binding activity.</b> A well from a 96-well PDL plate coated with streptavidin and blocked with bovine serum albumin (BSA). dsDNA with response element (RE) conjugated to biotin (B) binds with high affinity to streptavidin. Activated transcription factor (TR) from the samples with specific recognition to RE binds via its DNA binding site. A primary antibody specific for the TR binds, and secondary fluorescent antibody binds to the primary antibody. The fluorescent signal is detected and quantified in the Odyssey Clx imager.....	114
<b>Figure 36: Schematic illustration of the Xanthine oxidase reaction.</b> Xanthine oxidase catalyses with the production of hydrogen peroxide as a by-product. Structures were drawn in ChemSpider. ....	117
<b>Figure 37: Schematic illustration of the reaction in the Nox activity assay.</b> A) Nox catalyses the oxidation of NADPH while producing a superoxide anion. B) The reaction in which superoxide reduces nitroterazolium blue (NTB) to formazan. Structures are drawn in ChemSpider. ....	118
<b>Figure 38: Thiobarbiturate reactive substance (TBRS) assay</b> (adapted from (457)). Two molecules of 2-thiobarbituric acid (TBA) react with one molecule of Malondialdehyde (MDA) to form a coloured-end-product, which can be spectrophotometrically detected at $\lambda_{max}$ = 532 nm. Structures were drawn in ChemSpider. ....	119
<b>Figure 39: Elevated expression levels of LPHNs, FLRT3, Tim-3 and galectin-9 in breast tumour tissue</b> (adapted from (326)). Expression levels of Tim-3, galectin-9 (A),	

FLRT3, LPHN2 (B) and LPHN3 (C) were analysed in primary breast malignant tumours and compared with healthy breast tissues (HT) of five patients (n = 5) by WB. Illustration of the surface expression on BT (D). Molecular weight markers (MW) are expressed in kDa. Images are from one experiment representative of five, which gave similar results. Other results are shown as mean values  $\pm$  SEM. \*p < 0.05; \*\*p < 0.01, and \*\*\*when p < 0.001 vs. control (326)..... 122

**Figure 40. Expression and activity of components downstream of the LPHN receptor in primary human breast tumours** (from (326)). The  $\alpha$ -subunit of the Gq protein expression was analysed using WB (A). Activities of PLC, PKC $\alpha$ , and the levels of phospho-S2448 mTOR were detected as described in (326) (B and C). The amounts of phospho-S65 and total eIF4E-BP (mTOR substrate) were analysed using WB (D). These components were analysed in primary breast malignant tumours and healthy breast tissues (HT) of five patients (n = 5). Molecular weight markers (MW) are expressed in kDa. Images are from one experiment representative of five which gave similar results. Other results are shown as mean values  $\pm$  SEM. \*p < 0.05; \*\*p < 0.01, and \*\*\*when p < 0.001 vs. control (326)..... 124

**Figure 41: Expression, interaction and co-localization of Tim-3 and galectin-9 in primary human breast tumours** (directly from (326)). (A) Presence of the Tim-3-galectin-9 complex in primary normal and tumour tissue extracts was analysed using ELISA as described in (326). (B) Expression and co-localization of galectin-9 and Tim-3 were analysed in primary human breast tumours and healthy tissues of the same patients using confocal microscopy as described in (326). Images are from one experiment representative of five, which gave similar results. Scale bars correspond to 20  $\mu$ m (326). ..... 125

**Figure 42: The MCF-7 breast cancer cell line mirrors primary human breast tumours the most** (adapted from (326)). (A) The expression levels of FLRT3-LPHN-galectin-9-Tim-3 pathway in MCF-7 breast cancer cell line were analysed by WB with  $\beta$ -actin as a housekeeping protein. (B) Levels of galectin-9 mRNA were compared in healthy breast tissue (HT) and breast tumour tissues as well as in MCF-7 cells and normalised against those of  $\beta$ -actin. qRT-PCR for galectin-9 and  $\beta$ -actin were performed as described in (326). Images are from one experiment representative of at least three which gave similar results. Data are the mean values  $\pm$  SEM of five independent experiments. \*\*, p<0.01 and \*\*\* p<0.001 vs control (326)..... 127

**Figure 43: The FLRT3-LPHN pathway induces translocation of galectin-9 onto the surface of MCF-7 breast cancer cells** (from (326)). (A) Secondary structure and conformational changes of LPHN2 olfactomedin-like domain (FLRT3-binding region), FLRT3, and the complex of the two proteins mixed at the equimolar ratio was characterized using SRCD spectroscopy as outlined in the Materials and Methods of (326). An interaction between olfactomedin-like domain of LPHN3 and FLRT3 generated by Swiss PDB viewer [5 cmn.pdb file downloaded through PubMed database was used] is presented to illustrate the structural basis of FLRT3 interaction with LPHNs (326). (B) G $\alpha$ Q expression by WB in MCF-7 cells. (C) MCF-7 cells were stimulated 10 nM FLRT3 for 4 h and activities of PLC, PKC $\alpha$ , the levels of phospho-S2448 mTOR, the amounts of phospho-S65 and total eIF4E-BP (an mTOR substrate) were analysed as described in the Materials and Methods of (326). (D) MCF-7 cells were exposed for 4 h to 10 nM FLRT3 with or without 1 h pre-treatment with 30  $\mu$ M U73122 (PLC inhibitor) or 70 nM Gö6983 (PKC $\alpha$  inhibitor). Surface presence of galectin-9 was measured by on-cell assay. Images are from one experiment representative of at least three which gave similar results. Other

results are shown as mean values  $\pm$  SEM of at least three independent experiments. \* $p < 0.05$ ; \*\* $p < 0.01$  vs. control (326). ..... 129

**Figure 44: sTim-3 and galectin-9 suppress Jurkat T cell function.** Jurkat T cells were pre-treated with 100 nM PMA for 30 min followed by 24 h stimulation with 1  $\mu$ g/mL galectin-9 or Tim-3. Levels of released IFN $\gamma$ , TNF $\alpha$  and IL-2 were detected by ELISA. The catalytic activity of granzyme B was analysed in the cell lysates. Data are the mean values  $\pm$  SEM of four independent experiments ( $n=4$ ). ..... 133

**Figure 45: Galectin-9 protects MCF-7 cells against T cell-dependent cytotoxic immune attack.** (A) Illustrates that MCF-7 cells were co-cultured with Jurkat T cells (pre-treated with PMA) at a ratio of 2:1 for 4 h in the absence or presence of 5  $\mu$ g/mL galectin-9 neutralizing antibody. (B) Demonstrates the surface presence of Tim-3 and galectin-9 on Jurkat T cells and MCF-7, respectively. (C and D) After the experiment, MCF-7 cells and Jurkat T cells were assessed for granzyme B and caspases-3 activity as an indicator of granzyme B mediated apoptosis. Images are from one experiment representative of at least three, which gave similar results. Other results are presented as mean values  $\pm$  SEM of at least three independent experiments. \* $p < 0.05$  vs. control. .... 134

**Figure 46: Galectin-9 protects MCF-7 cells against T cell-dependent cytotoxic immune attack** (directly from (326)). (A) MCF-7 cells were co-cultured with TALL-104 cytotoxic T lymphocytes at a ratio of 4:1 for 16 h (the ratio was determined by the aggressive behaviour of TALL-104 cells) in the absence or presence of 5  $\mu$ g/mL galectin-9 neutralizing antibody or 5  $\mu$ g/mL isotype control antibody. (B) After the experiment, TALL-104 cells were lysed, and PARP cleavage, as an indicator of the rate of apoptotic cells, was measured using WB analysis. (C) CD8 expressions (reflecting the infiltration of TALL-104 into the MCF-7 layer) were measured by on-cell assay. (D) Galectin-9 surface presence was measured using an on-cell assay in resting MCF-7 cells and those co-cultured with TALL-104 cells. (E) Viability of MCF-7 cells was measured by MTS test. Images are from one experiment representative of five, which gave similar results. Other results are presented as mean values  $\pm$  SEM of five independent experiments. \* $p < 0.05$  vs. control (326). ..... 135

**Figure 47: Expression of Tim-3, galectin-9, LPHNs 1, 2, and 3 as well as FLRT3 proteins in various human cancer cell lines** (directly from (326)). Lysates of indicated cells were subjected to WB analysis as outlined in Materials and Methods (images are presented in Appendix Table 2). Detected infrared fluorescence of the bands divided by the total amount of protein loaded (measured using a Bradford assay) was used as a measure of protein quantity. Levels of Tim-3 & total galectin-9 (A) and LPHNs 1, 2, & 3 (B) were expressed as a % of the levels present in THP-1 cells (expressed as 100%). Since THP-1 cells lack FLRT3 expression, the levels of this protein were expressed as % RCC-FG1 (C), considering FLRT3 level in these cells as 100%. Bn, brain; CR, colorectal; Ki, kidney; BBM, blood, bone marrow and mast cells; Li, liver; Br, breast; Pr, prostate; Lu, lung; Sk, skin. Data are presented as mean values  $\pm$  SEM of three independent experiments (326). ..... 138

**Figure 48: Breast cancer cell-based patho-biochemical pathways showing LPHN-induced activation of PKC $\alpha$ , which triggers the translocation of Tim-3 and galectin-9 onto the cell surface which is required for immune escape** (directly from (326)). The interaction of FLRT3 with LPHN isoform leads to the activation of PKC $\alpha$ , most likely through the classic Gq-PLC-Ca $^{2+}$  pathway. Ligand-bound LPHN activates Gq, which in turn stimulates PLC. This leads to phosphatidyl-inositol-bisphosphate (PIP2) degradation and production of inositol-trisphosphate (IP3) and diacylglycerol (DAG). PKC $\alpha$  requires DAG

and cytosolic  $Ca^{2+}$  for its activation. Activated PKC $\alpha$  provokes the formation of SNARE complexes that tether vesicles to the plasma membrane. Galectin-9 impairs the cancer cell killing activity of cytotoxic T cells (and other cytotoxic lymphocytes) (326). Possible (not directly confirmed) interactions of galectin-9 with glycoside component and T cell receptor (TCR)/CD8, with MHC I, and the antigen are highlighted with question mark “?” to indicate the fact that it is a hypothetic interaction since TALL-104 cells used in the study kill tumour cells in an MHC-independent manner (326, 468). ..... 141

**Figure 49: Proposed model in which oxidative stress mediates HIF-1 and AP-1 activation, resulting in the production of TGF- $\beta$  and upregulation of galectin-9** (directly from (419)). The proposed pathway studied is summarised, and it is indicated that XOD and Nox produce ROS, which activates the transcription factor AP-1 through ASK1-controlled MAP kinase cascade. HIF-1 and AP-1 contribute to the activation of TGF- $\beta$  expression, which then displays autocrine activity and stimulates the activation of galectin-9 and possibly Tim-3 expression through Smad3 transcription factor (419). ..... 145

**Figure 50: Oxidative burst is increased in breast cancer tissue** (adapted from (419)). Tissue lysates from breast tumour and adjacent healthy breast tissue were subjected to measurement of xanthine oxidase and NADPH oxidase activities (A) and TBRS levels (B). As illustrated in the figure superoxide radicals may in the tumour tissue be caused by hypoxia, increased XOD or Nox activity. All quantities are expressed in respective units per 1 g of the tissue. In addition, normalisations against total protein for enzyme activities and TBRS assays were performed. These results are presented in Appendix, Figure 82. Images are from one experiment representative of five, which gave similar results. Data are shown as mean values  $\pm$  SEM of five independent experiments. \* -  $p < 0.05$  and \*\* -  $p < 0.01$  vs non-transformed peripheral tissue abbreviated as HT (healthy tissue) (419). .. 147

**Figure 51: Increased redox status, upregulated HIF-1 $\alpha$ , ATF-2 activation and TGF- $\beta$ /Smad3 pathways and Tim-3 and galectin-9 expression in breast tumour tissues compared to non-transformed peripheral tissues** (adapted from (419)). HIF-1 $\alpha$  accumulation, tissue-associated and phosphorylation of ATF-2 TGF- $\beta$  and phospho-S423/S425-Smad3 levels (A), as well as levels of tissue-associated Tim-3 and galectin-9 (B), were analysed in tissue lysates. All quantities are expressed in respective units per 1 g of the tissue. In addition, normalisations against total protein loaded (for WB) were performed. These results are presented in Appendix, Figure 82. Images are from one experiment representative of five which gave similar results. Data are shown as mean values  $\pm$  SEM of five independent experiments. \* -  $p < 0.05$  and \*\* -  $p < 0.01$  vs non-transformed peripheral tissue abbreviated as HT (healthy tissue) (419). ..... 148

**Figure 52: Increased redox status, upregulated HIF-1 $\alpha$  and TGF- $\beta$ -Smad3 pathways as well as Tim-3 and galectin-9 expression in primary human AML cells compared to non-transformed PBMCs** (from (419)). Measurements were conducted in primary human AML cells vs primary peripheral blood mononuclear cells (PBMCs, leukocytes) obtained from healthy donors. Activities of xanthine oxidase, NADPH oxidase and TBRS levels (A). Levels of accumulated HIF-1 $\alpha$  protein and phospho-S423/S425-Smad3 were assessed by WB (B). Levels of secreted TGF- $\beta$ , Tim-3 and galectin-9 were measured in cell culture medium using ELISA (C). Images are from one experiment representative of five, which gave similar results. Data are shown as mean values  $\pm$  SEM of five independent experiments. \* -  $p < 0.05$  and \*\* -  $p < 0.01$  vs PBMCs (419). ..... 149

**Figure 53: Levels of secreted TGF- $\beta$  in blood plasma of healthy donors, primary and metastatic breast cancer patients and AML patients** (directly from (419)). TGF- $\beta$  concentrations were measured in the blood plasma of healthy donors, patients with

primary breast tumours, patients with metastatic breast solid tumours and AML patients (n=6 for all donor types). Data are shown as mean values  $\pm$  SEM (data for each patient are shown). \* -  $p < 0.05$  vs healthy donors (419). ..... 150

**Figure 54: HMGB1, a TLR4 ligand triggers TLR4 mediated activation of the ROS signalling pathway** (directly from (419)). TLR4 triggers assembly and activation of NADPH oxidase using myeloid differentiation factor 88 (MyD88), TLR4 TIR domain-associated protein (TIRAP) and Bruton's tyrosine kinase (Btk). Activation of Btk by MyD88 and TIRAP leads to Btk-dependent phosphorylation of phospholipase C (PLC, mainly isoform 1 $\gamma$ ), which triggers activation of protein kinase C alpha (PKC $\alpha$ ). PKC $\alpha$  activates NADPH oxidase, which produces a superoxide anion radical, which activates ASK1 by releasing it from thioredoxin. The ASK1 pathway mediates activation of the AP-1 transcription factor (419). ..... 152

**Figure 55: Oxidative stress-induced activation of AP-1 in an ASK1-dependent manner and promotes TGF- $\beta$  and galectin-9 expression** (directly from (419)). THP-1 cells were exposed for 24 h to 1  $\mu$ g/mL HMGB1 with or without pre-treatment with 30  $\mu$ M DPI (NADPH oxidase inhibitor), 1  $\mu$ M SR11302 (AP-1 inhibitor) or transfection with a dominant-negative isoform of ASK1 ( $\Delta$ N-ASK1). Levels of secreted TGF- $\beta$  and galectin-9 were measured by ELISA (B). Data are shown as mean values  $\pm$  SEM of four independent experiments. \* -  $p < 0.05$  and \*\* -  $p < 0.01$  vs control (419). ..... 153

**Figure 56: Xanthine oxidase activation leads to increased oxidative stress and upregulation of the TGF- $\beta$ -Smad3 pathway and galectin-9 expression** (directly from (419)). MCF-7 human breast cancer cells were exposed to 100  $\mu$ g/mL ammonium molybdate for 24 h to induce xanthine oxidase activity in the absence or presence of 250  $\mu$ g/mL allopurinol (xanthine oxidase inhibitor). Xanthine oxidase activity, TBRS levels, HIF-1 $\alpha$  accumulation (A), secreted TGF- $\beta$  and cell-associated phospho-S423/S425-Smad3 (B), Tim-3 and galectin-9 (C) were analysed as outlined in the Materials and Methods. Images are from one experiment representative of four, which gave similar results. Data are shown as mean values  $\pm$  SEM of four independent experiments. \* -  $p < 0.05$  and \*\* -  $p < 0.01$  vs indicated events (419). ..... 155

**Figure 57: Schematic illustration of how xanthine oxidase derived ROS results in TGF- $\beta$  and galectin-9 production under the normoxic condition in MCF-7 cells** (from (419)). Xanthine oxidase activity is increased with the addition of molybdate, which results in increased ROS production. The increase in the oxidative burst is not enough to result in HIF-1 $\alpha$  accumulation, but there still is an augmented TGF- $\beta$ 1 secretion and galectin-9 expression, suggesting that the ASK1-p38-AP-1 pathway may contribute to TGF- $\beta$  production, and the subsequent TGF- $\beta$ 1 signalling results in upregulation of galectin-9 expression. ..... 156

**Figure 58: HIF-1 is involved in the production of TGF- $\beta$  and galectin-9** (from (419)). Cobalt chloride induces HIF-1 activation, TGF- $\beta$  and galectin-9 production. Wild type, HIF-1 $\alpha$  knockdown and random siRNA-transfected MCF-7 cells were exposed to 50  $\mu$ M cobalt chloride for 6 h followed by measurement of HIF-1 DNA binding activity, secreted (in cell culture medium) and cell-associated (in cell lysates) TGF- $\beta$  and cell-associated galectin-9. Images are from one experiment representative of three, which gave similar results. All quantitative data are shown as mean values  $\pm$  SEM (n=3-4). \* -  $p < 0.05$  and \*\* -  $p < 0.01$  vs indicated events (419). ..... 159

**Figure 59: Dynamics of cobalt chloride-induced HIF-1 activation, TGF- $\beta$  and galectin-9 accumulation in MCF-7 human breast cancer cells** (from (419)). MCF-7 cells were exposed to 50  $\mu$ M cobalt chloride for 1, 2, 3, 4, 5 and 6 h followed by

measurement of HIF-1 DNA binding activity, secreted and cell-associated TGF- $\beta$  and cell-associated galectin-9. Images are from one experiment representative of three, which gave similar results (in the case of TGF- $\beta$  – vs 1 h time-point since at zero point, cells cannot release any TGF- $\beta$ . At this time-point, fresh medium had just been supplied and measurement was obtained immediately to confirm zero TGF- $\beta$  levels). All quantitative data are shown as mean values  $\pm$  SEM (n=3-4). \* -  $p < 0.05$  and \*\* -  $p < 0.01$  vs indicated events (419)..... 160

**Figure 60: HIF-1-induced galectin-9 expression is mediated by TGF- $\beta$**  (from (419)). MCF-7 cells were exposed to 50  $\mu$ M cobalt chloride for 6 h with or without presence of TGF- $\beta$  neutralising or isotype control antibody. Galectin-9 expression was then assessed by WB. Images are from one experiment representative of three, which gave similar results. All quantitative data are shown as mean values  $\pm$  SEM (n=3-4). \* -  $p < 0.05$  and \*\* -  $p < 0.01$  vs indicated events (419)..... 161

**Figure 61: Smad3 is involved in TGF- $\beta$  and galectin-9 expression** (directly from (419)). Wild type, Smad3 knockdown and random siRNA-transfected MCF-7 cells were exposed to 2 ng/mL TGF- $\beta$  for 24 h followed by measurement of secreted (in cell culture medium) and cell-associated (in cell lysates) TGF- $\beta$  as well as cell-associated galectin-9 and phospho-S423/S425 Smad3. Images are from one experiment representative of three, which gave similar results. All quantitative data are shown as mean values  $\pm$  SEM (n=3-4). \* -  $p < 0.05$  and \*\* -  $p < 0.01$  vs indicated events (419)..... 162

**Figure 62: Scheme of the experiment performed showing studied effects.** CoCl<sub>2</sub> (Co), a chemical inducer of hypoxia, promotes HIF-1 $\alpha$  accumulation (possibly by inhibition of PHD and/or augment ROS production). HIF-1 $\alpha$  associates together with HIF-1 $\beta$  to form the HIF-1 transcription factor complex, which then translocate to the nucleus to induce transcription of TGF- $\beta$ . Secreted TGF- $\beta$  acts most likely locally in an autocrine manner binding to the TGF- $\beta$  receptors to activate TGF- $\beta$  signalling, which includes activation of the canonical Smad pathway. A direct downstream effector molecule of TGF- $\beta$  receptor activation is Smad3, which is phosphorylated and can then associate with other Smad molecules (such as Smad2 and possible Smad4) to form a complex, which is translocated to the nucleus to induce transcription of both TGF- $\beta$  gene and LGALS9 and consequently production of more TGF- $\beta$  and galectin-9 that can be used to escape immune surveillance. .... 163

**Figure 63: TGF- $\beta$  induces galectin-9 expression in human cancer but not healthy cells** (from (419)). THP-1 (AML), Colo-205 (colorectal cancer), MCF-7 (breast cancer) HaCaT (keratinocytes) and primary human keratinocytes (Prim KC) were exposed to 2 ng/mL human recombinant TGF- $\beta$  for 24 h. Levels of cell-associated Tim-3 and galectin-9 and secreted galectin-9 were measured. Images are from one experiment representative of four, which gave similar results. Data are shown as mean values  $\pm$  SEM of four independent experiments. \* -  $p < 0.05$  vs control (419)). .... 165

**Figure 64: The effects of TGF- $\beta$  on Smad3 phosphorylation in human cancer and non-malignant cells** (from (419)). (A) MCF-7 (breast cancer), (B) HaCaT (keratinocytes) and (C) primary human keratinocytes were exposed for 24 h to 2 ng/mL TGF- $\beta$  followed by WB analysis of phospho-S423/S425-Smad3 levels. Images are from one experiment representative of four, which gave similar results. Data are shown as mean values  $\pm$  SEM of four independent experiments (419). .... 166

**Figure 65: Proposed mechanism of the regulation of galectin-9 expression in human cancer at low and normal oxygen availability stages** (directly from (419)). The figure depicts the key processes taking place in malignant tumour growth during the initial low

oxygen availability (hypoxic) stage and later (normal oxygen availability) stages. The studied biochemical events are demonstrated in the right-hand panel. During the hypoxic stage, HIF-1 induces TGF- $\beta$  expression, which then displays autocrine activity and triggers galectin-9 expression in a Smad3-dependent manner. During the normal oxygen availability stage, oxidative stress may trigger activation of HIF-1 and AP-1, which contributes to TGF- $\beta$  expression, and it is self-triggered by TGF- $\beta$ . Galectin-9 upregulation is perpetually induced by the TGF- $\beta$ -Smad3 pathway (419)..... 173

**Figure 66: HMGB1 mediates TGF- $\beta$ , Tim-3 and galectin-9 secretion in THP-1 cells.** THP-1 cells were exposed to 1  $\mu$ g/mL recombinant human HMGB1 for 24 h followed by measurements of secreted TGF- $\beta$ , galectin-9 and Tim-3 detected by ELISA, protein expression of phospho-S423/S425 Smad3, galectin-9 and Tim-3 was determined by WB, and surface-based galectin-9 was examined by OCA. Images are from one experiment representative of at least three, which gave similar results. All quantitative data are shown as mean values  $\pm$  SEM \* -  $p < 0.05$  and \*\* -  $p < 0.01$  vs control. .... 177

**Figure 67: HMGB1 do not affect secretion of TGF- $\beta$ , galectin-9 or Tim-3, but translocate galectin-9 to the surface in Colo-205 cells.** Colo-205 cells were exposed to 1  $\mu$ g/mL recombinant human HMGB1 for 24 h followed by measurements of secreted TGF- $\beta$ , galectin-9 and Tim-3 detected by ELISA, protein expression of phospho-S423/S425 Smad3, galectin-9 and Tim-3 was determined by WB, and surface-based galectin-9 was examined by OCA. Images are from one experiment representative of at least three, which gave similar results. All quantitative data are shown as mean values  $\pm$  SEM \* -  $p < 0.05$  and \*\* -  $p < 0.01$  vs control. .... 180

**Figure 68: HMGB1 do not mediate any effect on TGF- $\beta$ , galectin-9 and Tim-3 in MCF-7 cells.** MCF-7 breast cancer cells were exposed to 1  $\mu$ g/mL recombinant human HMGB1 for 24 h followed by measurements of secreted TGF- $\beta$ , galectin-9 and Tim-3 detected by ELISA, protein expression of phospho-S423/S425 Smad3, galectin-9 and Tim-3 was determined by WB, and surface-based galectin-9 was examined by OCA. Images are from one experiment representative of four, which gave similar results. All quantitative data are shown as mean values  $\pm$  SEM (n=4) \* -  $p < 0.05$  and \*\* -  $p < 0.01$  vs control..... 181

**Figure 69: HMGB1 do not mediate any effect on TGF- $\beta$ , galectin-9 and Tim-3 in non-malignant HaCaT keratinocytes.** HaCaT keratinocytes were exposed to 1  $\mu$ g/mL recombinant human HMGB1 for 24 h followed by measurements of secreted TGF- $\beta$ , galectin-9 and Tim-3 detected by ELISA, protein expression of phospho-S423/S425 Smad3, galectin-9 and Tim-3 was determined by WB, and surface-based galectin-9 was examined by OCAs. Images are from one experiment representative of four which gave similar results. All quantitative data are shown as mean values  $\pm$  SEM (n=4) \* -  $p < 0.05$  and \*\* -  $p < 0.01$  vs control..... 182

**Figure 70: Constitutive expression of HMGB1 receptors, RAGE, TLR2, TLR4 and Tim-3.** All the four cell lines, THP-1 (model for human AML), Colo-205 (model for human colorectal cancer), MCF-7 (model for non-invasive human breast cancer) and HaCaT (a non-transformed human cell line which is model for human keratinocytes), were examined for expression of known HMGB1 surface receptor. The THP-1 cell line is the only analysed cell line expressing all four receptors. Colo-205 expressed all except for TLR4. MCF-7 and HaCaT cells only expressed RAGE and Tim-3. Images are from one experiment representative of three..... 183

**Figure 71: HMGB1-mediated effect on TGF- $\beta$  and galectin-9 is TLR4 dependent.** Colo-205 cells were transfected with MCD14-hTLR4 (a constitutive active TLR4 receptor) or empty vector as control and cultured for 24 h. Activation of AP-1 was determined by

expression of pT69/T71-ATF-2/total ATF-2, TGF- $\beta$ , and galectin-9 secretion as well as cell-associated galectin-9 were analysed by ELISA. Protein expression of phospho-S423/S425 Smad3, pT69/T71-ATF-2, Total ATF-2, galectin-9 and Tim-3 was determined by WB. Images are from one experiment representative of at least three, which gave similar results. All quantitative data are shown as mean values  $\pm$  SEM \* -  $p < 0.05$  and \*\* -  $p < 0.01$  vs control. .... 184

**Figure 72: HMGB1 do not mediate any effect on TGF $\beta$  or galectin-9 in primary human AML cells lacking TLR2 and TLR4 receptors.** Primary human AML cells were exposed to 2.5  $\mu$ g/mL recombinant human HMGB1 for 16 h followed by measurements of secreted TGF- $\beta$ , galectin-9 and Tim-3 detected by ELISA, protein expression of phospho-S423/S425 Smad3, galectin-9, Tim-3, TLR2 and TLR4 was determined by WB. Images are from one experiment representative of three, which gave similar results. All quantitative data are shown as mean values  $\pm$  SEM (n=3) \* -  $p < 0.05$  and \*\* -  $p < 0.01$  vs control. .... 186

**Figure 73: Cell death induce HMGB1 release from cancer cells.** (A) BH3I-1 (a Bcl-XL antagonist) induces apoptosis via the intrinsic pathway by promoting permeabilization of the mitochondrial outer membrane causing caspase activation and release of HMGB1. (B) THP-1, Colo-205 and MCF-7 cancer cell lines were analysed for HMGB1 secretion after exposure to 100  $\mu$ M BH3I-1 for 24 h. All quantitative data are shown as mean values  $\pm$  SEM (n=3) \* -  $p < 0.05$  and \*\* -  $p < 0.01$  vs control. .... 189

**Figure 74: Levels of secreted HMGB1 blood plasma of healthy donors, primary and metastatic breast cancer patients, and AML patients.** HMGB1 concentrations were measured in the blood plasma of healthy donors, patients with primary breast tumours, patients with metastatic breast solid tumours and AML patients (n=5 for all donor types). Data are shown as mean values  $\pm$  SEM (data for each patient are shown). \* -  $p < 0.05$  vs healthy donors. .... 189

**Figure 75: Stressed cell release HMGB1, which promote biological active TGF- $\beta$  secretion that can induce galectin-9 production.** To induce oxidative stress, THP-1 cells were exposed to 1 mM hydrogen peroxide (H<sub>2</sub>O<sub>2</sub>) for 24 h. Medium was collected from the cells and was split in two. One half of the medium was depleted for HMGB1 by nanoconjugates (NCJ) coated with anti-HMGB1 antibodies. THP-1 cells (which express TLR4) were then either treated with medium containing HMGB1 or HMGB1 depleted medium. Medium from these cells were collected, and the TGF- $\beta$  concentration was measured. The medium from the THP-1 cells that received HMGB1 containing medium were also split in two. Like HMGB1, TGF- $\beta$  was depleted from one half using NCJ coated with anti-TGF- $\beta$  antibodies. MCF-7 cells were then treated with TGF- $\beta$  containing medium or TGF- $\beta$  depleted medium for 24 h, and following the expression of galectin-9 was determined by WB. Images are from one experiment representative of at least three, which gave similar results. All quantitative data are shown as mean values  $\pm$  SEM \* -  $p < 0.05$  and \*\* -  $p < 0.01$  \*\*\*-  $p < 0.001$  vs indicated events. .... 190

**Figure 76: Schematic illustrating of a vicious cycle in which stress/dying tumour cells promote immune escape by HMGB1-mediated TGF- $\beta$ -induced galectin-9 production.** A solid tumour cell was damaged causing release of HMGB1. These tumours are often infiltrated by TLR4-positive myeloid cells (such as TAMs or MDSCs). HMGB1 released from the damage tumour cells stimulates TGF- $\beta$  production and secretion from the TLR4-positive myeloid cells. TGF- $\beta$ -derived from TLR4-possitive cells can promote galectin-9 production by the "healthy" and live tumour cells. This facilitates immune escape of cancer cells and thus completes the cycle. .... 195



**Figure 77: Expression of galectin-9 in primary human breast tumours** (from (326)). Expression levels of galectin-9 were analysed in primary BT and HT of five patients (n=5) by WB using 10 % PAGE. Images are from one experiment representative of five which gave similar results. Other results are shown as mean values  $\pm$  SEM. \*\*\*  $p < 0.001$  vs HT (326). .....a

**Figure 78: CD3 is barely detectable in tumour tissue** (from (326)). The levels of CD3 (biomarker of T cells) were also measured using lysate of Jurkat T cells as a positive control. Molecular weight markers (MW) are expressed in kDa. Images are from one experiment representative of five which gave similar results. Other results are shown as mean values  $\pm$  SEM. \* $p < 0.05$ ; \*\* $p < 0.01$ , and \*\*\*when  $p < 0.001$  vs. control (326) .....b

**Figure 79: Jurkat T cells express both Tim-3 and galectin-9 in resting conditions.** The expression of Tim-3 and galectin-9 were measured using lysate of Jurkat T cells in resting unstimulated condition. Molecular weight markers (MW) are expressed in kDa. Images are from one experiment. ....b

**Figure 80: AP-1, HIF-1 and Smad3 binding sites in the TGF- $\beta$  promoter region.** Using AP-1 consensus sequence TGTCTCA = grey and TGACTCT = cyan. Two possible AP-1 binding site was identified. Using HIF-1 consensus sequence (A/G)CGTG = red, 2 possible binding sites was identified. Smad3 has can bind to several motifs, including the Smad box consensus sequence GTCT=green and AGAC =yellow, CAGA motifs AGCCAGACA =red text, and 5 bp GC-rich motif GGCGC=blue and GGCCG=pink. Using these sequences 14 possible Smad3 binding sites were identified in the TGF- $\beta$  promoter. T=red marks transcription start site.....g

**Figure 81: Smad3 binding sites in the LGALS9 promoter region.** Using the Smad box consensus sequence GTCT=green and AGAC =yellow. There were no 5-bp GC-rich sequence found in LGALS9 promoter. We found 9 possible Smad3 binding sites upstream of T. T=red marks transcription start site. ....h

**Figure 82: Values presented in Figure 51 normalised against total protein loaded for WB data and per 1 mg of total tissue protein for enzyme activity and TBRs assays** (from (419)). Data are shown as mean values  $\pm$  SEM of five independent experiments. \* -  $p < 0.05$  and \*\* -  $p < 0.01$  vs non-transformed peripheral tissue abbreviated as HT (healthy tissue) (419).....i

**Figure 83: TGF- $\beta$  induces galectin-9 expression in K562 human cancer cells** (from (419)). K562 human chronic myeloid leukaemia cells were exposed for 24 h to 2, 4 or 8 ng/mL TGF- $\beta$  followed by detection of phospho-S423/S425-Smad3 and galectin-9 expression by WB. Galectin-9 release was analysed by ELISA. Images are from one experiment representative of three, which gave similar results. Data are shown as mean values  $\pm$  SEM of three independent experiments (419). .....j

**Figure 84: How nanoconjugate can be used to deplete HMGB1 (or TGF- $\beta$ ) from the medium.** Gold nanoparticles of the average size  $27.8 \pm 0.1$  nm have space to be coated with 6 anti-HMGB1 (or anti-TGF- $\beta$ ) antibodies which captures and deplete HMGB1 (or TGF- $\beta$ ) from the medium. ....k

## TABLES

**Table 1:** List of some of the HMGB1 mediated biological effects, upon interaction with different proteins both in the nucleus, cytosol and extracellular.....90

**Table 2: Expression of Tim-3, galectin-9, LPHNs 1, 2 and 3 as well as FLRT3 proteins in variety of cancer cell lines detectable by WB analysis. Tim-3** (directly from (326): lower band represents non-glycosylated protein, upper band(s), protein with differential levels of glycosylation; **galectin-9:** multiple bands represent different isoforms of the same protein; **FLRT3** – detectable between 80 and 95 kDa (upper band where applicable or the only visible band); another band (lower band; possibly extracellular domain) often appears at around 60 most likely reflecting levels of glycosylation in the first two cases and proteolytic processing in the third. **Traces** – detectable expression which requires loading of >100 µg protein per well (326). ..... e

**Table 3: The French-American-British (FAB) classification of Acute myeloid leukaemia (AML) (536).** French, American, and British leukaemia experts have divided AML into subtypes, M0 through M7, based on the type of cell the leukaemia develops from and how mature the cells are. The classification is largely based on how the leukaemia cancer cells looked under the microscope after routine staining. Subtypes M0 through M5 all start in immature forms of white blood cells. M6 AML starts in very immature forms of red blood cells, while M7 AML starts in immature forms of cells that make platelets. .... k

## ABBREVIATIONS

Abbreviation	Meaning
ADAM	A disintegrin and metalloproteinases
Ago-2	Argonaute-2
AIRE	Autoimmune regulator
AKT/PKB	Protein kinase B
AML	Acute myeloid leukaemia
AP	Adaptor protein
AP-1	Activator protein-1
APC	Antigen Presenting Cell
ASK1	Apoptosis signal-regulating kinase 1
ATF	Activating transcription factor
ATP	Adenosine triphosphate
$\beta$ 2M	$\beta$ 2-microglobulin
Bat3/Bag6/Scythe	HLA-B associated transcript 3
Bcl-2	B-cell lymphoma 2
Bcl-Xl	B-cell lymphoma-extra large
BH3l-1	5-[(4-bromophenyl)methylene]-a-(1-methylethyl)-4-oxo-2-thioxo-3-thiazolidineacetic acid
Bid	BH3 interacting-domain death agonist
BMP	Bone morphogenetic proteins
BSA	Bovine serum albumin
BT	Breast tumour tissue
Btk	Bruton's tyrosine kinase
BTLA	B- and T-lymphocyte attenuator
CAD	caspase-activated DNase
Cbl	Casitas B-lineage lymphoma - E3 ubiquitin ligase
CBP	CREB binding protein
CD	Cluster differentiation
CDK	Cyclin dependent kinase
cFLIP	cellular FLICE-inhibitory protein
Co-Smad	Common-Smad
CPT1A	Carnitine palmitoyltransferase IA
CRD	Carbohydrate recognition domain
CRT	Calreticulin
CTL	Cytotoxic T lymphocytes/cytotoxic T cell
CTLA-4/CD152	cytotoxic T-lymphocyte-associated protein 4
CXCL	CXC chemokine ligand
CXCR	CXC chemokine receptor
DAMP	Danger-associated molecular pattern
DAP	2,3-diaminophenazine
DC	Dendritic cell
DISC	Death-inducing signalling complex

DOTAP	1,2-dioleoyl-3-trimethylammoniumpropyl chloride
DPI-ELISA	DNA protein interaction- ELISA
DTT	Dithiothreitol
ECM	Extracellular matrix
EDTA	Ethylenediaminetetraacetic acid
EGF	Epidermal growth factor
eIF4E-BP	eIF4E binding protein
ELISA	Enzyme-linked immunosorbent assay
EMT	Epithelial mesenchymal transition
ER	Endoplasmic reticulum
ERK	Extracellular signal-regulated kinase
FAO	Fatty-acid b-oxidation
FBS	Foetal bovine serum
FIH	Factor inhibiting HIF
fICTLA-4	full-length CTLA-4
FLRT3	Fibronectin leucine-rich transmembrane protein 3
Foxo3	Forkhead box protein O3
Foxp3	Forkhead box P3
GDF	Growth differentiation factor
GM-SCF	Granulocyte-macrophage colony-stimulating factor
GPCR	G-protein coupled receptor
Grb2	Growth factor receptor-bound protein 2
HA	Hyaluronan
HBV	Hepatitis B virus
HCV	Hepatitis C virus
HIF	Hypoxia-inducible factor
HIV	Human immunodeficiency virus
HMG	High mobility group
HMGB1	High mobility group box 1
HRP	Horseradish peroxidase
HSP	Heat Shock Protein
HT	Healthy breast tissue
ICAD	Inhibitor of CAD
ICAM	Intracellular adhesion molecule
ICB	Immune checkpoint blockade
ICD	Immunogenic cell death
ICI	Immune checkpoint inhibitor
ICW	In-cell western
IDO	Indoleamine 2,3-dioxygenase
Ig	Immunoglobulin
IgV	Immunoglobulin variable domain
IKK	IkB Kinase
IL	Interleukin

INF $\gamma$	Interferon gamma
iNOS	Inducible nitric oxide synthase
irAEs	immune-related adverse effects
IS	Immunological synapse
I-Smad	Inhibitory-Smad
ITAM	Immunoreceptor tyrosine-based activation motif
ITIM	Immunoreceptor tyrosine-based inhibitory motif
iTreg	inducible Treg
JAK	Janus kinase
JNK	c-Jun N-terminal kinase
KIR	Killer-cell immunoglobulin-like receptors
KO	Knockout
KSFM	Keratinocyte basal serum-free medium
LAG-3	Lymphocyte activation gene-3
LAP	Latency-associated peptide
LAT	Linker for activation of T cells
Lck	Lymphocyte-specific protein tyrosine kinase
LCMV	Lymphocytic choriomeningitis virus
LFA-1	Lymphocyte function-associated antigen-1
LLC	Large latent complex
LPHN	Latrophilin
LPS	Lipopolysaccharid
LTBP	Latent TGF- $\beta$ binding protein
MAPK	Mitogen-activated protein kinase
MBC	Metastatic breast cancer
MDA	Malondialdehyde
MDM2	Mouse double minute 2 homolog
MDSC	Myeloid-derived suppressor cell
MH	Mad homology
MHC	Major histocompatibility complex
MIC	MHC class I chain-related protein
MMP	Matrix metalloproteinase
mRNA	messenger RNA
MS	Multiple sclerosis
mTOR	mammalian target of rapamycin
MW	Molecular weight
MyD88	Myeloid differentiation primary response 88
NBT	Nitrotetrazolium blue
NFAT	Nuclear factor of activated T-cells
NFIL-3/E4BP4	Nuclear factor Interleukin-3 regulated/E4 binding protein 4
NF $\kappa$ B	Nuclear factor kappa-light-chain-enhancer of activated B cells
NK	Natural killer cell
Nkex	exhausted NK cell

NKG2	Natural killer group 2
NKT	Natural killer T cell
NLPR3	NLR family pyrin domain containing 3
Nox	NADPH oxidase
NSCLC	Non-small cell lung cancer
nTreg	natural Treg
OCW/OCA	On-cell western / On-cell assay
OD	Optical density
OPD	Orto-phenylenediamine
OS	Overall survival
OXPPOS	Oxidative phosphorylation
P/S	Penicillin/Streptomycin
P2RX7	P2X purinoceptor 7
p38	p38 mitogen-activated protein kinase
PAMP	Pathogen-associated molecular pattern
PARP	Poly (ADP-ribose) polymerase
PBC	Primary breast cancer
PBMCs	Peripheral blood mononuclear cells
PBS	Phosphate-buffered saline
PD-1/CD279	Programme cell death protein-1
PDL	Poly-d-lysine
PD-L1/CD274/B7-H1	Programme cell death ligand-1
PHD	Prolyl hydroxylase
PHL	Primary human leukocytes
PI3K	Phosphoinositide 3-kinase
PKC	Protein kinase C
PLC	Phospholipase C
PMA	Phorbol 12-myristate 13-acetate
PMSF	Phenylmethylsulfonyl fluoride
PP2A	Protein phosphatase 2
PPR	Pattern-recognition receptor
PRMT1	Protein arginine N-methyltransferase 1
PS	Polystyrene
PSF	Progression-free survival
PtdSer	Phosphatidylserine
PTEN	Phosphatase and tensin homolog
RAGE	Receptor for advanced glycation end products
Rb	Retinoblastoma protein
RISC	RNA-inducing silencing complex
RNAi	RNA interference
ROR $\gamma$ T	RAR-related orphan receptor gamma
ROS	Reactive oxygen species
R-Smad	Receptor-regulated Smad

RT	Room temperature
Runx1	Runt-related transcription factor 1
SARA	Smad anchor for receptor activation
sCTLA-4	soluble CTLA-4
SDS-PAGE	Sodium dodecyl sulphate polyacrylamide gel electrophoresis
SH2	Src homology 2
SHP	Src homology 2 domain containing phosphatases
siRNA	small interfering RNA
SLC	Small Latent TGF- $\beta$ Complex
SMAC	Supramolecular activation cluster
Smurf	Smad ubiquitination regulatory factor - an E3 ubiquitin ligase
SOS	Son of sevenless homolog
Sp1	Specificity protein 1
STAT3	Signal transducer and activator of transcription 3
TAA	Tumour-associated antigen
TACE/ADAM17	Tumour necrosis factor $\alpha$ -converting enzyme
TAK1/MAP3K7	Mitogen-activated protein kinase kinase kinase 7
TALL	Acute lymphoblastic leukaemia
TAM	Tumour-associated macrophage
TBA	Thiobarbituric acid
TBRS	Thiobarbiturate reactive substance
T-bet/TBX21	T-box expressed in T cells/T-box transcription factor
TBRP	Transactivating response RNA-binding protein
TBST	Tris-buffered saline with tween20
Tc	Cytotoxic T cell
TCA	Trichloroacetic acid
TCD	Tologenic cell death
TCR	T Cell Receptor
Teff	Effector T cell
Tex	Exhausted T cell
TGF- $\beta$	Tumour Growth Factor beta
TGN	Trans-Golgi Network
Th	Helper T cell
TIF1 $\gamma$ / TRIM33	Transcriptional intermediary factor 1 gamma / Tripartite motif-containing 33
TIGIT	T cell immunoglobulin and ITIM domain
TIM-3 / HAVCR2	T-cell immunoglobulin and mucin-domain containing-3/Hepatitis A virus cellular receptor 2
TLR	Toll-Like Receptor
TME	Tumour microenvironment
Tmem	Memory T cell
TNF $\alpha$	Tumour necrosis factor alpha
TR	Transcription factor

TRAIL/CD253	TNF-related apoptosis-inducing ligand
TRAIL-R	TRAIL-receptor
Treg	Regulatory T cell
TRIF	TIR-domain-containing adapter-inducing interferon- $\beta$
Trx	Thioredoxin
TSA	Tumour-specific antigen
T $\beta$ R/ALK	TGF-beta receptor/Activin receptor-like kinase
ULBP	UL16 binding protein
VCAM	Vascular cell adhesion molecule
VEGF	Vascular endothelial growth factor
VHL	von Hippel-Lindau
VISTA	V-domain Ig suppressor of T cell activation
WB	Western blot
XOD	Xanthine oxidase
ZAP70	Zeta-chain-associated protein kinase 70



# 1 INTRODUCTION

The immune system consists of a network of different cells from the innate and adaptive immune system that collaborate to recognize and eliminate infectious agents and abnormal cells. Immune cells work in a complex system where they first must recognize and distinguish self-antigens from non-self-antigens before activating and initiating their immune effector functions. At the same time, they are under tight immunological control in order not to provoke unnecessary tissue damage when the pathogens have been cleared. Finally, once the adaptive immune system has been efficiently activated, it clears the remaining pathogens and is capable of generating immunological memory (protective immunity) (1).

For the most part, immune cells are successful at removing these harmful agents and cells, however, sometimes they fail, resulting in chronic infections or cancer, or they overreact, resulting in allergic or autoimmune disorders. The prevalence of cancer (2, 3), atopic (4, 5) and autoimmune (6-8) diseases is increasing. All three disorders have genetic and environmental causes where increased risk and prevalence of acquiring these conditions have been shown to be caused by changes in environmental exposure and, paradoxically, better health care (2, 3, 5, 7, 8). DNA mutations necessary for malignant transformation accumulate over time and, therefore, the mere fact that we are getting older, due to better health care, increases the risk of developing cancer (3). Moreover, a more industrialized civilisation and change of lifestyle habits increase the risk of getting cancer, atopic and autoimmune diseases. Risk factors applied for one or more of these conditions includes: air pollution, smoking, increased intake of antibiotics, reduced physical exercise and unhealthy diet resulting in obesity, vitamin D deficiency etc (2, 3, 5, 7, 8). With modernisation comes more “cleanliness” and a move away from farm life. The hygiene hypothesis suggests that increase in allergic and autoimmune disorders is due to lack of exposure to microorganisms when we are young, which then can train our immune system to distinguish between harmful and harmless irritants and self from non-self (9).

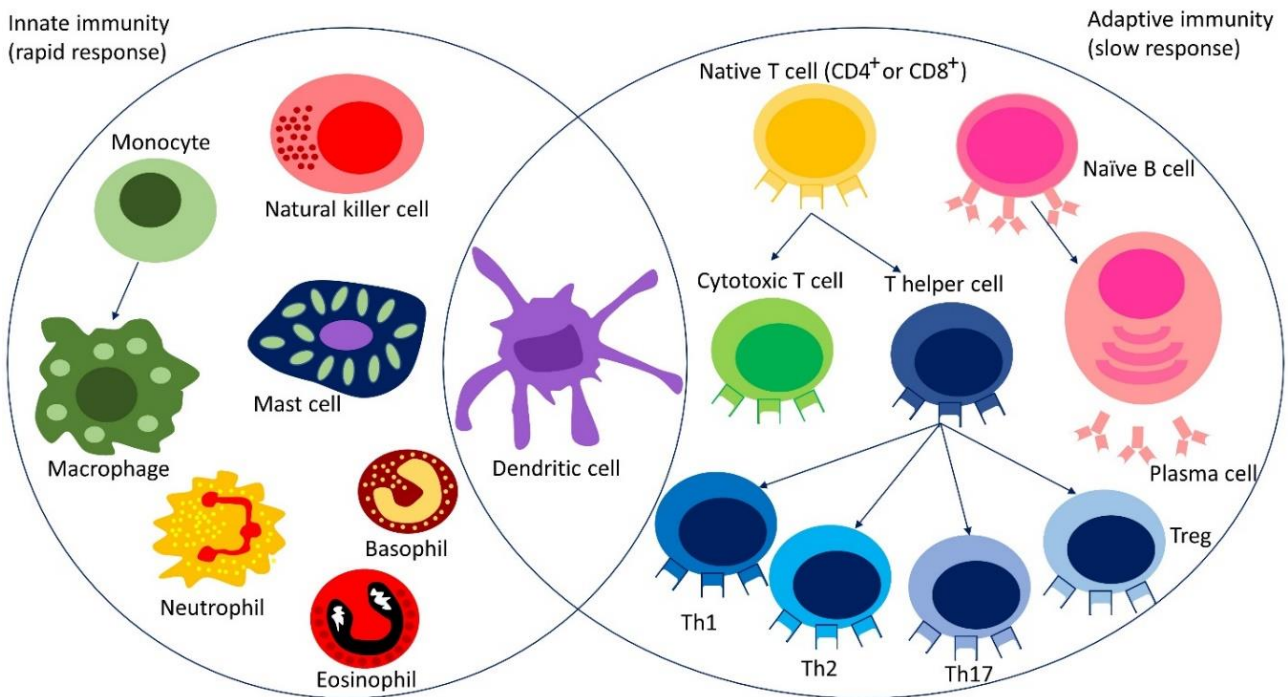
In the last few decades, great strides have been achieved in medical technologies and with that, a better understanding of the proteins and cells involved in immune responses, and many of these have been identified as potential targets for treatment. However, not everyone responds to the current therapies, whether it is a treatment for asthma (10),

cancer (11-15) or autoimmune disorder (16), and some of them cause short- and long-term side effects. Thus, the development of innovative therapeutic strategies with higher efficiency and lower toxicity is required. Newer therapies like immunotherapy and gene therapy show encouraging promises; however, the struggle is to molecular target these therapies (17, 18). This goal can possibly be achieved through better exploration of the differences of cells between the “healthy” and diseased conditions as well as their associated immune responses.

## 1.1 The Immune System

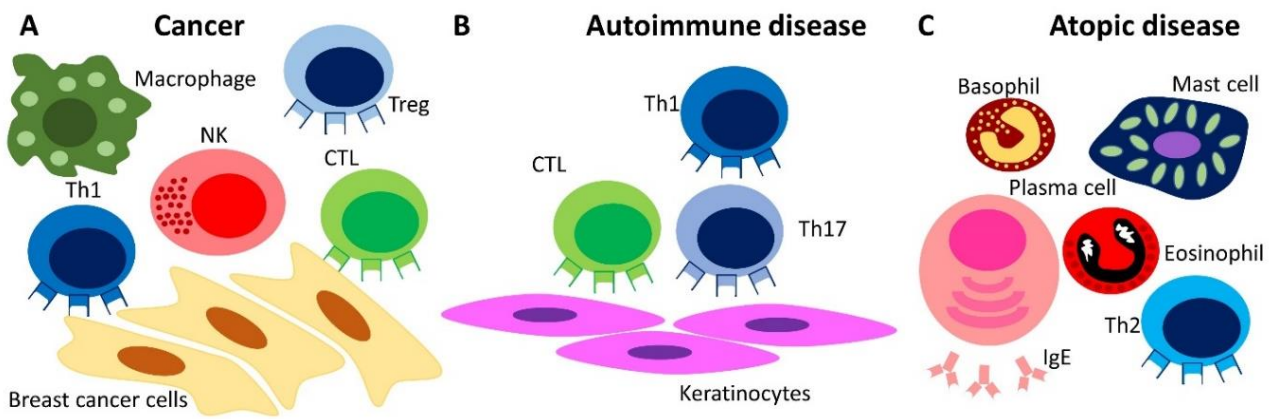
As mentioned, the immune system is a network of specialised cells that are divided into the innate and adaptive immune system, where the innate is the fast responding, and the adaptive is late responds, which also give rise to protective immunity (1) (Figure 1). The overall function is to protect the host from diseases by recognizing and/or eliminating infectious agents and abnormal cells (such as infected or transformed cells) without damaging adjacent host tissues and organs. Thus, a targeted attack is required to fight pathogens and invading malignant cells (1).

Both cells of the innate and adaptive immune system can distinguish non-self from self-antigens in order to avoid collateral tissue damage like an autoimmune reaction (1). The innate immune cells do this by expression of germline-encoded host sensors, called pattern recognition receptors (PPRs), although their expression is not excluded to innate cells. PPRs detect two classes of typical proteins of either microbial pathogens, known as pathogen-associated molecular patterns (PAMPs) or components of host cells that are released during cell damage or death, known as damage-associated molecular patterns (DAMPs) or alarmins (1). In contrast to innate immune cells, which recognize pathogens/PAMPs in broad “non-specific” manner, adaptive immune cells have antigen-specific receptors, which are capable of fine distinction between closely related proteins, thus there is a requirement of an enormous repertoire of antigen-specific receptors. These receptors are generated through a process of somatic cell gene rearrangement where each lymphocyte undergoes clonal selection and expresses just one type of antigen receptor (1).



**Figure 1: Simple overview of the innate and adaptive immune system.** The innate immune response occurs rapidly upon encounter with a pathogen. The dendritic cells (DCs) are innate cells but are crucial for the activation of the adaptive immune response, thus acting as a bridge between the innate and adaptive immune system. Once activated, the naïve lymphocytes, T and B cells undergo clonal expansion and differentiation to become effector cells and memory cells (not depicted), this process takes a few days. Naïve CD8<sup>+</sup> and CD4<sup>+</sup> T cells become cytotoxic T cells (T<sub>c</sub> or CTL) and T helper cells (T<sub>h</sub>), respectively, which further can differentiate into different subgroups of phenotypes. In addition, the immune system also encompasses other types of immune cells, such as Innate-like lymphocytes, regulatory B cells,  $\gamma\delta$  T cells and natural killer T (NKT) cells, and other newer subset of T helper cells, not shown here.

To elicit an immune response seems quite complex, however, it becomes more complicated as different types of pathogens or diseases are associated with their own distinct immune responses, which usually can be categorized as being overall Th1, Th2 and Th17 immune responses. Th1 immune response is for intracellular bacterial and viral infections, cancer and some autoimmune diseases, Th2 response is for extracellular parasitic infections, such as helminths that can cause atopic diseases, and Th17 response is for extracellular parasitic and fungal infections as well as autoimmune diseases (1). Thus, the immune system is trying to specifically target the problem causing antigens while maintaining tolerance. To achieve tolerance, the immune system operates in different layers of mechanisms that are categorized into central and peripheral tolerance (1, 19). However, in some pathologies, such as cancer, autoimmune and atopic diseases, there is a dysregulation of tolerance. Figure 2 depicts the major immune cells involved in different immune responses such as cancer, psoriasis and allergy. In all of these conditions, there is a dysregulation of immune tolerance.



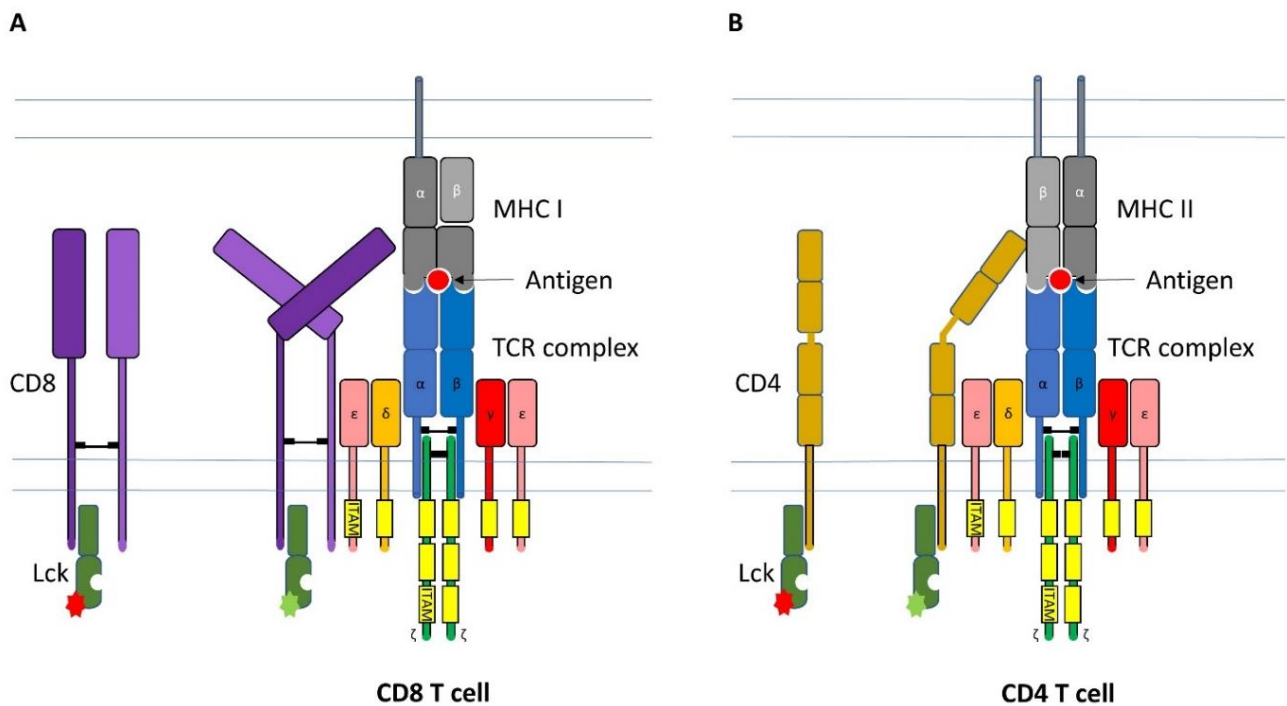
**Figure 2: A simple overview of the most common types of immune responses and how they in general relate to different diseases such as cancer, autoimmune disease and atopic conditions.** (A) The immune response mounted to fend off cancer, such as breast cancer, is a Th1 immune response where the major contributors are cytotoxic T lymphocytes (CTLs), natural killers (NK) cells, Th1 cells and macrophages. Although, the cancer cells can recruit and co-opt some immune cells such as T regulatory cells (Tregs), myeloid-derived suppressor cells (MDSCs) and tumour-associated macrophages (TAMs), which are M2-like macrophages to help them escape immune destruction. (B) On the other hand, a Th17 immune response is most common in autoimmune diseases, such as psoriasis, where CTLs and Th17 cells are the main players and to some extent also Th1 cells. (C) Finally, atopic disease, such as allergy, is characterized by a Th2 response where the predominating immune cells are mast cells, basophils, Th2 cells and eosinophils, and IgE-producing plasma cells.

## 1.2 Immune Tolerance

As discussed above, there is a number of molecular and cellular mechanisms operated at multiple levels that induce and maintain immune tolerance. Central tolerance takes place in the primary lymphoid organs, such as the bone marrow (for B cells) and thymus (for T cells). Here lymphocytes are conditioned during their development to discriminate between self and non-self in a process called negative selection in which strong binding of a self-antigen induces apoptosis. In contrast, intrinsic and extrinsic mechanisms of peripheral tolerance occur in peripheral tissue and are involved in proper contraction of the immune response as well as safeguards against autoimmunity. Intrinsic mechanisms are regulated by both co-stimulatory and co-inhibitory proteins and by anti-apoptotic and pro-apoptotic factors, which can induce T cell anergy, phenotype skewing or apoptosis, respectively. Whereas the main element of extrinsic mechanisms are the regulatory T cells (Tregs), which regulate the immune system by secretion of immune-suppressive cytokines, such as interleukin (IL)-10 and tumour growth factor (TGF)- $\beta$ , and can modulate the interaction of cluster differentiation (CD)4 and CD8 T cells and antigen presenting cells (APCs) creating tolerogenic cells (20, 21). The focus here is the activation of T cells and those components involved in the regulation of T cell tolerance as these processes often are dysregulated in cancer and autoimmune and atopic diseases.

### 1.2.1 Central Tolerance Is Programmed During T Cell Development

All the cellular elements of the blood, including the cells of the immune system, arise from pluripotent hematopoietic stem cells in the bone marrow. It is also here lymphoid progenitors are generated; however, T cell progenitors migrate to the thymus to mature into naïve CD4<sup>+</sup> or CD8<sup>+</sup> T cells(1). There are many processes occurring in the thymus, although, here are just briefly mentioned the highlights of conventional T cell development. Firstly, in the cortex of the thymus, the T cell receptor (TCR) is generated by somatic DNA recombination/gene rearrangement, which gives each thymocyte its unique antigen-receptor. The TCR is only expressed on the surface of the thymocytes when it forms a complex with the CD3 protein, which is also required for intracellular signalling mediated through the TCR via the presence of immunoreceptor-tyrosine-based associated motifs (ITAMs). Thus, the full TCR receptor is a complex of the TCR $\alpha$  and TCR $\beta$  chain, and the chains of the CD3 protein ( $\lambda$ ,  $\delta$ ,  $\epsilon$ , and  $\zeta$ ) (1, 20), which can be seen in Figure 3. Secondly, positive selection occurs, which targets the response restricted to the major histocompatibility complex (MHC). In this process cortical thymic epithelial cells present self-antigens (peptides) on either MHC I or MHC II, and only those thymocytes that interact weakly with self-antigens on MHC proteins will receive a survival signal, the rest will die through programmed cell death. It is also during this process they become committed to being either CD4<sup>+</sup> T cells or CD8<sup>+</sup> T cells (1, 20). The third step before maturation into a naïve T cell is negative selection, which occurs in the medulla of the thymus. Through their expression of the autoimmune regulator (AIRE), medullary thymic epithelial cells can express and present some tissue-specific proteins/self-antigens from tissues around the body. Most of the thymocytes that interact too strongly with self-antigen-MHC proteins are targeted for apoptosis, however, some of them become natural Tregs (nTregs). This process of negative selection is an important component of central tolerance and serves to prevent the formation of self-reactive T cells that are capable of inducing autoimmune diseases in the host(1, 20). Despite this negative selection, it may not remove all T cells reacting to self-antigens; however, several mechanisms are operating in the peripheral tissue that can prevent these possible autoreactive T cells from responding to a tissue-specific antigen. These are the intrinsic and extrinsic mechanism of peripheral tolerance (1, 20).

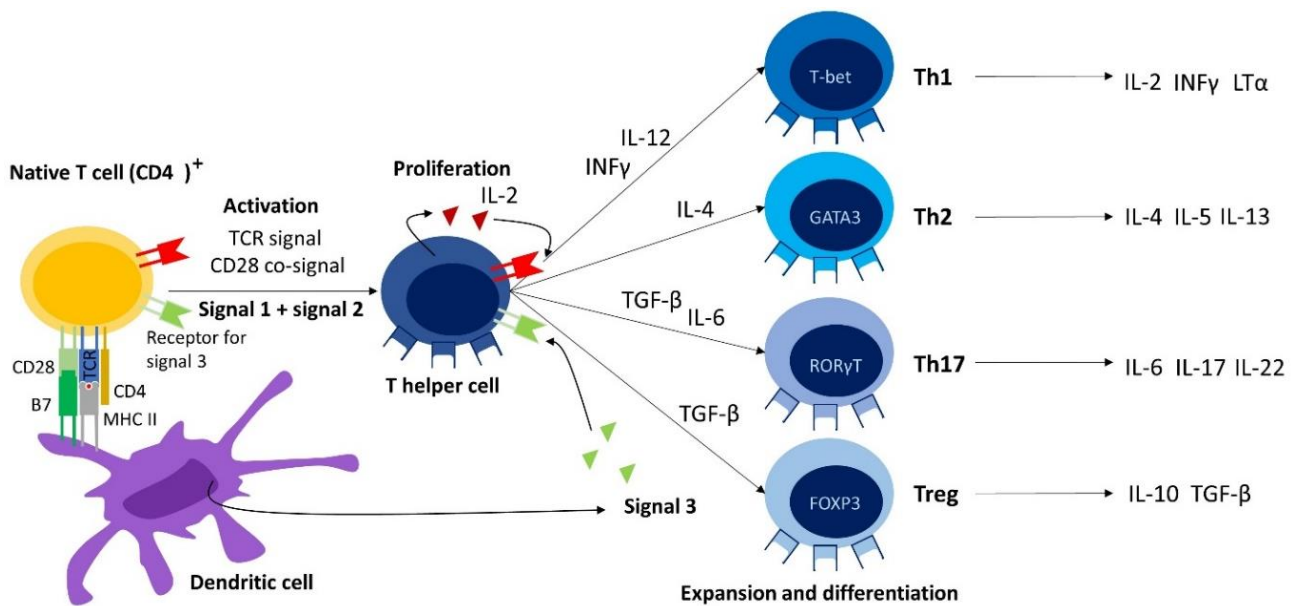


**Figure 3: T cell receptor complex with co-receptor and antigen presentation** (adapted from (1)). The T cell receptor complex (TCR) consists of the TCR $\alpha$  and TCR $\beta$  chain, and CD3 protein ( $\gamma$ ,  $\delta$ ,  $\epsilon$  and  $\zeta$ ), which is required for TCR surface expression and intracellular signalling with immunoreceptor tyrosine-based activator motif (ITAM). However, the TCR receptor complex does not have any intrinsic kinase ability. Thus, upon binding of an antigen-MHC complex, the co-receptor (either CD4 or CD8) partners with the TCR complex to facilitate TCR-mediated signalling as these co-receptors are constitutively associated with the non-receptor tyrosine kinase Lck (a Src family kinase). Upon TCR engagement Lck becomes activated. Lck is the kinase responsible for the phosphorylation of ITAMs, which allows the recruitment of other kinases and binding of adaptor/scaffold proteins that mediates downstream signalling (1, 19). (A) CD8 T cells are presented with antigen on MHC class I, which is expressed on any nucleated cell. (B) CD4 T cells are presented with antigen on MHC class II, which is expressed by APCs or by thymic epithelial cells during development.

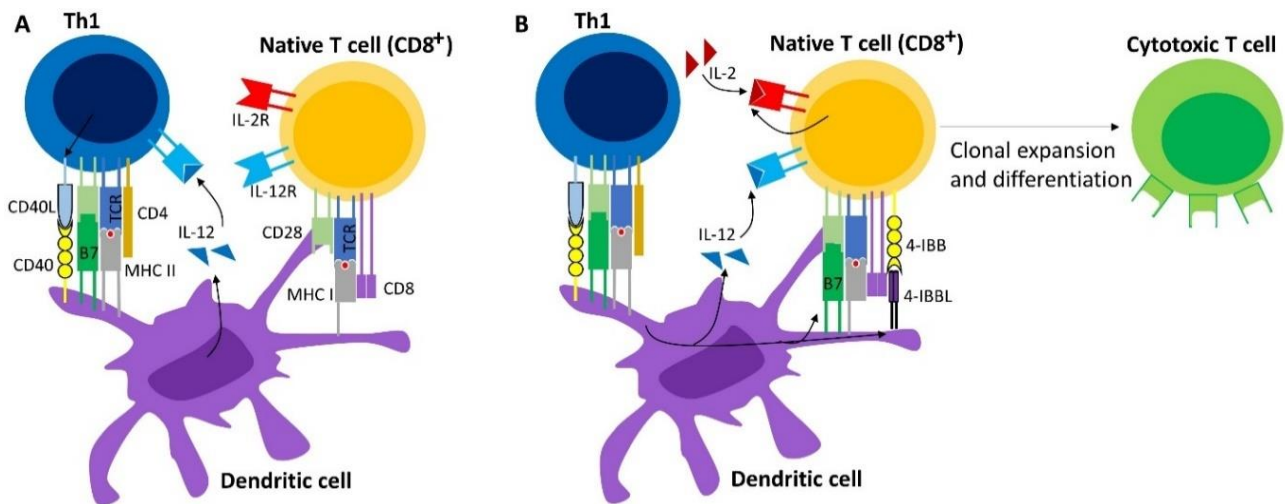
### 1.2.2 Mechanisms of Peripheral Tolerance Influence T Cell Response

For a successful immune response, there is a requirement for activation of adaptive immune cells, such as effector T cells (Teff), against foreign pathogens. To achieve their distinct effector function and formation of memory cells, the two main classes of naïve T cells must be activated and undergo clonal expansion and differentiation, and to do so, the naïve T cells requires three signals: signal 1 is an antigen-specific signal through the TCR complex, signal 2 is obtained by co-stimulation usually by co-ligation of the CD28, and signal 3 is a cytokine signal provided by APCs or influenced by the local cytokine milieu(1, 19). Naïve CD4 T cells differentiate into the different subset of CD4 T helper cells (Th), where the main functional classes are Th1, Th2, Th17 cells and Tregs (Figure 4) (1). As the name implies, it is thought that T helper cells are support cells, which produce different cytokines and co-stimulation for enhanced activation of macrophages, antibody

production, and formation of cytotoxic CD8 T cells and memory cells, although, some CD4 T cells also have cytotoxic activity (1, 19, 22). In contrast, naïve CD8 T cells differentiate into the cytotoxic T lymphocytes (CTLs or also sometimes abbreviated as Tc) (Figure 5), which function is to kill their target via different mechanisms, such as the production of interferon (INF)- $\gamma$ , release perforin and granzyme B or through Fas ligand-induced apoptosis, these are Tc1 (1, 19, 23). Yet, some CD8 T cells are more like other types of T helper cells and are denoted Tc2 and Tc17, and they secrete the Th-specific cytokines and have the ability of cell-mediated cytotoxic killing (19, 23-25). Since each of them has a distinct functional phenotype, each of them must be regulated differently.



**Figure 4: Differentiation of naive CD4 T cells** (adapted from Naïve CD4 T cells require three signals to be activated and undergo clonal expansion and differentiation. Signal 1 and signal 2 is provided by APCs through cell-cell interaction. Signal 1 is the recognition of antigen-peptide presented on MHC II protein, which induces signal through TCR receptor complex. Signal 2 is binding of B7 co-stimulatory molecules (B7-1/CD80 or B7-2/CD86) on the CD28 receptor, which aids the TCR signal in the generation of IL-2, which is required for proliferation and survival of activated T cells. Finally, signal 3 is a cytokine signal, where local cytokine milieu often provided by the APCs drives the expression of different lineage-specific transcription factors (such as T-box expressed in T cell (T-bet), GATA3, (RAR-related orphan receptor gamma) ROR $\gamma$ T and (Forkhead box p3) Foxp3) that promote the differentiation into distinct classes of T helper cells, e.g. Th1, Th2, Th17 cells and Tregs, other types are not depicted (1, 19). The required cytokines for Th1 differentiation are IL-12 and/or INF $\gamma$  (1, 26), for Th2 it is IL-4 (1), for Th17 cells, it is IL-6, TGF- $\beta$  and/or IL-1 $\beta$  (1, 27), and for Tregs, it is TGF- $\beta$  (1, 26). These T helper subsets are characterized by secretion of different cytokines, which assist in distinct function, such as activation of macrophages and CD8 T cells, B cell isotype switching, and suppression of the immune system (1).

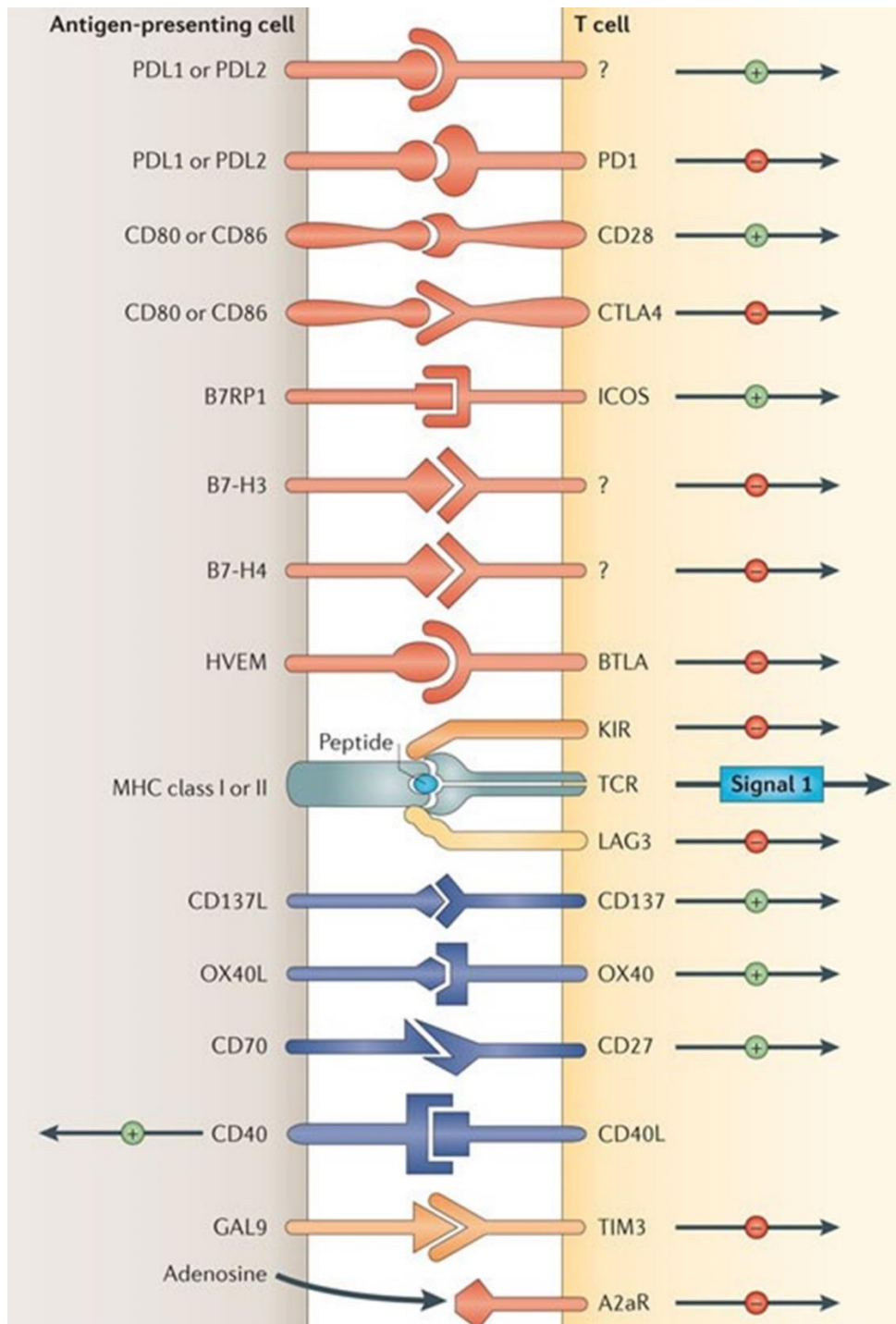


**Figure 5: Differentiation of naive CD8 T cells** (adapted from (1)). As the naïve CD4 T cells, Naïve CD8 T cells require three signals to become activated and undergo clonal expansion and differentiation (28). Here is shown differentiation of a Tc1/CTL cell, which amongst others is involved in viral and cancer clearing. As CD4 T cells, signal 1 (the antigen-specific signal) and signal 2 (co-stimulatory signal) are provided by cell-cell interaction by the APC, although the antigen is required to be presented on MHC class I protein. These two signals are enough for activation and proliferation for a few rounds; however, the cell becomes tolerant rather than gaining its cytolytic function. To obtain cytolytic function, a third cytokine signal from either IL-12 or type I interferons is required (29, 30). Most probably due to the damage that the cytolytic function can cause, the CD8 T cells require more positive co-stimulation to become activated. This is achieved in a 3-way dialogue between the naïve CD8 T cells, an APC (with low intrinsic co-stimulatory activity), and Th1 cells (which provide help by promoting more co-stimulatory signals and IL-2) (1). (A) In the T helper cells, signalling from TCR, CD28 and IL-12R induces production of IL-2 and expression of other co-stimulatory proteins, such as CD40L, which binds to the CD40 receptor on DCs. (B) The CD40L delivers a positive signal that enhances the surface expression of co-stimulatory proteins, such as B7s and 4-IBBL (CD137L) on DCs. These signals provide strong co-stimulatory signal required for activation of naïve CD8 T cells and induce induction of IL-2 and together with IL-12 or type 1 interferon they drive the proliferation and differentiation into effector cytotoxic T cells.

The nature of the T cell response is determined by the overall signal strength from the TCR complex. In general, the signal strength from any receptor is influenced by the affinity and the temporal and spatial abundance of ligand, which determines aspects, such as threshold, amplitude and duration. For example, a low-affinity interaction often induces a signal with lower amplitude and shorter duration than high-affinity interaction (1). In terms of T cells, the signal strength from the TCR complex is usually not only determined by the affinity to the ligand (peptide-MHC complex), but also from a balance between co-stimulation and co-inhibition originating from co-stimulatory and co-inhibitory receptors, respectively, which together with the ligand influence the differentiation of the T cells and regulate the threshold for a response, the amplitude (quality effect), and the duration of the T cell response (1, 31). Although, the dependency of co-stimulation is more evident in naïve T cells during priming, while less important in T<sub>eff</sub> and T memory cells (T<sub>mem</sub>) (32).



Co-stimulatory signals are thought to promote and sustain T cell response, and the importance of these positive signals can be seen when the TCR signal is engaged in the absence of co-stimulatory proteins (and/or high co-inhibitory proteins), it results in a non-responsive, anergic state or cell death (33-36). Many proteins can provide co-stimulatory signals, however, the best characterized of these co-stimulatory pathways is the B7-CD28 pathway, which is critical for naïve T cell activation, proliferation and survival as illustrated in Figure 4 and Figure 5 (21, 31). After clearance or control of the pathogen, the effector phase of the immune response needs to be terminated in order to minimize collateral tissue damage or chronic inflammation (31, 37). This is achieved by both inducing inhibition of T cell expansion and eliminating T cells by a process known as activation-induced cell death, the remaining cells survive as long-lived memory cells (37). Under normal physiological conditions, co-inhibitory signals modulate the duration and amplitude of immune responses in peripheral tissues, which include the inhibition of signal required for IL-2 production (a growth factor for T cells) (31). Furthermore, the co-inhibitory pathways together with Tregs represent a part of the intrinsic and extrinsic mechanisms of peripheral tolerance and thus are crucial for maintaining self-tolerance (that is, the prevention of autoimmunity) (21). As with the co-stimulatory pathways, the cells can be induced to express a variety of co-inhibitory pathways (also called immune checkpoints) to limit the immune response. The best characterised of these immune checkpoints are cytotoxic T-lymphocyte-associated protein 4 (CTLA-4) and programmed cell death protein 1 (PD-1), which pathways will be described in section 1.5.1 and 1.5.2, respectively (31). Figure 6 illustrates some of the co-stimulatory and co-inhibitory interactions that modulate the T cell response.

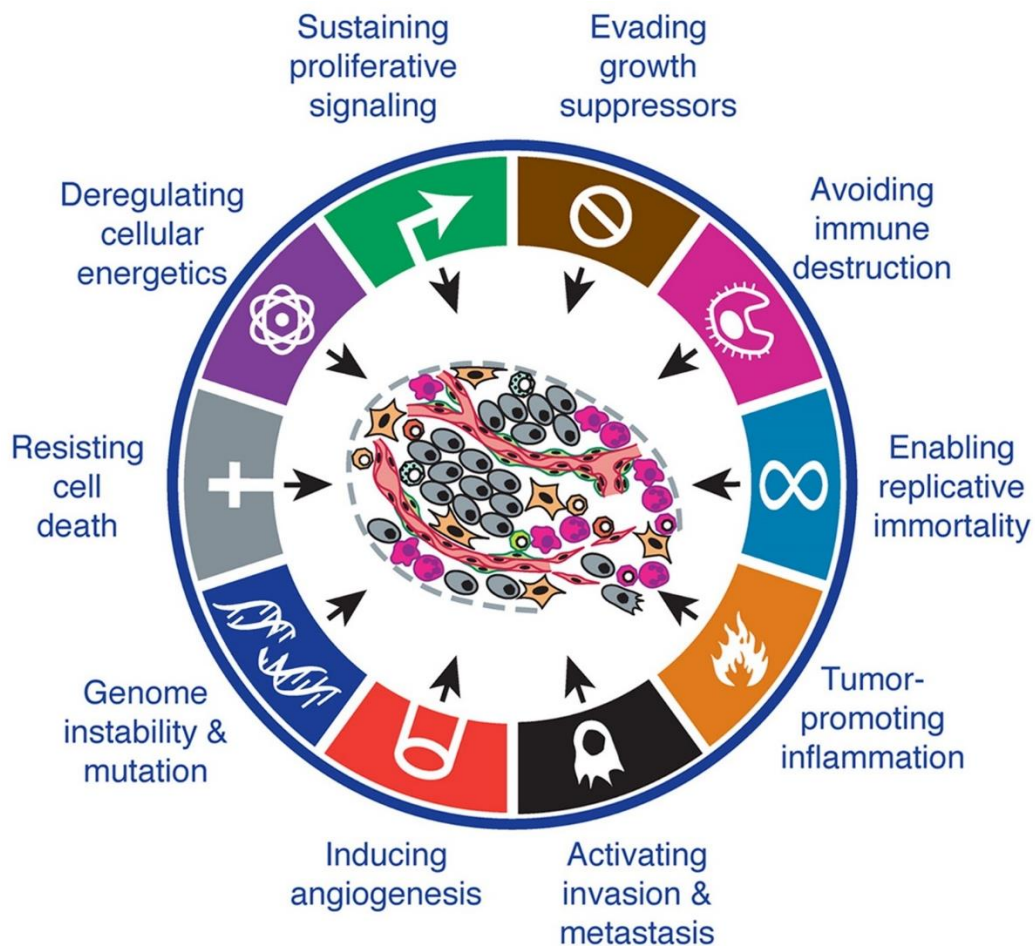


**Figure 6: Multiple co-stimulatory and co-inhibitory interactions regulate T cell responses** (adapted from (31)). Depicted are some ligands typically expressed by APCs (and/or tumours) and their cognitive receptor present on T cells. These interactions regulate the T cell response by providing either co-stimulatory or co-inhibitory signals when the T cells already have recognized its specific antigen-peptide bound on an MHC molecule. Not all receptors and ligands are constitutively present, some are present in resting state, and some are upregulated upon activation. In most cases, co-inhibitory receptors are upregulated upon activation.

### 1.3. Biochemical Pathways Operated by Cancer Cells to Escape Host Immune Surveillance

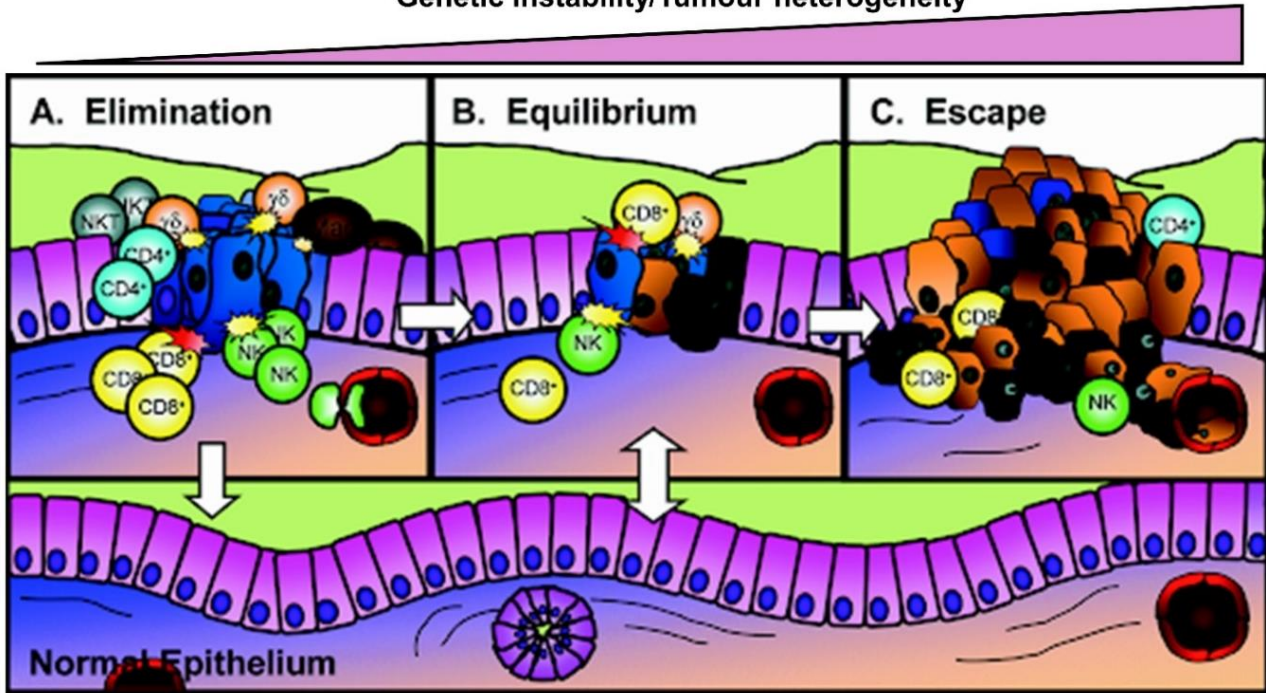
Tumourigenesis is a multistep process, and these steps reflect genetic and epigenetic alteration, which typically result in gain or loss of function in tumour oncogenes or tumour suppressor genes, respectively. E.g. mutations in tumour suppressor genes, which often are components of DNA repair mechanism, can result in genome instability and promote further accumulation of mutations, which drive the progressive transformation of a normal cell into a malignant one. Thus, gain or loss of function mutations, epigenetic changes and chromosomal translocation provide survival/growth benefit for the growing tumour cell (38, 39). In fact, Douglas Hanahan and Robert A. Weinberg proposed that there are specific traits or hallmarks, which reflect tumour intrinsic and extrinsic barriers that must be overcome for malignant transformation (Figure 7) (38, 39). The intrinsic barriers include that the cell must be able to grow autonomously, develop insensitivity to negative growth signals, be able to resist cell death, must circumvent restriction in multiplication to achieve unlimited replication potential, must be able to reprogramme energy metabolism, induce angiogenesis to keep up the nutrient and oxygen supply for the growing tumour, and establish competencies for invasive growth and metastasis (38, 39). Furthermore, there are tumour extrinsic barriers in which the malignant cells must be able to evade extrinsic tumour suppressor function of the immune system, and thus escape immune destruction. The tumour cells can in part do this by co-opting normal stromal cells and recruiting certain pro-tumour immune cells (Tregs, TAMs and MDSCs) to provide an immunosuppressive milieu in the tumour microenvironment (TME), and thus promote tumour progression (39, 40). Although, the anti-tumour immunity provided by immune cells, such as NKs and T cells, are fighting cancer cells and trying to promote tumour clearances, they may in the long run aid in tumour progression. Thus, the immune system has a paradoxical dual effect in both promoting and suppressing tumour progression. In search of an explanation of this dual function of the immune system, the cancer immunoediting hypothesis, the so-called three Es of cancers (elimination, equilibration and escape) has been formulated (Figure 8) (40, 41). It is believed that there are three phases of immune cancer interaction. The first is the elimination phase or immunosurveillance phase where cells of the innate and adaptive immune cells can recognize and eradicate the incipient tumour cells, and if successful, there is no development of cancer. Any tumour cell variant that survives the elimination phase enter a dynamic equilibrium phase, in which lymphocytes with their

effector function are able to contain tumour progression by being able to destroy some tumour cells, however, this relentless attack exerts a “Darwinian” selection pressure that sculpts tumour cell variants with reduced immunogenicity. These cells thus enter the last escape phase where they resist immune detection and/or elimination, thus allowing the tumour to expand and become clinical detectable (40, 41).



**Figure 7: TME and Hallmarks of cancers** (adapted from (39)). The TME consists of many cells, not only tumour cells. Inside the circle, the different cells of the TME are depicted, which consist of endothelial cells, pericytes, cancer-associated fibroblast, local and bone marrow-derived stromal stem cells and progenitor cells, cancer stem cells, cancer cells, both pro-tumour and anti-tumour immune cells, and invasive cancer cells. Collectively, they influence each other and are “corrupted” by the cancer cells to enable tumour growth and progression. The outer ring illustrates the specific traits or hallmarks, which reflect tumour intrinsic and extrinsic barriers, which must be overcome for malignant transformation.

## Genetic instability/Tumour heterogeneity



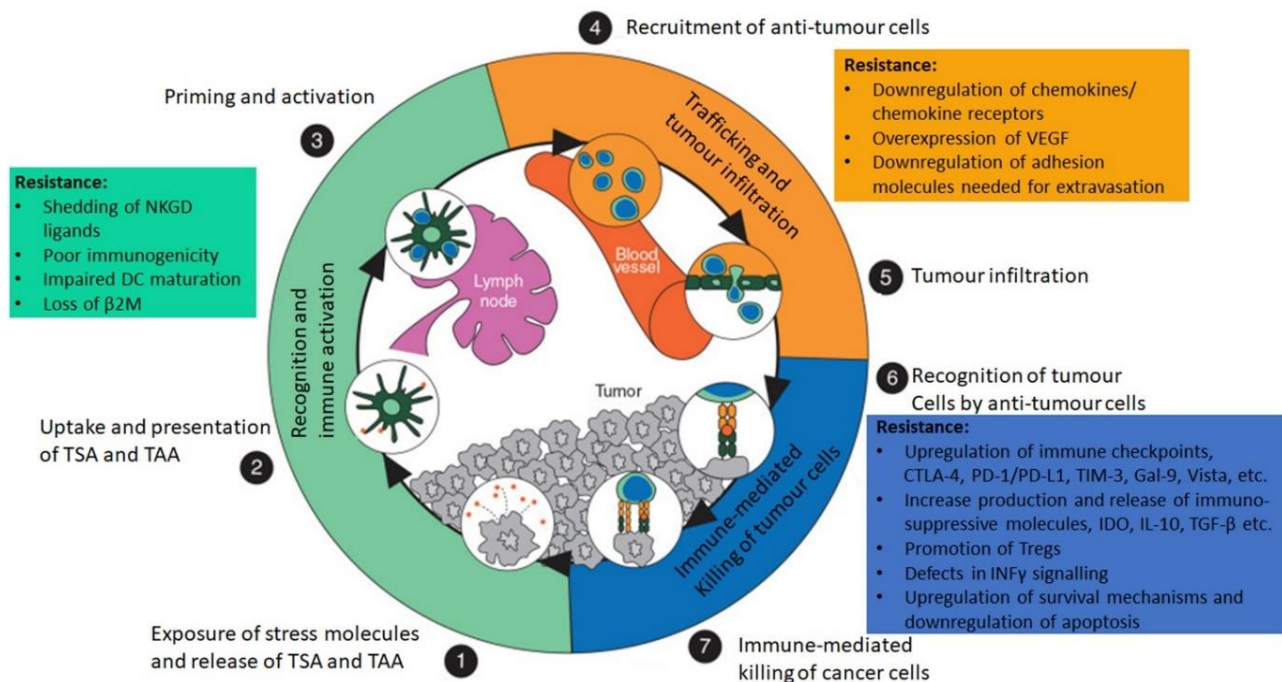
**Figure 8 – The cancer immunoeediting process – the three Es of cancer** (adapted from (40)). Equilibrium phase, the immune system has not been able to destroy all the tumour cells and surviving cancer cells try to proliferate while being under constant attack from the immune cells, which try to control and contain progression. C) Escape phase, at every stage the tumour increases its genetic instability and heterogeneity. This is caused by the immune pressure - “Darwinian” selection of tumour cells with new capabilities, such as reduced immunogenicity, and are able to promote an immunosuppressive TME and functional exhaustion of anti-tumour immune cells, which eventually result in escape from the immune system and tumour progression. In the elimination and equilibrium phase, the immune cells are sometimes successful, and the tissue returns to normal (white arrows).

How do cancer cells evade the immune system? In the last few decades with the development of gene targeting and transgenic mouse technologies as well as the capacity to produce highly specific blocking antibodies, it has been possible to study which immune cells and their effector components are involved in immune surveillance (40). Both innate (such as NK and NKT cells) and adaptive (like  $\alpha\beta$  T cells (both CD4 and CD8) and  $\gamma\delta$  T cells) immune cells are involved in immunosurveillance (40, 41), albeit their action, might depend on “the tumours cell type of origin, mechanism of transformation, anatomic localization and mechanism of immunological recognition” (40). Here, I will focus on NK and T cells in immunosurveillance and some of the escape mechanisms that cancer cells use to avoid immune destruction from these cells.

### 1.3.1 The Cancer-Immune Cycle

To initiate an anti-tumour immune response, “the cancer-immune cycle” must be initiated. Here, I will describe a modified version of Daniel S. Chen and Ira Mellman’s work (42) that will include not only T cells but also NKs and their role in the cancer-immune cycle. There

are three stages in this cycle: 1) recognition and immune cell activation, 2) trafficking and tumour infiltration, and 3) immune-mediated killing of tumour cells (Figure 9). Defects in any of these steps will most likely result in tumour immune escape. Cancer cells often utilize multiple immune evasion strategies, and this can affect response to treatment, thus, it is vital to identify the specific escape mechanism used by cancer in each patient for the most optimal treatment (13).



**Figure 9: The three stages of the Cancer-immune cycle** (adapted from (13, 42, 43)).

1) Recognition and immune activation. Here innate cells such as NKs recognize stress molecules, such as MHC class I chain-related protein (MICs), and target cancer cells for killing, or cancer cells die due to hypoxia. With the death of the cancer cells, tumour-specific antigens (TSA) and/or tumour-associated antigens (TAA) are released and can be taken up and presented by APCs, which prime and activate T cells to join the fight against the cancer cells. 2) Trafficking and tumour infiltration. Anti-tumour cells are recruited to the tumour bed by chemotactic signals, and to leave the blood stream, they need to extravasate into the tumour tissue. 3) immune-mediated killing of tumour cells. At this stage, anti-tumour cells, such as NK and especially T cells, recognize tumour cells displaying stressed signals and/or TSA/TAA and are target tumour cells for cell-mediated cytotoxic killing. This releases more and/or new TSA/TAA, and the cycle continues. In the boxes, some of the mechanisms, which the cancer cells use to escape anti-tumour immunity, are listed, which also promote resistance to therapy.

### 1) Recognition and immune activation.

MHC class I chain-related proteins MICA/MICB and UL16 binding protein (ULBP) proteins are rarely expressed in healthy tissues but induced by various cellular stresses, such as DNA damage, heat shock, or cellular transformation (44). In fact, many solid tumours, e.g. carcinomas of the lung, breast, kidney, ovary, prostate and colon, melanoma and hepatocellular carcinoma have been shown to have a

constitutive expression of MICA/MICB (40, 41). These ligands act as killing target for effector cells expressing the NKG2D activating receptor, such as NKs and most human  $\delta\gamma$  T cells and CD8+  $\alpha\beta$  T cells (40, 41). Once activated, these cells are able to perform cytotoxic cell-mediated killing of the tumour cells and secrete IFN $\gamma$ . A way for the tumour cells to escape is by promoting the shedding of NKG2D ligands, which is believed to attenuate the expression of NKG2D on host immune cells (40, 44).

The most predominant way that T cells recognize tumours is by their antigen-specific TCR (41). As the neoplastic cells evolve, there is usually an increase in mutational load that generates numerous neoantigens, which often result in abnormal or increased expression in proteins (45). A way for the antigen-specific T cells to recognize tumour cells is by their expression of these tumour antigens. Tumour antigens can be divided into tumour-specific antigen (TSA), which is only expressed by cancer cells and not healthy cells, and tumour-associated antigens (TAA), which is highly expressed by malignant cells, but only little is seen on healthy cells (46, 47). Tumour death due to cell-mediated killing by e.g. NKs, results in the release of tumour antigens that can be taken up by dendritic cells (DCs), which then matures, leading to increased expression of co-stimulatory proteins, and migrates to the lymph node where the tumour antigen can be presented to naïve T cells, and this results in T cell activation, differentiation, and clonal expansion (40, 48). As described above, it is crucial that the antigen is presented together with appropriate co-stimulation as the lack of co-stimulatory signal leads to T cell anergy and thus tolerance (49). The tumour cell and tumour-associated immune cells (Tregs, MDSCs and TAMs) can promote an immunosuppressive TME by secreting different factors, such as indoleamine 2,3-dioxygenase (IDO), vascular endothelial growth factor (VEGF), IL-10 and TGF- $\beta$ , which all have been shown to impair DCs maturation, which means that there are insufficient co-stimulatory proteins, such as CD80, CD86, CD40 and MHC proteins, expressed on the surface of DCs (13, 50-54). Furthermore, when CTLs home to tumour site, they kill tumour cells expressing tumour antigens presented on MHC I. However, the tumour can often lose particular tumour antigens, which is targeted by the immune system. This often happens after immunotherapy, or they can acquire a mutation in the antigen-presentation/processing machinery, e.g. loss of function mutation of  $\beta$ 2-microglobulin ( $\beta$ 2M) leading to loss of MHC I, both of which lead to reduced immunogenicity and thus evasion of immune detection (13, 40). Although, the

loss of MCH I makes the tumour susceptible for NK cell-mediated killing with the relief of the inhibitory HLA class I-binding receptor, killer-cell immunoglobulin-like receptors (KIRs) (44).

## 2) Trafficking and tumour infiltration.

Immune cell trafficking is driven by chemoattractant and adhesion molecules. Chemokines are chemotactic cytokines that control the trafficking of cells (especially immune cells) between tissues and the positioning interactions of cells within the tissue (55). Immune cell subsets differentially express chemokine receptors, which result in their selective recruitment that is tailored to infect pathogens or foreign bodies (55). E.g. during maturation of NKs or differentiation of naïve T cells to T<sub>eff</sub>, there is a change in chemokine receptor expression that allows them to home to the tumour site. One of these chemokine receptors that permits the recruitment of anti-tumour leukocytes into the tumour is CXCR3 and its ligands CXCL9, CXCL10 and CXCL11, which are inducible by IFN $\gamma$ , and to some extent by type I interferon (13, 40, 55). Dysregulated expression of chemokines receptors and their respective ligands are implicated in a broad range of human diseases, including autoimmune and inflammatory diseases and cancer (55). In fact, tumour cells have adopted escape mechanisms by preventing tumour infiltration of anti-tumour leukocytes (NKs,  $\alpha\beta$  T cells,  $\gamma\delta$  T cells and NKT cells), which is normally associated with a good prognosis, but at the same time promotes the recruitment of pro-tumour leukocytes (such as Tregs, TAMs, MDSCs, and immature DCs), which in many cancers have been linked with poor patient survival (47, 55). An example of preventing infiltration of anti-tumour cells can be mediated by epigenetic silencing of the chemokines CXCL9 and CXCL10. Another way is to acquire defects in the IFN $\gamma$  signal pathway, such as loss of function mutations in Janus kinase (JAK)1/2, which result in IFN $\gamma$ -insensitivity, and thus reduce IFN $\gamma$ -inducible genes (13, 40).

Chemokines are not the only factor necessary for cells to migrate into the tissue. For the leukocytes to be able to leave the blood vessels and enter the site of tissue damage or infection/tumour site, they have to perform extravasation (1). In this process many adhesion s are important, some of them are the intracellular adhesion (ICAM) and vascular adhesion (VCAM), which are expressed by endothelial cells and required for cell adhesion to the endothelium (1). To accommodate the requirement of



the growing tumour for oxygen and nutrients, tumour cells and tumour-associated cells release a high amount of VEGF. VEGF-A has been shown to inhibit ICAM and VCAM on endothelial cells, thus, preventing extravasation and homing to the tumour bed (13).

### 3) Immune-mediated killing of cancer cells.

Once the immune cells reach the tumour site, they can perform their effector function, which is direct or indirect tumour killing (40, 41). NKs, CTLs and Th1 cells can indirectly kill tumour cells by the production of IFN $\gamma$ . IFN $\gamma$  has many functions, which include induction of MHC I expression, and thus enhancing tumour immunogenicity, recruit tumour infiltrating lymphocytes by enhancing the secretion of IFN $\gamma$ -inducible chemokines, inhibit proliferation of tumour cells by inducing cell cycle inhibitors, such as cyclin-dependent kinase (CDKs) inhibitors, p21 and p27, and can promote apoptosis by inducing caspase-1, Fas, FasL and TNF-related apoptosis-inducing ligand (TRAIL) (40, 41). Although, it also induces programmed cell death ligand 1 (PD-L1), which acts as a co-inhibitory ligand to suppress and/or induce apoptosis of NK and effector T cells, and therefore associated with poor prognosis (56). PD-L1 can be upregulated in other ways, such as post-transcriptional upregulation by persistent phosphoinositide 3-kinase (PI3K)-protein kinase B (PKB also known as AKT) pathway or transcriptional upregulated by constitutive signal transducer and activator of transcription 3 (STAT3) signalling (57-60).

As mentioned, tumour cells can acquire a defect in the IFN $\gamma$  signal pathway to escape the mediated effects of IFN $\gamma$  and obtain capability to constitutive active PI3K/AKT and STAT3 to escape immunological control.

The direct cell-mediated tumour killing is mediated by death receptor pathways, such as tumour necrosis factor (TNF)/TNFR, FasL/Fas, TRAIL/TRAIL-Rs, and CTL-mediated cytotoxicity perforin/granzyme B pathway, which accounts for extrinsic and intrinsic paths to apoptosis, respectively (61). Cancer cells may escape apoptosis by promoting survival signals, e.g. by loss of phosphatase and tensin homolog (PTEN) promoting constitutive activation of the PI3K-AKT pathway (62), or frequently have constitutive active STAT3 activation, both of which can induce the upregulation of anti-apoptotic factors, such as B-cell lymphoma 2 (Bcl-2) and B-cell lymphoma-extra-large (Bcl-XL) (63), or cancer cells may acquire defects in death receptor signalling (49). When a ligand binds to a death receptor, it results in activation of caspase-8 by

cleaving its pro-part off and release of caspase-8 from death-inducing signalling complex (DISC). Caspase-8 will then initiate the caspase cascade to induce apoptosis of the extrinsic pathway. Various tumour cells have been shown to upregulate the caspase inhibitor cellular FLICE-inhibitory protein (cFLIP) as a way to resist death receptor-mediated apoptosis (49). Other ways to escape death receptor signalling are by a loss of Fas expression, loss of TRAIL receptor expression, and mutations in Fas-associated protein with death domain (FADD), which result in lack of signalling from DISC (49). Furthermore, tumours can also evade killing via the perforin/granzyme B pathway by overexpressing PI9, a serine protease inhibitor that inactivates granzyme B (49).

If it is assumed that recognition, activation and recruitment have happened successfully, and that there is no defect in effector signalling pathways, then it would be feasible to think that the anti-tumour immune response must be successful in the destruction of the tumour cells. However, this might not be the case. The tumour can express and release many different proteins, which influence the tumour microenvironment, which is now known to consist not only of cancer cells but also fibroblast, endothelial cells and even immune cells that are able to support tumour progression (38-40). As mentioned above, the tumour often changes its chemokine release in order to promote recruitment immunosuppressive immune cells as MDSCs, TAMs, and Tregs to the TME, and secretion of different mediators (which in itself often is immunosuppressive in TME), such as IDO, Granulocyte-macrophage colony-stimulating factor (GM-CSF), IL-1 $\beta$ , VEGF, TGF- $\beta$  and prostaglandin E<sub>2</sub>, enables them to expand and accumulate in the TME (47, 49, 51, 55). These immunosuppressive immune cells can then either directly or indirectly suppress the anti-tumour immune response. MDSCs have been shown to inhibit TILs and NKs and promote the recruitment of Tregs in the TME. MDSCs can do this by expression of many mediators, such as inducible nitric oxide synthase (iNOS), reactive oxygen species (ROS), arginase, IDO, TGF- $\beta$ , IL-10, and PD-L1 (51, 52). Arginase is involved in the conversion of L-arginine to urea, and IDO is involved in the conversion of tryptophan to kynurenine. Depletion of either L-arginine or tryptophan both inhibit T cell proliferation by arresting them G<sub>0</sub>/G<sub>1</sub> in the cell cycle (51). Kynurenine and other metabolic products of IDO activity have been shown to impair NK cell function (64), and inhibit both NK and T cell proliferation as well as induce apoptosis in thymocytes (65, 66). Arginase also

downregulates the CD3 $\zeta$ -chain of the TCR receptor, which is essential for TCR-mediated signalling, thus inhibits T cell activation (51). TGF- $\beta$  promotes induction and maintenance of inducible Tregs (iTregs) and nTregs, and suppresses the function of T cells, NKs, DCs and macrophages, e.g. by downregulating cytolytical proteins and co-stimulatory protein (54, 67). TGF- $\beta$  and its function in particular its contribution to cancer are described further in section 1.7.1. IL-10 inhibits DCs differentiation and maturation by downregulating MCH I and MCH II and or other components of the antigen-processing machinery, and thus impairs T cell priming. In addition, IL-10 down-modulates ICAM, which is required for mediated extravasation of leucocytes, and it also participates in the immunological synapse (IS) between T cells and APCs (1, 51, 68). In the TME, macrophages are often polarized to a phenotype that resembles the alternative activated M2 macrophage and are known as tumour-associated macrophages (TAMs). These cells exhibit many of the similar immunosuppressive effects as MDSCs as they also express ARG, IL-10, TGF- $\beta$  and VEGF (53). In addition to its function in promoting angiogenesis, VEGF has also been shown to impair DC differentiation and maturation (49). Tregs also secrete IL-10 and TGF- $\beta$  and consume a large amount of IL-2, which might compete with the need of CTLs (47, 69). Furthermore, Tregs also mediates its immunosuppressive effect by direct cell-to-cell contact where its expression of co-inhibitory receptors, such as CTLA-4 and PD-1, comes into play (47, 70-72). For example, they can downregulate the B7 co-stimulatory proteins necessary for full T cell activation (73). Thus, these immunosuppressive cells, their mediators and tumour-derived mediators contribute to a vicious cycle that promotes an immunosuppressive environment in the TME.

Finally, while combating cancer and trying to avoid immune suppression by external measures, the anti-tumour cells have an intrinsic program that can inhibit their function and display a progressively exhausted, dysfunctional state (74-76). As mentioned, the immune system has an incorporated multi-level tolerance system to avoid unnecessary tissue destruction and/or autoimmunity, e.g. following activation, T cells start to upregulate co-inhibitory receptors, such as CTLA-4 and PD-1, as a way to contract the effector phase of the immune response. However, upon repetitive exposure to antigens as in chronic inflammation, such as viral infections and cancer, the infiltrating lymphocytes acquire an exhausted T cell (Tex) phenotype with impaired functions, and they are marked with persistent high expression of co-inhibitory receptors on their surface, such as PD-1,

Lymphocyte-activation gene 3 (LAG-3), V-domain Ig suppressor of T cell activation (VISTA), CD244 (2B4), CD160, B- and T-lymphocyte attenuator (BTLA), CTLA-4 and Tim-3, and their long-term maintenance occurs in an antigen-dependent manner (74, 77, 78). Both CD4 and CD8 T cells, as well as NKs can become exhausted with a progressive loss of effector function (74-76, 79). Most of the knowledge obtained to date is obtained from exhausted CD8 T cells during viral chronic infections. Here, the CD8 T cell dysfunction occurs progressively with first losing its ability to produce IL-2 and reduced proliferation capacity, followed by a diminished ability to produce cytokines and chemokines, e.g. TNF $\alpha$  and IFN $\gamma$ , impair degranulation resulting in reduced release of granzyme B, and at the most terminal stage of exhaustion, these cells can be physically deleted (74, 75). The presence of tumour-infiltrating lymphocytes in the tumour is often associated with good prognosis, especially, if they are anti-tumour cells that can destroy cancer cells. However, even with the presence of these cells, the tumour manages to grow (75). This is because many of these cells display a similar exhausted phenotype as in chronic infections and thus are inefficient in fighting the cancer cells because of their impaired functions (75, 80).

As mentioned above, exhaustion is associated with displaying excessive-high amounts of co-inhibitory receptors, such as CTLA-4 and PD-1, and the accumulation of different co-inhibitory receptors, e.g. LAG-3, T cell immunoglobulin and ITIM domain (TIGIT), BTLA, VISTA, and Tim-3 in T cells, and NKG2A, TIGIT, PD-1 and Tim-3 in NKs, which reflect an exhausted state (75, 76). The phenomenon of the exhausted phenotype is still relatively new, however, T<sub>ex</sub>s has also been linked to an altered metabolism and a unique transcriptional program compared to functional T<sub>eff</sub>s and T<sub>mem</sub>s (75). This is most likely also true for NKs (76, 79).

The following section is about co-inhibitory receptors/ligands, which are considered as immunotherapeutic targets, and there is an overview of the molecular level on how these immune checkpoints are affecting the cells.

## 1.4 Biochemical Regulation of Activities of Immune Checkpoint Proteins Used as Potential Targets for Immunotherapy of Cancer and other Disorders.

As mentioned above, the balance between co-stimulatory and co-inhibitory receptors and their ligands is critical in determining if antigenic recognition will result in immune activation or induced peripheral immune tolerance (21, 31). Our understanding of these co-stimulatory and co-inhibitory proteins has shown that they are not only involved in controlling the response of naïve T cells, but also influence the response of T<sub>H</sub>17, T<sub>H</sub>22, T<sub>H</sub>1, T<sub>H</sub>2, T<sub>H</sub>9 and Treg (21). Furthermore, many of these receptors and ligands have been found on other immune cells, and even non-hematopoietic cells, and are also shown to be involved in their regulation (81). Although here, I will mainly focus on the role and expression of T cells. Even though, the first discovery of the co-stimulatory receptor CD28 and co-inhibitory receptor CTLA-4 occurred in the early 1980s and 1990s, respectively, the exact mechanism on how they perform their functions is still to some extent being unravelled (73, 82, 83). Furthermore, new costimulatory receptors, such as ICOS and 4-1BB, and co-inhibitory receptors, such as PD-1, Tim-3 and VISTA and their ligands have been identified, and these contribute to the complex regulation of the immune system (31, 81, 84). The physiological function of many of the co-inhibitory receptor pathways (also called immune checkpoints) is to serve as a negative feedback mechanism to downregulate/contract the immune response and thus minimize the risk of unintended immune-mediated tissue damage (31). However, cancer cells and some microbes have evolved to exploit these immune checkpoint pathways against the immune system, and thus escape immune destruction. Furthermore, co-inhibitory pathways have also been implicated in immune exhaustion leading to impaired effector function of T cells and NKs (85).

Understanding these immune checkpoint pathways will allow the development of new strategies for therapeutic intervention in immune-mediated diseases, such as cancer, atopic and autoimmune diseases, as it is now clear that they can be targeted to either enhance or possibly dampen the immune response (86).

Immune checkpoint blockade (ICB) immunotherapy using immune checkpoint inhibitors (ICI) have revolutionized anti-cancer treatments. ICI such as anti-CTLA-4 and anti-PD/anti-PD-L1 have shown that it can reverse the exhausted state of immune cells and thus

enhance the anti-tumour response in a variety of tumours (74-76). In fact, phase III trial in patients with metastatic melanoma, with the first ICI, ipilimumab (anti-CTLA-4), showed significant improvement in progression-free survival (PSF) and overall survival (OS) compared with gp100 (tumour antigen) vaccine or dacarbazine chemotherapy (13). However, this treatment is also associated with immune-related adverse effects (irAEs), such as various skin lesions (rash, pruritus and vitiligo) and colitis as the more common irAEs, but also other side effects are reported, albeit less frequently such as hypophysitis, thyroiditis and others (87). These irAEs reflect the role of CTLA-4s in the induction of tolerance and preventing autoimmunity. Pre-clinical models in mice, knockout (KO) of PD-1 showed less severe symptoms compared to KO of CTLA-4, hence, these pre-clinical experiments and the good clinical outcome of anti-CTLA-4 treatment led to the development of anti-PD-1 antibodies. Pre-clinical models in mice, knockout (KO) of PD-1 showed less severe symptoms compared to KO of CTLA-4, hence, from these pre-clinical experiments and the good clinical outcome of anti-CTLA-4 treatment led to the development of anti-PD-1 antibodies (21, 73, 88, 89). Indeed, pre-clinical experiments have shown that antibodies against PD-1 and/or PD-L1 can reinvigorate the functionality of some subset of T<sub>H</sub>1 (those that are T-bet<sup>hi</sup> Eomes<sup>low</sup> PD-1<sup>int</sup> and not Eomes<sup>hi</sup> T-bet<sup>low</sup> PD-1<sup>hi</sup> are functionally more exhausted and express higher levels of other inhibitory receptors, such as CD160, LAG-3 and Tim-3) during chronic infections (75, 90). Furthermore, an *in vitro* study found that PD-L1 blockade could augment human tumour-specific T cell response by enhancing the cytolytic effect of TAA-specific CTL and augment cytokine production of TAA-specific T helper cells (91). Moreover, PD-1 blockade could restore CD8 T cell effector function in only a subset of non-small cell lung cancer (NSCLC), in which TILs expressed intermediate levels of PD-1. In contrast, PD-1 blockade had only a marginal effect on T cells expressing high levels of PD-1(92). In addition to T cell exhaustion, PD-1 expression is associated with functional exhaustion of NKs, exhibiting impaired cytokine production, decreased cytolytic activity and poor proliferation, and also here blocking of the interactions of PD-L1-PD-1 could reverse dysfunction of NKs (76, 79). The reversal of NKexs is particularly important for MHC I deficient tumours, such as Hodgkin lymphoma (79). The good pre-clinical outcome of these experiments promoted head to head clinical trials assessing anti-PD1 and anti-CTLA-4 treatment. Pembrolizumab and nivolumab (anti-PD-1 antibodies) showed a further increase in response rates, PSF, OS compared to CTLA-4 blockade and less severe irAEs (13).

However, although ICB therapy has revolutionized cancer treatment, not all patients respond to treatment (they have primary resistance to therapy), and some patients show relapse after the initial response (they have acquired resistance to therapy) (13). In search of improving ICB therapy, understanding both the mechanistic action of these ICI and what causes resistance is essential. Resistance to immunotherapy, which tries to invigorate the host's own immunity to fight cancer, can reflect an escape mechanism in any of the steps in the cancer-immune cycle. As mentioned above, many of these exhausted immune cells express more than one type of co-inhibitory receptor, and it is believed that the upregulation of these receptors could be the cause of acquired resistance as the more co-inhibitory receptors they have, the more dysfunctional they are. A study examining the expression of co-inhibitory receptors, such as PD-1, CTLA-4, Tim-3, LAG-3 and BTLA, on CD8 T cells from NSCLC patients found that expression of PD-1 and Tim-3 increased with tumour stage. PD-1 expression is an early marker, whereas BTLA is upregulated at the late stage of T cell exhaustion (92). Furthermore, another study reported that tumour resistance to anti-CTLA-4 (ipilimumab) treatment in melanoma patients was caused by PD-L1 and represents a major resistance mechanism to therapy (75). Moreover, Tim-3 co-expression with PD-1 on tumour-specific CD8 T cells displayed a more dysfunctional phenotype than Tim-3<sup>-</sup> PD-1<sup>+</sup> and Tim-3<sup>-</sup> PD-1<sup>-</sup> both in mice and humans (93, 94). In support of this, recent studies reported that acquired resistance to PD-1 blockade is associated with upregulation of Tim-3 as alternative immune checkpoint (14, 15). Furthermore, this upregulation was found to be mediated by the PI3K-AKT pathway in head and neck cancer (15). In some cases, Tim-3 blockade alone could enhance CD8 T and/or CD4 T cell effector function, although, the most noticeable synergistic effect was with combination of blockade of the PD-L1-PD-1 pathway (14, 93-95). Persistent high expression of Tim-3 on NKs also promotes exhaustion of these cells as shown by the impaired cytokine production and cytolytic functions, and blockade of Tim-3 restored their function (79, 96-99).

In addition to co-inhibitory receptors, other factors like cytokines have been associated with exhaustion. Although further research is still needed on immunosuppressive proteins, such as IL-10 and TGF- $\beta$ , which have been linked to T cell exhaustion (74, 90). Studies of lymphocytic choriomeningitis virus (LCMV) infection in mice have shown that blockade of IL-10 enhances viral control and improves T cell responses (90). Another study found that phosphorylation of Smad2 (a downstream signalling protein of TGF- $\beta$ ) was higher in virus-

specific CD8<sup>+</sup> T cells from chronic LCMV infection than in virus-specific CD8<sup>+</sup> T cells obtained during well-controlled infection, and by abrogating TGF- $\beta$  signalling (by a dominant-negative receptor), it improved the functionality of CD8<sup>+</sup> T cells during chronic LCMV infection and prevented severe exhaustion (100). Furthermore, TGF- $\beta$  has been linked to chronic viral infection in humans (74). However, the molecular mechanism in which TGF- $\beta$  contributes to T cell exhaustion still remain elusive (74, 90, 101).

Thus, understanding the molecular escape mechanism deployed by the cancer cells is vital for new innovative strategies of treatment. The research is now focused on combinational approaches, such as dual blockade of CTLA-4 and PD-1, which has been shown to have a better clinical outcome than monotherapy although with increasing incidences of irAEs (13, 102), and/or dual blockade of PD-1 and Tim-3 (14, 15, 93, 94, 103), or combinational strategies that have ICI as the backbone and other immune escape mechanisms as a target, such as small molecule inhibitors, e.g. inhibition of soluble factors such as TGF- $\beta$  (104-106), and others such as chemotherapy, radiotherapy, vaccination, or CAR-T cell therapy, to overcome resistance to therapy (107, 108). Many of these combinations have been proven to be more effective and synergistic to enhance the anti-tumour immune response, however, precautionary measures have to be taken as combination therapies (especially targeting multiple immune checkpoints) also amplified irAEs (89, 106, 107).

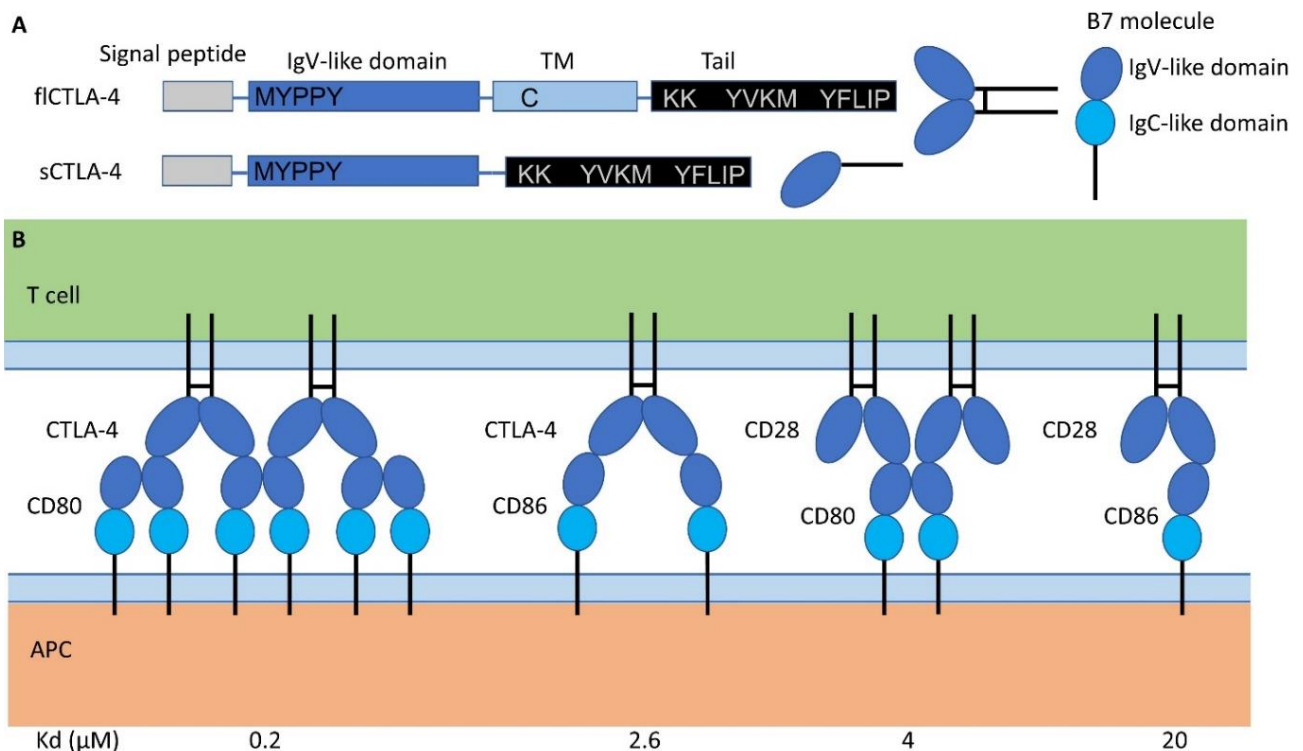
In the next subsections, I will highlight the biochemical signalling pathways for the two most studied co-inhibitory receptors, CTLA-4 and PD-1, which are already therapeutically targeted, clinically, and describe the current knowledge for the relatively newly identified co-inhibitory receptor Tim-3 and its ligand galectin-9.

#### 1.4.1 Cytotoxic T-lymphocyte-associated Protein 4 (CTLA-4)-mediated Signalling Pathways

CTLA-4 (also known as CD152) is a member of the CD28 family, which is part of the immunoglobulin (Ig) superfamily, as such, it shares a structure that consists of a single IgV-like extracellular domain, a stalk, a transmembrane domain and a cytoplasmic domain with one or more tyrosine signalling motif (21, 81). CTLA-4 shares some similarities with CD28, both of which has a cysteine amino acid in the stalk region that mediates homo-dimerization, and they both bind the same B7 ligands, which are B7-1 (CD80) and B7-2 (CD86) (21, 81). Both CD28 and CTLA-4 use the same conserved MYPPY binding motif,



however, CTLA-4 binds these ligands with much higher affinity (21, 81). The stronger binding by CTLA-4 is thought to be caused by the periodic arrangement in which bivalent CTLA-4 homodimer bridge with e.g. bivalent B7-1 homodimer that forms a zipper-like structure, which is in contrast to the monovalent binding of B7 molecules by CD28 (Figure 10) (81). Moreover, CD86 is constitutive expressed on resting APCs while CD80 is induced after activation, suggesting that CD28 favours interaction with CD86, and CTLA-4 prefers binding to CD80 (21). In support of this idea, it was demonstrated that B7-2 stabilizes the CD28 presence at the immunological synapse (IS) upon TCR stimulation and B7-1 mediated CTLA-4s recruitment to IS (109).



**Figure 10: CTLA-4 structure and binding to B7 molecules** (adapted from (110)). (A) full length (fl) CTLA-4 consists of 4 exons: exon 1 is the signal peptide, exon 2 the IgV-like domain including the MYPPV binding motive to B7 molecules, exon 3 is the transmembrane (TM) domain, which also contains a cysteine required for dimerization, and exon 4 is the cytoplasmic tail. There are no functional signalling domains, however, in its cytoplasmic tail, there are a lysine-rich motif and two tyrosine motives YVKM and YFLIP, which can recruit different proteins that mediate its immunosuppressive function. Soluble (s) CTLA-4 lacks exon 3 and thus the cysteine required for dimerization. Membrane-associated CTLA-4 is thus a dimer with two IgV-like domains and can interact with B7 molecules consisting of an IgV and IgC-like domain. (B) CD28 and CTLA-4 are quite similar and both have the MYPPV binding motive to bind CD80 (B7-1) and CD86 (B7-2), however, they have different affinities for each ligand, which is attributed to their distinct way of engaging with the ligands. Bivalent CTLA-4 dimer bridges with bivalent CD80 dime, whereas CD28 interacts monovalent with the B7 molecules.

In contrast to CD28, which is constitutively expressed on naïve T cells and then upregulated, CTLA-4 surface presence is tightly regulated, and its surface expression is only induced after T cell activation by TCR and CD28 ligation. Its upregulation is

proportional to the strength of TCR stimuli, although, it is constitutively expressed on Tregs (21, 73, 81). Although, CTLA-4 expression has long been thought to be restricted to T cells, it has also been reported in other cell types such as B cells, DCs, monocytes and even non-immune cells, such as placental fibroblasts (81). However, the focus here will be on T cells.

In conventional T cells at any given time, there are only low levels of surface CTLA-4, and the rest is found in intracellular compartments (such as the trans-Golgi network (TGN), endosome, and lysosome) (21, 81). It is here that the cytoplasmic tail comes into play as it contains a conserved YVKM motif, which is a consensus sequence for the adaptor protein (AP)1 and 2, and PI3K, and the binding depends on the phosphorylation of the tyrosine residue in the motif. As such, when tyrosine in the motif is dephosphorylated, it acts as a binding site for AP1 and AP2, where AP2 retains CTLA-4 in the TGN and mediates clathrin-dependent endocytosis of surface CTLA-4, and AP1 is involved in shuttling CTLA-4 from TGN to lysosome for degradation (21, 81). Tyrosine kinases such as Lymphocyte-specific protein tyrosine kinase (Lck), Lyn and Rlk, can phosphorylate the tyrosine at the YVKM motif, which stabilize its surface presence and may allow binding of PI3K (21).

CTLA-4 is thought to be crucial for the induction of T cell tolerance, and thus guard against autoimmunity. It is demonstrated by the striking phenotype of CTLA-4 deficient mice, which succumb within 3-4 weeks of birth due to lymphoproliferative disorder that also results in massive tissue infiltration and tissue destruction in multiple organs, which resembles a systemic autoimmune disease (81). This is also supported in humans where polymorphisms in the CTLA-4 gene is associated with autoimmune diseases (81). The overall function of CTLA-4 is generally regarded as an inhibitory regulator of T cell activation by increasing the threshold necessary for activation. Moreover, it has been shown to decrease T cell proliferation, downregulate cytokine production, and reduced T cell survival, by counteracting the effect of TCR-CD28-mediated signalling (111). Although, in settings of anergy, CTLA-4 has been shown to activate the PI3K-AKT pathways and rescue the anergic T cells from activation-induced cell death through inactivating pro-apoptotic Bad and increase expression of both anti-apoptotic Bcl-XI and Bcl-2, thus, promoting long-term tolerance (21). Furthermore, it is involved in CD4 T cell differentiation, where it has a role in suppressing Th2 and Th17 polarization while promoting Th1 differentiation (21). Even though, CTLA-4 was discovered in the early 1990s (82), the

mechanisms on how CTLA-4 mediates its "inhibitory" function is still unclear. The fact that CTLA-4 may or may not be required for induction of anergy (34, 36, 112), and that CTLA-4 might have "positive" effects (like the aforementioned activation of PI3K) in addition to its general inhibitory effects, and it is differentially regulated on various T cell subsets, such as upregulated on activated T cells, but constitutively expressed by Tregs and in fact, is required to mediate their suppressive effects, and may or may not require ligand binding to mediate its functions (21, 73), has made it difficult to come up with one model that explains all of the mediated functions of CTLA-4. This could also be attributed to reports of different splice variants of the CTLA-4 gene. To date, four variants have been reported in mice: 1) full-length (fICTLA-4) consists of all four exons (exon 1 encodes the signal peptide sequence, exon 2 contains the IgV-like domain with B7 binding motif, exon 3 consists of the transmembrane region, and exon 4 encodes the cytoplasmic tail with the tyrosine motif YVKM), 2) soluble CTLA-4 (sCTLA-4) lacks exon 3 and also lacks the cysteine residue required for covalent homodimerization, 3) ligand-independent CTLA-4 (liCTLA-4) lacks exon 2, and 4) a CTLA-4 variant has been reported that only has exon 1 and 4 (1/4 CTLA-4) (81). Only fICTLA-4 and sCTLA-4 have so far been found in humans (81). fICTLA-4 is constitutively expressed by Tregs, but in forkhead box p3 (Foxp3)<sup>-</sup> T cells, it is quickly upregulated after activation and becomes the predominant transcript. In contrast, in mice, liCTLA-4 appears to be downregulated upon activation (81). sCTLA-4 is mainly detected in resting T cells, and its exact function is unclear, however, CTLA-4 polymorphisms, such as CT60 and +49G>A, have been suggested to favour sCTLA-4 over fICTLA-4 (81), and elevated serum levels of sCTLA-4 are associated with autoimmune diseases, such as autoimmune thyroid diseases, systemic lupus erythematosus, systemic sclerosis, and others (113). In the autoimmune diseases associated with increased levels of sCTLA-4, the levels were for some disorders correlated with disease activity and clinical features, however, in other cases, they were not (113).

Although, the biochemical mechanism for CTLA-4 inhibitory effects is ambiguous, one thing seems to be certain: by blocking CTLA-4, the suppressive effects on T cell responses are reversed, and this is the grounds for the therapeutic intervention with anti-CTLA4, e.g. Ipilimumab in diseases such as cancer (13, 78). However, the underlying mechanism of how anti-CTLA-4 works is also unclear. It has been suggested that the enhanced anti-tumour effect is caused by antibody-dependent cell-mediated cytotoxicity

(ADCC)-mediated depletion of Tregs and to some extent de-repression of CTL function (114-117). Furthermore, the expression pattern of CTLA-4 by different CD4 T cell subsets might influence the efficacy of CTLA-4 blockade. It has been suggested that due to its high expression of CTLA-4 on Th17 cells compared to e.g. Th1 cells, Th17 cells are resistant to CTLA-4 blockade, and thus might contribute to CTLA-4 immune-related toxicities as these cells are often implicated in autoimmune responses (118, 119). Hence, improved understanding of the regulation and biochemical pathway of CTLA-4 involved in the inhibitory mediated effects would have profound implications in the immunomodulation strategy.

CTLA-4 inhibitory functions *in vivo* are thought to be mediated by both cell-intrinsic and cell-extrinsic mechanism, some of the underlying events have only been reported in conventional non-Tregs and some only in Tregs. Here, I will give an overview of the different models proposed of the inhibitory functions of CTLA-4 that reflect both cell-intrinsic and cell-extrinsic mechanisms (Figure 11), although, I will not discuss the ligand-independent action of CTLA-4 as these are not relevant to humans.

#### *Cell-intrinsic:*

- i) CTLA-4 competes with CD28 for B7 ligand binding.

A simple model that at least in part can explain the CTLA-4 and CD28 opposing effect is that CTLA-4 can outcompete CD28 for B7 ligand binding. This model is based on that CD28 and CTLA-4 share the same binding motif, and CTLA-4 has a much higher binding affinity to B7 molecules than CD28. This is thought to be mediated by the fact that CTLA-4 can bind bivalently to its ligands, while CD28 can only bind monovalent (81). In support of this notion, two studies (an *in vitro* study in human Jurkat T cells and a *in vivo* study in mice) have demonstrated that CTLA-4 inhibitory functions are mediated both by ectodomain competition and negative signalling by the cytoplasmic region (120, 121). In the *in vitro* study, it was demonstrated that truncated tailless CTLA-4 could sequester B7 ligands as its inhibition of IL-2 production was directly proportional to CTLA-4 surface presence (121). Furthermore, in the *in vivo* study truncated tailless, CTLA-4 could in part rescue the CTLA-4-deficient mice as these mice were long-lived with no signs of lymphocytes infiltration to multiple organs, although did still exhibit lymphadenopathy, suggesting that CTLA-4 ectodomain can compete for ligands,

and that the cytoplasmic domain is involved with regulating tissue infiltration (120). However, it has been demonstrated that CD28 co-stimulation is required for the manifestation of the disease phenotype of CTLA-4-deficient mice (73, 81). A way to explain this could be that CD80 and CD86 selectively regulate CD28 and CTLA-4 functions and stabilization at the immunological synapse (IS) by selective recruitment, of which CD86 is the main binding partner for CD28, and CD80 preferentially binds to CTLA-4 (109). CD28 recruitment to IS was reported independent of B7 proteins, however, its localization was not stabilized as it could be disrupted by CTLA-4. In contrast, B7 binding was critical for CTLA-4 recruitment to IS (109). This is supported by a recent study using molecular imaging analysis, which showed that there was a ligand-dependent recruitment of CTLA-4 to the central supramolecular activation cluster (c-SMAC) of the IS, and that CTLA-4 could compete for ligand binding, which ultimately results in the exclusion of CD28 from the c-SMAC (122). Moreover, it was found that this inhibitory mechanism was deployed both by Teffs and Tregs (122).

ii) Engagement of negative signalling protein by CTLA-4.

The TCR/CD28 co-ligation results in phosphorylation of TCR $\zeta$  by Lck, which promotes downstream phosphorylation of signalling intermediates, such as Zeta-chain-associated protein kinase 70 (ZAP70), Linker for activation of T cells (LAT) and others (19). In contrast, the engagement of CTLA-4-mediated inhibitory effects has been associated with dephosphorylation/reduced phosphorylation of signalling elements (21). Although, CTLA-4 does not have an immunoreceptor tyrosine-based inhibitory motif (ITIM) in the cytoplasmic tail, it has still been reported to be associated with phosphatases such as Protein phosphatase 2 (PP2A) and Src homology 2 domain containing phosphatases (SHP)-2 (81).

The roles of PP2A and SHP-2 serine/threonine phosphatase in CTLA-4 are unclear as both also binds to CD28 (123). Nevertheless, PP2A has been shown to have multiple binding sites at the cytoplasmic tail of CTLA-4, at three-lysine motif in the juxtamembrane portion of the cytoplasmic tail and at the YVKM motif, which is also crucial for PI3K and AP1/2 binding and at the YFLIP motif (123-125). CTLA-4 engagement has been shown to activate PP2A, which then inhibits AKT activation as this effect was ablated by the PP2A inhibitor okadaic acid (126). However, the regulatory unit of PP2A was shown to bind to the lysine-rich motif of

the CTLA-4 cytoplasmic tail as mutations in this motif could no longer co-precipitate PP2A and CTLA-4. Furthermore, the mutant cells were more efficient at inhibiting IL-2 gene transcription, suggesting that PP2A acts as a repressor of CTLA-4 (124).

The SHP-2 tyrosine phosphatase has been shown to associate with CTLA-4 and has been proposed to mediate the inhibitory proximal signalling events of CTLA-4 down-stream of TCR (127). This recruitment was proposed mediated by the phosphorylation of the YVKM motif (127), however, another study showed that the inhibitory functions of CTLA-4 are independent of the tyrosine phosphorylation, although it is critical for surface retention (128). Furthermore, if SHP-2 is associated with CTLA-4, this interaction is possibly indirect as it has been demonstrated that CTLA-4 has no binding sites for SHP-2 (129).

Other proposed mechanisms are activation of E3 ligases, such as Casitas B-lineage lymphoma (Cbl)-b or Itch. It has previously been reported that SHP-2 mediates some of the inhibitory effect of CTLA-4 by activating Itch. Itch can bind to the proline-rich residues of the SHP-2 tail, and SHP-2 dephosphorylates Itch, and it becomes activated (130). Suppression is mediated by ubiquitinating its different targets, such as Phospholipase C (PLC) $\gamma$ 1, Protein Kinase C (PKC) $\theta$  and JunB, which either target them for proteasome-dependent degradation or alternatively reduce their catalytic activity, or promote interaction with inhibitory proteins, or may alter sub-cellular localization (130). Although, CTLA-4-mediated suppression of IL-2 was unaffected in Itch-deficient cells, suggesting that additional proteins are involved in CTLA-4-mediated suppression of T cell response (130). In the case of Cbl-b, it appears that CD28 and CTLA-4 have opposing roles as TCR-CD28 co-ligation targets Cbl-b for degradation, whereas CTLA-4 is required for its re-expression, and it is correlated with decreased T cell proliferation (131). Furthermore, Cbl-b KO T cells were not susceptible to the inhibitory effects of CTLA-4 ligation, suggesting that expression of Cbl-b is necessary for the function of CTLA-4 (131). This is supported by the fact that both Cbl-b and CTLA-4-deficient cells are resistant in the induction of anergy (131). Recent evidence has pointed to Cbl-b being essential for induction of T cell anergy (132). Although, the role for CTLA-4 in the induction of anergy is heavily debated, there seems to be a

difference if the setup is *in vitro* or *in vivo* where CTLA-4 at least appears to be required for anergy *in vivo* (34, 36, 112).

iii) Inhibition of lipid-raft/microclusters formation by CTLA-4.

When T cells engage with antigen-bearing APCs there is a macromolecular rearrangement of protein structures that results in the formation of an interface called the immunological synapse (IS). A time frame of 5-10 min of active cytoskeleton processes is involved in forming the mature IS. When completed, the interface can be divided into zones consisting of the central, peripheral, and distal supramolecular activation cluster (SMAC), c-SMAC, p-SMAC and d-SMAC, respectively (133). These zones are enriched with different proteins, such as TCR, and CD28 in c-SMAC, integrins such as CD2, Lymphocyte function-associated antigen 1 (LFA-1) and cytoskeleton protein in p-SMAC and larger glycoproteins, such as CD43 and CD45, in the d-SMAC (133). Two models, the lipid-raft and the microcluster model, have been proposed to explain how the signal is initiated and maintained in the IS (134). The lipid-raft model proposes that as the IS forms, there is an enrichment of lipid-rafts forming in this interface (135). Lipid-rafts exist in a pre-assembled state in intracellular compartments, and TCR ligation promotes the release of these to the surface, which enables entry and aggregation of signalling proteins into TCR-associated lipid-rafts (135). However, recent studies have observed an increase in cellular phospho-tyrosine, intracellular calcium elevations, and cytoskeletal rearrangements, which were all initiated within seconds of receptor engagement and peaked within 2-3 min of TCR engagement, suggesting that these signals were derived from TCR ligation before the formation of c-SMAC (136). This has led to the formation of the microcluster model where microclusters containing TCR signalling components, such as CD3 $\zeta$ , ZAP70, SPL76, form within seconds of initial TCR engagement and sustain TCR-mediated signalling (136, 137). Nonetheless, these models are quite similar and a proposed mechanism on how CD28 and CTLA-4 can regulate the threshold for T cell activation by promoting or inhibiting lipid-raft/microcluster formation and thereby regulate the availability of key signal mediators necessary for efficient TCR signalling (135, 138). It was reported that CD28 could enhance raft formation upon TCR engagement, whereas CTLA-4 was shown to potently inhibit both TCR- and TCR/CD28-associated lipid-raft expression on the surface of T cells (135, 138,

139). Furthermore, CTLA has been found to disrupt ZAP70 microcluster formation (140).

- iv) CTLA-4 signal affect adhesion and motility (only Teff) – reverse stop-signal.

Another model that has been proposed is the reverse stop-signal model, which proposes that CTLA-4 promotes T cell motility, thereby limiting the dwell time between T cells and APCs resulting in a reduced level of T cell activation (134). It is believed that CTLA-4 mediates the inside-out signalling necessary for LFA-1 activation required for stable contact in the IS by activating the GTPases Rap1 (which is an integrin activator), and this increases the movement of T cells (141). Furthermore, it has been shown that CTLA-4 could override the stop-signal induced by TCR engagement, and thus reduce the dwell time between T cells and APCs. The reduced dwell time resulted in impaired ZAP70 microcluster formation and calcium mobilization concurrent with reduced cytokine production and proliferation (140, 142). However, this finding is only applicable to Teffs not Tregs as blocking CTLA-4 increases contact time between Teffs and APCs, but not in Tregs and APCs (143, 144).

- v) PKC- $\eta$  can bind to cytoplasmic domain and modulate Treg function (only Tregs).

By examining Teffs and Tregs, it is clear that although there are some intrinsic proximal TCR signalling that is the same, such as activation of TCR, Lck, PDK1, LAT and PLC $\gamma$ 1, although some are distinct, and this likely enables Tregs to perform its suppressive functions (70). As mentioned above, CTLA-4 is upregulated on activated T cells, but is constitutively expressed by Tregs and at a much higher level. This is in part attributed to CTLA-4 being a target of Foxp3 (71, 81). In addition, the interaction of Tregs and APCs in the IS is much stronger than in Teffs (145). Furthermore, upon activation, Teffs requires PKC $\theta$  as part of its positive signalling and is recruited to the IS. In contrast, PKC $\theta$  was sequestered away from the Tregs IS, and PKC $\theta$  is thought to inhibit Treg-mediated suppression (146). Instead, upon CTLA-4 engagement, Tregs recruit the novel PKC $\eta$  to the IS, where it is involved in the contact-dependent suppressive activity of Tregs (70). Furthermore, upon co-ligation of TCR/CTLA-4, a GIT-PIX-PAX complex is recruited to Treg IS, which was defective in PKC $\eta$ -deficient Tregs and was associated with reduced CD86 depletion from APCs. In this study, it was proposed that the GIT-PIX-PAX complex destabilises the Tregs-APCs contact and thus



enables Tregs mobility to engage with new APCs targets (70). This could be a related mechanism to what is seen in Teff, whereas mentioned, CTLA-4 has been reported to reverse the TCR stop-signal and promote motility of Teff by influencing LFA-1 affinity. Thus, the CTLA-4-bound PKC- $\eta$ -GIT-PIX-PAK complex is a Treg cell-intrinsic signalling, which plays a role in mediating the cell-extrinsic suppressive functions of Tregs (70).

#### *Cell-extrinsic:*

Many cell-extrinsic effects of CTLA-4 are mediated by Tregs.

i) CTLA-4 induction of IDO by APC.

It has been proposed that CTLA-4 can function in a cell-extrinsic manner via Tregs by initiating a reverse signal into APCs when binding to its ligands, and thus inducing IDO enzyme activity/functional IDO expression (73). IDO is an enzyme, which is involved in the rate-limiting step in the catabolism of tryptophan to kynurenine, which is then converted into various downstream metabolites (147).

It is thought that IDO inhibitory mediated effect is caused by various mechanisms, such as tryptophan depletion that inhibits T cell and NK proliferation, kynurenine-mediated inhibition of IL-2 signalling, kynurenine-promoted induction of iTregs, and some of the kynurenine metabolites have a cytotoxic effect and induce apoptosis of certain T cell subsets such as Th1 cells (148, 149). IDO expression can be induced by inflammatory cytokines such as type I and II interferons, however, induced expression does not necessarily mean that it is also active (147). It was first shown in *in vitro* experiments that IDO activity in DCs expressing B7 molecules could be induced by the CTLA-4-immunoglobulin (CTLA-4-Ig) recombinant fusion protein (73, 147). In addition, this was supported by studies demonstrating that mouse Tregs and human CD4 T cells (most likely Tregs) could induce functional IDO expression in a CTLA-4-B7 dependent manner (150, 151). IDO-deficient mice do not have the same disease phenotype as CTLA-4-deficient mice, which suggests that induction of IDO activity is not the only CTLA-4 dependent mechanism (73).

ii) CTLA-4 can induce TGF- $\beta$  expression.

The displayed similarities between TGF- $\beta$ -deficient and CTLA-4-deficient mice have led to the speculation that the inhibitory cell-extrinsic mechanism of CTLA-4

is mediated via the production of TGF- $\beta$  by Tregs (73). It has been reported that co-ligation of TCR-CTLA-4 could induce TGF- $\beta$  production by murine CD4 T cells (Th1, Th2 and Th0 subsets) (152). Moreover, anti-TGF- $\beta$  could partially reverse CTLA-4-mediated T cell suppression, suggesting that some of CTLA-4 mediated effects are through TGF- $\beta$  (152). In contrast, in another study, it was reported that CTLA-4 cross-linking did not result in the production of active nor latent TGF- $\beta$  by TCR transgenic T cells, and they also found that TGF- $\beta$  neutralizing antibody could not reverse CTLA-4-mediated suppressive effects, suggesting that CTLA-4 and TGF- $\beta$  represent distinct mechanisms for suppressing T cells (153). In support of this, another study reported that anti-CTLA-4 abrogated wild-type Tregs suppressive functions *in vitro* while neutralizing TGF- $\beta$  had no effect (154). However, in this study, it was also reported that CTLA-4-deficient Tregs *in vitro* develop a compensatory suppressive mechanism via CTLA-4-independent production of anti-inflammatory cytokines, such as IL-10 and TGF- $\beta$  (154). Tang and colleagues suggested that there are two distinct mechanisms in which CTLA-4 regulates Treg function, one during functional development of Treg and the other during the effector phase when the CTLA-4 signalling pathway is required for Treg suppressive activity (154). A third study suggested that the main mechanism of Treg suppressor effect is by the presence of surface-bound TGF- $\beta$ , and that CTLA-4 engagement of Tregs facilitates TGF- $\beta$  suppression by concentrating the TGF- $\beta$  at the point of cell-cell contact (155).

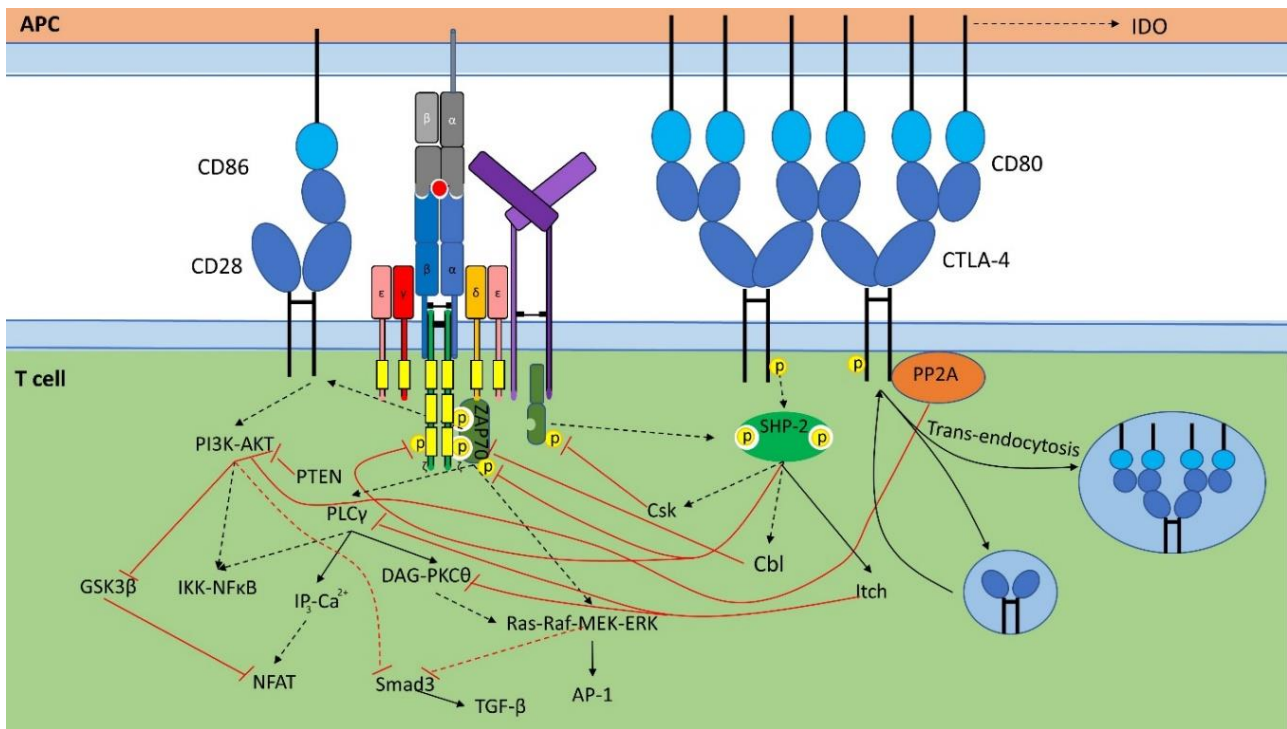
iii) CTLA-4-mediated modification of APC phenotype by trans-endocytosis.

The suppressive functions of Tregs are thought to be both indirect (secretion of suppressive cytokines) and direct by cell-cell contact. It has been reported that Tregs are able to impair the stimulatory capacity of DCs *in vitro* by downregulating B7 molecules (156). In support of this, another study from the same group reported that the *in vitro* down-modulation of B7 molecules on DCs occurs rapidly in a CTLA-4-dependent manner when co-cultured with Tregs, and this effect was reversed by blocking CTLA-4 (157). In support of this, another group found that Treg suppressive function was impaired *in vitro* and *in vivo* in Treg-specific CTLA-4 deficient cells (71). Finally, several recent studies have demonstrated a cell-extrinsic mechanism in which CTLA-4 is able to downregulate B7 molecules by the process of trans-endocytosis in which CTLA-4 captures the B7 ligands on the

opposing cell and internalizes it in vesicles, which then is degraded in CTLA-4-bearing cells (158-160). Qureshi and colleagues have shown that CTLA-4 blocking antibody hampered the down-modulation of CD86 on DCs in conjunction with the presence of CD86 in CTLA-4+ vesicles in T cells. The CTLA-4-mediated trans-endocytosis appeared to be specific to B7 co-stimulatory proteins as other co-stimulatory proteins, such as CD40, were unaffected on DCs (158). Furthermore, they demonstrated that CD28 was incapable of trans-endocytosis. Moreover, their data indicated that both Foxp3+ (Treg) and Foxp3- T cells have the capacity of trans-endocytosis (158). "In essence, trans-endocytosis represents an extension of the original ligand competition model whereby, in addition to competing at the cell surface for ligands, CTLA4 can also physically remove them" (73).

iv) Secretion of sCTLA-4.

As mentioned above, sCTLA-4 is a soluble monomeric form of CTLA-4, which is able to bind B7 molecules caused by an mRNA splice variant. sCTLA-4 transcript has been reported in secondary lymphoid organs (lymph node and spleen) as well as in T cells (both CD4 and CD8), B cells and monocytes (161). It is not clear what the function is, but elevated levels have been detected in patients suffering from autoimmune diseases and in some cases correlated with disease severity, while in other cases, they were not (113). The fact that it can bind B7 molecules suggests that it can sequester them from both CD28 and CTLA-4, this could explain the mixed outcome of clinical features (162). Simone and Saverino envisioned that "On one hand, sCTLA-4 may bind CD80/CD86 natural ligands expressed on APC and thus interfere with CD80/CD86-CD28-mediated co-stimulation of early T cell responses. On the other hand, sCTLA-4 may also be capable of interfering with CD80/CD86-CTLA-4 interactions, thereby blocking the negative signal imparted via the membrane-bound form of CTLA-4 in the later phases of T cell responses" (113). However, further investigations are necessary to clarify the role of sCTLA-4 in regulating T cell response.



**Figure 11: Some proposed CTLA-4 cell-intrinsic and extrinsic suppressive mechanisms.** CTLA-4 surface presence is tightly regulated by AP1 and AP2 adaptor proteins (not shown) and cycles between surface and endosome/lysosome, its surface expression becomes stable upon phosphorylation of the YVKM motif and engagement of ligand. CTLA-4 can activate PP2A, which inhibits AKT. Furthermore, CTLA-4 can indirectly mediate activation of SHP-2, which dephosphorylates TCR proximal signalling proteins and activates Cbl and Itch, which target their substrate for proteolytical degradation. This results in inhibition of the PI3K-AKT, PLCγ-PKCθ and the MEK-ERK MAPK pathways and consequently also attenuation of the transcription factors, such as NFAT, AP-1 and NFκB, but enhanced Smad3 activity, which promotes TGF-β production. It is thought that some of the CTLA-4-mediated immunosuppressive effects are via CTLA-4-induced TGF-β-mediated suppression. Another proposed mechanism is that CTLA-4 can reverse signal into APCs and induce IDO expression and activity, which also is immunosuppressive. Recently, CTLA-4 has been proposed to mediate trans-endocytosis and thus removing B7 ligands from the surface of APCs.

### 1.4.2 Programmed Cell Death Protein 1 (PD-1) Signalling Pathways

PD-1 (also known as CD279) was discovered in the early 1990s (163), and since then, research has identified it as a co-inhibitory receptor, which is critical in the induction and maintenance of peripheral tolerance by regulating T cell response of not only naïve T cells and Tregs, but also Tmems, Tregs as well as exhausted T cells (Texs) (163, 164). PD-1 and its ligands have also been found to be involved in central tolerance during thymocyte development where it influences fate decision at several stages of thymocyte maturation and modulates both positive and negative selection in the thymus (89, 164). Its importance is illustrated by PD-1 deficient mice, which in later stages of life eventually develop organ-specific autoimmune disease, which symptoms are dependent on the genetic background of the mice strain (89, 164). Furthermore, polymorphisms detected in the human PD-1 gene are associated with autoimmune disorders, cancer, and viral pathogenesis (81). PD-

1 and CTLA-4 are both co-inhibitory receptors and members of the same family. Engagement of either of these results in the attenuation TCR-CD28-mediated signalling, and thus diminishes T cell activation by reducing T cell proliferation, cell survival, and effector function, such as cytokine production and cytolytic activities (165, 166), as well as influencing T cell differentiation, which is due to metabolic reprogramming (167) and modulation of lineage-specific transcription factors (21, 81). Albeit the mechanisms in which CTLA-4 and PD-1 deploy to obtain their inhibitory effects are somewhat distinct (126). Although, CTLA-4-deficient mice display a more profound disease phenotype with severe systemic autoimmunity that results in fatality than PD-1 deficient mice. Experiments with DNA microarray analysis investigating the transcriptional profile of T cells have demonstrated that PD-1 is a more potent suppressor of CD3/CD28-mediated change of the T cell transcriptome than CTLA-4, where transcripts that were regulated five-fold or more by T cell activation were reduced by 67% and 90% upon CTLA-4 and PD-1 engagement, respectively (126). The contrast of the transcriptional profile and the phenotype of the diseased mice could possibly be explained by the distribution of CTLA-4 and PD-1 ligands and their roles in the induction and maintenance of peripheral tolerances, respectively (126). Furthermore, it appears that PD-1 signal attenuates more membrane-proximal signals, whereas CTLA-4 reduces more membrane-distal signals, for instance, both co-inhibitory receptors mediate some of their effects by targeting the PI3K-AKT pathway. However, it has been demonstrated that PD-1-mediated signalling directly blocks PI3K activity, whereas CTLA-4-mediated signalling blocks AKT, preserving PI3K activity and in doing so maintain the Bcl-xl survival factor (126). Another example is that both CTLA-4 and PD-1 signals are involved in reversing/blocking the TCR stop-signal required for stable contact between T cells and APCs. While in the priming phase of naïve T cells, CTLA-4 increases motility by affecting the cell adhesion molecule LFA-1, however, in anergic T cells, PD-1 but not CTLA-4 appears to have a role in attenuating the TCR-stop signal as assessed by blocking antibodies (168). In support of this, another study found that silencing of PD-L1 allowed enhanced clustering between DCs and CD8 T cells, suggesting that PD-1-mediated inhibition of TCR-induced stop-signal was abrogated (169). This is further supported by a study that demonstrated that in activated T cells, PD-1 microcluster formation and accumulation in c-SMAC upon ligation of PD-1 were implicated in interfering with TCR-stop-signal probably by reducing phosphorylation of TCR proximal signalling proteins (170).

As mentioned, PD-1, like CTLA-4, is a type 1 transmembrane protein and also a member of the CD28 family, and thus part of the immunoglobulin (Ig) superfamily. Consequently, some structural similarities are observed in the extracellular domain with a single N-terminal IgV-like domain, however, the cytoplasmic domain resembles more that of the Siglec family, which has an ITIM and an ITSM motif in the cytoplasmic tail (Figure 12) (171). PD-1 is encoded by the PDCD1 gene located on chromosome 2q37.3 and consists of 5 exons: exon 1 encodes the signal sequence, exon 2 consists of an IgV-like domain found in the extracellular region, exon 3 encodes the stalk and transmembrane region, and exon 4 and 5 form the cytoplasmic tail, which as mentioned consists of an ITIM and an ITSM motif, respectively (81). Unlike in CTLA-4, there are no cysteines found in the stalk region, which are important for CTLA-4 homo-dimerization, thus PD-1 is considered to act as a monomer (171). To date, there have been reported additional four splice variants of the PDCD1 gene, although their functions are unclear, albeit the splice variant (lacking exon 3) forming a soluble sPD-1 is implicated in autoimmune diseases, such as rheumatoid arthritis (RA), and may serve as a biomarker as increased levels in the synovial fluids and sera correlate with disease severity (81). PD-1 is inducible expressed on activated T cells (CD4, CD8 and Tregs), B cells, NKT cells, monocytes/macrophages, some subsets of DCs and NKs and chronic inflammation may enhance its expression (81). Although, here, I will mainly focus on its function in T cells.

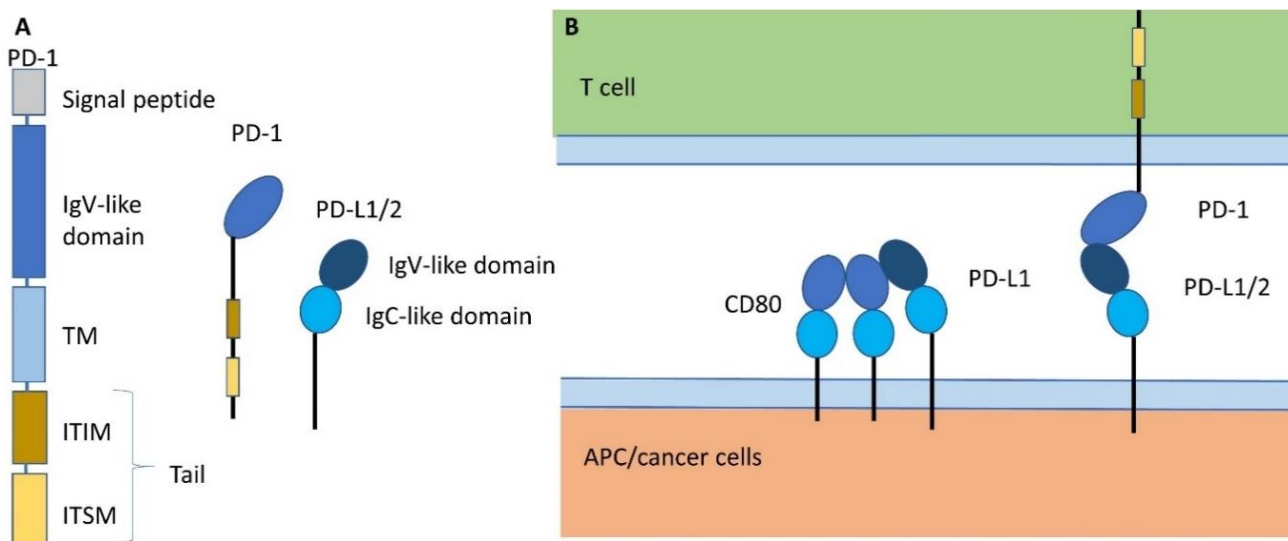
PD-1 expression is transiently induced by TCR signalling (and possibly TCR-CD28 co-ligation) as well as by cytokines from the common  $\gamma$ -chain family of cytokines (IL-2, IL-7, IL-15, IL-21 and IFN $\gamma$ ), where PD-1 surface presence is usually detectable 24 h after activation (81). Furthermore, the extent of PD-1-mediated inhibition depends on the strength of the TCR signal, where PD-1 inhibition appears more effective with weak TCR stimulation inhibiting both proliferation and cytokine production, but at strong TCR stimulation only inhibits cytokine production. This most likely reflects that PD-1 expression on activated T cells was highest in the cells that were weakly activated (172). In addition, when T cells are continuously stimulated by antigens, such as in chronic infections or cancer, PD-1 expression remains high, which results in T cell exhaustion (81).

PD-1-mediated signalling is activated upon ligation of its ligands, either PD-L1 (also known as B7-H1 or CD274) and PD-L2 (also called B7-DC or CD273), which both are part of the B7 family of ligands, and thus have structural similarities, such as an IgV- and an IgC-like

domain in their extracellular regions and a very short cytoplasmic tail of 30 amino acids (Figure 12) (81). PD-L1 is more widely expressed than PD-L2. PD-L1 is constitutively expressed by T cells, B cells, macrophages and DCs. Upon activation of these cells, PD-L1 is further upregulated, but it is also expressed by non-hematopoietic cells and cancer cells (164). PD-L2 is restricted to APCs (such as DCs and macrophages) and non-hematopoietic cells in the lung, as well as some tumour cells (164). Because of this more widely peripheral expression of PD-L1, it is thought that PD-1-PD-L1 is vital for maintaining peripheral tolerance in the tissue whereas CTLA-4, which ligands mainly are restricted to APCs, is thought to be more involved in the induction of peripheral tolerance (164). Various proinflammatory stimulations, such as type I and type II interferons, induce both PD-L1 and PD-L2 expression, and it is thought that in physiological conditions, it might serve as a negative feedback mechanism to down-modulate T cell response in the periphery and protect against immune-mediated tissue damage (81). In contrast, cancer cells appear to exploit this pathway with constitutively high expression of PD-L1 and use it to escape immune attack by multiple mechanisms, such as inducing apoptosis of T cells in a PD-1-independent manner (173), promote T cell exhaustion by suppression of T cell activation shown by reduced cell proliferation, cytokine production and cytolytic functions in PD-1 dependent manner (81, 165). Furthermore, in some tumours, it has also been reported that cancer cells can express PD-1 and use it to promote tumour growth (174).

Thus, PD-1 and PD-L1 appear to be possible targets for cancer immunotherapy. Pre-clinical and clinical trials using PD-1 and/or PD-L1 blockade have already proved to provide a durable and long-lasting effect for patients with different kinds of tumours and seem to be associated with a lower incidence of irAEs than blocking CTLA-4 (13, 89). Although, not all patients respond to treatment (primary resistance), and those who do often face a relapse after 3 years (acquired resistance) (13). To discern, which patients are more likely to respond, there is a need to identify biomarkers that can predict response, which might be related to resistance to therapy. Furthermore, to overcome the therapeutic resistance, an extensive knowledge of the molecular mechanisms of blocking antibodies are required, and accordingly, a more comprehensive understanding of the mechanism mediated by the PD-1 pathway and its ligands (13, 89). Some of the signalling components downstream of PD-1 are still being unfolded, although, recruitment of the tyrosine phosphatase SHP-2 seems to be the main driver of the inhibitory effects.

Furthermore, the roles for the multiple splice variants of not only PD-1 but also PD-L1 and PD-L2 need to be elucidated (81). Besides, PD-L1 and PD-L2 have both been reported to bind to other receptors than PD-1, which are B7-1 and RGMb, respectively (81), and these interactions should also be considered when using blocking antibodies, e.g. engagement of PD-L1 with B7-1 has been demonstrated to inhibit T cell proliferation (175), and PD-L2 has been suggested to promote airway hyperresponsiveness in allergic asthma and possibly has a role in other allergic conditions (176-178). In the next section, I will describe the inhibitory cell-intrinsic and cell-extrinsic mechanism mediated by the PD-1 signalling pathway in T cells.



**Figure 12: PD-1 and PD-L1 structure and binding** (adapted from (179)). PD-1 consists of 5 exons: exon 1 is the signal peptide, exon 2 encodes the IgV-like binding domain, exon 3 the TM, and exon 4 and exon 5 encode the cytoplasmic tail, which have two signalling motives, the ITIM and the ITSM. (B) PD-1 and PD-L1 binding. PD-1 is upregulated upon activation of T cells as a negative feedback mechanism to attenuate response and can engage with PD-L1 or PD-L2 expressed APCs or cancer cells. PD-L1 and PD-L2 have other binding partners. PD-L1 can interact with CD80 in cis (meaning that they need to be expressed by the same cell).

### PD-1 signalling

As previously described, PD-1 has two tyrosine-based motifs, an N-terminal sequence VDYGEL forming the ITIM and a C-terminal sequence TEYATI creating the ITSM motif (defined as V/I/LxYxxL and TxYxxL, respectively) (171). Live imaging has shown that upon TCR-PD-1 co-ligation, PD-1 co-localize with TCR microclusters in c-SMAC of IS (170). It has been suggested that this allows for Src family kinases (Lyn in B cells), Fyn and Lck in T cells) to phosphorylate the tyrosine-based motif in the PD-1 cytoplasmic tail (180-182). It was demonstrated that Fyn and Lck, but not ZAP70, phosphorylate the PD-1 cytoplasmic domain (182).



Although, the ITIM motif usually is found to recruit src homology-2 (SH2) domain-containing phosphatases, mutational studies have identified the ITSM motif to be critical for mediating PD-1 inhibitory effects by recruitment of phosphatases. It has been demonstrated *in vitro* that both SHP-1 and SHP-2 tyrosine phosphatases can bind to a phosphorylated ITSM motif. Moreover, SHP-2 was able to bind to ITIM, although the amount was lower (181, 183). SHP-1 is normally considered to be a negative regulator of T cell response, whereas SHP-2 is thought to promote positive signalling, however, in the case of PD-1 downstream signalling, it appears that SHP-2 is the main driver of the inhibitory effects as only SHP-2 has been found to associate with PD-1 microclusters (170). In fact, TCR stimulation alone allows for SHP-2 association to PD-1 cytoplasmic tail, and TCR-PD-1 co-ligation enhances the recruitment, however, PD-1 engagement is required for blocking TCR-CD28-mediated signals (183). This supports the need for the formation of PD-1-TCR microclusters, allowing PD-1 in proximity to TCR and/or CD28 (170). The amount of SHP-2 recruited to PD-1 is dependent on the strength of TCR stimulation (170).

Although, the ITSM motif is critical for PD-1 inhibitory effect, some studies have suggested that ITIM is still involved. For example, in one study, PD-1-mediated inhibition of IL-2 production was diminished by 50% if the ITSM was mutated, whereas the production was almost abrogated in T cells with a double mutation of both the ITSM and ITIM motif (184). Similarly, Chemenitz et al. reported that mutation in the ITSM motif severely reduced SHP-2 association, whereas the association was completely absent in double mutation of both ITSM and ITIM (183). A third study similarly reported that mutation of ITSM resulted in partial loss of SHP-2 association as well as suppressive activity of IL-2 production, while in the double mutant, there was a complete loss of physical association of SHP-2 to the cytoplasmic tail of PD-1, and PD-1 suppressive effect on IL-2 production was completely abrogated. Furthermore, both tyrosine-based motifs were liable for the instability of IS (170). Peled et al. reported that ITSM was crucial for SHP-2 recruitment, as opposed to ITIM, however, both motifs were indispensable for phosphatase activity, and consequently, PD-1 had an inhibitory effect on the cytokine production (185). Crystal structure and mutation analysis of SHP-2 support the notion that when SH-2 domains bind a bi-phosphorylated ligand, SHP-2 is in a phosphatase active conformation (181), thus, it has been suggested that SHP-2 only acquires phosphatase activity when engaged by both its

SH2 domains (186). This was supported by one study showing that SHP-2 was binding to both ITIM and ITSM of PD-1 cytoplasmic tail (181), however, another study demonstrated that SHP-2 acquires its phosphatase activity by forming a binding bridge between two PD-1 proteins forming a PD-1 dimer via the p-ITSM motif (182). Notwithstanding, upon TCR-PD-1 co-ligation, SHP-2 is transiently recruited to the cytoplasmic domain of PD-1, it engages both its SH2 domains to obtain phosphatase activity (170). In addition, TCR-PD-1 co-ligation results in rapid phosphorylation of SHP-2 (172), and this may enhance its catalytic activity or may allow for binding of adaptor proteins (187). Once activated, SHP-2 initiates dephosphorylation of TCR proximal signalling components, and reduced phosphorylation was observed of CD3 $\zeta$ , ZAP70, Vav1, PLC $\gamma$ 1, PKC $\theta$ , extracellular signal-regulated kinase (ERK), as well as PD-1 itself (170, 181). The exact substrates of SHP-2 are unclear, but it has been proposed to be CD3 $\zeta$ , ZAP70, and facilitate recruitment of Csk, which then inhibits the Src kinase Lck, which initiates the whole TCR signalling (181, 188, 189). No matter what the exact target of SHP-2 is, it is clear that in the presence of PD-1 associated SHP-2, there is a reduction of TCR proximal signalling, and consequently, it affects the activation of the major pathways which includes PI3K-AKT, RAS-mitogen-activated protein kinase (MAPK) (although only the RAS-MEK-ERK pathway, the p38-c-Jun N-terminal kinases (JNK) pathways are not affected), and PLC $\gamma$ -PKC $\theta$ , which consequently leads to the reduction of the transcription factors Nuclear factor kappa-light-chain-enhancer of activated B cells (NF $\kappa$ B), Activator protein-1 (AP-1) and Nuclear factor of activated T-cells (NFAT), which are required for IL-2 transcription (190). PD-1-mediated signalling also inhibits some of the lineage-specific transcription factors involved in T cell differentiation, such as T-bet (important for Th1 cells), GATA3 (required for Th2 cells) and Eomes (which together with T-bet is important for the formation of CD8 T cell effector and memory subsets) (81) and upregulating BATF (a transcription factor thought to be important for the transcriptional program of T cell exhaustion) (191).

Furthermore, by attenuating the activation of PI3K-AKT and RAS-MEK-ERK pathways and enhancing the activity of Smad3 (independently of TGF- $\beta$ ), PD-1 engagement indirectly blocks cell cycle progression by arresting the cells in the G1/S phase (190). This is mediated by several ways: PD-1 ligation has been shown to inhibit TCR-CD28-mediated upregulation of Casein Kinase 2 (CK2) as well as inhibit its activity (192), suppress hyperphosphorylation of Retinoblastoma (Rb) protein, and reduce transcription of cyclin A,

Cdc25A and Skp2 (190). In contrast, an accumulation of the CDK inhibitor p27, as well as enhanced Smad3 transcriptional activity and increased transcription of CDK inhibitor p15 were observed upon TCR-CD28 co-ligation in the presence of PD-1 engagement. Most of these effects are the result of PD-1-mediated attenuation of the PI3K-AKT and RAS-MAPK pathways due to dephosphorylation of TCR proximal signalling components (190). However, it is unclear how PD-1 regulates CK2 expression and enzymatic activity, nevertheless, CK2 is involved in cell proliferation and suppression of apoptosis by influencing the PI3K-AKT pathway (193). CK2 phosphorylates PTEN, which results in increased stability and abundance of PTEN, although at the cost of reduced phosphatase activity. Thus, when PD-1-mediated signalling inhibits CK2, it concomitantly decreases PTEN abundance but enhances its enzymatic activity and thereby inhibits the activation of PI3K (192). TCR/CD3 and CD28 cooperate to activate simultaneously both PI3K-AKT and the RAS-MEK-ERK pathway resulting in the down-modulation of the CDK inhibitor p27<sup>kip</sup> by targeting it for ubiquitin-dependent degradation by the E3 ubiquitin ligase SCF<sup>Skp2</sup> (194). p27 suppresses the activity of cyclin D/cdk4, cyclin E and/or cyclin A with cdk2 complex. In the absence of p27, the cyclin D/Cdk4/Cdk6 complex can hyperphosphorylate Rb, which relieves its suppression of the transcription factor E2F and initiates transcription of its target genes, such as cyclin A and Cdc25A (194). Cdc25A can activate Cdk2, 4 and 6, and cyclin complexes with either Cdk2 or 4 inhibit Smad3 transcriptional activity, which normally increases transcription of p15 and c-Myc while suppresses Cdc25A (190). Furthermore, cyclin complexes with cdk2 phosphorylate p27 and mediate its ubiquitin-dependent degradation by SCF<sup>Skp2</sup>. Skp2 is a component of SCF ubiquitin ligase, and its transcription is promoted by the transcription factors Sp1 and Elk1 and enhanced by E2F. Elk1 and E2F and downstream proteins of MAPK and PI3K-AKT pathways, which are activated upon T cell activation of TCR-CD28 signalling (195). Thus, PD-1 engagement blocks cell cycle transition from G1 to S phase by abrogation of RAS-MAPK and PI3K-AKT pathways, which results in reduced transcription of Skp2, and thus the accumulation of p27. As mentioned above, p27 inhibits cdk4 and cdk2 cyclin complexes, which results in enhanced transcriptional activity of Smad3, and thus an increase in p15 that inhibits cdk4 and cdk6 cyclin complexes (190).

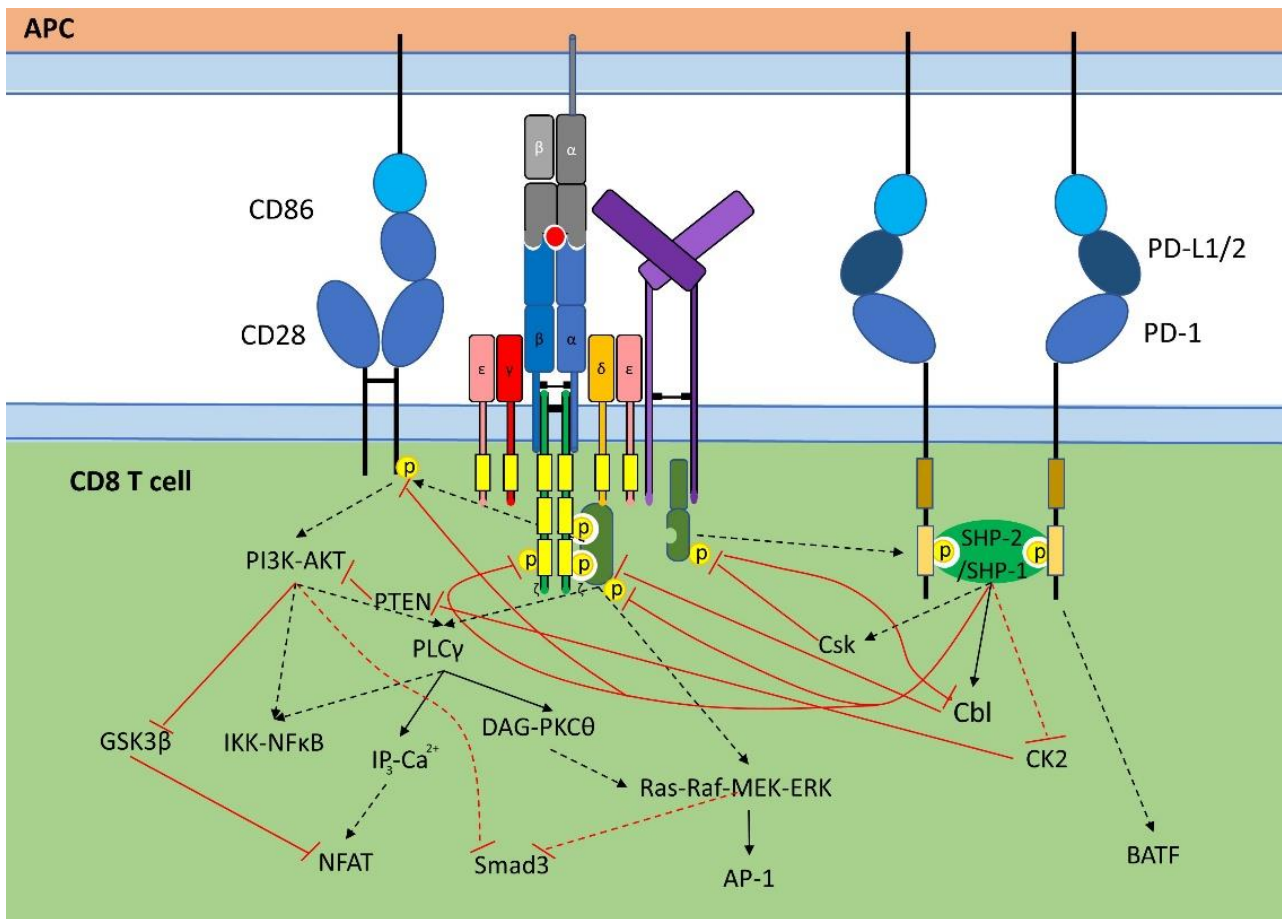
Another way for PD-1 signal transduction to regulate T cell activation at the level of antigen presentation is by ligand-induced TCR down-modulation, which then contracts TCR

signalling. This process is complex, but upon antigen presentation, MHC-peptide-bound TCRs are quickly internalized, and afterwards, other TCR-complexes (even those not engaged) are also downregulated. It was suggested that E3 ubiquitin ligases of the Cbl family are involved in this TCR downregulation as double Cbl KO T cells (deficient in both *c-cbl* and *cbl-b*) exhibit a reduced downregulation following antigen presentation, leading to sustained TCR signalling and hyperactivated T cells (196). However, the mechanisms that allow the Cbl family to down-modulate TCR levels are unclear. A study by Karwacz et al. (169). reported that PD-L1 silencing, as well as antibody blockade of either PD-L1 or PD-1, inhibited TCR down-modulation upon antigen presentation *in vitro* and *in vivo*, and this increase in TCR surface level resulted in persistent activation of TCR induced signalling proteins, such as ERK, which resulted in the expansion of hyperactivated CD8 T cells with increased production of IFN $\gamma$  and IL-17. This was mediated by impaired upregulation of RING finger family of Cbl E3 ubiquitin ligases, such as *c-Cbl* and in particular *Cbl-b* (169). Previously, it has been demonstrated that CD28 co-stimulation potentiates TCR-induced *Cbl-b* degradation, whereas CTLA-4-B7 interaction is required for *Cbl-b* re-expression by most likely promoting its transcription (131). There are possibly two types of CD28-mediated regulation of *Cbl-b*. The first is that HECT type E3 ubiquitin ligase, Nedd4, is induced to polyubiquitinate *Cbl-b*, and consequently mediates proteasomal degradation upon CD28 co-stimulation (197). This process might be facilitated by phosphorylation of *Cbl-b* by PKC $\theta$  (198). The other is that CD28 co-stimulation interferes with SHP-1 in association with *Cbl-b*. TCR signalling both activates *Cbl-b* and SHP-1 by Lck phosphorylation. Lck phosphorylation of *Cbl-b* allows for its autoubiquitination, but concomitantly phosphorylated SHP-1 remove the phosphate group from *Cbl-b*, thus with CD28 co-stimulation, *Cbl-b* autoubiquitination and degradation is favoured (199). In the same study, it was also shown that SHP-2 can bind *Cbl-b*, however, SHP-2 contribution was not the focus of the study (199). As PD-1 also has been reported to associate with SHP-1 (183), and a study with T cell specific SHP-2-deficient mice has demonstrated that SHP-2 is dispensable for T cell exhaustion and PD-1 signalling *in vivo* (200), it could be speculated that in this setting, SHP-1 accounts for the inhibitory effect of PD-1 by preventing Cbl degradation. Since PD-1 signalling has been shown mostly to inhibit CD28-mediated signalling (201-203), and both SHP-1/2 have been reported to be associated with PD-1, it is likely that it can target any of these mechanisms. For instance,

PD-1 signalling has been shown to regulate the activities of both PKC $\theta$  and Lck via SHP-2 as well as dephosphorylate CD28(181, 188, 204).

As described above, Cbl-b promotes TCR/CD3 $\zeta$  down-modulation, however, it has been demonstrated that it can operate with the HECT type E3 ligase, Itch, to regulate ubiquitination and phosphorylation in a proteolysis-independent manner. This study demonstrated that double KO of Cbl-b and Itch had the same level of TCR-down-modulation, but enhance phosphorylation of CD3 $\zeta$  (205). CTLA-4 has been demonstrated to activate Itch via SHP-2, although the exact recruitment of SHP-2 is controversial (130). However, it is clearly demonstrated that SHP-2 is a downstream mediator of PD-1, and it could therefore be speculated that PD-1 cooperatively regulates the activity of Cbl-b and Itch, and thus via ubiquitination facilitates reduced phosphorylation of the TCR proximal element CD3 $\zeta$ .

In summary, the signalling mechanisms behind PD-1 inhibitory function on T cells are ambiguous, but from the experiments just described, it is clear that SHP-2 and (possible also SHP-1) is involved. Figure 13 illustrates some of the mechanisms in which PD-1-mediated signalling suppresses T cell activation by attenuating the TCR-CD28 signalling pathways.



**Figure 13: PD-1 signalling pathway** (adapted from (206)). Upon activation, T cells upregulates PD-1 as a negative feedback mechanism. PD-1 can be phosphorylated at both ITIM and ITSM, although the latter has been shown to be the major contributor to its immunosuppressive activity. SHP-2 is recruited to PD-1 that has both phosphorylated ITIM and ITSM or to two PD-1 with phosphorylated on ITSM creating a form of dimer. Activated SHP-2 dephosphorylates TCR proximal signalling components, such as CD3 $\zeta$ , ZAP70 and CD28. By ligation of PD-1, SHP-2 is sequestered, and therefore it cannot prevent Csk recruitment and inactivation of Lck. PD-1 signalling also inhibits CK2, possibly through SHP-2. These effects result in inhibition of the PI3K-AKT, PLC $\gamma$ -PKC $\theta$  and the MEK-ERK MAPK pathways, and consequently attenuation of the transcription factors, such as NFAT, AP-1 and NF $\kappa$ B, but enhanced Smad3 activity. SHP-1 has also been associated to PD-1, however, its role is unclear in the PD-1 setting, but in other settings has been reported in dephosphorylating Cbl and thus prevent its degradation. Active Cbl, is involved in the down-modulation of the TCR expression and/or its phosphorylation status. PD-1 signalling is also involved in the upregulation of BATF transcription factor, which promotes T cell exhaustion by impairing T cell proliferation and cytokine secretion.

### PD-1 involved in the Formation of Tregs

In addition to the ascribed inhibitory function of naïve T cells Teffs, PD-L1/PD-1 signalling axis promotes the development, maintenance and function of Tregs (72). Francisco et al. demonstrated that PD-L1 stimulation synergises with TGF- $\beta$  to enhance iTreg development by lowering the threshold of TGF- $\beta$  signalling as minimal amount of TGF- $\beta$  was required. Furthermore, PD-L1 stimulation alone was sufficient in the conversion of naïve CD4 T cells to iTreg. They found that PD-1-mediated inhibition of PI3K-AKT and the RAS-MEK-ERK pathway were involved in this conversion (72). In support of this, a later

study found that PD-1-mediated attenuation of these pathways resulted in inhibition of cdk2-mediated phosphorylation of Smad3, and thus enhanced its transcriptional activity and thereby promoting transcription of the Treg-specific transcription factor Foxp3 (190). In further support of this, PD-L1 signalling was able to promote Foxp3 expression by suppression of the PI3K-AKT pathway (207) and able to enhance Treg suppressive effect at low Treg/Teff ratio, but had a less pronounced (but still improved) effect with a greater number of Tregs (72). PD-1-PD-L1 signalling axis can promote the development of iTregs from naïve CD4 T cells, but in a model of graves vs host disease, it has also been shown that PD-1 signalling can induce Th1 plasticity and conversion into Tregs(208). This is thought to be mediated by a default pathway, where PD-1-mediated signalling activates SHP-2 (or possible SHP-1) to dephosphorylate STAT1, and thus inhibits its activation. STAT1 is activated by TNF $\alpha$  or IFN $\gamma$  signalling and is the main contributor to Th1 stability by promoting T-bet (the lineage-specific transcription factor of Th1), and it has been shown to suppress Foxp3. By PD-1-mediated dephosphorylation of STAT1, Th1 cells were no longer able to maintain T-bet, and demethylation of the Foxp3 locus was observed (208).

#### *PD-1 and Metabolic Reprogramming*

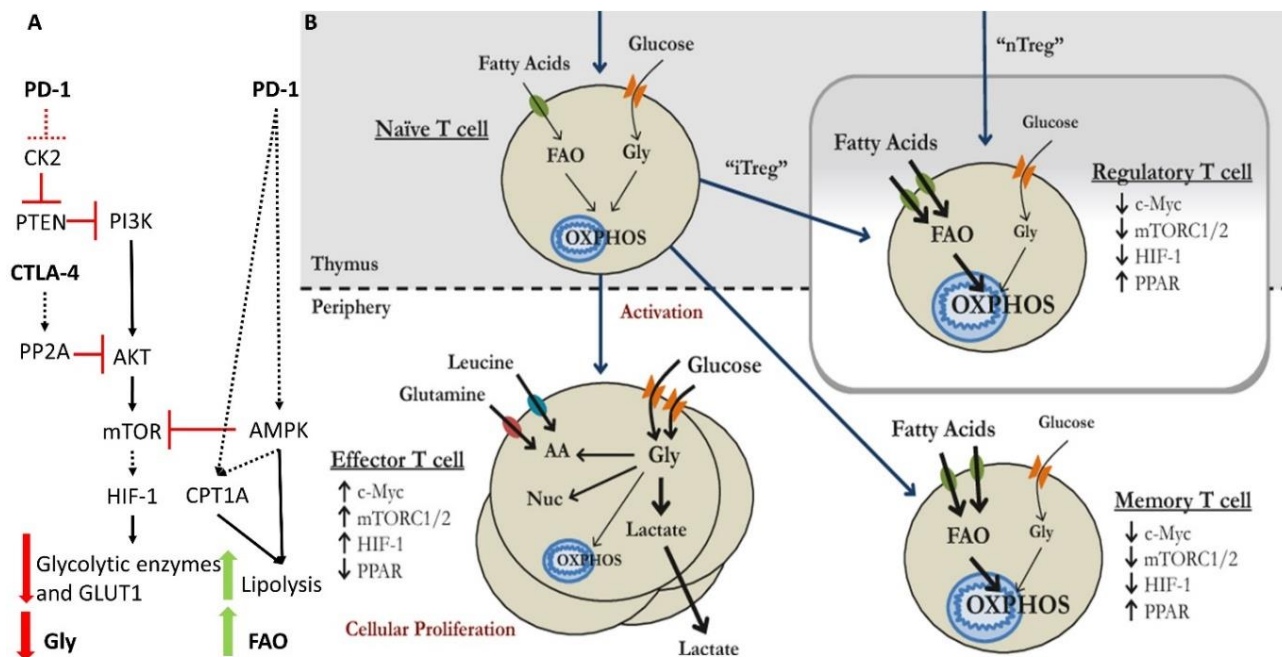
In addition to the ascribed inhibitory function of naïve and effector T cells and induction of iTregs, PD-1-PD-L1 signalling axis has been shown to perform metabolic reprogramming to inhibit Teff function, promote iTregs and support the longevity of Tregs (209-211).

During activation, T cells undergo metabolic reprogramming, which imprints distinct differentiation and functional fates. Naïve T cells utilize oxidative phosphorylation (OXPHOS) for energy generation, although, T cell activation switches the metabolic program to aerobic glycolysis, which is required to support their growth, effector differentiation and function (212). On the other hand, a switch to fatty acid  $\beta$ -oxidation (FAO) enables the conversion of Teff to long-lived quiescent Tmem (210, 213). This is mediated by the high activity of AMPK (AMP-activated protein kinase), which is a key energy sensor, and it regulates cellular metabolism to maintain energy homeostasis. AMPK increases the activity of carnitine palmitoyltransferase IA (CPT1A), and thus promotes FAO while indirectly inhibits mTORC1, which is required for Th1 and Th17 differentiation (212). Moreover, AMPK activates Ulk1, which is required for initiation of autophagy, and thus mitochondrial homeostasis and cell survival during starvation (214). Moreover, Treg differentiation has been shown to be dependent on FAO as it was

suppressed by blocking CPT1A. Furthermore, it has been shown that enforcing AMPK activation by metformin increases the frequency of Tregs in an allergic asthma model (210). The change in metabolic switch and how it affects T cell fate, PD-1 and CTLA-4 contribution to T cell metabolism are illustrated in Figure 14

TCR-CD28 co-ligation induces a metabolic switch to glycolysis by the activation of the PI3K-AKT-mammalian target of rapamycin (mTOR) pathway, which increases glucose transporter GLUT1 and glycolytic enzymes (212, 213). Both co-inhibitory receptors CTLA-4 and PD-1 can inhibit this pathway, thus inhibit Teff by suppressing glycolysis (211). Furthermore, PD-1 signalling can promote a metabolic switch from aerobic glycolysis to FAO by inducing AMPK, and thus upregulate the expression of CPT1A and promoting lipolysis while inhibiting glycolysis, glutaminolysis, and metabolism of branched-chain amino acids (209, 211, 214). Thus, PD-1 signalling induces the generation of Tregs by promoting FAO while suppressing the generation of Th1 and Th17 cells (171). In addition, when uncoupling adenosine triphosphate (ATP) from the electron transport chain, PD-1 stimulated T cells demonstrated substantial mitochondrial spare respiratory capacity (SRC), which was higher than for naïve T cells (211). "SRC is the extra mitochondrial capacity available in a cell to produce energy under conditions of increased work or stress and is thought to be important for long-term cell survival" (211). Interestingly, both increased levels of CTP1A expression and CTP1A-mediated increase of SRC are crucial for Tmem metabolism, survival and function, suggesting that PD-1 ligation enables T cells to survive as long-lived memory-like cells by utilizing a fat-based metabolism (211). This could have a great impact on the situation of chronic infections and cancer because here exhausted T cells are marked with a persistent high expression of PD-1, which then can facilitate their longevity (209, 211).





**Figure 14: CTLA-4 and PD-1 suppressive function includes alteration of cellular metabolism** (adapted from (213)). Changes in cellular metabolism influence the fate of the T cell. Naïve T cells use oxidative phosphorylation (OXPHOS) for ATP production. A metabolic switch to fatty-acid  $\beta$ -oxidation (FAO) promotes conversion to Treg or memory T cell. When naïve T cells are activated, there is a metabolic switch to glycolysis (Gly), which is mediated by activation of the PI3K-AKT-mTOR-HIF-1 pathway. Upon T cell activation, immunosuppressive receptors PD-1 and CTLA-4 are upregulated as a negative feedback mechanism to attenuate immune response; however, upon exhaustion of T cells, there are sustained expression of these immune checkpoints. Both CTLA-4 and PD-1 can inhibit Gly by suppressing the PI3K-AKT pathway, although through different targets. In addition, PD-1 can induce the conversion to iTreg by promoting a metabolic switch to FAO. This occurs by PD-1-induced AMPK increased expression of CPT1A. AMPK also inhibit mTORC1, which is required for Th1 and Th17 differentiation.

### 1.4.3 T-Cell Immunoglobulin and Mucin Domain 3 (Tim-3) and Galectin-9 Pathway

One of the new up and coming immune checkpoint inhibitors for the treatment of cancers is monoclonal antibodies against Tim-3. Pre-clinical trials already show great promise, especially in combination with blockade of the PD-1-PD-L1 signalling pathway. This section will focus on the Tim-3-Galectin-9 signalling pathway.

#### *Tim-3 Structure*

Tim-3 is a glycoprotein and is a member of the Tim-family consisting of Tim-1, Tim-3 and Tim-4 in humans and Tim-1-8 in mice and part of the Ig superfamily of receptors (215). Thus, its structural hallmark features are as follows: in the extracellular region, there is a membrane distal IgV-like domain subjected to O- and N-linked glycosylation and a membrane-proximal serine/threonine rich mucin-like domain of varying length that also contains sites for O- and N-linked glycosylation, which is followed by a single transmembrane domain and an intracellular C-terminal cytoplasmic tail. The cytoplasmic

tail contains no ITIM motifs, but has six conserved tyrosine residues, which are important for downstream signal transduction (216). Compared to mouse Tim-3, Human Tim-3 has fewer glycosylations with two N-linked glycosylations in each extracellular domain and one O-linked glycosylation site in the mucin domain (217). The molecular weight of Tim-3 is calculated to about 33 kDa, but depending on glycosylation level, it has also been detected as big as 70 kDa (218). Figure 15 illustrates Tim-3 structures and its binding partners.

Full-length flTim-3 is encoded by Hepatitis A virus cellular receptor 2 (HAVCR2) gene and consist of seven exons, where exon 1 encodes a signal peptide sequence, exon 2 the IgV domain, exon 3-5 the mucin domain, and exon 6-7 the cytoplasmic tail (219). In addition, in mice, but not in humans, a soluble splice variant sTim-3 has been reported and is missing exon 3-5 (219, 220). Furthermore, human flTim-3 has been shown to undergo shedding by matrix metalloproteinases (MMPs), such as a disintegrin and metalloproteinases (ADAM)10 and ADAM17 for monocytes and ADAM10 for CD8 T cells to release the ectodomain of Tim-3, sTim-3 (220-223).

### *Tim-3 Expression*

Tim-3 is a type I transmembrane receptor and was originally identified in a search for Th1-specific surface markers. It was found that Tim-3 was present on Th1 as well as Tc1 cells, but not Th2, Tc2 cells, nor naïve T cells (224). Since then, its expression has also been found on Th17, Tregs, B cells, and NKs as well as myeloid cells, such as monocytes/macrophages, DCs, mast cells and basophils (low expression) (223, 225, 226). Furthermore, Tim-3 can also be expressed on tumour cells, which may lead to tumour progression by multiple mechanisms (223, 227, 228). Tim-3 appears to be constitutively expressed in myeloid cells (229) as well as NKs (and can be further upregulated) (230). In contrast, in T cells, it is upregulated upon activation (224).

### *Tim-3 Ligands and Functions*

The HAVCR2 gene in humans is found on chromosome 5q33.2, a chromosomal region that has been repeatedly linked with atopic diseases and autoimmunity (225, 231). In mice, Tim-3 expression was not detected in Th2 cells but found on Th1 and to a lesser extent in Th17 cells (224, 232), and those two cell types are known to be involved in autoimmune diseases. Tim-3 expression was found to be involved in induction of peripheral tolerance, especially regulating Th1 immunity (219, 233) and promoting Tregs and their suppressive function (233-236). In addition, blockade of Tim-3 was found to

exacerbate disease in NOD mice model of type 1 diabetes (233), and in experimental autoimmune encephalomyelitis (EAE, a mouse model for human Multiple Sclerosis (MS), it also resulted in accelerated disease progression with both increased exacerbation of symptoms and mortality (224). This was the result of both a rise in numbers and activated levels of macrophages (224), which most likely were attributed to overreacting Th1 cells, as blocking Tim-3 with Tim-3-Ig fusion proteins resulted in hyperproliferating Th1 cells and enhanced production of Th1 cytokines (219). Furthermore, it was shown that Tim-3-Ig fusion proteins could abrogate the induction of Th1 tolerance (219). Tim-3 expression was also found on human activated CD4 T cells preferably on Th1 and to a lesser extent Th17, and blocking Tim-3 during T cell activation augmented secretion of INF $\gamma$ , IL-2, IL-6 and IL-17 cytokines, suggesting that Tim-3 regulates cytokine secretion of Th1 and Th17 cells (237).

Tim-3 expression on T cells appears to be dysregulated in patients suffering from multiple sclerosis (MS) (238, 239), and MS therapies may function in part by restoring Tim-3 expression and its modulatory effects on T cells (239). Also in Th1, Tc1 and Th17 from psoriasis patients, Tim-3 expression has been shown to be dysregulated having lower expression than healthy controls (240). Moreover, in humans, polymorphism of Tim-3 has been associated with rheumatoid arthritis (RA) (241, 242). Indeed, Tim-3 expression is negatively correlated with disease activity (243, 244). Collectively, these studies suggest that Tim-3 is involved in establishing peripheral tolerance and protecting against autoimmune diseases.

Genetic polymorphisms of the Tim-3 loci have also been associated with cancer (220). As mentioned, persistent high expression of Tim-3 has been implicated in the exhaustion of both T cells and NKs in both chronic infections and cancer, and blocking Tim-3 enhances anti-tumour/anti-viral response (64, 74-76, 79, 90, 93, 94, 97, 99, 103, 245-247). Especially, in cancer setting, the Tim-3 immune checkpoint has emerged as an interesting novel target where blockade alone or in combination with PD-1 blockade restored the functionality of the exhausted cells (64, 74-76, 79, 90, 93, 94, 97, 99, 103, 245-247), as well as relieving the suppression by Tim-3 expressing Tregs (236, 248, 249).

Tim-3-mediated effects are initiated upon engagement of its possible ligands, which includes galectin-9, carcinoembryonic antigen-related cell adhesion molecule 1

(Ceacam1), high-mobility group box 1 (HMGB1), and phosphatidylserine (PtdSer) (225). They all share an overlapping binding site except galectin-9 at the FG-CC loop in the Tim-3 IgV domain. Instead, galectin-9 binds to N-glycosylation sites at IgV domain (220). Here is a short outline of the main function and interactions:

Engagement of Tim-3 by PtdSer facilitates engulfment of apoptotic cells by phagocytes, such as DCs and macrophages, and promotes cross-presentation of antigens to CD8 T cells by DCs. PtdSer exposed on apoptotic cells can bind to Tim-3 expressing T cells; however, they are not engulfed (250). In addition, on DCs, Tim-3 binds to HMGB1, which interferes with their nucleic acid activation of intracellular Toll-like receptors (TLRs) (227). To date, no report has found that HMGB1 binds to Tim-3 on Tregs (216), however, in mice having hepatic viral infections, a Tim-3 expressing population of CD8 Tregs were found to suppress CD8 T cell expansion by TIM-3-mediated sequestration of HMGB1, which has a crucial role in stimulating the expansion of CD8 T cells after TCR activation (251). Recently, also Ceacam-1 has been reported to be a heterophilic ligand and regulates Tim-3-mediated T cell tolerance and exhaustion. In the same study, a crystal structure of their interaction was reported (252), but has later been retracted (253). Moreover, another group questioned if Ceacam1 is in fact a ligand for Tim-3 as their binding experiment could not prove any interactions (254). Galectin-9-Tim-3 interaction has been reported on T cells, NKs, macrophages and DCs where the pathway in a context-dependent manner promotes or suppresses their function (227, 230, 235, 237, 255-261). However, a single paper has also questioned if galectin-9 is a binding partner of Tim-3 (262).

There are some conflicting pieces of evidence as to if Tim-3 mediates positive or negative signalling in lymphoid and myeloid cells, and this appears to be context-dependent and most likely also influenced by its interaction with its different ligands (216). In the context of chronic conditions, such as viral infections and cancer, Tim-3 is mostly known for its inhibitory regulation of T cell response and are considered to be a co-inhibitory receptor (an immune checkpoint) (216). Although there is evidence that Tim-3 has a co-stimulatory function on T cells under conditions involving acute stimulations (216, 223, 263). Furthermore, there is evidence to suggest that Tim-3 signals differently in T cells compared to myeloid cells, such as DCs cell, as the tyrosine phosphorylation patterns on the cytoplasmic tail are different (229). This may also explain the reported difference of Tim-3-mediated effect upon ligation in the different cell types, wherein T cells, Tim-3 is

considered to be inhibitory especially suppressing Th1 immunity, whereas, in DCs, the Tim-3-Galectin-9 pathway can synergise with lipopolysaccharide (LPS) promoting TNF $\alpha$  secretion through activating NF $\kappa$ B (229). Although, another study found that in tumour settings, engagement of Tim-3 on tumour-associated DCs suppressed their nucleic acid-mediated activation of anti-tumour immunity. Tim-3 and nucleic acid compete with each other for binding to the A-box domain of HMGB1, and thus, Tim-3 interferes with HMGB1-dependent transfer of nucleic acid to the endosome where it would engage with intracellular TLR to elicit immune response (227). This has great implication when using chemotherapy as cancer treatment, which can induce a form of immunogenic cell death releasing DAMP, such as HMGB1, as well as nucleic acid from dying tumour cells. The data from this study “indicated that DC-specific Tim-3 served as a negative regulator of chemotherapy-induced anti-tumour responses by circumventing the nucleic acid-mediated innate immune pathways (227).

As mentioned above, upon activation of naive T cells, there is a metabolic change from oxidative phosphorylation to aerobic glycolysis. Both co-inhibitory proteins CTLA-4 and PD-1 have been shown to inhibit glucose metabolism, and PD-1 can furthermore promote metabolic reprogramming to FOA. A recent study has shown that also Tim-3 is linked with changes in glucose metabolism and lactate release. The CD4 T cell Jurkat cell line was stably transfected with Tim-3 and different truncated forms of Tim-3. This demonstrated that the cytoplasmic tail of Tim-3 is crucial for the regulation of glucose consumption by modulating Glut1 expression and thus glucose uptake (264). Since activation-induced glycolysis is essential for cytokine production, high persistent Tim-3 in chronic conditions may modulate glucose metabolism, and hence a decrease in cytokine production, such as IL-2 and INF $\gamma$ , is observed (264).

These data suggest that Tim-3-mediated effects are context-dependent even in the same cell type, and this may be attributed to many different ligands of Tim-3. The focus in the section below is to understand how Tim-3 and Galectin-9 regulate T and NK responses. However, first a description of its ligand Galectin-9.

### *Galectin-9 Structure*

Galectins (Gal) are a family of lectins which are characterized by the presence of one or two carbohydrate-recognition domains (CRDs) that bind to beta-galactoside-binding proteins (265). Galectins are evolutionary conserved from earlier vertebrate species, and

to date, 15 mammalian galectins have been identified, where 11 of them have been found in humans (gal-5, gal-6, gal-11, and gal-15 are not found in humans) (266, 267). Galectins are small soluble proteins, which are widely expressed in various cells, and their functions are mediated both intracellularly and extracellularly, although they lack a signal transport sequence and thereby non-classical secreted (267). By binding to both glycolipids and non-carbohydrate-containing proteins (266), galectins have been found to have a diverse set of functions, which includes the regulation of cell growth, apoptosis, pre-messenger RNA (mRNA) splicing, cell-cell and cell-matrix adhesion, cellular polarity, motility, differentiation, transformation, signal transduction and innate/adaptive immunity (267). The family of galectins can further be divided in three subgroups based on their structure and CRD: 1) prototype galectins, gal-1, gal-2, gal-5, gal-7, gal-10, gal-11, gal-13, gal-14 and gal-15, contain one CRD. 2) The chimeric-type gal-3 contains a CRD domain and an N-terminal extension. 3) tandem repeat-type galectins, gal-4, gal-6, gal-8, gal-9 and gal-12 contain two CRDs and are connected by a flexible linker (267). Many galectins are either bivalent or multivalent with regard to their carbohydrate-binding activities and thus can dimerise and/or oligomerise to increase their binding avidity (267).

Galectin-9 is a tandem-repeat type galectin and has two non-homologous N- and C-terminal CRDs, which have conserved amino acids involved in their binding capacity to  $\beta$ -galactoside, but overall, they have only 38% similarity with each other (268). The two CRDs are connected by a peptide-linker of variable length (short (S) 14 aa, medium (M) 26 aa, or long (L) 58 aa), and thus galectin-9 varies between 34-39 kDa (269). This linker domain influences the rotational freedom of both CRDs and mediates higher-order multimer formation and thereby increasing galectin-9 valence, which may result in different specificities and/or affinities for glycoconjugates (270). Figure 15 illustrates galectin-9 structure and its binding partners.

Galectin-9 is encoded by LGALS9 in humans and located on chromosome 17q11.2. Full-length flgalectin-9 = galectin-9L consists of 11 exons, the other splice variant reported is galectin-9 $\Delta$ 5 = galectin-9M, which lacks exon 5, and galectin-9 $\Delta$ 5/6 = galectin-9S lacks exon 5 and 6, however, also a short truncated form of galectin-9 lacking exon 10 has been reported, which is only found intracellularly (270). Galectin-9 can be found both intracellularly and extracellularly of the cell and appears to have distinct functions depending on its localization. Most studies have focused on the extracellular properties of

galectin-9, thus its intracellular functionality still needs further research (270). Intracellularly, galectin-9 can be found in the nucleus, the cytoplasm, and the cellular membrane network (ER-Golgi), and extracellularly, it is found on the plasma membrane or being secreted (270-272). However, like all galectins, galectin-9 lacks a signal sequence for transport into the classical ER-Golgi cargo machinery, thus, galectin-9 is being non-classically secreted, e.g. via exosomes from the cytoplasm to extracellular milieu (268), or it has also been proposed that Tim-3 might act as its trafficker where their exocytosis to the plasma membrane depends on PKC $\alpha$  (64, 272). Furthermore, galectin-9 can be shredded off together with Tim-3 or alone by MMP such as ADAM10/17 (64, 272).

The linker peptide of galectin-9 provides it with bi/multivalent binding properties, which have great physiological functions as it heightens its potency compared to proto-type galectins with just one CRD (268). Although, galectin-9L has in its linker domain a protease-cleavage-site for MMP3/stromelysin, elastases and thrombin (268). Cleavage of the linker region may generate free N- and C-CRDs, which can homo-oligomerize and bind to different glycoconjugates to exert their own distinct biological outcomes; for instance, the N-CRD of galectin-9 is efficient in activating DCs, whereas C-CRD oligomerization can contribute to T-cell death (268).

#### *Galectin-9 Expression and Regulation*

In basal physiological conditions, low levels of galectin-9 is ubiquitously expressed in most tissues (with the greatest abundance in the thymus and kidney) (273-275). It can be expressed by a wide variety of cell types, including immune and cancer cells (268). Although, there are some tissue/cell specificities because the microenvironment greatly influences the expression of galectin-9. Galectin-9 expression can cell-specifically be induced by different stimuli, such as IFN $\gamma$  in fibroblast, endothelial cells and astrocytes (276-278), IL-1 $\beta$  and TNF $\alpha$  in astrocytes and synovial fibroblast (278, 279), TGF- $\beta$  in iTregs (273-275), Phorbol 12-myristate 13-acetate (PMA), e.g. in Jurkat T cells (272), and others stimuli such as some agonists of TLRs in synovial fibroblast (279).

#### *Galectin-9 Receptors and Functions*

The human galectin-9 has been shown to have a higher affinity for branched N-glycan-type oligosaccharides than linear structured oligolactosamines (1–3-linked poly-N-acetyl-lactosamines). Its cellular functions depend on its intra- or extracellular localization, its availability (concentration) and its binding partners (268).

A role for galectin-9 function has been reported in cell adhesion, cell surface recognitions, migration, chemoattraction and a modulator of important signalling between growth and apoptosis (268). Thus, depending on the context and the cell type, it has a suppressive or stimulatory effect.

The involvement of galectin-9 has been observed in many pathologies, e.g. infections, autoimmune disorders, graft rejections, allergic responses, and cancer (280). In certain acute infections, galectin-9 was shown to stimulate anti-microbial immunity (259), whereas in chronic infections, such as human immunodeficiency virus (HIV) and hepatitis B virus (HBV) infection as well as virus-associated tumours, galectin-9 is associated with immune cell exhaustion (281-284). In addition, in the autoimmune disease MS, high galectin-9 levels were found in the cerebrospinal fluid of MS patients compared to healthy controls, and it correlated with the number of lesions (285). Furthermore, when comparing active and inactive MS lesion, galectin-9 displays a distinctly different intracellular localization in microglia/macrophages, being restricted to the nuclei in the active lesions, and primarily localized in the cytoplasm in inactive lesions (286), which could suggest different functionality. Moreover, in EAE, a model of MS, galectin-9 was found to improve symptoms by inducing apoptosis of auto-reactive T cells. Supporting this role, it was also found that knockdown of galectin-9 exacerbated symptoms (255, 287). Soluble galectin-9 reduced symptoms in mice model of IL-23-induced psoriasis-like skin inflammation, which was also associated with reduced IL-17 and IL-22 production, suggesting suppression of Th17 cells (288). In RA, galectin-9 appears to be both suppressing and promoting pathogenesis. The levels of galectin-9 are increased in serum as well as the synovial fluids of RA patients (289, 290). In mouse collagen-induced arthritis (CIA, a model for human RA), galectin-9 was shown to induce apoptosis of Th17 cells and promote the generation of Tregs (291). Furthermore, exogenously administrated galectin-9 was shown to induce apoptosis of synovial fibroblasts (289), on the other hand, the presence of endogenous galectin-9 was shown to suppress apoptosis and enhance the viability of synovial fibroblasts (279). Moreover, in granulocytes, it was shown that galectin-9 upregulated expression of the enzyme peptidyl arginine deiminase 4, which is required for RA-associated citrullination of proteins, and consequently, an increase of citrullinated autoantigens was observed. This suggests that galectin-9 may participate in the initiation the pathogenesis of RA (290). In studying graft rejections, galectin-9 was shown to



promote tolerance, e.g. prolonging survival of skin graft by promoting Tregs (235, 292, 293) and protecting the foetus from the mothers immune cells, diminishing the chance of miscarries by suppressing Teff and NKs (294-296). Galectin-9 may also contribute to allergic responses. Originally galectin-9 was identified as a chemoattractant for eosinophils *in vitro*, but in some cases, exogenous galectin-9 was found to induce apoptosis of activated eosinophils (297). Furthermore, galectin-9 was reported to reduce airway hyperresponsiveness in allergic asthma model by preventing CD44-hyaluronic acid (HA) interaction, and thus leukocyte adhesion and migration to the lungs (298). In mast cells, it was found to prevent degranulation while enhancing cytokine secretion (299, 300). In cancer, galectin-9 has been reported both to suppress and promote tumour progression (268). For instance, in hepatocellular carcinoma, melanoma, and breast cancer, it has been shown to have anti-metastatic potential promoting tumour aggregations stabilizing cell-cell adhesion junctions while blocking CD44-hyaluronic acid interaction to adhesion molecules on endothelium and extracellular matrix (ECM) (301-303). In contrast, it is involved in immune escape of acute myeloid leukaemia (AML) and breast cancer where it suppresses anti-tumour immunity by impairing and/or inducing apoptosis of T cell, and impairs NK function (64, 304, 305). It has also been reported to promote highly suppressive iTregs as well as MSDCs in TME, both of which also suppress the function of Teffs and NKs (273, 275, 291, 306, 307). All of these effects are mediated by the engagement of galectin-9 to different binding partners intracellularly or extracellularly.

Like Tim-3, galectin-9 has been shown to have multiple binding partners. Extracellular binding partners include 4-1BB (CD137), CD40, CD44, IgE, disulphide isomerases, dectin-1, Forssman glycosphingolipid, glucose transporter 2, glucagon receptor and Tim-3 (268). In this context, I will mostly describe its function in T cells and highlight its interaction with Tim-3.

Galectin-9 influence both the effector and regulatory phases of the immune response. Briefly described, galectin-9 has been shown to promote DC maturation, which in turn induces Th1 and Tc1 polarization (260, 308), enhances cytokine secretion from activated T cells (271, 309, 310), and can induce apoptosis of Th1, Th17 and CD8 T cells (255, 291, 311, 312). It suppresses Th17 differentiation and promotes iTreg generation (235, 275, 291, 312). Thus, it has both stimulatory and inhibitory effects on T cells. In NKs, galectin-9 also has bi-modal effects where some have reported that it increases INF $\gamma$ , and others

say it suppresses NK cytotoxicity both in Tim-3-dependent and -independent manner (96, 230, 282, 313). As mentioned, the effect of galectin-9 is context-dependent, concentration-dependent, and receptor interaction-dependent. A low concentration galectin-9 was shown to increase cytokine production by activated T cells. In contrast, at high concentration, galectin-9 induces apoptosis of activated CD4 and CD8 T cells (309-311).

It has long been known that galectin-9 mediates cell death by mechanisms of both apoptosis and necrosis. Galectin-9-induced cell death has been reported in many different cell lines, such as T cells (MOLT-4 and Jurkat), B cells (BALL-1), monocytes (THP-1), myelocytes (HL-60), and different types of primary cells, such as activated eosinophils, activated human CD4, and CD8 T cells, some cancer cells etc. Trying to elucidate the mechanisms in which it carry out cell death, it has been studied in cell lines. In MOLT-4 (a T cell line), galectin-9 induced apoptosis in a  $Ca^{2+}$ -calpain-caspase-1-dependent manner (311), whereas in Jurkat (another T cell line), galectin-9 did induced calcium mobilization, but using calcium chelators and blocking calpain, it was found that the galectin-9-induced cell death pathway was not the same as in MOLT-4 T cells (314). In Jurkat T cells, it was found that N-link glycosylations and the dimeric structure of galectin-9 were important for its function (314). Furthermore, in Jurkat T cells, it was demonstrated that galectin-9-induced cell death involved both mitochondrial caspase-dependent pathway and caspase-independent pathway. In the caspase-dependent pathway, mitochondrial proteins, such as Smac/DIABLO and caspase-3, were involved. In the caspase-independent pathways, the galectin-9-induced cell death was caused by altered mitochondrial membrane potential and release of the caspase-independent death effector protein apoptosis-inducing factor (AIF), which induced chromatin condensation and DNA fragmentation (314). In support of this, another study examining galectin-9-*induce* cell death in Jurkat T cells found that this was induced in a caspase-dependent manner (caspase-3 and 7) It was also found that galectin-9 induced calcium mobilization, but it was not associated with cell death (271). Instead, calcium was mobilized in a TCR $\beta$ -CD3-Lck-dependent manner, which resulted in upregulation of Th-1 related cytokines, e.g. IL-2 and INF $\gamma$ . This suggests that galectin-9 could induce a moderate antigen-independent activation of T cells. These results were also confirmed on human CD4 T cells isolated from PBMCs (271). In these studies, no receptor for galectin-9 was identified, however, in 2005, Zhu et al. demonstrated that galectin-9 was a ligand for Tim-3, and in an *in vitro* mouse model could induce Th1

aggregation and cell death (by both apoptotic and necrotic mechanisms), which was likely mediated by an intracellular calcium flux upon Tim-3 engagement (255). They also found that galectin-9 binds to Tim-3 in a glycosylation-dependent manner, because when treating sTim-3-Ig fusion protein with PNGase F (de-glycosylating), the interaction was ablated, suggesting that galectin-9 recognizes N-linked glycosylations of the IgV domain of Tim-3 (as sTim-3 is missing the mucin domain) (225, 255). Cooperating the notion that galectin-9 is a ligand for Tim-3, another group using two different biochemical assays, surface plasmon resonance and galectin-9 affinity precipitation, found that human galectin-9 is a physiological ligand for human Tim-3 (315). In support of this, our group demonstrated using surface plasmon resonance analysis that galectin-9 binds to the extracellular domain of Tim-3 with  $K_d = 2.79 \times 10^{-8}$  M (226). Furthermore, Zhu et al. found evidence to suggest that galectin-9 might be able to use other receptors as well to induce Th1 cell death, as it was not completely abolished in Tim-3 deficient cells (255). Lhuillie et al. found that Jurkat galectin-9-induced cell death is Tim-3-independent as these cells even after PMA stimulation did not express Tim-3 (assessed by WB) (271). Also another study found that in activated T cells expressing CD40, high concentration of galectin-9 could induce necrotic cell death by binding to CD40 (316). Moreover, galectin-9 was *in vivo* shown to reduce disease severity and mortality in mice with EAE, and this was mediated by depleting INF $\gamma$  producing CD4 T cells, suggesting that the Tim-3-galectin-9 pathway regulates Th1 immunity by selectively delete antigen-specific Th1 cells (255).

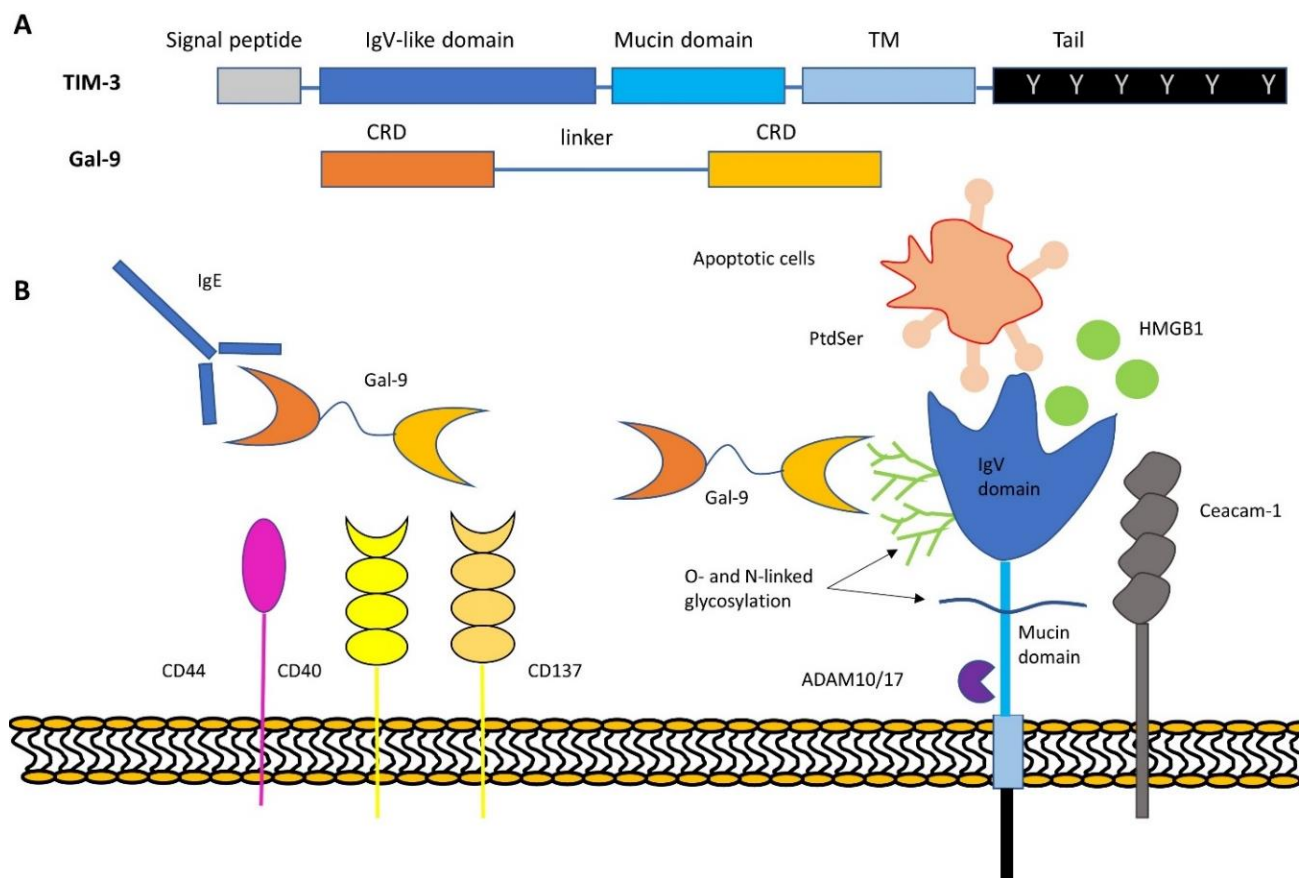
Since galectin-9 first was identified as a ligand for Tim-3, it has later been found to suppress Th1-related cytokines, such as IL-12 and INF $\gamma$  as well as IL-17, a Th17 cytokine in CIA (291). It was suggested that the attenuation of cytokine secretion was attributed to galectin-9-mediated cell death of the respective T cells. It was shown that galectin-9 mediated early apoptosis in Th17-skewed cells, and there was a decrease in Tim-3 expressing CD4 T cells, suggesting that cell death of both Th1 and Th17 cells was mediated through galectin-9-Tim-3 interactions (291). As in mice, Tim-3 (as well as galectin-9) expression was found on activated human CD4 T cells, and blockade of Tim-3 resulted in augmented secretion of both Th1- and Th17-related cytokines, such as INF $\gamma$ , IL-2, IL-6, and IL-17. The fact that galectin-9 expression also was found could suggest that this was mediated by galectin-9 engagement by Tim-3 (237). However, unlike in mice, no effect on CD4 T cell death was observed, suggesting if there is a galectin-9-Tim-3

interaction, the signal pathway do not promote cell death in human CD4 T cells (237), or the concentration of galectin-9 was too low to induce apoptosis. As mentioned, chronic conditions, e.g. viral infections like HIV, HBV, hepatitis C virus (HCV) and cancer have dysfunctional T cells, which are marked with high expression of Tim-3 (231). Furthermore, human sera from these patients have elevated levels of galectin-9 (317). In HBV both CD4 and CD8, T cells were susceptible to galectin-9-triggered cell death *in vitro* (281). Also in tumours, such as colon cancer, the Tim-3-galectin-9 pathway has been shown to induce apoptosis of Tim-3 expressing CD8 TILs (257).

Galectin-9 was shown to inhibit Th17 differentiation and to synergize with TGF- $\beta$ 1 to upregulate Foxp3 and promotes the induction of iTreg in CIA (291). Moreover, Wu et al. showed that galectin-9 synergies with TGF- $\beta$ -Smad3 in a feedforward loop promoting iTreg differentiation and maintenance (273, 274). This happens in a Tim-3-independent manner, instead, galectin-9 bound to CD44 (a hyaluronan-binding protein), which can form complex with T $\beta$ RI. This interaction-mediated phosphorylation of Smad3 and LGALS9-deficient T cells was found to be defective in phosphorylation of Smad3, and consequently, Smad3 showed reduced interaction with the CNS1 enhancer region of Foxp3 (273, 274). Furthermore, galectin-9 was found to be important for iTreg suppressive activity, as galectin-9-deficient iTreg was less efficient in suppressing the proliferative response of T<sub>eff</sub> and had reduced production of the immunosuppressive cytokine IL-10. Moreover, galectin-9 promoted the stability of iTreg by increasing the accessibility (increased acetylation) of the enhancer element to Foxp3 locus, as in its absent, iTreg preferentially converted to Th1 cells (273, 274). Although, another group studying allogenic skin graft rejections has found that Tim-3 is expressed on Tregs, and engagement of galectin-9 augmented their suppressive activity and prolonged survival of skin graft (235). In addition, they found that 100  $\mu$ g/mL galectin-9-induced cell death of both activated Tim-3 expressing CD4 and CD8 INF $\gamma$  producing T cells, but even low galectin-9 concentration 1-10  $\mu$ g/mL can suppress INF $\gamma$  production. Blockade of Tim-3 abrogated all galectin-9-mediated effects (292, 293).

Furthermore, galectin-9 is found at a high level in the sera of healthy pregnant women compared to non-pregnant women, and galectin-9 is expressed by the placenta itself as well as the peripheral and decidual immune cells (294). In addition, the galectin-9-Tim-3 pathway has a role during pregnancy in the feto-maternal interface protecting the implant

from the mother's immune response, especially by decidual NKs and CD8 T cells (223, 294-296, 318).



**Figure 15: Tim-3 and galectin-9 structure and some of their respective binding partners** (adapted from (215, 216)). (A) Structure of Tim-3 and galectin-9. Tim-3 consists of a signal peptide and an IgV-like binding domain, a mucin domain, TM and a cytoplasmic tail with six conserved tyrosine residues (Y), which are important for downstream signalling. Human Tim-3 has two N-linked glycosylation in the IgV domain and one O-glycosylation in the mucin domain. Galectin-9 consists of two non-homologues carbohydrate recognition domains (CRD) and a variable linker region. It does not have a signal sequence and thus requires a trafficker to be externalized and secreted. (B) Tim-3 and galectin-9 binding partners. Both Tim-3 and galectin-9 can interact with multiple binding partners. As galectin-9 binds to sugar groups, it has been reported to interact with many different proteins, of which only some is portrayed here, such as IgE, CD40, CD44, CD137 and Tim-3. However, not all effects of galectin-9 can be blocked by lactose (which diminished the carbohydrate binding interaction), suggesting that it in some circumstances may bind to other non-glycosylate proteins. Tim-3 has been reported to interact with PtdSer presented on apoptotic cells, HMGB1, Ceacam-1 and galectin-9. Furthermore, MMPs, such as ADAM10 and ADAM 17, have been shown to cleave Tim-3 either alone or in complex with galectin-9, secreting soluble (s)Tim-3 and galectin-9.

### Galectin-9-Tim-3 Pathway in Cancer

Physiologically, the TIM-3-galectin-9 pathway has evolved as a negative feedback mechanism to contract the immune response to avoid collateral tissue damage or safeguard against autoimmunity and “transplant rejection” where such a natural phenomenon is during pregnancy. However, multiple types of cancers have been shown to exploit this pathway as a way to escape anti-tumour immune response by multiple

mechanisms, e.g. 1) promoting tumour progression, 2) impaired function of exhausted T cells and NKs, and 3) promoting highly suppressive Tregs in TME.

1) Tim-3 on tumour cells can in itself promote tumour progression. For instance, normal hematopoietic stem cells (HSCs) do not express Tim-3; however, Tim-3 was identified as a possible TAA on AML cells, which originate from leukemic stem cells, although with the exception of acute promyelocytic leukaemia (319). Our group found that both primary AML cells and healthy PBMCs express Tim-3, although the expression is higher in AML cells. In addition, most of the Tim-3 in PBMCs was expressed intracellularly, whereas in AML cells most was present on the surface (320). Furthermore, high serum levels of galectin-9 were observed in patients and mice suffering from AML compared to healthy controls (321). Moreover, SCF is known to be involved in the progression of AML, and our group has recently shown that engagement of Tim-3 triggers growth factor type response similar to that of SCF in both THP-1 cells (a model for AML) and primary AML cells. Galectin-9 (or agonistic Tim-3 antibody)-induced phosphorylation of Bruton's tyrosine kinase (Btk) and activation of the PLC-1-PI3K pathway lead to calcium mobilization and activation of the AKT-mTOR pathway, resulting in phosphorylation of p70S6K and eIF4E binding protein (eIF4E-BP)1 as well as increased upregulation of hypoxia inducible factor 1 (HIF-1, a transcription factor involved in upregulation of glycolysis and production of VEGF, which can promote angiogenesis). Indeed, Tim-3 engagement was also associated with increased expression and release of VEGF as well as TNF $\alpha$  (which is due to NF $\kappa$ B activation) (226, 320). Not only the galectin-9-Tim-3 interaction triggers a growth factor-like response, but it was also found that the interaction contributes to an autocrine loop, which promotes self-renewal of AML leukaemic stem cells and their development through the co-activation of both NF $\kappa$ B and  $\beta$ -catenin signalling (321). Furthermore, our group has shown that Tim-3 is a cell-specific trafficker of galectin-9 in AML cells, and that Tim-3 alone or in complex with galectin-9 is shredded from the surface of AML and used to escape anti-tumour immunity (64, 322). IL-2 is a cytokine required for both activation of CTLs and NKs, and its secretion was attenuated by sTim-3 by T cells, and galectin-9 was shown to impair NK-mediated cytotoxicity (64). Moreover, it was found that latrophilin (LPHN)1, a biomarker for AML cells, is specifically upregulated in these cells by cortisol. When LPHN1 is engaged by fibronectin leucine-rich transmembrane protein 3 (FLRT3), it triggers calcium mobilization and activation of PKC $\alpha$ , which results in mTOR activation that

controls the translation of Tim-3 and galectin-9. In addition, to control their translation, this pathway also triggers their exocytosis to the surface of the cell (64, 323, 324). In support of the TIM-3-galectin-9 pathway is used as cancer escape mechanism, a study found that AML patients, who failed chemotherapy, expressed much higher levels of Tim-3 and galectin-9 (325). Also, solid tumours like colon cancer use the Tim-3-galectin-9 pathway for immune escape, as galectin-9 induces apoptosis of Tim-3 expressing CD8 TIL. In further support that Tim-3-galectin-9 might be a general pathway operated by many types of malignancies for immune escape, our group, with myself as co-author, has recently demonstrated that breast cancer cells (cell lines and primary tumours) and many other types of malignant cell lines, such as brain, liver, kidney etc., express Tim-3 and galectin-9 as well as at least one of the three LPHN forms (1, 2, or 3) and FLRT3 (ligand for LPHN) (326). Furthermore, when studying the biochemical mechanism in detail in MCF-7 breast cancer, it was found that FLRT3 engagement of LPHN induces translocation of the TIM-3-galectin-9 complex on to the surface of breast cancer cells in a PLC-PKC $\alpha$ -dependent manner. These cells did not shed galectin-9; however, membrane-bound galectin-9 was still able to protect breast cancer cells from cytotoxic immune attack (326). Moreover, there was evidence that other mechanisms might be involved in diminishing immune attack as co-culture with cytotoxic T<sub>H</sub>1-104 cells significantly upregulated galectin-9 on the surface of MCF-7 cells (326).

2) Tumour-specific antigen stimulation promotes the persistent high expression of Tim-3 on both CD4 and CD8 TIL with impaired effector function, such as INF $\gamma$  production (327). It is found that Tim-3 and PD-1 co-expression mark highly exhausted TILs in both mice and humans in many types of tumours, such as colon, gastric, lung, breast, kidney, cervical and oesophageal cancer and melanoma (14, 93, 94, 103, 246, 257, 328-331). In support of this, recent studies reported that acquired resistance to PD-1 blockade is associated with upregulation of Tim-3 as an alternative immune checkpoint (14, 15). In head and neck cancer, it was found that this upregulation was mediated by the PI3K-AKT pathway (15). AKT suppresses the TSC1/TSC2 complex and promotes mTOR signalling. In line with this, our group's own observation demonstrated that FLRT3 engagement of LPHN1 on AML cells promotes calcium mobilization, and PKC $\alpha$  activation is required for translation of galectin-9 and Tim-3 and induces their exocytosis to the plasma membrane. PKC $\alpha$  also

suppresses the TSC1/TSC2 complex promoting activation of mTOR translational pathway and phosphorylates Munc18 (an exocytosis regulator protein) (64).

3) High Tim-3 expression of CD4 TILs in cancer may not mark dysfunctional cells, but rather Tregs. It was found in several human tumours that high numbers of Tim-3 expressing CD4 TILs actually are CD4+Tim-3+Foxp3+Tregs (248, 327, 332), which are found in close contact with galectin-9 expressing cells in the tumour nest (332). Furthermore, these TIL Tim-3+Foxp3 Tregs were able to suppress CD8 T cell proliferation and cytokine production *in vitro* (332). Their immunosuppressive capacity was about 2-fold greater than in Tim-3-Foxp3 Tregs, and they produced more IL-10 and expressed more perforin, granzyme A and G (248). Moreover, Tregs derived from TME have been shown to induce cell death of NK and CD8 T cells in perforin-granzyme B-dependent manner (333, 334). In addition, it was demonstrated that Tim-3+ Tregs preceded the appearance of exhausted CD8 TIM-3+PD-1+ TILs, and they actually supported the development of exhausted CD8 T cells, as depletion of these Tregs showed functional Tim-3 expressing CD8 T cells (Tim-3 was expressed as a consequence of their activation and differentiation towards INF $\gamma$ -producing effector cell) (248). Moreover, dual blockade of Tim-3 and PD-1 downregulated Treg effector proteins. Thus, co-blockade of Tim-3 and PD-1 not only reverse the CD8 exhausted phenotype, but also mediates inhibition of the suppressive Treg functions (248).

### *Galectin-9 -Tim-3 Signalling*

As mentioned, Tim-3-mediated effects on T cells are context-dependent and in an acute situations often stimulatory, whereas in a chronic conditions, such as cancer, it is thought to be inhibitory on CD4 and CD8 effector cells, but augments the suppressive capacity of Tregs. However, it might not even be as simple as stimulatory or inhibitory effects. Recently, it was proposed by Ferris et al. that Tim-3 might contribute to T cell exhaustion by enhancing TCR signalling (263). Tim-3 is already being explored as a therapeutic target, however, although enhancement is seen on the anti-tumour response, the mechanisms that bring this about is still not fully understood. To clarify this, an in-depth understanding of the biochemical-signalling pathway is required, and if it differs between which ligands, it is engaged by and in which cells it is found on. Here, I will highlight some of the biochemical signalling mechanisms found upon activation of the galectin-9-Tim-3 pathway (Figure 16) with focus on T cells.



As mentioned above, Tim-3 is transiently upregulated upon T cell activation, and it has been reported to be incorporated into SMAC at the IS (335, 336) upon activation in a ligand-independent manner, however, its TM domain is crucial for TIM-3s localization to IS (336). As already described in the structure section of TIM-3, it does not have any signalling motif, such as ITAM (co-stim), ITIM or ITSM (co-inhib). However, in its cytoplasmic tail, it has six conserved tyrosine residues (337). Two Y residues appear particularly important, which are Y256 and Y263 in mice (337), and the corresponding residues in humans are Y265 and Y272 where Y265/256 is predicted to be in the middle of a highly conserved SH2-domain (338). Upon Tim-3 crosslinking by galectin-9, it was found that these sites were phosphorylated (335). In support of this, Tim-3 engagement by galectin-9 was shown to induce Y265 phosphorylation by Itk, a Tec family kinase (338). Furthermore, Src family kinase proteins, such as Fyn and Lck, have been reported to phosphorylate these sites (337).

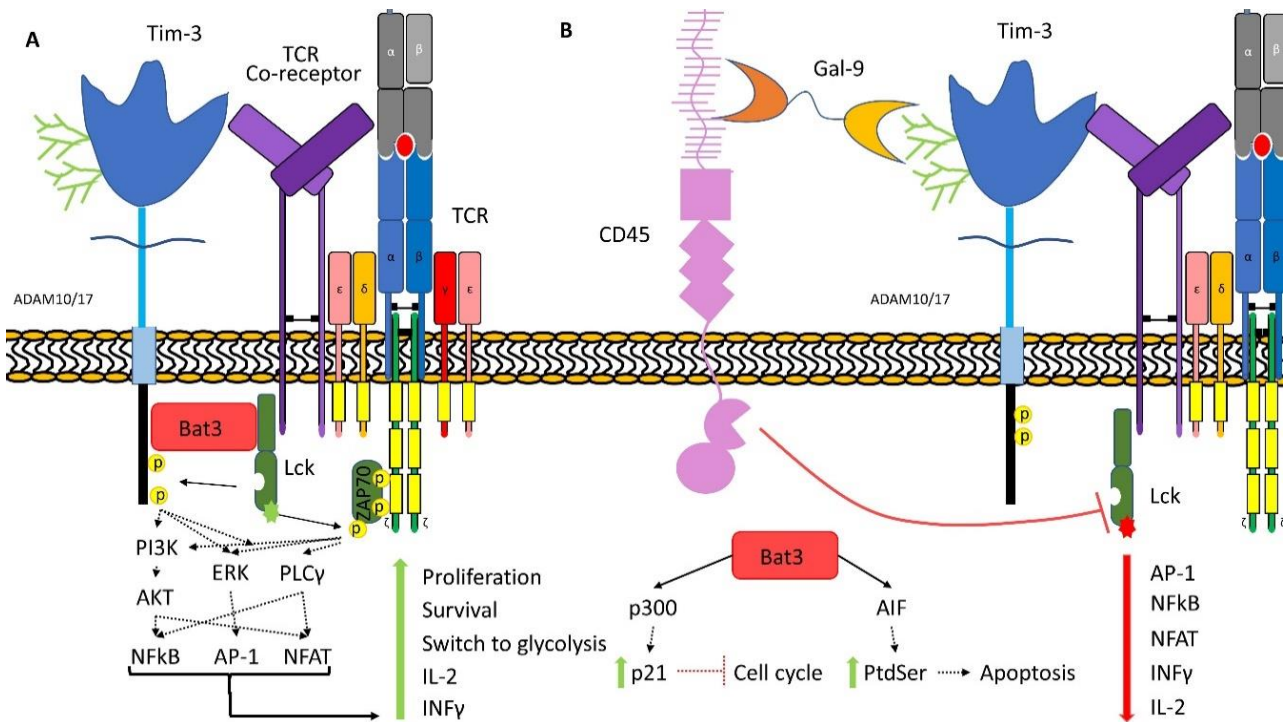
When Tim-3 is not engaged by ligand, it was demonstrated that these tyrosine residues allow binding of HLA-B associated transcript 3 (Bat3) in a phosphorylation-independent manner. However, upon ligation by galectin-9, there is induced phosphorylation of these residues, which releases Bat3 from the cytoplasmic tail of Tim-3 (335). Furthermore, they found that Bat3 expression was enriched in Th1 cells, but not in Th0, Th2 or Th17 cells (335). Bat3 is known to modulate apoptosis, survival and proliferation in a context-dependent manner (339-342). Interestingly, the researchers found that Bat3 in Th1 cells modulated their activity by Tim-3. For example, in an overexpressing system of Bat3, there was an increase of Th1-related cytokines IL-2 and INF $\gamma$ , which could accelerate the onset of EAE. Moreover, galectin-9-induced cell death was lower in Th1 cells overexpressing Bat3. Conversely, loss of Bat3 decreased INF $\gamma$  production and was associated with a decrease in the severity of EAE (335). Importantly, Bat3-deficient CD4 T cells displayed an exhausted phenotype with diminished proliferation and low production of IL-2 and INF $\gamma$ , and an increase of IL-10, which was also associated with an upregulation of markers linked to exhaustion, such as transcription factors Prdm1 and Pbx3 as well as surface immune checkpoints, such as Tim-3 and LAG-3 (335). Furthermore, highly exhausted TILs TIM-3<sup>+</sup>PD-1<sup>+</sup> had lower amounts of Bat3 mRNA compared to lesser exhausted TILs TIM-3<sup>+</sup>PD-1<sup>+</sup> in mice tumour models. Similar results were seen in exhausted CD4 T cells of HIV infected patients (335). Moreover, it was found that upon T cell activation, Tim-3 is

recruited to SMAC, which intracellularly allows for the Bat3 (a proline-rich protein) to interact with catalytically active Lck (pY394) via its SH3 domain to promote TCR signalling. Although, upon Tim-3 ligation, this interaction is abrogated, and Lck is released from Bat3, which results in the accumulation of inactive Lck (pY505). These data suggest that Bat3 protects Th1 cells from Tim-3 inhibitory regulation, such as galectin-9-induced cell death, and suppresses progression to exhaustion phenotype most likely by modulating the activity of Lck (335). In support of this, Lee et al. demonstrated that in Jurkat T cells transfected with TIM-3, the presence of Tim-3 upon T cell activation enhances TCR-mediated signalling, where Fyn and especially Lck were required for optimal Tim-3 function by phosphorylation of Tim-3 cytoplasmic tail at Y256 and Y263 (337). This promoted recruitment and activation of SH2-containing protein, such as PI3K p85 and PLC $\gamma$ 1 as well as ERK and p70S6K, and further downstream also enhancement of NF $\kappa$ B, AP-1 and NFAT, transcription factors required for IL-2 production, and thus conversely an increase of IL-2 was seen. Furthermore, primary murine Th1 cells showed an increase in INF $\gamma$  production in the presence of Tim-3 (336, 337). However, upon crosslinking with agonistic Tim-3 antibody, all the stimulatory effect was inhibited. This suggests that initially under acute stimulation of T cells, Tim-3 may augment TCR signalling, but upon Tim-3 ligation, there is rapid inhibition of T cell activation (336, 337). Interestingly, exogenously administration of galectin-9 to Jurkat T cells has shown that galectin-9 operates two distinct pathways, one involving apoptosis and one involving calcium mobilization and cytokine production where TCR proximal signalling proteins, such as LCK, are required for calcium mobilization (271). In mast cells, Tim-3 expression was found to enhance Fc $\epsilon$ RI signalling upon antigen activation leading to enhance Th2 cytokine production and degranulation (343). Fc $\epsilon$ RI like TCR/CD3 complex has an ITAM motif and these signal transduction pathways share many of the same signalling proteins. It was found that Tim-3 cytoplasmic tail with especially the two tyrosine phosphorylation sites at Y256 and Y263 was needed for the co-stimulatory effect, which most likely was attributed to Lyn or Fyn and resulted in downstream activation of PLC $\gamma$ 1 and p70S6K as well as activation of transcription factors, e.g. NF $\kappa$ B, NFAT and AP-1 (343).

In contrast to the positive Tim-3-mediated signalling just described, Lee et al. reported that in Jurkat stable cells transfected with Tim-3, activation of these cells with PMA/ionomycin decreased production of IL-2 due to decreased activation of NFAT and AP-1, and this was

dependent on the Tim-3 cytoplasmic tail (344). They confirmed their results in human CD4 T cells, which were stimulated with PMA/ionomycin for a week to express high amount of Tim-3. The researchers explain their contradicting finding by that these T cells already may have begun their transition to an exhausted phenotype (344). Although, in support of a Tim-3-mediated negative outcome of TCR signalling, Tomkowicz et al. show in Jurkat T cells stably expressing Tim-3 and in primary human CD8 T cells that the presence of Tim-3 upon T cell activation inhibited IL-2 production due to a diminished activation of NFAT and NF $\kappa$ B activation (345). They found that in basal state of Tim-3 expressing CD8 T cells, Tim-3 co-immunoprecipitated with Vav1, AKT, SLP76, ZAP70, Syk, P85 $\alpha$ -PI-3K, Fyn, and the adaptor proteins 3-BP2 and SH2D2A. However, T cell activation induced by anti-CD3/CD28 beads changed this pattern; in this case, there was no longer an association between Tim-3 and Vav1, AKT, SLP76, ZAP70, Syk, P85 $\alpha$ -PI-3K and Fyn. Although, there was an association between Tim-3 with Lck and PLC- $\gamma$ 1. This suggests that the mechanism used by Tim-3 to suppress NF $\kappa$ B and NFAT activity might be by the ability of the cytoplasmic tail of Tim-3 to sequester Lck and PLC $\gamma$ 1 (345). These studies suggest that the presence of Tim-3 (without the engagement of ligand) has a negative effect on T cell activation. In support of Tim-3 as a negative regulator of T cell function, Clayton et al. reported that Tim-3 was found in lipid-rafts, and upon T cell activation (triggered by galectin-9 expressing APCs) was recruited to c-SMAC in the IS to interfere with stable IS formation in primary human CD8 T cells expressing high amount of Tim-3. In resting condition, Tim-3 was found to associate with Lck in a phosphorylation-independent manner (315). Probably by interacting with Bat3 as Rangachari et al. have demonstrated (335). Upon Tim-3 ligation in the IS, catalytically active Lck was excluded from Tim-3 localization. They demonstrated that galectin-9 could bind to other proteins, e.g. receptor type phosphatases, such as CD45 and CD148, in a carbohydrate-specific manner in addition to Tim-3, and this allowed for co-localization of these phosphatases to Tim-3 in the IS upon T cell activation (315). Lck activity is known to be regulated by CD45 depending on its expression level. High levels of CD45 result in dephosphorylation of Y394, thus, decreasing Lck activity, whereas low-to-intermediate expression results in dephosphorylation of Y505, which increases the Lck activity (346). Thus, galectin-9 engagement of Tim-3 leads to co-recruitment of CD45 to SMAC, which then results in accumulation of inactive Lck that will dampen the TCR signalling (315).

In support of the Bat3 modulatory function of Tim-3 demonstrated by Rangachari et al. (335), Ji and colleagues found that long-non-coding-Tim-3 (Lnc-Tim-3) RNA was upregulated in exhausted tumour-infiltrating CD8 T cells of HCC patients, and that Lnc-Tim-3 could interfere with Tim-3-Bat3 interaction, releasing Bat3, which resulted in inhibition of TCR signalling by accumulating catalytic inactive Lck, and hence, reduction of NFAT and AP-1 needed for cytokine production, such as IL-2 and IFN $\gamma$  (347). Furthermore, with the release of Bat3, it was free to engage with p300 and promotes its nuclear translocation. Nuclear Bat3 enhances recruitment of p53 and RelA to p300, which promotes expression of p21 (a cell cycle checkpoint inhibitor) and anti-apoptosis proteins, mouse double minute 2 homolog (MDM2) and Bcl-2, thus this may induce replicative senescence and promote survival of these exhausted CD8 T cells (347). On the other hand, Bat3 in Jurkat has also been shown to have a role in apoptosis when interacting with AIF promoting PtdSer exposure (342).



**Figure 16: Tim-3-galectin-9 signalling pathway** (adapted from (348)). (A) T cell activation promotes T cell proliferation, survival and a metabolic switch to glycolysis, which is triggered by the activation of the PI3K-AKT, MAPK (ERK) and PLC $\gamma$  pathways. These pathways signal downstream to activate transcription factors, such as AP-1, NF $\kappa$ B and NFAT, which is required of cytokine production such IL-2 and IFN $\gamma$ . T cell activation also results in the upregulation of Tim-3, albeit without engagement of ligand, it functions to enhance TCR signalling. Active Lck (in a phosphorylation-independent manner) can interact with Bat3, which is associated to Tim-3 and this mediated phosphorylation of Tim-3 cytoplasmic tail that allows for recruitment and activation of proteins, such as ERK, PI3K and PLC $\gamma$ , and thus enhanced production of cytokines is observed. (B) When Tim-3 is engaged by galectin-9, this mediates phosphorylation of the region where Bat3 interacts with Tim-3 and releases Bat3. Bat3 can interact with p300 and translocate to the nucleus where it mediates transcription of CDK inhibitor p21 and thus inhibits cell cycle progression. Bat3 can also interact with AIFs and this promotes PtdSer exposure, which is involved in the uptake of apoptotic cells. Furthermore, galectin-9 has two binding regions, which allows the possibility of recruitment of other proteins to the vicinity of the TCR receptors, such as receptor phosphatase, CD45. CD45 can then inactivate Lck, (which is main initiator of TCR signalling), and thus the abrogation of TCR signalling pathway and TCR-mediated cytokine production is observed.

## 1.5 Background (in short) and Rationale for Studying Galectin-9

The functions of Tim-3 and galectin-9 have recently been studied in diseases relating especially to autoimmune diseases and cancer where the expression of one or both proteins appear dysregulated and promote pathogenesis. In autoimmune diseases, the upregulation of immune checkpoints is intended to protect against autoimmune attack, however, due to often a dysregulated low expression of Tim-3 on immune cells and a low expression of galectin-9 on healthy cells, the immune cells are uncontrolled. In cancer, co-inhibitory receptors (immune checkpoints), e.g. CTLA-4, PD-1 and/or their ligands, such as PD-L1, are upregulated and associated with immune suppression and exhaustion of immune cells (86). Monoclonal antibodies targeting either receptor or ligand to block their interaction have proven to be beneficial for many types of cancers, promoting increase of patient survival with less severe side effect than the standard treatment, such as chemotherapy or radiotherapy (13, 78). However, ICB immunotherapy is extremely expensive as it is not easy to produce monoclonal antibodies. Furthermore, not all patients respond to treatment, and those who do often acquire resistance to therapy by upregulating alternative immune checkpoints such as Tim-3 (14). Indeed, the persistent high expression has been shown on tumour-infiltrating lymphocytes, such as CTL and NKs, and this is associated with exhaustion and impaired effector functions (74-76). Moreover, galectin-9, a Tim-3 ligand, has been reported to be upregulated on both tumour cells themselves, but also an increase in galectin-9 expression is found in sera from patients(326, 349) The overall function of the Tim-3-galectin-9 pathway in cancer is to promote immune escape by: 1) immune suppression of anti-tumour immunity, and 2) promoting factors for tumour progression. Suppression of anti-tumour immunity is the result of the ability of Tim-3-galectin-9 pathway to impair the function of both NK and T cells and induce T cell death (64, 304, 326). Activation of the Tim-3-galectin-9 pathway can also mediate tumour progression by the production of promoting factors, such as the angiogenic factor VEGF, and/or generation of immune suppressive cells, e.g. MDSCs and Tregs (275, 320, 350), which they in themselves and their mediators promote an immunosuppressive TME facilitating tumour progression and metastasis (351).

Overall, this points to the Tim-3-galectin-9 pathway being a therapeutic target where blocking the pathway is essential for enhancing anti-tumour immunity in cancer, whereas upregulating the pathway could be therapeutically beneficial in autoimmune diseases.

Antagonist anti-Tim-3 antibodies have shown in collaboration with blockade of PD-1 to reverse exhaustion of immune cells and promote tumour rejection (14, 93, 95). In contrast, some drug treatments for MS have shown to work by increasing the expression of Tim-3 (239). However, the understanding of the mechanism on how these treatments work is still mostly elusive as there is still a lack of understanding of the galectin-9-Tim-3 signalling in acute and chronic conditions, and how these proteins are regulated. Thus, a clearer in-depth understanding of galectin-9 and Tim-3 regulation and signalling is required.

Research studying the mechanism involved in Tim-3 regulation has started to emerge, and here factors, such as TNF $\alpha$ , IL27/NFIL3 (nuclear factor Interleukin-3 regulated) and T-bet, appear to be involved in the induction of Tim-3 in NKs and T cells, respectively (99, 352), and induction by common  $\gamma$ -chain cytokines, such as IL-2, IL-7, IL-15 and IL-21 and IL-12 and IL-18, have been found relevant in the induction of Tim-3 in T cells and NKs (230, 353). In many of these situations, the transcription factor T-bet has been found as a direct transcriptional inducer of Tim-3 (354). Furthermore, in liquid tumours and solid tumours, such as AML and breast cancer, respectively, the PI3K-PKC $\alpha$ -mTOR pathway appears to be involved in exocytosis, and thus translocation of the Tim-3 either alone or in complex with galectin-9 to the plasma membrane of the surface of cancer cells (64, 326). Galectin-9 is widely expressed in many tissues and cells, however, factors upregulating galectin-9 appear to be cell-specific, i.e. INF $\gamma$ , TNF $\alpha$ , IL-1 $\beta$  can induce it in certain cells, but not in others (270, 276-278), and direct transcription factors have yet to be clarified. Since galectin-9 is more ubiquitously expressed compared to Tim-3, and galectin-9 has been shown to have an inhibitory effect on NKs and T cells that are independent of Tim-3. This suggests that blocking of galectin-9 rather than Tim-3 might be more effective in the case of cancer. Moreover, galectin-9 blockade is also more affordable since functions of galectin-9 are dependent on its two CRDs, which can easily be blocked by peptides or  $\beta$ -galactoside, such as lactose (which is more cost-effective). Thus, this warrants the rationale for studying the biochemical regulation of galectin-9 in detail.

## 1.6 Looking for Regulators of Galectin-9

In the literature search for possible regulators of galectin-9 for solid tumours, such as breast cancer, and healthy cells, such as keratinocytes, a few possible candidates are highlighted in this context.

IFN $\gamma$  has been shown to upregulate galectin-9 expression in fibroblast, endothelial cells and astrocytes (276-278). TNF $\alpha$  was identified as the main regulator of galectin-9 in astrocytes (278). Our group's previous work found that in AML, cortisol upregulates LPHN1, which promotes surface expression of galectin-9 (324). Furthermore, looking at the promoter region of the LGALS9 gene, several Smad3 response elements were found, suggesting a possible role for regulation by TGF- $\beta$  (Appendix Figure 81). TGF- $\beta$  (especially TGF- $\beta$ 1) is a well-known immunosuppressive cytokine/growth factor often produced by many types of tumours and found at high levels in TME (355).

### 1.6.1 Transforming Growth Factor-beta (TGF- $\beta$ )

TGF- $\beta$  was discovered in the late 1970s as a secreted factor of cancer cells, which promoted growth and transformation of fibroblast, hence its name (356). Although, it can stimulate cell proliferation depending on the cell type and the environmental setting, its stimulatory effect on proliferation is modest compared to other growth factors. Actually, the name is somewhat misleading, because in most physiological settings, it is a potent inhibitor of proliferation of various cell types including epithelial, endothelial and cells derived from hematopoietic stem cells, such as immune cells (357).

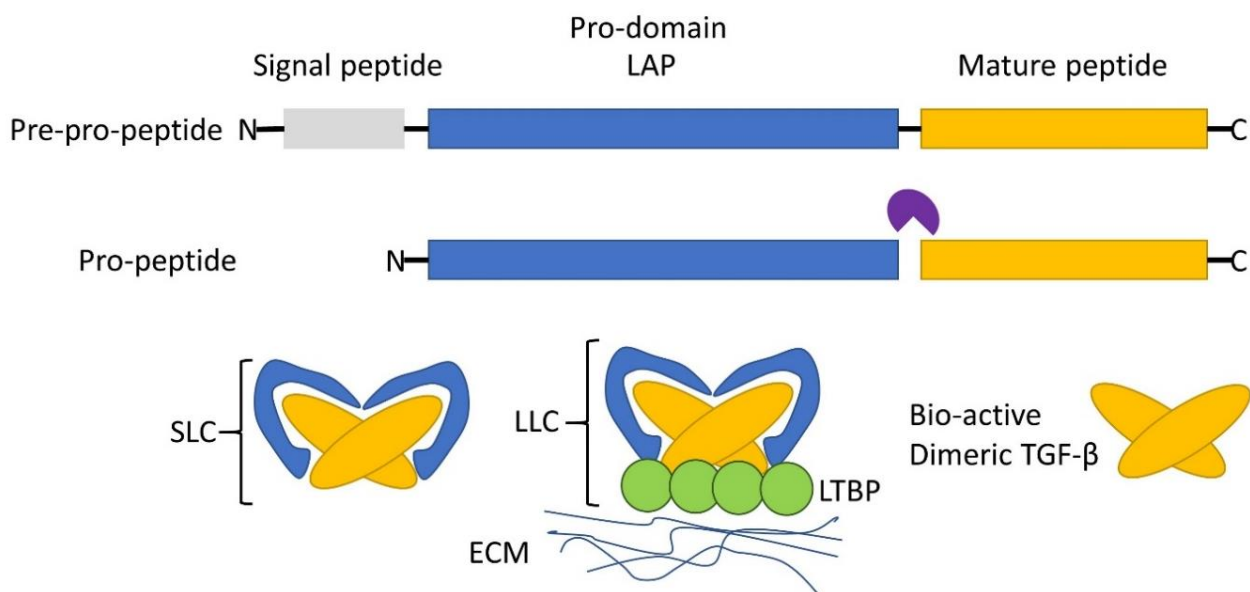
TGF- $\beta$  is part of the TGF- $\beta$  superfamily, which consists of 33 genes that translate into many related proteins, such as bone morphogenetic proteins (BMPs), growth differentiation factors (GDFs), activins/inhibins, myostatin etc., and they act as homodimers and/or heterodimers (357). There are three different isoforms of TGF- $\beta$ : TGF- $\beta$ 1, TGF- $\beta$ 2, and TGF- $\beta$ 3, which is expressed in a cell-specific manner, although, TGF- $\beta$ 1 is the most abundantly expressed and also the most studied (357). Here the focus is on TGF- $\beta$ 1.

#### *TGF- $\beta$ Ligand Structure and Its Receptors*

TGF- $\beta$  proteins are synthesized as precursor proteins consisting of a signal peptide required for secretion, a pro-domain also known as latency-associated peptide (LAP), which is required for proper folding and secretion of the TGF- $\beta$ , and the growth factor domain (mature polypeptide) (357-359). The pro-peptide is processed by proteolytical cleavage (typically by furin proteases, which often occur in the endoplasmic reticulum (ER)), thus separating the pro-domain from the mature polypeptide, although it remains non-covalently associated. This complex is known as small latent TGF- $\beta$  complex (SLC). The mature polypeptide form disulphide-linked dimerization. SLC can associate with latent



TGF- $\beta$  binding protein (LTBP) and forms the large latent complex (LLC), which is then secreted and associated with ECM components (357-359) or with plasma membrane-associated glycoprotein-A repetitions predominant (GARP) on Tregs (357). Proteolytic degradation of ECM proteins by e.g. MMPs can occur during physiological remodelling or in response to injury or cell invasion and is thought to activate TGF- $\beta$ 1 by releasing it from LTBP and LAP, and consequently it becomes biologically active and binds to its receptor. However, other processes have shown to activate TGF- $\beta$ 1, such as through contact with integrins and thrombospondin (357). Figure 17 illustrates the TGF- $\beta$  structure and its inactive and bio-active states.



**Figure 17: TGF- $\beta$  structure** (adapted from (357, 358)). TGF- $\beta$  is synthesized as precursor protein consisting of a signal peptide, a pro-domain also known as latency-associated peptide (LAP), and the growth factor domain (mature polypeptide). The pro-peptide is processed by proteolytical cleavage, thus separating the pro-domain from the mature polypeptide, although it remains non-covalently associated, this complex is known as small latent TGF- $\beta$  complex (SLC). The mature polypeptide form disulfide-linked dimerization. SLC can associate with latent TGF- $\beta$  binding protein (LTBP) and forms the large latent complex (LLC), which is then secreted and associated with the extracellular matrix (ECM) components. Proteolytic degradation of ECM proteins by e.g. MMPs is thought to activate TGF- $\beta$ 1 by releasing it from LTBP and LAP, and consequently it becomes bioactive and able to bind to its receptors.

TGF- $\beta$  mediates its effect by binding to TGF- $\beta$  receptors (T $\beta$ Rs), which are continuously internalized via clathrin-dependent or lipid-raft dependent endocytosis (359). Furthermore, the expression of the receptors is under post-translational control, such as N-linked (and possible O-linked) glycosylations, which facilitate receptor transport to the surface, and thus enhance receptor availability and increase TGF- $\beta$  responsiveness (357). There are three main T $\beta$ Rs: TGF- $\beta$  type I receptor (T $\beta$ RI), TGF- $\beta$  type II receptor (T $\beta$ RII) and the accessory receptor (T $\beta$ RIII). There have been reported seven types of T $\beta$ RI and five

types of T $\beta$ RII, and each TGF- $\beta$  family member uses a distinct combination of these receptors, which result in a specific combination of Smad effector proteins, which are reflected in the different outcomes of TGF- $\beta$  stimulation (357, 360). TGF- $\beta$  utilizes the type I receptors known as ALK1 and ALK5 and the type II receptor known as T $\beta$ RII (357). Of the three TGF- $\beta$  receptors, T $\beta$ RI and T $\beta$ RII are required for signal transduction and contain serine/threonine protein kinases in their cytoplasmic domains, although they also have a low ability to phosphorylate tyrosine (357). T $\beta$ RIII (e.g. betaglycan and endoglin) acts as a co-receptor and has no kinase activity. Betaglycan can bind all three TGF- $\beta$ s, but is especially important for TGF- $\beta$ 2 as it has a lower affinity for both T $\beta$ RI and T $\beta$ RII. Here, betaglycan facilitates the loading of TGF- $\beta$ 2 to T $\beta$ RII and stabilises its association to T $\beta$ RI (357-359). Endoglin is highly expressed on human endothelial cells and is involved in determining the outcome of the TGF- $\beta$  signal. It facilitates the interaction of TGF- $\beta$ 1 already bound to T $\beta$ RII with T $\beta$ RI, also known as ALK-1, thus favouring an ALK-1-mediated proliferative and invasive response and promotes angiogenesis (the formation of new blood vessels). In the absence of endoglin, interaction with T $\beta$ RI known as ALK-5 is favoured and results in inhibition of proliferation and migration (357, 358). However, the ectodomain of both betaglycan and endoglin can also be cleaved and released to sequester TGF- $\beta$ , thus lowering responsiveness to TGF- $\beta$  (357).

### *TGF- $\beta$ Signalling and Canonical Smad Signalling*

TGF- $\beta$  ligation can result in canonical Smad signalling pathway as well as alternative non-Smad signalling. However, in general, Smad proteins are thought to be the main effectors upon TGF- $\beta$  binding. Smad proteins are divided into groups depending on their function: Receptor-regulated Smad (R-Smad) consists of Smad 1, 2, 3, 5, and 8, common mediator (Co-Smad) Smad4, inhibitory Smad (I-Smad) Smad 6 and 7. Smad2 and Smad3 act as R-Smads for activin and TGF- $\beta$  signalling, whereas Smad1, Smad5 and Smad8 mediate responses to BMPs and GDFs (358).

R-Smads consist of two structural domains fused by a linker region. The mad homology (MH)1 domain allows for DNA binding, although the most predominant form of Smad2 has an insert in the MH1 domain, which renders it unable to bind DNA (361). MH1 allows for interaction with other transcription factors, such as Jun, activating transcription factor (ATF)-3, specificity protein 1 (Sp1) and runt-related transcription factor (Runx) (358). The linker region is a hotspot for phosphorylation-sites, which serve as docking-sites for other

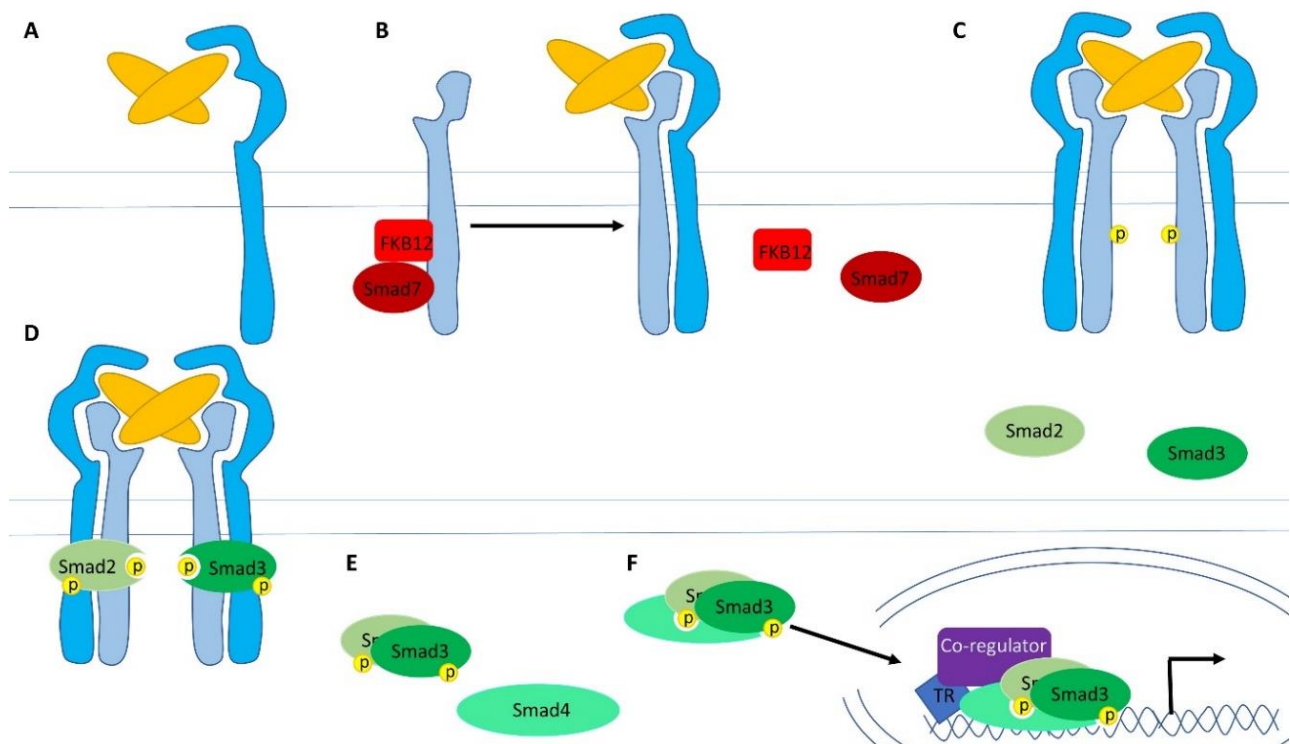
proteins and influence the stability, nuclear localization, and other properties of these Smads, and it also contains a PPxY motif, which acts as binding site for E3 ubiquitin ligases, such as Smad ubiquitination regulatory factor (Smurf) (358). The MH2 domain allows for protein-protein interactions, e.g. Smad-Receptor, Smad-Smad or Smad DNA binding co-regulators (361). One example is the conserved SxS motif in the MH2 domain, which can be phosphorylated by the T $\beta$ RI and promote the formation of oligomeric Smad complexes (358). The Smad hetero-trimers bind to DNA through their MH1 domains, but due to the weak interaction, they interact with other DNA-binding factors/co-regulators to achieve high affinity and selectivity to either repress or activate gene transcription (358).

Active dimeric TGF- $\beta$ 1 mediates effect by signalling through TGF- $\beta$  receptors forming a heterotetrameric complex with two T $\beta$ RI and two T $\beta$ RII. First, TGF- $\beta$ 1 binds to T $\beta$ RII, causing a conformational change, which allows a stable association to T $\beta$ RI. This results in three effects: 1) protein arginine N-methyltransferase 1 (PRMT1), which is associated to T $\beta$ RII, is able to methylate I-Smads (such as Smad7), and then dissociates from the T $\beta$ RI relieving inhibitory pressure allowing R-Smads to be recruited. 2) the cytoplasmic domains of the type I and type II receptors are brought in close proximity and enable T $\beta$ RII to phosphorylate T $\beta$ RI in the GS domain (Glycine-Serine regulatory region) of its cytoplasmic tail, and this results in the release of inhibitory immunophilin FKBP12 and hence the activation of T $\beta$ RI (357, 358). 3) Both type I and type II receptors can upon ligand-binding induce autophosphorylation, which enhances their kinase activity (357).

Phosphorylation of the GS domain of T $\beta$ RI also acts as docking-site for R-Smad proteins. The cytoplasmic retention protein Smad anchor for receptor activation (SARA) facilitates the interactions between R-Smad and T $\beta$ RI, which then phosphorylates R-Smads on two C-terminal serines (SxS motif). Which R-Smads that are recruited depend on ligand and receptor combination (357, 358). As mentioned, Smad2 and Smad3 act as R-Smad for both TGF- $\beta$  and activin, whereas BMPs and GDFs mediate their effect through Smad1, Smad5 and Smad8 (357). Once R-Smads are phosphorylated, they detach from the receptor and are generally thought to form complex with Co-Smad (Smad4), generating a trimeric complex and then translocate to the nucleus where the Smad complex cooperates with other transcription factors and co-regulators (histones acetyltransferases (HATs) and histone deacetylases (HDACs)) to activate or repress target genes. Smad complexes can recruit the HATs p300 and CREB binding protein (CBP) to modulate epigenetic changes

that allow for transcription of target genes as well as RNA processing (357, 358). In addition, it was recently reported that Smad2 and Smad3 could form complex with TIF1 $\gamma$  instead of Smad4 in human hematopoietic progenitor cells, and this resulted in a different TGF- $\beta$  outcome than with Smad4 (362). TGF- $\beta$  signalling is a transient response as upon its activation, negative feedback mechanisms are also set in motion. Phosphorylated Smads are the target for E3 ubiquitin ligases, such as Smurf1/2, which target them for degradation. Moreover, TGF- $\beta$  signalling promotes transcription of I-Smads, which with Smurfs operation can target the TGF- $\beta$  receptors for proteolytical degradation (359).

TGF- $\beta$  family proteins are not the only proteins, which can activate Smad, even though they are thought to be the main downstream effector proteins. There has been reported crosstalk from various other signalling pathways, such as Wnt signalling, MAPK signalling and CDK signalling pathways. Various kinases from these pathways are able to phosphorylate R-Smads on serines and/or threonines in their linker regions. Depending on the phosphorylation site at the linker region, it influences both nuclear translocation and activation of R-Smads. In addition, other posttranslational modifications may also contribute to this. As mentioned, such phosphorylation may also be a target of Smurfs or other E3 ubiquitin ligases, such as Nedd4L, which targets the R-Smad for degradation (357).



**Figure 18: TGF- $\beta$  mediated Smad dependent signalling** (adapted from (357, 358)). (A) bioactive TGF- $\beta$  binds to T $\beta$ RII possibly facilitated by T $\beta$ RIII (not shown). (B) T $\beta$ RI then associated with T $\beta$ RII and binds TGF- $\beta$ , which induces conformational change and stable association as well as the release of Smad7 and FKBP12, which inhibit T $\beta$ RI. (C) When TGF- $\beta$  binds, it creates a hetero-tetrameric complex of two T $\beta$ RI and two T $\beta$ RII receptors. With the release of inhibitors and the cytoplasmic tails of the two receptors in proximity, T $\beta$ RII activates T $\beta$ RI by phosphorylation. (D) Activation of T $\beta$ RI allows recruitment of R-Smad, such as Smad2 and Smad3, which becomes phosphorylated. (E) Phosphorylated R-Smad dissociates from the T $\beta$ Rs. (F) Activated R-Smad forms a trimeric complex with Smad4 (or possibly TIF1 $\gamma$ ), which allows for translocation to the nucleus where it with other transcription factors (TR) and co-regulators mediates activation (or repression) of target genes. Activation of Smad3 can induce more TGF- $\beta$ .

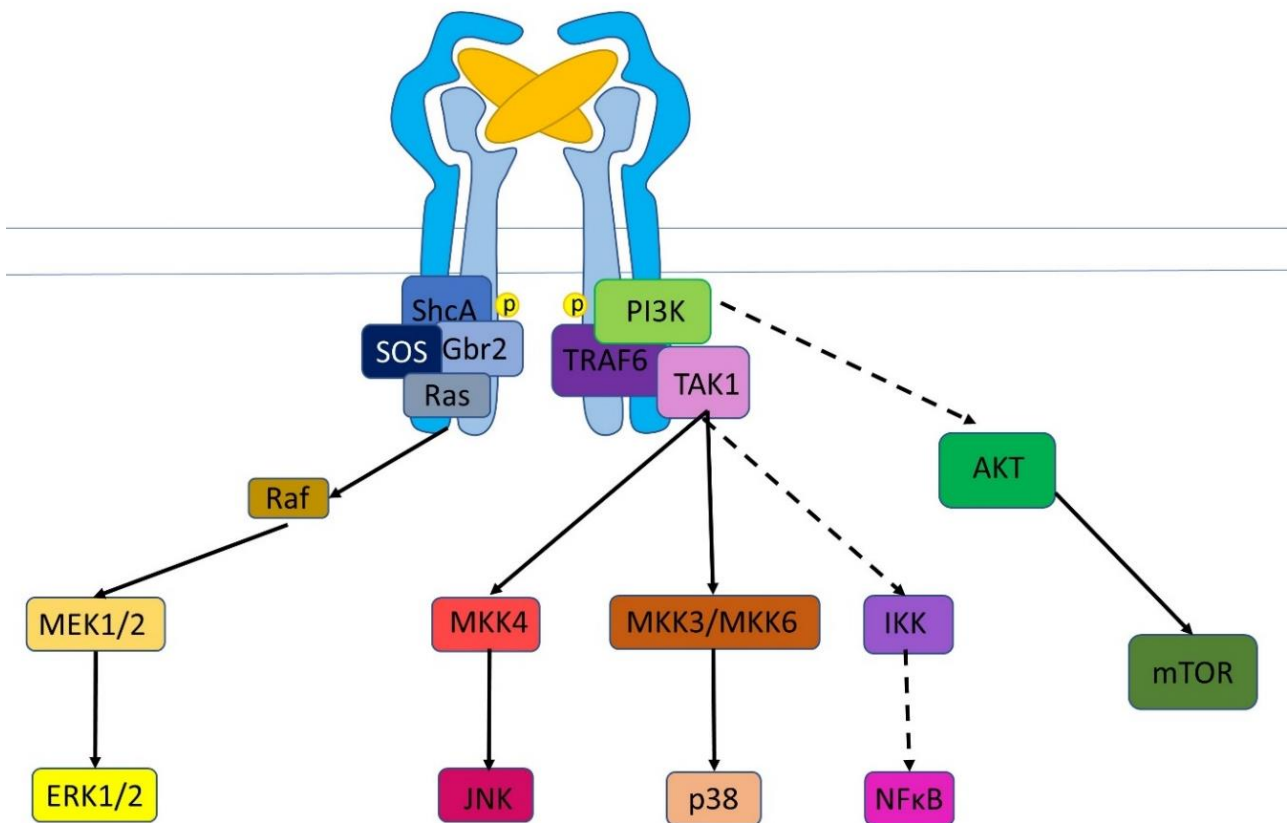
### **Alternative Non-Smad Signalling**

TGF- $\beta$  family receptors are also able to activate other signalling pathways, including the MAPK pathways (both ERK, p38 and JNK), PI3K–AKT–mTOR pathways and others (359). This is not the focus as our work has focused on TGF- $\beta$ -mediated Smad signalling, and therefore, it will only be briefly described (Figure 19).

As mentioned above, ligation of TGF- $\beta$  can result in tyrosine phosphorylation of T $\beta$ RI, which acts as docking-site for the ShcA adaptor protein. TGF- $\beta$ -induces tyrosine phosphorylation of ShcA and recruits growth factor receptor-bound protein 2 (Grb2) and son of sevenless homolog (SOS), forming a ShcA-Grb2-SOS complex resulting in Ras activation, which further leads to MEK1/2 activation, and finally ERK activation. It should be noted that ShcA and Smad3 compete for T $\beta$ RI association, thus this pathway also represses TGF- $\beta$ -induced Smad3 activation (357).

TGF- $\beta$  ligation induces association of TGF- $\beta$  receptor complexes with the RING domain E3 ubiquitin ligases TRAF6 or TRAF4, which undergo polyubiquitination that functions as a scaffold for TAK1 recruitment and activation. TAK1 is a MAP3K, which can activate both MKK4 and MKK3/MKK6, resulting in JNK and p38 activation, respectively. These pathways are possibly involved in damping the TGF- $\beta$  response as they promote the metalloprotease tumour necrosis factor  $\alpha$ -converting enzyme (TACE, also known as ADAM17), which has been reported to cleave the T $\beta$ RI, resulting in shedding of the ectodomain and attenuating T $\beta$ RI responses (357).

TGF- $\beta$ -induced PI3K-AKT activation can occur through the association of the p85 (the regulatory unit of PI3K) with T $\beta$ RII and T $\beta$ RI, or as with p38 and JNK through association with TRAF6. Activation of the PI3K-AKT-mTOR pathway could be important in regulating TGF- $\beta$  responsiveness by forming a positive feedback loop as this pathway controls glucose metabolism, and high glucose concentration (25 mM) promotes N- and O-glycosylations of proteins, which increase TGF- $\beta$  receptor availability (357).



**Figure 19: TGF- $\beta$  mediated non-Smad signalling** (adapted from (357)). Although the TGF $\beta$  receptors are mainly classified as serine/threonine kinases, they possess the ability to phosphorylate tyrosine as well, and are thus considered as dual-specificity kinases. Therefore, engagement of T $\beta$ Rs can also result in tyrosine phosphorylation, which allows for recruitment of ShcA and Grb2 adaptor proteins, which form complex with the guanine exchange factor SOS to activate the GTPase Ras. Ras activates the MAPK pathway Raf-MEK-ERK. TGF- $\beta$  ligation also induces association with the RING domain E3 ubiquitin ligases TRAF6, which undergo polyubiquitination that allows recruitment and activation of TAK1, which can activate both MKK4 and MKK3/MKK6, resulting in JNK and p38 activation, respectively. All of the MAPK pathways can lead to AP-1 activation, which has been reported to be involved in TGF- $\beta$  production. TAK1 also leads to activation of the I $\kappa$ B (IKK) complex, which mediates release and activation of NF $\kappa$ B. Crosslinking TGF- $\beta$  receptors can also activate the PI3K-AKT-mTOR pathway either through direct association with the p85 (the regulatory unit of PI3K) or with p38 and JNK through association with TRAF6. Activation of the PI3K-AKT-mTOR pathway can lead to translation of HIF-1 $\alpha$ , which is involved in TGF- $\beta$  production

### TGF- $\beta$ Functions

TGF- $\beta$  is considered to be a pleiotropic cytokine/growth factor with multifunctional activities that are involved in cell cycle control, regulation of early development, differentiation, extracellular matrix formation, haematopoiesis, angiogenesis (both pro-angiogenic and anti-angiogenic dependent on context), chemotaxis, modulator of immune functions, wound healing and apoptosis (both protecting and promoting depending on context (357, 363, 364)). TGF- $\beta$  has been implicated in many different diseases such as fibrosis, asthma, vascular and autoimmune diseases, as well as cancer (357, 363, 364). In this section, the

focus will be on the role of TGF- $\beta$  in cancer. TGF- $\beta$  has a paradoxical dual role both as a tumour suppressor and as a tumour promoter depending on the cancer stage (359).

### **TGF- $\beta$ as a Tumour Suppressor**

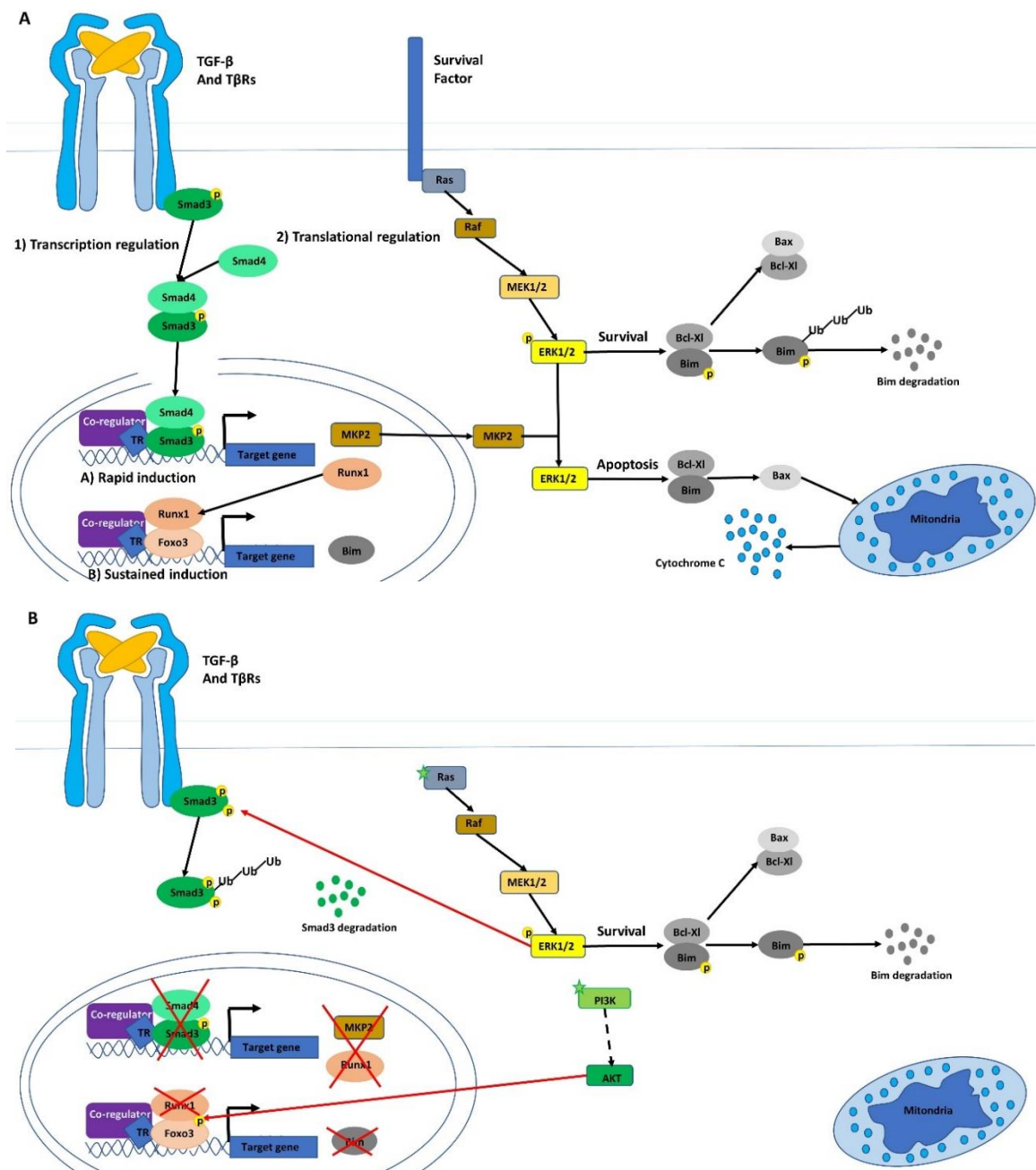
In normal cells, such as epithelial cells and early stages of cancer, TGF- $\beta$  acts as a tumour suppressor by inhibiting cell cycle progression, promoting apoptosis and suppression of growth factor, cytokine and chemokine expression (355).

TGF- $\beta$  suppresses tumour growth by attenuating the expression of c-Myc, a transcription factor, which upregulates pro-proliferative genes and abrogating the function of cyclin-dependent kinases (CDKs) by inducing the expression of CDK inhibitors, such as p15, p21 and p27. These effects occur in a Smad3-dependent manner (359).

Multiple apoptotic mediators and signalling pathways have been implicated in TGF $\beta$ -induced apoptosis, e.g. Smad, JNK, p38 pathway and many others (365). TGF- $\beta$  promotes Smad3 activation, which induces Runx1, a transcription factor that operates with forkhead box protein O3 (Foxo3) to mediate transcriptional induction of Bim (a pro-apoptotic member of Bcl-2 family and a sensor of apoptotic stimuli). Furthermore, TGF- $\beta$  induced Smad3 activation also promotes transcription of MKP2 (a MAPK phosphatase), which attenuates ERK1/2 activation that would normally phosphorylate Bim and target it for proteolytical degradation. Bim interacts with pro-survival Bcl-2 family members, freeing Bax and Bak to oligomerize and mediate mitochondrial outer membrane permeabilization and release cytochrome C, and thus activate the intrinsic (mitochondrial) pathway of apoptosis (365). TGF- $\beta$  mediated apoptosis by Bim regulation is depicted in

Figure 20.

In cancer, there is often an overexpression and/or a constitutive activation of AKT, MAPK, and CDKs, which facilitate tumour progression. For instance, AKT inhibits Foxo3, and thereby prevents the induction of Bim, ERK1/2 phosphorylates Bim and targets it for degradation, hence, promoting survival and inhibiting apoptosis of cancer cells (365). In addition, ERKs and CDKs (Cdk2 and Cdk4) phosphorylate Smad3 in the linker region, which retains it in the cytosol and target it for Smurf-mediated degradation, and thereby reduces TGF- $\beta$  responsiveness of tumour cells (190). These are some of the ways that tumours can escape TGF- $\beta$ -mediated growth inhibition.



**Figure 20: TGF- $\beta$ -mediated apoptosis by Bim regulation** (adapted from (365)). (A) When the cell receives survival signal, Bim (a pro-apoptotic factor) is released from its binding partner Bcl-XI (an anti-apoptotic factor), and Bim is targeted for proteolytical degradation by phosphorylation-dependent ubiquitination, mediated by the activation of the Raf-MEK-ERK MAKP pathway. TGF- $\beta$  regulates Bim both at transcriptional and translational level. At translational level, TGF- $\beta$ -mediated Smad3 activation induces Runx1 and MKP2. MKP2 dephosphorylates ERK1/2 and thus inactivates it, which prevents proteolytical degradation of Bim. Prolonged TGF- $\beta$  treatment induces a sustained induction of Bim. Bim mediates intrinsic pathway to apoptosis by sequestering Bcl-XL, and thus allows pro-apoptotic effector proteins, such as Bax and Bak, to oligomerize and mediate mitochondrial outer membrane permeabilization, which releases cytochrome C and induces the intrinsic apoptosis programme. (B) Cancer escapes from TGF- $\beta$ -mediated apoptosis. Cancer cells frequently have mutations that result in overexpression or constitutively active RAS, PI3K and CDKs. ERK is downstream of RAS and alone or together with Cdk2/4 can phosphorylate Smad3 and target it for ubiquiting-mediated proteolytical degradation. AKT is downstream of PI3K and it mediates inhibitory phosphorylation of Foxo3. In both cases, there is no transcription of Bim, and whatever Bim there is, is targeted for degradation.



## **TGF- $\beta$ Promotes Tumour Progression**

At late stages of cancer, the tumour resists TGF- $\beta$ -mediated growth inhibition (cytostatic effect) while concomitantly uses TGF- $\beta$  to exert tumour-promoting effects by suppressing immune surveillance of anti-tumour immune cells, mediating infiltration of pro-tumour-associated immune cells, inducing angiogenesis, increasing tumour invasiveness and metastasis (366). The switch from tumour suppressor to tumour promoter often occurs due to aberrant expression of TGF- $\beta$  signalling elements that cause decreased or altered TGF- $\beta$  responsiveness and increased expression or activation of the TGF- $\beta$  ligand. Somatic mutations, such as loss-of-function mutation or phosphorylations that cause downregulation in T $\beta$ RI, T $\beta$ RII or Smad signalling proteins are often found in human cancers and are often associated with poor prognosis and a more malignant tumour phenotype (355). Although, at some stage, there might be enhanced TGF- $\beta$  signalling caused by constitutive active T $\beta$ RI or TGF- $\beta$  ligand, which leads to an increase in metastasis. This reflects TGF- $\beta$  involvement in driving epithelial-mesenchymal transition (EMT) (367).

It was originally thought that the SMAD dependent pathways mediated the growth inhibition; whereas the SMAD independent pathways probably contributed to the tumour-promoting effect at a later stage of tumour progression. However, recent data demonstrate that SMAD-dependent pathway is also involved in the tumour-promoting activities of TGF- $\beta$  (355).

TGF- $\beta$  has an adverse effect on anti-tumour immunity and significantly inhibits host tumour immune surveillance. In addition, it promotes pro-tumour immune cells, such as MDSC and Tregs (355).

TGF- $\beta$  inhibits cell proliferation of anti-tumour cells, such as NKs and T cells. Furthermore, it represses the cytotoxic gene programme such as perforin, and granzymes of CTLs and NKs, thus prevents them from replenishing the granule content. This reduces tumour clearance as they are unable to attack the next set of cancer cells. Furthermore, TGF- $\beta$  decreases the expression of the activating natural killer group 2 (NKG2)D receptor of both CD8 T cells and NKs and attenuate the expression of its ligand MICA, thus reducing the ability of anti-tumour cells to recognize the cancer cells (355).

TGF- $\beta$  regulates the production of chemokines/chemokine receptors that are important in inflammatory cell recruitment. The loss of T $\beta$ RII in tumours, such as breast cancer, results in increased expression of the chemokines CXCL1 and CXCL5, which promotes infiltration of MDSCs that produce high levels of MMPs, TGF- $\beta$ 1 and VEGF, which are major contributors to enhance tumour invasion, metastasis and angiogenesis. These MDSCs also inhibit the function of NKs and T cells through the production of arginase and ROS as well as secrete factors that prevent maturation of DCs and promote polarization of TAMs (M2-like phenotype macrophages). Furthermore, TGF- $\beta$  induces Foxp3 expression, resulting in generation and differentiation of Tregs, which also suppresses NKs and T effs (355).

Cancer cells deploy various mechanisms to inhibit or kill immune cells. As described above, one of these mechanisms is by use of galectin-9 (64, 326). Furthermore, galectin-9 is known to induce apoptosis of T cells (255, 304). Chen et al. reported that apoptotic T cells releases TGF- $\beta$ , which contributed to an immunosuppressive environment (368). This may be important, as it could be speculated that galectin-9 could induce apoptosis of T cells and boost the immunosuppressive TME by release of TGF- $\beta$ . Thus, targeting TGF- $\beta$  signalling as cancer therapy appears promising. The goal is to abolish the tumour-promoting effect of TGF- $\beta$  while maintaining its tumour-suppressive properties. Until now, approaches include a variety of neutralizing antibodies, and small molecular inhibitors are being explored (355).

### 1.6.2 Immunogenic Cell Death (ICD)

Our body consists of billions of cells if not more, and every day many of these cells die due to natural turnover in order to maintain homeostasis (369). However, infected cells and/or malignant cells are targeted to be killed by the immune system, or if our skin is damaged, cells are injured and may die, and wound healing is set in motion (1). Thus, billions of cells die every day for different reasons, and therefore, there are also several types of cell death. The three main types of cell death are apoptosis, necrosis/necroptosis and autophagy, although the latter is mostly considered a survival mechanism, which failed outcome ends in cell death. All of these for the most part require active death signalling (370). Furthermore, depending on the circumstances, a cell death can invoke an immune response, also known as immunogenic cell death (ICD), or the cell can die without

involving the immune system, known as non-immunogenic or tolerogenic cell death (TCD) (371). However, what factors are involved in ICD, and can it be used, for example, to promote cancer clearing? And in an autoimmune setting, is it possible to remove or block the factors that cause an ICD, revert back to TCD and thereby attenuating the autoimmune response?

Originally, it was thought that apoptosis induces TCD whereas necrosis induces an ICD, however, further studies have found evidence that dependent on the circumstances both forms of cell death can result in both ICD and TCD (371). It is now believed that immunogenic cell death depends on the combination of antigenic factors (e.g. neo-antigens from tumours) and adjuvants, such as danger signals, also known as danger-associated-molecular patterns (DAMPs) (372). DAMPs are endogenous proteins, which are normally sequestered within the live cells (inside the nucleus, cytosol or with biological membranes). These proteins are exposed on the cell surface or secreted and released by stress, damaged or dying cells. Some of the externalized DAMPs have immunostimulatory properties whereas others are inhibitory (373). Depending on the type of DAMP, it has different abilities, e.g. facilitating opsonization/phagocytosis, assist in antigen processing and antigen presentation, maturation of DCs, activation of immune cells, such as DCs macrophages, T cells and NKs, and aid inflammatory processes by inducing inflammatory gene programmes (373). Regardless of the circumstances of the cell death, the cell needs to be cleared by phagocytes as uncleared cells may promote autoimmunity (369). For the elimination of dying or dead cells, several processes are required. Most living cells express “don’t eat me” signal, such as CD47, which can inhibit the engulfment of cells displaying PtdSer (369). Therefore “don’t eat me” signals have to be removed before engulfment, although the mechanism behind the removal still remain unknown (371). As mentioned, dying cells must emit DAMPs, so-called alarmins, some of which act as “find me” and “eat me” signals and others as adjuvants. “Find me” signals function as chemotactic signals that recruit monocytes/macrophages and immature DCs to the dying cell. For the phagocytic engulfment to take place, the dying cells also need to show an “eat me” signal. The most studied “eat me” signal is the cell surface exposure of PtdSer. The cell is then engulfed and enters a compartment known as the phagosome where it undergoes degradation. Post engulfment and upon TCD, the phagocyte will then secrete anti-inflammatory cytokines (369).

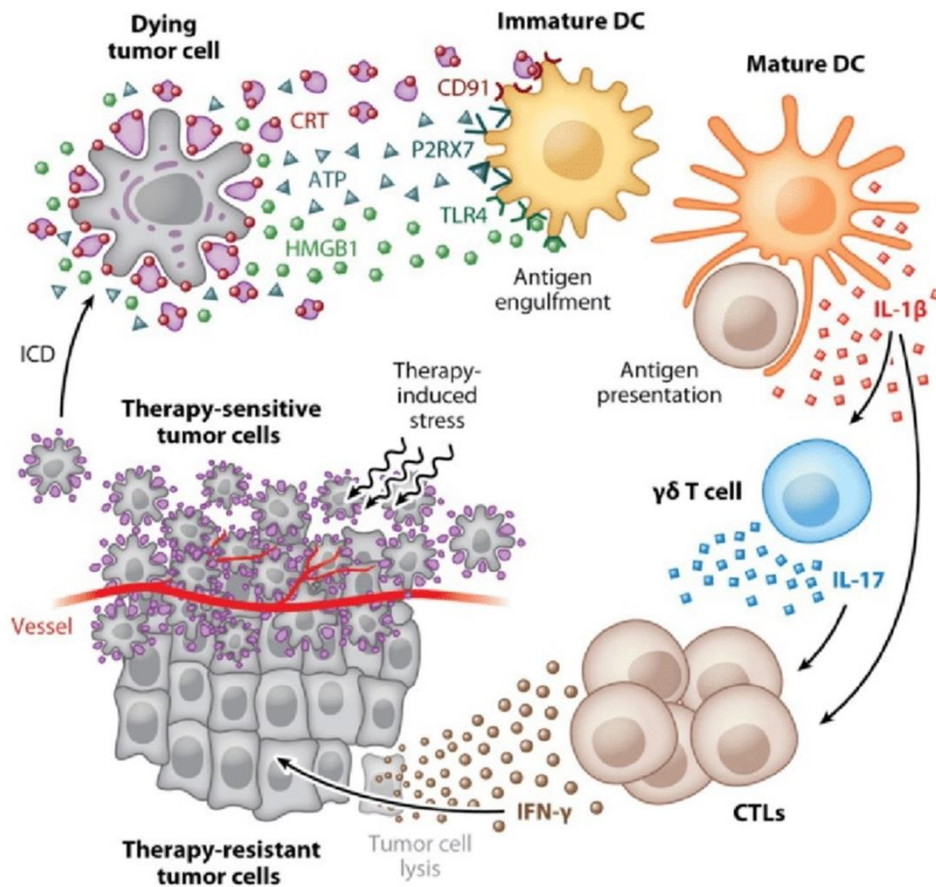
Dependent on the initial inducer, dying cancer cells under some circumstances can promote ICD and induce an anti-tumour immune response, thus operate as a form of vaccine promoting its clearance (374). To do this, it has to down-modulate “don’t eat me” signals. It has been shown that many types of cancer cells overexpress “don’t eat me signals”, CD47 and CD24 and blocking antibodies targeting these signals improved immunogenicity (375). It also needs to emit DAMPs corresponding to a “find me” signal and an “eat me” signal as well as an adjuvant that aids in antigen processing and presentation and/or DC maturation (372, 376). It has been observed that only certain chemotherapeutic agents promote ICD, and for those drugs that did, it was found that two types of stress, namely ER stress and autophagy obligatorily preceded ICD (374). These processes are necessary for the exposure and release of DAMPs associated with ICD. DAMPs associated with ICD of dying tumour cells include the exposure of calreticulin (CRT), secretion of ATP and the release of HMGB1, which interacts with CD91, P2X purinoceptor 7 (P2RX7) and TLR4 on DCs, respectively (Figure 21) (374, 376).

Studies have shown that only certain chemotherapeutic agents, such as anthracycline, support the development of ICD by inducing ER stress, which initiates the translocation of CRT to the cell surface during the pre-apoptotic stage of cell death, and CRT acts as a “eat me” signal that then facilitates the uptake of dying cells by DCs expressing the receptor CD91 (377). The importance of CRT of anthracycline-induced ICD is demonstrated by siRNA or neutralizing antibodies against CRT, which resulted in lost ability to promote ICD. Furthermore, it was shown that external supply or enforced expression of CRT with chemotherapeutic regimens that not normally promote exposure of CRT, improved efficacy and converted TCD to ICD (377). However, CRT exposure alone is not sufficient to elicit an anti-tumour immune response, as live cells that ectopically express CRT are unable to induce DC maturation and antigen presentation to initiate the tumour-antigen specific immune response (377). Thus, other signals are also necessary for the promotion of ICD.

Michaud et al. showed that autophagy is dispensable for apoptosis but required for ICD. Suppression of autophagy did not affect CRT exposure nor HMGB1 release; however, it did inhibit secretion of ATP from dying tumour cells during apoptosis. Furthermore, only autophagy-competent cancer cells were able to attract DCs and T cells to the tumour bed, indicating that ATP acts as a “find me” signal (378). ATP do not only act as a short-range

chemoattractant, but also stimulates the anti-tumour immune response. By engaging its receptor, P2RX7, on APCs, it initiates signalling that activates the NLR family pyrin domain containing 3 (NLPR3)-dependent caspase-1 activation complex also known as the inflammasome, which in turn allows for secretion of IL-1 $\beta$  (379). IL-1 $\beta$  enhances expansion, differentiation of antigen-specific CD4 and CD8 T cells, as well as augments effector function, memory response of antigen-specific CD8 T cells, and promotes IL-17 producing  $\gamma\delta$  T cells (380-382). Many neoplastic cancers have disabled the autophagy machinery as a part of malignant transformation, although, at a later stage of cancer, it regains its ability to perform autophagy (378), thus, depending on the stage of cancer, the dying cancer cells can help to promote clearance by stimulating an anti-tumour immune response. Although, studies have found that by implementing manoeuvres that increase extracellular ATP concentrations, it can potentially improve the efficacy of chemotherapies in cancers with disabled autophagy (378).

Seemingly, ICD improves the efficacy of conventional cancer treatment, such as chemotherapy and radiotherapy, by invoking an anti-tumour response that can control remaining tumour cells, and possibly eliminates remaining cancer stem cells (374). Understanding the underlying grounds of ICD and which components are involved enables its exploitation and thereby improves the immunogenicity of current treatments. Following permeabilization of the plasma membrane, dying cells can release several proteins including DAMPs. Many DAMPs have been identified and more are continuously being discovered. Although, not all are involved in ICD, in fact, some may be involved in TCD or both (371, 373, 383, 384). A DAMP that has been shown to be involved in both tumour progression and limits tumour growth is the nuclear protein high-mobility-group-box 1 (HMGB1), which is released from injured/stressed/dying cells. Originally, it was thought to be released from the nucleus only during primary necrosis; however, recent data indicate that it can be post-apoptotic released during secondary necrosis (371, 374, 385).



**Figure 21: Immunogenic cell death** (directly from (374)). Therapy-induced ICD promotes exposure of CRT at the surface of dying cells at a pre-apoptotic stage, induces secretion of ATP during apoptosis and release HMGB1 during secondary necrosis (when their membranes become permeabilized). CRT, ATP and HMGB1 bind to their respective receptors on DC, which are CD91, P2RX7 and TLR4. ATP acts as a find me signal facilitating the recruitment of DC into the tumour bed. Here, it engulfs dying tumour cells showing CRT on the surface (eat me signal) and with the exposure to HMGB1, they obtained the capacity for processing and presentation of the tumour antigens as well as maturation, and thus optimally activates T cells. This results in IL-1 $\beta$  and IL-17-dependent and IFN $\gamma$ -mediated anti-tumour immune response involving both  $\gamma\delta$  T cells and CTLs, which have been suggested to eliminate residual chemotherapy resistant tumour cells.

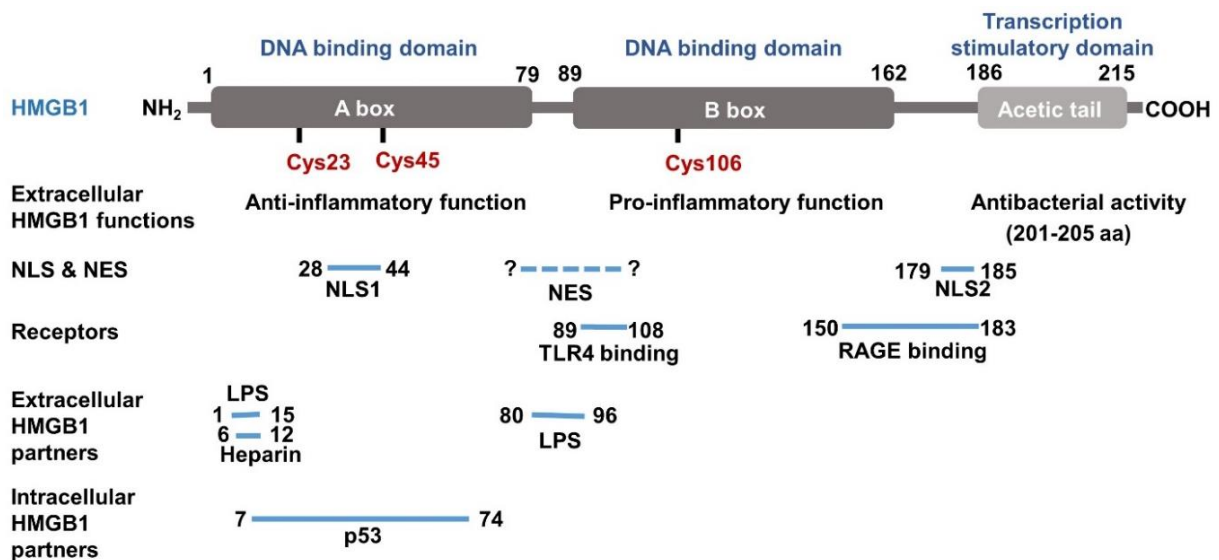
### 1.7.2.1 High Mobility Group Box 1 (HMGB1)

The high mobility group (HMG) superfamily of proteins consists of nucleosome-binding protein, which mostly resides in the cell nucleus where they exert various functions, such as controlling chromatin architecture and dynamics, modifying the transcription of certain genes, regulating DNA repair/genome stability, and cell differentiation (386). Protein members of the HMG superfamily all contain a characteristic C-terminal acidic tail. Based on the functional motifs, the superfamily can be divided into three families, the HMGA, HMGB and HMGN, in which HMGB is distinct by expressing 2 DNA-binding domains known as Box A and Box B. The HMGB family consists of HMGB1, HMGB2 and HMGB3,

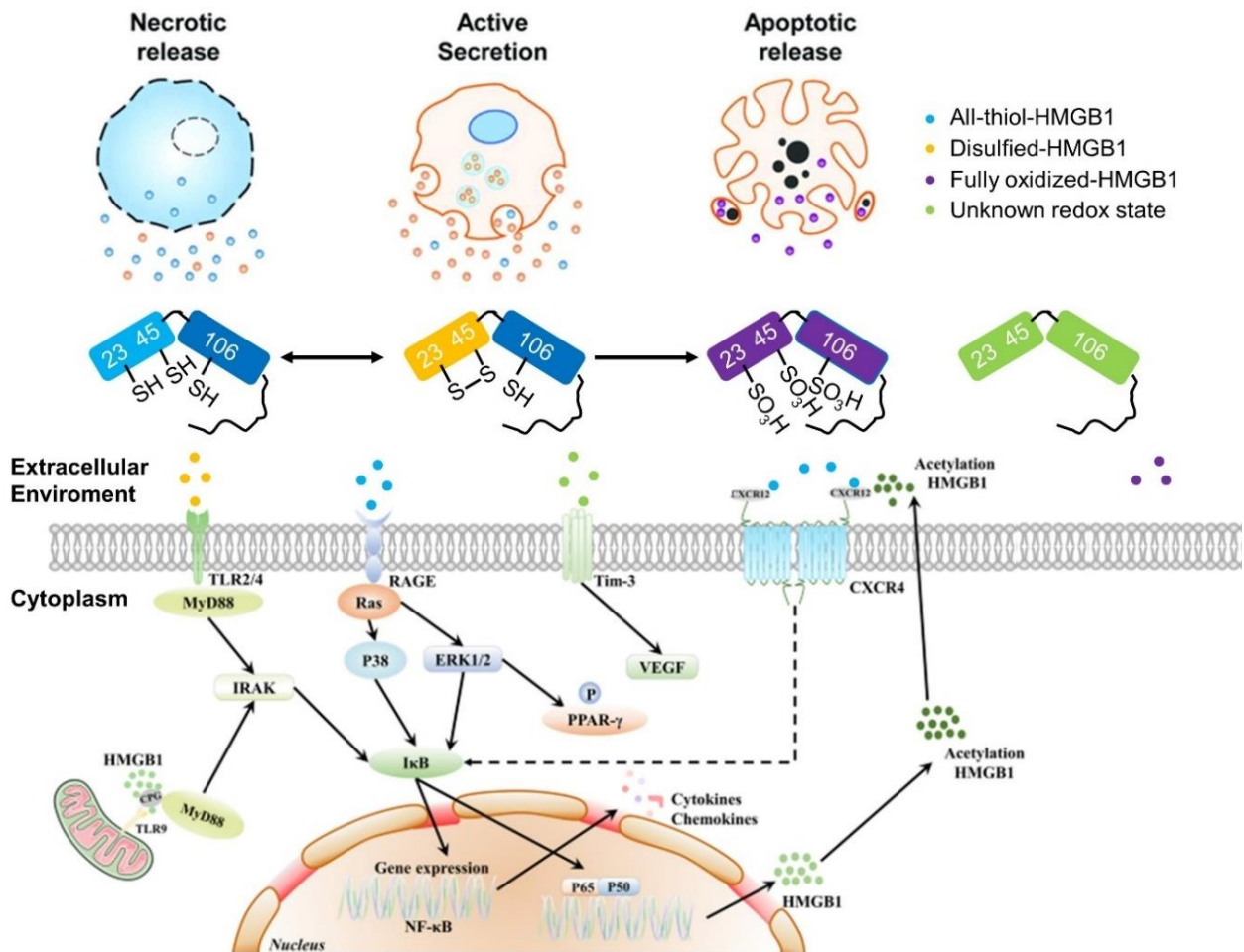
and they are able to bind DNA without sequence specificity (386). I will mainly focus on HMGB1 and its function as an alarmin.

### **HMGB1 Structure and Its Binding Partners**

HMGB1 is characterized as ubiquitous non-histone nuclear protein, which has two functional DNA binding domains, the A box and B box, and a C-terminal acidic tail that modulates the DNA binding activity. In addition, it has three conserved cysteine residues, which have functional importance (Figure 22 illustrates the structure of HMGB1) (384). HMGB1 mostly resides in the nucleus due to two nuclear localisation signals, although it also contains a nuclear export signal. Its localisation in the cytosol or nucleus is determined by its post-translational modifications and the transport proteins karyopherin- $\alpha$ 1 and chromosome-region-maintenance-1, which mediate transport to the nucleus or cytosol, respectively (384). HMGB1 can undergo various post-translation modifications, such as acetylation, phosphorylation, ADP-ribosylation, methylation and oxidation, which increase its cytoplasmic accumulation and extracellular secretion. However, the best-characterized modification is oxidation (384, 387). HMGB1 has three conserved cysteine residues (Cys23, Cys45, and Cys106) in its functional domain and can take three forms: all-thiol, disulphide and fully oxidized (384). The oxidative state of HMGB1 is important as it determines the interaction with its receptors and its DNA-binding affinity (384). Intracellular all-thiol is usually located in the nucleus whereas disulfide is found in the cytosol. Extracellular HMGB1 can take all three forms where all-thiol and disulfide HMGB1 take part in signalling from PPRs, whereas fully oxidized HMGB1 is inert inducing immune tolerance (Figure 23) (384).



**Figure 22: HMGB1 structure** (adapted from (384)). HMGB1 structure illustrating two functional DNA binding domains designated A box and B box, and a C-terminal acidic tail, which is flexible allowing modularly ability. HMGB1 is a multi-binding protein, which interacts with both intracellular and extracellular partners and surface receptors. Intracellular HMGB1 is able to interact with Beclin-1 and p53, regulating autophagy and apoptosis. Extracellular HMGB1 can interact with partners, such as LPS, heparin, ITA, C1q, IL-1 $\beta$ , CXCL12, ssDNA and nucleosomes. Finally, HMGB1 is able to engage different receptors, including receptor for advanced glycation endproducts (RAGE), TLR2, TLR4, TLR9 and CD24-Siglec10.





**Figure 23: HMGB1 redox status mediates different biological effects by interacting with different receptors** (adapted from (384, 388)). HMGB1 can be passively released by necrotic or apoptotic cells or actively secreted from activated immune cells or stressed cancer cells. Dependent of its redox state, HMGB1 mediated different functional effects. Some of the most important receptors and their simplified signalling pathways are illustrated here. All-thiol (reduced) HMGB1 can interact with CXCL12 and engage CXCR4 to promote **chemotaxis and recruitment of inflammatory cells**. All-thiol form of HMGB1 can directly engage the RAGE receptor to induce **autophagy and pro-inflammatory cytokines**. Disulfided (semi oxidised) HMGB1 can directly bind to TLR4 to promote production of **pro-inflammatory cytokines**. HMGB1 has also been shown to bind to TLR2, TLR9 and Tim-3, although the redox form of HMGB1 upon interaction with these receptors has not been identified. Like with RAGE and TLR4, engagement of TLR2 and TLR9 activates NFκB, which induces **production of inflammatory cytokines**. When HMGB1 interacts with Tim-3, it has been shown to prevent binding of nucleotide and thus **inhibiting nucleic acid-mediated immune response as well as inducing production of VEGF, promoting angiogenesis**. Apoptosis promotes mitochondrial ROS and release of oxidized HMGB1. Fully oxidized (sulfonate cysteines) HMGB1 is immunological inert and thus mediates **immune tolerance**. HMGB1 can undergo post-translational modification, such as acetylation and oxidation, which increases its cytoplasmic accumulation and extracellular secretion.

HMGB1 has both intercellular and extracellular binding partners and can by itself interact with a number of receptors, but in complex with binding partners, it can engage other receptors. Thus, the possible functional effect of HMGB1 is vast (384, 387). Table 1 and Figure 23 list a short overview of some of the biological effects of HMGB1. In the next part, I will mainly focus on extracellular HMGB1 and its function as an alarmin.

Ligand/ligand complex	Receptor	Functional effect
<b>Extracellular</b>		
HMGB1	TLR4/MD2/CD14 complex	Acting as a cytokine promote activation of macrophages and induce secretion of pro-inflammatory cytokine (387, 389, 390). This occurs due to activation of transcription factors, in particular NFκB (350, 387, 391).
HMGB1	TLR2	Increases activation of NFκB and enhanced expression of pro-inflammatory cytokines (350, 387, 391).
All-thiol HMGB1	RAGE	Regulates cell migration by activating Rac1/CDC42 inducing cytoskeletal changes as well as promoting inflammation by activation of NFκB and mediates expression of MMPs such as MMP2 and MMP9 (387, 392).  Promoting autophagy in Beclin-1 dependent manner (387, 393).

HMGB1	TIM-3	On tumour-infiltrating DCs, Tim-3 compete with nucleic acid for binding to A box of HMGB1 and interfere with HMGB1-dependent transfer of nucleic acid to the endosome thereby suppress the nucleic acid-mediated immune response. This is particularly important as it was shown to diminish chemotherapy-induced anti-tumour response by circumventing the nucleic acid-mediated innate immune pathways (227). HMGB1 induces secretion of VEGF from AML cells and possibly promote angiogenesis (350).
HMGB1 complex with CXCL12	CXCR4	Promotes the recruitment of inflammatory leukocytes, such as monocytes (394).
HMGB1-CD24	Siglec-10	Selectively represses tissue damage-induced inflammation (384).
HMGB1 complex with nucleic acid	TLR3, TLR7, TLR9	Activating nucleic acid-mediated innate immune response and enhance cytokine production (227, 395-397).
<b>Cytoplasmic</b>		
HMGB1	Beclin-1	Inducing autophagy and inhibiting apoptosis, by attenuating interaction of Beclin-1 and Bcl-2 (398, 399).
<b>Nuclear</b>		
HMGB1	p53	Increases nuclear accumulation of p53/HMGB1, and possibly assist in p53-mediated damage response (400).

**Table 1:** List of some of the HMGB1 mediated biological effects, upon interaction with different proteins both in the nucleus, cytosol and extracellular.

Extracellular HMGB1 has been identified as an alarmin, which can be actively secreted from immune cells and stressed cancer cells, or passively released from damaged/dying cells (387). Furthermore, autophagy promotes the release of HMGB1 (393, 401). In many cancer settings, HMGB1 has been shown to be overexpressed, and here it may either promote or limit cancer growth.

### **HMGB1 as an Alarmin that Limits Tumour Growth**

In addition to directly killing cancer cells by conventional anti-cancer therapies, such as chemotherapy and radiotherapy, HMGB1 can promote ICD, which elicits an anti-tumour response that can clear or control remaining tumour cells, and thus improve the efficacy of the treatment. I have already described ATP as a "find me" signal, and its stimulatory effect on immune cells by activating the inflammasome along with CRT as an "eat me" signal, which is only exposed in association with ICD. Apetoh et al. conducted further experiments. They have shown that TLR4-deficient mice and/or depletion of DCs resulted in abrogation of T cell priming and TLR4-deficient DCs failed to activate T cells. This suggests that TLR4 expressing DCs are required for activating the immune response upon chemotherapy/radiotherapy (402). Furthermore, they found that endogenous HMGB1 was released by dying tumour cells following anti-cancer treatment, and it could bind to TLR4 on DCs and invoke an anti-tumour response. Downstream signalling from TLR4 can induce TIR-domain-containing adapter-inducing interferon- $\beta$  (TRIF)-dependent or myeloid differentiation primary response 88 (MyD88)-dependent signalling. They found that the MyD88 pathway was required for this response as MyD88<sup>-/-</sup> DCs had a similar phenotype to TLR4<sup>-/-</sup> DCs. In DCs, TLR4-MyD88 signalling regulates processing and antigen-presentation of tumour-antigens by inhibited lysosomal dependent degradation of the phagosome and preventing the destruction of the antigens (402). The importance of HMGB1 was illustrated by a knockdown experiment with siRNA and a neutralization experiment with antibodies targeting HMGB1. Both experiments resulted in the attenuation of the capacity of DCs to mediate antigen-presentation. These results indicate that HMGB1 is a DAMP required for ICD to promote anti-tumour response (402).

Besides assisting in antigen processing and presentation by DCs, extracellular HMGB1 has been shown to be able to stimulate DC maturation and secretion of pro-inflammatory cytokines, such as IL-12, and thus promoting Th1 polarization. Although, receptor engagement to mediate DC maturation was not studied, they showed that these changes were mediated by an NF $\kappa$ B-independent and p38 mitogen-activated protein kinases (p38)-dependent mechanism (403). The ability of HMGB1 to stimulate DC maturation and Th1 response may be important for anti-tumour immunity.

Nuclear HMGB1 has been shown to act as a tumour suppressor when interacting with retinoblastoma protein (Rb). HMGB1 can bind RB via an LxCxE motif-dependent

mechanism. This enhances Rb affinity of E2F and cyclin A transcriptional repression. Thus, HMGB1-Rb interaction mediates cell growth inhibition by preventing G1 cell cycle progression. Another role as a tumour suppressor is the ability of HMGB1 to participate in DNA repair and regulating telomerase, which maintains genome stability. Loss of HMGB1 results in instability of genome and leads to tumorigenesis (387, 404).

### **HMGB1 as an Alarmin that Promotes Tumour Progression**

As mentioned, HMGB1 can be released from dying cells following necrosis or apoptosis with subsequent secondary necrosis (371, 374). However, HMGB1 can also be actively secreted from immune cells and stressed cancer cells (387). I have just described HMGB1 as a DAMP associated with immunogenic cell death that promotes anti-tumour immunity induced by radiotherapy or chemotherapy. However, HMGB1 has also been reported to be involved in tumorigenesis, cancer invasion and metastasis (387). This difference might be dependent on the presence or absence of other DAMPs and receptors expressed by tumour and tumour-infiltrating immune cells.

Although, in some circumstances, HMGB1 promotes anti-tumour immune response following chemotherapy or radiotherapy. He et al. reported that HMGB1 could contribute to repopulation and cell proliferation of surviving cancer cells following irradiation. They found that this effect was mediated by HMGB1 ligation to RAGE and downstream activation of ERK and p38. Blocking of RAGE and/or HMGB1 or genetic ablated HMGB1 suppresses tumour cell proliferation (405).

As described, elevated Tim-3 expression is quite common in cancer settings on both cancer cells and immune cells. Chiba et al. reported that chemotherapy-induced anti-tumour response could be circumvented when HMGB1 engages Tim-3 on tumour-infiltrating DCs by diminishing nucleic acid-mediated innate immune response and reduces cytokine secretion due to suppressing the activation of TLR3, TLR7 and TLR9. This did not affect HMGB1 binding to TLR2 or TLR4. The mechanism is that Tim-3 competes with nucleic acid binding to the A box domain of HMGB1. Blocking of Tim-3 improved the efficacy of treatment (227).

Our group's own results showed that in AML cells, HMGB1-Tim-3 interaction could possibly promote angiogenesis by stimulating secretion of VEGF. This was Tim-3 dependent as blocking of Tim-3 results in reduced secretion. In addition, to a Tim-3-

dependent VEGF secretion, HMGB1 stimulation of AML induced activation of the PI3K-AKT-mTOR-pathway and subsequent accumulation of hypoxia-inducible factor (HIF)-1 $\alpha$ , along with an increase in TNF $\alpha$  secretion (350). Although, the TNF $\alpha$  secretion is known to be induced by NF $\kappa$ B downstream of RAGE, TLR2 and TLR4 (387, 392). In AML cells, TLR2 and TLR4 were the main contributors. TNF $\alpha$  secretion stimulates IL-1 $\beta$  secretion from healthy leukocytes, and IL-1 $\beta$  promotes production of SCF, which is crucial for proliferation of AML cells (350).

The PI3K-AKT-mTOR pathway is known to regulate multiple physiological activities, such as cell proliferation (cell cycle progression), promote autophagy and inhibit apoptosis (pro-survival) (406). Also in breast cancer, HMGB1 has been shown to promote tumour progression by inducing angiogenesis and tumour migration. This occurred by HMGB1-mediated activation of the PI3K-AKT-mTOR axis and nuclear accumulation of HIF-1 $\alpha$  with subsequent production of VEGF (407). This mechanism may be important as in the initial phase of tumour growth there is an induction of hypoxia due to the growing number of tumour cells, which also results in necrotic tumour cells that may release HMGB1. HMGB1 and hypoxia-mediated increase in HIF-1 $\alpha$  may facilitate tumour growth by angiogenesis de novo.

In lung cancer, HMGB1 promotes tumour progression by stimulating tumour migration and invasion. It was shown that HMGB1-mediated NF $\kappa$ B activation results in the production of MMP2, which aids in the degradation of ECM, leading to tumour cell invasion and metastasis (408).

Nuclear, cytoplasmic and extracellular HMGB1 can promote autophagy and inhibit apoptosis by transcription-dependent and independent pathways (409). Tumour cells have been shown to induce chemotherapy resistance by inducing autophagy (409-411). Nuclear HMGB1 has been reported to upregulate heat shock protein (HSP)27 to induce autophagy (409). Furthermore, HMGB1 can form complex with p53 to regulate autophagy and apoptosis (400). Stimuli that promote oxidative stress and enhance the production of ROS, promote cytosol translocation of HMGB1. Cytoplasmic disulfide HMGB1 is then able to induce and sustain autophagy by binding to autophagic protein Beclin-1 and displace Bcl-2 in the process, which suppress cell-death mediated by apoptosis (399). Most anti-cancer therapies, such as radiation and chemotherapeutic drugs, induce apoptosis, but also

promote autophagy while generating ROS (412, 413). HMGB1 has been shown to induce autophagy in response to oxidative stress (414). Extracellular all-thiol (reduced) form of HMGB1 has also been shown to induce the Beclin1-dependent autophagy by engaging the RAGE receptor and not TLR4. Furthermore, with the inhibition of HMGB1 release, there is a decrease in autophagy and improved treatment efficacy (393). In support of this, RAGE was shown to be an important regulator of autophagy during oxidative stress and promote pancreatic tumour cell survival by sustaining autophagy and limit apoptosis (405, 415). Moreover, in leukaemia cells, extracellular HMGB1 was shown to confer resistance to chemotherapy by promoting autophagy through the PI3K–MEK–ERK pathway (411). On the other hand, oxidized HMGB1 promotes apoptosis in cancer cells (393). Furthermore, apoptosis promotes mitochondrial ROS production, which can oxidize HMGB1 released from dying cells, this form of HMGB1 is inert promoting immune tolerance (416).

ROS does not only promote oxidative stress and release of HMGB1. HMGB1 can also promote ROS production. It has been reported that HMGB1-stimulated neutrophils caused TLR4-dependent activation of NADPH oxidase (Nox) and an increase in ROS production by both MyD88-IRAK4-p38 MAPK and MyD88-IRAK4-AKT signalling pathways (417).

Altogether, these studies demonstrate that depending on the circumstances and the oxidative milieu, dying tumour cells can promote tumour progression or promote tumour clearance by release of HMGB1.

## 2 AIMS AND OBJECTIVES

The aim of this PhD programme was to investigate the biochemical regulation of the Tim-3-galectin-9 immunosuppressive pathway in human malignant cells, such as AML and breast cancer cells, as well as healthy/non-malignant cells and elucidate the biochemical functions of its crucial components.

The following objectives were addressed in order to achieve this aim:

- 1) To study the expression and activity of the Tim-3-galectin-9 immunosuppressive pathway in human solid tumour cells in order to understand whether it is either unique for AML or ubiquitous to a variety of malignant tumours.
- 2) To study differential mechanisms that are involved in the regulation of TIM-3 and galectin-9. In particular:
  - a. Examine if and how the FLRT3/LPHN pathway regulates TIM-3 and galectin-9 in breast cancer cells as it does in AML cells.
  - b. Explore the role of oxidative stress, hypoxic and TGF- $\beta$ -dependent signalling pathways in biochemical regulation of galectin-9 expression in breast and colorectal cancer as well as AML cells.
  - c. Investigate how stressed/damaged or dying cells, which release the alarmin HMGB1, can contribute to anti-cancer immune evasion.

## 3 MATERIALS AND METHODS

### 3.1 Materials

Culture medium and reagents were purchased from Sigma-Aldrich. DOTAP liposomal transfection reagent, small interfering RNA (siRNA) for HIF-1, and random siRNA were acquired from Sigma (Suffolk, UK). Compounds used for stimulation such as cortisol, cobalt chloride, phorbol 12-myristate 13-acetate (PMA) were bought commercially. Human recombinant TGF- $\beta$ 1 was obtained from ELISA kit R&D Systems (Abingdon, UK) and human recombinant HMGB1 (350) was a kind gift from Dr Luca Varani (Institute for research in Biomedicine, Bellinzona, Switzerland).

Commercially available kits for caspase-3 colorimetric assay and ELISA-based assay kits for the detection of galectin-9, Tim-3, IL-2, IFN $\gamma$ , TNF $\alpha$ , and TGF $\beta$ 1 were purchased from R&D Systems (Abingdon, UK). Substrate for granzyme B (Ac-IEPD-AFC) was acquired from Sigma (Suffolk, UK). These techniques, as well as Bradford, were run in 96-well flat-bottom plates either polystyrene (PS) or poly-d-lysine (PDL) from Greiner bio-one and Oxley Hughes Ltd, respectively.

Antibodies for Western blotting were purchased from different companies. The following primary antibodies directed at different targets were acquired from Abcam (Cambridge, UK): mouse monoclonal antibody TLR4 (ab22048), TLR2 (ab9100), HIF-1 $\alpha$  (ab1),  $\beta$ -actin (ab3280), as well as rabbit polyclonal antibody against galectin-9 (ab69630), RAGE (ab3611), ATF-2 (ab47476), and rabbit monoclonal antibody targeting phosphor-smad3 (ab52903) and  $\beta$ -actin (ab179467). Phospho-ATF-2 (9225) rabbit polyclonal antibody was acquired from Cell Signaling. Mouse monoclonal antibody against FLRT3 (Sc-514482) was obtained from Santa Cruz Biotechnology.  $\beta$ -actin (66009-1-Ig) mouse monoclonal antibody was purchased from Proteintech. The polyclonal rabbit anti-peptide antibody, (PAL2) against LPHN2 (418) and Anti-Tim-3 mouse monoclonal antibody (226) were gifted from Professor Yuri Ushkaryov and Dr Luca Varani, respectively. Secondary Goat anti-mouse and goat anti-rabbit fluorescence dye-labelled antibodies were obtained from LICOR.

All other chemicals purchased were of the highest grade of purity and commercially available from either Sigma-Aldrich or Thermo Fisher Scientific.



## 3.2 Cell Lines, Primary Cells, and Primary Tissue

### 3.2.1 Cell Lines

All cultured cells were kept 37°C and 5% CO<sub>2</sub>.

Jurkat T, THP-1, Colo-205 and MCF-7 cells were obtained from the European Collection of Cell Cultures and HaCaT non-malignant keratinocytes from CLS Cell Lines Service GmbH. All of them were cultured in RPMI-1640 medium containing 2 g/L glucose, 0.3 g/L L-glutamine and supplemented with 10% foetal bovine serum (FBS) and 1.5% penicillin/streptomycin (P/S) (penicillin (50 IU/mL) and streptomycin sulphate (50 µg/mL)).

TALL-104 cytotoxic T lymphocytes derived from human acute lymphoblastic leukemia (ALL) were purchased from the American Tissue Culture Collection. They were cultured in Iscove's Modified Dulbecco's medium with the addition of 100 units/mL recombinant human IL-2; 2.5 µg/mL human albumin; 0.5 µg/mL D-mannitol and FBS to a final concentration of 20%.

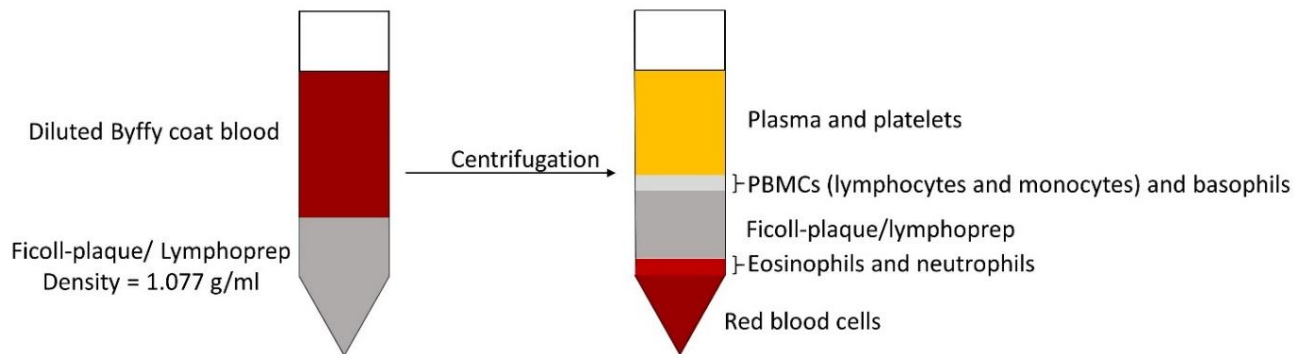
### 3.2.2 Primary Cells

Primary human keratinocytes isolated from cleft lip palate patients (children) were gifted from Elizaveta Fasler-Kan and Steffen Berger affiliated with the Department of Pediatric Surgery, Department of Biomedical Research, Children's Hospital, Inselspital, University of Bern, Switzerland. Isolation of human keratinocytes was approved by the Kantonale Ethikkommission of Bern, Switzerland, protocol number 2017-01394). Written informed consent was obtained from the parents of the children involved (419). The primary keratinocytes were cultured in keratinocyte basal serum-free medium (KSFM, Gibco), supplemented with epidermal growth factor (EGF), bovine pituitary extract, 1.5% P/S and 30 mM calcium chloride (CaCl<sub>2</sub>).

Primary human AML plasma samples and cells were obtained from the sample bank of the University Medical Centre Hamburg-Eppendorf (Ethik-Kommission der Ärztekammer Hamburg, reference: PV3469). Primary AML cells were incubated in RPMI1640 medium containing 10% FBS and 1.5% P/S. Both the primary keratinocytes and AML cells were kept at 37°C and 5% CO<sub>2</sub>.

Buffy coat blood samples from healthy donors were obtained from the National Health Blood and Transfusion Service (NHSBT, UK) following ethical approval (REC

reference:16-SS-033). The buffy coats were used to isolate primary human leukocytes (PHL). Isolation of PHL was performed by enrichment of peripheral blood mononuclear cells (PBMCs) using density gradient centrifugation with Ficoll-Plaque or lymphoprep (Figure 24). From the first step of the enrichment process plasma samples from healthy donors were obtained



**Figure 24: Density gradient centrifugation.** Lymphoprep and Ficoll-Paque-Plus have a density of 1.077 g/mL. A density gradient centrifugation will result in three layers, a bottom layer of erythrocytes and granulocytes, an intermediate layer of PBMCs and an upper layer of plasma (420, 421).

### 3.2.3 Primary Tissue

Primary human breast tumour tissue (BT) samples and paired peripheral tissues (also called “normal” or “healthy” breast tissue (HT)) of the same patients were collected surgically from breast cancer patients treated at the Colchester General Hospital, following informed, and written consent obtained before surgery. HT was selected at a safe distance from the site of the matching primary tumour; these tissues were microscopically inspected to confirm normal histology. Blood samples were also collected before breast surgery from patients with primary breast cancer (PBC) and before treatment from patients with metastatic breast cancer (MBC). Samples from healthy donors (individuals with no diagnosed pathology) were collected and used as control samples. “Blood separation was performed using buoyancy density method employing Histopaque 1119-1 (Sigma, St. Louis, MO) according to the manufacturer's protocol. Ethical approval documentation for these studies was obtained from the NRES Essex Research Ethics Committee and the Research & Innovation Department of the Colchester Hospitals University, NHS Foundation Trust [MH 363 (AM03) and 09/H0301/37]” (326).

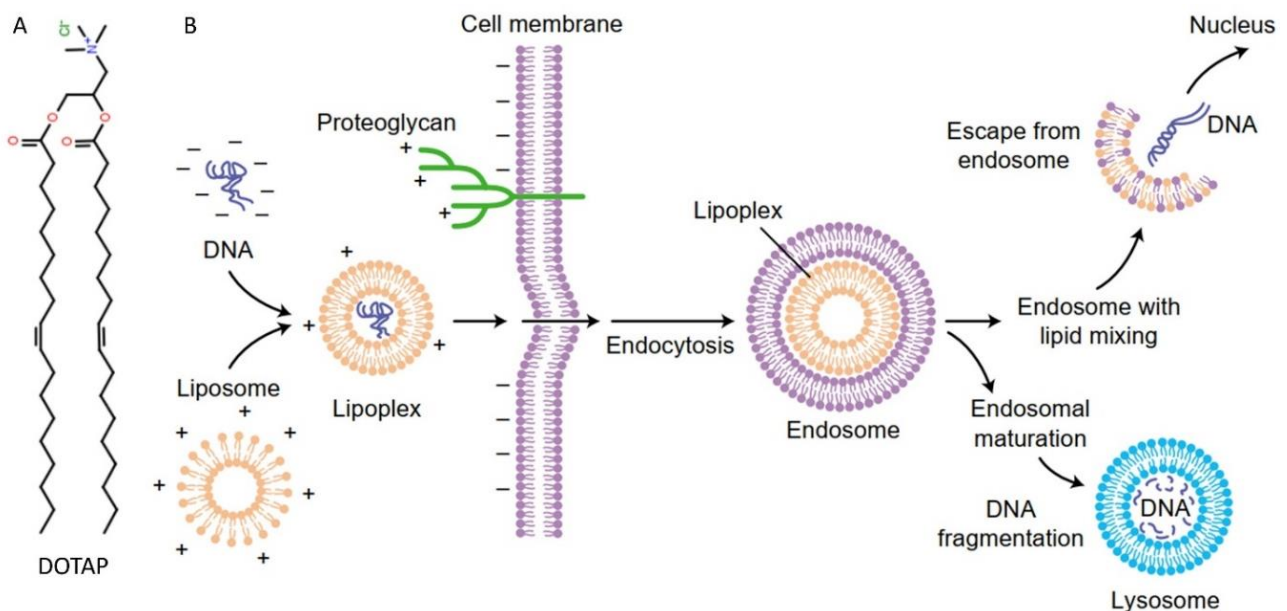
### 3.3 DOTAP Transfection

Transfection is a process in which DNA or RNA is introduced to eukaryotic cells. There are different ways to accomplish this, such as lipofection, which is applied in this study. For

lipofection (liposome transfection), the cationic-lipid DOTAP reagent (1,2-dioleoyl-3-trimethylammoniumpropyl chloride) was applied to introduce the siRNA.

Principle for lipofection is illustrated in Figure 25. The cationic-lipids form liposomes in aqueous solution and mixed with RNA (or DNA) they interact and form complexes known as lipoplexes. These lipoplex complexes are taken up by the cell either through fusing with the cell membrane or by endocytosis (422-424).

Firstly, the lipoplexes are formed by mixing reagent A (5  $\mu$ l of HIF-1 $\alpha$ , Smad3 or Random siRNA, in 50  $\mu$ l of 1M HEPES) and reagent B (30  $\mu$ l DOTAP reagent in 70  $\mu$ l of 1M HEPES) and left for 30 min at room temperature (RT). Then for each small culture dish with 2 mL of medium, 30  $\mu$ l of the lipoplex mixture were added and the cell culture was incubated overnight at 37°C with 5% CO<sub>2</sub>. The next day the medium was changed with treatment.



**Figure 25: Lipofection** (adapted from (422)). (A) Chemical structure of the cationic-lipid transfection reagent 1,2-dioleoyl-3-trimethylammoniumpropyl chloride (DOTAP) (423). (B) Schematic illustration of Lipoplex-mediated transfection and endocytosis (422). The lipoplex complex structure (consisting of liposomes and DNA) fuse with the cell membrane where it is internalised by endocytosis, resulting in the formation of a double-layer inverted micellar vesicle. During the maturation of the endosome into a lysosome, the endosomal wall might rupture, releasing the contained DNA into the cytoplasm and potentially towards the nucleus. DNA imported into the nucleus might result in gene expression. Alternatively, DNA might be degraded within the lysosome (422). In this study, siRNA is transfected instead of DNA and this is accumulated in the cytosol where it causes gene silencing when interacting with the RNA-inducing silencing complex (RISC). The chemical structure was drawn in ChemSpider.

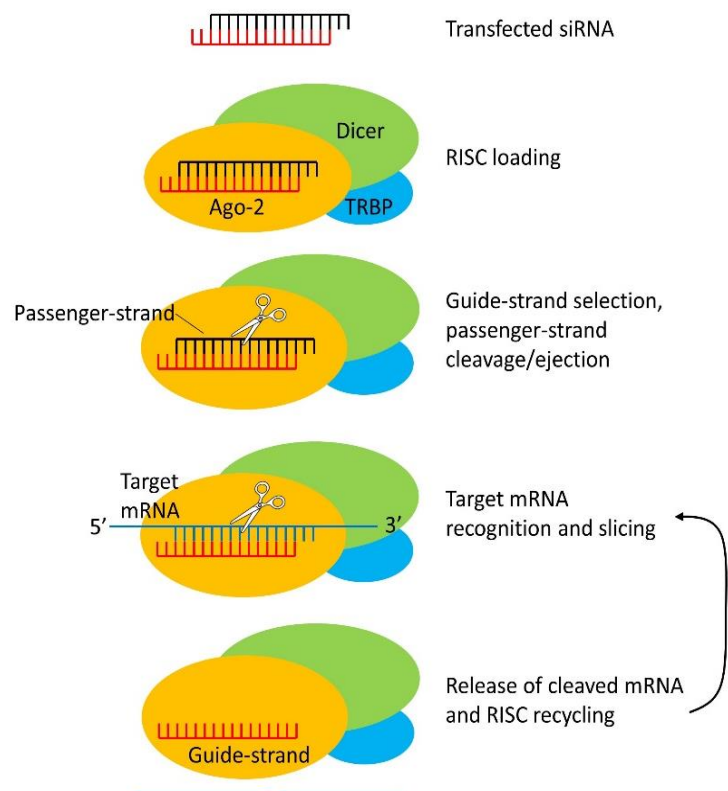
### 3.3.1 Plasmid Transfection with Dominant-negative ASK1 or Constitutive Active TLR4

Plasmid encoding hemagglutinin (HA)-tagged human ASK1 with kinase-dead domain (dominant-negative form),  $\Delta$ N-ASK1, was a kind gift of Professor Ichijo (University of Tokyo, Tokyo, Japan). Plasmid encoding constitutively active human TLR4 (murine CD4 fused to human TLR4) was generously provided by Professor Medzhitov (Yale University, New Haven, USA). Both plasmids were amplified using *E. coli* XL10 Gold® (Stratagene Europe, Amsterdam, The Netherlands) and isolated/purified using the GenElute™ plasmid purification kit according to the manufacturer's protocol. Purified plasmids and empty vectors as control were then transfected into THP-1 and/or Colo-205 cells using DOTAP transfection as described above (425).

### 3.3.2 Gene Knockdown

Gene knockdown is an experimental technique to reduce gene expression (gene silencing). There are different techniques to accomplish this. In this study, RNA interference (RNAi) is used with the means of small double-stranded (ds) interfering RNAs (siRNA) to knockdown HIF-1 $\alpha$  and Smad3.

The silencing process with siRNA is depicted in Figure 26. Once the siRNA is inside the cell, it is processed by RNA-inducing silencing complex (RISC), which is composed of Dicer, transactivating response RNA-binding protein (TBRP) and Argonaute-2 (Ago-2). TBRP contains the dsRNA binding domains which aid in binding and loading the RNA to Dicer and Ago-2. Dicer is an RNA III endonuclease that processes the long dsRNA into small dsRNA fragments of 21-25 nucleotides (nt), which is referred to



as siRNA (however, here siRNA is transfected directly). Ago-2 cleaves the passenger-strand which is then discarded, and the guide-strand of the siRNA is used to cleave sequence-specific complementary

**Figure 26: Schematic illustration of gene knockdown with RNAi.** Transfected siRNA is loaded on to Ago-2 in the RISC. Once loaded the passenger-strand is discarded and the remaining strand is used as the guide-strand to find and cleave mRNA with complementary sequence (424, 426).

mRNA with its RNase-H-like activity. The cleaved mRNA is no longer protected and will quickly degrade (424, 426, 427).

### 3.3.2.1 Knockdown of HIF-1 $\alpha$ and Smad3 by DOTAP-transfected siRNA

HIF-1 $\alpha$ , Smad3 and/or Random siRNA were transfected into MCF-7 cells using DOTAP transfection reagent.

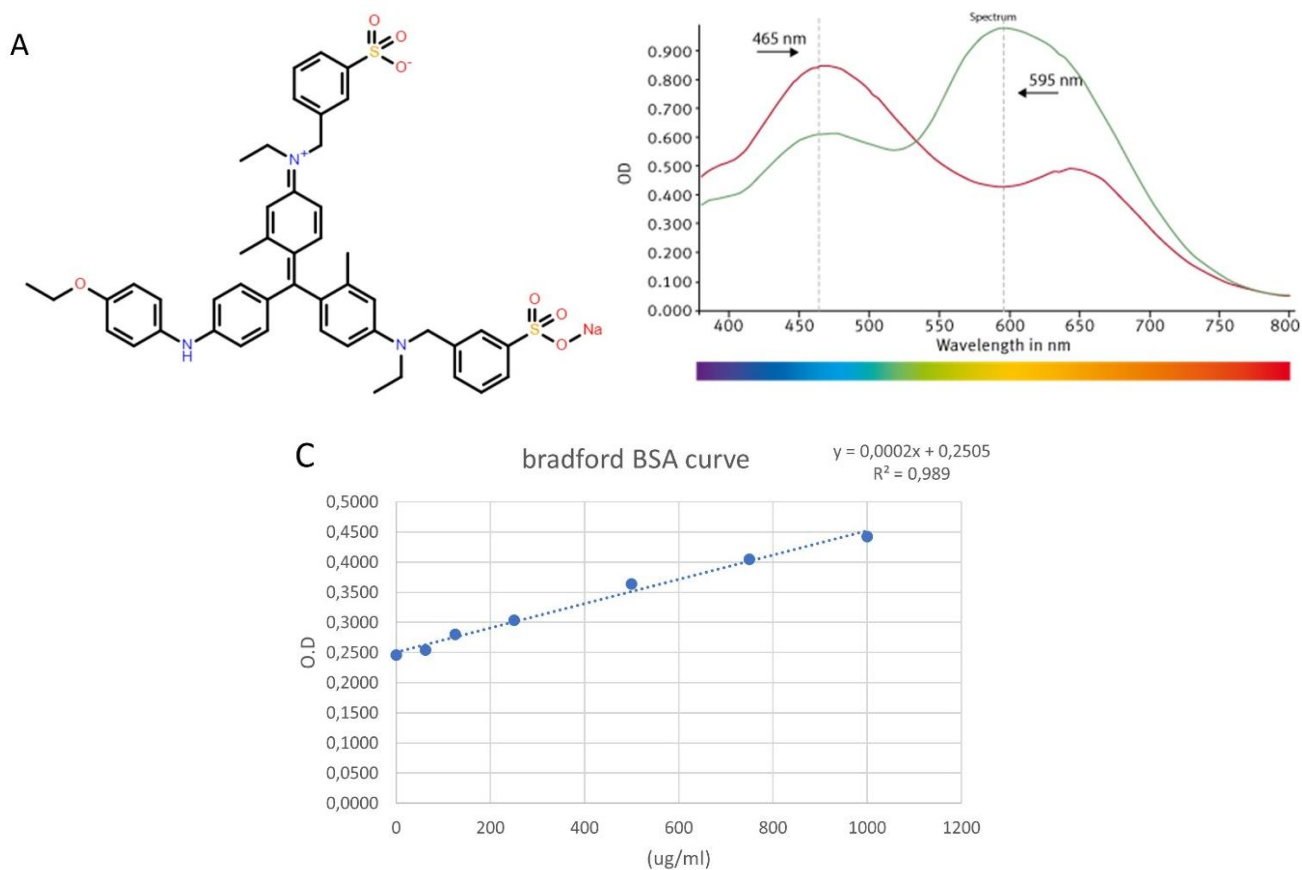
A HIF-1 $\alpha$ -specific siRNA target sequence (ugu gag uuc gca ucu uga u dtdt), which was localised at position 146 bases downstream of the HIF-1 $\alpha$  start codon, was employed.

Smad3 siRNA was a commercially available reagent purchased from Ambion (ID 107876) through Thermo Fisher Scientific (Waltham, Massachusetts, USA).

For all knockdown experiments, random siRNA with the following sequence (uac acc guu agc aga cac c dtdt) was used as a negative control.

## 3.4 Protein Quantification

The method used for protein quantification is called Bradford assay or sometimes Coomassie assay. The method was first described in 1976 by Bradford hence its name (428). It allows the quantification of the protein due to a shift in the absorption maximum of the dye (Coomassie Brilliant Blue G-250) from 465 nm to 595 nm, from red to blue, upon binding with protein (Figure 27). Mix 5  $\mu$ L cell lysate or protein standard which in this case is bovine serum albumin (BSA), with 150  $\mu$ L of Bradford reagent (0.01% (w/v) Coomassie Brilliant Blue G-250, 4.7% (w/v) ethanol, and 8.5% (w/v) phosphoric acid) and incubated for 10 min in a 96-well plate. The optical density (OD) is ideally measured at 595 nm, however, variation is allowed for microplate readers, although this will decrease the sensitivity (429). Here OD was read at 620 nm in the plate reader. A BSA standard curve was used to determine the protein concentration of the sample. If sample OD values were out of linear range, the samples were diluted in either PBS or lysis buffer. Protein concentration was then used for normalization of granzyme B, caspase 3, Nox, Xanthine oxidase (NOD), TBRS, and ELISA assay when counting of cells was not possible.



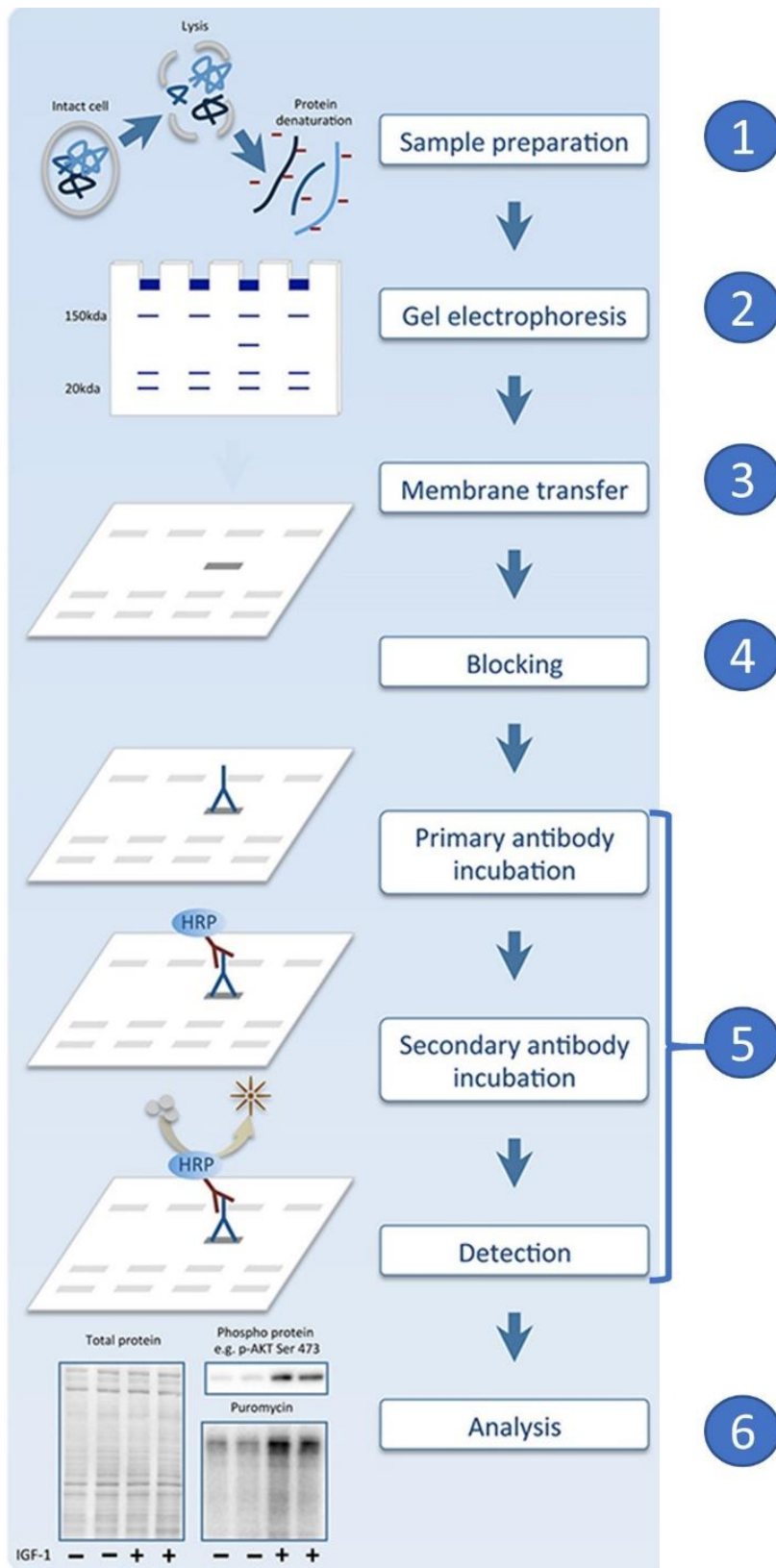
**Figure 27: Chemical structure and spectrum of Coomassie Brilliant Blue G-250 (adapted from (430)).** (A) Chemical structure of Coomassie Brilliant Blue G-250. (B) The spectrum from unbound (red line) and protein-bound (green line) Coomassie Brilliant Blue. After binding the absorbance maximum of the dye shifts from 465 nm to 595 nm (430). (C) An example of BSA standard curve, which is used to calculate the protein concentration from an unknown sample. The chemical structure was drawn in ChemSpider

### 3.5 Western Blot Analysis

Western blot (WB), also known as immunoblotting is a semi-quantitative process that has diverse application for investigating regulatory molecular processes in physiological, pathological and experimental conditions, such as relative protein abundance, cellular localization, protein-protein interaction (Co-Immune precipitation) and post-translational modification (like phosphorylation, and glycosylation etc.) (431). The underlying principle for the process is that: Proteins are separated electrophoretically according to their size, and then the specific protein of interest can be identified using antibodies. This technique has multiple steps: 1) extraction of cellular proteins and sample denaturation in sample buffer, 2) running evenly loaded samples (determined by Bradford) on sodium dodecyl sulphate polyacrylamide gel electrophoresis (SDS-PAGE), 3) semi-dry or wet transfer, 4) blocking the membrane to avoid unspecific binding of antibodies, 5) detection (using primary and secondary antibodies) and imaging, and 6) Quantification using densitometry

software and analysis (431). The whole WB process is outlined in Figure 28, and in the subsections below, each step is explained in more details.

The components of the Tim-3-galectin-9, FLRT3-LPHN, HMGB1 and TGF- $\beta$  signalling pathways were detected in cell and tissue lysates by WB, and the relative protein expression was determined by normalization to the levels of housekeeping protein,  $\beta$ -actin, to confirm equal protein loading.



**Figure 28: The sequential stage of the western blot process** (adapted from (431)). 1) Sample preparation, 2) SDS-PAGE, 3) transfer, 4) blocking, 5) detection and imaging, and 6) quantitative analysis. Here is shown enhance chemiluminescent detection (ECL) with horseradish peroxidase (HRP), however, in this study, fluorescent detection was used.



### 3.5.1 Sample Preparation

#### 3.5.1.1 Cell Lysates

The cells were incubated according to the indicated time points in the results section. After incubation, the cells were harvested and centrifuged for 5 min at 232g (1200 rpm). The media was collected and stored at -20°C until further use, and the pellet was re-suspended in cell lysis buffer, a slightly modified NP-40 lysis buffer (432) (50 mM Tris-HCl, 5 mM Ethylenediaminetetraacetic acid (EDTA), 150 mM NaCl, 0.5% Nonidet-40, 1 mM phenylmethylsulphonyl fluoride (PMSF – a serine protease inhibitor), pH 8.0). The samples were incubated on ice for 60 min with mixing every 10 min. On occasion when interested in transcription factors, samples during lysis also underwent sonication. When lysis was completed, the samples were centrifuged 5 min at 13,200 rpm and used straight after or stored at -20°C until future use. The cell lysis buffer is gentler, and thus maintains enzyme activity, furthermore, it is effective for extracting water-soluble proteins.

#### 3.4.1.2 Tissue Lysates

Depending on the proteins of interest the primary tissues were lysed in tissue lysis buffer (for Tim-3 and galectin-9) or cell lysis buffer (PKC $\alpha$ , PLC-1, XOD, Nox, TBRS, Smad3, and ATF-2). The cell lysis buffer is gentler and thus keeps enzyme activity, furthermore, it is good for extracting water-soluble proteins.

Tissue lysis procedures were described in our recent publication (326): “Briefly, 100 mg of frozen tissues were grounded into a powder in dry ice, followed by the addition of 100  $\mu$ L of the tissue lysis buffer (20 mM Tris/HEPES pH 8.0, 2 mM EDTA, 0.5 M NaCl, 0.5% sodium deoxycholate, 0.5% Triton X-100, 0.25 M Sucrose, supplemented with 50 mM 2-mercaptoethanol, 50  $\mu$ M PMSF, 1  $\mu$ M pepstatin supplied just before use). Tissues were homogenized using a Polytron Homogenizer (Capitol Scientific, USA), and a syringe was used to acquire a homogenous cell suspension. These tissue suspensions were then filtered through medical gauzes and centrifuged at +4°C at 10,000 g for 15 min. Proteins present in supernatants were precipitated by incubation of the samples on ice for 30 min with equal volumes of ice-cold acetone. Protein pellets were obtained by centrifugation at +4°C, 10,000 g for 15 min followed by air drying at RT and then lysed” (326).

Primary tissues lysed with cell lysis buffer were weighed and homogenized mechanically on dry ice. When the tissue pieces were small enough cell lysis buffer was added (9 times

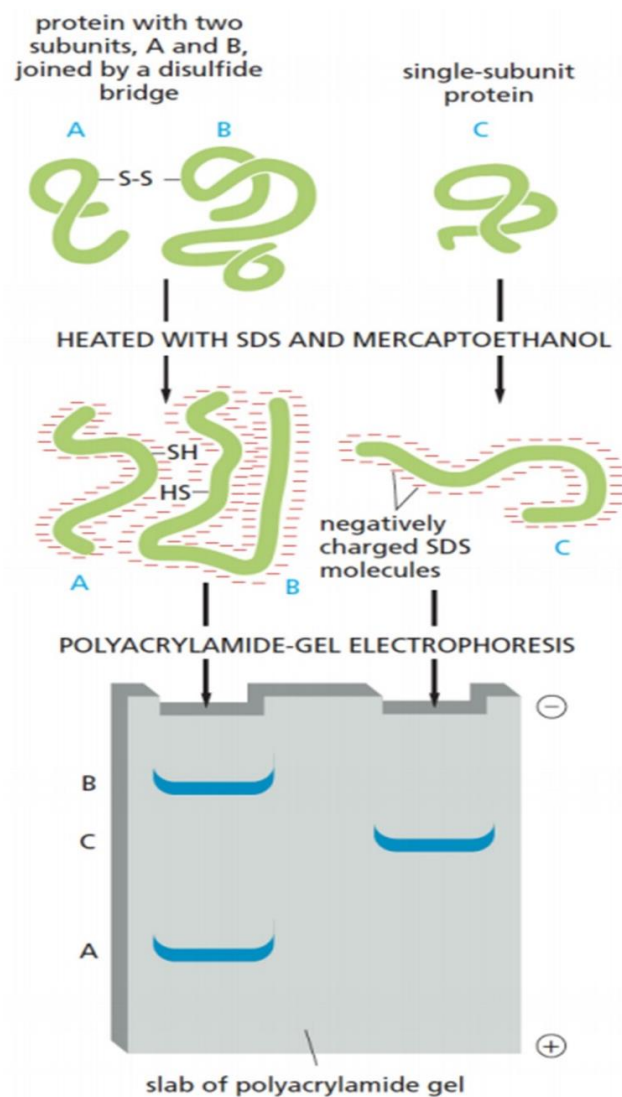
more than the tissue weight) and the sample was placed on ice. The rest of the process was similar to cell lysis described in Section 3.5.1.1.

### 3.5.2 SDS-PAGE

The mixture of proteins in the cell or tissue lysate was then separated according to their molecular weight using discontinuous Tris-glycine SDS-PAGE system (431, 432). To do this, lysates depending on the protein concentration were first prepared in 2x or 4x “home-made” Laemmli sample buffer containing Tris-HCl, SDS, glycerine/glycerol, dithiothreitol (DTT), and bromophenol blue (for recipe see Appendix 7.6.1) and boiled for 5 min at 95°C for denaturation. During denaturation, the reducing agent DTT cleaves disulphide bonds (S-S bonds), destabilizing the secondary and tertiary structure and helps to unfold the protein, while SDS is an anionic (negatively charged) detergent that binds to the primary structure of proteins (in the ratio 1.4 g per 1 g of protein). The process allows the proteins to be in their primary amino acid structure with the

same charge-to-mass ratio, so they can migrate through an electric field from the cathode (negative pole) to anode (positive pole) according to their molecular weight as shown in Figure 29 (431).

The discontinuous Tris-glycine SDS-PAGE system used, is comprised of a 4% Tris-HCl stacking gel (pH 6.8), and Tris-HCl separation gel (pH 8.8) (for preparation of the gel see



**Figure 29: Principle of SDS-PAGE** (adapted from (433)). In this study, DTT was used as a reducing agent instead of  $\beta$ -mercaptoethanol.

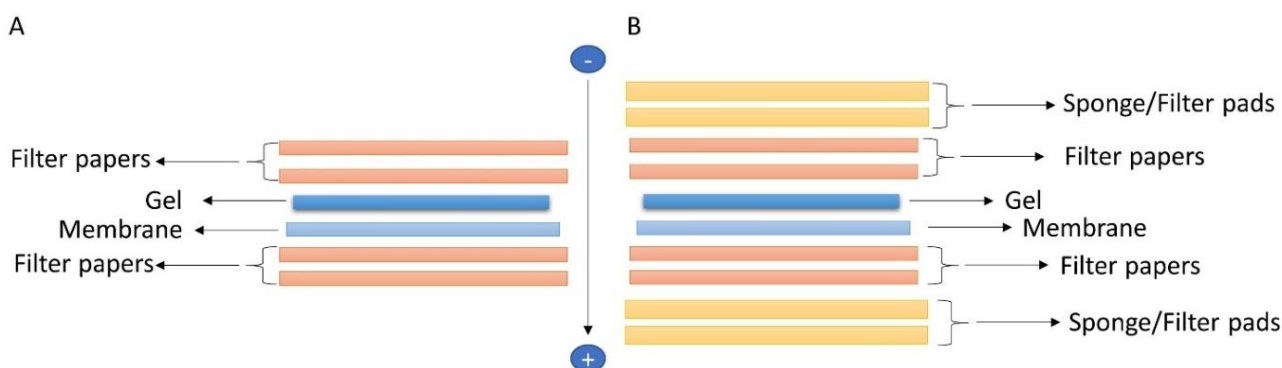
Appendix 7.6.2). Separation gel percentage was chosen according to the molecular weight of the target protein:

Protein target, (kDa)	>250	90-250	50-90	20-50	<20
Gel%	5	7.5	10	12	15

Gels were casted using either the BioRad or the Invitrogen system depending on the volume of the protein sample that was loaded, max 20  $\mu\text{L}$  or 40  $\mu\text{L}$  respectively. The gel or gels were placed in the gel tank and submerged in running buffer (for recipe see Appendix 7.6.1) and WB samples together with a pre-stained protein marker (for recipe see Appendix 7.6.1) were loaded in the wells of the gel. Empty lanes were loaded with sample buffer diluted in lysis buffer. A constant voltage (V) of initial 50 V was applied for the first 10 min, then 150 V for the main part, and at the end, 200 V were applied for 3-5 min until the dye front was at the bottom of the gel.

### 3.5.3 Transfer

After performing SDS-PAGE, the separated proteins in the gel were electrophoretically blotted on to a nitrocellulose membrane using semi-dry (BioRad system) or wet (Invitrogen system) transfer at constant voltage and 0.07 Amp (semi-dry transfer) or 0.1 Amp (wet transfer) for about 1 h. Filter paper and/or filter pads together with nitrocellulose membrane were soaked in transfer buffer and assembled with the gel into a sandwich as illustrated in Figure 30. For semi-dry transfer, the sandwich was placed directly in the transfer machine, whereas in wet transfer, the sandwich was assembled in the blotting module, which then was positioned in the gel tank and then immersed with transfer buffer.

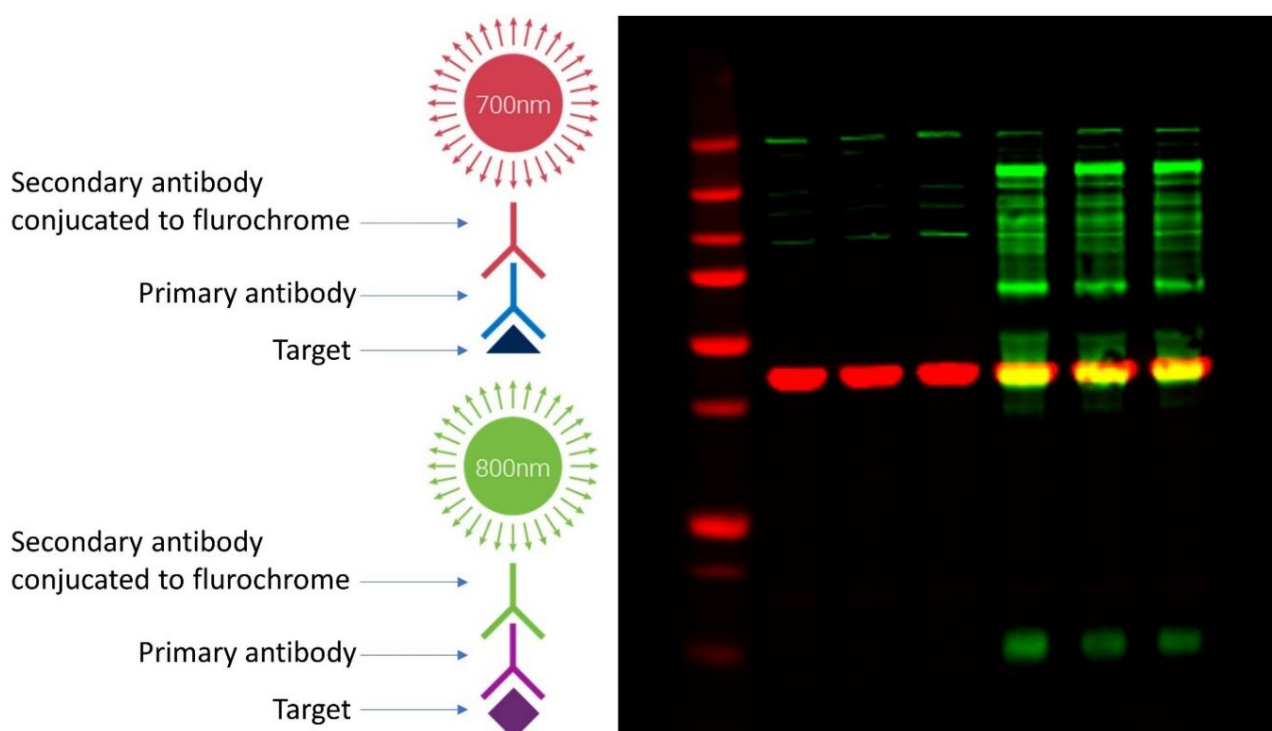


**Figure 30: Schematic representation of the sandwich assembly in (A) semidry and (B) wet transfer.** For semi-dry transfer, the sandwich is placed directly in the transfer machine, whereas in wet transfer, the sandwich is assembled in the blotting module, which is positioned in the gel tank and then immersed with transfer buffer.

### 3.5.4 Blocking, Detection and Imaging

All incubations were under constant agitation at RT, except for overnight incubation, which occurred 1 h at RT, and then left in the fridge overnight at 4°C and again the following morning for 30-60 min at RT.

After transfer, the membrane was washed in TBST (tris-buffered saline, 0.1% Tween 20 (TBST) striving to remove the remaining gel pieces that could disturb quantification. Then, the membranes were blocked with blocking buffer (2% BSA in TBST) for 1 h at RT. The primary antibody for the target protein was diluted in blocking buffer, added to the membrane, and incubated for at least 2 h at RT or overnight at 4°C. This was followed by washing the membrane with TBST 3x5 min. Li-Cor goat secondary antibodies, conjugated with fluorescent dyes, were diluted in blocking buffer and incubated for 1 h and again followed by a wash procedure for 3x5 min. Upon completion, the membrane was scanned using the SA or Clx Odyssey imager from Li-Cor to visualise the proteins of interest. The machine has a 685 nm (red) and a 785 nm (green) laser, and when the laser hit the fluorophore of IRDye 680RD or IRDye 800CW, there is an emission signal at 700 nm and 800 nm, respectively ( Figure 31).



**Figure 31: Multiplex detection using a near-infrared (NIR) fluorescent WB** (adapted from LI-Cor's webpage). Secondary antibodies IRDy680RD = red, and IRDye800CW = green detect the fluorescent signal at 700 nm and 800 nm, respectively. Yellow depicts overlapping signal between the green and red channel (434).

Some membranes were stripped using a ReBlot™ Plus Kit (Chemicon International) according to the manufacturer's protocol or with "home-made" stripping buffer (Appendix 7.6.1). Membranes were then blocked and scanned using the Li-Cor Odyssey imaging system to ensure that the stripping was successfully completed. Then the membranes were re-probed to detect new proteins.

### 3.5.5 WB Analysis

The WB data were subjected to quantitative analysis using Odyssey software. To determine the relative protein expression of specific target protein, values should be normalized to a loading control/housekeeping protein, which was  $\beta$ -actin in this case.

## 3.6 On-Cell Western Assay (OCA)

In-Cell Western (ICW) and On-Cell Western (OCW) assays (also known as on-cell assay (OCA)) are cell-based assays that detect proteins in-situ in a relevant cellular context and can measure relative protein levels in a 96- or 384-well format (435, 436). ICW, as implied by its name, is a bit like a WB, however, no lysis or gel running are required. It detects proteins that are fixed and permeabilized in cell culture, using target-specific primary antibodies and IRDye labelled secondary antibody. Permeabilization is required for the antibodies to enter the cell and bind to their target, however, permeabilization can compromise the detection of antigens on the cell membrane (surface protein/receptors) (435). Thus a modified version with no permeabilization (with or without fixation), known as OCA, is adapted for detection of surface protein, ligand binding to cell surface receptors, or receptor internalization and recycling (436).

In this study, OCA (without fixation) was used to analyse the surface expression of Tim-3 and galectin-9. An example of how OCA works is illustrated in Figure 32.

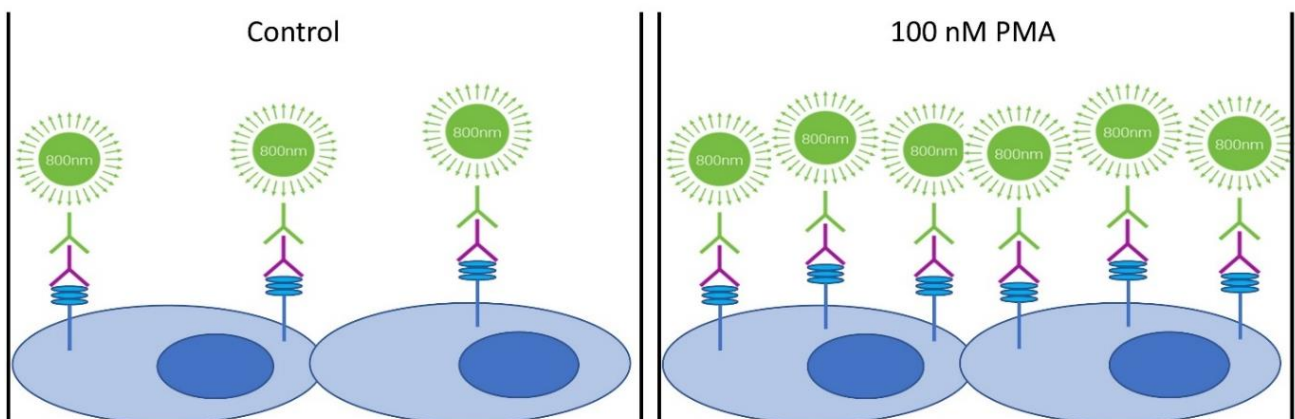
### 3.6.1 OCA on Suspension Cells

Cells were cultured and treated according to the experimental design in cell culture dishes. The cell suspension was transferred to appropriate tubes and centrifuged at 5000 rpm (small centrifuge) or 1200 rpm (big centrifuge) for 5 min. The pellet was resuspended in fresh media containing 1.5  $\mu$ l/mL primary anti-Tim-3 (3 mg/mL) for 2 h at 37°C and 5% CO<sub>2</sub>. The cell suspension was centrifuged and washed 1-2 times with fresh media without disturbing the pellet. The pellet was then resuspended in fresh media with 1.5  $\mu$ l/mL

secondary IRDye 800CW antibody and incubated for 1 h at 37°C and 5% CO<sub>2</sub>. This was followed for further washing 1-2 times, and the pellet was resuspended in fresh media. A small aliquot was sampled from each tube for cell counting and the cell number was normalized to the lowest count. Hereafter, 100 µl/well was loaded in replica to a PS flat-bottom 96-well plate and the plate was scanned with the Odyssey SA or CLx imager.

### 3.6.2 OCA on Adherent Cells

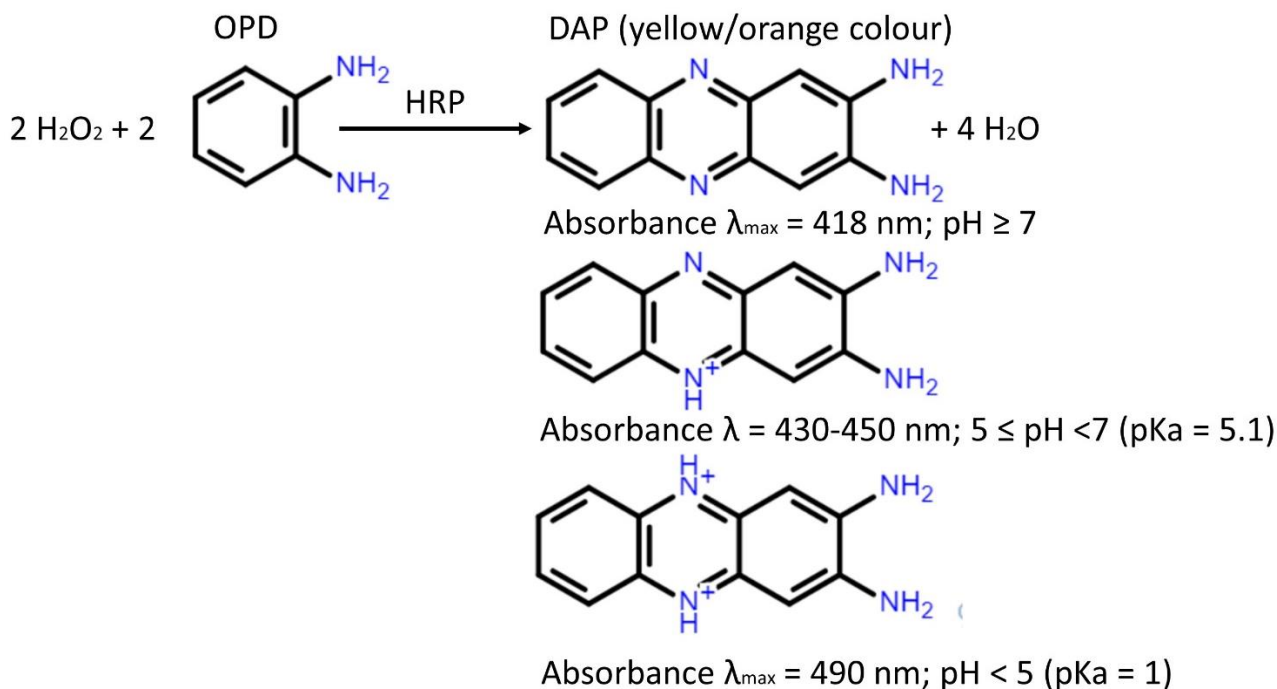
Cells were cultured and treated according to experimental design in cell culture dishes. When confluency was about 80%, the cells were harvested by scraping the cells, as trypsin can disturb surface protein expression (437). The harvested cell suspension was transferred to appropriate tubes and centrifuged at 5000 rpm (small centrifuge) or 1200 rpm (big centrifuge) for 5 min. Then, pellet was resuspended in fresh media containing 1.2 µl/mL primary anti-galectin-9 for 2-4 h under constant agitation at RT. Next, the cell suspension was centrifuged, and the pellet was resuspended in fresh media with 1.5 µl/mL secondary IRDye 800CW antibody and incubated for 2 h under constant agitation at RT. This was followed by centrifugation, wash procedure and resuspension in fresh media. Hereafter, 100 µL/well were loaded in replica to a PS flat-bottom 96-well plate and the plate was scanned with the Odyssey SA or CLx imager. As with the suspension cells, normalization is required. However, every time adherent cells were counted there were clumps, making cell count less reliable. Therefore, the values from the scan were normalized to protein concentration in the lysate before primary Ab was added.



**Figure 32: On-Cell Western assay (OCA).** The illustration is an example of detection of Tim-3 on the surface of Jurkat T cells. Cultured cells with or without treatment are exposed to primary antibody (which in this case anti-Tim-3) followed by incubation with secondary antibody conjugated to a fluorophore (in this case the green fluorophore IRDye 800CW was used as the secondary antibody).

### 3.7 Enzyme-linked immunoSorbent Assay (ELISA)

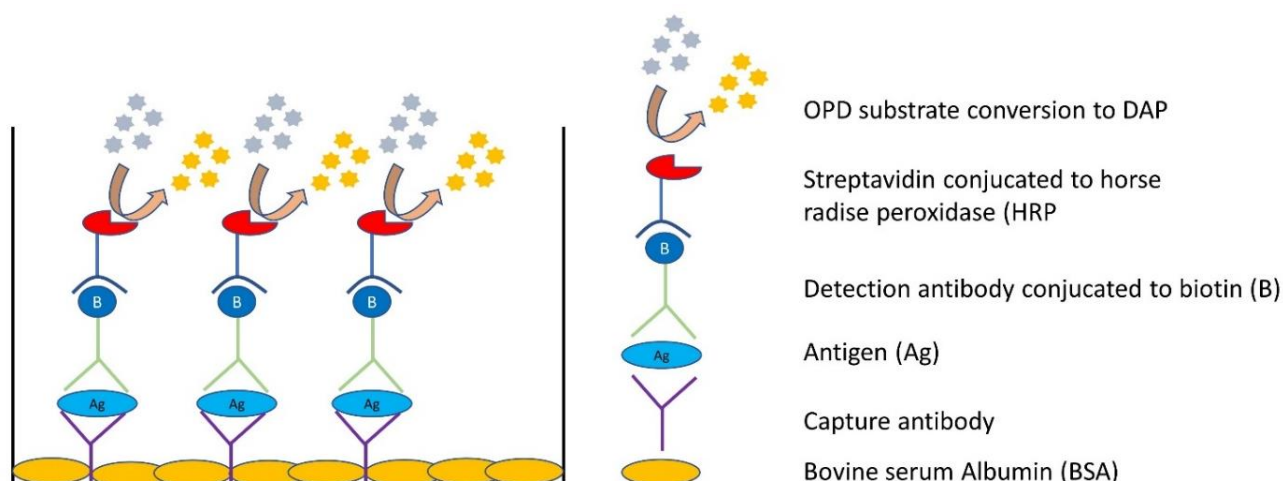
Enzyme-Linked ImmunoSorbent Assay (ELISA) is a technique that uses a solid-phase immunoassay to immobilize a soluble antigen in a biological sample, such as peptides, proteins, antibodies, and hormones. The amount of antigen can then be directly or indirectly colorimetrically detected by antibodies linked to a reporter enzyme which in this case is horse radish peroxidase (HRP). The principle of colorimetric detection is that the HRP catalyses the oxidation of orto-phenylenediamine (OPD) (colourless) with hydrogen peroxide ( $\text{H}_2\text{O}_2$ ) acting as an oxidant, aiding to the formation of 2,3-diaminophenazine (DAP) a yellow/orange product (438, 439). The maximum absorbance wavelength of DAP depends on the pH of the solution and its related protonated structures (Figure 33) (439-441). The stop solution sulphuric acid ( $\text{H}_2\text{SO}_4$ ) leads to the irreversible inactivation of HRP and a pH change, hence, the acidified chromophore, di-protonated DAP, can be measured around 490 nm (438-441).



**Figure 33: Schematic illustration of the HRP reaction.** *o*-phenylenediamine (OPD) oxidation catalysed by HRP leads to the formation of 2,3-diaminophenazine (DAP), which can absorb at three different wavelengths, depending on pH and its protonated structure. The structure can have a neutral charge, be mono-cation or di-cation and the absorbance for these are respectively, 418 nm, 430-450 nm and 490 nm (439-441). Structures were drawn in ChemSpider.

ELISA was used for the detection and quantification of target proteins in the cell culture media, human plasma, and cell and tissue lysates. In this study, indirect sandwich ELISA (shown in Figure 34) was used to quantify the concentration of galectin-9, Tim-3, IL-2,

IFN $\gamma$ , TNF $\alpha$ , and TGF $\beta$  using ELISA kits from R&D Systems (Minnapolis, Minnesota, USA).



**Figure 34: Schematic illustration of indirect sandwich ELISA.** Well from a 96-well poly-D-lysine (PDL) plate coated with capture antibody and blocked with BSA. Antigen (Ag) from the samples binds to the captured antibody and detection antibody conjugated to biotin (B) binds to the antigen creating a sandwich with antigen in the middle. Streptavidin, which is conjugated to horseradish peroxidase (HRP), has a high affinity to B. HRP together with H<sub>2</sub>O<sub>2</sub> catalyse the conversion of o-phenylenediamine (OPD) to 2,3-diaminophenazine (DAP). The signal is measured at 492 nm in a plate-reader.

### 3.7.1 Quantification of Galectin-9, Tim-3, IL-2, IFN $\gamma$ , and TNF $\alpha$ Concentrations in Cell Lysates and Culture Medium

For every step described below, 100  $\mu$ L of solution were added per well except for washing where 150  $\mu$ L was applied. All incubation occurred under constant agitation at RT, except for capture antibody incubation which was just at RT.

The procedure is as follow: 1) Capture antibody was diluted in phosphate-buffered saline (PBS) solution according to the manufacturer's protocol and 100  $\mu$ L of capture antibody for specific target protein were added to each well of a PDL 96-well microplate, which was then incubated overnight. 2) After incubation with the capture antibody, the wells were blocked with ELISA blocking buffer for media (PBS/BSA 1%) for 1 h. 3). Samples (cell-cultured media (collected as described in Section 3.5.1.1 or human blood plasma) were then added to each well and left for 2 h. Following the incubation with the samples, the wells were washed three times with TBST. 4) Then specific biotinylated detection antibody diluted in blocking buffer was added and incubated for 2 h, which was followed by another washing. 5) Next, streptavidin labelled with HRP diluted in blocking buffer was incubated for at least 30 min (usually 1 h) with a subsequent wash procedure. 6) Finally, the detection was made possible with the addition of substrate solution (0.2% H<sub>2</sub>O<sub>2</sub>, 56 mM



OPD) incubated for about 10 min (until a slight yellow colour was observed). The reaction was stopped by adding 1.8 M H<sub>2</sub>SO<sub>4</sub> in each well, and this caused a change to an intense orange colour. Optical density (OD) was measured at 492 nm, and it is directly proportional to the concentration of the protein of interest contained in the sample

### 3.7.2 Quantification of TGFβ Concentrations in Cell Lysates and Culture Medium

The ELISA procedure to measure TGF-β1 is similar to what is described in section 3.7.1. However, since TGF-β1 is produced in its latent inactive form, activation (performed by acidification) is required as the detection antibody only recognises the active form (442). Activation steps are as follows: For 100 μL of cell supernatant or media control, 20 μL of 1 M HCl are added, mixed and incubated for 10 min at RT. The sample is neutralized by adding 20 μL of 1.2M NaOH/0.5M HEPES resulting in a total volume of 140 μL, however, only 100 μL were loaded in the well immediately after activation. The concentration read off from the standard curve must be multiplied by the dilution factor, 1.4. The need for a medium control is because FBS contains TGF-β1, and thus “conditioned medium containing 10% FBS can be expected to have a TGF-β1 concentration of about 1600 pg/mL. The background level of TGF-β1 in control medium can be determined and subtracted from samples of conditioned medium” (442).

For determining TGF-β1 in the cell lysate (obtained from 3.5.1.1), the cell lysate was diluted 5-6 times in PBS, and a similar practice as described above was adopted. However, instead of using 1% BSA/PBS as blocking buffer, a 2% BSA/PBS solution was produced. For the initial experiment with cell lysate, there was no significant change observed in the concentration of TGF-β1 ± activation, thus hence no activation of TGF-β1 was performed in cell lysate samples

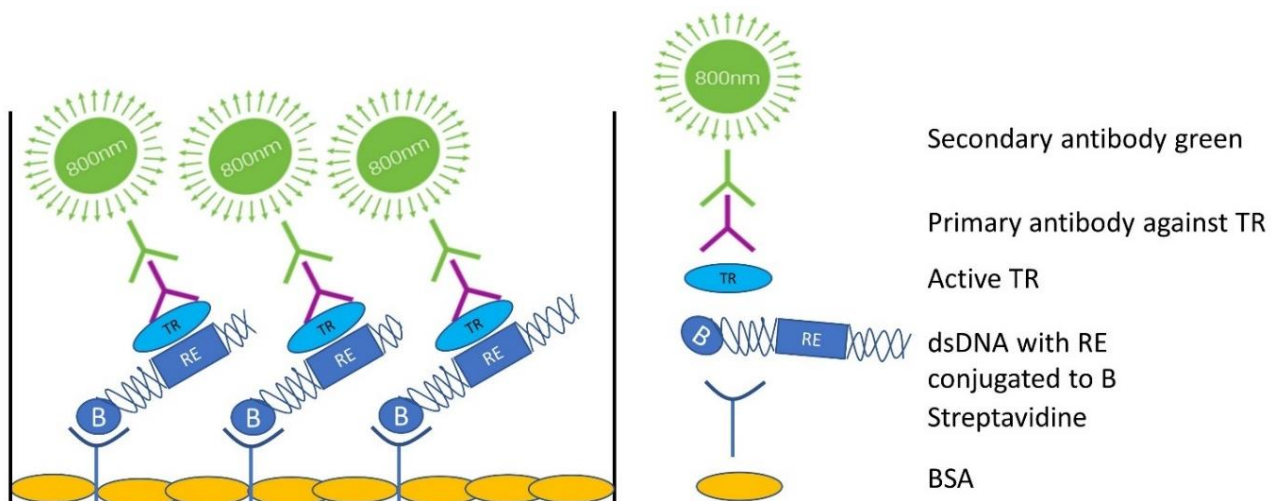
### 3.8 DNA Protein Interaction (DPI)-ELISA - DNA Binding Activity Assay

There exist different methods to investigate DNA protein interaction (DPI), such as electrophoretic mobility shift assay (EMSA), yeast-one-hybrid screening approach, and DPI-ELISA. As the name implies, the DPI-ELISA is an ELISA-based assay, which is cost-efficient, less time-consuming than other methods, and thus suitable for screening and provides a qualitative and quantitative readout by either colorimetric, chemiluminescent or

fluorescent detection (443-445). In this study, DPI-ELISA (depicted in Figure 35) was applied to examine the DNA binding activity of HIF-1 after knockdown of HIF-1 $\alpha$ .

For each step, 100  $\mu$ L solution were added per well except for washing where 150  $\mu$ L were used, and the dsDNA was loaded directly to blocking buffer. After each step, 3x wash procedure was performed except for between streptavidin and blocking.

To perform DPI-ELISA, a PDL 96-well flat-bottom plate was coated with streptavidin (1  $\mu$ g/well) overnight. Next morning, the plate was blocked with blocking buffer (2% BSA/TBST) for 1 h at RT under constant agitation. Equivalent molar of single-stranded (ss) DNA conjugated to biotin was annealed at 95 $^{\circ}$ C on the heating block for 5 min to form dsDNA containing response element (RE) conjugated to biotin. The dsDNA (2 pmol/well of biotinylated 2HRE-containing oligonucleotide) was added directly in the well with blocking buffer and incubated for 1 h. After washing 100  $\mu$ L sample/well were loaded and left to incubate for 1 h and 30 min at 37 $^{\circ}$  (this is the biological process where only active transcription factor (TR) will bind to RE). Then target-specific primary antibody which was diluted in blocking buffer (anti-HIF-1 $\alpha$  1:1000) is added to the wells and incubated for 2 h at RT under constant agitation. This is followed by binding of the secondary antibody diluted in blocking buffer which also occurs for 2 h at RT under constant agitation. After thorough washing, the plate was finally scanned using the Odyssey Clx imager (with the plate setting 3.0 mm).



**Figure 35: Schematic illustration of DPI-ELISA for detection of DNA binding activity.** A well from a 96-well PDL plate coated with streptavidin and blocked with bovine serum albumin (BSA). dsDNA with response element (RE) conjugated to biotin (B) binds with high affinity to streptavidin. Activated transcription factor (TR) from the samples with specific recognition to RE binds via its DNA binding site. A primary antibody specific for the TR binds, and secondary fluorescent antibody binds to the primary antibody. The fluorescent signal is detected and quantified in the Odyssey Clx imager.

### 3.9 Granzyme B and Caspase-3 Activity Assay

Apoptosis known as programmed cell death can be initiated by the extrinsic pathway (e.g. TNF/TNFR or FasL/Fas) or by the intrinsic pathway (mitochondrial pathway) both of which leads to activation of one of the initiator caspases that then cleaves and activates one of the effector caspases. The effector caspase-3 is part of both the extrinsic (activation by caspases 8, 9 or 10) and intrinsic pathway (activation by the apoptosome). The killing mechanism of cytotoxic lymphoid cells (CTL), such as CD8+ T cells and NKs, are thought to be mediated not only through receptor-mediated killing like Fas and TNF but also through granzyme B-mediated killing. Granzyme B is a serine protease, which was thought to be exclusively expressed by cytotoxic lymphoid cells (CTL/NKs), but now it is widely accepted that other cells, e.g. CD4 T cells, Treg, basophils, mast cells, smooth muscle cells and keratinocytes etc., can express it, although in these cases granzyme B is thought to be involved inflammation and anoikis (a form of programmed cell death due to loss of cell-ECM contact). However, granzyme B is best known for its function in mediating apoptosis in different ways: 1) Caspase-dependent with direct cleavage of caspase 3, 7, 8 and 10, 2) activation of the mitochondrial pathway with cytochrome C release through cleavage of BH3 interacting-domain death agonist (Bid), 3) Caspase-independent pathway (with cleavage of inhibitor of CAD (ICAD) and release caspase-activated DNase (CAD) resulting in DNA fragmentation and increase in mitochondrial ROS) (370, 446-449).

In this study, granzyme B-mediated killing activity by cytotoxic T lymphocytes (CTLs) and overall apoptosis by caspase-3 activity were investigated. Both enzyme activities were normalized to protein concentration in the lysate measured by a Bradford assay.

#### 3.9.1 Sample Preparation

The cells were incubated according to the indicated time points in the result section. After the incubation, the cells were harvested and centrifuged for 5 min at 232 g (1200 rpm). The medium was collected and stored at -20°C until further use, and the pellet was re-suspended in caspase-3 lysis buffer (caspase-3 colourimetric kit cat#BF3100 R&D systems) and then incubated on ice for 30 min with mixing every 10 min. When lysis was completed samples were centrifuged for 5 min at 13,200 rpm, and the supernatant was transferred to a clean tube and used straight after or stored at -20°C until future use.

### 3.9.2 Granzyme B Activity Assay

To measure granzyme B activity, its ability to cleave a fluorogenic substrate is used. The substrate for granzyme B employed is Ac-IEPD-AFC (N-acetyl-Ile-Glu-Pro-Asp-(7-amino-4-trifluoromethyl-coumarin)) (obtained from Sigma), where Ac-IEPD is the recognition motif of granzyme B and AFC is the fluorophore. When AFC is attached to the peptide Ac-IEPD, the fluorophore is quenched, however, after granzyme B cleavage of Ac-IEPD-AFC, AFC is released and thus can fluoresce. By using an excitation wavelength of (Ex) = 400 nm and emission wavelength (Em) = 505 nm (as recommended by the manufacturer), the amount of AFC can be measured, and this is proportional to granzyme B activity (450).

First, a stock of reaction buffer (10 mM DTT, 150 mM NaCl and 6 mM EDTA in PBS) and substrate solution is mixed. Then 27.5  $\mu$ L of reaction buffer/substrate solution and 25  $\mu$ L of cell lysate or 300  $\mu$ L of medium is loaded per well in a PS 96-well flat bottom plate. This corresponds to a final granzyme B substrate concentration per well of 0.19 mM and 30  $\mu$ M for cell lysate and media, respectively. The plate was incubated in the dark for 1-4 h at 37°C or overnight at RT. Finally, the plate was scanned using a plate-reader at fluorescence excitation at 400 nm and emission at 505 nm.

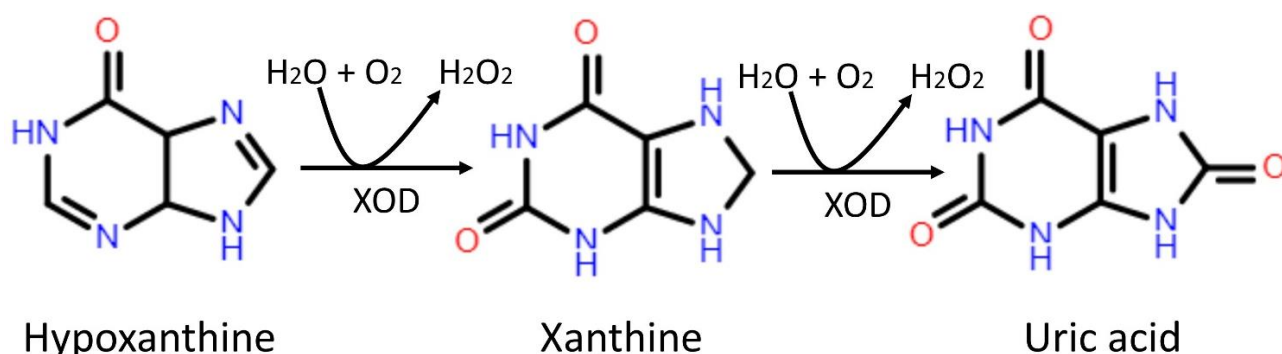
### 3.9.3 Caspase-3 Activity Assay

For caspase-3 cleavage, the chromogenic substrate Ac-DEVD-pNa (N-acetyl-Asp-Glu-Val-Asp-p-nitroaniline) is applied, where Ac-DEVD is the recognition motif of caspase-3, and pNa is the chromophore (reporter molecule). When pNa is attached to the peptide Ac-DEVD, the chromophore is quenched. However, after caspase-3 cleavage of Ac-DEVD-pNa, pNa is released, and it can absorb light. By using an absorbance wavelength of  $\lambda_{max}$  = 405 nm, the amount of pNa can be measured, and this is proportional to caspase-3 activity (451).

Firstly, a stock of reaction buffer (10 mM DTT, 150 mM NaCl and 6 mM EDTA in PBS) and substrate solution are mixed. Then 27.5  $\mu$ L of reaction buffer/substrate solution and 25  $\mu$ L of cell lysate are loaded per well in a PS 96-well flat bottom plate. This corresponds to a final caspase-3 substrate concentration per well of 0.19 mM and 30  $\mu$ M for cell lysate and medium, respectively. The plate was incubated in the dark for 2-5 h at 37°C. Finally, the plate was scanned using a plate-reader absorbance of 405 nm.

### 3.11 Xanthine Oxidase (XOD) Activity Assay

Xanthine Oxidase (XOD) catalyses the degradation of hypoxanthine to xanthine and then to uric acid. In this process reactive oxygen species (ROS) like hydrogen peroxide ( $\text{H}_2\text{O}_2$ ) is produced (Figure 36). However, it can also act on certain other purines and aldehyde where a superoxide anion ( $\text{O}_2^-$ ) is generated instead (452). XOD activity assay indirectly measures how much  $\text{H}_2\text{O}_2$  is produced when XOD catalyses xanthine to uric acid. Then HRP catalyses the reaction of  $\text{H}_2\text{O}_2$  oxidizing OPD and the end product of this reaction, DAB, can be measured spectrophotometrically at the wavelength 492 nm (as illustrated in Figure 33).

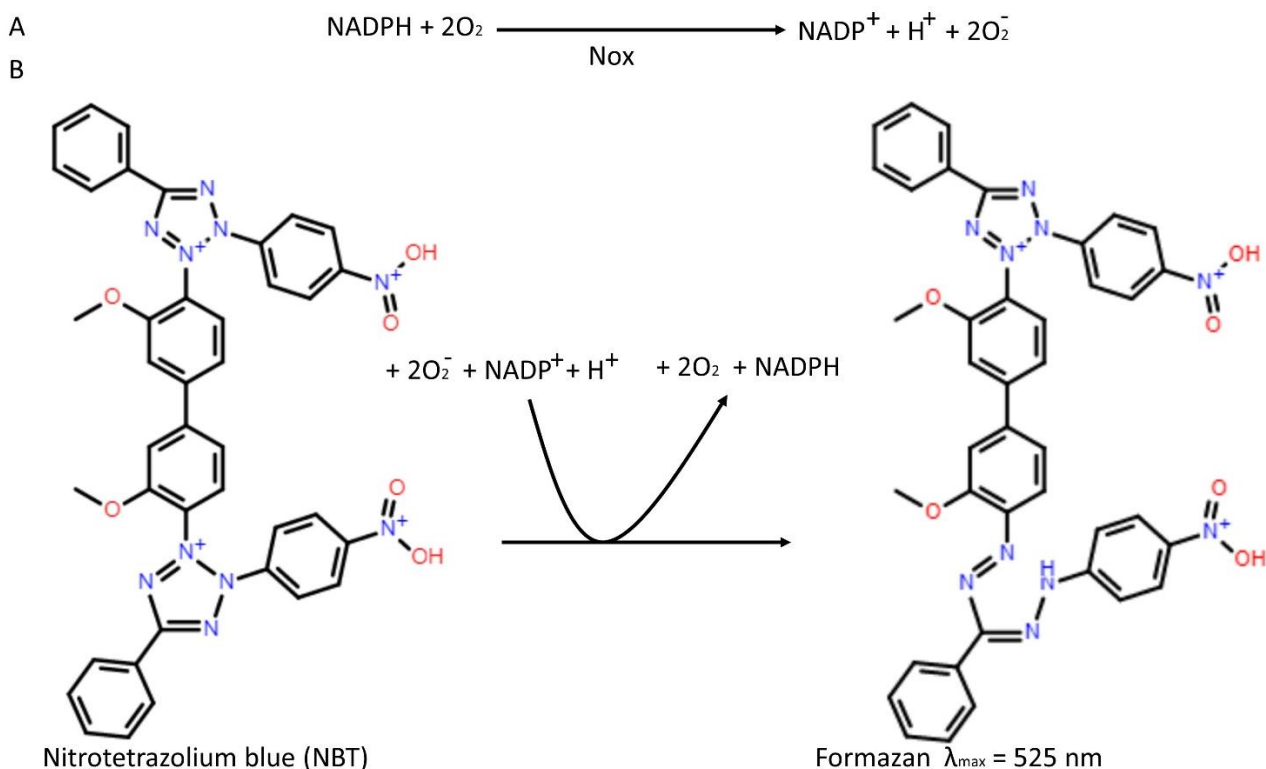


**Figure 36: Schematic illustration of the Xanthine oxidase reaction.** Xanthine oxidase catalyses with the production of hydrogen peroxide as a by-product. Structures were drawn in ChemSpider.

A working solution of 60  $\mu\text{L}$  0.1 M Tris-HCl buffer containing 40 mg/L HRP pH 7.5 (this pH is perfectly suitable for both XOD and HRP), 20  $\mu\text{L}$  4 mol Xanthine (substrate) and 10  $\mu\text{L}$  OPD (6 mg/mL) were mixed. In a PS 96-well flat bottom plate 90  $\mu\text{L}$  of working solution and 10  $\mu\text{L}$  of cell lysate were loaded per well and incubated for 1 h at 40°C (temperature optimum for XOD). To stop the reaction 100  $\mu\text{L}$  1.8 M  $\text{H}_2\text{SO}_4$  were added. The plate was measured in the plate-reader at 492 nm.

### 3.12 NADPH oxidase (Nox) activity assay

NADPH oxidase (Nox) can contribute to ROS production as it catalyses the production of superoxide anion radicals ( $\text{O}_2^-$ ) by transferring electrons to molecular oxygen from NADPH (453). The production of superoxide can be detected by measuring the ability of Nox to reduce nitrotetrazolium blue (NBT) to biz-formazan which purple colour can be measured spectrophotometrically at the wavelength 525 nm. The colour intensity is proportional to the enzyme activity (454, 455). The reactions are shown in Figure 37.



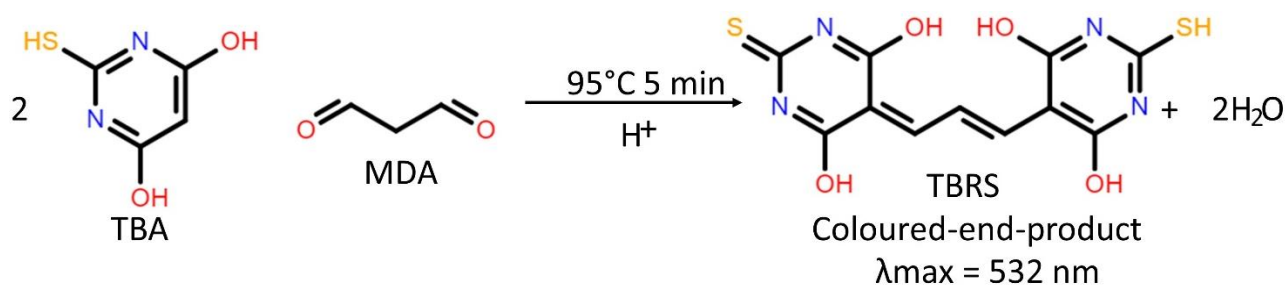
**Figure 37: Schematic illustration of the reaction in the Nox activity assay.** A) Nox catalyses the oxidation of NADPH while producing a superoxide anion. B) The reaction in which superoxide reduces nitrotetrazolium blue (NTB) to formazan. Structures are drawn in ChemSpider.

Firstly, a working solution consisting of 200  $\mu\text{L}$  NADPH reagent (1 mM EDTA, 0.1 M NADPH in PBS) and 50  $\mu\text{L}$  of 10 mg/mL NBT was produced. In a PS 96-well flat bottom plate, 190  $\mu\text{L}$  of working solution and 10  $\mu\text{L}$  cell lysate were added per well, and the plate was left to incubate for 10-30 min at 37-40°C until a colour development occurred. The plate was then measured at 525 nm in a plate-reader.

### 3.13 Thiobarbiturate Reactive Substance (TBRS) Assay

The generation of ROS can be difficult to measure directly due to short lifespan, yet, it is possible to perform an indirect measurement of ROS by examining oxidative damage, such as lipid damage, mediated by oxidative stress. An indicator for such ROS-mediated damage to the cell membrane is lipid peroxidation (456). The more common term of TBRS is Thiobarbituric acid reactive substance (TBARS) assay, however, as the end product is technically not an acid, the term TBRS is used in this context. It measures the formation of certain aldehydes due to lipid peroxidation. The majority of aldehyde formed by the degradation of lipids is malondialdehyde (MDA) (456). The more MDA generated the greater the oxidative burst. Thiobarbituric acid (TBA) reacts with these aldehydes, such

as MDA, to form TBRS a red coloured end-product which can be measured spectrophotometrically at wavelength 532 nm (Figure 38) (456).



**Figure 38: Thiobarbiturate reactive substance (TBRS) assay** (adapted from (457)). Two molecules of 2-thiobarbituric acid (TBA) react with one molecule of Malondialdehyde (MDA) to form a coloured-end-product, which can be spectrophotometrically detected at  $\lambda_{\text{max}} = 532 \text{ nm}$ . Structures were drawn in ChemSpider.

The TBRS assay was performed as follows: firstly, proteins in the sample were precipitated with trichloroacetic acid (TCA) (50  $\mu\text{L}$  of  $\text{dH}_2\text{O}$ , 40  $\mu\text{L}$  of 10% TCA and 10  $\mu\text{L}$  cell lysate were mixed together for each reaction) and incubated for 5-10 min at RT. The tube was centrifuged at 13,200 rpm for 5 min. Then the pellet was discarded, and the supernatant, 90  $\mu\text{L}$ , was transferred to a new tube where 45  $\mu\text{L}$  0.8% TBA (in glacial acetic acid) were added to the tube. The tube was boiled for 5-10 min at 95°C to facilitate the reaction formation, and after cooling on ice, the samples were loaded in PS 96-well flat bottom plate with 90  $\mu\text{L}$ /well. The plate was measured in the plate-reader at 532 nm.

### 3.14 Statistical Analysis

Each experiment was performed at least three times. Statistical analyses were performed using two-tailed Student's t-test when comparing two events at a time. In cases when multiple comparisons (more than two groups) were performed, an ANOVA test was used. Where applicable, a post-hoc Bonferroni correction was used. Statistical probabilities (p) reflecting significant differences between individual events were expressed as \* where  $p < 0.05$ , \*\* where  $p < 0.01$ , and \*\*\* where  $p < 0.001$ .

## 4 RESULTS AND DISCUSSIONS

Most of the data presented in section 4.1 and 4.2 have been published in "The Tim-3-Galectin-9 Pathway and Its Regulatory Mechanisms in Human Breast Cancer" (326) and "Transforming growth factor beta type 1 (TGF- $\beta$ ) and hypoxia-inducible factor 1 (HIF-1) transcription complex as master regulators of the immunosuppressive protein galectin-9 expression in human cancer and embryonic cells" (419). The data presented in section 4.3 are in the process of being a manuscript for

publication. I have contributed to some of the experiments in section 4.1 and most of the experiments in section 4.2 and section 4.3. Experiments provided by fellow PhD students or collaborators were included to tell a coherent story and fill out the puzzle of the biochemical regulation of galectin-9.

#### 4.1 The FLRT3-LPHN and Galectin-9-Tim-3 Signalling Pathways – a Possible Common Mechanism in Different Types of Cancer to Mediate Immune Escape

As mentioned in the introduction, Tim-3 and galectin-9 are known as an immunosuppressive immune checkpoint pathway, and in various types of cancer, it has been implicated with immune exhaustion of anti-tumour cells leading to immune escape. Recently, it was reported that AML cells ectopically expressed the neuronal latrophilin 1 (LPHN1), and when it is engaged with its ligand, fibronectin leucine-rich transmembrane protein 3 (FLRT3), it increases translation and exocytosis of Tim-3 and galectin-9 and thereby promotes immune escape (64, 323). Latrophilin is a G-protein coupled receptor (GPCR), which has been reported to have three isoforms denoted LPHN1, LPHN2 and LPHN3, where LPHN1 and LPHN3 usually are brain-specifically expressed, and LPHN2 is expressed ubiquitously (458). Cancer can be divided into solid or liquid (haematological) tumours, where breast cancer and acute myeloid leukaemia (AML) represent each category, respectively. Like AML, breast cancer has been shown to express an LPHN isoform, the LPHN2 mRNA (encoded by LPHN1 gene), which was reported to be upregulated compared to normal breast tissue (459). Furthermore, in breast cancer, galectin-9 has been suggested to have anti-metastatic potential as it increases cellular aggregation (302). Moreover, it has been shown that different breast cancer cell lines upon PD-1-PD-L1 blockade upregulate immune checkpoints, such as Tim-3 on CD4 T cells (460). In addition, conditioned-tumour-derived media from certain types of breast cancer can in a contact independent manner upregulate Tim-3 on Jurkat T cells (461). Since it has been reported in many cancer types that Tim-3 and galectin-9 are upregulated on TILs (T cells and NKs) and tumour cells, respectively (64, 225, 257, 267, 325, 462), it is speculated that the FLRT3-LPHN pathway may be a common mechanism involved in regulating Tim-3-galectin-9 in cancer cells of different origin. To investigate a possible role of FLRT3-LPHN-galectin-9-Tim-3 in immune escape for solid tumours, focus was directed towards breast cancer.

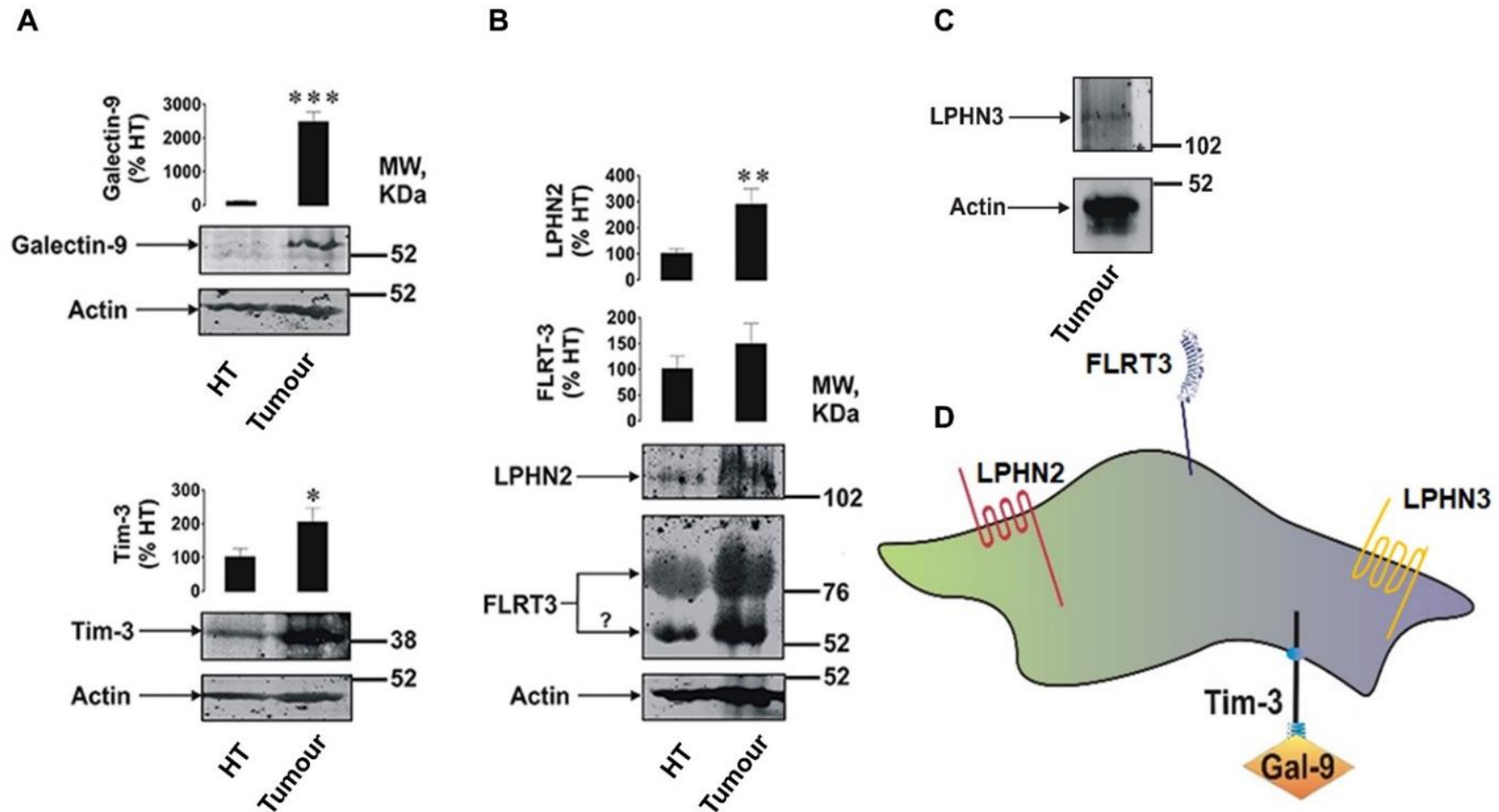


#### 4.1.1 Breast Tumour Cells Have Elevated Levels of Expression of LPHN, FLRT3, Tim-3 and galectin-9.

Initially, the expression levels of galectin-9, Tim-3, FLRT3 and different forms of LPHN expression in primary breast tumour tissue (BT) and adjacent healthy breast tissue (HT) were investigated. The results showed that BT expressed galectin-9, Tim-3, FLRT3, LPHN2 and LPHN3, and the expression level was significantly higher (about 15-20-fold for galectin-9,  $p < 0.001$ , 2-fold for Tim-3,  $p < 0.05$  and 2.5-3 fold for LPHN2,  $p < 0.01$ ) in tumours compared to HT isolated from the same patient (Figure 39A, B). FLRT3 expression tended to be greater expressed in BT compared to HT. Furthermore, BT had detectable amounts of LPHN3 (Figure 39C), whereas the expression was undetectable in HT (data not shown). LPHN1 was not detected in HT nor BT (data not shown).

A band specific for galectin-9 appeared at around 55 kDa when 12% SDS-PAGE gel was used (this is the gel concentration normally used for galectin-9 detection). The band had a higher molecular weight than the reported isoforms of galectin-9, which is between 34-39 kDa. This could indicate that it is the secreted TIM-3-galectin-9 complex formation, which in AML cells has been reported to have a size of about 52 kDa (64). However, in each case, it was not detectable by the anti-Tim-3 antibody. This suggests that it is not the TIM-3-galectin-9 complex, but probably a galectin-9 isoform bound to carbohydrates (as a lectin), which is unlikely to be secreted. To confirm this, the samples were re-run using 10% SDS-PAGE, and the specific band appeared above 31 kDa molecular weight marker (Appendix, Figure 77). This indicates that in a 12% gel protein running was “delayed”. The cause for the delay was possibly the presence of glycosides or other post-translational modifications affecting the protein properties/shape, but not the molecular weight.

An interesting observation was that the FLRT3 antibody detected two bands, one corresponding to a specific FLRT3 band and a band around 55 kDa (highlighted by a question mark). This may represent FLRT3, which underwent proteolytic processing (324).



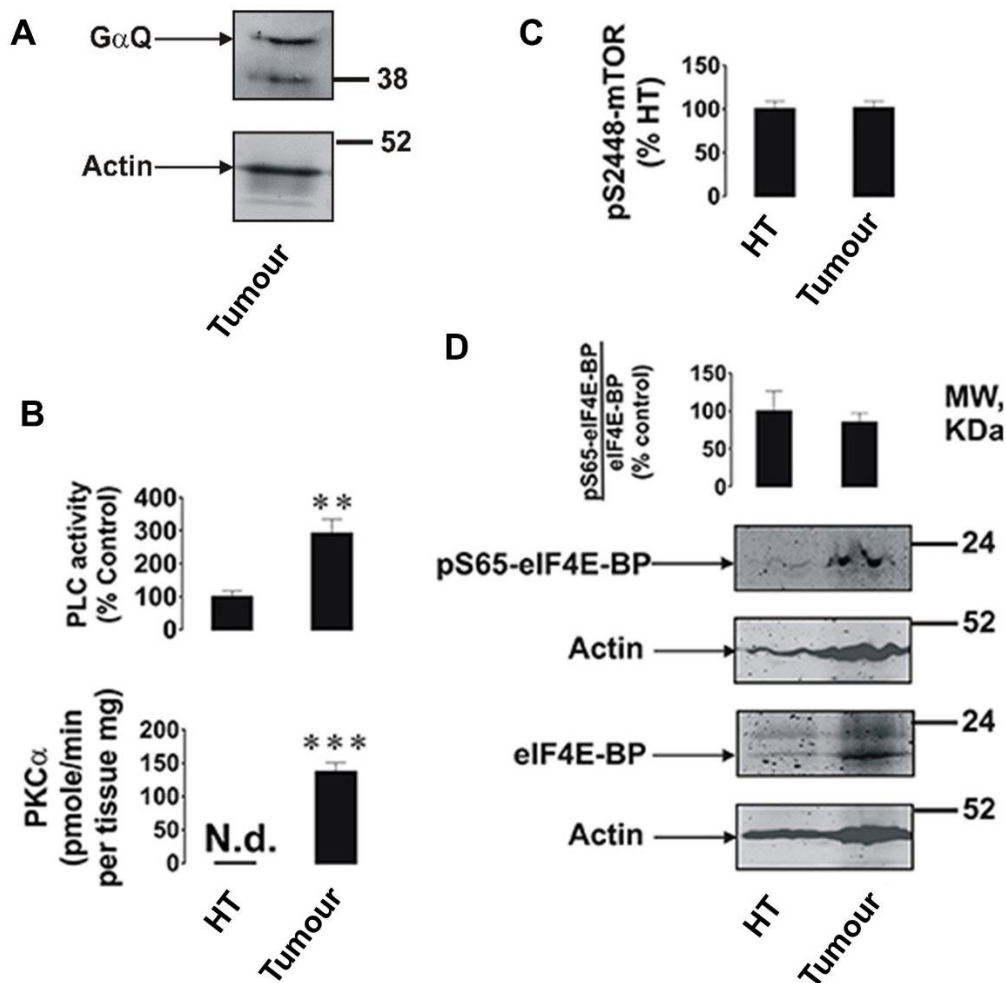
**Figure 39: Elevated expression levels of LPHNs, FLRT3, Tim-3 and galectin-9 in breast tumour tissue** (adapted from (326)). Expression levels of Tim-3, galectin-9 (A), FLRT3, LPHN2 (B) and LPHN3 (C) were analysed in primary breast malignant tumours and compared with healthy breast tissues (HT) of five patients ( $n = 5$ ) by WB. Illustration of the surface expression on BT (D). Molecular weight markers (MW) are expressed in kDa. Images are from one experiment representative of five, which gave similar results. Other results are shown as mean values  $\pm$  SEM. \* $p < 0.05$ ; \*\* $p < 0.01$ , and \*\*\*when  $p < 0.001$  vs. control (326).

#### 4.1.2 Breast Tumour Cells Have Increased Activity of PLC and PKC $\alpha$ , not mTOR Activity.

From a previous study on AML cells (64), it was found that the downstream component of the FLRT3-LPHN1 pathway was via Gq protein, PLC, PKC $\alpha$ , mTOR and eIF4E-BP (a substrate of mTOR). Therefore, the expression and activity of these signal proteins were investigated in breast tumour tissue and compared with adjacent healthy breast tissue.

Figure 40 shows that BT did express G $\alpha$ q, PLC, PKC $\alpha$ , mTOR and eIF4E-BP. Unlike in AML cells (64), the S2448 phosphorylation level of mTOR was similar in both healthy and tumour tissues (Figure 40C, D). The ratio between phospho-S65 eIF4E-BP and its total amount was likewise comparable in both tissue types, although the amount of both phospho-S65 and total eIF4E-BP was higher in tumour tissues (Figure 40D). The activity of PLC and PKC $\alpha$  was significantly higher ( $p < 0.01$  for PLC and  $p < 0.001$  for PKC $\alpha$ ) in BT compared to HT) (Figure 40B).

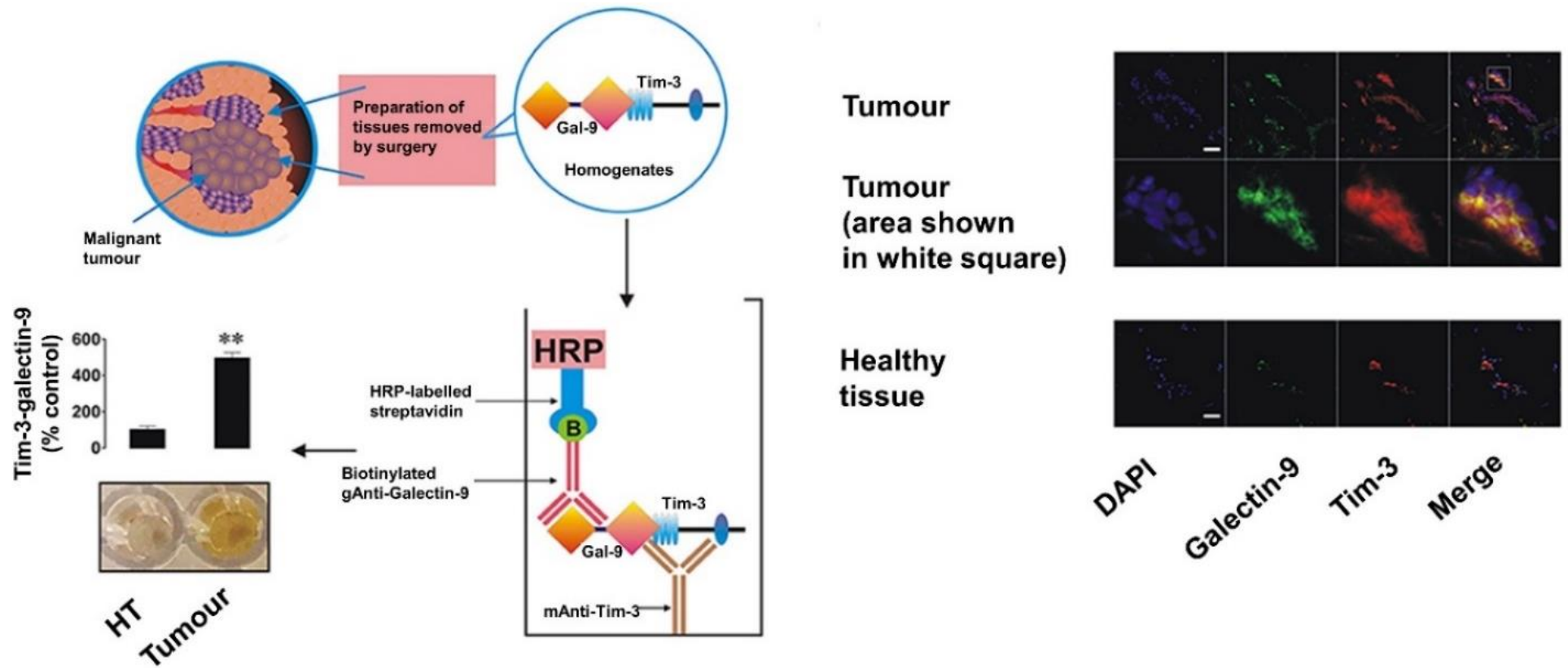
As described in the introduction, the TME contain both tumour cells and tumour-infiltrating immune cells, such as T cells, which in tumours are known to express high amount of Tim-3 and galectin-9. Therefore, the expression of CD3 (a marker of T cells) was analysed to determine the contribution from these cells. It was demonstrated that this protein is undetectable in healthy and barely detectable in tumour tissue lysates (Appendix, Figure 78). This suggests that the analysed proteins are mainly expressed by breast tumour cells and not by TILs.



**Figure 40. Expression and activity of components downstream of the LPHN receptor in primary human breast tumours** (from (326)). The  $\alpha$ -subunit of the Gq protein expression was analysed using WB (A). Activities of PLC,  $PKC\alpha$ , and the levels of phospho-S2448 mTOR were detected as described in (326) (B and C). The amounts of phospho-S65 and total eIF4E-BP (mTOR substrate) were analysed using WB (D). These components were analysed in primary breast malignant tumours and healthy breast tissues (HT) of five patients ( $n = 5$ ). Molecular weight markers (MW) are expressed in kDa. Images are from one experiment representative of five which gave similar results. Other results are shown as mean values  $\pm$  SEM. \* $p < 0.05$ ; \*\* $p < 0.01$ , and \*\*\*when  $p < 0.001$  vs. control (326).

#### 4.1.3 Breast Tumour Cells Express Tim-3 and galectin-9 as a Complex

In order to assess if Tim-3 and galectin-9 are co-localized and complexed together as in AML cells (64), detection of the Tim-3-galectin-9 complex was performed in tissue homogenates from BT and HT (by the method described in (326)). The complex was scarcely observed in HT, but clearly detectable in BT extracts (Figure 41A). Confocal microscopy is another way to determine if Tim-3 and galectin-9 are co-localized. In line with the data shown in Figure 39, both proteins were abundant in tumour tissue slices and are co-localized (Figure 41B).

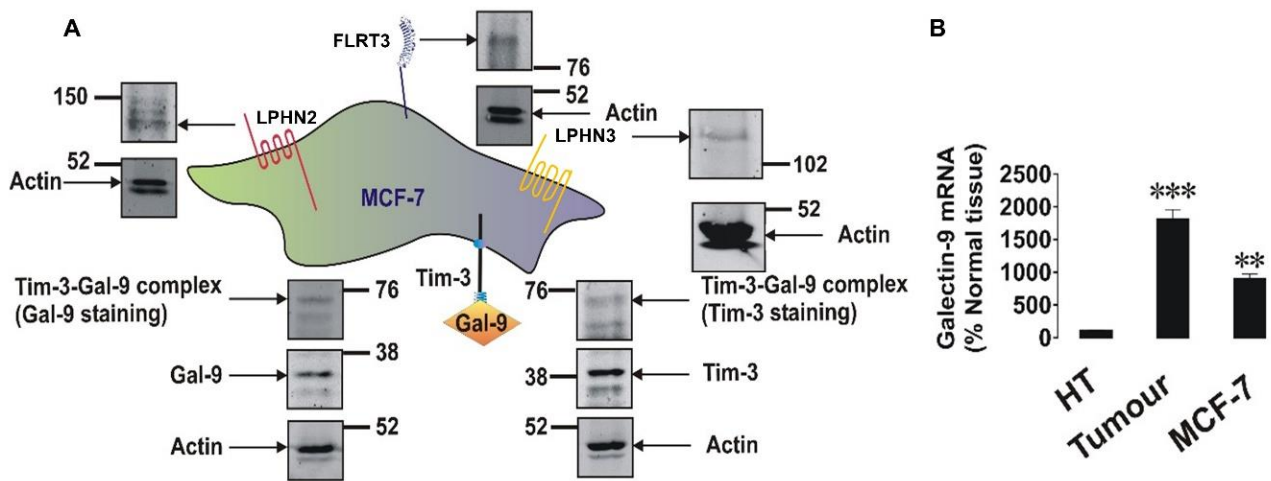


**Figure 41: Expression, interaction and co-localization of Tim-3 and galectin-9 in primary human breast tumours** (directly from (326)). (A) Presence of the Tim-3-galectin-9 complex in primary normal and tumour tissue extracts was analysed using ELISA as described in (326). (B) Expression and co-localization of galectin-9 and Tim-3 were analysed in primary human breast tumours and healthy tissues of the same patients using confocal microscopy as described in (326). Images are from one experiment representative of five, which gave similar results. Scale bars correspond to 20  $\mu$ m (326).

#### 4.1.4 MCF-7 Express Similar Components of the FLRT3-LPHN-galectin-9-Tim-3 Pathway and Act as a Model for Breast Cancer

To study the biochemical mechanism by which FLRT3-LPHN-galectin-9-Tim-3 pathway is mediating immune escape in solid tumours in particular breast cancer, human breast cancer cell lines were used as models. The expression of galectin-9, Tim-3, FLRT3 and LPHNs was analysed in three breast cancer cell lines, MCF-7, BC-8701, and MDA-MB-231. All the analysed cell lines expressed Tim-3, galectin-9, FLRT3, and at least one LPHN isoform (Figure 42 and Appendix Table 2). None of the three cell lines expressed LPHN1 (Appendix, Table 2 and data not shown for MCF-7). MDA-MB-231 cells expressed LPHN2, but not LPHN3. In contrast, BC-8701 cells expressed LPHN3, but not LPHN2. MCF-7 cells expressed both LPHN2 and LPHN3 in comparable amount with primary breast tumour.

Of the analysed cell lines, the MCF-7 breast cancer cell line was the only model which expressed detectable amounts of both LPHN2 and LPHN3 as well as Tim-3, galectin-9 and the Tim-3-galectin-9 complex (Figure 42A), thus being more similar to primary breast tumours (Figure 39). This cell line was therefore selected to study the mechanism of Tim-3-galectin-9 regulation in further details. In addition to protein levels, the expression of galectin-9 mRNA was analysed by qRT-PCR. Galectin-9 mRNA levels were significantly higher in both MCF-7 cells and primary breast tumours (Figure 42B), and the ratio of galectin-9 mRNA in tumour and normal tissues was comparable to the respective levels of protein detected (Figure 39A). These results indicated that the expressed galectin-9 was identical between MCF-7 cells, HT, and BT (tumour) thus, re-confirming that the same protein was detected by WB (Figure 39A and Figure 42A).



**Figure 42: The MCF-7 breast cancer cell line mirrors primary human breast tumours the most (adapted from (326)). (A) The expression levels of FLRT3-LPHN-galectin-9-Tim-3 pathway in MCF-7 breast cancer cell line were analysed by WB with  $\beta$ -actin as a housekeeping protein. (B) Levels of galectin-9 mRNA were compared in healthy breast tissue (HT) and breast tumour tissues as well as in MCF-7 cells and normalised against those of  $\beta$ -actin. qRT-PCR for galectin-9 and  $\beta$ -actin were performed as described in (326). Images are from one experiment representative of at least three which gave similar results. Data are the mean values  $\pm$  SEM of five independent experiments. \*\*,  $p < 0.01$  and \*\*\*  $p < 0.001$  vs control (326).**

#### 4.1.5 The FLRT3-LPHN Pathway Induces Translocation of Galectin-9 onto the Surface of MCF-7 Breast Cancer Cells

It has recently been reported that LPHN1 is ectopically expressed in AML cells and that FLRT3-mediated activation of LPHN1 promotes translation and secretion of Tim-3 and galectin-9 (64, 324). Although, no LPHN1 expression was observed on breast cancer cell lines (BC-8701, MDA-MD-231 and MCF-7, Figure 47 and data not shown), although as mentioned, they expressed at least one other LPHN isoform and MCF-7 was observed to express both LPHN2 and LPHN3. FLRT3 has also been reported to bind to LPHN3 (463, 464), and it has been suggested that it may bind to the olfactomedin-like domain that are similar to all LPHNs (3D illustration

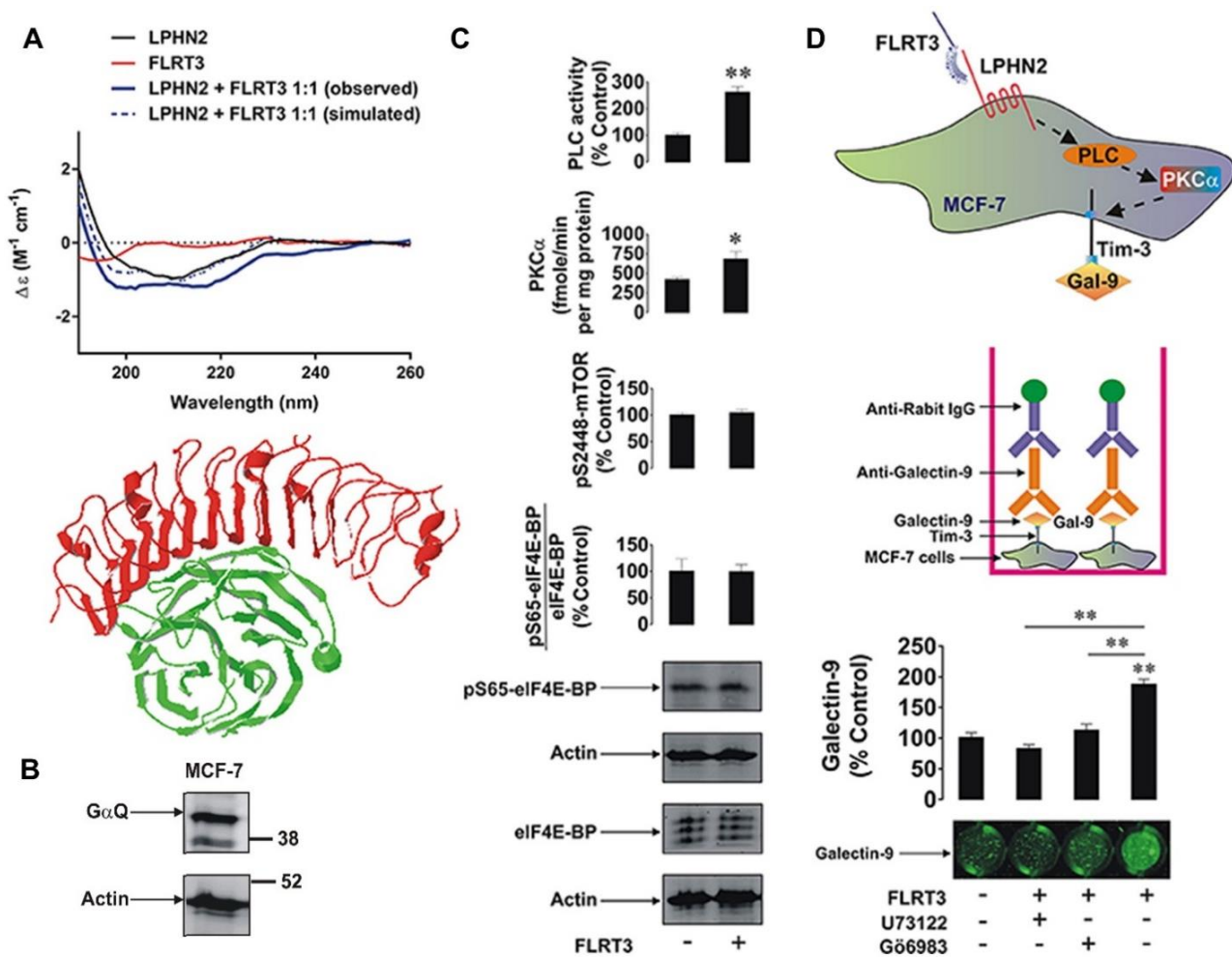
Figure 43A). To confirm that FLRT3 similarly interact with LPHN2, equivalent molar of the olfactomedin-like domain of LPHN2 and FLRT3 alone were analysed using Synchrotron radiation circular dichroism (SRCD) spectroscopy. In

Figure 43A the secondary structures are visualized for both LPHN2 and FLRT3 and there is observed a conformational change when the two are combine indicating that there is a binding interaction.

In line with FLRT3 binding to LPHN isoforms, which are GPCR proteins, the expression of  $G\alpha$  was examined as it is required for signal transduction.  $G\alpha_Q$  and it has been reported to

function downstream of LPHN1 (64) and therefore the expression of this protein was examined. Like primary breast tumour (Figure 40A), MCF-7 cells expressed GαQ (Figure 43B). Subsequently, it was explored what other signal components that might be involved in the upregulation of galectin-9. MCF-7 cells were stimulated with 10 nM FLRT3 for 4 h followed by detection of phospho-S65/total eIF4E-BP, phospho-S2448 mTOR, activities of PLC and PKCα as well as cell surface presence of galectin-9. As shown in Figure 43C, exposure to FLRT3 did not affect mTOR activity nor phospho-S65/total eIF4E-BP expression levels, however, the exposure significantly upregulated the activities of PLC and PKCα. Galectin-9 surface presence was significantly upregulated in response to FLRT3 as measured by OCA (Figure 43D). Pre-treatment of the cells for 1 h with 30 μM U73122 (PLC inhibitor) and 70 nM Gö6983 (PKCα inhibitor) before 4 h exposure to 10 nM FLRT3 attenuated FLRT3-induced galectin-9 translocation onto the cell surface (Figure 43D). This confirms that FLRT3-induced translocation of galectin-9 onto the surface of MCF-7 cells, and it is controlled by the LPHN-PLC-PKCα pathway.





**Figure 43: The FLRT3-LPHN pathway induces translocation of galectin-9 onto the surface of MCF-7 breast cancer cells** (from (326)). (A) Secondary structure and conformational changes of LPHN2 olfactomedin-like domain (FLRT3-binding region), FLRT3, and the complex of the two proteins mixed at the equimolar ratio was characterized using SRCD spectroscopy as outlined in the Materials and Methods of (326). An interaction between olfactomedin-like domain of LPHN3 and FLRT3 generated by Swiss PDB viewer [5 cmn.pdb file downloaded through PubMed database was used] is presented to illustrate the structural basis of FLRT3 interaction with LPHNs (326). (B) G $\alpha$ Q expression by WB in MCF-7 cells. (C) MCF-7 cells were stimulated 10 nM FLRT3 for 4 h and activities of PLC, PKC $\alpha$ , the levels of phospho-S2448 mTOR, the amounts of phospho-S65 and total eIF4E-BP (an mTOR substrate) were analysed as described in the Materials and Methods of (326). (D) MCF-7 cells were exposed for 4 h to 10 nM FLRT3 with or without 1 h pre-treatment with 30  $\mu$ M U73122 (PLC inhibitor) or 70 nM Gö6983 (PKC $\alpha$  inhibitor). Surface presence of galectin-9 was measured by on-cell assay. Images are from one experiment representative of at least three which gave similar results. Other results are shown as mean values  $\pm$  SEM of at least three independent experiments. \* $p < 0.05$ ; \*\* $p < 0.01$  vs. control (326).

#### 4.1.6 Galectin-9 Protects Breast Cancer Cells Against Cytotoxic Immune Attack

It has previously been reported that the galectin-9-Tim-3 pathway is used as an immune escape mechanism by AML cells (64). sTim-3 is able to suppress IL-2 production by T cells which is necessary for activation of both T cells and NKs. Furthermore, galectin-9 can

attenuate AML killing by NKs, and it is known to induce apoptosis of T cells (64, 255, 304). To investigate if this is the case for solid tumours such as breast cancer, it was required to establish a co-culture system. It has been reported for some solid tumours, that the main infiltrating cytotoxic cells are T cells (465, 466), therefore, a co-culture system with T cells rather than NKs was chosen.

To assess, if T cells are able to perform cytotoxic-cell-dependent killing of MCF-7 cells, and if galectin-9 is used as an escape mechanism, it was decided to study the Jurkat T cell line. Jurkat T is a CD4 T cell line, which expresses both granzyme B and IFN $\gamma$ , and thus are functional CD4 cytotoxic T cells, albeit are not as efficient in killing as cytotoxic CD8 T cells, and therefore enable to study the killing mechanism. Although some studies have reported that Jurkat is not ideal for this kind of study as it does not express Tim-3 (271). We found that Jurkat T cell express both Tim-3 and galectin-9 in resting condition (Appendix Figure 79). To confirm that Jurkat T cell function was affected and behaved similarly as cytotoxic lymphoid cells in a cancer setting, Jurkat cells were pre-treated with 100 nM PMA (to induce activation) for 30 min followed by 24 h stimulation with 1  $\mu$ g/mL galectin-9 or sTim-3. sTim-3 significantly reduced IL-2 release, confirming previous findings (64). In Jurkat T cells, galectin-9 promoted IFN $\gamma$  and TNF $\alpha$  release, and at the same time, there was an increase in granzyme B activity inside the cells (Figure 44). These results demonstrated that Jurkat is equally affected by sTim-3 and galectin-9 as reported in other more cytotoxic lymphoid cells (64).

Tumour-infiltrating T cells in the TME have upregulated expression of Tim-3 (due to activation-induced upregulation or persistent high expression due to exhaustion). Therefore, Jurkat T cells were pre-treated with 100 nM PMA for 4 h to induce T cell activation and upregulate Tim-3 surface expression. Tim-3 surface presence on Jurkat T cells was then analysed and confirmed by OCA (Figure 45B). This contrasts with other studies, which could not detect Tim-3 even with PMA stimulation. It was furthermore confirmed that MCF-7 cells express galectin-9 on their surface (Figure 45B). MCF-7 cells and PMA pre-treated Jurkat T cells were cultured alone or 4 h co-culture with or without galectin-9 neutralizing antibody, followed by measurement of granzyme B activity and caspase-3 activity as an indicator of apoptosis. Surprisingly, MCF-7 cells by themselves had some granzyme B activity, but cultured with Jurkat T cells, the activity significantly increased, suggesting that Jurkat T cells had released some of their granule content with

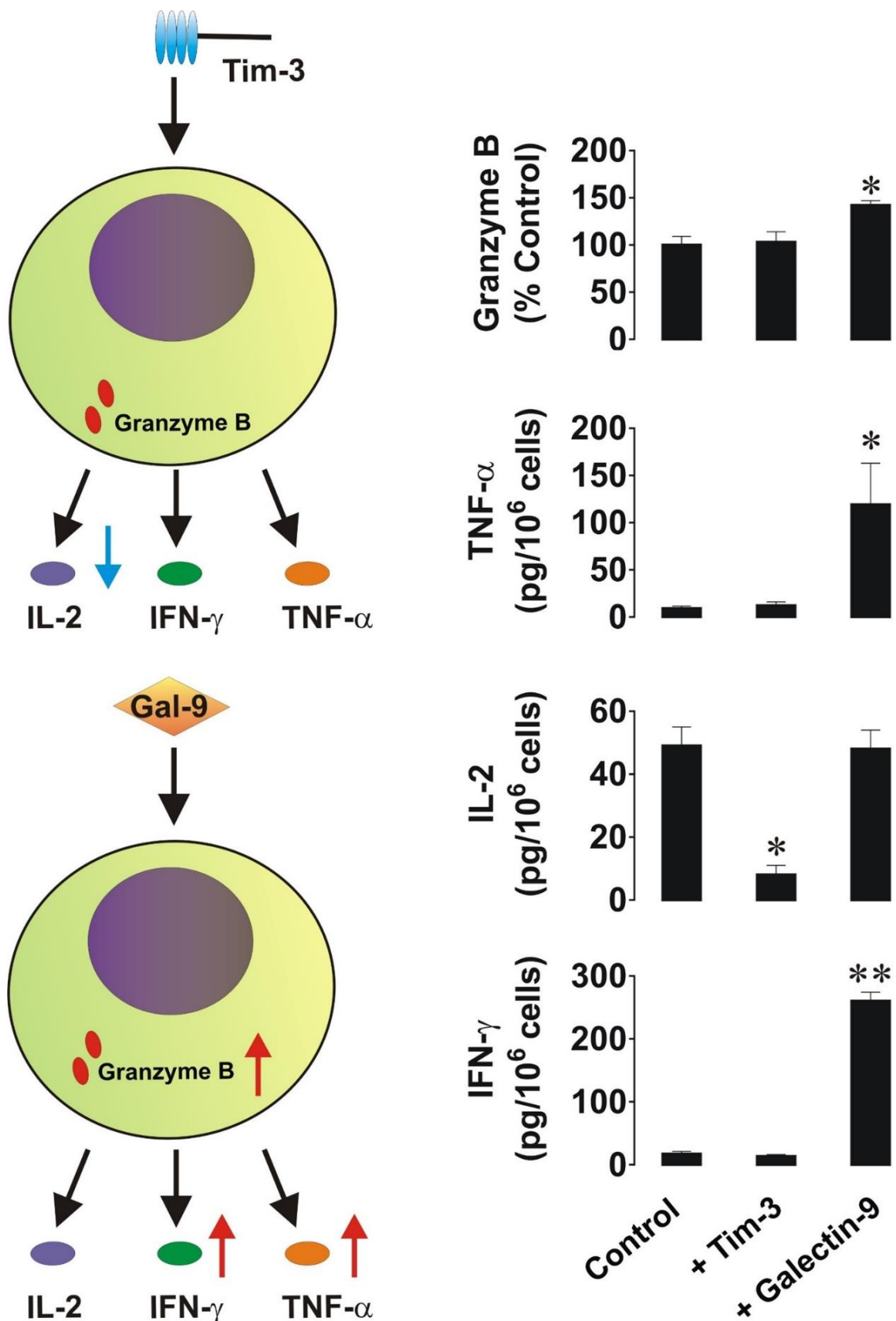
granzyme B into MCF-7 cells (Figure 45C). Jurkat T cells alone also had granzyme B activity (not a surprise), but when co-cultured with MCF-7, the activity significantly increased, and this was attenuated by galectin-9 neutralising antibody (Figure 45D low), suggesting that granules with granzyme B might have exploded inside the T cells in the presence of galectin-9-derived from cancer cells. This was to some extent supported by analysis of caspase-3 activity as there was a tendency to an increase in caspase-3 activity when co-cultured with MCF-7, and the activity decreased again with anti-galectin-9 (Figure 45D top). However, as apoptosis takes time, and the cells were only co-cultured 4 h before harvesting, this might not be enough time to activate all caspase-3 proteins.

With having established a successful co-culture system that allows analysis of cytotoxic cell-dependent killing, the next step was to perform a similar experiment, but using the more cytotoxic T cell line, TALL-104, which expresses CD8 and thus resemble CTL. MCF-7 cells were co-cultured with TALL-104 cells for 16 h at a ratio of 4 MCF-7 cells: 1 TALL-104 cell (Figure 46A, this ratio was selected experimentally to achieve moderate effects in order to be able to trace biochemical mechanisms). To assess the contribution of surface-based galectin-9, the co-culture experiment was performed in either the absence or presence of 5 µg/mL galectin-9 neutralizing antibody. Following the treatment, TALL-104 cells were collected, lysed, and subjected to WB analysis of full-length and cleaved poly (ADP-ribose) polymerase (PARP) (a marker of apoptosis). The higher the level of PARP cleavage is, the greater the number of apoptotic cells. In TALL-104 cells co-cultured with MCF-7 cells, the level of PARP cleavage was significantly increased (about 3 fold,  $p < 0.05$ ), and the presence of anti-galectin-9 antibody attenuated the effect (Figure 46B).

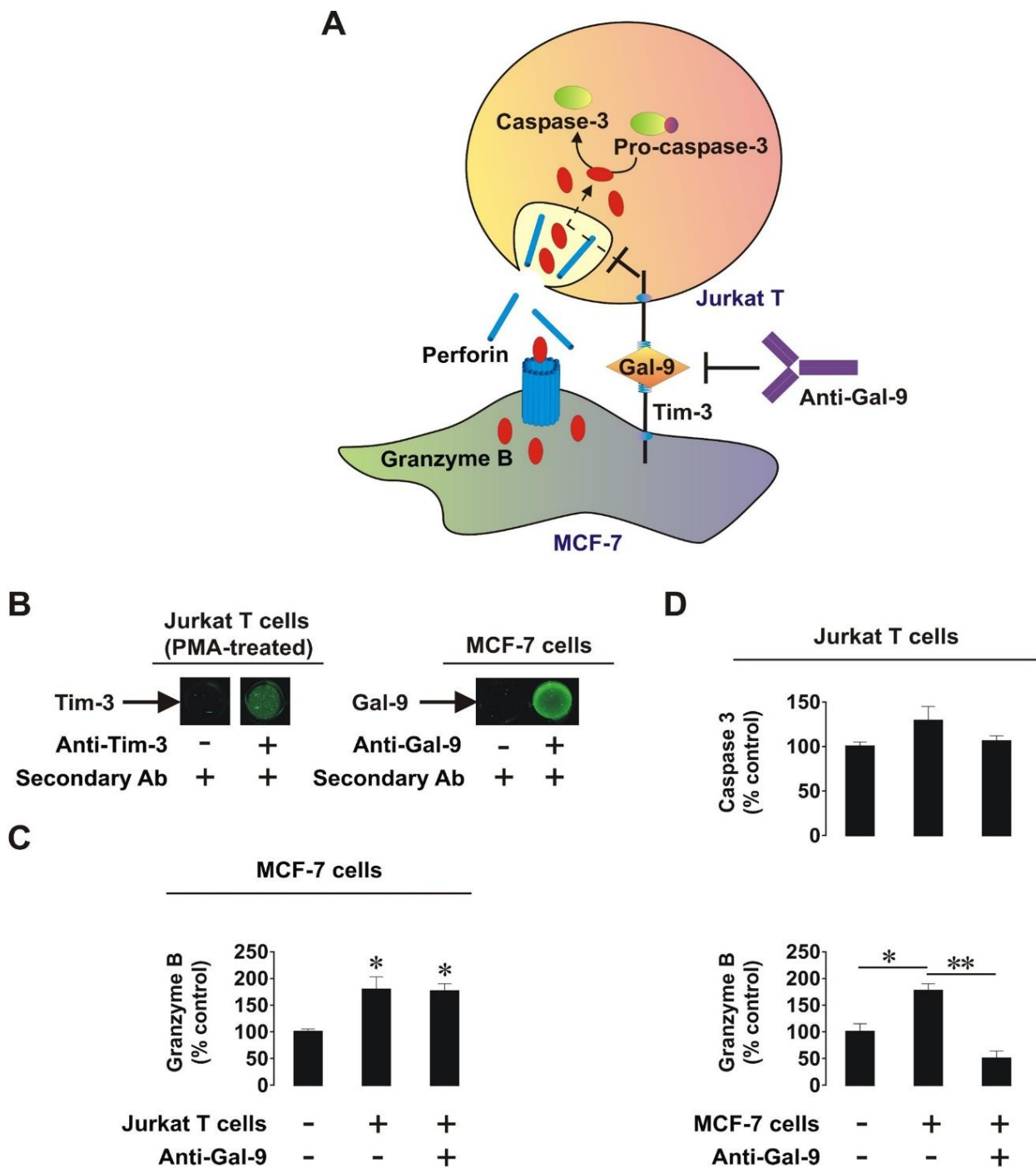
OCA was used to evaluate the level of infiltration of TALL-104 cells into the MCF-7 cell monolayer. It was observed that CD8 was absent in the MCF-7 cells when cultured on their own. As CD8 was detected when MCF-7 cells were co-cultured with TALL-104, it suggests some infiltration by the T cells. It was further significantly augmented when the cells were co-cultured in the presence of galectin-9 neutralizing antibody, suggesting that the ability of TALL-104 cells to infiltrate and attack MCF-7 cells is increased when galectin-9 activity is disabled (Figure 46C top). Isotype control antibody (used at the same concentration of 5 µg/mL) did not affect interactions between TALL-104 and MCF-7 cells, confirming the role of galectin-9 in this process (Figure 46C bottom). To confirm that T cells attack MCF-7 when infiltrating them, the viability of MCF-7 cells was assessed using

MTS test. The presence of TALL-104 cells and galectin-9 neutralizing antibody (but not isotype control) attenuated the viability of MCF-7 (Figure 46E), suggesting that MCF-7 cells are killed in the absence of galectin-9. Interestingly, cell surface presence of galectin-9 was significantly upregulated in the presence of TALL-104 cells as measured by OCA (Figure 46D).

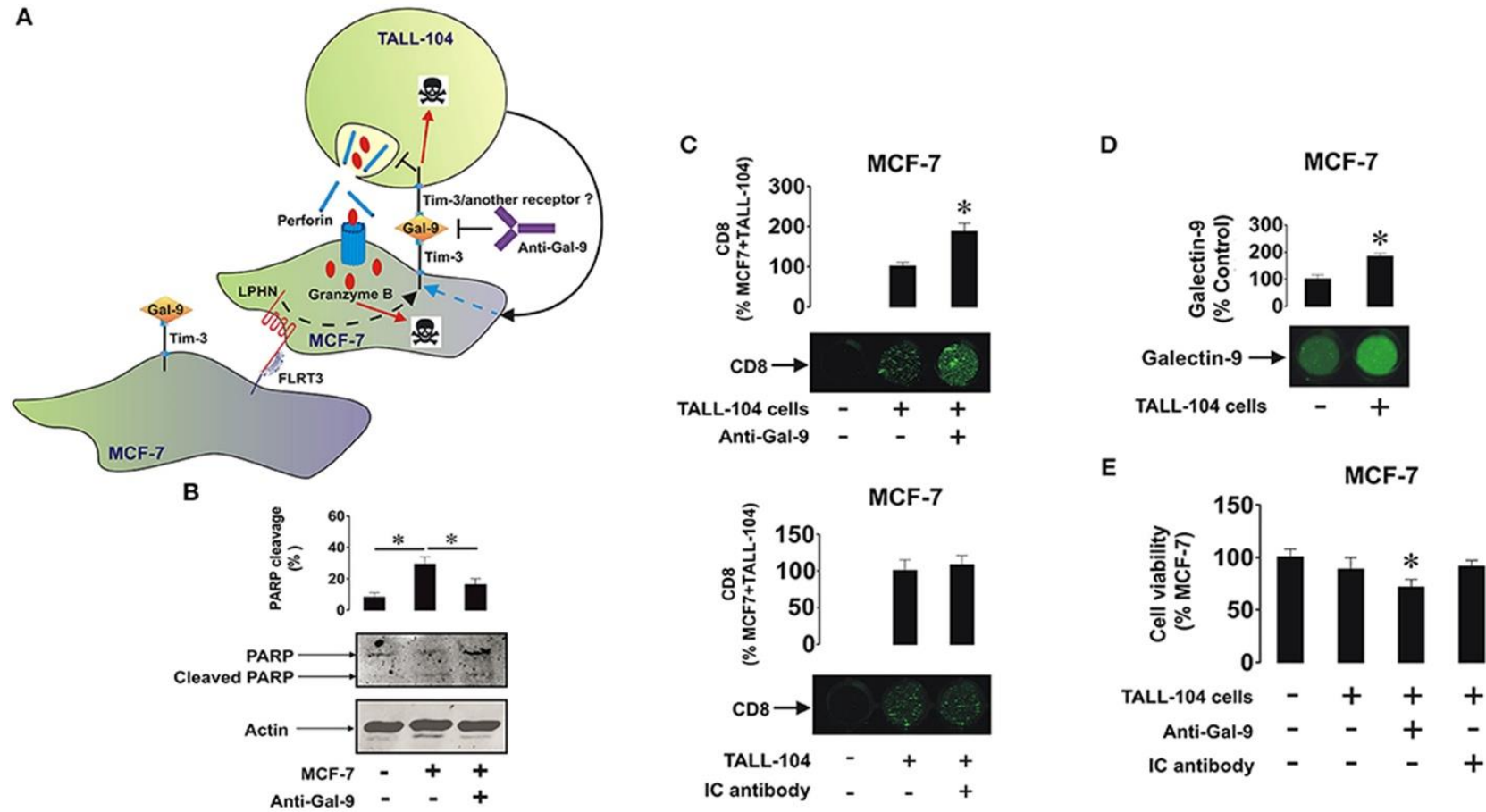
Altogether, these results strongly indicate that galectin-9 is capable of protecting breast tumour cells against cytotoxic cell-dependent killing from T cells.



**Figure 44: sTim-3 and galectin-9 suppress Jurkat T cell function.** Jurkat T cells were pre-treated with 100 nM PMA for 30 min followed by 24 h stimulation with 1  $\mu$ g/mL galectin-9 or Tim-3. Levels of released IFN $\gamma$ , TNF $\alpha$  and IL-2 were detected by ELISA. The catalytic activity of granzyme B was analysed in the cell lysates. Data are the mean values  $\pm$  SEM of four independent experiments (n=4).



**Figure 45: Galectin-9 protects MCF-7 cells against T cell-dependent cytotoxic immune attack.** (A) Illustrates that MCF-7 cells were co-cultured with Jurkat T cells (pre-treated with PMA) at a ratio of 2:1 for 4 h in the absence or presence of 5  $\mu\text{g}/\text{mL}$  galectin-9 neutralizing antibody. (B) Demonstrates the surface presence of Tim-3 and galectin-9 on Jurkat T cells and MCF-7, respectively. (C and D) After the experiment, MCF-7 cells and Jurkat T cells were assessed for granzyme B and caspases-3 activity as an indicator of granzyme B mediated apoptosis. Images are from one experiment representative of at least three, which gave similar results. Other results are presented as mean values  $\pm$  SEM of at least three independent experiments. \* $p < 0.05$  vs. control.

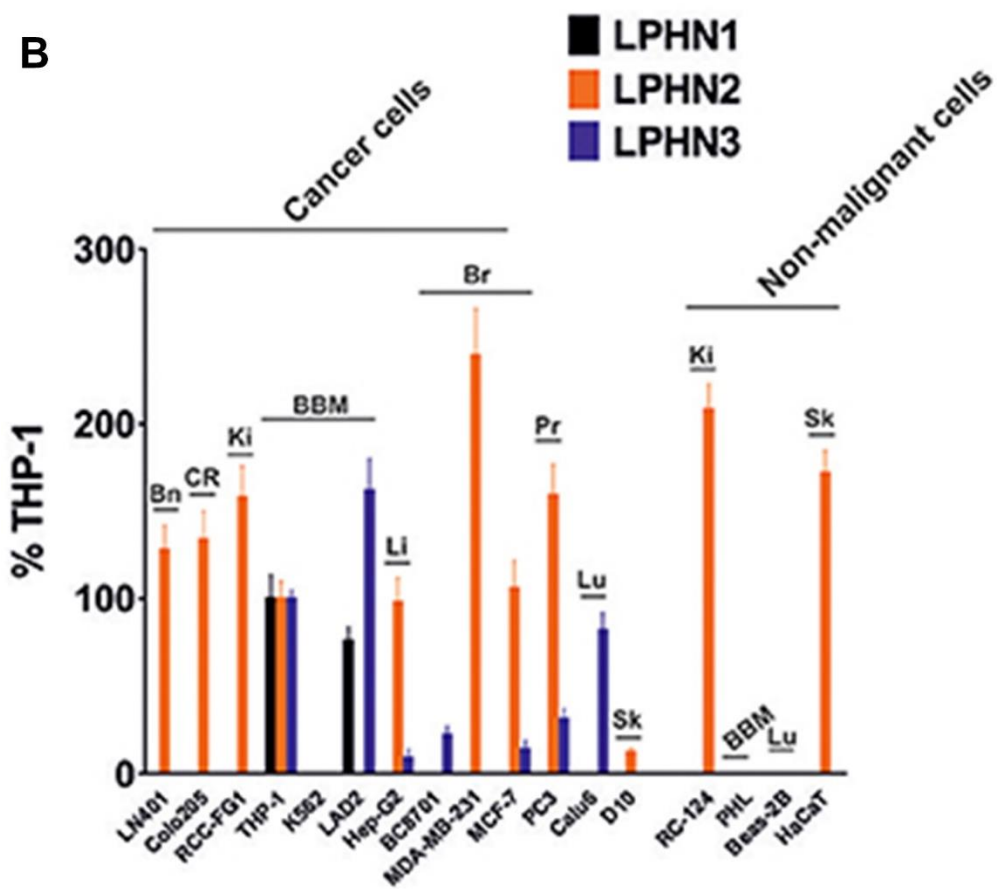
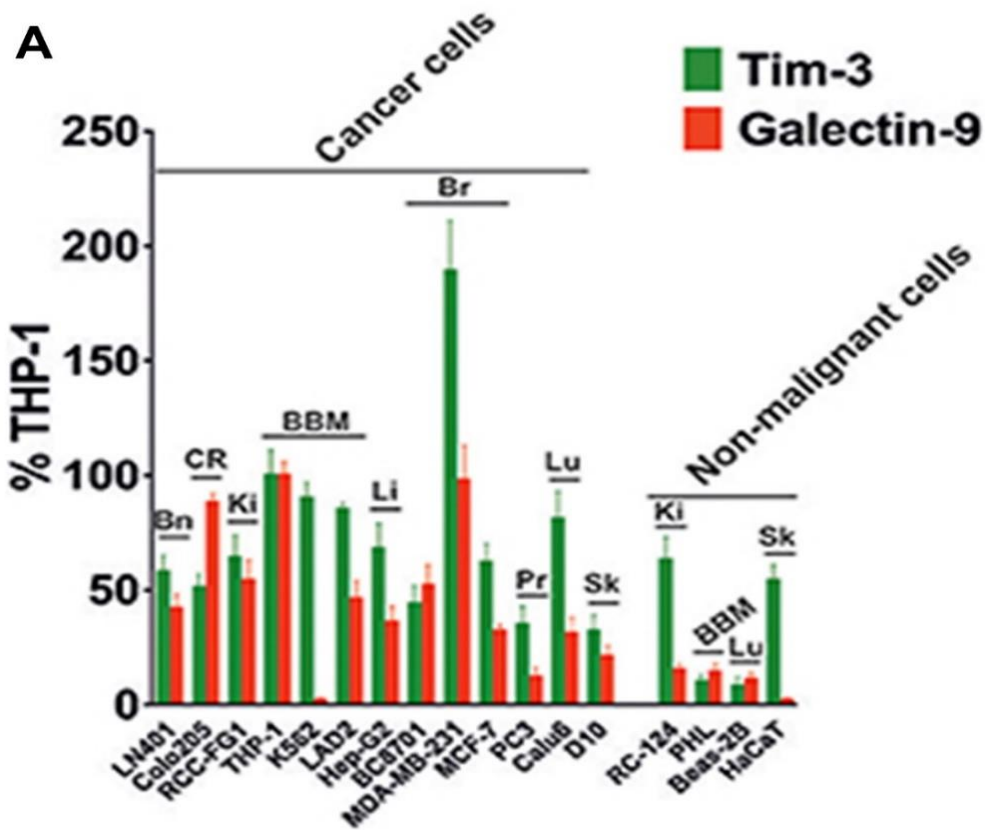


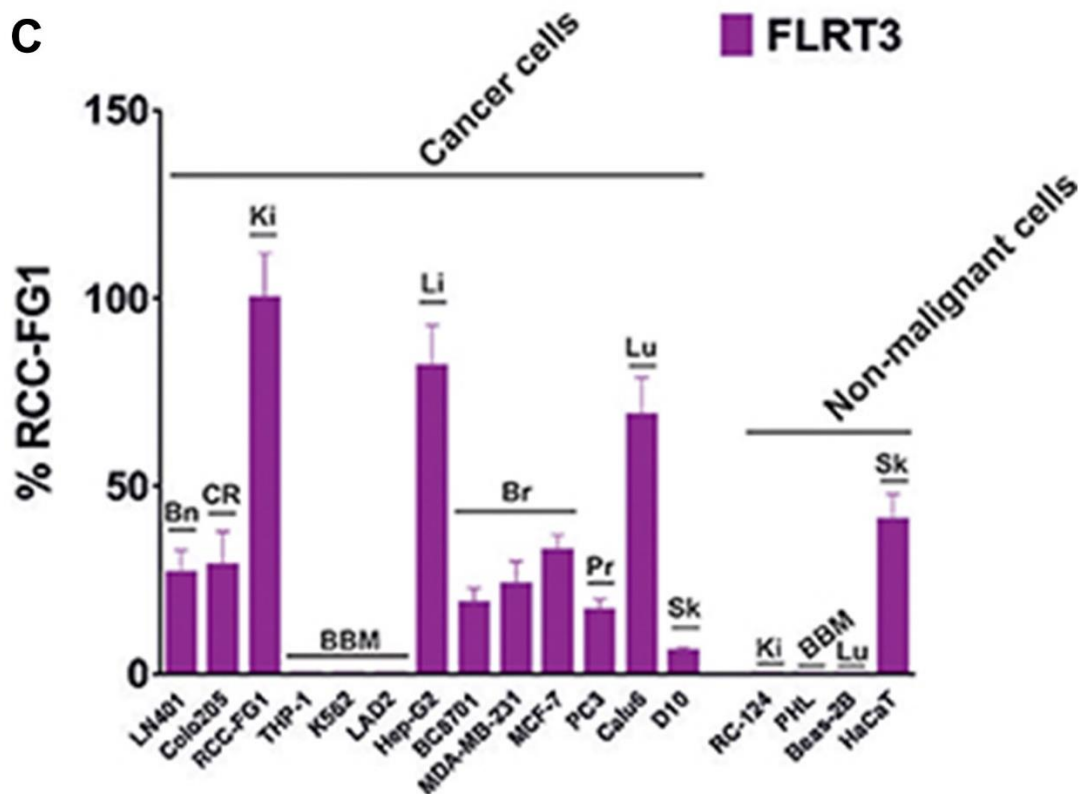
**Figure 46: Galectin-9 protects MCF-7 cells against T cell-dependent cytotoxic immune attack** (directly from (326)). (A) MCF-7 cells were co-cultured with TALL-104 cytotoxic T lymphocytes at a ratio of 4:1 for 16 h (the ratio was determined by the aggressive behaviour of TALL-104 cells) in the absence or presence of 5  $\mu\text{g}/\text{mL}$  galectin-9 neutralizing antibody or 5  $\mu\text{g}/\text{mL}$  isotype control antibody. (B) After the experiment, TALL-104 cells were lysed, and PARP cleavage, as an indicator of the rate of apoptotic cells, was measured using WB analysis. (C) CD8 expressions (reflecting the infiltration of TALL-104 into the MCF-7 layer) were measured by on-cell assay. (D) Galectin-9 surface presence was measured using an on-cell assay in resting MCF-7 cells and those co-cultured with TALL-104 cells. (E) Viability of MCF-7 cells was measured by MTS test. Images are from one experiment representative of five, which gave similar results. Other results are presented as mean values  $\pm$  SEM of five independent experiments. \* $p < 0.05$  vs. control (326).

#### 4.1.7 The Majority of Solid and Liquid Tumours Expresses Key Components of the FLRT3-LPHN-Galectin-9-Tim-3 Pathway

It has previously been reported that galectin-9-Tim-3 pathway is used by AML cells (liquid/haematological tumour) as an immune escape mechanism and in this study, it was found that this also holds true for breast cancer (solid tumour). In both cases, the surface presence appears to be regulated by the FLRT3-LPHN pathway. As many cancer cells of different origins have been reported to have elevated levels of galectin-9/Tim-3, it suggests that this may be a common immune escape mechanism for different types of cancer, and accordingly, the regulation of it might be similar. Therefore, the expression of FLRT3-LPHN-galectin-9-Tim-3 pathway components was investigated by WB analysis in cancer cells of different origins: various human cancer cell lines (derived from brain, colorectal, kidney, blood/mast cell, liver, breast, prostate, lung, and skin tumours) and various non-malignant cell lines and primary cells. Comparative WB analysis was performed by normalizing the measured infrared fluorescence of the bands by dividing with the total quantity of the loaded protein. This approach was followed because the cells analysed originated from different tissues, and thus the levels of each housekeeping protein (such as beta-actin) varied depending on the origin of the cells. Results of quantitative analysis are summarized in Figure 47, and WB images are presented in Appendix, Table 2. All the studied cancer cells, except for the chronic myeloid leukaemia (CML) cell line, K562 expressed Tim-3 and galectin-9. K562 expressed Tim-3, but only traces of galectin-9 in agreement with previously reported observations (64). The levels of secreted galectin-9 were measured in different cell lines, and variations were observed dependent on their origin (Appendix, Table 2). The highest levels of galectin-9 were measured in haematological (except for K562 cells) and colorectal cancer cells. Other cell types expressed moderate levels, and prostate cancer cells expressed lower, but still detectable levels of at least one isoform of galectin-9 (Appendix, Table 2). Compared to cancerous cells, non-malignant cells of similar origins expressed lower amounts of galectin-9 and Tim-3. Furthermore, the majority of the cells expressed at least one LPHN isoform as well as the ligand, FLRT3. Some of the cells did not express FLRT3, but expressed LPHN isoforms (Appendix, Table 2). This most likely implies that these LPHN expressing cells use blood-based soluble FLRT3 to trigger the pathway since the other LPHN ligand, teneurin-2, is not found in blood (323).







**Figure 47: Expression of Tim-3, galectin-9, LPHNs 1, 2, and 3 as well as FLRT3 proteins in various human cancer cell lines** (directly from (326)). Lysates of indicated cells were subjected to WB analysis as outlined in Materials and Methods (images are presented in Appendix Table 2). Detected infrared fluorescence of the bands divided by the total amount of protein loaded (measured using a Bradford assay) was used as a measure of protein quantity. Levels of Tim-3 & total galectin-9 (A) and LPHNs 1, 2, & 3 (B) were expressed as a % of the levels present in THP-1 cells (expressed as 100%). Since THP-1 cells lack FLRT3 expression, the levels of this protein were expressed as % RCC-FG1 (C), considering FLRT3 level in these cells as 100%. Bn, brain; CR, colorectal; Ki, kidney; BBM, blood, bone marrow and mast cells; Li, liver; Br, breast; Pr, prostate; Lu, lung; Sk, skin. Data are presented as mean values  $\pm$  SEM of three independent experiments (326).

#### 4.1.8 Discussion

Growing evidence shows that the galectin-9-Tim-3 pathway is involved in immune escape in both liquid and solid tumours (for example in AML and colorectal cancer) (64, 257). In this study, it was demonstrated that the FLRT3-LPHN-galectin-9-Tim-3 immunosuppressive pathway is activated in breast cancer tissue (solid tumour) and protects malignant cells from cytotoxic immune attack (illustrated in Figure 48). Using SRCD, it was found that FLRT3, as the LPHN1 and LPHN3, can also bind to LPHN2 (Figure 43A). MCF-7 expresses both LPHN2 and LPHN3 (Figure 42A). Moreover, it was found that FLRT3 (by binding to LPHNs on the cell surface) induced the upregulation of PLC and PKC $\alpha$  activities intracellularly, which leads to a significant increase in galectin-9 surface expression (

Figure 43).

TALL-104 and Jurkat T cells were used as model for tumour-infiltrating T cells. Jurkat T cells have in other studies been reported not to express Tim-3 even after PMA stimulation assessed with WB (271). However, the present study clearly shows that Jurkat T cells express Tim-3 on their surface (Figure 45B), and expression in resting condition has also been demonstrated by WB (Appendix, Figure 79). This discrepancy might possibly be explained by the applied antibody. If they for example used an antibody that only recognizes the native form of Tim-3 in the WB, it might not be recognized.

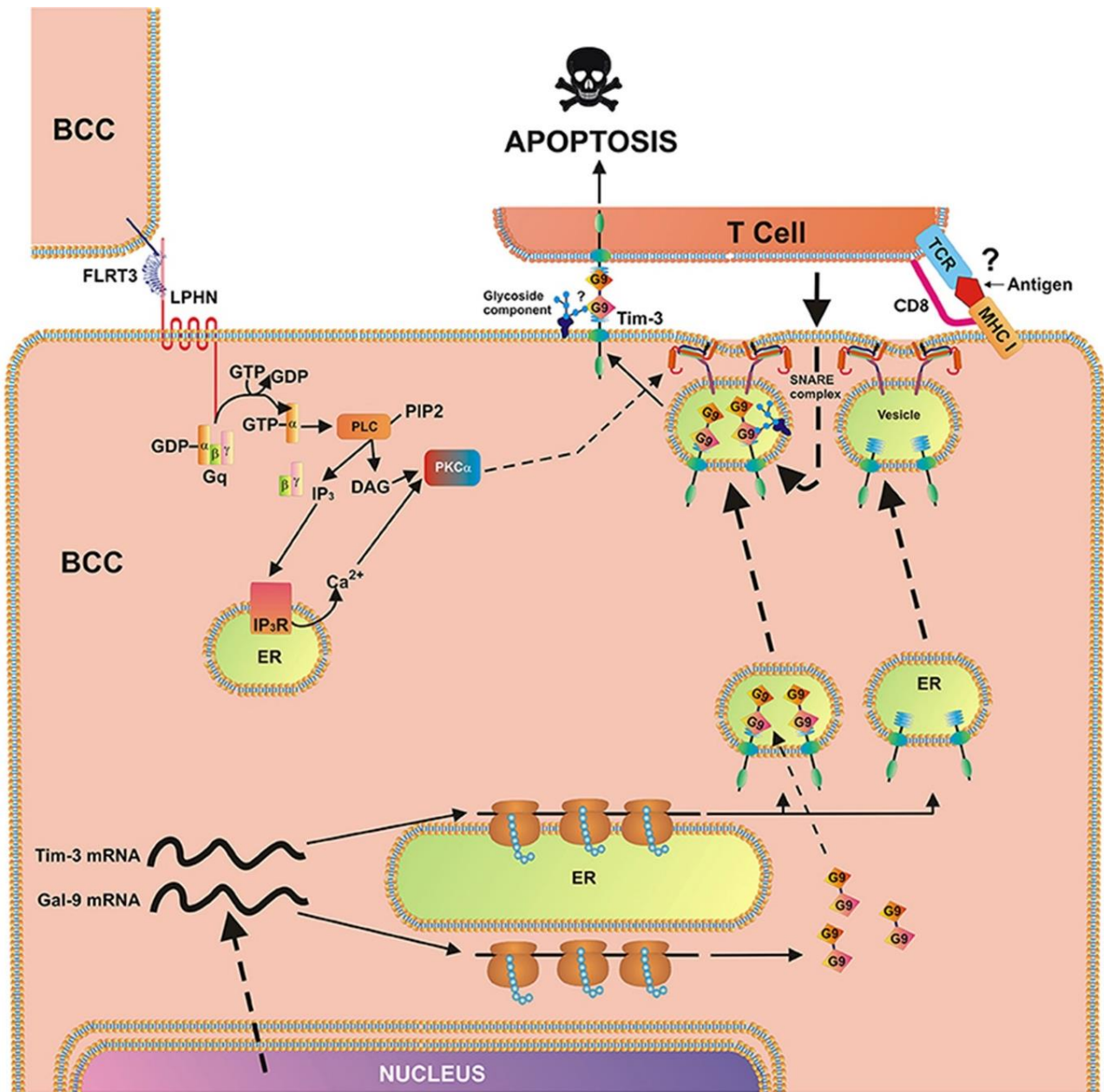
Both Jurkat T cells and the more cytotoxic T cell line TALL-104 were applied to confirm that, as in AML, breast cancer cells use galectin-9 to attenuate the cytotoxic activity of immune cells by increasing granzyme B activity inside them, resulting in apoptosis (as indicated by caspase-3 activity and/or PARP cleavage) (Figure 45 and Figure 46). Although the mechanism behind the galectin-9-induced intracellular granzyme B activity is unclear. Albeit, recently, our group have reported that in AML secreted galectin-9 together with VISTA and Tim-3 form a multicomplex barrier on the T cells leading to a change in plasma membrane potential, which prevents granzyme B release, and thus its activity is increased inside the CTLs, resulting in their apoptosis (304). Here, the observed effects are most likely attributed to the membrane-bound form of galectin-9 complex with Tim-3, as demonstrated by WB in Figure 39 and Figure 78. Galectin-9 was probably associated to carbohydrates (as a lectin), therefore, it is unlikely to be secreted. Furthermore, all three breast cancer cell lines analysed were unable to secrete galectin-9 (Appendix, Table 2 and data not shown for MCF-7). In addition, MCF-7 cells expressed a Tim-3-galectin-9 complex with molecular weight of about 74 kDa (Figure 42A), which is almost similar to the 70 kDa of the membrane-associated form that was reported in AML cells (64). As galectin-9/Tim-3 is not continuously secreted by breast cancer cells, and thus does not need to be replenished, it may explain why there was no difference in mTOR activity in healthy and breast tumour tissue, and when MCF-7 cells were stimulated with FLRT3 (Figure 40C and Figure 43C).

In this study, the expression of key components of FLRT3-LPHN-galectin-9-Tim-3 pathway was analysed in malignant and non-malignant cells of different origin. In general, cancer cells express a higher amount of Tim-3 and galectin-9 compared to healthy (non-

malignant) cells (Figure 47), and they express at least one isoform of LPHNs. Most cancer cells also express FLRT3 or might use blood-based soluble FLRT3. This indicates that the FLRT3-LPHN-galectin-9-Tim-3 pathway may be operational in cancer cells of different origins, and thus, targeting these pathways could be promising anti-cancer immunotherapies.

In addition, our group recently reported that the LPHN1 expression in AML is upregulated by cortisol, but not in healthy leukocytes (324). Furthermore, abnormal cortisol levels have also been associated with poor breast cancer survival with a reduction in NKs count and function (467). Hence, it could be speculated that cortisol may also dysregulate the expression of other LPHN receptors and contribute to immune escape via galectin-9. However, our own work (data not shown) indicates that cortisol does not regulate LPHN2 expression in non-malignant HaCaT cells, but there was a tendency towards an increase in FLRT3 expression and a significant increase on galectin-9 surface level. Therefore, in the future, it would be interesting to investigate if cortisol in other types of cancer (other than AML) may contribute to a dysregulated expression and activity of the FLRT3-LPHN2 pathway that stimulates aberrant expression of the galectin-9-Tim-3 pathway, which leads to immune escape.

On the other hand, there may be additional pathways operated by breast cancer cells to suppress the activity of cytotoxic immune cells. For example, the presence of TALL-104 cells significantly upregulates galectin-9 surface presence in MCF-7 breast cancer cells (Figure 46D). However, biochemical pathways underlying this phenomenon remain elusive.



**Figure 48: Breast cancer cell-based patho-biochemical pathways showing LPHN-induced activation of PKC $\alpha$ , which triggers the translocation of Tim-3 and galectin-9 onto the cell surface which is required for immune escape (directly from (326)).** The interaction of FLRT3 with LPHN isoform leads to the activation of PKC $\alpha$ , most likely through the classic Gq-PLC-Ca<sup>2+</sup> pathway. Ligand-bound LPHN activates Gq, which in turn stimulates PLC. This leads to phosphatidyl-inositol-bisphosphate (PIP2) degradation and production of inositol-trisphosphate (IP3) and diacylglycerol (DAG). PKC $\alpha$  requires DAG and cytosolic Ca<sup>2+</sup> for its activation. Activated PKC $\alpha$  provokes the formation of SNARE complexes that tether vesicles to the plasma membrane. Galectin-9 impairs the cancer cell killing activity of cytotoxic T cells (and other cytotoxic lymphocytes) (326). Possible (not directly confirmed) interactions of galectin-9 with glycoside component and T cell receptor (TCR)/CD8, with MHC I, and the antigen are highlighted with question mark “?” to indicate the fact that it is a hypothetical interaction since TALL-104 cells used in the study kill tumour cells in an MHC-independent manner (326, 468).

## 4.2 Transforming Growth Factor-beta Type 1 (TGF- $\beta$ ) and Hypoxia-inducible Factor 1 (HIF-1) Transcription Complex as Master Regulators of the Immunosuppressive Protein Galectin-9 Expression in Human Cancer Cells

Human cancer cells express in most cases much higher levels of galectin-9 compared to non-transformed cells and use it to escape immune attack (64, 326). In the previous section 4.1, it is described that one of the mechanisms in which cancer upregulates galectin-9 is by the FLRT3-LPHN pathway, which is downstream dependent on PLC and PKC $\alpha$  for solid tumours, such as breast cancer (326). However, liquid tumours, such as AML, are also dependent on mTOR activity (which regulates protein synthesis) in addition to PLC and PKC $\alpha$  as galectin-9 needs to be replenished due to secretion (64). Other pathways may also be involved as it was observed that co-culture with cytotoxic T cells and breast cancer cells upregulated galectin-9 surface presence on cancer cells (326). However, biochemical pathways underlying this phenomenon remain elusive.

Early tumourigenesis of solid tumours is followed by hypoxia and the induction of the transcription factor hypoxia-inducible factor 1 (HIF-1) (consisting of HIF-1 $\alpha$  and HIF-1 $\beta$ ), which promote angiogenesis, erythropoiesis and glycolysis to keep the growing tumour oxygenated and nourished (469, 470). Hypoxia is linked to oxidative stress by promoting the production of mitochondrial ROS as well as by mitochondrial independent mechanisms, such as Xanthine oxidase (XOD) (471, 472). Hypoxia could act to increase activity of XOD and modulate its expression via HIF-1 (472, 473). Furthermore, ROS can be generated under normoxic conditions, e.g. enzymatically by NADPH oxidase (Nox) and/or XOD, and ROS derived from these enzymes has been implicated in tumorigenesis and progression (425, 471, 472, 474-476). The expression and or activity of these enzymes are increased in some types of cancers. Nox, for example, is regulated by the GTPase Rac1, which is downstream of proto-oncogene Ras that is frequently mutated to be constitutive active in some cancer types (476, 477). As many types of protein, TLR4 has a dual effect on cancer, both promoting anti-tumour immunity and facilitating tumour growth and immune escape (478). LPS (a TLR4 ligand) has been reported to increase activity of Nox and XOD as well as regulate XOD expression (425, 473, 479). Thus, ROS from different sources contributes to oxidative stress in cancer.

ROS levels have been reported to be greater in tumour cells as opposed to healthy cells (476, 480). ROS (such as hydroxyl radicals) in itself could contribute to tumourigenesis as it promotes genome instability by damaging DNA (471). However, ROS is involved in mediating signalling by activating kinases or inhibiting phosphatases, and it thus could activate pathways like MAPK and PI3K-AKT pathways (471). Indeed, ROS has been shown to activate the apoptosis signal-regulating kinase 1 (ASK1)-p38 pathway, which can mediate apoptosis in cells with severe oxidative stress (476, 481, 482), however, it has also been reported to promote stabilization of HIF-1 $\alpha$  (425, 479). Another way for ROS to participate in the stabilization of HIF-1 $\alpha$  is most likely by inhibiting prolyl hydroxylase (PHD) and/or factor inhibiting HIF (FIH) (470, 483-485). HIF-1 $\alpha$ , which as part of the HIF-1 complex, promotes transcription of genes associated with tumour growth, angiogenesis, metastasis and resistance to therapy (471). In addition, a recent study has reported elevated plasma levels of HIF-1 $\alpha$  in breast cancer patients (486). In fact, HIF-1 $\alpha$  has been shown to promote breast cancer invasion by CSRP2, an invadopodial actin-bundling protein (487), and promote cancer progression by inhibiting apoptosis and inducing cell proliferation by HIF-1-mediated TGF- $\beta$  signalling (486). Furthermore, TGF- $\beta$  signalling primes breast tumour metastasis to the lungs by induction of angiopoietin-like 4 (488). Hypoxia-induced HIF-1 and TGF- $\beta$  signalling have been linked to different diseases, such as fibrosis and various cancers (476). Both hypoxia/ROS-mediated HIF-1 and TGF- $\beta$  have been implicated in the induction of EMT and metastasis and resistance to radiotherapy and chemotherapy (366, 470, 471, 480).

As mentioned, TGF- $\beta$  is a growth factor-like cytokine, which has a dual role in cancer settings. In early stages, it acts as a tumour suppressor whereas in later stages it contributes to tumour progression by inducing EMT and facilitates tumour invasion and metastasis (489). Elevated plasma levels of TGF- $\beta$  have been correlated with poor prognosis in different types of cancer including hepatocellular carcinoma, lung, prostate and colorectal cancer (359, 490). The prognostic value of TGF- $\beta$  plasma level in breast cancer is debatable as some studies report it elevated (491, 492), and others report no difference compared to healthy control (493, 494). Although, there is a consensus that TGF- $\beta$  is elevated in breast tumour tissue and breast cancer cell lines, and this contributes to breast tumour progression and metastasis (367, 486, 488, 490, 495-497). Furthermore, TGF- $\beta$  contributes to an immunosuppressive TME as it inhibits immune surveillance by

multiple mechanisms (355, 490, 498, 499). TGF- $\beta$  mediates its effect by binding to TGF- $\beta$  receptors and activates classical Smad signalling and alternative non-Smad signalling, such as PI3K-AKT and MAPK pathways (357). Classical Smad signalling initiated by TGF- $\beta$  activates Smad2 and Smad3, which can complex with, e.g. Smad4 or transcription intermediary factor 1-gamma (TIF-1 $\gamma$ , also known as tripartite motif-containing factor 33 (TRIM33)), together with other co-regulators to induce or repress transcription of target genes (362, 500). Computational analysis reveals several Smad3 response elements in the TGF- $\beta$  promoter region (Appendix, Figure 80), and thus could upregulate TGF- $\beta$  expression in an autocrine manner capable of supporting itself without external signals. In addition, several Smad3 response elements were identified in the LGALS9 promoter region (Appendix, Figure 81), suggesting that TGF- $\beta$  might be involved in the regulation of galectin-9. This is supported by a study on iTregs demonstrating that Smad3 can bind to the LGALS9 promoter region to induce production of galectin-9 (273).

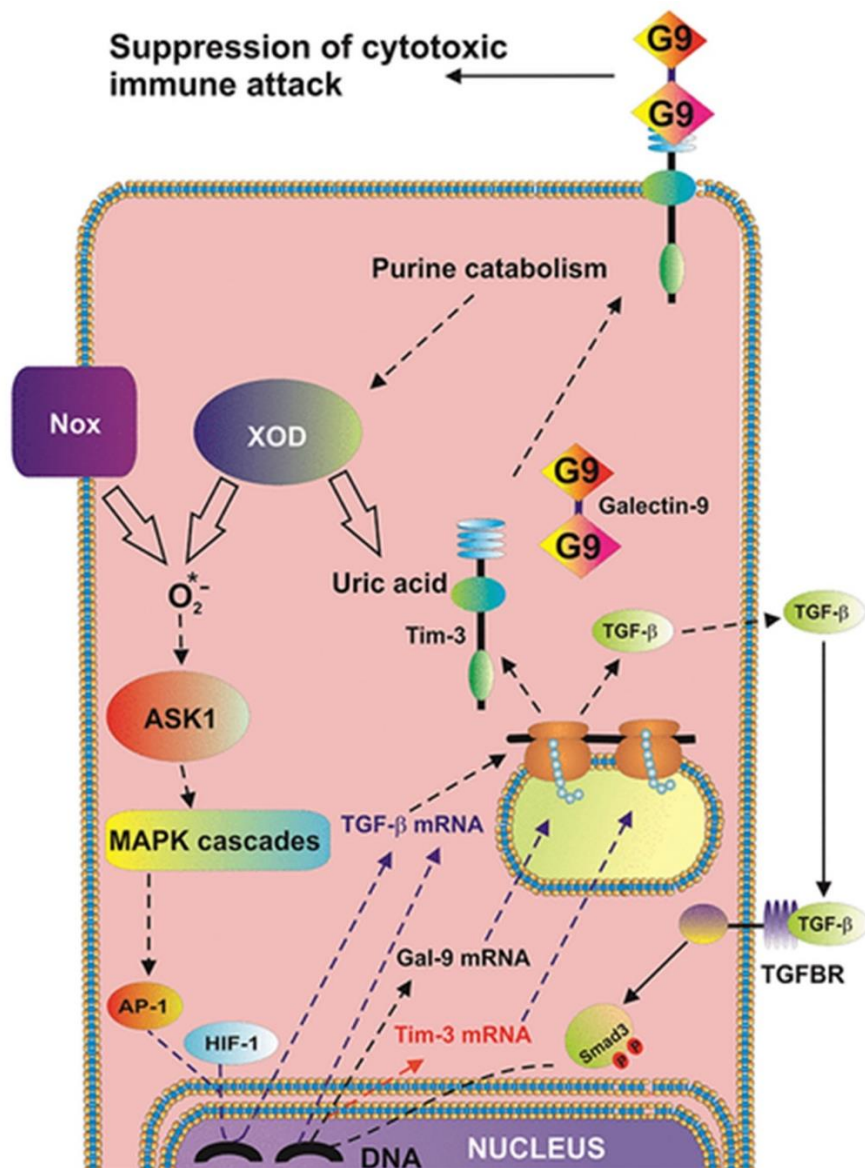
Since hypoxia and increased oxidative stress is associated with cancer resulting in increased levels of HIF-1-induced TGF- $\beta$ , and TGF- $\beta$  at least in some setting is able to induce galectin-9, it could be speculated that HIF-1-mediated TGF- $\beta$  induction could be involved in galectin-9 regulation and thus facilitate immune escape and possible resistance to therapy.

#### 4.2.1 Oxidative Stress, HIF-1, TGF- $\beta$ , Smad3 and Galectin-9 are Upregulated in Primary Human Cancers

Characterization of the human TGF- $\beta$ 1 promoter region has identified several possible regulators, among these are AP-1, HIF-1 and Smad3 (Appendix, Figure 80). It was hypothesised that in cancer cells, oxidative stress (caused by hypoxia or increased activity of Nox and/or XOD) could stabilize HIF-1 $\alpha$ , as well as initiation of ASK1 signalling, resulting in activation of p38 and JNK (stress sensors) and formation of the AP-1 complex, which either alone or in synergy with HIF-1 can induce TGF- $\beta$ 1 transcription and translation. TGF- $\beta$  is proposed to enhance its own production in an autocrine manner via activation of Smad3, and this TGF- $\beta$ -mediated Smad3 activation is suggested to promote the induction of galectin-9, which can be used to escape cytotoxic immune attack. This hypothesis is illustrated in

Figure 49.



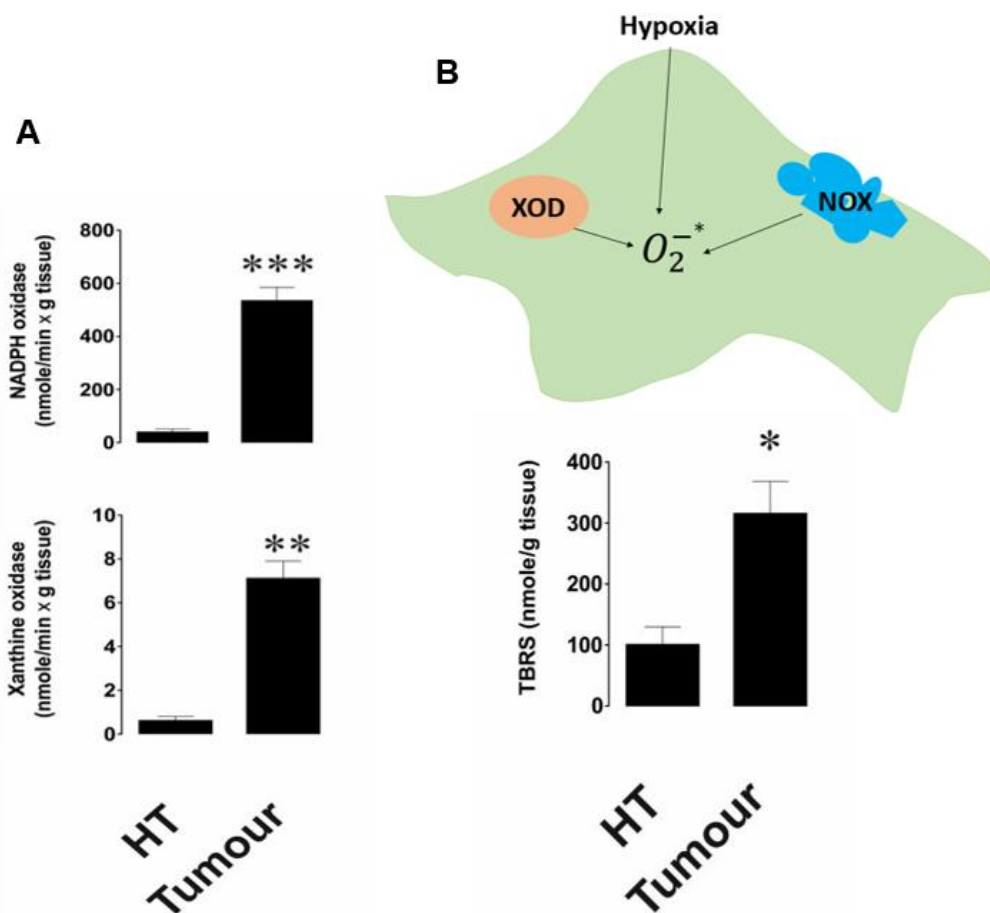


**Figure 49: Proposed model in which oxidative stress mediates HIF-1 and AP-1 activation, resulting in the production of TGF- $\beta$  and upregulation of galectin-9 (directly from (419)).** The proposed pathway studied is summarised, and it is indicated that XOD and Nox produce ROS, which activates the transcription factor AP-1 through ASK1-controlled MAP kinase cascade. HIF-1 and AP-1 contribute to the activation of TGF- $\beta$  expression, which then displays autocrine activity and stimulates the activation of galectin-9 and possibly Tim-3 expression through Smad3 transcription factor (419).

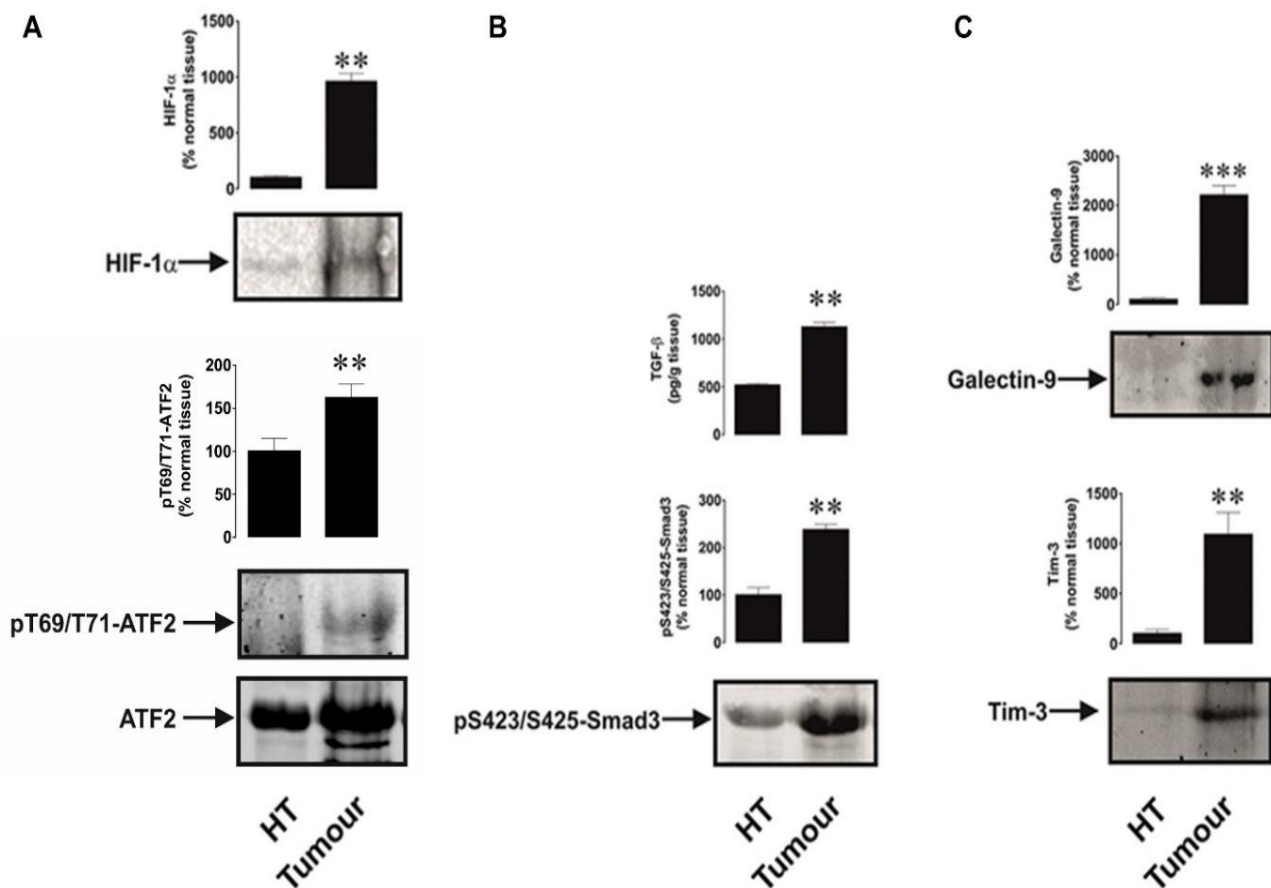
The hypothesis was first tested in breast cancer. Primary breast tumour tissue (BT) and adjacent healthy breast tissue (HT) from five patients were resected, homogenised, and lysed as described in the method section. Experiments were set up to assess Nox and NOD activity, which produces ROS, and measurement of thiobarbiturate reactive substance (TBRS) assay was performed. TBRS is a product of lipid peroxidation and acts as an indicator of oxidative stress (456), thus the higher the value, the more ROS has been produced, and the greater the oxidative burst. As shown in Figure 50A, both Nox and

XOD activity are significantly increased in BT compared to HT, suggesting increased oxidative burst, and it is reflected by a significant increase in TBRS levels (Figure 50B). This indicates that ROS levels are higher in breast tumour tissue compared to healthy tissue. The ATF-2 phosphorylation (part of active AP-1 complex), HIF-1 $\alpha$  accumulation, TGF- $\beta$ 1 expression and Smad3 phosphorylation (an indicator of active TGF- $\beta$  signalling) were assessed. The results showed an increased level of HIF-1 $\alpha$  accumulation and ATF-2 phosphorylation as well as increased production of TGF- $\beta$ 1 and Smad3 activation in BT compared to HT (Figure 22A and B). HIF-1 $\alpha$  is normally hydroxylated by PHD, which targets it for proteasomal degradation by von Hippel-Lindau (VHL) E3 ubiquitin ligase complex (470, 484, 485). HIF-1 $\alpha$  expression is stabilized and accumulated upon hypoxia and hypoxia-independent mechanisms such as PI3K-AKT activation and generation of ROS (470, 472, 484, 485). Thus, the fact that higher levels of ROS and an increase in HIF-1 $\alpha$  accumulation were observed in BT compared to HT suggested that these data confirm previous reported studies. ROS is known to act as an oxidant and thereby activates kinases or inhibits phosphatases to induce signal transduction (471). ASK1 is a redox-sensitive kinase, which is normally inhibited by thioredoxin (Trx). For Trx-ASK1 binding, the reactive SH-groups of Trx must be in the reduced form. Upon oxidation of Trx reactive thiol groups, ASK1 dissociates from Trx, followed by its activation (homodimerization and autophosphorylation). ASK1 mediates activation of the MAPK pathways that trigger p38 and JNK activation, which result in c-jun and ATF-2 activation respectively, which together form the AP-1 transcriptional complex (481). Several studies have implicated HIF-1 in the induction of TGF- $\beta$ , including a recent study on breast cancer (486). In addition, computational analysis reveals several HIF-1 response elements in the TGF- $\beta$  promoter, supporting the role of HIF-1 in the induction of TGF- $\beta$  (Appendix, Figure 80). Other transcription factors, such as AP-1, have been reported to be involved in TGF- $\beta$  induction (501, 502). In support of this, at least two possible AP-1 binding sites were identified in the TGF- $\beta$ 1 promoter (Appendix, Figure 80). TGF- $\beta$  has been reported to promote its own production in an autocrine manner (501). Although, TGF- $\beta$  can mediate non-Smad signalling that leads to activation of AP-1, Smad signalling may be the major contributor to TGF- $\beta$  production as a substantial higher number of Smad3 binding sites was identified in the promoter region (Appendix, Figure 80). This suggests that ROS mediated activation of HIF-1 and AP-1 may promote initial TGF- $\beta$ 1 production but is enhanced by TGF- $\beta$  signalling itself. In fact, TGF- $\beta$  signalling mediates positive feedback as it has been

reported to both induce AP-1(c-Jun) and HIF-1 $\alpha$  (470, 485, 501, 503, 504). Furthermore, TGF- $\beta$  signalling is autocrine as it induces its own production as well as its receptors, which boost TGF- $\beta$  responsiveness and enhance Smad3 phosphorylation (505-507). Smad3 has many different targets, one of them has been suggested to be galectin-9, and several Smad3 response elements have been found in the LGALS9 promoter region (Appendix, Figure 81). In addition to an elevated TGF- $\beta$  production and increase activation of Smad3 (Figure 51B), an augmented expression was observed of both galectin-9 and Tim-3 in BT compared to HT (Figure 51C). This could suggest that TGF- $\beta$ 1 signalling promotes galectin-9.



**Figure 50: Oxidative burst is increased in breast cancer tissue** (adapted from (419)). Tissue lysates from breast tumour and adjacent healthy breast tissue were subjected to measurement of xanthine oxidase and NADPH oxidase activities (A) and TBRS levels (B). As illustrated in the figure superoxide radicals may in the tumour tissue be caused by hypoxia, increased XOD or Nox activity. All quantities are expressed in respective units per 1 g of the tissue. In addition, normalisations against total protein for enzyme activities and TBRS assays were performed. These results are presented in Appendix, Figure 82. Images are from one experiment representative of five, which gave similar results. Data are shown as mean values  $\pm$  SEM of five independent experiments. \* -  $p < 0.05$  and \*\* -  $p < 0.01$  vs non-transformed peripheral tissue abbreviated as HT (healthy tissue) (419).

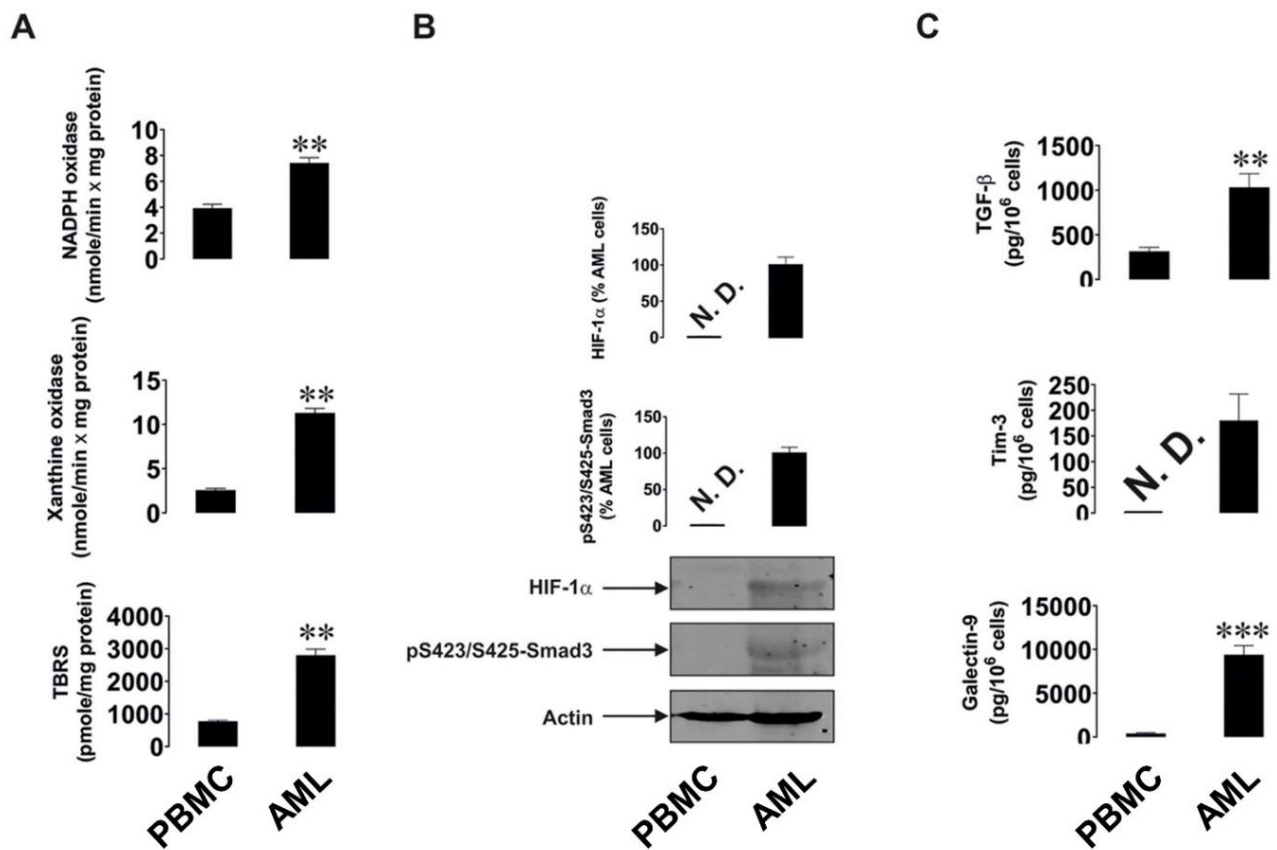


**Figure 51: Increased redox status, upregulated HIF-1 $\alpha$ , ATF-2 activation and TGF- $\beta$ /Smad3 pathways and Tim-3 and galectin-9 expression in breast tumour tissues compared to non-transformed peripheral tissues** (adapted from (419)). HIF-1 $\alpha$  accumulation, tissue-associated and phosphorylation of ATF-2 TGF- $\beta$  and phospho-S423/S425-Smad3 levels (A), as well as levels of tissue-associated Tim-3 and galectin-9 (B), were analysed in tissue lysates. All quantities are expressed in respective units per 1 g of the tissue. In addition, normalisations against total protein loaded (for WB) were performed. These results are presented in Appendix, Figure 82. Images are from one experiment representative of five which gave similar results. Data are shown as mean values  $\pm$  SEM of five independent experiments. \* -  $p < 0.05$  and \*\* -  $p < 0.01$  vs non-transformed peripheral tissue abbreviated as HT (healthy tissue) (419).

It was previously reported (Section 4.1) that the FLRT3-LPHN-PLC-PKC $\alpha$  is a pathway used by several types of cancer to upregulate galectin-9/Tim-3 expression. In this study, focus was on other possible pathways that upregulate galectin-9. The present study reports that primary breast cancer (solid tumour) may activate the ROS-HIF-1-TGF- $\beta$ -Smad3 pathway to upregulate galectin-9. Therefore, it was relevant to investigate if this pathway may be used by other various forms of cancer such as AML (liquid/haematological tumour).

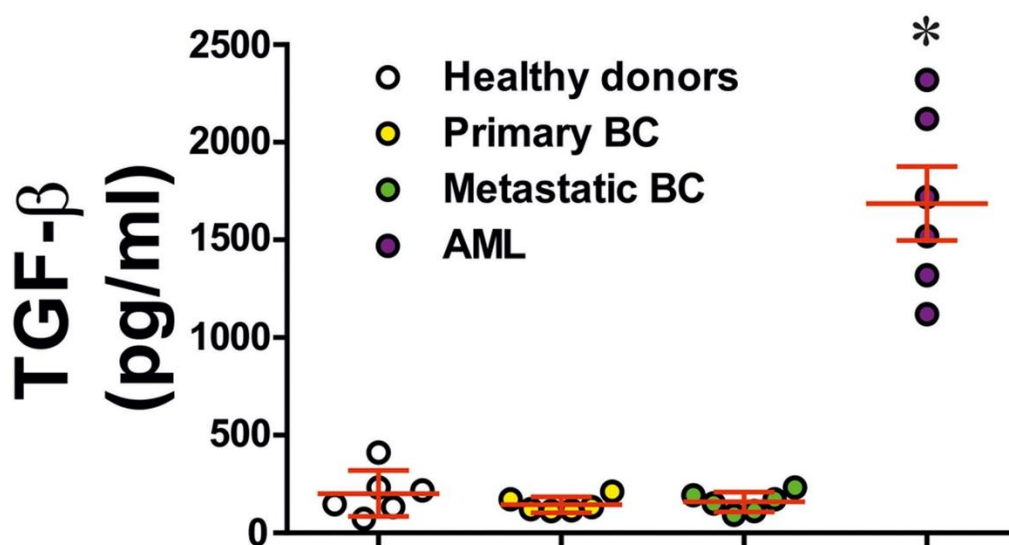
AML cells isolated from newly diagnosed patients were compared with primary PBMCs isolated from healthy donors upon culturing them for 24 h. As in breast cancer tissue, there was an increased activity of both Nox and XOD in AML cells compared to PBMCs, and this

was further reflected with a significant increase in TBRS levels (Figure 52A), suggesting that these cells had more oxidative stress than PBMCs. AML cells showed an increase in HIF-1 $\alpha$  accumulation (Figure 52B) most likely due to the augmented ROS production. Furthermore, there was an increase in the production of TGF- $\beta$ 1 and Smad3 phosphorylation in AML compared to PBMCs (Figure 52C and Figure 52B). Although, PBMCs produced some TGF- $\beta$ , there was undetectable sign of active TGF- $\beta$  signalling. As reported previously, since AML is a haematological form of cancer, these cancer cells fend off an immune attack from afar by secreting Tim-3 and galectin-9, therefore, the secreted levels by these cells were assessed. AML cells had an increase of secreted galectin-9 and Tim-3 compared to PBMCs (Figure 52C). This suggests that the ROS-HIF-1-TGF- $\beta$ -Smad3 pathway may be used by AML cells to promote galectin-9 secretion.



**Figure 52: Increased redox status, upregulated HIF-1 $\alpha$  and TGF- $\beta$ -Smad3 pathways as well as Tim-3 and galectin-9 expression in primary human AML cells compared to non-transformed PBMCs (from (419)).** Measurements were conducted in primary human AML cells vs primary peripheral blood mononuclear cells (PBMCs, leukocytes) obtained from healthy donors. Activities of xanthine oxidase, NADPH oxidase and TBRS levels (A). Levels of accumulated HIF-1 $\alpha$  protein and phospho-S423/S425-Smad3 were assessed by WB (B). Levels of secreted TGF- $\beta$ , Tim-3 and galectin-9 were measured in cell culture medium using ELISA (C). Images are from one experiment representative of five, which gave similar results. Data are shown as mean values  $\pm$  SEM of five independent experiments. \* -  $p < 0.05$  and \*\* -  $p < 0.01$  vs PBMCs (419).

Elevated plasma levels of TGF- $\beta$  have been reported for some cancer types (359). To understand the role of TGF- $\beta$ , blood plasma was analysed of healthy donors and cancer patients (six subjects of each category were analysed: healthy, primary breast cancer, metastatic breast cancer, and AML. In cases of primary and metastatic breast cancers, blood plasma levels of TGF- $\beta$  were similar to those in healthy donors. However, in AML patients they were strikingly and significantly elevated (Figure 53). These results suggest that in solid tumours, e.g primary and metastatic breast tumours, produced TGF- $\beta$  most likely remains in the tumour microenvironment. In contrast, in AML, TGF- $\beta$  is secreted into the peripheral blood and can be employed by circulating AML cells.



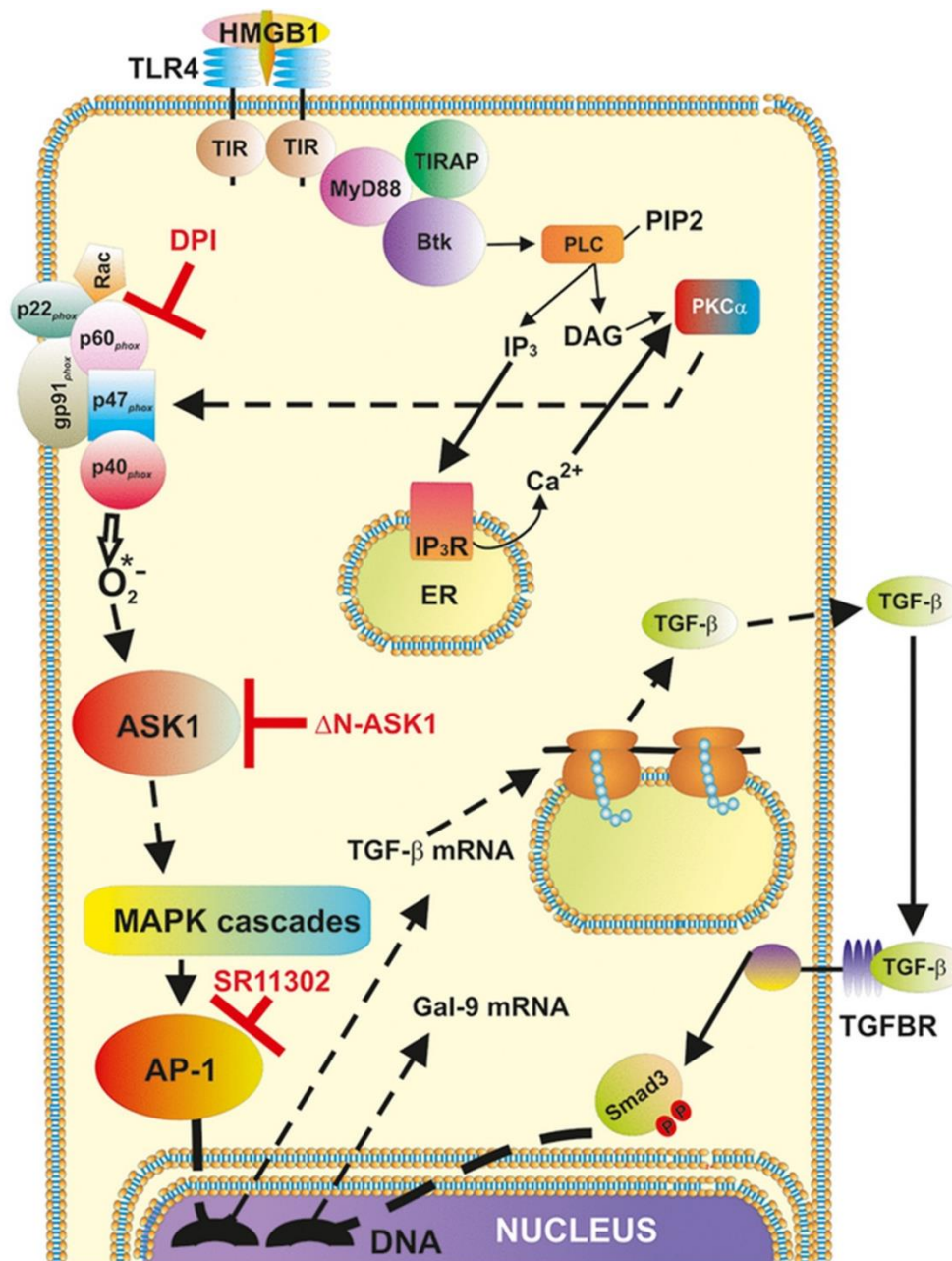
**Figure 53:** Levels of secreted TGF- $\beta$  in blood plasma of healthy donors, primary and metastatic breast cancer patients and AML patients (directly from (419)). TGF- $\beta$  concentrations were measured in the blood plasma of healthy donors, patients with primary breast tumours, patients with metastatic breast solid tumours and AML patients ( $n=6$  for all donor types). Data are shown as mean values  $\pm$  SEM (data for each patient are shown). \* -  $p < 0.05$  vs healthy donors (419).

#### 4.2.2 Redox-dependent Mechanisms Contribute to TGF- $\beta$ and Galectin-9 Expression in Models of Human Cancers

To understand the ability of redox-dependent ASK1-mediated activation of AP-1 in TGF- $\beta$  and galectin-9 production, THP-1 cells were used (a model for human acute myeloid leukaemia cells), which express Toll-like receptor 4 (TLR4). AP-1 is a complex in which composition can vary, however, one of them is the ATF-2-c-Jun complex (481, 508). c-JUN and ATF-2 are induced by JNK and p38 activation, respectively, which can be activated by ASK1 (481). ASK1 has been reported activated by ROS through the

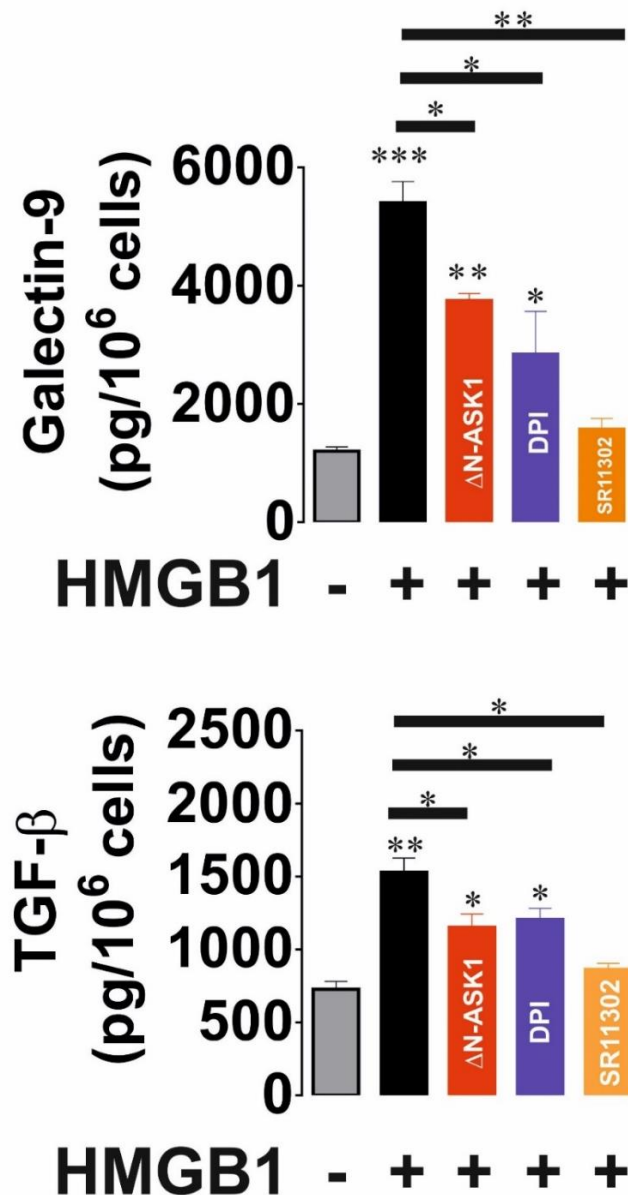
dissociation of Trx, and in the following activation, it recruits TRAF2 and/or TRAF6 to initiate MAPK cascade (481, 482). LPS-induced activation of TLR4 has been reported to induce ROS-TRAF6-ASK1-p38 activation in a MyD88-dependent mechanism (482), and stimulating this pathway can lead to AP-1 and HIF-1 accumulation (425, 482). The ROS generation by activated TLR4 has been suggested to be due to assembly of Nox, by Btk-PLC-PKC $\alpha/\beta$  dependent mechanism (479). As the study is interested in the effect of galectin-9, and galectin-9 is a carbohydrate-binding protein, and LPS has sugars, it might interfere with the detection of galectin-9. Therefore, it was decided to use the endogenous natural ligand, HMGB1 (which also have been reported elevated in cancer), to activate TLR4. The pathway investigated is illustrated in Figure 54.

THP-1 cells were stimulated with 1  $\mu\text{g}/\text{mL}$  HMGB1 protein for 24 h. It was found that HMGB1 induced the secretion of TGF- $\beta$  and galectin-9 by THP-1 cells (Figure 55). To evaluate the contribution of the Nox-ASK1-AP-1 redox-dependent pathway to TGF- $\beta$  expression, the cells were pre-treated with 30  $\mu\text{M}$  diphenyleneiodonium chloride (DPI) (a Nox inhibitor) or 1  $\mu\text{M}$  SR11302 (AP-1 inhibitor which blocks all forms of AP-1 as it binds to the DNA binding motif) for 1 h before exposing them to HMGB1 for 24 h (Figure 55). Another set of cells was subjected to transfection with dominant-negative ASK1 ( $\Delta\text{N-ASK1}$ ) to block the activity of this enzyme prior to 24 h stimulation with HMGB1. The result showed that HMGB1 induced TGF- $\beta$  as well as galectin-9 secretion (Figure 55). DPI, SR11302 and  $\Delta\text{N-ASK1}$  decreased the effect, suggesting that ROS-induced ASK1-mediated AP-1 activation leads to an augmented TGF- $\beta$  and galectin-9 production and secretion by THP-1 cells.



**Figure 54: HMGB1, a TLR4 ligand triggers TLR4 mediated activation of the ROS signalling pathway (directly from (419)).** TLR4 triggers assembly and activation of NADPH oxidase using myeloid differentiation factor 88 (MyD88), TLR4 TIR domain-associated protein (TIRAP) and Bruton's tyrosine kinase (Btk). Activation of Btk by MyD88 and TIRAP leads to Btk-dependent phosphorylation of phospholipase C (PLC, mainly isoform 1 $\gamma$ ), which triggers activation of protein kinase C alpha (PKC $\alpha$ ). PKC $\alpha$  activates NADPH oxidase, which produces a superoxide anion radical, which activates ASK1 by releasing it from thioredoxin. The ASK1 pathway mediates activation of the AP-1 transcription factor (419).



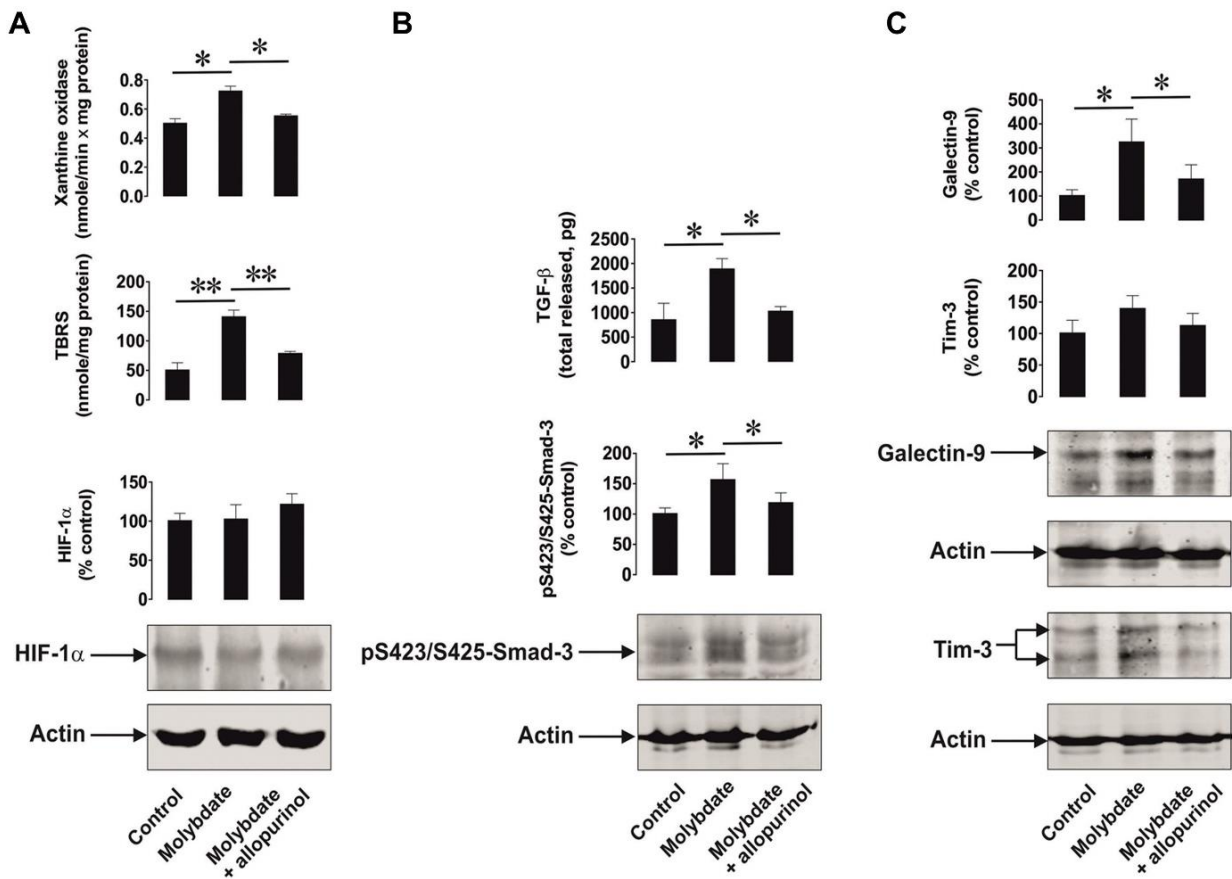


**Figure 55: Oxidative stress-induced activation of AP-1 in an ASK1-dependent manner and promotes TGF-β and galectin-9 expression** (directly from (419)). THP-1 cells were exposed for 24 h to 1 μg/mL HMGB1 with or without pre-treatment with 30 μM DPI (NADPH oxidase inhibitor), 1 μM SR11302 (AP-1 inhibitor) or transfection with a dominant-negative isoform of ASK1 (ΔN-ASK1). Levels of secreted TGF-β and galectin-9 were measured by ELISA (B). Data are shown as mean values ± SEM of four independent experiments. \* -  $p < 0.05$  and \*\* -  $p < 0.01$  vs control (419).

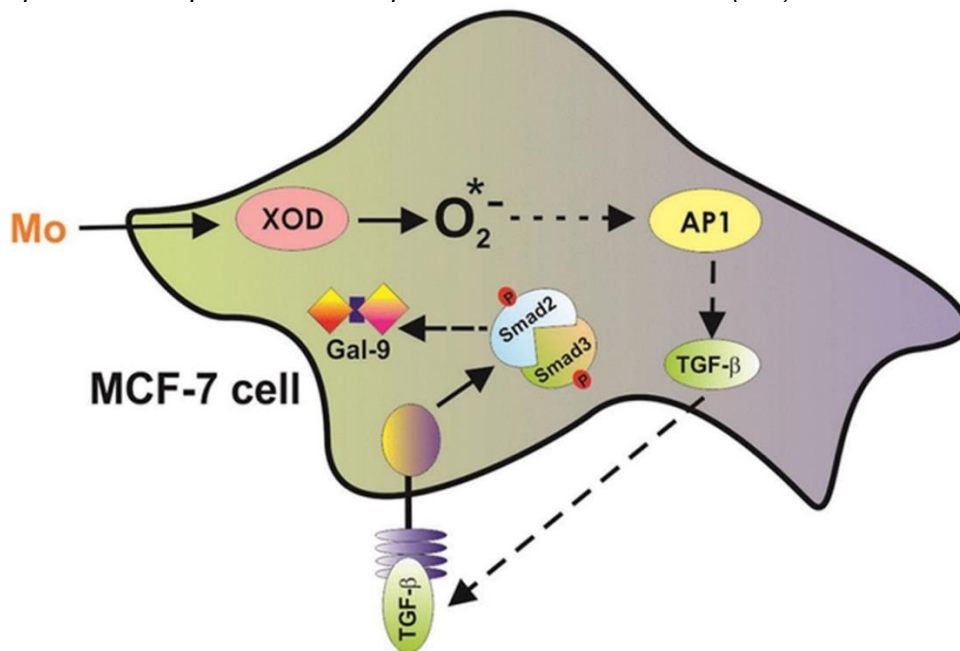
XOD is involved in purine catabolism catalysing hypoxanthine to xanthine and then to uric acid and as a by-product generates intracellular ROS in the form of  $O_2^-$  and  $H_2O_2$  (509). XOD dysregulation is observed in cancer, and as many other proteins, it has an ambiguous role, both promoting anti-oncogenic activities as well as cancer development. The latter is thought to contribute to XOD-derived ROS (452, 510). XOD expression is regulated at transcriptional and post-transcriptional levels by various stimuli, including hypoxia (510). Cobalt chloride ( $CoCl_2$ ), a chemical inducer of hypoxia, has been reported

to work by promoting XOD activity without affecting expression (472). The increased XOD activity results in ROS, which was sufficient to induce HIF-1 $\alpha$  accumulation in cancers with glycolytic-dependent phenotype such as the glioma cell line U251-MG (472).

Thus, the ability of XOD to upregulate TGF- $\beta$  production and galectin-9 expression was studied. MCF-7 breast cancer cells, which express XOD (473), were applied, and its activity was induced by ammonium molybdate under normoxic conditions. XOD is a molybdenum-containing enzyme, thus, excess of molybdenum converts all the available XOD enzymes into their active form. To confirm the specificity of the effect, MCF-7 cells were exposed to 100  $\mu$ g/mL ammonium molybdate for 24 h in the absence or presence of 250  $\mu$ g/mL allopurinol, a specific XOD inhibitor. Figure 26A shows that XOD activity was significantly upregulated by molybdate in MCF-7 cells, which resulted in a subsequent increase of oxidative burst based on increased TBRS levels (Figure 26A). Under the normoxic cultured condition, XOD activation was not able to induce HIF-1 $\alpha$  accumulation (Figure 56A). However, the level of secreted TGF- $\beta$  was still significantly increased (Figure 56B), suggesting that this increase may be mediated by other pathways, such as the ROS-ASK1-p38-AP-1 pathway (Figure 57). The increase in TGF- $\beta$  secretion was associated with a significant upregulation of Smad3 S423/S425 phosphorylation reflecting activation of TGF- $\beta$  signalling (Figure 56B). As a result, galectin-9 expression was significantly increased, albeit Tim-3 was not. (Figure 56C). Allopurinol attenuated all these effects (Figure 56), indicating a specific role for XOD in the processes outlined above. A schematic of the XOD pathway in MCF-7 is illustrated in Figure 57.



**Figure 56: Xanthine oxidase activation leads to increased oxidative stress and upregulation of the TGF- $\beta$ -Smad3 pathway and galectin-9 expression** (directly from (419)). MCF-7 human breast cancer cells were exposed to 100  $\mu$ g/mL ammonium molybdate for 24 h to induce xanthine oxidase activity in the absence or presence of 250  $\mu$ g/mL allopurinol (xanthine oxidase inhibitor). Xanthine oxidase activity, TBRS levels, HIF-1 $\alpha$  accumulation (A), secreted TGF- $\beta$  and cell-associated phospho-S423/S425-Smad3 (B), Tim-3 and galectin-9 (C) were analysed as outlined in the Materials and Methods. Images are from one experiment representative of four, which gave similar results. Data are shown as mean values  $\pm$  SEM of four independent experiments. \* -  $p < 0.05$  and \*\* -  $p < 0.01$  vs indicated events (419)



**Figure 57: Schematic illustration of how xanthine oxidase derived ROS results in TGF- $\beta$  and galectin-9 production under the normoxic condition in MCF-7 cells (from (419)).** Xanthine oxidase activity is increased with the addition of molybdate, which results in increased ROS production. The increase in the oxidative burst is not enough to result in HIF-1 $\alpha$  accumulation, but there still is an augmented TGF- $\beta$ 1 secretion and galectin-9 expression, suggesting that the ASK1-p38-AP-1 pathway may contribute to TGF- $\beta$  production, and the subsequent TGF- $\beta$ 1 signalling results in upregulation of galectin-9 expression.

#### 4.2.3 The HIF-1 Transcription Complex Triggers Galectin-9 Expression by Inducing TGF- $\beta$ Production; Smad3 is Involved in both TGF- $\beta$ and Galectin-9 Expression

As mentioned above, HIF-1 $\alpha$  is under normoxic conditions expressed at low levels due to continuous hydroxylation by PHD, which targets it for proteolytical degradation (470, 484, 485). Furthermore, the activity of whatever little HIF-1 is present is repressed by FIH-mediated hydroxylation (470, 485). Both PHD and FIH requires several cofactors, such as Fe<sup>2+</sup> (iron), ascorbate (as an iron reductant), 2-oxoglutarate and O<sub>2</sub>, as substrates to hydroxylate HIF-1 $\alpha$  (485, 511). Under hypoxic condition, it is generally thought that the mitochondrial electron transport chain produce ROS, which leads to HIF-1 $\alpha$  stabilization and accumulation, although the exact mechanism is still unclear, however, it has been suggested that it is by inhibiting FIH and/or PHD (484, 485). To understand HIF-1 contribution, it was required to promote HIF-1 $\alpha$  accumulation and transcriptional activity. Due to lack of hypoxic chamber, hypoxia is mimicked by administrating cobalt chloride (CoCl<sub>2</sub>) to the cell culture under normoxic condition (485). Several mechanisms have been proposed in which CoCl<sub>2</sub> leads to HIF-1 $\alpha$  accumulation and increased transcriptional activity. Among the proposed models are the replacement hypothesis, the ascorbate and/or Fe<sup>2+</sup> oxidation hypothesis, and the hypothesis in which Co<sup>2+</sup> has been suggested to interfere with the interaction between VHL and HIF-1 $\alpha$  (485). The replacement hypothesis is the most accepted, and here Co<sup>2+</sup> is thought to replace Fe<sup>2+</sup> in its active site and thereby inhibiting PHD activity and thus leading to HIF-1 $\alpha$  stabilization (485). The ascorbate and/or Fe<sup>2+</sup> oxidation model proposes that CoCl<sub>2</sub> produces ROS by mitochondrial independent mechanisms, e.g. through XOD. ROS can oxidize ascorbate, which is normally used as an iron reductant and thereby prevent Fe<sup>3+</sup> to return to Fe<sup>2+</sup> inhibiting both PHD and FIH activity leading to HIF-1 $\alpha$  accumulation and increase transcriptional activity (485). Depending on the concentration of CoCl<sub>2</sub>, there are different effects. Low levels can lead to increased transcriptional activity without an increase in protein expression, whereas high levels result in both increase in protein expression (due to decreased degradation)

and upregulation of activity (485). Finally,  $\text{Co}^{2+}$  has been suggested to bind to PAS domain of HIF-1 $\alpha$  preventing its ubiquitination and/or  $\text{Co}^{2+}$  can bind to Cul2 a component of VHL and inhibits its activity (485). Humans cannot by themselves produce ascorbic acid, and the intake is dependent on vitamin C (512), and since ascorbate is not added to these experiments, one of the other two hypothesis must be relevant here.

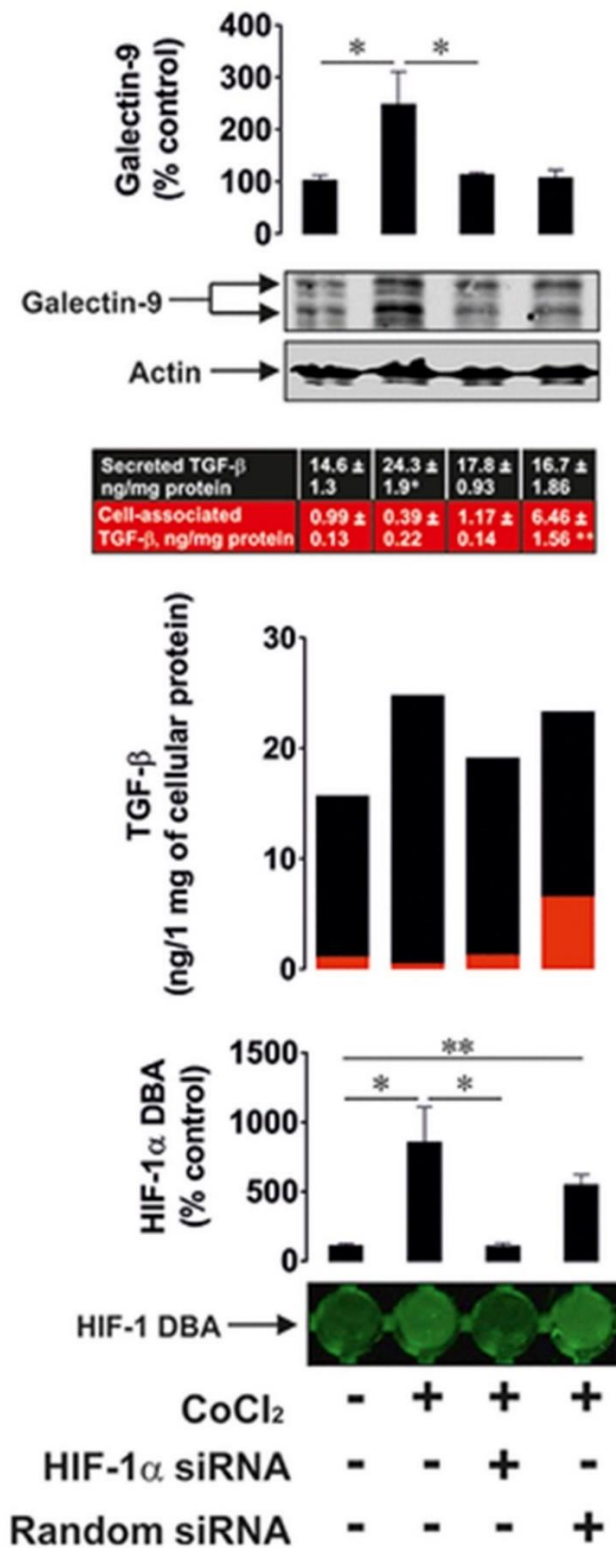
To investigate the effect of HIF-1 activation on TGF- $\beta$  production and its subsequent effect on galectin-9 expression, wildtype and HIF-1 $\alpha$  knockdown (obtained by transfection of HIF-1 $\alpha$  siRNA) MCF-7 cells were exposed and those transfected with random siRNA to 50  $\mu\text{M}$   $\text{CoCl}_2$  for 6 h. Following stimulation, HIF-1 DNA-binding activity, cell-associated and secreted TGF $\beta$  (ELISA) as well as cellular galectin-9 levels (WB) were measured. As described in the previous result section, MCF-7 cells do not secrete galectin-9 and were therefore not assessed. It was found that  $\text{CoCl}_2$  induced significant upregulation of HIF-1 DNA-binding activity in wild type and random siRNA-transfected MCF-7 cells (Figure 58). No effect was observed in HIF-1 $\alpha$  knockdown cells (Figure 58). In wild type cells, but not in HIF-1 $\alpha$  knockdown cells,  $\text{CoCl}_2$  induced significant upregulation of secreted and total levels of TGF- $\beta$  (Figure 58). The level of total TGF- $\beta$  was upregulated similarly in both MCF-7 cells transfected with random siRNA and in wild type cells when exposed to  $\text{CoCl}_2$ . However, the combination with the application of DOTAP to transfect these cells with random siRNA and  $\text{CoCl}_2$  slowed down the process of TGF- $\beta$  secretion. As a result, the level of galectin-9 was only upregulated in wild type MCF-7 cells treated with  $\text{CoCl}_2$  (Figure 58). These results suggest that  $\text{CoCl}_2$  promotes HIF-1 $\alpha$  accumulation, and that HIF-1 induces the expression of TGF- $\beta$ , which then facilitates the upregulation of galectin-9 expression.

To further investigate this assumption, the dynamics of the process were studied. Wild type MCF-7 cells were exposed to 50  $\mu\text{M}$   $\text{CoCl}_2$  for 1, 2, 3, 4, 5 and 6 h time points and HIF-1 DNA-binding activity, levels of secreted TGF- $\beta$  and cellular galectin-9 expressions were detected. The data in Figure 59 demonstrate that HIF-1 DNA-binding activity was rapidly increased after 1 h of stimulation to  $\text{CoCl}_2$ , while the levels of secreted TGF- $\beta$  were significantly increased after 3 h of exposure. The cellular galectin-9 level was significantly upregulated following 6 h of exposure to  $\text{CoCl}_2$  (Figure 59).

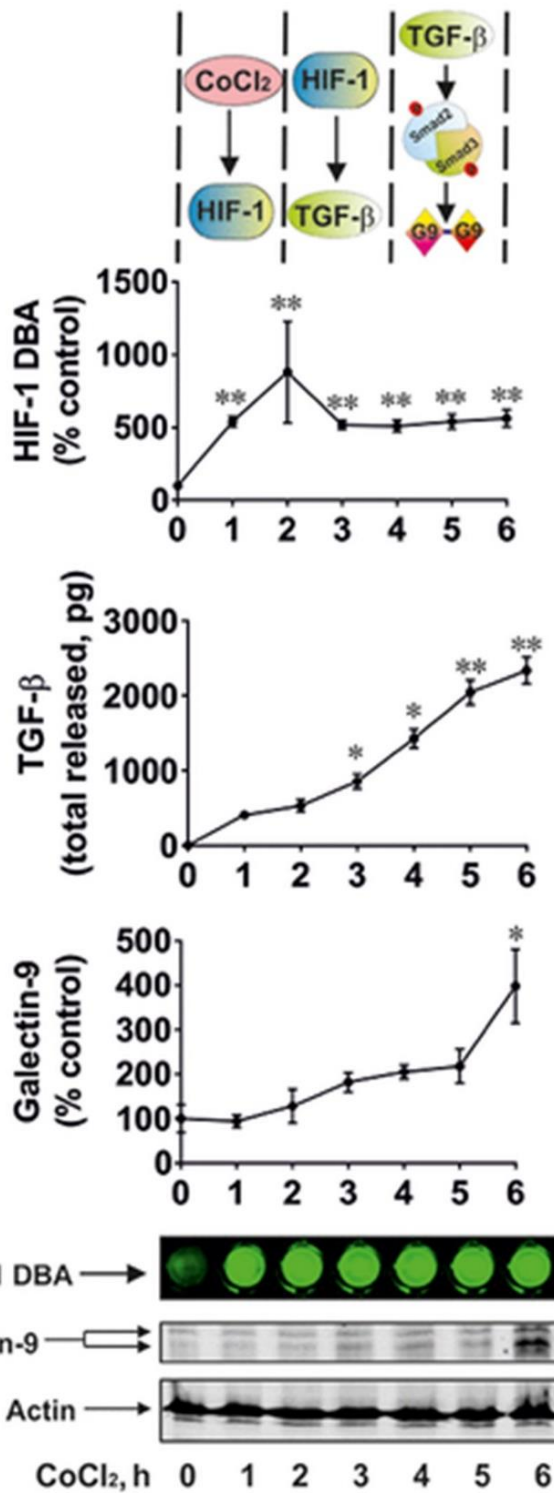
To specifically confirm the contribution of TGF- $\beta$  in regulating galectin-9 expressions, wild type MCF-7 cells were exposed to 50  $\mu$ M CoCl<sub>2</sub> for 6 h in the absence or presence of TGF- $\beta$  neutralising antibody or isotype control antibody. It was found that TGF- $\beta$  neutralising antibody, but not the isotype control, attenuated CoCl<sub>2</sub>-induced galectin-9 upregulation in MCF-7 cells (Figure 60), suggesting that autocrine TGF- $\beta$  signalling is involved in CoCl<sub>2</sub>-mediated increase of galectin-9.

As mentioned, Smad3 has been implicated in the regulation of both TGF- $\beta$  and galectin-9, thus, to confirm the role of Smad3 in both TGF- $\beta$  and galectin-9 expression, wild type and Smad3 knockdown MCF-7 cells were applied. As a control for reagents, MCF-7 cells transfected with random siRNA were used. Cells were subjected to 2 ng/mL TGF- $\beta$  for 24 h and cell-associated (in cell lysates), and the levels of secreted (in cell culture medium) TGF- $\beta$  were measured by ELISA. To confirm successful Smad3 knockdown and to assess the effects on galectin-9 expression, phospho-S423/S425-Smad3 and galectin-9 were measured in cell lysates (Figure 61). The presence of TGF- $\beta$  led to an increase in secreted TGF- $\beta$  levels in wild type MCF-7 cells, but not in Smad3 knockdown cells (Figure 61). The same was applicable to the levels of galectin-9 (Figure 61). This suggests that TGF- $\beta$  promotes its own induction via Smad3 activation, which simultaneously induces galectin-9. It was observed that MCF-7 cells transfected with random siRNA displayed increased levels of cell-associated as well as secreted TGF- $\beta$ , which subsequently also resulted in upregulation of galectin-9 expression (Figure 61). However, MCF-7 cells transfected with random siRNA in the presence of CoCl<sub>2</sub> displayed higher levels of cell-associated TGF- $\beta$  and lower levels of secreted protein compared to similar cells treated with TGF- $\beta$ . This indicates that the presence of DOTAP reagent in combination with cobalt cations reduces the ability of MCF-7 cells to secrete de novo produced TGF- $\beta$ .

All these findings clearly demonstrate that HIF-1 induces TGF- $\beta$  production, which displays autocrine activity and by acting through Smad3 triggers galectin-9 expression (Figure 62).

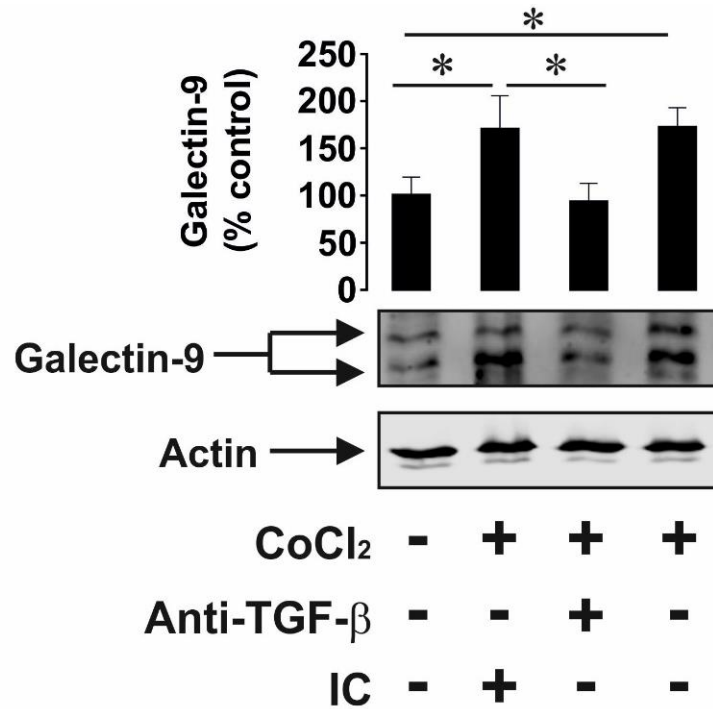


**Figure 58: HIF-1 is involved in the production of TGF-β and galectin-9** (from (419)). Cobalt chloride induces HIF-1 activation, TGF-β and galectin-9 production. Wild type, HIF-1α knockdown and random siRNA-transfected MCF-7 cells were exposed to 50 μM cobalt chloride for 6 h followed by measurement of HIF-1 DNA binding activity, secreted (in cell culture medium) and cell-associated (in cell lysates) TGF-β and cell-associated galectin-9. Images are from one experiment representative of three, which gave similar results. All quantitative data are shown as mean values ± SEM (n=3-4). \* - p < 0.05 and \*\* - p < 0.01 vs indicated events (419).



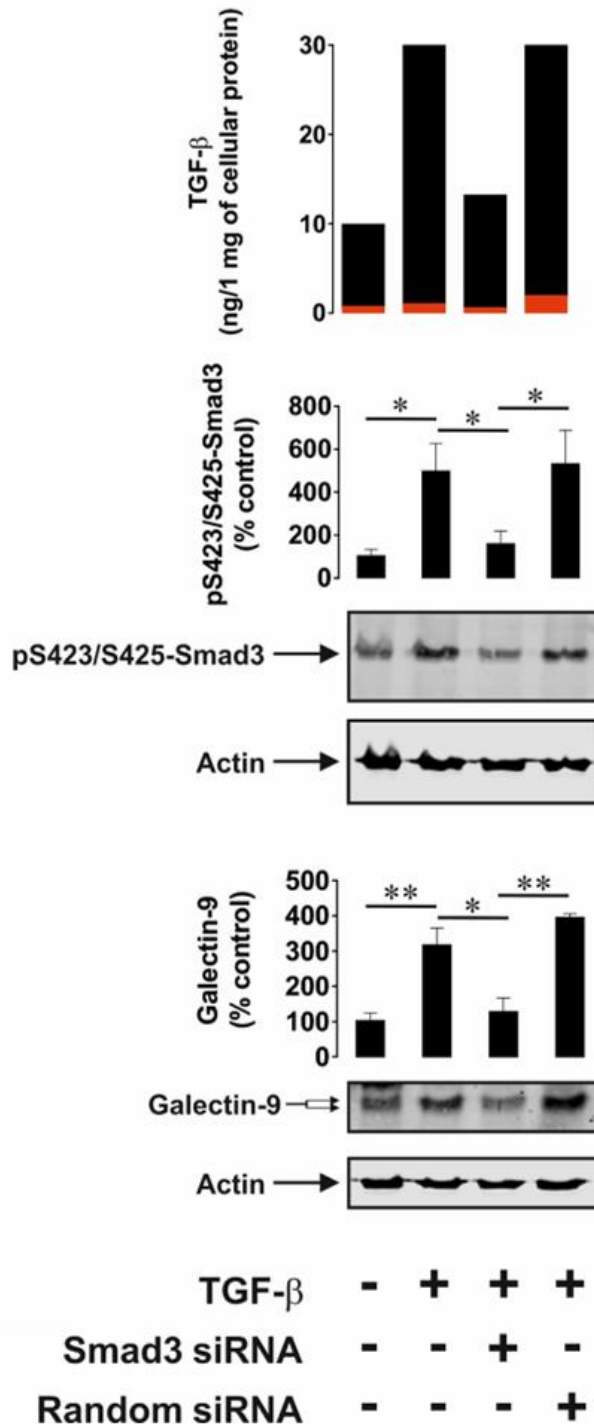
**Figure 59: Dynamics of cobalt chloride-induced HIF-1 activation, TGF-β and galectin-9 accumulation in MCF-7 human breast cancer cells** (from (419)). MCF-7 cells were exposed to 50 μM cobalt chloride for 1, 2, 3, 4, 5 and 6 h followed by measurement of HIF-1 DNA binding activity, secreted and cell-associated TGF-β and cell-associated galectin-9. Images are from one experiment representative of three, which gave similar results (in the case of TGF-β – vs 1 h time-point since at zero point, cells cannot release any TGF-β. At this time-point, fresh medium had just been supplied and measurement was obtained immediately to confirm zero TGF-β levels). All quantitative data are shown as mean values ± SEM (n=3-4). \* -  $p < 0.05$  and \*\* -  $p < 0.01$  vs indicated events (419).



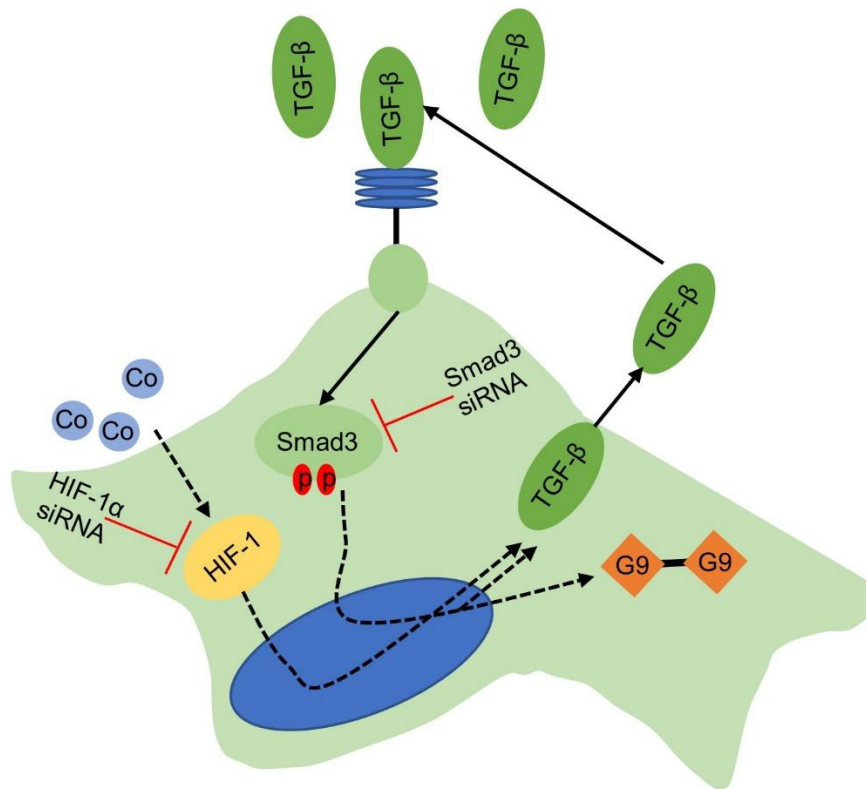


**Figure 60: HIF-1-induced galectin-9 expression is mediated by TGF-β** (from (419)). MCF-7 cells were exposed to 50 μM cobalt chloride for 6 h with or without presence of TGF-β neutralising or isotype control antibody. Galectin-9 expression was then assessed by WB. Images are from one experiment representative of three, which gave similar results. All quantitative data are shown as mean values ± SEM (n=3-4). \* - p < 0.05 and \*\* - p < 0.01 vs indicated events (419).

Secreted TGF- $\beta$ ng/mg protein	9.2 $\pm$ 1.2	32.8 $\pm$ 5.2**	12.6 $\pm$ 3.1	28.1 $\pm$ 4.4**
Cell-associated TGF- $\beta$ , ng/mg protein	0.65 $\pm$ 0.17	0.98 $\pm$ 0.26	0.52 $\pm$ 0.08	1.89 $\pm$ 0.41**



**Figure 61: Smad3 is involved in TGF- $\beta$  and galectin-9 expression** (directly from (419)). Wild type, Smad3 knockdown and random siRNA-transfected MCF-7 cells were exposed to 2 ng/mL TGF- $\beta$  for 24 h followed by measurement of secreted (in cell culture medium) and cell-associated (in cell lysates) TGF- $\beta$  as well as cell-associated galectin-9 and phospho-S423/S425 Smad3. Images are from one experiment representative of three, which gave similar results. All quantitative data are shown as mean values  $\pm$  SEM ( $n=3-4$ ). \* -  $p < 0.05$  and \*\* -  $p < 0.01$  vs indicated events (419).



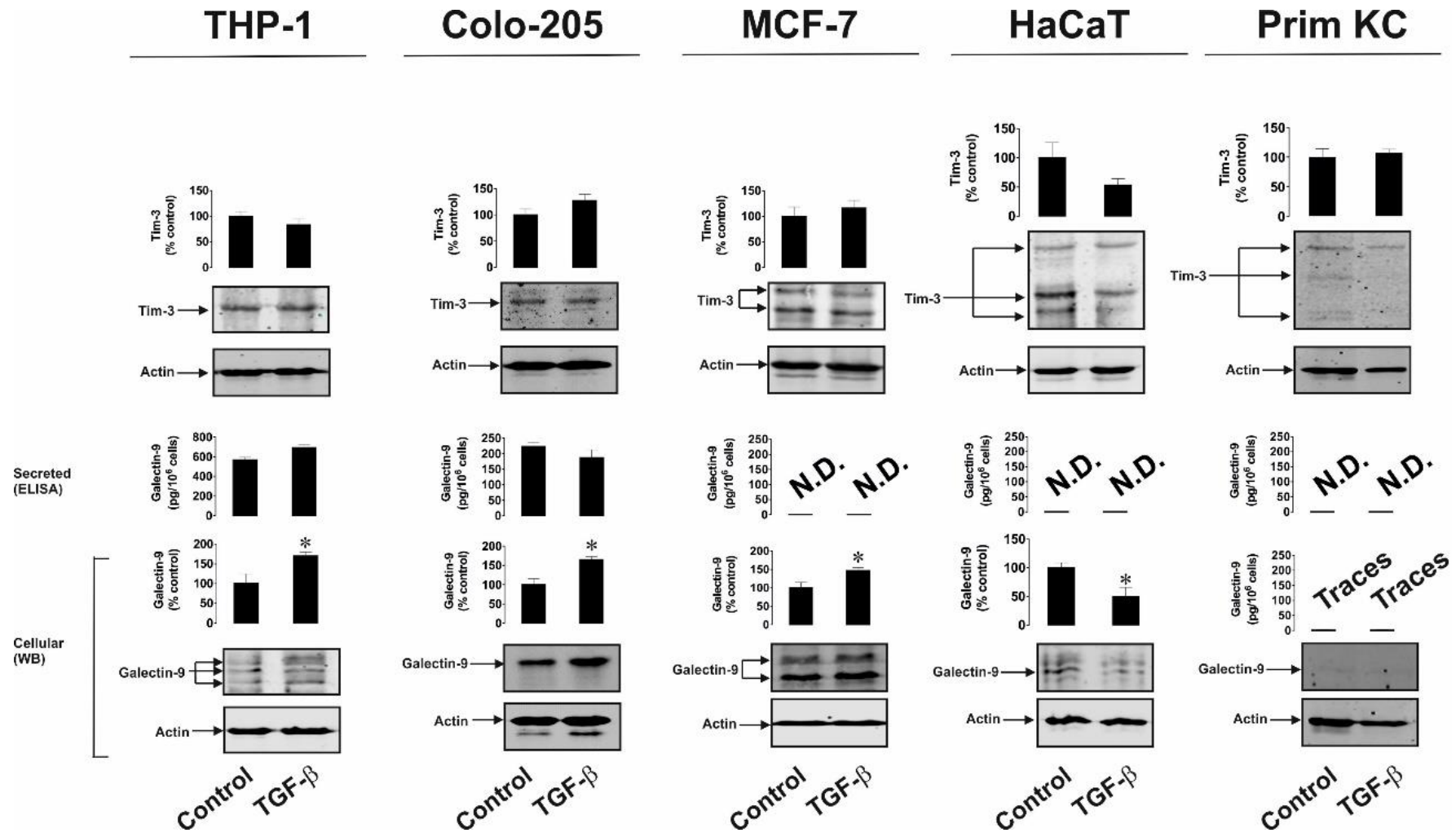
**Figure 62: Scheme of the experiment performed showing studied effects.**  $\text{CoCl}_2$  (Co), a chemical inducer of hypoxia, promotes HIF-1 $\alpha$  accumulation (possibly by inhibition of PHD and/or augment ROS production). HIF-1 $\alpha$  associates together with HIF-1 $\beta$  to form the HIF-1 transcription factor complex, which then translocate to the nucleus to induce transcription of TGF- $\beta$ . Secreted TGF- $\beta$  acts most likely locally in an autocrine manner binding to the TGF- $\beta$  receptors to activate TGF- $\beta$  signalling, which includes activation of the canonical Smad pathway. A direct downstream effector molecule of TGF- $\beta$  receptor activation is Smad3, which is phosphorylated and can then associate with other Smad molecules (such as Smad2 and possible Smad4) to form a complex, which is translocated to the nucleus to induce transcription of both TGF- $\beta$  gene and LGALS9 and consequently production of more TGF- $\beta$  and galectin-9 that can be used to escape immune surveillance.

#### 4.2.4 TGF- $\beta$ Induces Galectin-9 Expression in Human Cancer

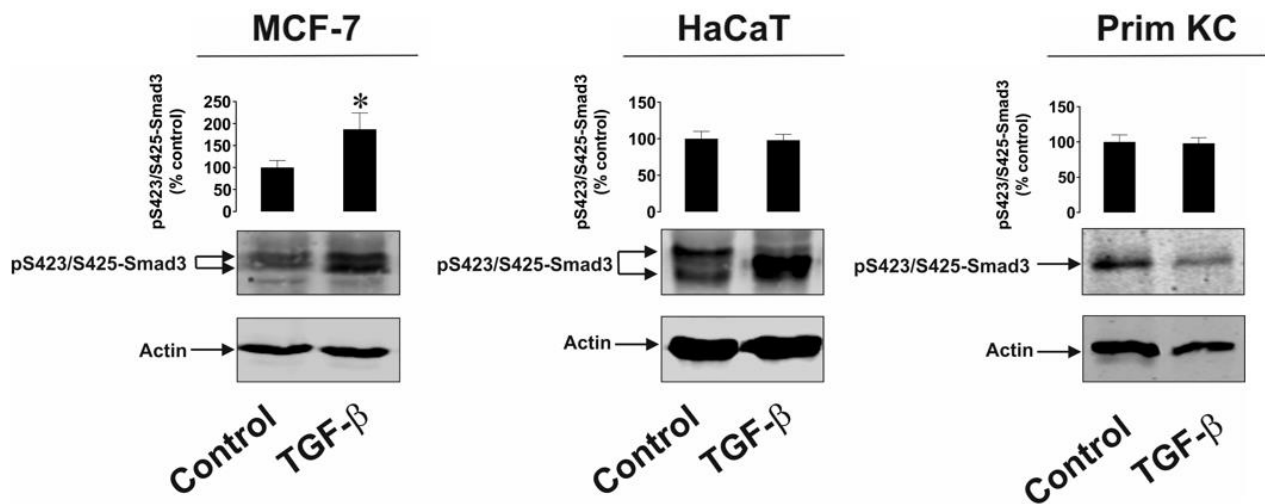
To confirm and study the differential effects of TGF- $\beta$  on galectin-9 expression on various cancer cells and healthy non-malignant cells, the following types of cells: THP-1 (a model for human AML), Colo-205 (a model for human colorectal cancer), MCF-7 (a model for human breast cancer), HaCaT (non-malignant human keratinocytes model) cells, as well as primary healthy human keratinocytes were treated with 2 ng/mL human recombinant TGF- $\beta$ 1 for 24 h. Cellular and secreted levels of galectin-9 and Tim-3 were then determined. In all types of analysed human cancer cells, TGF- $\beta$  upregulated the amounts of expressed galectin-9, but not Tim-3 (Figure 63), indicating that while galectin-9 is under TGF- $\beta$  regulation, Tim-3 is not. However, in non-malignant cells (both types of keratinocytes), no upregulation of either galectin-9 or Tim-3 expression was observed in

response to TGF- $\beta$  (Figure 63). Furthermore, both types of keratinocytes expressed Tim-3 and scarce amounts of galectin-9, and this was not inducible by TGF- $\beta$ . To determine whether such a phenomenon (the inability to induce galectin-9 expression by TGF- $\beta$ ) also applies to cancer cells, K562 chronic myeloid leukaemia cells were used, as they only express traces of galectin-9 protein compared to for example THP-1 or other AML cells (Figure 47). Stimulating these cells with increasing concentrations of TGF- $\beta$  for 24 h led to a clear induction of galectin-9 expression (Appendix, Figure 83), suggesting differential responses of cancer and non-transformed mature human cells in their ability to induce galectin-9. Phospho-S423/S425 Smad-3 levels were undetectable in resting K562 cells and were clearly noticeable in TGF- $\beta$ -treated cells (Appendix, Figure 83). Regardless of the treatment, K562 cells did not release detectable amounts of galectin-9 (Appendix, Figure 83).

Since Smad3 is the transcription factor activated by TGF- $\beta$ , which then induces galectin-9 expression, a comparison of TGF- $\beta$ -induced activation of Smad3 and the phosphorylation status of S423/S425 on Smad3 were conducted in malignant and non-malignant human cells. MCF-7 breast cancer cells, non-malignant HaCaT cells and primary keratinocytes were exposed for 24 h to 2 ng/mL TGF- $\beta$  followed by detection of phospho-S423/S425 Smad3. Significant upregulation of phospho-S423/S425-Smad3 levels was only detected in MCF-7 cells, but not in non-malignant healthy keratinocytes (Figure 64). Moreover, the visual profile of the phospho-S423/S425-Smad3 band was different in malignant and non-malignant cells (Figure 64). Taken together, these results suggest that TGF- $\beta$ -induced Smad3-mediated galectin-9 expression takes place mainly in human cancer cells. The responses associated with TGF- $\beta$ -induced S423/S425 Smad3 phosphorylation are clearly different in cancer and mature non-malignant human keratinocytes cells.



**Figure 63: TGF- $\beta$  induces galectin-9 expression in human cancer but not healthy cells** (from (419)). THP-1 (AML), Colo-205 (colorectal cancer), MCF-7 (breast cancer) HaCaT (keratinocytes) and primary human keratinocytes (Prim KC) were exposed to 2 ng/mL human recombinant TGF- $\beta$  for 24 h. Levels of cell-associated Tim-3 and galectin-9 and secreted galectin-9 were measured. Images are from one experiment representative of four, which gave similar results. Data are shown as mean values  $\pm$  SEM of four independent experiments. \* -  $p < 0.05$  vs control (419).



**Figure 64: The effects of TGF- $\beta$  on Smad3 phosphorylation in human cancer and non-malignant cells** (from (419)). (A) MCF-7 (breast cancer), (B) HaCaT (keratinocytes) and (C) primary human keratinocytes were exposed for 24 h to 2 ng/mL TGF- $\beta$  followed by WB analysis of phospho-S423/S425-Smad3 levels. Images are from one experiment representative of four, which gave similar results. Data are shown as mean values  $\pm$  SEM of four independent experiments (419).

#### 4.2.5 Discussion

Many types of cancer cells express significantly higher amounts of galectin-9 compared to non-transformed cells of similar origin (64, 326). Galectin-9 plays a crucial role in cancer progression as it is used to escape immune surveillance (64, 304, 326). Cell surface-based or secreted galectin-9 can impair anti-cancer activities of NK and cytotoxic T cells (64, 304, 326). Galectin-9 (like other galectins) lacks a secretion signal sequence and thus requires trafficking in order to be externalised onto the cell surface or secreted (64, 326). Tim-3 acts as a receptor and has been proposed as a possible trafficker for galectin-9 in certain cancer cells such as AML cells (322). Recently, the FLRT3-LPHN pathway has been identified as a mechanism involved in the regulation of galectin-9 and Tim-3 expression in cancer (64, 326). Furthermore, it was clear that other mechanisms might also be involved in regulating the Tim-3-galectin-9 pathway. Although, other biochemical mechanisms underlying galectin-9 regulation remain to be elucidated. Understanding galectin-9 regulation may provide a therapeutic target for the treatment of cancer, and thus, the investigation of pathways controlling galectin-9 expression was the main goal of this study.

Smad3, a downstream transcription factor of TGF- $\beta$  signalling, has been reported to bind to the LGALS9 promoter region and induce galectin-9 in iTregs (273, 274). In support of this, many putative Smad3 binding sites have been identified in the LGALS9 promoter

(Appendix, Figure 81). Similar to galectin-9, TGF- $\beta$  is an autocrine growth factor, which is highly upregulated in cancer (357, 359, 490). It was therefore speculated that TGF- $\beta$  could be responsible for the upregulation of galectin-9 expression in cancer cells. Thus, the aim was to elucidate what factors that contributed to high aberrant TGF- $\beta$  levels in cancer, and how it may contribute to increased level of galectin-9. Several studies have reported that HIF-1 is involved in the induction of TGF- $\beta$ , and it was recently also confirmed in breast cancer cells (486). Furthermore, AP-1 has been implicated in the autoinduction of TGF- $\beta$  (501, 502). Thus, HIF-1 and AP-1 are transcription factors that may be involved in the regulation of TGF- $\beta$ . Both of these transcription factors are activated by oxidative stress signalling (425, 481).

Human breast tumour cells and AML cells produced significantly higher levels of TGF- $\beta$  compared to healthy cells of similar origin (Figure 51B and Figure 52C). Interestingly, the levels of oxidative stress and activities of ROS producing enzymes (Nox and XOD) were significantly higher in cancer cells/tissues (Figure 50 and Figure 52A). Oxidative stress normally leads to activation of the AP-1 transcription complex (481), which contributes to TGF- $\beta$  expression (502). In this study, phosphorylation of ATF-2 (a component of AP-1) was significantly increased (Figure 51A), suggesting that AP-1 indeed had been activated. Furthermore, the levels of HIF-1 $\alpha$  accumulation were much higher in cancer samples (Figure 51A and Figure 52B). HIF-1 $\alpha$  associates with HIF-1 $\beta$  to form the HIF-1 transcription complex, which directly activates the expression of TGF- $\beta$  (486, 513). The data of this study suggest that TGF- $\beta$  may act locally in the microenvironment, and for solid tumours such as breast cancer, it remains in the TME, whereas in liquid tumours such as AML, TGF- $\beta$  is found in the circulation where it can act on the cancer cells (Figure 53). In the studied cancer cells/tissues, augmented TGF- $\beta$  levels resulted in a subsequent increase in active Smad3 (phosphorylated at S423/S425) (Figure 51B and Figure 52B). Furthermore, the levels of galectin-9 and its receptor Tim-3 were upregulated in all the studied cancer cell types (Figure 51C and Figure 52C). These data suggest that oxidative stress (due to increased enzyme activity of XOD and Nox) leads to activation of HIF-1 and AP-1, which both can contribute to increased TGF- $\beta$  production, which may consequently lead to enhanced activation of Smad3 that could augment galectin-9 expression (

Figure 49). To confirm this hypothesis and investigate the mechanistic, the cancer cell lines MCF-7 and THP-1 were applied, which are models for breast cancer and AML, respectively.

It was confirmed that upregulation of both Nox and XOD is capable of increasing TGF- $\beta$  production. HMGB1-induced Nox activation led to upregulated TGF- $\beta$  and galectin-9 production by THP-1 human AML cells. Blockade of Nox activity, ASK1 kinase activity or AP-1 transcriptional activity decreased HMGB1-induced effects (Figure 54 and Figure 55). From our group's previous work, it is known that HMGB1 acts through Toll-like receptors (TLRs) 2 and 4 causing oxidative stress and inducing HIF-1 activation (350), and hypoxia response elements (HREs) are found in TGF- $\beta$  promoter region (Appendix, Figure 80). AP-1 is known to be required for TGF- $\beta$  expression (501, 502), and putative AP-1 binding sites are found in the promoter region (Appendix, Figure 80). Specific activation of XOD in MCF-7 human breast cancer cells under normoxic condition upregulated the level of oxidative burst, however, it was insufficient to induce HIF-1 $\alpha$  accumulation (Figure 56A). Despite this, TGF- $\beta$ , phospho-S423/425-Smad3 and galectin-9 levels were significantly upregulated suggesting the contribution of the ROS-ASK1-MAPK-AP-1 pathway (Figure 56 and Figure 57).

The role of HIF-1 in TGF- $\beta$  expression was confirmed by exposing MCF-7 breast cancer cells to CoCl<sub>2</sub>. CoCl<sub>2</sub> mediates HIF-1 $\alpha$  stabilisation by inhibiting degradative hydroxylation of HIF-1 $\alpha$ , leading to HIF-1 activation (485). CoCl<sub>2</sub> is known to promote oxidative stress, and the mechanism has been suggested to be either inducing opening of the mitochondrial transition pore and/or through mitochondrial independent mechanisms such as activation of XOD, and consequently ROS generation leading to HIF-1 $\alpha$  stabilization (472, 514). ROS triggers ASK1-mediated AP-1 activation (481) and HIF-1 $\alpha$  accumulation (425, 484). These experiments demonstrated the importance of HIF-1 in regulating TGF- $\beta$  expression. The results showed that CoCl<sub>2</sub> induced TGF- $\beta$  and galectin-9 expression in wild type but not in HIF-1 $\alpha$  knockdown MCF-7 cells. This confirmed the involvement of HIF-1 in CoCl<sub>2</sub>-induced TGF- $\beta$  expression. MCF-7 cells transfected with random siRNA had an augmented TGF- $\beta$  expression, although DOTAP transfection and the presence of CoCl<sub>2</sub> slowed down the secretion process of TGF- $\beta$ , and consequently, galectin-9 expression was not increased, suggesting that it might depend on the autocrine activity of secreted TGF- $\beta$  (Figure 58). When studying the process in dynamics, it was found that CoCl<sub>2</sub> rapidly induced HIF-1



activation in MCF-7 cells (after 1 h of exposure, a significant increase in HIF-1 DNA-binding activity was clearly detectable, Figure 59). Secreted TGF- $\beta$  levels were significantly elevated after 3-4 h of CoCl<sub>2</sub> stimulation, whereas galectin-9 levels were significantly upregulated after 6 h. This supports the notion that CoCl<sub>2</sub>-induced galectin-9 expression depends on the autocrine activity of TGF- $\beta$ , the expression, which is induced by the HIF-1 transcription complex. This study specifically confirmed the role of HIF-1-induced TGF- $\beta$  production in upregulating the expression of galectin-9 in MCF-7 cells. Wild type MCF-7 cells were subjected to 50  $\mu$ M CoCl<sub>2</sub> in the absence or presence of TGF- $\beta$ -neutralising antibody or isotype control antibody. Since TGF- $\beta$ -neutralising antibody, but not isotype control, attenuated CoCl<sub>2</sub>-induced galectin-9 expression (Figure 60), it demonstrates that the autocrine activity of this growth factor controls the expression of galectin-9. It was confirmed that Smad3 transcription factors are involved in TGF- $\beta$  autoinduction and galectin-9 production as MCF-7 Smad3 knockdown cells were unable to increase TGF- $\beta$  or galectin-9 in response to TGF- $\beta$  stimuli (Figure 61). The whole pathway includes activation of HIF-1, which upregulates TGF- $\beta$  expression; TGF- $\beta$  is then secreted and displays autocrine activity leading to activation of Smad3 and autoinduction of TGF- $\beta$  along with induction of galectin-9 expression in MCF-7 breast cancer cells (Figure 62).

This study further demonstrated that TGF- $\beta$  induces galectin-9 expression (but not Tim-3) in human AML, breast and colorectal cancer cells but not in the studied healthy (non-transformed) human cells (Figure 63). In healthy human cells (keratinocytes expressing minimal amounts of galectin-9), TGF- $\beta$  cannot induce galectin-9 expression, while in cancer cells (for example K562 chronic myeloid leukaemia cells expressing only traces of galectin-9), TGF- $\beta$  can induce expression of this protein (Appendix, Figure 83). This suggests a differential regulation of galectin-9 in malignant and non-malignant cells. The investigations further confirmed that TGF- $\beta$  induces S423/S425-phosphorylation of Smad3 in the studied cancer cells but not in healthy human cells. Moreover, phospho-S423/S425-Smad3 WB band profiles vary between malignant and non-malignant human cells (Figure 64). These results suggest a differential response to TGF- $\beta$  between malignant and healthy cells.

It could be speculated that a reason for these differences in responses could be in differential reactivity of the cells in terms of expression of TGF- $\beta$  receptors (T $\beta$ Rs) or their downstream signalling. For example, a previous clinical study has demonstrated that high

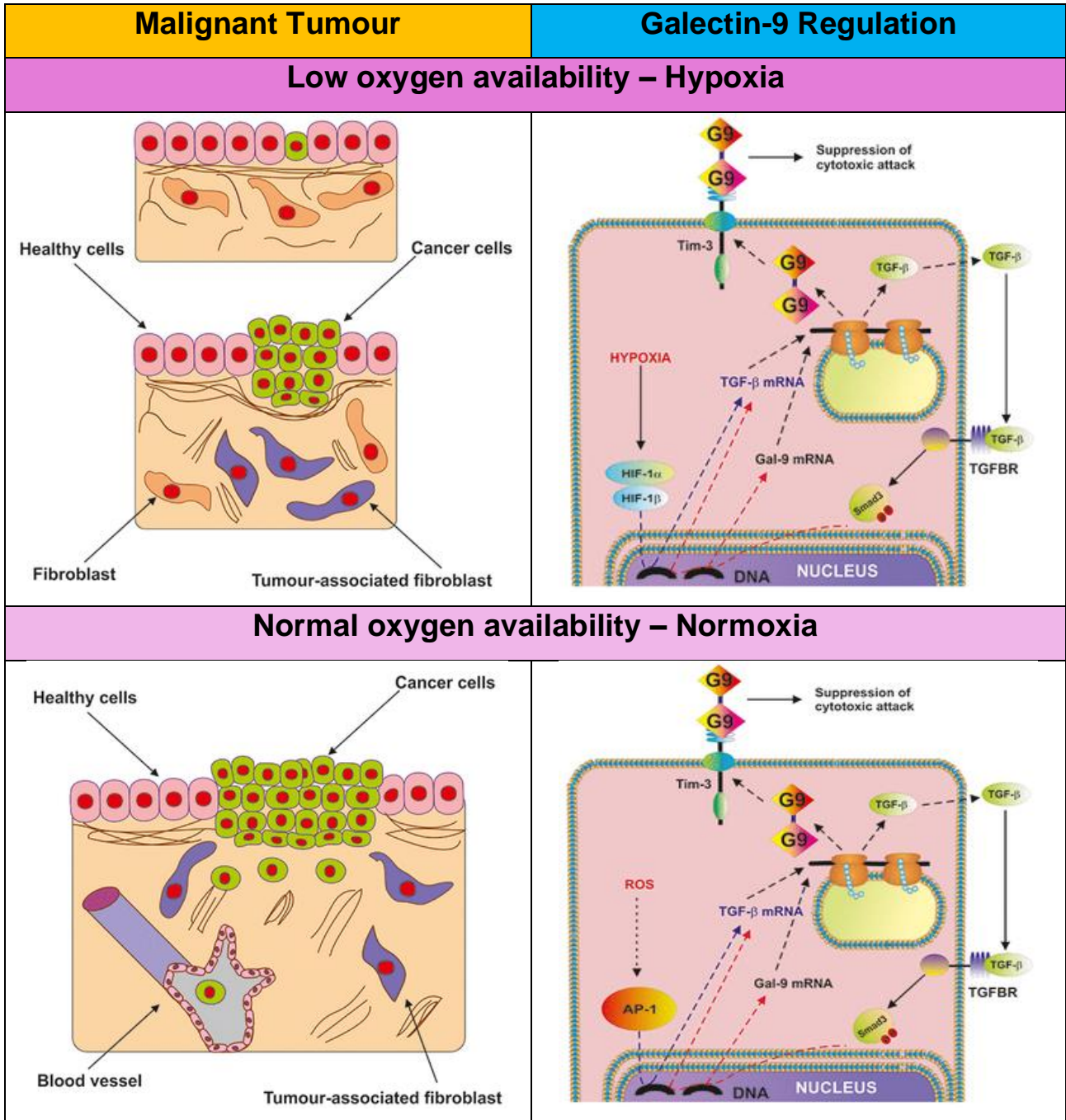
expression levels of T $\beta$ Rs are associated with poor prognosis for AML patients and have a significant negative impact on complete remission achievement and long-term survival of these patients (515). Moreover, somatic mutation of Smad molecules has been reported in various cancers, which could influence responsiveness to TGF- $\beta$ . In physiological setting, TGF- $\beta$  is known to induce growth arrest of epithelial cells. This has likewise been reported for HaCaT keratinocytes in a Smad3 dependent manner (TGF- $\beta$  induced Smad-3 phosphorylation, which mediated growth arrest) (516, 517). Albeit longer incubation with TGF- $\beta$  has been reported to reduce total Smad3 in HaCaT, but not in MCF-7 cells (518). Brown et al. further demonstrated that short stimuli of TGF- $\beta$  increase p-Smad2 in HaCaT, but not in MCF-7 cells, suggesting that other factors that can interact with Smad3 may contribute to the differential response between healthy and malignant cells (518). Furthermore, data have shown that TGF- $\beta$  in fibroblast from WT mice, but not in LGALS9 KO mice, enhances Smad3, AKT and MAPK(EKR) phosphorylation in response to TGF- $\beta$  (519). In line with this, a previous study reported that in iTregs (from mice), galectin-9 was found to synergize with TGF- $\beta$  to promote enhanced phosphorylation of Smad2/Smad3 as well as ERK1/2. A later study reported that this was mediated by the ability of galectin-9 binding to CD44 associated with T $\beta$ RI, and this interaction promoted enhanced phosphorylation of Smad3 (273, 274). CD44 and T $\beta$ RI have also been found to be associated in the human breast cancer cell line MDA-MB-231 when activated by hyaluronan (HA), and this interaction increased Smad2/Smad3 phosphorylation facilitating tumour progression and migration/metastasis (496). Galectin-9 has been reported to inhibit HA and CD44 interaction in metastatic B16F10 melanoma and Colon26 colon mouse cancer cells, which suppressed tumour migration (520). Moreover, in a murine allergic asthma model, galectin-9 was reported to prevent CD44 and HA interaction and thus inhibited allergic airway inflammation (298). Collectively, data from these different studies suggest that galectin-9 could aid in its own production, hence, since cancer cells have high expression of galectin-9, it could augment the phosphorylation of Smad3 from TGF- $\beta$  stimulation, and since cancer cells (at least reported in MCF-7) retain high expression of Smad3, there are plenty to phosphorylate. However, healthy keratinocytes have low expression of galectin-9 (barely detectable), and the TGF- $\beta$  mediated Smad3 phosphorylation may not be enhanced. In addition, as Smad3 expression declines with TGF- $\beta$  stimulation in keratinocytes, there may be less to phosphorylate, and thus after 24 h, no difference is detected. As mentioned, other factors associated with Smad3 may be

involved in the differential response. For instance in this study, it was demonstrated that in hypoxia mimicking condition and/or increased oxidative stress, Smad3 phosphorylation is increased in MCF-7 breast cancer cells. However, when HaCaT is exposed to TGF- $\beta$  under hypoxic condition, Smad3 is specifically dephosphorylated by PP2A (521). Another possibility for differential response is the involvement of different co-activator proteins recruited by Smad3 in distinct cell types (362). There are two main co-activators of Smad3: TIF-1 $\gamma$  and Smad4 (362). Both co-activators and some other binding partners (for example Smad2) are known to interact with Smad3, which influences the response that Smad3 will trigger, and this can occur in a cell-specific manner (505, 517, 522-524). Galectin-9 may be differently regulated in specific cell types, e.g. in iTregs, Smad3 promoted galectin-9, but this was not the case in Th0 cells (273). Moreover, IFN $\gamma$  has been reported to upregulate galectin-9 in fibroblast, however, Igawa and colleagues (525) as well as our own work (data not shown) have demonstrated that IFN $\gamma$  stimulation decreases galectin-9 expression in epidermal keratinocytes/HaCaT cells. In future work, it will be important to understand which co-activators/co-regulators/chaperons are involved in galectin-9 expression in different cell types, and how galectin-9 presence may influence TGF- $\beta$  mediated signalling.

The observations of this study suggest that during the early stages of tumour growth when the cells pass through a low oxygen availability stage, activation of HIF-1 induces TGF- $\beta$  expression. TGF- $\beta$  can then display autocrine activity and induce galectin-9 expression in a Smad3 dependent manner (a summary is shown in Figure 65). At later stages, when angiogenesis addresses the issue of low oxygen availability and normalises it, oxidative stress may activate AP-1. This contributes to TGF- $\beta$  production, which again displays autocrine activity and can induce its own expression through the Smad3 transcription factor. Concomitantly, Smad3 can induce the expression of galectin-9 (Figure 65). Therefore, it is proposed that cancer cells studied here operate a self-supporting autocrine mechanism, which is a two-stage process. During the early stage, hypoxia may activate the HIF-1 transcription complex, which most likely induces the initial expression of TGF- $\beta$ , and at later stages, TGF- $\beta$  triggers self-expression. At both stages, TGF- $\beta$  induces galectin-9 expression through the Smad3 pathway. TGF- $\beta$  can display both tumour-promoting and tumour-suppressing biochemical activities. However, tumour suppressive

activities of the TGF- $\beta$  are often avoided by tumours through acquiring mutations in critical signalling proteins or by simply inhibiting TGF- $\beta$ -induced anti-proliferative responses.

These findings demonstrate a TGF- $\beta$ -mediated self-supporting mechanism of galectin-9 expression operated by human AML and breast and colorectal cancer cells. The results suggest the possibility of using TGF- $\beta$  signalling as a potential highly efficient target for cancer immunotherapy.



**Figure 65: Proposed mechanism of the regulation of galectin-9 expression in human cancer at low and normal oxygen availability stages** (directly from (419)). The figure depicts the key processes taking place in malignant tumour growth during the initial low oxygen availability (hypoxic) stage and later (normal oxygen availability) stages. The studied biochemical events are demonstrated in the right-hand panel. During the hypoxic stage, HIF-1 induces TGF- $\beta$  expression, which then displays autocrine activity and triggers galectin-9 expression in a Smad3-dependent manner. During the normal oxygen availability stage, oxidative stress may trigger activation of HIF-1 and AP-1, which contributes to TGF- $\beta$  expression, and it is self-triggered by TGF- $\beta$ . Galectin-9 upregulation is perpetually induced by the TGF- $\beta$ -Smad3 pathway (419).

### 4.3 HMGB1 Derived From Dying Tumour Cells Can Promote Immune Escape Inducing TGF- $\beta$ in TLR4 Dependent Mechanism, which Signalling Upregulate Galectin-9

Human cancer cells in most cases express higher levels of galectin-9 compared to non-transformed cells and use it to escape immune surveillance by inhibiting cytotoxic activities of NKs and killing T cells (64, 304, 326). It has hitherto been found that the FLRT3-LPHN pathway is a common mechanism in cancer cells to upregulate galectin-9, and it is used to facilitate immune escape, by e.g. inducing granzyme B release inside attacking cytotoxic T cells and thus killing them (Section 4.1). Furthermore, it was found that oxidative stress is increased in cancer cells compared to non-transformed cells of similar origin. In addition, oxidative stress triggered HIF-1 and AP-1 activation which could promote TGF- $\beta$ -induced galectin-9 production in cancer cells (Section 4.2). Interestingly, co-culture of cytotoxic T cells and MCF-7 breast cancer cells promoted the upregulation of galectin-9 surface presence (Figure 46D). However, the biochemical mechanism for this phenomenon is unknown.

In the investigation of ROS-mediated induction of TGF- $\beta$ , it was demonstrated that HMGB1 stimulation of THP-1 human AML cells was able to promote TGF- $\beta$  production and secretion as a consequence upregulated galectin-9 secretion (Figure 54 and Figure 55). HMGB1 is known as an alarmin or DAMP, which is released passively from either dead, dying/injured cells or secreted by immune/cancer cells in response to endogenous and/or exogenous stimuli, e.g. hypoxia, endotoxin and anti-cancer treatments (387, 526, 527). During the course of tumour development, the cancer cells experience cellular stress, which may eventually lead to cell death (528). Furthermore, cancer treatments such as radiotherapy and some chemotherapies are cytotoxic by promoting directly or indirectly DNA damage, e.g. through oxidative stress. If DNA damage and/or adaptation to stress not occur, it may eventually lead to cell death, e.g. by apoptosis or necrosis (529, 530). To improve the efficacy of these treatments, understanding how they may promote tumour clearance is important. Research has shown that some agents are more effective than others because they promote immunogenic cell death (ICD) of cancer cells (531). ICD is important as it invokes an immune response to the dying cells by processes described in section 1.7.2. ICD is thought to aid in tumour clearing by promoting immune cell mediated

killing of the residual cancer cells after treatment. Different factors, such as exposure of CRT, secretion of ATP and release of HMGB1, are known to be required for dying cells to undergo ICD (531). However, as TGF- $\beta$ , HMGB1 has a dual function acting as both tumour suppressor and promoter, which depends on the circumstance and the oxidative milieu (387). In line with HMGB1 contribution to cancer development, HMGB1 has been reported elevated in AML as well as other cancer types, and in most cases it is associated with poor prognosis (532).

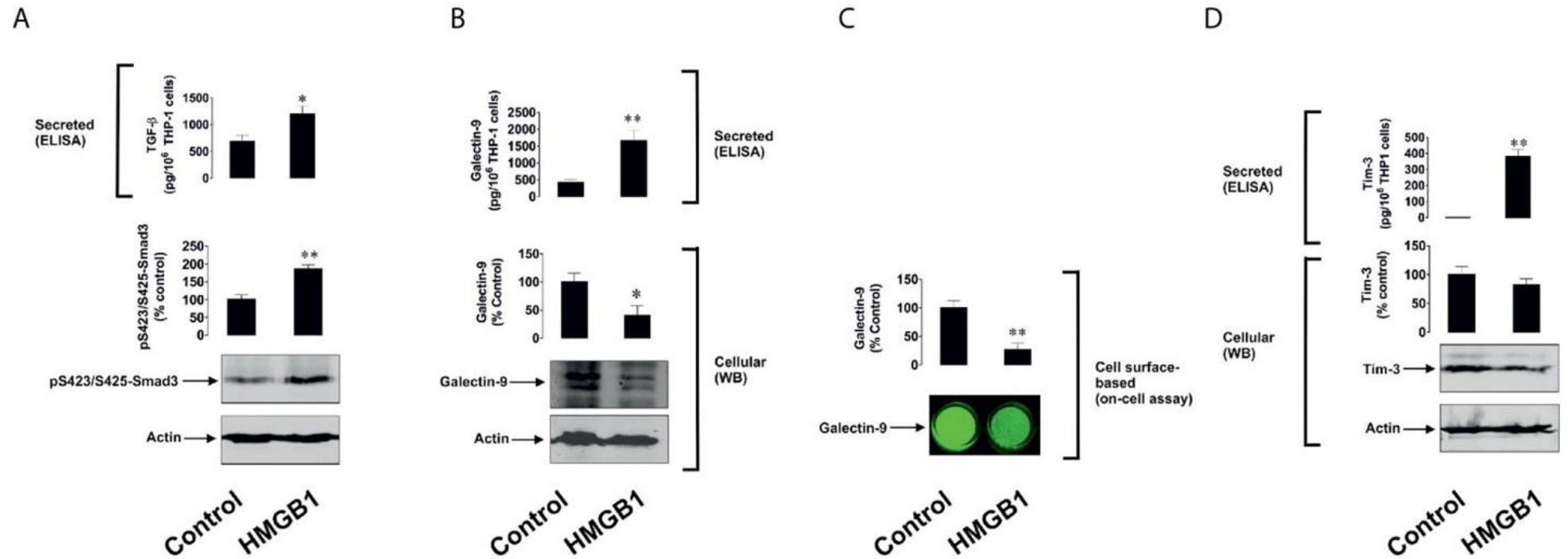
Extracellular HMGB1 is important for ICD assisting in antigen processing and presentation by DCs as well as stimulating DC maturation and secretion of pro-inflammatory cytokines, such as IL-12, and thus promoting a Th1 response (402, 403). However, as a tumour promoter, HMGB1 has been reported to be involved in tumorigenesis, cancer invasion and metastasis and resistance to therapy (387). Our group has recently reported that HMGB1 promotes AML progression by triggering TNF $\alpha$  release through activation of TLR2 and TLR4, which induces IL-1 $\beta$  that can stimulate the release of SCF required for survival and proliferation of AML cells (350). Furthermore, through a Tim-3-dependent manner, HMGB1 induced the secretion of VEGF, which is an angiogenic factor that contributes to tumour metastasis (350). Moreover, HMGB1 (cytoplasmic and extracellular forms) is involved in inducing and sustaining autophagy, and it is this ability that is the major contributor to therapy resistance, as rather than undergoing apoptosis the cancer cells survive (387, 411). Cancer treatments, such as radiotherapy and chemotherapy, are known to promote ROS (412, 474), and oxidative stress has been shown to mediate HMGB1 release (387). As showed in the previous result section in THP-1 cells (a model of AML) HMGB1-mediated ROS production, which promoted a TGF- $\beta$  induced galectin-9 secretion. Both ROS and TGF- $\beta$  have been associated with resistance to therapy. Thus, it could be speculated that stressed or dying cancer cells may contribute to immune escape and resistance to treatment by HMGB1-mediated TGF- $\beta$  induction of galectin-9 expression. This is the hypothesis that the present study aims to investigate.

#### 4.3.1 HMGB1 Promote Increased TGF- $\beta$ Production and Secretion and Its Autocrine Signalling Augment Galectin-9 Secretion in THP-1 cells

To confirm our previous finding, THP-1 cells were stimulated for 24 h with 1  $\mu$ g/mL HMGB1 and following secretion of TGF- $\beta$ , galectin-9 and Tim-3 were assessed using

ELISA, expression of phosphor-Smad3, galectin-9 and Tim-3 was determined by WB, and surface presence of galectin-9 was measured by OCA. Compared to the control, HMGB1-mediated a significantly increase in TGF- $\beta$  secretion, which autocrine activity subsequently resulted in an upregulation of active Smad3 (phosphor-S423/S425) (Figure 66A). This supports our previous experiment in Figure 54 and Figure 55 that HMGB1-TLR4 activation increases TGF- $\beta$  secretion in a ROS-ASK1-AP-1-dependent manner. It has previously been reported that THP-1 cells secrete galectin-9 in order to protect the cells from cytotoxic immune attack (64). Furthermore, as galectin-9 lacks the secretory domain, it needs a trafficker to be able to be exocytosed in a non-classical way. In THP-1 cells, Tim-3 has been suggested to acts as galectin-9 trafficker (322). In line with this, HMGB1 significantly augmented the secretion of galectin-9 and Tim-3, with a concomitant reduction in galectin-9 expression and surface-level (Figure 66B, C and D). This was in agreement with our previous findings that HMGB1 upregulated galectin-9 secretion, and this was found to be dependent on HMGB1-TLR4 activation of the ROS-ASK1-AP-1 pathway. As mentioned, galectin-9 can be shed off alone or in complex with Tim-3 by MMPs such as ADAM10 and ADAM17 (64, 272). Stimulation of TLR4 is known to activate various MMPs including ADAM17 supporting the notion that TLR4 activation promotes secretion of galectin-9-Tim-3 (533, 534).





**Figure 66: HMGB1 mediates TGF- $\beta$ , Tim-3 and galectin-9 secretion in THP-1 cells.** THP-1 cells were exposed to 1  $\mu$ g/mL recombinant human HMGB1 for 24 h followed by measurements of secreted TGF- $\beta$ , galectin-9 and Tim-3 detected by ELISA, protein expression of phospho-S423/S425 Smad3, galectin-9 and Tim-3 was determined by WB, and surface-based galectin-9 was examined by OCA. Images are from one experiment representative of at least three, which gave similar results. All quantitative data are shown as mean values  $\pm$  SEM \* -  $p < 0.05$  and \*\* -  $p < 0.01$  vs control.

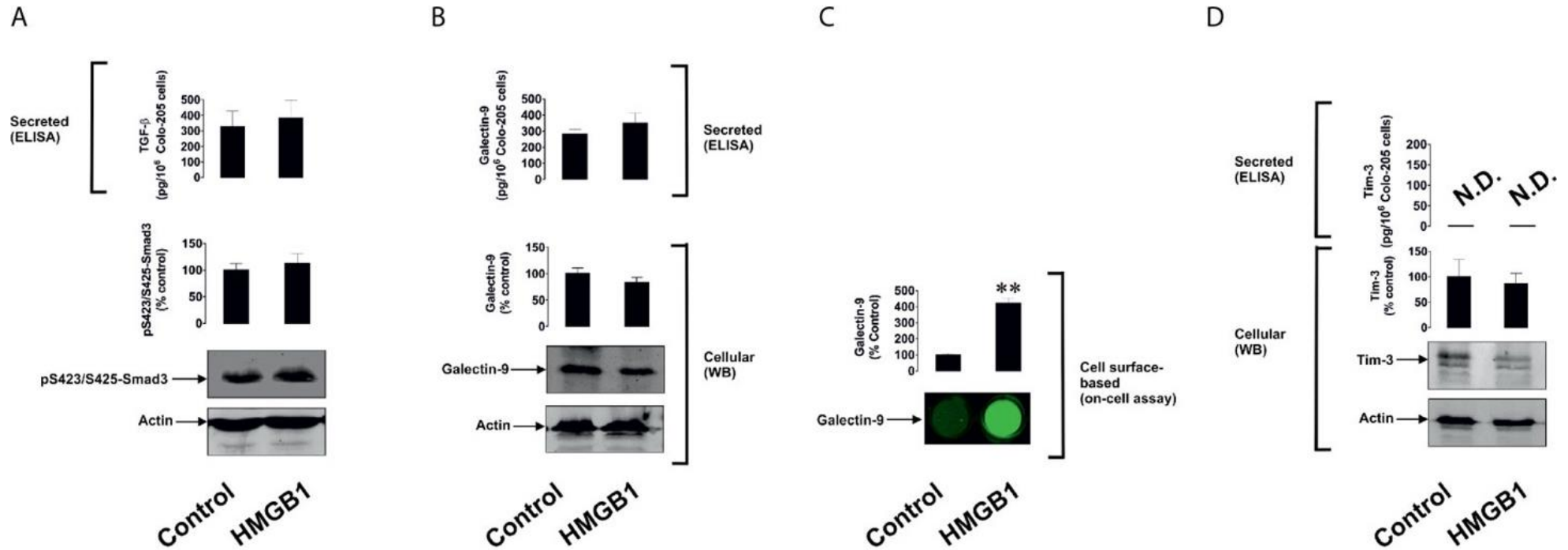
#### 4.3.2 HMGB1 Do not Increase Galectin-9 Expression in Adherent Cells

Subsequently, an investigation on HMGB1 effect on galectin-9 regulation in other cancer cells was undertaken. As with AML, galectin-9 has previously been reported to be used as an immune escape mechanism targeting cytotoxic T cells to undergo cell death in both breast cancer and colon cancer (257, 326). Therefore, the HMGB1 effect on galectin-9 was investigated in the human breast cancer cell line MCF-7 and human colorectal cancer cell line Colo-205, as well as human non-malignant healthy cell line HaCaT (keratinocytes), which like MCF-7 and Colo-205 are epithelial cells. All three cell lines were stimulated with 1  $\mu\text{g}/\text{mL}$  HMGB1 for 24 h, and following TGF- $\beta$ , galectin-9 and Tim-3 secretion were assessed by ELISA, active Smad3, galectin-9 and Tim-3 expression were measured by WB and surface presence of galectin-9 was determined by OCA. In all three cell lines (Colo-205, MCF-7 and HaCaT), HMGB1 did not affect TGF- $\beta$  secretion, phosphor-Smad3, galectin-9 and Tim-3 secretion and expression (Figure 67, Figure 68 and Figure 69 panel A, B and D). Interestingly, HMGB1 stimulated Colo-205 showed a significant increase in surface galectin-9 levels (Figure 67C), suggesting an increase in surface-translocation.

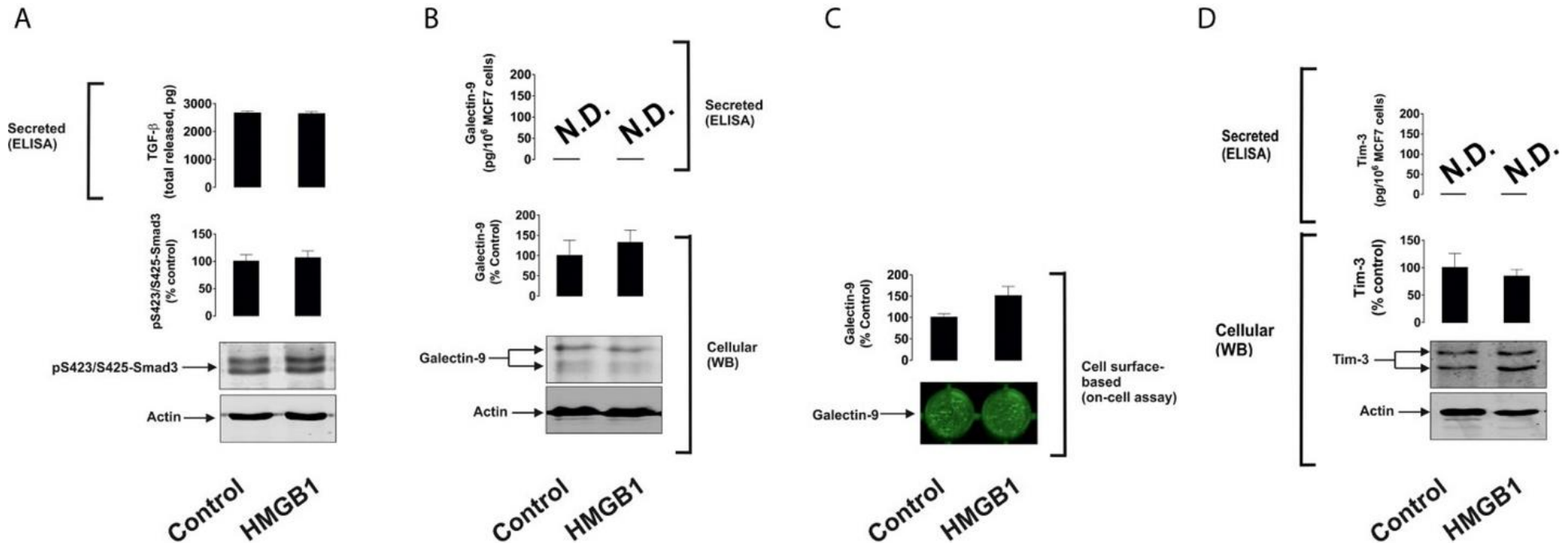
It was questioned why HMGB1 stimulation of the three cell lines had no effect on TGF- $\beta$  and galectin-9 (except for surface presence in Colo-205). HMGB1 is a multi-binding protein and can bind different receptors either directly or indirectly(384, 387). The surface receptors that have been reported to interact with HMGB1 directly are RAGE, TLR2, TLR4 and Tim-3 (384, 387). Although, which receptor HMGB1 binds to is dependent on the redox status of the HMGB1 ligand (Figure 23) (384). For instance, the all-thiol (fully reduced) form has been reported to bind to RAGE, the disulfide form (disulfide bridge C23 and C45, and reduced C106) has been demonstrated to interact with TLR4, and the fully terminal oxidized (sulfonate cysteines) form is unable to engage any of them (384). Which form of HMGB1 is binding to TLR2 or Tim-3 has not been reported. Although our group has previously reported that recombinant HMGB1 was able to trigger the secretion of TNF $\alpha$  in a TLR2 and TLR-4, but not in a RAGE dependent manner in THP-1 cells (350). This suggests that the recombinant HMGB1 from this experiment may have been in a disulfide form as it could trigger TLR4 activation, but not RAGE. Furthermore, it suggests that the disulfide form might bind to TLR2. Moreover, in the same study, recombinant HMGB1 was able to induce VEGF in a Tim-3 dependent manner in THP-1 cells,

suggesting that the disulfide form might bind to Tim-3 (350). The redox status of the recombinant HMGB1 applied in this study was not examined, but as it is added to the cell culture medium (which in itself is an oxidative milieu) (535), it is most likely that at least some of it will be in an oxidized state. As it is the same batch used in previously published paper (350), we assume that at least some of the HMGB1 is in a disulfide form able to trigger TLR4 signalling and possible TLR2 and Tim-3 activation as well (535).

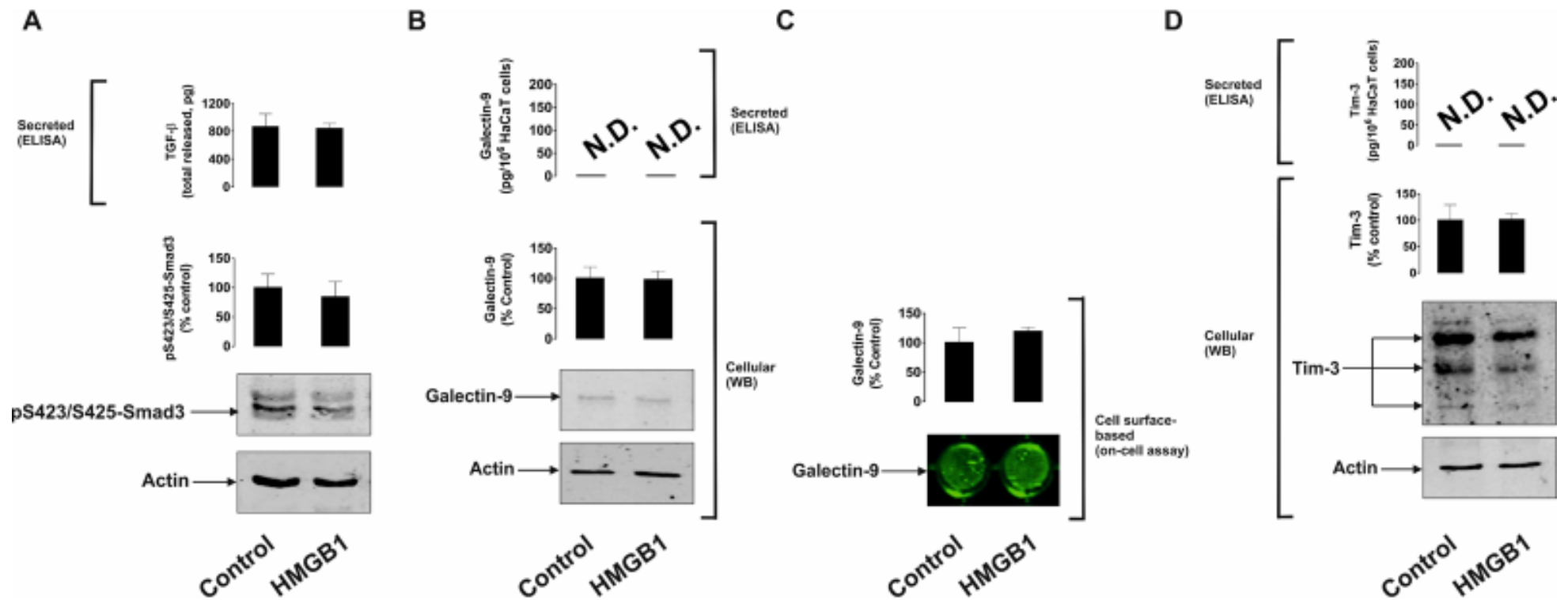
The constitutive expression of HMGB1 receptors was examined on all the four cell lines (THP-1, Colo-205, MCF-7, and HaCaT) using WB. All four cell lines expressed RAGE and Tim-3 in resting conditions. Moreover, Colo-205 and THP-1 expressed TLR2, whereas THP-1 was the only analysed cell line which expressed TLR4 (Figure 70).



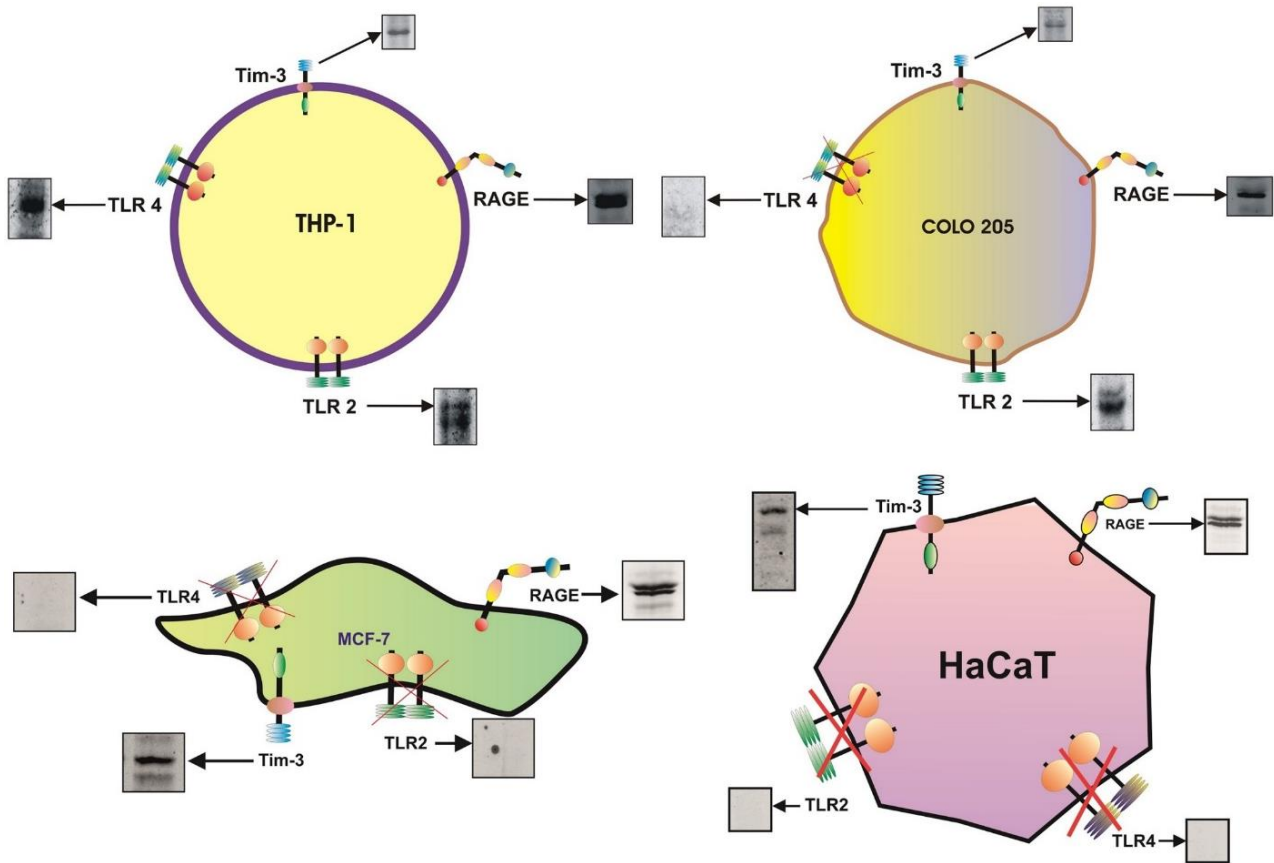
**Figure 67: HMGB1 do not affect secretion of TGF- $\beta$ , galectin-9 or Tim-3, but translocate galectin-9 to the surface in Colo-205 cells.** Colo-205 cells were exposed to 1  $\mu$ g/mL recombinant human HMGB1 for 24 h followed by measurements of secreted TGF- $\beta$ , galectin-9 and Tim-3 detected by ELISA, protein expression of phospho-S423/S425 Smad3, galectin-9 and Tim-3 was determined by WB, and surface-based galectin-9 was examined by OCA. Images are from one experiment representative of at least three, which gave similar results. All quantitative data are shown as mean values  $\pm$  SEM \* -  $p < 0.05$  and \*\* -  $p < 0.01$  vs control.



**Figure 68: HMGB1 do not mediate any effect on TGF- $\beta$ , galectin-9 and Tim-3 in MCF-7 cells.** MCF-7 breast cancer cells were exposed to 1  $\mu$ g/mL recombinant human HMGB1 for 24 h followed by measurements of secreted TGF- $\beta$ , galectin-9 and Tim-3 detected by ELISA, protein expression of phospho-S423/S425 Smad3, galectin-9 and Tim-3 was determined by WB, and surface-based galectin-9 was examined by OCA. Images are from one experiment representative of four, which gave similar results. All quantitative data are shown as mean values  $\pm$  SEM ( $n=4$ ) \* -  $p < 0.05$  and \*\* -  $p < 0.01$  vs control.



**Figure 69: HMGB1 do not mediate any effect on TGF- $\beta$ , galectin-9 and Tim-3 in non-malignant HaCaT keratinocytes.** HaCaT keratinocytes were exposed to 1  $\mu$ g/mL recombinant human HMGB1 for 24 h followed by measurements of secreted TGF- $\beta$ , galectin-9 and Tim-3 detected by ELISA, protein expression of phospho-S423/S425 Smad3, galectin-9 and Tim-3 was determined by WB, and surface-based galectin-9 was examined by OCAs. Images are from one experiment representative of four which gave similar results. All quantitative data are shown as mean values  $\pm$  SEM (n=4) \* -  $p < 0.05$  and \*\* -  $p < 0.01$  vs control.

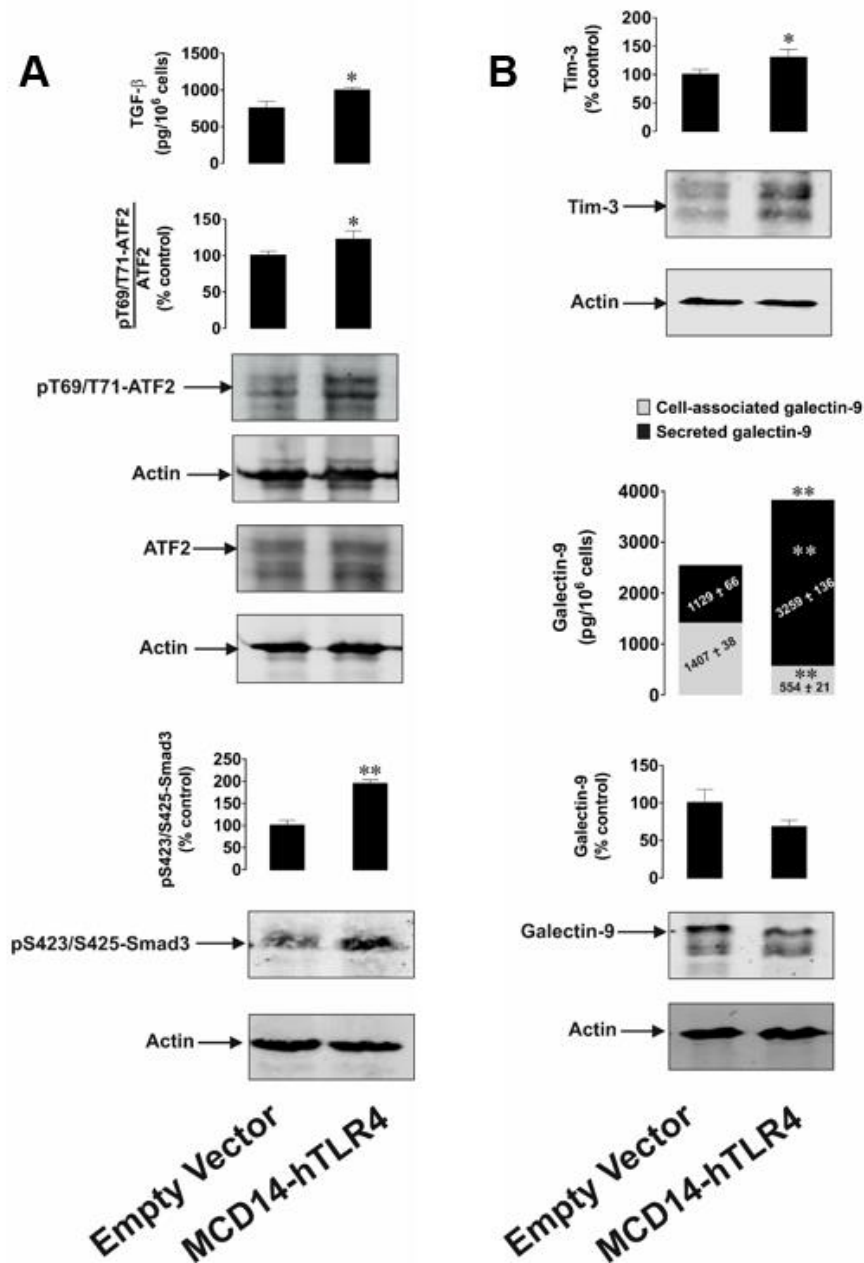


**Figure 70: Constitutive expression of HMGB1 receptors, RAGE, TLR2, TLR4 and Tim-3.** All the four cell lines, THP-1 (model for human AML), Colo-205 (model for human colorectal cancer), MCF-7 (model for non-invasive human breast cancer) and HaCaT (a non-transformed human cell line which is model for human keratinocytes), were examined for expression of known HMGB1 surface receptor. The THP-1 cell line is the only analysed cell line expressing all four receptors. Colo-205 expressed all except for TLR4. MCF-7 and HaCaT cells only expressed RAGE and Tim-3. Images are from one experiment representative of three.

#### 4.3.3 HMGB1 Mediated Effects on Galectin-9 is Dependent on TLR4 expression

Giving that THP-1 was the only cell line that had HMGB1-mediated effect on TGF- $\beta$  and galectin-9 (except for Colo-205 regarding galectin-9 surface presence), and it was the only cell line analysed that expressed TLR4, it was speculated that these effects were TLR4 dependent. To confirm this hypothesis, Colo-205 was transfected with constitutively active TLR4 or empty vector as control. Colo-205 was chosen as these cells similar to AML express TLR2, but unlike MCF-7 and HaCaT, are able to secrete galectin-9. Colo-205 with constitutively active TLR4 responded similarly to THP-1 cells stimulated with HMGB1. The cells transfected with active TLR4 significantly upregulated phospho-ATF-2 (Figure 71A), indicating an active AP-1 complex, which is known to contribute to TGF- $\beta$  production. In

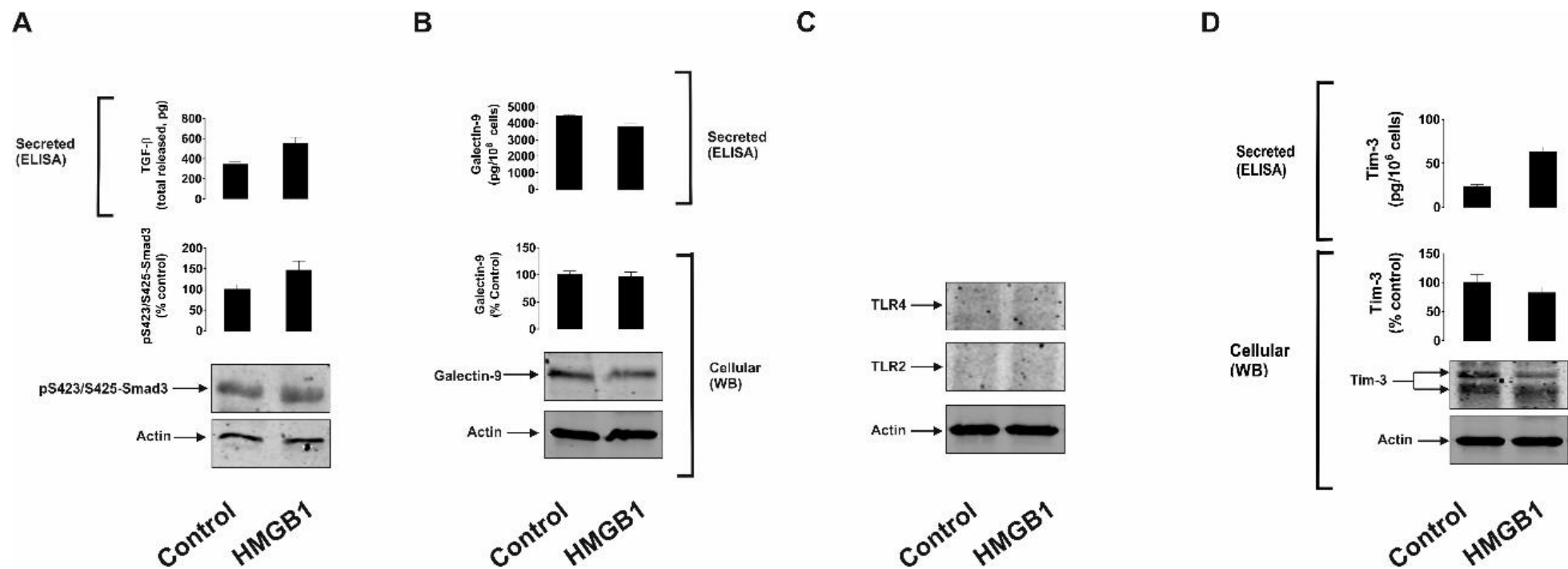
support of this, a significant increase in TGF- $\beta$  secretion and activation of Smad3 were seen (Figure 71A). Furthermore, there was an increase in Tim-3 expression and enhanced secretion of galectin-9 with a subsequent reduction in galectin-9 expression (Figure 71B). These data suggest that the HMGB1 induces TGF- $\beta$  along with galectin-9 production and secretion in a TLR4 dependent manner.



**Figure 71: HMGB1-mediated effect on TGF- $\beta$  and galectin-9 is TLR4 dependent.** Colo-205 cells were transfected with MCD14-hTLR4 (a constitutive active TLR4 receptor) or empty vector as control and cultured for 24 h. Activation of AP-1 was determined by expression of pT69/T71-ATF-2/total ATF-2. TGF- $\beta$ , and galectin-9 secretion as well as cell-associated galectin-9 were analysed by ELISA. Protein expression of phospho-S423/S425 Smad3, pT69/T71-ATF-2, Total ATF-2, galectin-9 and Tim-3 was determined by WB. Images are from one experiment representative of at least three, which gave similar results. All quantitative data are shown as mean values  $\pm$  SEM \* -  $p < 0.05$  and \*\* -  $p < 0.01$  vs control.



To verify the HMGB1-TLR4 effect on TGF- $\beta$  and galectin-9 in primary human AML cells, primary AML cells were stimulated with 2.5  $\mu\text{g}/\text{mL}$  HMGB1 for 16 h, secreted proteins were determined by ELISA, and the expression levels of protein were assessed by WB. No significant changes were observed in TGF- $\beta$ , galectin-9 or Tim-3 (Figure 72A, B and D). This unresponsiveness could be explained by the lack of TLR2 and TLR4 receptors (Figure 72C). The fact that this patient's AML cells do not express TLR2 and TLR4, and the THP-1 cells do, could be because the cells are derived from a different subtype of AML. AML can be categorized into nine different subtypes which are based on the cells that the leukaemia developed from (536). The subtypes are listed in Appendix, Table 3. Different studies have analysed the mRNA expression level of TLR2 and TLR4. One study reported higher levels of mRNA in promyelocytic (M3) AML cells compared to others (537, 538), whereas another study reported higher levels of mRNA in myelomonocytic (M4) and monoblastic AML cells (538). THP-1 is known to be derived from the monocytic (M5) AML cells (539). Thus, the primary AML cells analysed could be derived from an earlier stage where the cells did not express TLR2 or TLR4, and therefore no change was observed in the analysed parameters.



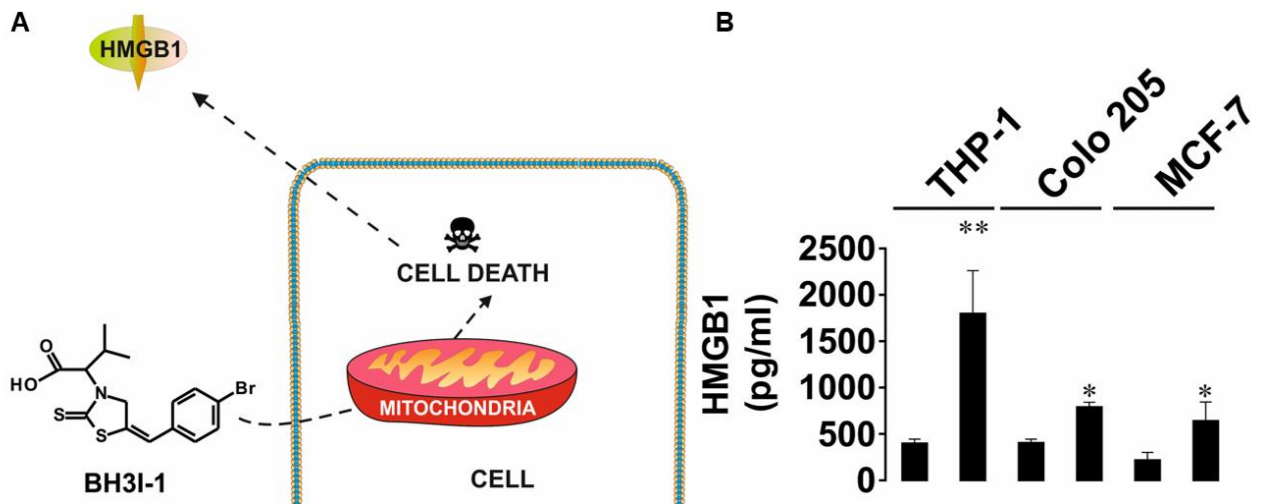
**Figure 72: HMGB1 do not mediate any effect on TGF $\beta$  or galectin-9 in primary human AML cells lacking TLR2 and TLR4 receptors.** Primary human AML cells were exposed to 2.5  $\mu$ g/mL recombinant human HMGB1 for 16 h followed by measurements of secreted TGF- $\beta$ , galectin-9 and Tim-3 detected by ELISA, protein expression of phospho-S423/S425 Smad3, galectin-9, Tim-3, TLR2 and TLR4 was determined by WB. Images are from one experiment representative of three, which gave similar results. All quantitative data are shown as mean values  $\pm$  SEM (n=3) \* -  $p < 0.05$  and \*\* -  $p < 0.01$  vs control.

#### 4.3.4 Stressed/dying Cancer Cells Promote the Release of HMGB1, which Can Induce TGF- $\beta$ -mediated Galectin-9 Production

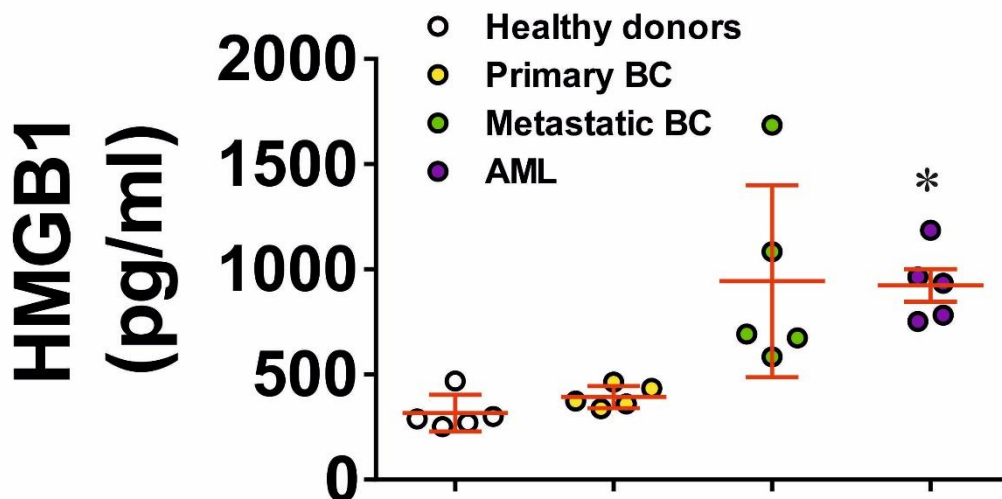
As reported previously, cancer cells are exposed to various forms of stress (e.g. hypoxia, or anti-cancer treatment etc.), which can promote oxidative stress and/or cell death. HMGB1 is a DAMP, which is released from stressed or dying cells. It was hypothesised that released HMGB1 can promote HMGB1-induced TGF- $\beta$ -mediated galectin-9 production in TLR4 expressing cancer cells, and thus evade immune surveillance. To investigate, if stressed/dying/death cancer cells can contribute to immune escape, it was examined if cancer cells release HMGB1 upon exposure to BH3I-1(5-[(4-bromophenyl)methylene]- $\alpha$ -(1-methylethyl)-4-oxo-2-thioxo-3-thiazolidineacetic acid), a known inducer of apoptosis (Figure 73A). BH3I-1 is a Bcl-XL antagonist, which induces apoptosis via the intrinsic pathway by promoting permeabilization of the mitochondrial outer membrane, leading to cytochrome C release, the formation of the apoptosome and activation of caspase-9 and caspase-3 (540). THP-1, Colo-205 and MCF-7 cells were stimulated with 100  $\mu$ M BH3I-1 for 24 h, following the detection of secreted HMGB1. In all three cell lines, there were observed an augmented secretion of HMGB1 upon exposure to BH3I-1, where interestingly, THP-1 cells release the highest levels (Figure 73B).

Subsequently, the HMGB1 plasma levels were investigated from five patients with AML, five patient suffering from metastatic breast cancer and five patients with primary breast cancer and from five healthy donors. HMGB1 plasma levels were significantly elevated in AML patients compared to healthy controls (Figure 74). However, there was no significant difference in plasma levels from healthy control and primary or metastatic breast tumour patients (Figure 74). These data suggest that as TGF- $\beta$ , HMGB1 stays in the microenvironment, thus release from circulating cells is found in the bloodstream, whereas it stays in the TME when released from solid tumour cells. This could maybe explain why THP-1 cells release more HMGB1 upon apoptosis than MCF-7 cells. It could be speculated that because these cells are further apart, more HMGB1 is released to increase chances of other adjacent cells are exposed to HMGB1. In breast tissue, the next adjacent cell is literally right beside the cell, and therefore it could be that less HMGB1 is needed to target the next cell.

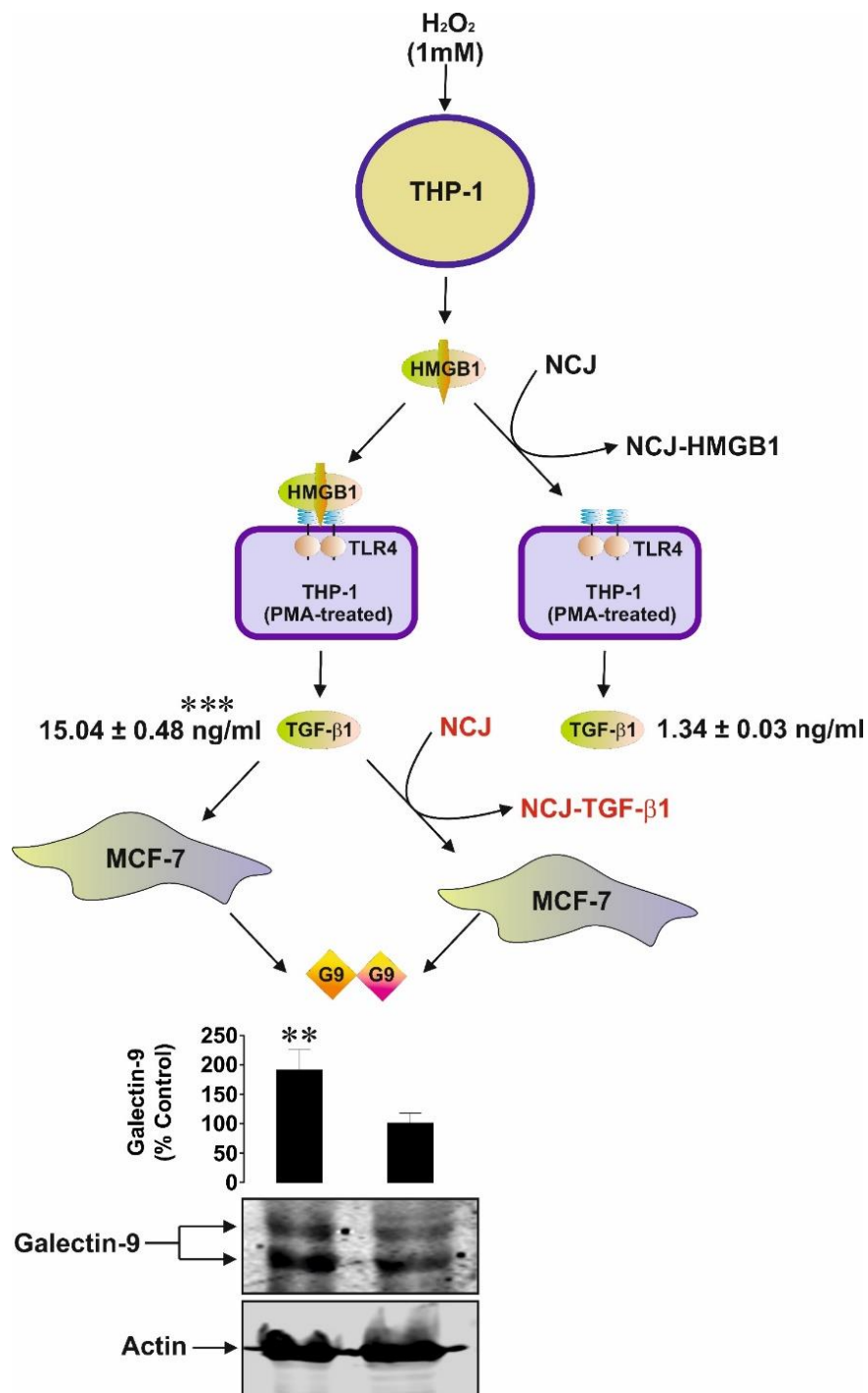
In order to confirm that stressed cells release HMGB1, and it can be deployed to induced TGF- $\beta$ -mediated galectin-9 production, THP-1 cells were chosen as they release the highest amount of HMGB1 (Figure 73) and were responding to HMGB1 stimulation through TLR-4 (Figure 66). THP-1 cells were exposed to oxidative stress, stimulating them with 1 mM hydrogen peroxide. The medium and secretory products collected from these cells were divided into two. One was used as direct stimuli on THP-1 cells, and the other was depleted for HMGB1 using nanoparticle coated with HMGB1 antibody to capture the HMGB1 in the medium (Appendix, Figure 84). The levels of secreted TGF- $\beta$  were then determined by ELISA from THP-1 receiving biological HMGB1 medium or THP-1 exposed to HMGB1-depleted medium. The cells that were given biological HMGB1 medium secreted significantly higher TGF- $\beta$  levels than the cells that received the HMGB1-depleted medium, and these cells hardly released any TGF- $\beta$  (Figure 75). The media and secretory products collected from the cells that were exposed to biological HMGB1 medium were likewise divided into two. Here, one was used as direct stimuli on MCF-7 cells, and the other was depleted for TGF- $\beta$  released upon HMGB1 stimulation. Galectin-9 expression in MCF-7 cells was then assessed by WB after exposure to biological TGF- $\beta$  medium or TGF- $\beta$ -depleted medium. The MCF-7 cells exposed to biological TGF- $\beta$  medium significantly upregulated galectin-9 expression compared to those that received TGF- $\beta$ -depleted medium (Figure 75). These data suggest that stressed or dying cancer cells can release HMGB1, which promotes TGF- $\beta$ -induced galectin-9 production that can be deployed as an immune escape mechanism, although, HMGB1 only promote TGF- $\beta$  in TLR4 expressing cells.



**Figure 73: Cell death induce HMGB1 release from cancer cells.** (A) BH3I-1 (a Bcl-XL antagonist) induces apoptosis via the intrinsic pathway by promoting permeabilization of the mitochondrial outer membrane causing caspase activation and release of HMGB1. (B) THP-1, Colo-205 and MCF-7 cancer cell lines were analysed for HMGB1 secretion after exposure to 100  $\mu$ M BH3I-1 for 24 h. All quantitative data are shown as mean values  $\pm$  SEM ( $n=3$ ) \* -  $p < 0.05$  and \*\* -  $p < 0.01$  vs control.



**Figure 74: Levels of secreted HMGB1 blood plasma of healthy donors, primary and metastatic breast cancer patients, and AML patients.** HMGB1 concentrations were measured in the blood plasma of healthy donors, patients with primary breast tumours, patients with metastatic breast solid tumours and AML patients ( $n=5$  for all donor types). Data are shown as mean values  $\pm$  SEM (data for each patient are shown). \* -  $p < 0.05$  vs healthy donors.



**Figure 75: Stressed cell release HMGB1, which promote biological active TGF- $\beta$  secretion that can induce galectin-9 production.** To induce oxidative stress, THP-1 cells were exposed to 1 mM hydrogen peroxide (H<sub>2</sub>O<sub>2</sub>) for 24 h. Medium was collected from the cells and was split in two. One half of the medium was depleted for HMGB1 by nanoconjugates (NCJ) coated with anti-HMGB1 antibodies. THP-1 cells (which express TLR4) were then either treated with medium containing HMGB1 or HMGB1 depleted medium. Medium from these cells were collected, and the TGF- $\beta$  concentration was measured. The medium from the THP-1 cells that received HMGB1 containing medium were also split in two. Like HMGB1, TGF- $\beta$  was depleted from one half using NCJ coated with anti-TGF- $\beta$  antibodies. MCF-7 cells were then treated with TGF- $\beta$  containing medium or TGF- $\beta$  depleted medium for 24 h, and following the expression of galectin-9 was determined by WB. Images are from one experiment representative of at least three, which gave similar results. All quantitative data are shown as mean values  $\pm$  SEM \* -  $p < 0.05$  and \*\* -  $p < 0.01$  \*\*\*-  $p < 0.001$  vs indicated events.

### 4.3.5 Discussion

Cancer cells upregulate galectin-9 and use it to escape immune surveillance (64, 304, 326). The mechanisms in which cancer cells deploy to upregulate galectin-9 are currently being investigated. Recently, it was reported that FLRT3-LPHN-PLC-PKC $\alpha$  and ROS-TGF- $\beta$ -Smad3 are common mechanisms used by various cancer cells to upregulate galectin-9, but not in healthy cells (326, 419). In section 4.2, it was found that HMGB1-mediated TLR4 activation resulted in the initiation of the ROS-ASK1-AP-1 pathway to promote TGF- $\beta$  and galectin-9 secretion. HMGB1 is a DAMP, which is passively released from stressed/dying cells or actively from immune/cancer cells (387). Furthermore, anti-cancer treatments such as radiotherapy and some chemotherapeutic agents are known to promote the release of HMGB1 (372, 374). Extracellular HMGB1 can directly bind to various receptors to mediate its effect, including TLR4 (Figure 23). In some settings, HMGB1 has been shown to aid in tumour clearance via TLR4-dependent mechanism (402). However, in other settings, HMGB1 is associated with resistance to therapy by promoting autophagy (387, 405). Many cancer types have elevated levels of HMGB1, and in most cases, it is associated with poor prognosis (532). Like HMGB1, TLR4 has been associated with both promoting anti-tumour immunity, on the other hand, it has been suggested to facilitate escape from host immune surveillance (541-544). Furthermore, the expression of TLR4-MyD88 was associated with poor clinical outcome (545, 546). This prompted a speculation if dying tumour cells could aid resistance to therapy by boosting immune escape via HMGB1-mediated upregulation of galectin-9.

It was previously demonstrated that recombinant HMGB1 can bind TLR4, resulting in signalling that promotes ROS production, which activates ROS-ASK1-MAPK-AP-1 pathway to induce TGF- $\beta$  (Figure 54 and Figure 55). Furthermore, the data from Section 4.2 demonstrate that TGF- $\beta$  is able to promote autocrine signalling that activates Smad3, a transcription factor that can induce galectin-9. It was therefore thought that the HMGB1-mediated increase in galectin-9 secretion from THP-1 cells, observed in Figure 55, was due to a Smad3-mediated increase in galectin-9 expression and then secretion. As previously shown, TGF- $\beta$  augments galectin-9 expression in THP-1 cells, and there was a tendency to an enhanced secretion of galectin-9 as well (Figure 63). In this study, it was demonstrated that HMGB1 significantly increased TGF- $\beta$  and galectin-9 production and secretion in a TLR4-dependent manner since only cells expressing TLR4 (THP-1 or Colo-

205 transfected with constitutive active TLR4) are able to do this (Figure 66, Figure 71 and Figure 70). Furthermore, galectin-9 surface presence was upregulated in Colo-205 cells, which express TLR2 (Figure 67 and Figure 70). This suggests that HMGB1-TLR2 activation could stimulate galectin-9 translocation to the surface. It was previously reported that PKC $\alpha$  is implicated in the translocation of galectin-9 (64, 326), and PKC $\alpha$  is known to act downstream of both TLR2 and TLR4 (547). The fact that galectin-9 surface presence was reduced in THP-1 cells, which express both TLR2 and TLR4, could be that galectin-9 was shed off more rapidly than it was replenished, or HMGB1 has different binding affinity to the two receptors and favouring ligation to TLR4, which promote secretion.

TLR4 has been implicated in tumour progression and metastasis in various cancers, such as AML, breast cancer and colon cancer (548-550). Therefore, it was a surprise that only functional TLR4 was detected in THP-1 cells (a model of AML), and not in Colo-205 (a model for colon cancer) and MCF-7 (a model for non-invasive breast cancer) (Figure 70). Suzuki et al. reported that Colo-205 had barely detectable TLR4 mRNA, however, this was upregulated with IFN $\gamma$  stimulation, and TLR4 protein expression was clearly detectable after treatment (551). Since the Colo-205 cells in this study had not undergone any prior treatment upon analysing the expression of HMGB1 receptors, it could be why TLR4 is not detected.

Regarding MCF-7 cells, one study reported no mRNA expression of TLR2 in both MCF-7 and the highly invasive cancer cell line MDA-MB-231 (541), supporting the findings that TLR2 is not expressed by MCF-7 cells. It was further demonstrated that MCF-7 cells barely expressed detectable TLR4 mRNA, in contrast, it was clearly detectable in MDA-MB-231 cells (541). In support of this, another study examined the expression of TLR4 and MyD88 (a downstream signalling protein of TLR4) and demonstrated that in contrast to MDA-MB-231 cells (which expressed high levels), MCF-7 expressed low levels of both TLR4 and MyD88 mRNA and protein (assessed by WB and confocal microscopy) (545). Although, the mRNA expression of HMGB1 was similar for the two cell lines. This indicates that the expression of TLR4 and MyD88 could correlate with the metastatic potential (which was confirmed in breast cancer patients) (545). Furthermore, a third study reported TLR4 protein expression in both MCF-7 and MDA-MB-231 (552). In neither the second or third study, the researchers did clarify what the molecular weight of TLR4 they detected was. An explanation could be that they detected degradation products and not functional



receptors as when TLR4 was detected in this study, there were also other bands observed than the functional TLR4 band (which molecular weight is 95-120 kDa). Although Li et al. demonstrated the migration of cancer cells in both cell lines when stimulated with LPS (a TLR4 ligand), suggesting a functional receptor (552). Zhou et al. also reported that LPS in combination with H<sub>2</sub>O<sub>2</sub> could enhance and sustain TGF- $\beta$ 1 mediated signalling, which could promote metastatic potential in MCF-7 cells, although this required culture for at least four days and up to 8 days (495). In this study, expression of TLR4 was not examined, but as response was observed when treated for longer periods, this could indicate that TLR4 receptors could be induced in MCF-7 cells. Albeit, in our current study, MCF-7 cells were only exposed to TLR4 ligand HMGB1 for 24 h, and maybe not long enough for inducing TLR4.

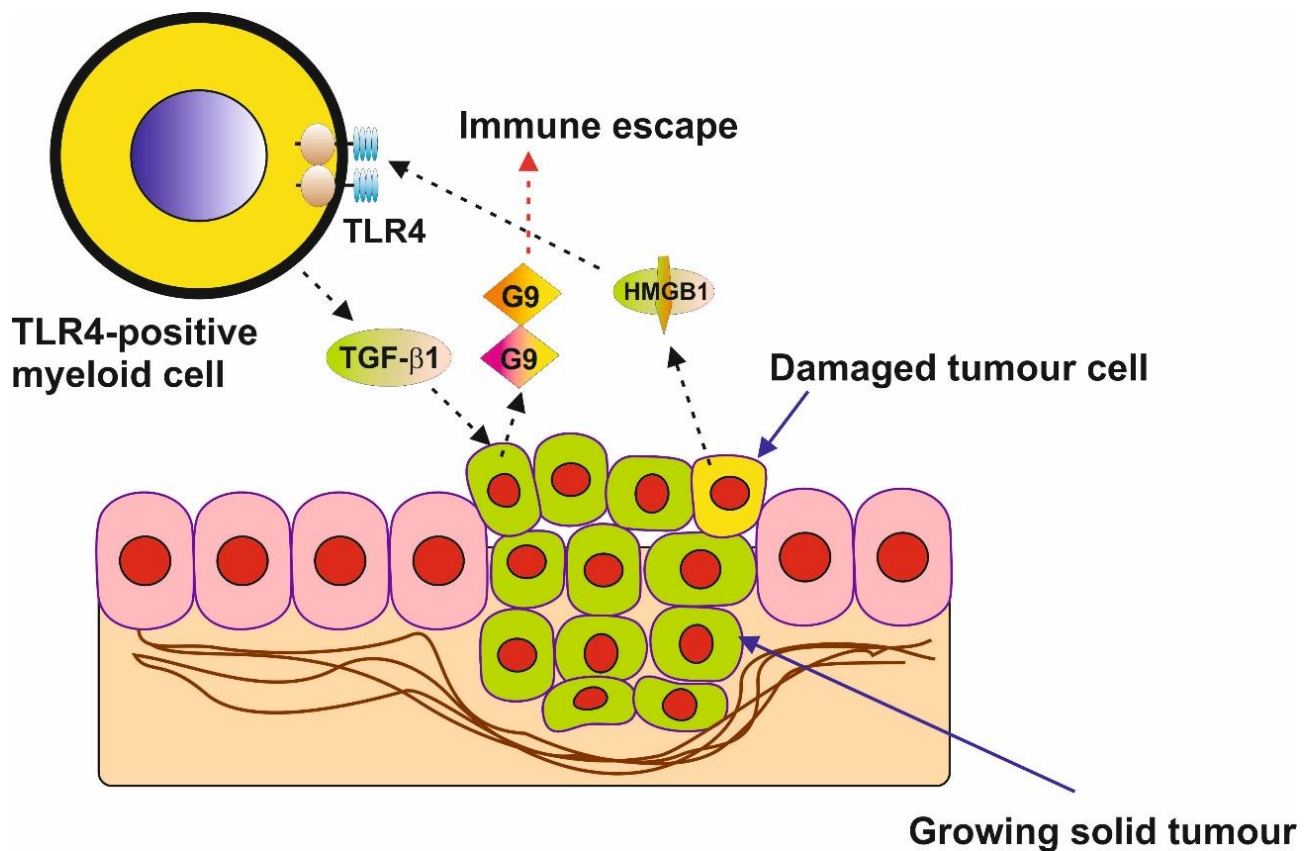
Keratinocytes have long been considered to be just a component of the physical barrier that prevents pathogenic entry. However, currently they are considered to be sentinel cells, which monitor changes in barrier integrity, the intrusion of microbial components and stress molecules and continuously communicate the status to the immune system. To do this, they are equipped with PPRs, among these are TLRs (553, 554). Primary human keratinocytes have been reported to express various TLRs, including TLR2 and TLR4 (although for TLR4, there are some discrepancies) (555-559). HaCaT keratinocytes have further been reported to express TLR2 and TLR4 mRNA (although lower levels of TLR4) (555). Pivarcsi et al. reported that the expression of TLR2 and TLR4 (assessed by qRT-PCR and flow cytometry) increases with differentiation of HaCaT keratinocytes (560). Köllisch and colleagues reported TLR4 mRNA in HaCaT, but not in primary human keratinocytes, although, TLR4 was not functional as LPS did not stimulate IL-8 release (558). This was most likely attributed to lack of MD2 expression as TLR4 both requires CD14 and MD2 co-receptors to initiate LPS-TLR4 mediated signalling (558). In all the studies regarding HaCaT keratinocytes just described none of them detected TLR4 expression using WB, which is a better characterizer of the functionality of TLR4 at the right molecular weight about 95 kDa (un-glycosylated) and about 120 kDa (glycosylated). The one study demonstrating TLR4 protein expression on HaCaT used differentiated HaCaT and flow cytometry (560). The difference between the present study and this could be that the HaCaT used had not undergone a differentiation process, or the flow cytometry antibody bound un-specifically.

I am not able to clearly explain the discrepancy in TLR4 expression between the previous reported studies with MCF-7 and HaCaT and what is observed in this study. Although, it should be noted that they used a different culture medium from ours. However, in any case, the lack of change in the analysed parameters in response to HMGB1 reflects very well the absence of TLR4 in the MCF-7 and HaCaT cells applied in this study.

Although HMGB1 can bind TLR4, TLR2, RAGE and Tim-3, the fact that no response was observed in the analysed parameters in cells only expressing RAGE and Tim-3 (Figure 67, Figure 68, Figure 69, and Figure 72) suggests that HMGB1-mediated effect on TGF- $\beta$  and galectin-9 is not through any of these receptors. As mentioned, there was an upregulated surface presence of galectin-9 in cancer cells expressing TLR2 when exposed to HMGB1 (Figure 67). This suggests that HMGB1 from stressed/dying cancer cells could promote immune escape in solid tumours expressing TLR2. That HMGB1 could augment TGF- $\beta$  secretion, Smad3 activation and galectin-9 production and secretion in THP-1 cells (expressing TLR4) and Colo-205 transfected with constitutive active TLR4, suggests that HMGB1-mediated TGF- $\beta$ -induced galectin-9 production is TLR4 dependent (Figure 54, Figure 55, Figure 66, and Figure 71). Moreover, it was clear that TGF- $\beta$  provided by HMGB1-stimulated THP-1 cells could increase galectin-9 expression in MCF-7 cells (Figure 75). This could suggest that HMGB1 release from stressed/dying solid tumour cells may aid in immune evasion by stimulating TLR4-expressing myeloid cells (e.g. TAM and MDSCs) to produce TGF- $\beta$ , and thus upregulate galectin-9 in cancer cells. This hypothesis is illustrated in Figure 76.

Furthermore, it should be noted that HMGB1 may in itself facilitate immune escape as it has been demonstrated to recruit MDSCs, promote their differentiation and augment their immunosuppressive activities (561, 562). In addition, HMGB1 can block phagocytosis of apoptotic cells by macrophages by binding to PtdSer (563), which might prevent the initiation of the adaptive immune response to neo-antigens. On the other hand, ingestion of apoptotic cells exposing PtdSer induces TGF- $\beta$  secretion by macrophages (564-566), indicating that dead cancer cells can aid in immune escape by promoting TGF- $\beta$ -induced galectin-9 production in live cancer cells. As mentioned, some solid tumours are mainly infiltrated by cytotoxic T cells (465, 466), and previous results (Figure 46) show that cytotoxic T cells in co-cultures with MCF-7 exposing galectin-9 had increased levels of cleaved PARP, suggesting that there are undergoing apoptosis. Apoptotic T cells have

been shown to release bio-active TGF- $\beta$  (368), this could suggest that CTL trying to attack tumour cells can be killed and facilitate immune escape by the release of TGF- $\beta$ , which can promote galectin-9 in cancer cells. In support of this, it was observed that MCF-7 cells in co-culture with cytotoxic Tall-104 T cells increased the surface level of galectin-9 (Figure 46). Overall, these studies suggest that dying cancer cells/immune cells can promote immune evasion by release of TGF- $\beta$  and/or HMGB1-induced TGF- $\beta$ , which may upregulate galectin-9 production in cancer cells that can be used to suppress NKs and kill T cells. Thus, blocking HMGB1 and/or TGF- $\beta$  mediated signalling should be considered as a therapeutic target for cancer treatment.



**Figure 76: Schematic illustrating of a vicious cycle in which stress/dying tumour cells promote immune escape by HMGB1-mediated TGF- $\beta$ -induced galectin-9 production.** A solid tumour cell was damaged causing release of HMGB1. These tumours are often infiltrated by TLR4-positive myeloid cells (such as TAMs or MDSCs). HMGB1 released from the damage tumour cells stimulates TGF- $\beta$  production and secretion from the TLR4-positive myeloid cells. TGF- $\beta$ -derived from TLR4-possitive cells can promote galectin-9 production by the “healthy” and live tumour cells. This facilitates immune escape of cancer cells and thus completes the cycle.

## 5 CONCLUSIONS

The following can be concluded from this work:

- 1) The majority of cancer cells, solid tumours, as well as liquid/haematological tumours, express Tim-3 and galectin-9 and the expression is higher than in non-malignant cells of similar origins. Similarly to AML a solid tumour like breast cancer has an active Tim-3-galectin-9 pathway and is used to protect malignant cells from host immune attack. This indicates that the Tim-3-galectin-9 pathway and is used to protect malignant cells from host immune attack. Indicating that Tim-3-galectin-9 pathway is a common way for malignant tumours to escape immune surveillance. Unlike AML, which secretes both galectin-9 and soluble Tim-3, breast cancer cells do not secrete these components, but as protection upregulates surface-bound galectin-9. It was demonstrated that galectin-9 induced increase intracellular activity of granzyme B in T cells results in their death (as indicated by apoptosis markers). Although, the mechanism behind this aberrant granzyme B activity is unclear, and further investigations are required to clarify if the role of membrane-associated galectin-9 in the increase in intracellular granzyme B activity in CTLs is similar to secreted galectin-9. With further understanding of this mechanism, it might be possible to prevent the death of CTLs and therefore promote cancer patients' outcome.
- 2) Cancer cells can deploy different mechanisms to regulate galectin-9 expression and localization and may be differentially regulated from Tim-3.
  - a. Like AML, breast cancer cells express FLRT3 and at least one isoform of LPHN. In breast cancer cells, FLRT3 engagement of LPHN triggers translocation of Tim-3-galectin-9 to the cell surface in a PLC and PKC $\alpha$ , but not in an mTOR dependent manner. Surface-based Tim-3-galectin-9 complex is used to protect breast cancer cells from cytotoxic immune attack. The FLRT3-LPHN pathway is expressed in the majority of cancer cell lines and thus may be a common mechanism for regulating galectin-9 (and Tim-3) for a variety of malignant tumours.
  - b. Oxidative stress (mediated by hypoxia or enhanced activity of ROS producing enzymes such as Xanthine oxidase and NADPH oxidase) is

increased in cancer cells compared to healthy cells. ROS triggers stabilization of HIF-1 $\alpha$  and consequently HIF-1 activity as well as promotes activation of the ASK-MAPK-AP-1 pathway. AP-1 and HIF-1 are involved in the induction of TGF- $\beta$ . TGF- $\beta$  displays autocrine activity and induces galectin-9 expression, but not Tim-3 expression, in a Smad3 dependent manner, in human cancer cells, but not in healthy cells.

- c. Induction of apoptosis or oxidative stress promotes the release of HMGB1 from cancer cells. HMGB1 triggers TGF- $\beta$ -induced galectin-9 production and secretion only in TLR4 expressing cells. In cancers that do not express TLR4, HMGB1 release may promote TGF- $\beta$  by TLR4 expressing infiltrating immune cells, such as myeloid-derived immune cells. The TGF- $\beta$  derived from infiltrating immune cells could promote galectin-9 production in live cancer cells.

Although further work is needed the data presented in this thesis have identified several promising targets for novel anti-cancer immunotherapies, such as galectin-9, FLRT3, TGF- $\beta$ , HMGB1 and their respective receptors.

The fact that galectin-9 expression and secretion are differentially regulated in cancer cells compared to healthy cells also poses further interest. It could be speculated that healthy cells express certain gene suppressor proteins, which do not allow for the upregulation of galectin-9. If these suppressors were identified, it might be possible to inhibit galectin-9 gene suppression in healthy cells, thus, allow for more expression of galectin-9 and protection against autoimmune attack.

## 6 BIBLIOGRAPHY

1. Murphy K. Janeway's Immunobiology. 8th ed: Garland Science; 2012.
2. WHO. Cancer 2018 [Available from: <https://www.who.int/news-room/factsheets/detail/cancer>].
3. Jones G. Why are cancer rates increasing: Cancer Research UK; 2015 [Available from: <https://scienceblog.cancerresearchuk.org/2015/02/04/why-are-cancer-rates-increasing/>].
4. AAAAI. Allergy statistic: American Academy of Allergy, Asthma & Immunology; [Available from: <https://www.aaaai.org/about-aaaai/newsroom/allergy-statistics>].
5. AAAAI TP. INCREASING RATES OF ALLERGIES AND ASTHMA: American Academy of Allergy, Asthma & Immunology; [Available from: <https://www.aaaai.org/conditions-and-treatments/library/allergy-library/prevalence-of-allergies-and-asthma>].
6. immunology Bsf. Report reveals the rising rates of autoimmune conditions: British society for immunology; 2018 [
7. Nakazawa DJ. The Autoimmune Epidemic - Foreword. The Autoimmune Epidemic 2007.
8. Love T. Why Are Autoimmune Diseases on the Rise? 2019 [Available from: <https://elemental.medium.com/autoimmunity-is-a-disorder-of-our-time-a7f1c45d6907>].
9. Okada H, Kuhn C, Feillet H, Bach JF. The 'hygiene hypothesis' for autoimmune and allergic diseases: an update. *Clinical and experimental immunology*. 2010;160(1):1-9.
10. Chapman KR, McIvor A. Asthma that is unresponsive to usual care. *CMAJ : Canadian Medical Association journal = journal de l'Association medicale canadienne*. 2010;182(1):45-52.
11. Alfarouk KO, Stock CM, Taylor S, Walsh M, Muddathir AK, Verduzco D, et al. Resistance to cancer chemotherapy: failure in drug response from ADME to P-gp. *Cancer cell international*. 2015;15:71.
12. Riganti C, Contino M. New Strategies to Overcome Resistance to Chemotherapy and Immune System in Cancer. *International journal of molecular sciences*. 2019;20(19).
13. Gide TN, Wilmott JS, Scolyer RA, Long GV. Primary and Acquired Resistance to Immune Checkpoint Inhibitors in Metastatic Melanoma. *Clinical cancer research : an official journal of the American Association for Cancer Research*. 2018;24(6):1260-70.
14. Koyama S, Akbay EA, Li YY, Herter-Sprie GS, Buczkowski KA, Richards WG, et al. Adaptive resistance to therapeutic PD-1 blockade is associated with upregulation of alternative immune checkpoints. *Nature communications*. 2016;7:10501.
15. Shayan G, Srivastava R, Li J, Schmitt N, Kane LP, Ferris RL. Adaptive resistance to anti-PD1 therapy by Tim-3 upregulation is mediated by the PI3K-Akt pathway in head and neck cancer. *Oncoimmunology*. 2017;6(1):e1261779.
16. Tanaka Y, Tsujimura S. [Multi-drug resistance in the treatments of autoimmune diseases]. *Nihon Rinsho Men'eki Gakkai kaishi = Japanese journal of clinical immunology*. 2006;29(5):319-24.
17. Arruebo M, Vilaboa N, Sáez-Gutierrez B, Lambea J, Tres A, Valladares M, et al. Assessment of the evolution of cancer treatment therapies. *Cancers*. 2011;3(3):3279-330.
18. Kau AL, Korenblat PE. Anti-interleukin 4 and 13 for asthma treatment in the era of endotypes. *Current opinion in allergy and clinical immunology*. 2014;14(6):570-5.
19. Pennock ND, White JT, Cross EW, Cheney EE, Tamburini BA, Kedl RM. T cell responses: naive to memory and everything in between. *Advances in physiology education*. 2013;37(4):273-83.
20. Xing Y, Hogquist KA. T-cell tolerance: central and peripheral. *Cold Spring Harbor perspectives in biology*. 2012;4(6).
21. Bour-Jordan H, Esensten JH, Martinez-Llordella M, Penaranda C, Stumpf M, Bluestone JA. Intrinsic and extrinsic control of peripheral T-cell tolerance by costimulatory molecules of the CD28/B7 family. *Immunological reviews*. 2011;241(1):180-205.
22. Takeuchi A, Saito T. CD4 CTL, a Cytotoxic Subset of CD4(+) T Cells, Their Differentiation and Function. *Frontiers in immunology*. 2017;8:194.

23. Dobrzanski MJ, Reome JB, Hollenbaugh JA, Dutton RW. Tc1 and Tc2 effector cell therapy elicit long-term tumor immunity by contrasting mechanisms that result in complementary endogenous type 1 antitumor responses. *Journal of immunology (Baltimore, Md : 1950)*. 2004;172(3):1380-90.
24. Eysteinsdóttir JH, Sigurgeirsson B, Ólafsson JH, Fridriksson T, Agnarsson BA, Davíðsson S, et al. The role of Th17/Tc17 peripheral blood T cells in psoriasis and their positive therapeutic response. *Scandinavian journal of immunology*. 2013;78(6):529-37.
25. Srenathan U, Steel K, Taams LS. IL-17+ CD8+ T cells: Differentiation, phenotype and role in inflammatory disease. *Immunology Letters*. 2016;178:20-6.
26. Zhu J, Yamane H, Paul WE. Differentiation of effector CD4 T cell populations (\*). *Annual review of immunology*. 2010;28:445-89.
27. Miossec P, Korn T, Kuchroo VK. Interleukin-17 and type 17 helper T cells. *The New England journal of medicine*. 2009;361(9):888-98.
28. Mescher MF, Curtsinger JM, Agarwal P, Casey KA, Gerner M, Hammerbeck CD, et al. Signals required for programming effector and memory development by CD8+ T cells. *Immunological reviews*. 2006;211:81-92.
29. Curtsinger JM, Lins DC, Mescher MF. Signal 3 determines tolerance versus full activation of naive CD8 T cells: dissociating proliferation and development of effector function. *The Journal of experimental medicine*. 2003;197(9):1141-51.
30. Curtsinger JM, Valenzuela JO, Agarwal P, Lins D, Mescher MF. Type I IFNs provide a third signal to CD8 T cells to stimulate clonal expansion and differentiation. *Journal of immunology (Baltimore, Md : 1950)*. 2005;174(8):4465-9.
31. Pardoll DM. The blockade of immune checkpoints in cancer immunotherapy. *Nature Reviews Cancer*. 2012;12(4):252-64.
32. Berard M, Tough DF. Qualitative differences between naïve and memory T cells. *Immunology*. 2002;106(2):127-38.
33. Gimmi CD, Freeman GJ, Gribben JG, Gray G, Nadler LM. Human T-cell clonal anergy is induced by antigen presentation in the absence of B7 costimulation. *Proceedings of the National Academy of Sciences of the United States of America*. 1993;90(14):6586-90.
34. Perez VL, Van Parijs L, Biuckians A, Zheng XX, Strom TB, Abbas AK. Induction of peripheral T cell tolerance in vivo requires CTLA-4 engagement. *Immunity*. 1997;6(4):411-7.
35. Wells AD, Walsh M, Turka LA. TWO DISTINCT FORMS OF T CELL ANERGY ARE INDUCED BY LACK OF COSTIMULATION VS. CELL DIVISION DURING PRIMARY ACTIVATION. *Transplantation*. 1998;65(12):S9.
36. Frauwirth KA, Alegre ML, Thompson CB. Induction of T cell anergy in the absence of CTLA-4/B7 interaction. *Journal of immunology (Baltimore, Md : 1950)*. 2000;164(6):2987-93.
37. Viganò S, Perreau M, Pantaleo G, Harari A. Positive and negative regulation of cellular immune responses in physiologic conditions and diseases. *Clinical & developmental immunology*. 2012;2012:485781.
38. Hanahan D, Weinberg RA. The hallmarks of cancer. *Cell*. 2000;100(1):57-70.
39. Hanahan D, Weinberg RA. Hallmarks of cancer: the next generation. *Cell*. 2011;144(5):646-74.
40. Dunn GP, Old LJ, Schreiber RD. The three Es of cancer immunoediting. *Annual review of immunology*. 2004;22:329-60.
41. Dunn GP, Old LJ, Schreiber RD. The immunobiology of cancer immunosurveillance and immunoediting. *Immunity*. 2004;21(2):137-48.
42. Chen DS, Mellman I. Oncology meets immunology: the cancer-immunity cycle. *Immunity*. 2013;39(1):1-10.
43. Kim JM, Chen DS. Immune escape to PD-L1/PD-1 blockade: seven steps to success (or failure). *Annals of oncology : official journal of the European Society for Medical Oncology*. 2016;27(8):1492-504.

44. Chester C, Fritsch K, Kohrt HE. Natural Killer Cell Immunomodulation: Targeting Activating, Inhibitory, and Co-stimulatory Receptor Signaling for Cancer Immunotherapy. *Frontiers in immunology*. 2015;6:601.
45. Liontos M, Anastasiou I, Bamias A, Dimopoulos MA. DNA damage, tumor mutational load and their impact on immune responses against cancer. *Annals of translational medicine*. 2016;4(14):264.
46. Janelle V, Rulleau C, Del Testa S, Carli C, Delisle J-S. T-Cell Immunotherapies Targeting Histocompatibility and Tumor Antigens in Hematological Malignancies. *Frontiers in immunology*. 2020;11(276).
47. Vesely MD, Kershaw MH, Schreiber RD, Smyth MJ. Natural innate and adaptive immunity to cancer. *Annual review of immunology*. 2011;29:235-71.
48. Kim R, Emi M, Tanabe K. Cancer immunoediting from immune surveillance to immune escape. *Immunology*. 2007;121(1):1-14.
49. Khong HT, Restifo NP. Natural selection of tumor variants in the generation of "tumor escape" phenotypes. *Nat Immunol*. 2002;3(11):999-1005.
50. Pitt JM, Marabelle A, Eggermont A, Soria JC, Kroemer G, Zitvogel L. Targeting the tumor microenvironment: removing obstruction to anticancer immune responses and immunotherapy. *Annals of oncology : official journal of the European Society for Medical Oncology*. 2016;27(8):1482-92.
51. Fleming V, Hu X, Weber R, Nagibin V, Groth C, Altevogt P, et al. Targeting Myeloid-Derived Suppressor Cells to Bypass Tumor-Induced Immunosuppression. *Frontiers in immunology*. 2018;9:398.
52. Park SM, Youn JI. Role of myeloid-derived suppressor cells in immune checkpoint inhibitor therapy in cancer. *Archives of pharmacal research*. 2019;42(7):560-6.
53. Chen Y, Song Y, Du W, Gong L, Chang H, Zou Z. Tumor-associated macrophages: an accomplice in solid tumor progression. *Journal of Biomedical Science*. 2019;26(1):78.
54. Yoshimura A, Wakabayashi Y, Mori T. Cellular and molecular basis for the regulation of inflammation by TGF-beta. *J Biochem*. 2010;147(6):781-92.
55. Chow MT, Luster AD. Chemokines in cancer. *Cancer immunology research*. 2014;2(12):1125-31.
56. Jiang X, Wang J, Deng X, Xiong F, Ge J, Xiang B, et al. Role of the tumor microenvironment in PD-L1/PD-1-mediated tumor immune escape. *Molecular Cancer*. 2019;18(1):10.
57. Bai J, Gao Z, Li X, Dong L, Han W, Nie J. Regulation of PD-1/PD-L1 pathway and resistance to PD-1/PD-L1 blockade. *Oncotarget*. 2017;8(66):110693-707.
58. Song M, Chen D, Lu B, Wang C, Zhang J, Huang L, et al. PTEN loss increases PD-L1 protein expression and affects the correlation between PD-L1 expression and clinical parameters in colorectal cancer. *PloS one*. 2013;8(6):e65821.
59. Chen J, Jiang CC, Jin L, Zhang XD. Regulation of PD-L1: a novel role of pro-survival signalling in cancer. *Annals of Oncology*. 2016;27(3):409-16.
60. Zerdes I, Wallerius M, Sifakis EG, Wallmann T, Betts S, Bartish M, et al. STAT3 Activity Promotes Programmed-Death Ligand 1 Expression and Suppresses Immune Responses in Breast Cancer. *Cancers*. 2019;11(10).
61. Thiery J, Safta TB, Ziani L, Chouaib S. Mechanisms of Cytotoxic Lymphocyte-Mediated Apoptosis and Relationship with the Tumor Suppressor p53. *Critical reviews in immunology*. 2015;35(6):433-49.
62. Wang Y, Hays E, Rama M, Bonavida B. Cell-mediated immune resistance in cancer. *Cancer Drug Resistance*. 2020;3(2):232-51.
63. Lee H, Jeong AJ, Ye SK. Highlighted STAT3 as a potential drug target for cancer therapy. *BMB reports*. 2019;52(7):415-23.
64. Gonçalves Silva I, Yasinska IM, Sakhnevych SS, Fiedler W, Wellbrock J, Bardelli M, et al. The Tim-3-galectin-9 Secretory Pathway is Involved in the Immune Escape of Human Acute Myeloid Leukemia Cells. *EBioMedicine*. 2017;22:44-57.



65. Frumento G, Rotondo R, Tonetti M, Damonte G, Benatti U, Ferrara GB. Tryptophan-derived catabolites are responsible for inhibition of T and natural killer cell proliferation induced by indoleamine 2,3-dioxygenase. *The Journal of experimental medicine*. 2002;196(4):459-68.
66. Terness P, Bauer TM, Röse L, Dufter C, Watzlik A, Simon H, et al. Inhibition of allogeneic T cell proliferation by indoleamine 2,3-dioxygenase-expressing dendritic cells: mediation of suppression by tryptophan metabolites. *The Journal of experimental medicine*. 2002;196(4):447-57.
67. Thomas DA, Massagué J. TGF-beta directly targets cytotoxic T cell functions during tumor evasion of immune surveillance. *Cancer cell*. 2005;8(5):369-80.
68. Dustin ML. The immunological synapse. *Cancer immunology research*. 2014;2(11):1023-33.
69. Busse D, de la Rosa M, Hobiger K, Thurley K, Flossdorf M, Scheffold A, et al. Competing feedback loops shape IL-2 signaling between helper and regulatory T lymphocytes in cellular microenvironments. *Proceedings of the National Academy of Sciences*. 2010;107(7):3058.
70. Kong KF, Fu G, Zhang Y, Yokosuka T, Casas J, Canonigo-Balancio AJ, et al. Protein kinase C- $\eta$  controls CTLA-4-mediated regulatory T cell function. *Nat Immunol*. 2014;15(5):465-72.
71. Wing K, Onishi Y, Prieto-Martin P, Yamaguchi T, Miyara M, Fehervari Z, et al. CTLA-4 control over Foxp3+ regulatory T cell function. *Science (New York, NY)*. 2008;322(5899):271-5.
72. Francisco LM, Salinas VH, Brown KE, Vanguri VK, Freeman GJ, Kuchroo VK, et al. PD-L1 regulates the development, maintenance, and function of induced regulatory T cells. *The Journal of experimental medicine*. 2009;206(13):3015-29.
73. Walker LS, Sansom DM. The emerging role of CTLA4 as a cell-extrinsic regulator of T cell responses. *Nature reviews Immunology*. 2011;11(12):852-63.
74. Wherry EJ. T cell exhaustion. *Nature Immunology*. 2011;12(6):492-9.
75. Pauken KE, Wherry EJ. Overcoming T cell exhaustion in infection and cancer. *Trends in immunology*. 2015;36(4):265-76.
76. Bi J, Tian Z. NK Cell Exhaustion. *Frontiers in immunology*. 2017;8:760.
77. Topalian SL, Drake CG, Pardoll DM. Immune checkpoint blockade: a common denominator approach to cancer therapy. *Cancer cell*. 2015;27(4):450-61.
78. Liu D, Jenkins RW, Sullivan RJ. Mechanisms of Resistance to Immune Checkpoint Blockade. *American journal of clinical dermatology*. 2019;20(1):41-54.
79. Zhang C, Liu Y. Targeting NK Cell Checkpoint Receptors or Molecules for Cancer Immunotherapy. *Frontiers in immunology*. 2020;11:1295.
80. Ahmadzadeh M, Johnson LA, Heemskerk B, Wunderlich JR, Dudley ME, White DE, et al. Tumor antigen-specific CD8 T cells infiltrating the tumor express high levels of PD-1 and are functionally impaired. *Blood*. 2009;114(8):1537-44.
81. Schildberg FA, Klein SR, Freeman GJ, Sharpe AH. Coinhibitory Pathways in the B7-CD28 Ligand-Receptor Family. *Immunity*. 2016;44(5):955-72.
82. Auchincloss H, Turka LA. CTLA-4: not all costimulation is stimulatory. *Journal of immunology (Baltimore, Md : 1950)*. 2011;187(7):3457-8.
83. Bjørgo E, Taskén K. Novel mechanism of signaling by CD28. *Immunol Lett*. 2010;129(1):1-6.
84. Chen L, Flies DB. Molecular mechanisms of T cell co-stimulation and co-inhibition. *Nature Reviews Immunology*. 2013;13(4):227-42.
85. . !!! INVALID CITATION !!! (74-76).
86. Schnell A, Bod L, Madi A, Kuchroo VK. The yin and yang of co-inhibitory receptors: toward anti-tumor immunity without autoimmunity. *Cell research*. 2020;30(4):285-99.
87. Bertrand A, Kostine M, Barnette T, Truchetet ME, Schaevebeke T. Immune related adverse events associated with anti-CTLA-4 antibodies: systematic review and meta-analysis. *BMC medicine*. 2015;13:211.
88. Fife BT, Bluestone JA. Control of peripheral T-cell tolerance and autoimmunity via the CTLA-4 and PD-1 pathways. *Immunological reviews*. 2008;224:166-82.

89. Iwai Y, Hamanishi J, Chamoto K, Honjo T. Cancer immunotherapies targeting the PD-1 signaling pathway. *J Biomed Sci.* 2017;24(1):26.
90. Wherry EJ, Kurachi M. Molecular and cellular insights into T cell exhaustion. *Nature reviews Immunology.* 2015;15(8):486-99.
91. Blank C, Kuball J, Voelkl S, Wiendl H, Becker B, Walter B, et al. Blockade of PD-L1 (B7-H1) augments human tumor-specific T cell responses in vitro. *International journal of cancer.* 2006;119(2):317-27.
92. Thommen DS, Schreiner J, Müller P, Herzig P, Roller A, Belousov A, et al. Progression of Lung Cancer Is Associated with Increased Dysfunction of T Cells Defined by Coexpression of Multiple Inhibitory Receptors. *Cancer immunology research.* 2015;3(12):1344-55.
93. Sakuishi K, Apetoh L, Sullivan JM, Blazar BR, Kuchroo VK, Anderson AC. Targeting Tim-3 and PD-1 pathways to reverse T cell exhaustion and restore anti-tumor immunity. *The Journal of experimental medicine.* 2010;207(10):2187-94.
94. Fourcade J, Sun Z, Benallaoua M, Guillaume P, Luescher IF, Sander C, et al. Upregulation of Tim-3 and PD-1 expression is associated with tumor antigen-specific CD8+ T cell dysfunction in melanoma patients. *The Journal of experimental medicine.* 2010;207(10):2175-86.
95. Ngiow SF, von Scheidt B, Akiba H, Yagita H, Teng MWL, Smyth MJ. Anti-TIM3 Antibody Promotes T Cell IFN- $\gamma$ -Mediated Antitumor Immunity and Suppresses Established Tumors. *Cancer Research.* 2011;71(10):3540-51.
96. Ndhlovu LC, Lopez-Vergès S, Barbour JD, Jones RB, Jha AR, Long BR, et al. Tim-3 marks human natural killer cell maturation and suppresses cell-mediated cytotoxicity. *Blood.* 2012;119(16):3734-43.
97. da Silva IP, Gallois A, Jimenez-Baranda S, Khan S, Anderson AC, Kuchroo VK, et al. Reversal of NK-cell exhaustion in advanced melanoma by Tim-3 blockade. *Cancer immunology research.* 2014;2(5):410-22.
98. Gallois A, Silva I, Osman I, Bhardwaj N. Reversal of natural killer cell exhaustion by TIM-3 blockade. *Oncoimmunology.* 2014;3(12):e946365.
99. Zheng Y, Li Y, Lian J, Yang H, Li F, Zhao S, et al. TNF- $\alpha$ -induced Tim-3 expression marks the dysfunction of infiltrating natural killer cells in human esophageal cancer. *Journal of Translational Medicine.* 2019;17(1):165.
100. Tinoco R, Alcalde V, Yang Y, Sauer K, Zuniga EI. Cell-intrinsic transforming growth factor-beta signaling mediates virus-specific CD8+ T cell deletion and viral persistence in vivo. *Immunity.* 2009;31(1):145-57.
101. Leng Q, Bentwich Z, Borkow G. Increased TGF-beta, Cbl-b and CTLA-4 levels and immunosuppression in association with chronic immune activation. *International immunology.* 2006;18(5):637-44.
102. Rotte A. Combination of CTLA-4 and PD-1 blockers for treatment of cancer. *Journal of Experimental & Clinical Cancer Research.* 2019;38(1):255.
103. Zhou Q, Munger ME, Veenstra RG, Weigel BJ, Hirashima M, Munn DH, et al. Coexpression of Tim-3 and PD-1 identifies a CD8+ T-cell exhaustion phenotype in mice with disseminated acute myelogenous leukemia. *Blood.* 2011;117(17):4501-10.
104. Ravi R, Noonan KA, Pham V, Bedi R, Zhavoronkov A, Ozerov IV, et al. Bifunctional immune checkpoint-targeted antibody-ligand traps that simultaneously disable TGF $\beta$  enhance the efficacy of cancer immunotherapy. *Nature communications.* 2018;9(1):741.
105. Sow HS, Ren J, Camps M, Ossendorp F, Ten Dijke P. Combined Inhibition of TGF- $\beta$  Signaling and the PD-L1 Immune Checkpoint Is Differentially Effective in Tumor Models. *Cells.* 2019;8(4).
106. Bai X, Yi M, Jiao Y, Chu Q, Wu K. Blocking TGF- $\beta$  Signaling To Enhance The Efficacy Of Immune Checkpoint Inhibitor. *OncoTargets and therapy.* 2019;12:9527-38.

107. Wang M, Liu Y, Cheng Y, Wei Y, Wei X. Immune checkpoint blockade and its combination therapy with small-molecule inhibitors for cancer treatment. *Biochimica et Biophysica Acta (BBA) - Reviews on Cancer*. 2019;1871(2):199-224.
108. Huemer F, Leisch M, Geisberger R, Melchardt T, Rinnerthaler G, Zaborsky N, et al. Combination Strategies for Immune-Checkpoint Blockade and Response Prediction by Artificial Intelligence. *International journal of molecular sciences*. 2020;21(8).
109. Pentcheva-Hoang T, Egen JG, Wojnoonski K, Allison JP. B7-1 and B7-2 selectively recruit CTLA-4 and CD28 to the immunological synapse. *Immunity*. 2004;21(3):401-13.
110. Collins AV, Brodie DW, Gilbert RJ, Iaboni A, Manso-Sancho R, Walse B, et al. The interaction properties of costimulatory molecules revisited. *Immunity*. 2002;17(2):201-10.
111. Schneider H, Valk E, Leung R, Rudd CE. CTLA-4 activation of phosphatidylinositol 3-kinase (PI 3-K) and protein kinase B (PKB/AKT) sustains T-cell anergy without cell death. *PloS one*. 2008;3(12):e3842.
112. Greenwald RJ, Boussiotis VA, Lorsch RB, Abbas AK, Sharpe AH. CTLA-4 regulates induction of anergy in vivo. *Immunity*. 2001;14(2):145-55.
113. Saverino D, Simone R, Bagnasco M, Pesce G. The soluble CTLA-4 receptor and its role in autoimmune diseases: an update. *Auto-immunity highlights*. 2010;1(2):73-81.
114. Liu Y, Zheng P. How Does an Anti-CTLA-4 Antibody Promote Cancer Immunity? *Trends in immunology*. 2018;39(12):953-6.
115. Simpson TR, Li F, Montalvo-Ortiz W, Sepulveda MA, Bergerhoff K, Arce F, et al. Fc-dependent depletion of tumor-infiltrating regulatory T cells co-defines the efficacy of anti-CTLA-4 therapy against melanoma. *The Journal of experimental medicine*. 2013;210(9):1695-710.
116. Du X, Tang F, Liu M, Su J, Zhang Y, Wu W, et al. A reappraisal of CTLA-4 checkpoint blockade in cancer immunotherapy. *Cell research*. 2018;28(4):416-32.
117. Sharma A, Subudhi SK, Blando J, Scutti J, Vence L, Wargo J, et al. Anti-CTLA-4 Immunotherapy Does Not Deplete FOXP3(+) Regulatory T Cells (Tregs) in Human Cancers. *Clinical cancer research : an official journal of the American Association for Cancer Research*. 2019;25(4):1233-8.
118. Krummey SM, Cheeseman JA, Conger JA, Jang PS, Mehta AK, Kirk AD, et al. High CTLA-4 expression on Th17 cells results in increased sensitivity to CTLA-4 coinhibition and resistance to belatacept. *American journal of transplantation : official journal of the American Society of Transplantation and the American Society of Transplant Surgeons*. 2014;14(3):607-14.
119. von Eeuw E, Chodon T, Attar N, Jalil J, Koya RC, Comin-Anduix B, et al. CTLA4 blockade increases Th17 cells in patients with metastatic melanoma. *Journal of Translational Medicine*. 2009;7(1):35.
120. Masteller EL, Chuang E, Mullen AC, Reiner SL, Thompson CB. Structural analysis of CTLA-4 function in vivo. *Journal of immunology (Baltimore, Md : 1950)*. 2000;164(10):5319-27.
121. Carreno BM, Bennett F, Chau TA, Ling V, Luxenberg D, Jussif J, et al. CTLA-4 (CD152) can inhibit T cell activation by two different mechanisms depending on its level of cell surface expression. *Journal of immunology (Baltimore, Md : 1950)*. 2000;165(3):1352-6.
122. Yokosuka T, Kobayashi W, Takamatsu M, Sakata-Sogawa K, Zeng H, Hashimoto-Tane A, et al. Spatiotemporal basis of CTLA-4 costimulatory molecule-mediated negative regulation of T cell activation. *Immunity*. 2010;33(3):326-39.
123. Rudd CE, Taylor A, Schneider H. CD28 and CTLA-4 coreceptor expression and signal transduction. *Immunological reviews*. 2009;229(1):12-26.
124. Baroja ML, Vijaykrishnan L, Bettelli E, Darlington PJ, Chau TA, Ling V, et al. Inhibition of CTLA-4 function by the regulatory subunit of serine/threonine phosphatase 2A. *Journal of immunology (Baltimore, Md : 1950)*. 2002;168(10):5070-8.
125. Teft WA, Chau TA, Madrenas J. Structure-Function analysis of the CTLA-4 interaction with PP2A. *BMC Immunol*. 2009;10:23.
126. Parry RV, Chemnitz JM, Frauwirth KA, Lanfranco AR, Braunstein I, Kobayashi SV, et al. CTLA-4 and PD-1 receptors inhibit T-cell activation by distinct mechanisms. *Molecular and cellular biology*. 2005;25(21):9543-53.

127. Marengère LE, Waterhouse P, Duncan GS, Mittrücker HW, Feng GS, Mak TW. Regulation of T cell receptor signaling by tyrosine phosphatase SYP association with CTLA-4. *Science (New York, NY)*. 1996;272(5265):1170-3.
128. Baroja ML, Luxenberg D, Chau T, Ling V, Strathdee CA, Carreno BM, et al. The inhibitory function of CTLA-4 does not require its tyrosine phosphorylation. *Journal of immunology (Baltimore, Md : 1950)*. 2000;164(1):49-55.
129. Schneider H, Rudd CE. Tyrosine Phosphatase SHP-2 Binding to CTLA-4: Absence of Direct YVKM/YFIP Motif Recognition. *Biochemical and Biophysical Research Communications*. 2000;269(1):279-83.
130. Hoff H, Kolar P, Ambach A, Radbruch A, Brunner-Weinzierl MC. CTLA-4 (CD152) inhibits T cell function by activating the ubiquitin ligase Itch. *Molecular immunology*. 2010;47(10):1875-81.
131. Li D, Gál I, Vermes C, Alegre ML, Chong AS, Chen L, et al. Cutting edge: Cbl-b: one of the key molecules tuning CD28- and CTLA-4-mediated T cell costimulation. *Journal of immunology (Baltimore, Md : 1950)*. 2004;173(12):7135-9.
132. Jeon MS, Atfield A, Venuprasad K, Krawczyk C, Sarao R, Elly C, et al. Essential role of the E3 ubiquitin ligase Cbl-b in T cell anergy induction. *Immunity*. 2004;21(2):167-77.
133. Klammt C, Lillemeier BF. How membrane structures control T cell signaling. *Frontiers in immunology*. 2012;3:291.
134. Rudd CE. The reverse stop-signal model for CTLA4 function. *Nature reviews Immunology*. 2008;8(2):153-60.
135. Rudd CE, Martin M, Schneider H. CTLA-4 negative signaling via lipid rafts: A new perspective. *Science's STKE : signal transduction knowledge environment*. 2002;2002(128):pe18.
136. Bunnell SC, Hong DI, Kardon JR, Yamazaki T, McGlade CJ, Barr VA, et al. T cell receptor ligation induces the formation of dynamically regulated signaling assemblies. *The Journal of cell biology*. 2002;158(7):1263-75.
137. Yokosuka T, Sakata-Sogawa K, Kobayashi W, Hiroshima M, Hashimoto-Tane A, Tokunaga M, et al. Newly generated T cell receptor microclusters initiate and sustain T cell activation by recruitment of Zap70 and SLP-76. *Nat Immunol*. 2005;6(12):1253-62.
138. Chikuma S, Imboden JB, Bluestone JA. Negative regulation of T cell receptor-lipid raft interaction by cytotoxic T lymphocyte-associated antigen 4. *The Journal of experimental medicine*. 2003;197(1):129-35.
139. Martin M, Schneider H, Azouz A, Rudd CE. Cytotoxic T lymphocyte antigen 4 and CD28 modulate cell surface raft expression in their regulation of T cell function. *The Journal of experimental medicine*. 2001;194(11):1675-81.
140. Schneider H, Smith X, Liu H, Bismuth G, Rudd CE. CTLA-4 disrupts ZAP70 microcluster formation with reduced T cell/APC dwell times and calcium mobilization. *European journal of immunology*. 2008;38(1):40-7.
141. Schneider H, Valk E, da Rocha Dias S, Wei B, Rudd CE. CTLA-4 up-regulation of lymphocyte function-associated antigen 1 adhesion and clustering as an alternate basis for coreceptor function. *Proceedings of the National Academy of Sciences of the United States of America*. 2005;102(36):12861-6.
142. Schneider H, Downey J, Smith A, Zinselmeyer BH, Rush C, Brewer JM, et al. Reversal of the TCR stop signal by CTLA-4. *Science (New York, NY)*. 2006;313(5795):1972-5.
143. Brunner-Weinzierl MC, Rudd CE. CTLA-4 and PD-1 Control of T-Cell Motility and Migration: Implications for Tumor Immunotherapy. *Frontiers in immunology*. 2018;9:2737.
144. Lu Y, Schneider H, Rudd CE. Murine regulatory T cells differ from conventional T cells in resisting the CTLA-4 reversal of TCR stop-signal. *Blood*. 2012;120(23):4560-70.
145. Wardell CM, MacDonald KN, Levings MK, Cook L. Cross talk between human regulatory T cells and antigen-presenting cells: Lessons for clinical applications. *European journal of immunology*. 2021;51(1):27-38.
146. Zanin-Zhorov A, Ding Y, Kumari S, Attur M, Hippen KL, Brown M, et al. Protein kinase C-theta mediates negative feedback on regulatory T cell function. *Science (New York, NY)*. 2010;328(5976):372-6.

147. Mellor AL, Munn DH. IDO expression by dendritic cells: tolerance and tryptophan catabolism. *Nature reviews Immunology*. 2004;4(10):762-74.
148. Routy JP, Routy B, Graziani GM, Mehraj V. The Kynurenine Pathway Is a Double-Edged Sword in Immune-Privileged Sites and in Cancer: Implications for Immunotherapy. *International journal of tryptophan research : IJTR*. 2016;9:67-77.
149. Fallarino F, Grohmann U, Vacca C, Bianchi R, Orabona C, Spreca A, et al. T cell apoptosis by tryptophan catabolism. *Cell death and differentiation*. 2002;9(10):1069-77.
150. Fallarino F, Grohmann U, Hwang KW, Orabona C, Vacca C, Bianchi R, et al. Modulation of tryptophan catabolism by regulatory T cells. *Nat Immunol*. 2003;4(12):1206-12.
151. Munn DH, Sharma MD, Mellor AL. Ligation of B7-1/B7-2 by human CD4+ T cells triggers indoleamine 2,3-dioxygenase activity in dendritic cells. *Journal of immunology (Baltimore, Md : 1950)*. 2004;172(7):4100-10.
152. Chen W, Jin W, Wahl SM. Engagement of cytotoxic T lymphocyte-associated antigen 4 (CTLA-4) induces transforming growth factor beta (TGF-beta) production by murine CD4(+) T cells. *The Journal of experimental medicine*. 1998;188(10):1849-57.
153. Sullivan TJ, Letterio JJ, van Elsas A, Mamura M, van Amelsfort J, Sharpe S, et al. Lack of a role for transforming growth factor-beta in cytotoxic T lymphocyte antigen-4-mediated inhibition of T cell activation. *Proceedings of the National Academy of Sciences of the United States of America*. 2001;98(5):2587-92.
154. Tang Q, Boden EK, Henriksen KJ, Bour-Jordan H, Bi M, Bluestone JA. Distinct roles of CTLA-4 and TGF-beta in CD4+CD25+ regulatory T cell function. *European journal of immunology*. 2004;34(11):2996-3005.
155. Oida T, Xu L, Weiner HL, Kitani A, Strober W. TGF-beta-mediated suppression by CD4+CD25+ T cells is facilitated by CTLA-4 signaling. *Journal of immunology (Baltimore, Md : 1950)*. 2006;177(4):2331-9.
156. Cederbom L, Hall H, Ivars F. CD4+CD25+ regulatory T cells down-regulate co-stimulatory molecules on antigen-presenting cells. *European journal of immunology*. 2000;30(6):1538-43.
157. Oderup C, Cederbom L, Makowska A, Cilio CM, Ivars F. Cytotoxic T lymphocyte antigen-4-dependent down-modulation of costimulatory molecules on dendritic cells in CD4+ CD25+ regulatory T-cell-mediated suppression. *Immunology*. 2006;118(2):240-9.
158. Qureshi OS, Zheng Y, Nakamura K, Attridge K, Manzotti C, Schmidt EM, et al. Trans-endocytosis of CD80 and CD86: a molecular basis for the cell-extrinsic function of CTLA-4. *Science (New York, NY)*. 2011;332(6029):600-3.
159. Hou TZ, Qureshi OS, Wang CJ, Baker J, Young SP, Walker LS, et al. A transendocytosis model of CTLA-4 function predicts its suppressive behavior on regulatory T cells. *Journal of immunology (Baltimore, Md : 1950)*. 2015;194(5):2148-59.
160. Ovcinnikovs V, Ross EM, Petersone L, Edner NM, Heuts F, Ntavli E, et al. CTLA-4-mediated transendocytosis of costimulatory molecules primarily targets migratory dendritic cells. *Science Immunology*. 2019;4(35):eaaw0902.
161. Oaks MK, Hallett KM, Penwell RT, Stauber EC, Warren SJ, Tector AJ. A native soluble form of CTLA-4. *Cellular immunology*. 2000;201(2):144-53.
162. Rita S, Daniele S. The Soluble CTLA-4 Receptor and its Emerging Role in Autoimmune Diseases. *Current Immunology Reviews (Discontinued)*. 2009;5(1):54-68.
163. Bardhan K, Anagnostou T, Boussiotis VA. The PD1:PD-L1/2 Pathway from Discovery to Clinical Implementation. *Frontiers in immunology*. 2016;7:550.
164. Okazaki T, Honjo T. The PD-1-PD-L pathway in immunological tolerance. *Trends in immunology*. 2006;27(4):195-201.
165. Riley JL. PD-1 signaling in primary T cells. *Immunological reviews*. 2009;229(1):114-25.
166. Iwai Y, Ishida M, Tanaka Y, Okazaki T, Honjo T, Minato N. Involvement of PD-L1 on tumor cells in the escape from host immune system and tumor immunotherapy by PD-L1 blockade. *Proceedings of the National Academy of Sciences of the United States of America*. 2002;99(19):12293-7.

167. Lim AR, Rathmell WK, Rathmell JC. The tumor microenvironment as a metabolic barrier to effector T cells and immunotherapy. *eLife*. 2020;9.
168. Fife BT, Pauken KE, Eagar TN, Obu T, Wu J, Tang Q, et al. Interactions between PD-1 and PD-L1 promote tolerance by blocking the TCR-induced stop signal. *Nat Immunol*. 2009;10(11):1185-92.
169. Karwacz K, Bricogne C, MacDonald D, Arce F, Bennett CL, Collins M, et al. PD-L1 co-stimulation contributes to ligand-induced T cell receptor down-modulation on CD8+ T cells. *EMBO molecular medicine*. 2011;3(10):581-92.
170. Yokosuka T, Takamatsu M, Kobayashi-Imanishi W, Hashimoto-Tane A, Azuma M, Saito T. Programmed cell death 1 forms negative costimulatory microclusters that directly inhibit T cell receptor signaling by recruiting phosphatase SHP2. *The Journal of experimental medicine*. 2012;209(6):1201-17.
171. Boussiotis VA, Chatterjee P, Li L. Biochemical signaling of PD-1 on T cells and its functional implications. *Cancer journal (Sudbury, Mass)*. 2014;20(4):265-71.
172. Latchman Y, Wood CR, Chernova T, Chaudhary D, Borde M, Chernova I, et al. PD-L2 is a second ligand for PD-1 and inhibits T cell activation. *Nat Immunol*. 2001;2(3):261-8.
173. Dong H, Strome SE, Salomao DR, Tamura H, Hirano F, Flies DB, et al. Tumor-associated B7-H1 promotes T-cell apoptosis: a potential mechanism of immune evasion. *Nature medicine*. 2002;8(8):793-800.
174. Kleffel S, Posch C, Barthel SR, Mueller H, Schlapbach C, Guenova E, et al. Melanoma Cell-Intrinsic PD-1 Receptor Functions Promote Tumor Growth. *Cell*. 2015;162(6):1242-56.
175. Butte MJ, Keir ME, Phamduy TB, Sharpe AH, Freeman GJ. Programmed death-1 ligand 1 interacts specifically with the B7-1 costimulatory molecule to inhibit T cell responses. *Immunity*. 2007;27(1):111-22.
176. Singh AK, Stock P, Akbari O. Role of PD-L1 and PD-L2 in allergic diseases and asthma. *Allergy*. 2011;66(2):155-62.
177. Lewkowich IP, Lajoie S, Stoffers SL, Suzuki Y, Richgels PK, Dienger K, et al. PD-L2 modulates asthma severity by directly decreasing dendritic cell IL-12 production. *Mucosal immunology*. 2013;6(4):728-39.
178. Xiao Y, Yu S, Zhu B, Bedoret D, Bu X, Francisco LM, et al. RGMb is a novel binding partner for PD-L2 and its engagement with PD-L2 promotes respiratory tolerance. *The Journal of experimental medicine*. 2014;211(5):943-59.
179. Chaudhri A, Xiao Y, Klee AN, Wang X, Zhu B, Freeman GJ. PD-L1 Binds to B7-1 Only In Cis on the Same Cell Surface. *Cancer immunology research*. 2018;6(8):921-9.
180. Okazaki T, Maeda A, Nishimura H, Kurosaki T, Honjo T. PD-1 immunoreceptor inhibits B cell receptor-mediated signaling by recruiting src homology 2-domain-containing tyrosine phosphatase 2 to phosphotyrosine. *Proceedings of the National Academy of Sciences of the United States of America*. 2001;98(24):13866-71.
181. Sheppard KA, Fitz LJ, Lee JM, Benander C, George JA, Wooters J, et al. PD-1 inhibits T-cell receptor induced phosphorylation of the ZAP70/CD3zeta signalosome and downstream signaling to PKCtheta. *FEBS letters*. 2004;574(1-3):37-41.
182. Patsoukis N, Duke-Cohan JS, Chaudhri A, Aksoylar HI, Wang Q, Council A, et al. Interaction of SHP-2 SH2 domains with PD-1 ITSM induces PD-1 dimerization and SHP-2 activation. *Communications biology*. 2020;3(1):128.
183. Chemnitz JM, Parry RV, Nichols KE, June CH, Riley JL. SHP-1 and SHP-2 associate with immunoreceptor tyrosine-based switch motif of programmed death 1 upon primary human T cell stimulation, but only receptor ligation prevents T cell activation. *Journal of immunology (Baltimore, Md : 1950)*. 2004;173(2):945-54.
184. Chatterjee P, Patsoukis N, Freeman GJ, Boussiotis VA. Distinct Roles Of PD-1 Itsm and ITIM In Regulating Interactions With SHP-2, ZAP-70 and Lck, and PD-1-Mediated Inhibitory Function. *Blood*. 2013;122(21):191-.

185. Peled M, Tocheva AS, Sandigursky S, Nayak S, Philips EA, Nichols KE, et al. Affinity purification mass spectrometry analysis of PD-1 uncovers SAP as a new checkpoint inhibitor. *Proceedings of the National Academy of Sciences of the United States of America*. 2018;115(3):E468-e77.
186. Pluskey S, Wandless TJ, Walsh CT, Shoelson SE. Potent stimulation of SH-PTP2 phosphatase activity by simultaneous occupancy of both SH2 domains. *The Journal of biological chemistry*. 1995;270(7):2897-900.
187. Lu W, Gong D, Bar-Sagi D, Cole PA. Site-specific incorporation of a phosphotyrosine mimetic reveals a role for tyrosine phosphorylation of SHP-2 in cell signaling. *Molecular cell*. 2001;8(4):759-69.
188. Bardhan K, Patsoukis N, Sari D, Anagnostou T, Chatterjee P, Freeman GJ, et al. PD-1 Inhibits TCR Proximal Signaling By Sequestering SHP-2 Phosphatase and Facilitating Csk-Mediated Inhibitory Phosphorylation of Lck. *Blood*. 2015;126(23):283-.
189. Zuazo M, Gato-Cañas M, Llorente N, Ibañez-Vea M, Arasanz H, Kochan G, et al. Molecular mechanisms of programmed cell death-1 dependent T cell suppression: relevance for immunotherapy. *Annals of translational medicine*. 2017;5(19):385.
190. Patsoukis N, Brown J, Petkova V, Liu F, Li L, Boussiotis VA. Selective effects of PD-1 on Akt and Ras pathways regulate molecular components of the cell cycle and inhibit T cell proliferation. *Science signaling*. 2012;5(230):ra46.
191. Quigley M, Pereyra F, Nilsson B, Porichis F, Fonseca C, Eichbaum Q, et al. Transcriptional analysis of HIV-specific CD8+ T cells shows that PD-1 inhibits T cell function by upregulating BATF. *Nature medicine*. 2010;16(10):1147-51.
192. Patsoukis N, Li L, Sari D, Petkova V, Boussiotis VA. PD-1 increases PTEN phosphatase activity while decreasing PTEN protein stability by inhibiting casein kinase 2. *Molecular and cellular biology*. 2013;33(16):3091-8.
193. Husain K, Williamson TT, Nelson N, Ghansah T. Protein kinase 2 (CK2): a potential regulator of immune cell development and function in cancer. *Immunological medicine*. 2020:1-16.
194. Appleman LJ, van Puijenbroek AA, Shu KM, Nadler LM, Boussiotis VA. CD28 costimulation mediates down-regulation of p27kip1 and cell cycle progression by activation of the PI3K/PKB signaling pathway in primary human T cells. *Journal of immunology (Baltimore, Md : 1950)*. 2002;168(6):2729-36.
195. Appleman LJ, Chernova I, Li L, Boussiotis VA. CD28 costimulation mediates transcription of SKP2 and CKS1, the substrate recognition components of SCFSkp2 ubiquitin ligase that leads p27kip1 to degradation. *Cell cycle (Georgetown, Tex)*. 2006;5(18):2123-9.
196. Naramura M, Jang IK, Kole H, Huang F, Haines D, Gu H. c-Cbl and Cbl-b regulate T cell responsiveness by promoting ligand-induced TCR down-modulation. *Nat Immunol*. 2002;3(12):1192-9.
197. Yang B, Gay DL, MacLeod MK, Cao X, Hala T, Sweezer EM, et al. Nedd4 augments the adaptive immune response by promoting ubiquitin-mediated degradation of Cbl-b in activated T cells. *Nat Immunol*. 2008;9(12):1356-63.
198. Gruber T, Hermann-Kleiter N, Hinterleitner R, Fresser F, Schneider R, Gastl G, et al. PKC-theta modulates the strength of T cell responses by targeting Cbl-b for ubiquitination and degradation. *Science signaling*. 2009;2(76):ra30.
199. Xiao Y, Qiao G, Tang J, Tang R, Guo H, Warwar S, et al. Protein Tyrosine Phosphatase SHP-1 Modulates T Cell Responses by Controlling Cbl-b Degradation. *Journal of immunology (Baltimore, Md : 1950)*. 2015;195(9):4218-27.
200. Rota G, Niogret C, Dang AT, Barros CR, Fonta NP, Alfei F, et al. Shp-2 Is Dispensable for Establishing T Cell Exhaustion and for PD-1 Signaling In Vivo. *Cell reports*. 2018;23(1):39-49.
201. O'Donnell JS, Smyth MJ, Teng MWL. PD1 functions by inhibiting CD28-mediated co-stimulation. *Clinical & translational immunology*. 2017;6(5):e138.
202. Kamphorst AO, Wieland A, Nasti T, Yang S, Zhang R, Barber DL, et al. Rescue of exhausted CD8 T cells by PD-1-targeted therapies is CD28-dependent. *Science (New York, NY)*. 2017;355(6332):1423-7.
203. Mizuno R, Sugiura D, Shimizu K, Maruhashi T, Watada M, Okazaki IM, et al. PD-1 Primarily Targets TCR Signal in the Inhibition of Functional T Cell Activation. *Frontiers in immunology*. 2019;10:630.

204. Hui E, Cheung J, Zhu J, Su X, Taylor MJ, Wallweber HA, et al. T cell costimulatory receptor CD28 is a primary target for PD-1-mediated inhibition. *Science (New York, NY)*. 2017;355(6332):1428-33.
205. Huang H, Jeon MS, Liao L, Yang C, Elly C, Yates JR, 3rd, et al. K33-linked polyubiquitination of T cell receptor-zeta regulates proteolysis-independent T cell signaling. *Immunity*. 2010;33(1):60-70.
206. Sharpe AH, Pauken KE. The diverse functions of the PD1 inhibitory pathway. *Nature reviews Immunology*. 2018;18(3):153-67.
207. Sauer S, Bruno L, Hertweck A, Finlay D, Leleu M, Spivakov M, et al. T cell receptor signaling controls Foxp3 expression via PI3K, Akt, and mTOR. *Proceedings of the National Academy of Sciences of the United States of America*. 2008;105(22):7797-802.
208. Amarnath S, Mangus CW, Wang JC, Wei F, He A, Kapoor V, et al. The PDL1-PD1 axis converts human TH1 cells into regulatory T cells. *Science translational medicine*. 2011;3(111):111ra20.
209. Patsoukis N, Chatterjee P, Sari D, Petkova V, Li L, Boussiotis VA. PD-1 Induces Metabolic Reprogramming Of Activated T Cells From Glycolysis To Lipid Oxidation. *Blood*. 2013;122(21):187-.
210. Michalek RD, Gerriets VA, Jacobs SR, Macintyre AN, MacIver NJ, Mason EF, et al. Cutting edge: distinct glycolytic and lipid oxidative metabolic programs are essential for effector and regulatory CD4+ T cell subsets. *Journal of immunology (Baltimore, Md : 1950)*. 2011;186(6):3299-303.
211. Patsoukis N, Bardhan K, Chatterjee P, Sari D, Liu B, Bell LN, et al. PD-1 alters T-cell metabolic reprogramming by inhibiting glycolysis and promoting lipolysis and fatty acid oxidation. *Nature communications*. 2015;6:6692.
212. Gerriets VA, Rathmell JC. Metabolic pathways in T cell fate and function. *Trends in immunology*. 2012;33(4):168-73.
213. Vignali PDA, Barbi J, Pan F. Metabolic Regulation of T Cell Immunity. *Advances in experimental medicine and biology*. 2017;1011:87-130.
214. Chatterjee P, Patsoukis N, Sari D, Boussiotis VA. PD-1 Couples Glucose Starvation with Autophagy and Survival Through AMPK-Mediated Phosphorylation of Ulk1. *Blood*. 2012;120(21):836-.
215. Du W, Yang M, Turner A, Xu C, Ferris RL, Huang J, et al. TIM-3 as a Target for Cancer Immunotherapy and Mechanisms of Action. *International journal of molecular sciences*. 2017;18(3).
216. Gorman JV, Colgan JD. Regulation of T cell responses by the receptor molecule Tim-3. *Immunologic research*. 2014;59(1-3):56-65.
217. Freeman GJ, Casasnovas JM, Umetsu DT, DeKruyff RH. TIM genes: a family of cell surface phosphatidylserine receptors that regulate innate and adaptive immunity. *Immunological reviews*. 2010;235(1):172-89.
218. Scientific TF. TIM3 Monoclonal Antibody (4C4G3) [Available from: <https://www.thermofisher.com/antibody/product/TIM3-Antibody-clone-4C4G3-Monoclonal/60355-1-IG>].
219. Sabatos CA, Chakravarti S, Cha E, Schubart A, Sánchez-Fueyo A, Zheng XX, et al. Interaction of Tim-3 and Tim-3 ligand regulates T helper type 1 responses and induction of peripheral tolerance. *Nat Immunol*. 2003;4(11):1102-10.
220. Das M, Zhu C, Kuchroo VK. Tim-3 and its role in regulating anti-tumor immunity. *Immunological reviews*. 2017;276(1):97-111.
221. Möller-Hackbarth K, Dewitz C, Schweigert O, Trad A, Garbers C, Rose-John S, et al. A disintegrin and metalloprotease (ADAM) 10 and ADAM17 are major sheddases of T cell immunoglobulin and mucin domain 3 (Tim-3). *The Journal of biological chemistry*. 2013;288(48):34529-44.
222. Clayton KL, Douglas-Vail MB, Nur-ur Rahman AK, Medcalf KE, Xie IY, Chew GM, et al. Soluble T cell immunoglobulin mucin domain 3 is shed from CD8+ T cells by the sheddase ADAM10, is increased in plasma during untreated HIV infection, and correlates with HIV disease progression. *Journal of virology*. 2015;89(7):3723-36.
223. Banerjee H, Kane LP. Immune regulation by Tim-3. *F1000Research*. 2018;7:316.
224. Monney L, Sabatos CA, Gaglia JL, Ryu A, Waldner H, Chernova T, et al. Th1-specific cell surface protein Tim-3 regulates macrophage activation and severity of an autoimmune disease. *Nature*. 2002;415(6871):536-41.



225. He Y, Cao J, Zhao C, Li X, Zhou C, Hirsch FR. TIM-3, a promising target for cancer immunotherapy. *OncoTargets and therapy*. 2018;11:7005-9.
226. Prokhorov A, Gibbs BF, Bardelli M, Ruegg L, Fasler-Kan E, Varani L, et al. The immune receptor Tim-3 mediates activation of PI3 kinase/mTOR and HIF-1 pathways in human myeloid leukaemia cells. *The international journal of biochemistry & cell biology*. 2015;59:11-20.
227. Chiba S, Baghdadi M, Akiba H, Yoshiyama H, Kinoshita I, Dosaka-Akita H, et al. Tumor-infiltrating DCs suppress nucleic acid-mediated innate immune responses through interactions between the receptor TIM-3 and the alarmin HMGB1. *Nat Immunol*. 2012;13(9):832-42.
228. Friedlaender A, Addeo A, Banna G. New emerging targets in cancer immunotherapy: the role of TIM3. *ESMO Open*. 2019;4(Suppl 3):e000497.
229. Anderson AC, Anderson DE, Bregoli L, Hastings WD, Kassam N, Lei C, et al. Promotion of tissue inflammation by the immune receptor Tim-3 expressed on innate immune cells. *Science (New York, NY)*. 2007;318(5853):1141-3.
230. Gleason MK, Lenvik TR, McCullar V, Felices M, O'Brien MS, Cooley SA, et al. Tim-3 is an inducible human natural killer cell receptor that enhances interferon gamma production in response to galectin-9. *Blood*. 2012;119(13):3064-72.
231. Anderson AC, Joller N, Kuchroo VK. Lag-3, Tim-3, and TIGIT: Co-inhibitory Receptors with Specialized Functions in Immune Regulation. *Immunity*. 2016;44(5):989-1004.
232. Nakae S, Iwakura Y, Suto H, Galli SJ. Phenotypic differences between Th1 and Th17 cells and negative regulation of Th1 cell differentiation by IL-17. *Journal of leukocyte biology*. 2007;81(5):1258-68.
233. Sánchez-Fueyo A, Tian J, Picarella D, Domenig C, Zheng XX, Sabatos CA, et al. Tim-3 inhibits T helper type 1-mediated auto- and alloimmune responses and promotes immunological tolerance. *Nat Immunol*. 2003;4(11):1093-101.
234. Gupta S, Thornley TB, Gao W, Larocca R, Turka LA, Kuchroo VK, et al. Allograft rejection is restrained by short-lived TIM-3+PD-1+Foxp3+ Tregs. *The Journal of clinical investigation*. 2012;122(7):2395-404.
235. Wang F, Wan L, Zhang C, Zheng X, Li J, Chen ZK. Tim-3-Galectin-9 pathway involves the suppression induced by CD4+CD25+ regulatory T cells. *Immunobiology*. 2009;214(5):342-9.
236. Banerjee H, Nieves-Rosado H, Kulkarni A, Murter B, Chandran UR, Chang A, et al. Expression of Tim-3 drives naïve Treg to an effector-like state with enhanced suppressive activity. *bioRxiv*. 2020:2020.07.31.230714.
237. Hastings WD, Anderson DE, Kassam N, Koguchi K, Greenfield EA, Kent SC, et al. TIM-3 is expressed on activated human CD4+ T cells and regulates Th1 and Th17 cytokines. *European journal of immunology*. 2009;39(9):2492-501.
238. Koguchi K, Anderson DE, Yang L, O'Connor KC, Kuchroo VK, Hafler DA. Dysregulated T cell expression of TIM3 in multiple sclerosis. *The Journal of experimental medicine*. 2006;203(6):1413-8.
239. Yang L, Anderson DE, Kuchroo J, Hafler DA. Lack of TIM-3 immunoregulation in multiple sclerosis. *Journal of immunology (Baltimore, Md : 1950)*. 2008;180(7):4409-14.
240. Kanai Y, Satoh T, Igawa K, Yokozeki H. Impaired expression of Tim-3 on Th17 and Th1 cells in psoriasis. *Acta dermato-venereologica*. 2012;92(4):367-71.
241. Chae SC, Park YR, Shim SC, Yoon KS, Chung HT. The polymorphisms of Th1 cell surface gene Tim-3 are associated in a Korean population with rheumatoid arthritis. *Immunol Lett*. 2004;95(1):91-5.
242. Liu R, Wang X, Chen X, Wang S, Zhang H. TIM-3 rs1036199 polymorphism increases susceptibility to autoimmune diseases: evidence based on 4200 subjects. *Bioscience reports*. 2018;38(6).
243. Liu Y, Shu Q, Gao L, Hou N, Zhao D, Liu X, et al. Increased Tim-3 expression on peripheral lymphocytes from patients with rheumatoid arthritis negatively correlates with disease activity. *Clinical immunology (Orlando, Fla)*. 2010;137(2):288-95.
244. Lee J, Oh JM, Hwang JW, Ahn JK, Bae EK, Won J, et al. Expression of human TIM-3 and its correlation with disease activity in rheumatoid arthritis. *Scandinavian journal of rheumatology*. 2011;40(5):334-40.

245. Xu L, Huang Y, Tan L, Yu W, Chen D, Lu C, et al. Increased Tim-3 expression in peripheral NK cells predicts a poorer prognosis and Tim-3 blockade improves NK cell-mediated cytotoxicity in human lung adenocarcinoma. *International immunopharmacology*. 2015;29(2):635-41.
246. Cai C, Xu YF, Wu ZJ, Dong Q, Li MY, Olson JC, et al. Tim-3 expression represents dysfunctional tumor infiltrating T cells in renal cell carcinoma. *World journal of urology*. 2016;34(4):561-7.
247. Takano S, Saito H, Ikeguchi M. An increased number of PD-1+ and Tim-3+ CD8+ T cells is involved in immune evasion in gastric cancer. *Surgery today*. 2016;46(11):1341-7.
248. Sakuishi K, Ngiow SF, Sullivan JM, Teng MW, Kuchroo VK, Smyth MJ, et al. TIM3(+)FOXP3(+) regulatory T cells are tissue-specific promoters of T-cell dysfunction in cancer. *Oncoimmunology*. 2013;2(4):e23849.
249. Liu JF, Wu L, Yang LL, Deng WW, Mao L, Wu H, et al. Blockade of TIM3 relieves immunosuppression through reducing regulatory T cells in head and neck cancer. *Journal of experimental & clinical cancer research : CR*. 2018;37(1):44.
250. DeKruyff RH, Bu X, Ballesteros A, Santiago C, Chim YL, Lee HH, et al. T cell/transmembrane, Ig, and mucin-3 allelic variants differentially recognize phosphatidylserine and mediate phagocytosis of apoptotic cells. *Journal of immunology (Baltimore, Md : 1950)*. 2010;184(4):1918-30.
251. Dolina JS, Braciale TJ, Hahn YS. Liver-primed CD8+ T cells suppress antiviral adaptive immunity through galectin-9-independent T-cell immunoglobulin and mucin 3 engagement of high-mobility group box 1 in mice. *Hepatology (Baltimore, Md)*. 2014;59(4):1351-65.
252. Huang YH, Zhu C, Kondo Y, Anderson AC, Gandhi A, Russell A, et al. CEACAM1 regulates TIM-3-mediated tolerance and exhaustion. *Nature*. 2015;517(7534):386-90.
253. Huang YH, Zhu C, Kondo Y, Anderson AC, Gandhi A, Russell A, et al. Corrigendum: CEACAM1 regulates TIM-3-mediated tolerance and exhaustion. *Nature*. 2016;536(7616):359.
254. De Sousa Linhares A, Kellner F, Jutz S, Zlabinger GJ, Gabius HJ, Huppa JB, et al. TIM-3 and CEACAM1 do not interact in cis and in trans. *European journal of immunology*. 2020.
255. Zhu C, Anderson AC, Schubart A, Xiong H, Imitola J, Khoury SJ, et al. The Tim-3 ligand galectin-9 negatively regulates T helper type 1 immunity. *Nat Immunol*. 2005;6(12):1245-52.
256. Sehrawat S, Reddy PBJ, Rajasagi N, Suryawanshi A, Hirashima M, Rouse BT. Galectin-9/TIM-3 Interaction Regulates Virus-Specific Primary and Memory CD8+ T Cell Response. *PLoS pathogens*. 2010;6(5):e1000882.
257. Kang C-W, Dutta A, Chang L-Y, Mahalingam J, Lin Y-C, Chiang J-M, et al. Apoptosis of tumor infiltrating effector TIM-3+CD8+ T cells in colon cancer. *Scientific reports*. 2015;5(1):15659.
258. Ju Y, Hou N, Meng J, Wang X, Zhang X, Zhao D, et al. T cell immunoglobulin- and mucin-domain-containing molecule-3 (Tim-3) mediates natural killer cell suppression in chronic hepatitis B. *Journal of hepatology*. 2010;52(3):322-9.
259. Jayaraman P, Sada-Ovalle I, Beladi S, Anderson AC, Dardalhon V, Hotta C, et al. Tim3 binding to galectin-9 stimulates antimicrobial immunity. *The Journal of experimental medicine*. 2010;207(11):2343-54.
260. Nagahara K, Arikawa T, Oomizu S, Kontani K, Nobumoto A, Tateno H, et al. Galectin-9 increases Tim-3+ dendritic cells and CD8+ T cells and enhances antitumor immunity via galectin-9-Tim-3 interactions. *Journal of immunology (Baltimore, Md : 1950)*. 2008;181(11):7660-9.
261. Kanzaki M, Wada J, Sugiyama K, Nakatsuka A, Teshigawara S, Murakami K, et al. Galectin-9 and T cell immunoglobulin mucin-3 pathway is a therapeutic target for type 1 diabetes. *Endocrinology*. 2012;153(2):612-20.
262. Leitner J, Rieger A, Pickl WF, Zlabinger G, Grabmeier-Pfistershammer K, Steinberger P. TIM-3 does not act as a receptor for galectin-9. *PLoS pathogens*. 2013;9(3):e1003253.
263. Ferris RL, Lu B, Kane LP. Too much of a good thing? Tim-3 and TCR signaling in T cell exhaustion. *Journal of immunology (Baltimore, Md : 1950)*. 2014;193(4):1525-30.
264. Lee MJ, Yun SJ, Lee B, Jeong E, Yoon G, Kim K, et al. Association of TIM-3 expression with glucose metabolism in Jurkat T cells. *BMC Immunol*. 2020;21(1):48.

265. Yang RY, Rabinovich GA, Liu FT. Galectins: structure, function and therapeutic potential. *Expert reviews in molecular medicine*. 2008;10:e17.
266. Johannes L, Jacob R, Leffler H. Galectins at a glance. *Journal of Cell Science*. 2018;131(9):jcs208884.
267. Chou FC, Chen HY, Kuo CC, Sytwu HK. Role of Galectins in Tumors and in Clinical Immunotherapy. *International journal of molecular sciences*. 2018;19(2).
268. John S, Mishra R. Galectin-9: From cell biology to complex disease dynamics. *Journal of biosciences*. 2016;41(3):507-34.
269. Sato M, Nishi N, Shoji H, Seki M, Hashidate T, Hirabayashi J, et al. Functional analysis of the carbohydrate recognition domains and a linker peptide of galectin-9 as to eosinophil chemoattractant activity. *Glycobiology*. 2002;12(3):191-7.
270. Heusschen R, Griffioen AW, Thijssen VL. Galectin-9 in tumor biology: A jack of multiple trades. *Biochimica et Biophysica Acta (BBA) - Reviews on Cancer*. 2013;1836(1):177-85.
271. Lhuillier C, Barjon C, Niki T, Gelin A, Praz F, Morales O, et al. Impact of Exogenous Galectin-9 on Human T Cells: CONTRIBUTION OF THE T CELL RECEPTOR COMPLEX TO ANTIGEN-INDEPENDENT ACTIVATION BUT NOT TO APOPTOSIS INDUCTION. *The Journal of biological chemistry*. 2015;290(27):16797-811.
272. Chabot S, Kashio Y, Seki M, Shirato Y, Nakamura K, Nishi N, et al. Regulation of galectin-9 expression and release in Jurkat T cell line cells. *Glycobiology*. 2002;12(2):111-8.
273. Wu C, Thalhamer T, Franca RF, Xiao S, Wang C, Hotta C, et al. Galectin-9-CD44 interaction enhances stability and function of adaptive regulatory T cells. *Immunity*. 2014;41(2):270-82.
274. Cummings Richard D. T Cells Are Smad'ly in Love with Galectin-9. *Immunity*. 2014;41(2):171-3.
275. Lv K, Zhang Y, Zhang M, Zhong M, Suo Q. Galectin-9 promotes TGF- $\beta$ 1-dependent induction of regulatory T cells via the TGF- $\beta$ /Smad signaling pathway. *Mol Med Rep*. 2013;7(1):205-10.
276. Asakura H, Kashio Y, Nakamura K, Seki M, Dai S, Shirato Y, et al. Selective eosinophil adhesion to fibroblast via IFN-gamma-induced galectin-9. *Journal of immunology (Baltimore, Md : 1950)*. 2002;169(10):5912-8.
277. Imaizumi T, Kumagai M, Sasaki N, Kurotaki H, Mori F, Seki M, et al. Interferon-gamma stimulates the expression of galectin-9 in cultured human endothelial cells. *Journal of leukocyte biology*. 2002;72(3):486-91.
278. Steelman AJ, Smith R, 3rd, Welsh CJ, Li J. Galectin-9 protein is up-regulated in astrocytes by tumor necrosis factor and promotes encephalitogenic T-cell apoptosis. *The Journal of biological chemistry*. 2013;288(33):23776-87.
279. Pearson MJ, Bik MA, Ospelt C, Naylor AJ, Wehmeyer C, Jones SW, et al. Endogenous Galectin-9 Suppresses Apoptosis in Human Rheumatoid Arthritis Synovial Fibroblasts. *Scientific reports*. 2018;8(1):12887.
280. Wiersma VR, de Bruyn M, Helfrich W, Bremer E. Therapeutic potential of Galectin-9 in human disease. *Medicinal research reviews*. 2013;33 Suppl 1:E102-26.
281. Nebbia G, Peppas D, Schurich A, Khanna P, Singh H, Cheng Y, et al. Upregulation of the Tim-3/Galectin-9 Pathway of T Cell Exhaustion in Chronic Hepatitis B Virus Infection. *PloS one*. 2012;7:e47648.
282. Motamedi M, Shahbaz S, Fu L, Dunsmore G, Xu L, Harrington R, et al. Galectin-9 Expression Defines a Subpopulation of NK Cells with Impaired Cytotoxic Effector Molecules but Enhanced IFN- $\gamma$  Production, Dichotomous to TIGIT, in HIV-1 Infection. *ImmunoHorizons*. 2019;3(11):531-46.
283. Shahbaz S, Dunsmore G, Koleva P, Xu L, Houston S, Elahi S. Galectin-9 and VISTA Expression Define Terminally Exhausted T Cells in HIV-1 Infection. *Journal of immunology (Baltimore, Md : 1950)*. 2020;204(9):2474-91.
284. Okoye I, Xu L, Motamedi M, Parashar P, Walker JW, Elahi S. Galectin-9 expression defines exhausted T cells and impaired cytotoxic NK cells in patients with virus-associated solid tumors. *J Immunother Cancer*. 2020;8(2).

285. Burman J, Svenningsson A. Cerebrospinal fluid concentration of Galectin-9 is increased in secondary progressive multiple sclerosis. *Journal of neuroimmunology*. 2016;292:40-4.
286. Stancic M, van Horssen J, Thijssen VL, Gabius HJ, van der Valk P, Hoekstra D, et al. Increased expression of distinct galectins in multiple sclerosis lesions. *Neuropathology and applied neurobiology*. 2011;37(6):654-71.
287. Afshar B, Khalifehzadeh-Esfahani Z, Seyfizadeh N, Rezaei Danbaran G, Hemmatzadeh M, Mohammadi H. The role of immune regulatory molecules in multiple sclerosis. *Journal of neuroimmunology*. 2019;337:577061.
288. Niwa H, Satoh T, Matsushima Y, Hosoya K, Saeki K, Niki T, et al. Stable form of galectin-9, a Tim-3 ligand, inhibits contact hypersensitivity and psoriatic reactions: A potent therapeutic tool for Th1- and/or Th17-mediated skin inflammation. *Clinical Immunology*. 2009;132(2):184-94.
289. Seki M, Sakata KM, Oomizu S, Arikawa T, Sakata A, Ueno M, et al. Beneficial effect of galectin 9 on rheumatoid arthritis by induction of apoptosis of synovial fibroblasts. *Arthritis and rheumatism*. 2007;56(12):3968-76.
290. Wiersma VR, Clarke A, Pouwels SD, Perry E, Abdullah TM, Kelly C, et al. Galectin-9 Is a Possible Promoter of Immunopathology in Rheumatoid Arthritis by Activation of Peptidyl Arginine Deiminase 4 (PAD-4) in Granulocytes. *International journal of molecular sciences*. 2019;20(16).
291. Seki M, Oomizu S, Sakata KM, Sakata A, Arikawa T, Watanabe K, et al. Galectin-9 suppresses the generation of Th17, promotes the induction of regulatory T cells, and regulates experimental autoimmune arthritis. *Clinical immunology (Orlando, Fla)*. 2008;127(1):78-88.
292. Wang F, He W, Zhou H, Yuan J, Wu K, Xu L, et al. The Tim-3 ligand galectin-9 negatively regulates CD8+ alloreactive T cell and prolongs survival of skin graft. *Cellular immunology*. 2007;250(1-2):68-74.
293. Wang F, He W, Yuan J, Wu K, Zhou H, Zhang W, et al. Activation of Tim-3-Galectin-9 pathway improves survival of fully allogeneic skin grafts. *Transplant immunology*. 2008;19(1):12-9.
294. Miko E, Meggyes M, Bogar B, Schmitz N, Barakonyi A, Várnagy A, et al. Involvement of Galectin-9/TIM-3 Pathway in the Systemic Inflammatory Response in Early-Onset Preeclampsia. *PloS one*. 2013;8:e71811.
295. Meggyes M, Miko E, Polgar B, Bogar B, Farkas B, Illes Z, et al. Peripheral blood TIM-3 positive NK and CD8+ T cells throughout pregnancy: TIM-3/galectin-9 interaction and its possible role during pregnancy. *PloS one*. 2014;9(3):e92371.
296. Li YH, Zhou WH, Tao Y, Wang SC, Jiang YL, Zhang D, et al. The Galectin-9/Tim-3 pathway is involved in the regulation of NK cell function at the maternal-fetal interface in early pregnancy. *Cellular & molecular immunology*. 2016;13(1):73-81.
297. Rao SP, Ge XN, Sriramarao P. Regulation of Eosinophil Recruitment and Activation by Galectins in Allergic Asthma. *Frontiers in medicine*. 2017;4:68.
298. Katoh S, Ishii N, Nobumoto A, Takeshita K, Dai SY, Shinonaga R, et al. Galectin-9 inhibits CD44-hyaluronan interaction and suppresses a murine model of allergic asthma. *American journal of respiratory and critical care medicine*. 2007;176(1):27-35.
299. Kojima R, Ohno T, Iikura M, Niki T, Hirashima M, Iwaya K, et al. Galectin-9 enhances cytokine secretion, but suppresses survival and degranulation, in human mast cell line. *PloS one*. 2014;9(1):e86106.
300. Niki T, Tsutsui S, Hirose S, Aradono S, Sugimoto Y, Takeshita K, et al. Galectin-9 is a high affinity IgE-binding lectin with anti-allergic effect by blocking IgE-antigen complex formation. *The Journal of biological chemistry*. 2009;284(47):32344-52.
301. Kageshita T, Kashio Y, Yamauchi A, Seki M, Abedin MJ, Nishi N, et al. Possible role of galectin-9 in cell aggregation and apoptosis of human melanoma cell lines and its clinical significance. *International journal of cancer*. 2002;99(6):809-16.
302. Irie A, Yamauchi A, Kontani K, Kihara M, Liu D, Shirato Y, et al. Galectin-9 as a prognostic factor with antimetastatic potential in breast cancer. *Clinical cancer research : an official journal of the American Association for Cancer Research*. 2005;11(8):2962-8.

303. Zhang ZY, Dong JH, Chen YW, Wang XQ, Li CH, Wang J, et al. Galectin-9 acts as a prognostic factor with antimetastatic potential in hepatocellular carcinoma. *Asian Pacific journal of cancer prevention : APJCP*. 2012;13(6):2503-9.
304. Yasinska IM, Meyer NH, Schlichtner S, Hussain R, Siligardi G, Casely-Hayford M, et al. Ligand-Receptor Interactions of Galectin-9 and VISTA Suppress Human T Lymphocyte Cytotoxic Activity. *Frontiers in immunology*. 2020;11(3015).
305. Yasinska IM, Gonçalves Silva I, Sakhnevych S, Gibbs BF, Raap U, Fasler-Kan E, et al. Biochemical mechanisms implemented by human acute myeloid leukemia cells to suppress host immune surveillance. *Cellular & molecular immunology*. 2018;15(11):989-91.
306. Zhang C-x, Huang D-j, Baloche V, Zhang L, Xu J-x, Li B-w, et al. Galectin-9 promotes a suppressive microenvironment in human cancer by enhancing STING degradation. *Oncogenesis*. 2020;9(7):65.
307. Dardalhon V, Anderson AC, Karman J, Apetoh L, Chandwaskar R, Lee DH, et al. Tim-3/galectin-9 pathway: regulation of Th1 immunity through promotion of CD11b+Ly-6G+ myeloid cells. *Journal of immunology (Baltimore, Md : 1950)*. 2010;185(3):1383-92.
308. Dai SY, Nakagawa R, Itoh A, Murakami H, Kashio Y, Abe H, et al. Galectin-9 induces maturation of human monocyte-derived dendritic cells. *Journal of immunology (Baltimore, Md : 1950)*. 2005;175(5):2974-81.
309. Gooden MJ, Wiersma VR, Samplonius DF, Gerssen J, van Ginkel RJ, Nijman HW, et al. Galectin-9 activates and expands human T-helper 1 cells. *PloS one*. 2013;8(5):e65616.
310. Su EW, Bi S, Kane LP. Galectin-9 regulates T helper cell function independently of Tim-3. *Glycobiology*. 2011;21(10):1258-65.
311. Kashio Y, Nakamura K, Abedin MJ, Seki M, Nishi N, Yoshida N, et al. Galectin-9 induces apoptosis through the calcium-calpain-caspase-1 pathway. *Journal of immunology (Baltimore, Md : 1950)*. 2003;170(7):3631-6.
312. Oomizu S, Arikawa T, Niki T, Kadowaki T, Ueno M, Nishi N, et al. Galectin-9 suppresses Th17 cell development in an IL-2-dependent but Tim-3-independent manner. *Clinical immunology (Orlando, Fla)*. 2012;143(1):51-8.
313. Golden-Mason L, McMahan RH, Strong M, Reisdorph R, Mahaffey S, Palmer BE, et al. Galectin-9 functionally impairs natural killer cells in humans and mice. *Journal of virology*. 2013;87(9):4835-45.
314. Lu L-H, Nakagawa R, Kashio Y, Ito A, Shoji H, Nishi N, et al. Characterization of Galectin-9-Induced Death of Jurkat T Cells. *The Journal of Biochemistry*. 2006;141(2):157-72.
315. Clayton KL, Haaland MS, Douglas-Vail MB, Mujib S, Chew GM, Ndhlovu LC, et al. T cell Ig and mucin domain-containing protein 3 is recruited to the immune synapse, disrupts stable synapse formation, and associates with receptor phosphatases. *Journal of immunology (Baltimore, Md : 1950)*. 2014;192(2):782-91.
316. Vaitaitis G, Wagner D. Galectin-9 Controls CD40 Signaling through a Tim-3 Independent Mechanism and Redirects the Cytokine Profile of Pathogenic T Cells in Autoimmunity. *PloS one*. 2012;7:e38708.
317. Merani S, Chen W, Elahi S. The bitter side of sweet: the role of Galectin-9 in immunopathogenesis of viral infections. *Reviews in medical virology*. 2015;25(3):175-86.
318. Wang S, Sun F, Li M, Qian J, Chen C, Wang M, et al. The appropriate frequency and function of decidual Tim-3+CTLA-4+CD8+ T cells are important in maintaining normal pregnancy. *Cell Death & Disease*. 2019;10(6):407.
319. Kikushige Y, Miyamoto T. TIM-3 as a novel therapeutic target for eradicating acute myelogenous leukemia stem cells. *International journal of hematology*. 2013;98(6):627-33.
320. Gonçalves Silva I, Gibbs BF, Bardelli M, Varani L, Sumbayev VV. Differential expression and biochemical activity of the immune receptor Tim-3 in healthy and malignant human myeloid cells. *Oncotarget*. 2015;6(32):33823-33.

321. Kikushige Y, Miyamoto T, Yuda J, Jabbarzadeh-Tabrizi S, Shima T, Takayanagi S, et al. A TIM-3/Gal-9 Autocrine Stimulatory Loop Drives Self-Renewal of Human Myeloid Leukemia Stem Cells and Leukemic Progression. *Cell stem cell*. 2015;17(3):341-52.
322. Gonçalves Silva I, Rüegg L, Gibbs BF, Bardelli M, Fruehwirth A, Varani L, et al. The immune receptor Tim-3 acts as a trafficker in a Tim-3/galectin-9 autocrine loop in human myeloid leukemia cells. *Oncoimmunology*. 2016;5(7):e1195535.
323. Sumbayev VV, Gonçalves Silva I, Blackburn J, Gibbs BF, Yasinska IM, Garrett MD, et al. Expression of functional neuronal receptor latrophilin 1 in human acute myeloid leukaemia cells. *Oncotarget*. 2016;7(29):45575-83.
324. Sakhnevych SS, Yasinska IM, Bratt AM, Benlaouer O, Gonçalves Silva I, Hussain R, et al. Cortisol facilitates the immune escape of human acute myeloid leukemia cells by inducing latrophilin 1 expression. *Cellular & molecular immunology*. 2018;15(11):994-7.
325. Dama P, Tang M, Fulton N, Kline J, Liu H. Gal9/Tim-3 expression level is higher in AML patients who fail chemotherapy. *Journal for ImmunoTherapy of Cancer*. 2019;7.
326. Yasinska IM, Sakhnevych SS, Pavlova L, Teo Hansen Selnø A, Teuscher Abeleira AM, Benlaouer O, et al. The Tim-3-Galectin-9 Pathway and Its Regulatory Mechanisms in Human Breast Cancer. *Frontiers in immunology*. 2019;10:1594.
327. Gao X, Zhu Y, Li G, Huang H, Zhang G, Wang F, et al. TIM-3 expression characterizes regulatory T cells in tumor tissues and is associated with lung cancer progression. *PloS one*. 2012;7(2):e30676.
328. Li X, Wang R, Fan P, Yao X, Qin L, Peng Y, et al. A Comprehensive Analysis of Key Immune Checkpoint Receptors on Tumor-Infiltrating T Cells From Multiple Types of Cancer. *Frontiers in Oncology*. 2019;9(1066).
329. Kuai W, Xu X, Yan J, Zhao W, Li Y, Wang B, et al. Prognostic Impact of PD-1 and Tim-3 Expression in Tumor Tissue in Stage I-III Colorectal Cancer. *BioMed Research International*. 2020;2020:5294043.
330. Granier C, Dariane C, Combe P, Verkarre V, Urien S, Badoual C, et al. Tim-3 Expression on Tumor-Infiltrating PD-1<sup>+</sup>CD8<sup>+</sup> T Cells Correlates with Poor Clinical Outcome in Renal Cell Carcinoma. *Cancer Research*. 2017;77(5):1075.
331. Datar I, Sanmamed MF, Wang J, Henick BS, Choi J, Badri T, et al. Expression Analysis and Significance of PD-1, LAG-3, and TIM-3 in Human Non-Small Cell Lung Cancer Using Spatially Resolved and Multiparametric Single-Cell Analysis. *Clinical Cancer Research*. 2019;25(15):4663.
332. Yan J, Zhang Y, Zhang JP, Liang J, Li L, Zheng L. Tim-3 expression defines regulatory T cells in human tumors. *PloS one*. 2013;8(3):e58006.
333. Cao X, Cai SF, Fehniger TA, Song J, Collins LI, Piwnica-Worms DR, et al. Granzyme B and perforin are important for regulatory T cell-mediated suppression of tumor clearance. *Immunity*. 2007;27(4):635-46.
334. Arce-Sillas A, Álvarez-Luquín DD, Tamaya-Domínguez B, Gomez-Fuentes S, Trejo-García A, Melo-Salas M, et al. Regulatory T Cells: Molecular Actions on Effector Cells in Immune Regulation. *Journal of immunology research*. 2016;2016:1720827.
335. Rangachari M, Zhu C, Sakuishi K, Xiao S, Karman J, Chen A, et al. Bat3 promotes T cell responses and autoimmunity by repressing Tim-3-mediated cell death and exhaustion. *Nature medicine*. 2012;18(9):1394-400.
336. Kataoka S, Manandhar P, Workman CJ, Banerjee H, Szymczak-Workman AL, Kvorjak M, et al. The co-stimulatory activity of Tim-3 requires Akt and MAPK signaling and immune synapse recruitment. *bioRxiv*. 2019:2019.12.30.878520.
337. Lee J, Su EW, Zhu C, Hainline S, Phuah J, Moroco JA, et al. Phosphotyrosine-dependent coupling of Tim-3 to T-cell receptor signaling pathways. *Molecular and cellular biology*. 2011;31(19):3963-74.

338. van de Weyer PS, Muehlfeit M, Klose C, Bonventre JV, Walz G, Kuehn EW. A highly conserved tyrosine of Tim-3 is phosphorylated upon stimulation by its ligand galectin-9. *Biochem Biophys Res Commun.* 2006;351(2):571-6.
339. Yong ST, Wang XF. A novel, non-apoptotic role for Scythe/BAT3: a functional switch between the pro- and anti-proliferative roles of p21 during the cell cycle. *PloS one.* 2012;7(6):e38085.
340. Sebti S, Prébois C, Pérez-Gracia E, Bauvy C, Desmots F, Pirot N, et al. BAT3 modulates p300-dependent acetylation of p53 and autophagy-related protein 7 (ATG7) during autophagy. *Proceedings of the National Academy of Sciences of the United States of America.* 2014;111(11):4115-20.
341. Desmots F, Russell HR, Lee Y, Boyd K, McKinnon PJ. The reaper-binding protein scythe modulates apoptosis and proliferation during mammalian development. *Molecular and cellular biology.* 2005;25(23):10329-37.
342. Preta G, Fadeel B. AIF and Scythe (Bat3) Regulate Phosphatidylserine Exposure and Macrophage Clearance of Cells Undergoing Fas (APO-1)-Mediated Apoptosis. *PloS one.* 2012;7(10):e47328.
343. Phong BL, Avery L, Sumpter TL, Gorman JV, Watkins SC, Colgan JD, et al. Tim-3 enhances FcεRI-proximal signaling to modulate mast cell activation. *The Journal of experimental medicine.* 2015;212(13):2289-304.
344. Lee MJ, Woo M-Y, Chwae Y-J, Kwon M-H, Kim K, Park S. Down-regulation of interleukin-2 production by CD4+ T cells expressing TIM-3 through suppression of NFAT dephosphorylation and AP-1 transcription. *Immunobiology.* 2012;217(10):986-95.
345. Tomkowicz B, Walsh E, Cotty A, Verona R, Sabins N, Kaplan F, et al. TIM-3 Suppresses Anti-CD3/CD28-Induced TCR Activation and IL-2 Expression through the NFAT Signaling Pathway. *PloS one.* 2015;10(10):e0140694.
346. McNeill L, Salmond RJ, Cooper JC, Carret CK, Cassady-Cain RL, Roche-Molina M, et al. The differential regulation of Lck kinase phosphorylation sites by CD45 is critical for T cell receptor signaling responses. *Immunity.* 2007;27(3):425-37.
347. Ji J, Yin Y, Ju H, Xu X, Liu W, Fu Q, et al. Long non-coding RNA Lnc-Tim3 exacerbates CD8 T cell exhaustion via binding to Tim-3 and inducing nuclear translocation of Bat3 in HCC. *Cell Death Dis.* 2018;9(5):478.
348. Yang R, Hung MC. The role of T-cell immunoglobulin mucin-3 and its ligand galectin-9 in antitumor immunity and cancer immunotherapy. *Science China Life sciences.* 2017;60(10):1058-64.
349. Moar P, Tandon R. Galectin-9 as a biomarker of disease severity. *Cellular immunology.* 2021;361:104287.
350. Yasinska IM, Goncalves Silva I, Sakhnevych SS, Ruegg L, Hussain R, Siligardi G, et al. High mobility group box 1 (HMGB1) acts as an "alarmin" to promote acute myeloid leukaemia progression. *Oncoimmunology.* 2018;7(6):e1438109.
351. Haist M, Stege H, Grabbe S, Bros M. The Functional Crosstalk between Myeloid-Derived Suppressor Cells and Regulatory T Cells within the Immunosuppressive Tumor Microenvironment. *Cancers.* 2021;13(2).
352. Zhu C, Sakuishi K, Xiao S, Sun Z, Zaghoulani S, Gu G, et al. An IL-27/NFIL3 signalling axis drives Tim-3 and IL-10 expression and T-cell dysfunction. *Nature communications.* 2015;6:6072.
353. Mujib S, Jones RB, Lo C, Aidarus N, Clayton K, Sakhdari A, et al. Antigen-independent induction of Tim-3 expression on human T cells by the common  $\gamma$ -chain cytokines IL-2, IL-7, IL-15, and IL-21 is associated with proliferation and is dependent on the phosphoinositide 3-kinase pathway. *Journal of immunology (Baltimore, Md : 1950).* 2012;188(8):3745-56.
354. Anderson AC, Lord GM, Dardalhon V, Lee DH, Sabatos-Peyton CA, Glimcher LH, et al. T-bet, a Th1 transcription factor regulates the expression of Tim-3. *European journal of immunology.* 2010;40(3):859-66.
355. Yang L, Pang Y, Moses HL. TGF-beta and immune cells: an important regulatory axis in the tumor microenvironment and progression. *Trends in immunology.* 2010;31(6):220-7.

356. Moses HL, Roberts AB, Derynck R. The Discovery and Early Days of TGF- $\beta$ : A Historical Perspective. *Cold Spring Harbor perspectives in biology*. 2016;8(7).
357. Derynck R, Budi E. Specificity, versatility, and control of TGF- $\beta$  family signaling. *Science signaling*. 2019;12:eaav5183.
358. Bastien D. Gomperts IMK, Peter E.R. *Tatham Signal Transduction*. 2nd ed 2009.
359. Kubiczko Besse L, Sedlaříková L, Hajek R, Sevcikova S. TGF- $\beta$  – an excellent servant but a bad master. *Journal of Translational Medicine*. 2012;10.
360. Shi Y, Massagué J. Mechanisms of TGF-beta signaling from cell membrane to the nucleus. *Cell*. 2003;113(6):685-700.
361. Massagué J, Wotton D. Transcriptional control by the TGF-beta/Smad signaling system. *The EMBO journal*. 2000;19(8):1745-54.
362. He W, Dorn DC, Erdjument-Bromage H, Tempst P, Moore MA, Massagué J. Hematopoiesis controlled by distinct TIF1 $\gamma$  and Smad4 branches of the TGFbeta pathway. *Cell*. 2006;125(5):929-41.
363. Syed V. TGF- $\beta$  Signaling in Cancer. *Journal of cellular biochemistry*. 2016;117(6):1279-87.
364. Tirado-Rodriguez B, Ortega E, Segura-Medina P, Huerta-Yeppez S. TGF-  $\beta$ : an important mediator of allergic disease and a molecule with dual activity in cancer development. *Journal of immunology research*. 2014;2014:318481.
365. Ramesh S, Wildey GM, Howe PH. Transforming growth factor beta (TGFbeta)-induced apoptosis: the rise & fall of Bim. *Cell cycle (Georgetown, Tex)*. 2009;8(1):11-7.
366. Hao Y, Baker D, Ten Dijke P. TGF- $\beta$ -Mediated Epithelial-Mesenchymal Transition and Cancer Metastasis. *International journal of molecular sciences*. 2019;20(11).
367. Zarzynska JM. Two faces of TGF-beta1 in breast cancer. *Mediators of inflammation*. 2014;2014:141747.
368. Chen W, Frank ME, Jin W, Wahl SM. TGF-beta released by apoptotic T cells contributes to an immunosuppressive milieu. *Immunity*. 2001;14(6):715-25.
369. Ravichandran KS. Find-me and eat-me signals in apoptotic cell clearance: progress and conundrums. *The Journal of experimental medicine*. 2010;207(9):1807-17.
370. Green DR, Llambi F. Cell Death Signaling. *Cold Spring Harbor perspectives in biology*. 2015;7(12).
371. Green DR, Ferguson T, Zitvogel L, Kroemer G. Immunogenic and tolerogenic cell death. *Nature reviews Immunology*. 2009;9(5):353-63.
372. Galluzzi L, Buqué A, Kepp O, Zitvogel L, Kroemer G. Immunogenic cell death in cancer and infectious disease. *Nature reviews Immunology*. 2017;17(2):97-111.
373. Garg AD, Dudek AM, Agostinis P. Cancer immunogenicity, danger signals, and DAMPs: what, when, and how? *BioFactors (Oxford, England)*. 2013;39(4):355-67.
374. Kroemer G, Galluzzi L, Kepp O, Zitvogel L. Immunogenic cell death in cancer therapy. *Annual review of immunology*. 2013;31:51-72.
375. Barkal AA, Brewer RE, Markovic M, Kowarsky M, Barkal SA, Zaro BW, et al. CD24 signalling through macrophage Siglec-10 is a target for cancer immunotherapy. *Nature*. 2019;572(7769):392-6.
376. Zhou J, Wang G, Chen Y, Wang H, Hua Y, Cai Z. Immunogenic cell death in cancer therapy: Present and emerging inducers. *Journal of cellular and molecular medicine*. 2019;23(8):4854-65.
377. Obeid M, Tesniere A, Ghiringhelli F, Fimia GM, Apetoh L, Perfettini JL, et al. Calreticulin exposure dictates the immunogenicity of cancer cell death. *Nature medicine*. 2007;13(1):54-61.
378. Michaud M, Martins I, Sukkurwala AQ, Adjemian S, Ma Y, Pellegatti P, et al. Autophagy-dependent anticancer immune responses induced by chemotherapeutic agents in mice. *Science (New York, NY)*. 2011;334(6062):1573-7.
379. Ghiringhelli F, Apetoh L, Tesniere A, Aymeric L, Ma Y, Ortiz C, et al. Activation of the NLRP3 inflammasome in dendritic cells induces IL-1 $\beta$ -dependent adaptive immunity against tumors. *Nature medicine*. 2009;15(10):1170-8.



380. Ben-Sasson SZ, Hu-Li J, Quiel J, Cauchetaux S, Ratner M, Shapira I, et al. IL-1 acts directly on CD4 T cells to enhance their antigen-driven expansion and differentiation. *Proceedings of the National Academy of Sciences of the United States of America*. 2009;106(17):7119-24.
381. Ben-Sasson SZ, Hogg A, Hu-Li J, Wingfield P, Chen X, Crank M, et al. IL-1 enhances expansion, effector function, tissue localization, and memory response of antigen-specific CD8 T cells. *The Journal of experimental medicine*. 2013;210(3):491-502.
382. Ma Y, Aymeric L, Locher C, Mattarollo SR, Delahaye NF, Pereira P, et al. Contribution of IL-17-producing gamma delta T cells to the efficacy of anticancer chemotherapy. *The Journal of experimental medicine*. 2011;208(3):491-503.
383. Birge RB, Boeltz S, Kumar S, Carlson J, Wanderley J, Calianese D, et al. Phosphatidylserine is a global immunosuppressive signal in efferocytosis, infectious disease, and cancer. *Cell Death & Differentiation*. 2016;23(6):962-78.
384. Kwak MS, Kim HS, Lee B, Kim YH, Son M, Shin JS. Immunological Significance of HMGB1 Post-Translational Modification and Redox Biology. *Frontiers in immunology*. 2020;11:1189.
385. Sachet M, Liang YY, Oehler R. The immune response to secondary necrotic cells. *Apoptosis : an international journal on programmed cell death*. 2017;22(10):1189-204.
386. Yang D, Tewary P, de la Rosa G, Wei F, Oppenheim JJ. The alarmin functions of high-mobility group proteins. *Biochimica et biophysica acta*. 2010;1799(1-2):157-63.
387. Kang R, Zhang Q, Zeh HJ, 3rd, Lotze MT, Tang D. HMGB1 in cancer: good, bad, or both? *Clinical cancer research : an official journal of the American Association for Cancer Research*. 2013;19(15):4046-57.
388. Yuan S, Liu Z, Xu Z, Liu J, Zhang J. High mobility group box 1 (HMGB1): a pivotal regulator of hematopoietic malignancies. *Journal of Hematology & Oncology*. 2020;13(1):91.
389. Yang H, Hreggvidsdottir HS, Palmblad K, Wang H, Ochani M, Li J, et al. A critical cysteine is required for HMGB1 binding to Toll-like receptor 4 and activation of macrophage cytokine release. *Proceedings of the National Academy of Sciences of the United States of America*. 2010;107(26):11942-7.
390. Yang H, Lundbäck P, Ottosson L, Erlandsson-Harris H, Venereau E, Bianchi ME, et al. Redox modification of cysteine residues regulates the cytokine activity of high mobility group box-1 (HMGB1). *Molecular medicine (Cambridge, Mass)*. 2012;18(1):250-9.
391. Park JS, Svetkauskaite D, He Q, Kim JY, Strassheim D, Ishizaka A, et al. Involvement of toll-like receptors 2 and 4 in cellular activation by high mobility group box 1 protein. *The Journal of biological chemistry*. 2004;279(9):7370-7.
392. van Beijnum JR, Buurman WA, Griffioen AW. Convergence and amplification of toll-like receptor (TLR) and receptor for advanced glycation end products (RAGE) signaling pathways via high mobility group B1 (HMGB1). *Angiogenesis*. 2008;11(1):91-9.
393. Tang D, Kang R, Cheh CW, Livesey KM, Liang X, Schapiro NE, et al. HMGB1 release and redox regulates autophagy and apoptosis in cancer cells. *Oncogene*. 2010;29(38):5299-310.
394. Venereau E, Casalgrandi M, Schiraldi M, Antoine DJ, Cattaneo A, De Marchis F, et al. Mutually exclusive redox forms of HMGB1 promote cell recruitment or proinflammatory cytokine release. *The Journal of experimental medicine*. 2012;209(9):1519-28.
395. Ivanov S, Dragoi AM, Wang X, Dallacosta C, Louten J, Musco G, et al. A novel role for HMGB1 in TLR9-mediated inflammatory responses to CpG-DNA. *Blood*. 2007;110(6):1970-81.
396. Tian J, Avalos AM, Mao SY, Chen B, Senthil K, Wu H, et al. Toll-like receptor 9-dependent activation by DNA-containing immune complexes is mediated by HMGB1 and RAGE. *Nat Immunol*. 2007;8(5):487-96.
397. Yanai H, Ban T, Wang Z, Choi MK, Kawamura T, Negishi H, et al. HMGB proteins function as universal sentinels for nucleic-acid-mediated innate immune responses. *Nature*. 2009;462(7269):99-103.
398. Kang R, Zeh HJ, Lotze MT, Tang D. The Beclin 1 network regulates autophagy and apoptosis. *Cell death and differentiation*. 2011;18(4):571-80.

399. Tang D, Kang R, Livesey KM, Cheh CW, Farkas A, Loughran P, et al. Endogenous HMGB1 regulates autophagy. *The Journal of cell biology*. 2010;190(5):881-92.
400. Livesey KM, Kang R, Vernon P, Buchser W, Loughran P, Watkins SC, et al. p53/HMGB1 complexes regulate autophagy and apoptosis. *Cancer Res*. 2012;72(8):1996-2005.
401. Thorburn J, Horita H, Redzic J, Hansen K, Frankel AE, Thorburn A. Autophagy regulates selective HMGB1 release in tumor cells that are destined to die. *Cell death and differentiation*. 2009;16(1):175-83.
402. Apetoh L, Ghiringhelli F, Tesniere A, Obeid M, Ortiz C, Criollo A, et al. Toll-like receptor 4-dependent contribution of the immune system to anticancer chemotherapy and radiotherapy. *Nature medicine*. 2007;13(9):1050-9.
403. Messmer D, Yang H, Telusma G, Knoll F, Li J, Messmer B, et al. High mobility group box protein 1: an endogenous signal for dendritic cell maturation and Th1 polarization. *Journal of immunology (Baltimore, Md : 1950)*. 2004;173(1):307-13.
404. Tang D, Kang R, Zeh HJ, 3rd, Lotze MT. High-mobility group box 1 and cancer. *Biochimica et biophysica acta*. 2010;1799(1-2):131-40.
405. He S, Cheng J, Sun L, Wang Y, Wang C, Liu X, et al. HMGB1 released by irradiated tumor cells promotes living tumor cell proliferation via paracrine effect. *Cell Death Dis*. 2018;9(6):648.
406. Liu R, Chen Y, Liu G, Li C, Song Y, Cao Z, et al. PI3K/AKT pathway as a key link modulates the multidrug resistance of cancers. *Cell Death & Disease*. 2020;11(9):797.
407. He H, Wang X, Chen J, Sun L, Sun H, Xie K. High-Mobility Group Box 1 (HMGB1) Promotes Angiogenesis and Tumor Migration by Regulating Hypoxia-Inducible Factor 1 (HIF-1 $\alpha$ ) Expression via the Phosphatidylinositol 3-Kinase (PI3K)/AKT Signaling Pathway in Breast Cancer Cells. *Medical science monitor : international medical journal of experimental and clinical research*. 2019;25:2352-60.
408. Wu X, Wang W, Chen Y, Liu X, Wang J, Qin X, et al. High Mobility Group Box Protein 1 Serves as a Potential Prognostic Marker of Lung Cancer and Promotes Its Invasion and Metastasis by Matrix Metalloproteinase-2 in a Nuclear Factor- $\kappa$ B-Dependent Manner. *Biomed Res Int*. 2018;2018:3453706.
409. Xu T, Jiang L, Wang Z. The progression of HMGB1-induced autophagy in cancer biology. *OncoTargets and therapy*. 2019;12:365-77.
410. White E, DiPaola RS. The double-edged sword of autophagy modulation in cancer. *Clinical cancer research : an official journal of the American Association for Cancer Research*. 2009;15(17):5308-16.
411. Liu L, Yang M, Kang R, Wang Z, Zhao Y, Yu Y, et al. HMGB1-induced autophagy promotes chemotherapy resistance in leukemia cells. *Leukemia*. 2011;25(1):23-31.
412. Ozben T. Oxidative stress and apoptosis: impact on cancer therapy. *Journal of pharmaceutical sciences*. 2007;96(9):2181-96.
413. Kim SJ, Kim HS, Seo YR. Understanding of ROS-Inducing Strategy in Anticancer Therapy. *Oxidative medicine and cellular longevity*. 2019;2019:5381692.
414. Tang D, Kang R, Livesey KM, Zeh HJ, 3rd, Lotze MT. High mobility group box 1 (HMGB1) activates an autophagic response to oxidative stress. *Antioxidants & redox signaling*. 2011;15(8):2185-95.
415. Kang R, Tang D, Livesey KM, Schapiro NE, Lotze MT, Zeh HJ, 3rd. The Receptor for Advanced Glycation End-products (RAGE) protects pancreatic tumor cells against oxidative injury. *Antioxidants & redox signaling*. 2011;15(8):2175-84.
416. Kazama H, Ricci JE, Herndon JM, Hoppe G, Green DR, Ferguson TA. Induction of immunological tolerance by apoptotic cells requires caspase-dependent oxidation of high-mobility group box-1 protein. *Immunity*. 2008;29(1):21-32.
417. Fan J, Li Y, Levy RM, Fan JJ, Hackam DJ, Vodovotz Y, et al. Hemorrhagic shock induces NAD(P)H oxidase activation in neutrophils: role of HMGB1-TLR4 signaling. *Journal of immunology (Baltimore, Md : 1950)*. 2007;178(10):6573-80.
418. Davydov, II, Fidalgo S, Khaustova SA, Lelyanova VG, Grebenyuk ES, Ushkaryov YA, et al. Prediction of epitopes in closely related proteins using a new algorithm. *Bulletin of experimental biology and medicine*. 2009;148(6):869-73.

419. Selnø ATH, Schlichtner S, Yasinska IM, Sakhnevych SS, Fiedler W, Wellbrock J, et al. Transforming growth factor beta type 1 (TGF- $\beta$ ) and hypoxia-inducible factor 1 (HIF-1) transcription complex as master regulators of the immunosuppressive protein galectin-9 expression in human cancer and embryonic cells. *Aging*. 2020;12(23):23478-96.
420. Technologies S. Lymphoprep - Density gradient medium for the isolation of mononuclear cells [Available from: <https://www.stemcell.com/lymphoprep.html>].
421. Science GHCL. Ficoll-Paque™ PLUS [Available from: <https://www.cytivalifesciences.co.jp/catalog/pdf/11003135ac.pdf>].
422. Parker AL, Newman C, Briggs S, Seymour L, Sheridan PJ. Nonviral gene delivery: techniques and implications for molecular medicine. *Expert reviews in molecular medicine*. 2003;5(22):1-15.
423. Meisel JW, Gokel GW. A Simplified Direct Lipid Mixing Lipoplex Preparation: Comparison of Liposomal-, Dimethylsulfoxide-, and Ethanol-Based Methods. *Scientific reports*. 2016;6:27662.
424. Dana H, Chalbatani GM, Mahmoodzadeh H, Karimloo R, Rezaiean O, Moradzadeh A, et al. Molecular Mechanisms and Biological Functions of siRNA. *International journal of biomedical science : IJBS*. 2017;13(2):48-57.
425. Sumbayev VV. LPS-induced Toll-like receptor 4 signalling triggers cross-talk of apoptosis signal-regulating kinase 1 (ASK1) and HIF-1 $\alpha$  protein. *FEBS letters*. 2008;582(2):319-26.
426. Jinek M, Doudna JA. A three-dimensional view of the molecular machinery of RNA interference. *Nature*. 2009;457(7228):405-12.
427. Wilson RC, Doudna JA. Molecular mechanisms of RNA interference. *Annual review of biophysics*. 2013;42:217-39.
428. Bradford MM. A rapid and sensitive method for the quantitation of microgram quantities of protein utilizing the principle of protein-dye binding. *Analytical Biochemistry*. 1976;72(1):248-54.
429. Kruger NJ. The Bradford method for protein quantitation. *Methods in molecular biology (Clifton, NJ)*. 1994;32:9-15.
430. LABTECH B. Bradford assay performed on BMG LABTECH microplate readers - application note AN158 2007 [Available from: <https://www.bmglabtech.com/bradford-assay-performed-on-bmg-labtech-microplate-readers/>].
431. Bass JJ, Wilkinson DJ, Rankin D, Phillips BE, Szewczyk NJ, Smith K, et al. An overview of technical considerations for Western blotting applications to physiological research. *Scandinavian journal of medicine & science in sports*. 2017;27(1):4-25.
432. MacPhee DJ. Methodological considerations for improving Western blot analysis. *Journal of pharmacological and toxicological methods*. 2010;61(2):171-7.
433. Alberts AJ, J. Lewis, M. Raff, K. Roberts, and P. Walter. *Molecular Biology of the Cell*. 5th ed: Garland science; 2008.
434. Li-Cor. See multiple target on the same western blot on Odessey Clx 2020 [Available from: <https://www.licor.com/bio/odyssey-clx/>].
435. Li-Cor. In-Cell Western Assay 2020 [Available from: <https://www.licor.com/bio/applications/in-cell-western-assay>].
436. Li-Cor. On-Cell Western Assay 2020 [Available from: <https://www.licor.com/bio/applications/on-cell-western-assay>].
437. Kurashina Y, Imashiro C, Hirano M, Kuribara T, Totani K, Ohnuma K, et al. Enzyme-free release of adhered cells from standard culture dishes using intermittent ultrasonic traveling waves. *Communications biology*. 2019;2:393.
438. Bovaird JH, Ngo TT, Lenhoff HM. Optimizing the o-phenylenediamine assay for horseradish peroxidase: effects of phosphate and pH, substrate and enzyme concentrations, and stopping reagents. *Clinical chemistry*. 1982;28(12):2423-6.
439. Fornera S, Walde P. Spectrophotometric quantification of horseradish peroxidase with o-phenylenediamine. *Anal Biochem*. 2010;407(2):293-5.

440. Brown KC, Corbett JF, Loveless NP. Spectrophotometric studies on the protonation of hydroxy and aminophenazines in aqueous solution. *Spectrochimica Acta Part A: Molecular Spectroscopy*. 1979;35(5):421-3.
441. Hinterberger V, Wang W, Damm C, Wawra S, Thoma M, Peukert W. Microwave-assisted one-step synthesis of white light-emitting carbon dot suspensions. *Optical Materials*. 2018;80:110-9.
442. R&D-Systems. Product information on Human TGF- $\beta$ 1 ELISA kit cat #DY240 [Available from: [https://www.rndsystems.com/products/human-tgf-beta-1-duoset-elisa\\_dy240](https://www.rndsystems.com/products/human-tgf-beta-1-duoset-elisa_dy240)].
443. Renard P, Ernest I, Houbion A, Art M, Le Calvez H, Raes M, et al. Development of a sensitive multi-well colorimetric assay for active NF $\kappa$ B. *Nucleic acids research*. 2001;29(4):E21.
444. Rosenau C, Emery D, Kaboord B, Qoronfleh MW. Development of a high-throughput plate-based chemiluminescent transcription factor assay. *Journal of biomolecular screening*. 2004;9(4):334-42.
445. Brand LH, Kirchler T, Hummel S, Chaban C, Wanke D. DPI-ELISA: a fast and versatile method to specify the binding of plant transcription factors to DNA in vitro. *Plant methods*. 2010;6:25.
446. Jan R, Chaudhry GE. Understanding Apoptosis and Apoptotic Pathways Targeted Cancer Therapeutics. *Advanced pharmaceutical bulletin*. 2019;9(2):205-18.
447. Hiebert PR, Granville DJ. Granzyme B in injury, inflammation, and repair. *Trends in molecular medicine*. 2012;18(12):732-41.
448. Cullen SP, Brunet M, Martin SJ. Granzymes in cancer and immunity. *Cell death and differentiation*. 2010;17(4):616-23.
449. Boivin WA, Cooper DM, Hiebert PR, Granville DJ. Intracellular versus extracellular granzyme B in immunity and disease: challenging the dogma. *Laboratory investigation; a journal of technical methods and pathology*. 2009;89(11):1195-220.
450. Sigma-Aldrich. Granzyme B Activity Assay Kit 2014 [Available from: <https://www.sigmaaldrich.com/content/dam/sigma-aldrich/docs/Sigma/Bulletin/2/mak176bul.pdf>].
451. Sigma. Caspase 3 Assay Kit, Colorimetric [Available from: <https://www.sigmaaldrich.com/content/dam/sigma-aldrich/docs/Sigma/Bulletin/casp3cbul.pdf>].
452. Battelli MG, Polito L, Bortolotti M, Bolognesi A. Xanthine Oxidoreductase-Derived Reactive Species: Physiological and Pathological Effects. *Oxidative medicine and cellular longevity*. 2016;2016:3527579.
453. Belambri SA, Rolas L, Raad H, Hurtado-Nedelec M, Dang PM, El-Benna J. NADPH oxidase activation in neutrophils: Role of the phosphorylation of its subunits. *European journal of clinical investigation*. 2018;48 Suppl 2:e12951.
454. Javvaji PK, Dhali A, Francis JR, Kolte AP, Mech A, Roy SC, et al. An Efficient Nitroblue Tetrazolium Staining and Bright-Field Microscopy Based Method for Detecting and Quantifying Intracellular Reactive Oxygen Species in Oocytes, Cumulus Cells and Embryos. *Frontiers in cell and developmental biology*. 2020;8:764.
455. Yusra H Al-Araji JKS, and Ahmed A Ahmed. CHEMISTRY OF FORMAZAN. *INTERNATIONAL JOURNAL OF RESEARCH IN PHARMACY AND CHEMISTRY*. 2015.
456. Katerji M, Filippova M, Duerksen-Hughes P. Approaches and Methods to Measure Oxidative Stress in Clinical Samples: Research Applications in the Cancer Field. *Oxidative medicine and cellular longevity*. 2019;2019:1279250.
457. Aguilar Diaz De Leon J, Borges CR. Evaluation of Oxidative Stress in Biological Samples Using the Thiobarbituric Acid Reactive Substances Assay. *Journal of visualized experiments : JoVE*. 2020(159).
458. Silva JP, Ushkaryov YA. The latrophilins, "split-personality" receptors. *Advances in experimental medicine and biology*. 2010;706:59-75.
459. White GR, Varley JM, Heighway J. Isolation and characterization of a human homologue of the latrophilin gene from a region of 1p31.1 implicated in breast cancer. *Oncogene*. 1998;17(26):3513-9.
460. Saleh R, Toor SM, Khalaf S, Elkord E. Breast Cancer Cells and PD-1/PD-L1 Blockade Upregulate the Expression of PD-1, CTLA-4, TIM-3 and LAG-3 Immune Checkpoints in CD4(+) T Cells. *Vaccines*. 2019;7(4).

461. Yun SJ, Lee B, Komori K, Lee MJ, Lee BG, Kim K, et al. Regulation of TIM-3 expression in a human T cell line by tumor-conditioned media and cyclic AMP-dependent signaling. *Molecular immunology*. 2019;105:224-32.
462. Wang Y, Zhao E, Zhang Z, Zhao G, Cao H. Association between Tim-3 and Gal-9 expression and gastric cancer prognosis. *Oncology reports*. 2018;40(4):2115-26.
463. O'Sullivan ML, de Wit J, Savas JN, Comoletti D, Otto-Hitt S, Yates JR, 3rd, et al. FLRT proteins are endogenous latrophilin ligands and regulate excitatory synapse development. *Neuron*. 2012;73(5):903-10.
464. Lu YC, Nazarko OV, Sando R, 3rd, Salzman GS, Li NS, Südhof TC, et al. Structural Basis of Latrophilin-FLRT-UNC5 Interaction in Cell Adhesion. *Structure (London, England : 1993)*. 2015;23(9):1678-91.
465. Halama N, Braun M, Kahlert C, Spille A, Quack C, Rahbari N, et al. Natural killer cells are scarce in colorectal carcinoma tissue despite high levels of chemokines and cytokines. *Clinical cancer research : an official journal of the American Association for Cancer Research*. 2011;17(4):678-89.
466. Habif G, Crinier A, André P, Vivier E, Narni-Mancinelli E. Targeting natural killer cells in solid tumors. *Cellular & molecular immunology*. 2019;16(5):415-22.
467. Sephton SE, Sapolsky RM, Kraemer HC, Spiegel D. Diurnal cortisol rhythm as a predictor of breast cancer survival. *Journal of the National Cancer Institute*. 2000;92(12):994-1000.
468. Cerignoli F, Abassi YA, Lamarche BJ, Guenther G, Santa Ana D, Guimet D, et al. In vitro immunotherapy potency assays using real-time cell analysis. *PLoS one*. 2018;13(3):e0193498.
469. Balamurugan K. HIF-1 at the crossroads of hypoxia, inflammation, and cancer. *International journal of cancer*. 2016;138(5):1058-66.
470. Tam SY, Wu VWC, Law HKW. Hypoxia-Induced Epithelial-Mesenchymal Transition in Cancers: HIF-1 $\alpha$  and Beyond. *Front Oncol*. 2020;10:486.
471. Weinberg F, Chandel NS. Reactive oxygen species-dependent signaling regulates cancer. *Cellular and molecular life sciences : CMLS*. 2009;66(23):3663-73.
472. Griguer CE, Oliva CR, Kelley EE, Giles GI, Lancaster JR, Jr., Gillespie GY. Xanthine oxidase-dependent regulation of hypoxia-inducible factor in cancer cells. *Cancer Res*. 2006;66(4):2257-63.
473. Abooli M, Lall GS, Coughlan K, Lall HS, Gibbs BF, Sumbayev VV. Crucial involvement of xanthine oxidase in the intracellular signalling networks associated with human myeloid cell function. *Scientific reports*. 2014;4(1):6307.
474. Perillo B, Di Donato M, Pezone A, Di Zazzo E, Giovannelli P, Galasso G, et al. ROS in cancer therapy: the bright side of the moon. *Experimental & Molecular Medicine*. 2020;52(2):192-203.
475. Piszczatowska K, Przybylska D, Sikora E, Mosieniak G. Inhibition of NADPH Oxidases Activity by Diphenyliodonium Chloride as a Mechanism of Senescence Induction in Human Cancer Cells. *Antioxidants (Basel, Switzerland)*. 2020;9(12).
476. Brown NS, Bicknell R. Hypoxia and oxidative stress in breast cancer. *Oxidative stress: its effects on the growth, metastatic potential and response to therapy of breast cancer*. *Breast cancer research : BCR*. 2001;3(5):323-7.
477. Finkel T. Redox-dependent signal transduction. *FEBS letters*. 2000;476(1-2):52-4.
478. Oblak A, Jerala R. Toll-like receptor 4 activation in cancer progression and therapy. *Clinical & developmental immunology*. 2011;2011:609579.
479. Sumbayev VV, Nicholas SA. Hypoxia-inducible factor 1 as one of the "signaling drivers" of Toll-like receptor-dependent and allergic inflammation. *Archivum immunologiae et therapiae experimentalis*. 2010;58(4):287-94.
480. Hielscher A, Gerecht S. Hypoxia and free radicals: role in tumor progression and the use of engineering-based platforms to address these relationships. *Free Radic Biol Med*. 2015;79:281-91.
481. Sumbayev VV, Yasinska IM. Regulation of MAP kinase-dependent apoptotic pathway: implication of reactive oxygen and nitrogen species. *Archives of biochemistry and biophysics*. 2005;436(2):406-12.

482. Matsuzawa A, Saegusa K, Noguchi T, Sadamitsu C, Nishitoh H, Nagai S, et al. ROS-dependent activation of the TRAF6-ASK1-p38 pathway is selectively required for TLR4-mediated innate immunity. *Nature Immunology*. 2005;6(6):587-92.
483. Nicholas SA, Sumbayev VV. The role of redox-dependent mechanisms in the downregulation of ligand-induced Toll-like receptors 7, 8 and 4-mediated HIF-1 alpha prolyl hydroxylation. *Immunology and cell biology*. 2010;88(2):180-6.
484. Movafagh S, Crook S, Vo K. Regulation of hypoxia-inducible factor-1a by reactive oxygen species: new developments in an old debate. *Journal of cellular biochemistry*. 2015;116(5):696-703.
485. Muñoz-Sánchez J, Chánez-Cárdenas ME. The use of cobalt chloride as a chemical hypoxia model. *Journal of applied toxicology : JAT*. 2019;39(4):556-70.
486. Peng J, Wang X, Ran L, Song J, Luo R, Wang Y. Hypoxia-Inducible Factor 1 $\alpha$  Regulates the Transforming Growth Factor  $\beta$ 1/SMAD Family Member 3 Pathway to Promote Breast Cancer Progression. *Journal of breast cancer*. 2018;21(3):259-66.
487. Hoffmann C, Mao X, Brown-Clay J, Moreau F, Al Absi A, Wurzer H, et al. Hypoxia promotes breast cancer cell invasion through HIF-1 $\alpha$ -mediated up-regulation of the invadopodial actin bundling protein CSRP2. *Scientific reports*. 2018;8(1):10191.
488. Padua D, Zhang XH, Wang Q, Nadal C, Gerald WL, Gomis RR, et al. TGFbeta primes breast tumors for lung metastasis seeding through angiopoietin-like 4. *Cell*. 2008;133(1):66-77.
489. Neel J-C, Humbert L, Lebrun J-J. The Dual Role of TGF $\beta$  in Human Cancer: From Tumor Suppression to Cancer Metastasis. *ISRN Molecular Biology*. 2012;2012:381428.
490. Pardali K, Moustakas A. Actions of TGF-beta as tumor suppressor and pro-metastatic factor in human cancer. *Biochimica et biophysica acta*. 2007;1775(1):21-62.
491. Kong FM, Anscher MS, Murase T, Abbott BD, Iglehart JD, Jirtle RL. Elevated plasma transforming growth factor-beta 1 levels in breast cancer patients decrease after surgical removal of the tumor. *Annals of surgery*. 1995;222(2):155-62.
492. Ivanović V, Todorović-Raković N, Demajo M, Nesković-Konstantinović Z, Subota V, Ivanisević-Milovanović O, et al. Elevated plasma levels of transforming growth factor-beta 1 (TGF-beta 1) in patients with advanced breast cancer: association with disease progression. *European journal of cancer (Oxford, England : 1990)*. 2003;39(4):454-61.
493. Wakefield LM, Letterio JJ, Chen T, Danielpour D, Allison RS, Pai LH, et al. Transforming growth factor-beta1 circulates in normal human plasma and is unchanged in advanced metastatic breast cancer. *Clinical cancer research : an official journal of the American Association for Cancer Research*. 1995;1(1):129-36.
494. Sminia P, Barten AD, van Waarde MA, Vujaskovic Z, van Tienhoven G. Plasma transforming growth factor beta levels in breast cancer patients. *Oncology reports*. 1998;5(2):485-8.
495. Zhou YH, Liao SJ, Li D, Luo J, Wei JJ, Yan B, et al. TLR4 ligand/H<sub>2</sub>O<sub>2</sub> enhances TGF- $\beta$ 1 signaling to induce metastatic potential of non-invasive breast cancer cells by activating non-Smad pathways. *PLoS one*. 2013;8(5):e65906.
496. Bourguignon LY, Singleton PA, Zhu H, Zhou B. Hyaluronan promotes signaling interaction between CD44 and the transforming growth factor beta receptor I in metastatic breast tumor cells. *The Journal of biological chemistry*. 2002;277(42):39703-12.
497. Barcellos-Hoff MH, Akhurst RJ. Transforming growth factor-beta in breast cancer: too much, too late. *Breast cancer research : BCR*. 2009;11(1):202.
498. Wrzesinski SH, Wan YY, Flavell RA. Transforming growth factor-beta and the immune response: implications for anticancer therapy. *Clinical cancer research : an official journal of the American Association for Cancer Research*. 2007;13(18 Pt 1):5262-70.
499. Li MO, Wan YY, Sanjabi S, Robertson AK, Flavell RA. Transforming growth factor-beta regulation of immune responses. *Annual review of immunology*. 2006;24:99-146.
500. Massagué J. TGF $\beta$  signalling in context. *Nature Reviews Molecular Cell Biology*. 2012;13(10):616-30.

501. Kim SJ, Angel P, Lafyatis R, Hattori K, Kim KY, Sporn MB, et al. Autoinduction of transforming growth factor beta 1 is mediated by the AP-1 complex. *Molecular and cellular biology*. 1990;10(4):1492-7.
502. Martin M, Vozenin MC, Gault N, Crechet F, Pfarr CM, Lefaix JL. Coactivation of AP-1 activity and TGF-beta1 gene expression in the stress response of normal skin cells to ionizing radiation. *Oncogene*. 1997;15(8):981-9.
503. Wong C, Rougier-Chapman EM, Frederick JP, Datto MB, Liberati NT, Li JM, et al. Smad3-Smad4 and AP-1 complexes synergize in transcriptional activation of the c-Jun promoter by transforming growth factor beta. *Molecular and cellular biology*. 1999;19(3):1821-30.
504. Shih SC, Claffey KP. Role of AP-1 and HIF-1 transcription factors in TGF-beta activation of VEGF expression. *Growth factors (Chur, Switzerland)*. 2001;19(1):19-34.
505. Kashiwagi I, Morita R, Schichita T, Komai K, Saeki K, Matsumoto M, et al. Smad2 and Smad3 Inversely Regulate TGF- $\beta$  Autoinduction in Clostridium butyricum-Activated Dendritic Cells. *Immunity*. 2015;43(1):65-79.
506. Zhang Y, Handley D, Kaplan T, Yu H, Bais AS, Richards T, et al. High throughput determination of TGF $\beta$ 1/SMAD3 targets in A549 lung epithelial cells. *PloS one*. 2011;6(5):e20319.
507. Duan D, Derynck R. Transforming growth factor- $\beta$  (TGF- $\beta$ )-induced up-regulation of TGF- $\beta$  receptors at the cell surface amplifies the TGF- $\beta$  response. *The Journal of biological chemistry*. 2019;294(21):8490-504.
508. Lopez-Bergami P, Lau E, Ronai Ze. Emerging roles of ATF2 and the dynamic AP1 network in cancer. *Nature Reviews Cancer*. 2010;10(1):65-76.
509. Chen C, Lü JM, Yao Q. Hyperuricemia-Related Diseases and Xanthine Oxidoreductase (XOR) Inhibitors: An Overview. *Medical science monitor : international medical journal of experimental and clinical research*. 2016;22:2501-12.
510. Battelli MG, Polito L, Bortolotti M, Bolognesi A. Xanthine oxidoreductase in cancer: more than a differentiation marker. *Cancer medicine*. 2016;5(3):546-57.
511. Strowitzki MJ, Cummins EP, Taylor CT. Protein Hydroxylation by Hypoxia-Inducible Factor (HIF) Hydroxylases: Unique or Ubiquitous? *Cells*. 2019;8(5).
512. Nishikimi M, Yagi K. Molecular basis for the deficiency in humans of gulonolactone oxidase, a key enzyme for ascorbic acid biosynthesis. *The American journal of clinical nutrition*. 1991;54(6 Suppl):1203s-8s.
513. Mingyuan X, Qianqian P, Shengquan X, Chenyi Y, Rui L, Yichen S, et al. Hypoxia-inducible factor-1 $\alpha$  activates transforming growth factor- $\beta$ 1/Smad signaling and increases collagen deposition in dermal fibroblasts. *Oncotarget*. 2018;9(3):3188-97.
514. Battaglia V, Compagnone A, Bandino A, Bragadin M, Rossi CA, Zanetti F, et al. Cobalt induces oxidative stress in isolated liver mitochondria responsible for permeability transition and intrinsic apoptosis in hepatocyte primary cultures. *The international journal of biochemistry & cell biology*. 2009;41(3):586-94.
515. Otten J, Schmitz L, Vettorazzi E, Schultze A, Marx AH, Simon R, et al. Expression of TGF- $\beta$  receptor ALK-5 has a negative impact on outcome of patients with acute myeloid leukemia. *Leukemia*. 2011;25(2):375-9.
516. Buschke S, Stark HJ, Cerezo A, Prätzel-Wunder S, Boehnke K, Kollar J, et al. A decisive function of transforming growth factor- $\beta$ /Smad signaling in tissue morphogenesis and differentiation of human HaCaT keratinocytes. *Molecular biology of the cell*. 2011;22(6):782-94.
517. Kretschmer A, Moepert K, Dames S, Sternberger M, Kaufmann J, Klippel A. Differential regulation of TGF- $\beta$  signaling through Smad2, Smad3 and Smad4. *Oncogene*. 2003;22(43):6748-63.
518. Brown KA, Aakre ME, Gorska AE, Price JO, Eltom SE, Pietenpol JA, et al. Induction by transforming growth factor-beta1 of epithelial to mesenchymal transition is a rare event in vitro. *Breast cancer research : BCR*. 2004;6(3):R215-31.
519. Hsu YA, Chang CY, Lan JL, Li JP, Lin HJ, Chen CS, et al. Amelioration of bleomycin-induced pulmonary fibrosis via TGF- $\beta$ -induced Smad and non-Smad signaling pathways in galectin-9-deficient mice and fibroblast cells. *J Biomed Sci*. 2020;27(1):24.

520. Nobumoto A, Nagahara K, Oomizu S, Katoh S, Nishi N, Takeshita K, et al. Galectin-9 suppresses tumor metastasis by blocking adhesion to endothelium and extracellular matrices. *Glycobiology*. 2008;18(9):735-44.
521. Heikkinen PT, Nummela M, Leivonen SK, Westermarck J, Hill CS, Kähäri VM, et al. Hypoxia-activated Smad3-specific dephosphorylation by PP2A. *The Journal of biological chemistry*. 2010;285(6):3740-9.
522. Yan X, Xiong X, Chen YG. Feedback regulation of TGF- $\beta$  signaling. *Acta biochimica et biophysica Sinica*. 2018;50(1):37-50.
523. Shen X, Hu PP, Liberati NT, Datto MB, Frederick JP, Wang XF. TGF-beta-induced phosphorylation of Smad3 regulates its interaction with coactivator p300/CREB-binding protein. *Molecular biology of the cell*. 1998;9(12):3309-19.
524. Verrecchia F, Vindevoghel L, Lechleider RJ, Uitto J, Roberts AB, Mauviel A. Smad3/AP-1 interactions control transcriptional responses to TGF-beta in a promoter-specific manner. *Oncogene*. 2001;20(26):3332-40.
525. Igawa K, Satoh T, Hirashima M, Yokozeki H. Regulatory mechanisms of galectin-9 and eotaxin-3 synthesis in epidermal keratinocytes: possible involvement of galectin-9 in dermal eosinophilia of Th1-polarized skin inflammation. *Allergy*. 2006;61(12):1385-91.
526. Huber R, Meier B, Otsuka A, Fenini G, Satoh T, Gehrke S, et al. Tumour hypoxia promotes melanoma growth and metastasis via High Mobility Group Box-1 and M2-like macrophages. *Scientific reports*. 2016;6:29914.
527. Song Y, Zou X, Zhang D, Liu S, Duan Z, Liu L. Self-enforcing HMGB1/NF- $\kappa$ B/HIF-1 $\alpha$  Feedback Loop Promotes Cisplatin Resistance in Hepatocellular Carcinoma Cells. *Journal of Cancer*. 2020;11(13):3893-902.
528. Brancolini C, Iuliano L. Proteotoxic Stress and Cell Death in Cancer Cells. *Cancers*. 2020;12(9).
529. Ricci MS, Zong WX. Chemotherapeutic approaches for targeting cell death pathways. *The oncologist*. 2006;11(4):342-57.
530. Baskar R, Dai J, Wenlong N, Yeo R, Yeoh KW. Biological response of cancer cells to radiation treatment. *Frontiers in molecular biosciences*. 2014;1:24.
531. Garg AD, Agostinis P. Cell death and immunity in cancer: From danger signals to mimicry of pathogen defense responses. *Immunological reviews*. 2017;280(1):126-48.
532. Wu T, Zhang W, Yang G, Li H, Chen Q, Song R, et al. HMGB1 overexpression as a prognostic factor for survival in cancer: a meta-analysis and systematic review. *Oncotarget*. 2016;7(31):50417-27.
533. Yang WS, Kim JJ, Lee MJ, Lee EK, Park SK. ADAM17-Mediated Ectodomain Shedding of Toll-Like Receptor 4 as a Negative Feedback Regulation in Lipopolysaccharide-Activated Aortic Endothelial Cells. *Cellular physiology and biochemistry : international journal of experimental cellular physiology, biochemistry, and pharmacology*. 2018;45(5):1851-62.
534. Yang WS, Kim JJ, Lee MJ, Lee EK, Park SK. Ectodomain Shedding of RAGE and TLR4 as a Negative Feedback Regulation in High-Mobility Group Box 1-Activated Aortic Endothelial Cells. *Cellular physiology and biochemistry : international journal of experimental cellular physiology, biochemistry, and pharmacology*. 2018;51(4):1632-44.
535. Halliwell B. Oxidative stress in cell culture: an under-appreciated problem? *FEBS letters*. 2003;540(1-3):3-6.
536. Society AC. Acute Myeloid Leukemia (AML) Subtypes and Prognostic Factors 2018 [Available from: <https://www.cancer.org/cancer/acute-myeloid-leukemia/detection-diagnosis-staging/how-classified.html>].
537. Ramzi M, Khalafi-Nezhad A, Iravani Saadi M, Jowkar Z. Association between TLR2 and TLR4 Expression and Response to Induction Therapy in Acute Myeloid Leukemia Patients. *International journal of hematology-oncology and stem cell research*. 2018;12(4):303-12.



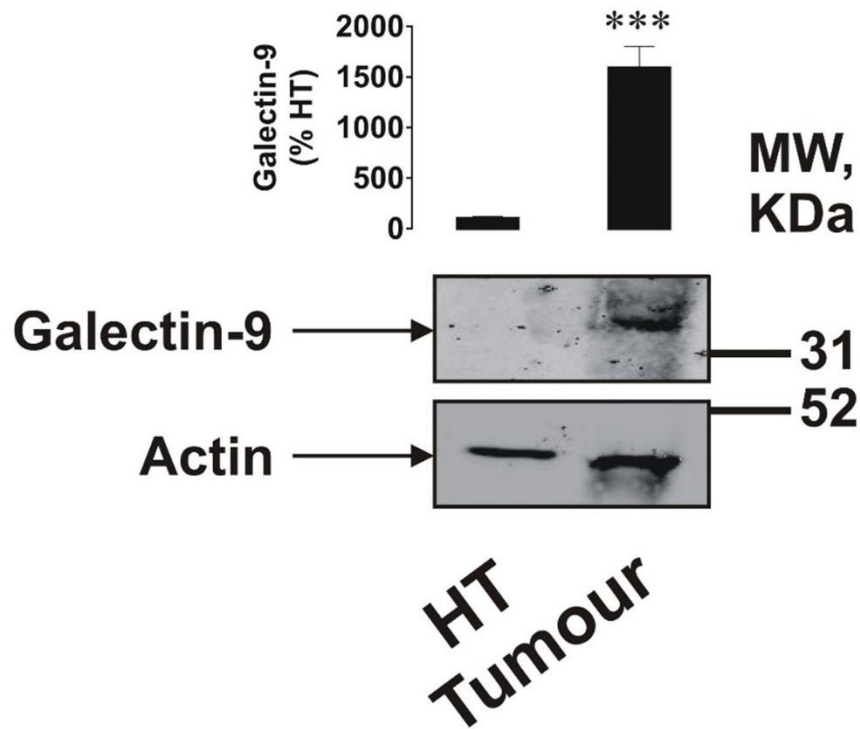
538. Rybka J, Butrym A, Wróbel T, Jaźwiec B, Stefanko E, Dobrzyńska O, et al. The expression of Toll-like receptors in patients with acute myeloid leukemia treated with induction chemotherapy. *Leukemia research*. 2015;39(3):318-22.
539. Bosshart H, Heinzelmann M. THP-1 cells as a model for human monocytes. *Annals of translational medicine*. 2016;4(21):438.
540. Stucki D, Brenneisen P, Reichert AS, Stahl W. The BH3 mimetic compound BH3I-1 impairs mitochondrial dynamics and promotes stress response in addition to its pro-apoptotic key function. *Toxicology letters*. 2018;295:369-78.
541. He W, Liu Q, Wang L, Chen W, Li N, Cao X. TLR4 signaling promotes immune escape of human lung cancer cells by inducing immunosuppressive cytokines and apoptosis resistance. *Molecular immunology*. 2007;44(11):2850-9.
542. Qi HM, Zhu TM, Wang J. [Regulation of immune suppressive cytokines by TLR4 activation in colon cancer cells]. *Zhonghua wei chang wai ke za zhi = Chinese journal of gastrointestinal surgery*. 2009;12(4):413-5.
543. Sun Z, Luo Q, Ye D, Chen W, Chen F. Role of toll-like receptor 4 on the immune escape of human oral squamous cell carcinoma and resistance of cisplatin-induced apoptosis. *Mol Cancer*. 2012;11:33.
544. Domenis R, Cifù A, Marinò D, Fabris M, Niazi KR, Soon-Shiong P, et al. Toll-like Receptor-4 Activation Boosts the Immunosuppressive Properties of Tumor Cells-derived Exosomes. *Scientific reports*. 2019;9(1):8457.
545. Wu K, Zhang H, Fu Y, Zhu Y, Kong L, Chen L, et al. TLR4/MyD88 signaling determines the metastatic potential of breast cancer cells. *Mol Med Rep*. 2018;18(3):3411-20.
546. Li Z, Block MS, Vierkant RA, Fogarty ZC, Winham SJ, Visscher DW, et al. The inflammatory microenvironment in epithelial ovarian cancer: a role for TLR4 and MyD88 and related proteins. *Tumour biology : the journal of the International Society for Oncodevelopmental Biology and Medicine*. 2016;37(10):13279-86.
547. Asehounne K, Strassheim D, Mitra S, Yeol Kim J, Abraham E. Involvement of PKC $\alpha$ /beta in TLR4 and TLR2 dependent activation of NF-kappaB. *Cellular signalling*. 2005;17(3):385-94.
548. Hao B, Chen Z, Bi B, Yu M, Yao S, Feng Y, et al. Role of TLR4 as a prognostic factor for survival in various cancers: a meta-analysis. *Oncotarget*. 2018;9(16):13088-99.
549. El-Zayat SR, Sibaii H, Mannaa FA. Toll-like receptors activation, signaling, and targeting: an overview. *Bulletin of the National Research Centre*. 2019;43(1):187.
550. Baakhlagh S, Kashani B, Zandi Z, Bashash D, Moradkhani M, Nasrollahzadeh A, et al. Toll-like receptor 4 signaling pathway is correlated with pathophysiological characteristics of AML patients and its inhibition using TAK-242 suppresses AML cell proliferation. *International immunopharmacology*. 2020;90:107202.
551. Suzuki M, Hisamatsu T, Podolsky DK. Gamma interferon augments the intracellular pathway for lipopolysaccharide (LPS) recognition in human intestinal epithelial cells through coordinated up-regulation of LPS uptake and expression of the intracellular Toll-like receptor 4-MD-2 complex. *Infection and immunity*. 2003;71(6):3503-11.
552. Li J, Yin J, Shen W, Gao R, Liu Y, Chen Y, et al. TLR4 Promotes Breast Cancer Metastasis via Akt/GSK3 $\beta$ / $\beta$ -Catenin Pathway upon LPS Stimulation. *Anatomical record (Hoboken, NJ : 2007)*. 2017;300(7):1219-29.
553. Klicznik MM, Szenes-Nagy AB, Campbell DJ, Gratz IK. Taking the lead - how keratinocytes orchestrate skin T cell immunity. *Immunol Lett*. 2018;200:43-51.
554. Jiang Y, Tsoi LC, Billi AC, Ward NL, Harms PW, Zeng C, et al. Cytokines: the diverse contribution of keratinocytes to immune responses in skin. *JCI insight*. 2020;5(20).
555. Kawai K, Shimura H, Minagawa M, Ito A, Tomiyama K, Ito M. Expression of functional Toll-like receptor 2 on human epidermal keratinocytes. *Journal of dermatological science*. 2002;30(3):185-94.

556. Pivarcsi A, Bodai L, Réthi B, Kenderessy-Szabó A, Koreck A, Széll M, et al. Expression and function of Toll-like receptors 2 and 4 in human keratinocytes. *International immunology*. 2003;15(6):721-30.
557. Baker BS, Ovigne JM, Powles AV, Corcoran S, Fry L. Normal keratinocytes express Toll-like receptors (TLRs) 1, 2 and 5: modulation of TLR expression in chronic plaque psoriasis. *The British journal of dermatology*. 2003;148(4):670-9.
558. Köllisch G, Kalali BN, Voelcker V, Wallich R, Behrendt H, Ring J, et al. Various members of the Toll-like receptor family contribute to the innate immune response of human epidermal keratinocytes. *Immunology*. 2005;114(4):531-41.
559. Lebre MC, van der Aar AM, van Baarsen L, van Capel TM, Schuitemaker JH, Kapsenberg ML, et al. Human keratinocytes express functional Toll-like receptor 3, 4, 5, and 9. *The Journal of investigative dermatology*. 2007;127(2):331-41.
560. Pivarcsi A, Koreck A, Bodai L, Széll M, Szeg C, Belso N, et al. Differentiation-regulated expression of Toll-like receptors 2 and 4 in HaCaT keratinocytes. *Archives of dermatological research*. 2004;296(3):120-4.
561. Parker KH, Sinha P, Horn LA, Clements VK, Yang H, Li J, et al. HMGB1 enhances immune suppression by facilitating the differentiation and suppressive activity of myeloid-derived suppressor cells. *Cancer Res*. 2014;74(20):5723-33.
562. Jin S, Yang Z, Hao X, Tang W, Ma W, Zong H. Roles of HMGB1 in regulating myeloid-derived suppressor cells in the tumor microenvironment. *Biomarker Research*. 2020;8(1):21.
563. Liu G, Wang J, Park YJ, Tsuruta Y, Lorne EF, Zhao X, et al. High mobility group protein-1 inhibits phagocytosis of apoptotic neutrophils through binding to phosphatidylserine. *Journal of immunology (Baltimore, Md : 1950)*. 2008;181(6):4240-6.
564. Huynh ML, Fadok VA, Henson PM. Phosphatidylserine-dependent ingestion of apoptotic cells promotes TGF-beta1 secretion and the resolution of inflammation. *The Journal of clinical investigation*. 2002;109(1):41-50.
565. Xiao YQ, Freire-de-Lima CG, Schiemann WP, Bratton DL, Vandivier RW, Henson PM. Transcriptional and Translational Regulation of TGF- $\beta$  Production in Response to Apoptotic Cells. *The Journal of Immunology*. 2008;181(5):3575-85.
566. Xiong W, Frasch SC, Thomas SM, Bratton DL, Henson PM. Induction of TGF- $\beta$ 1 synthesis by macrophages in response to apoptotic cells requires activation of the scavenger receptor CD36. *PLoS one*. 2013;8(8):e72772.
567. Seldeen KL, McDonald CB, Deegan BJ, Farooq A. Single nucleotide variants of the TGACTCA motif modulate energetics and orientation of binding of the Jun-Fos heterodimeric transcription factor. *Biochemistry*. 2009;48(9):1975-83.
568. Kim SJ, Glick A, Sporn MB, Roberts AB. Characterization of the promoter region of the human transforming growth factor-beta 1 gene. *The Journal of biological chemistry*. 1989;264(1):402-8.
569. Xia X, Kung AL. Preferential binding of HIF-1 to transcriptionally active loci determines cell-type specific response to hypoxia. *Genome biology*. 2009;10(10):R113.
570. Schödel J, Oikonomopoulos S, Ragoussis J, Pugh CW, Ratcliffe PJ, Mole DR. High-resolution genome-wide mapping of HIF-binding sites by ChIP-seq. *Blood*. 2011;117(23):e207-17.
571. Zavel L, Dai JL, Buckhaults P, Zhou S, Kinzler KW, Vogelstein B, et al. Human Smad3 and Smad4 are sequence-specific transcription activators. *Molecular cell*. 1998;1(4):611-7.
572. Itoh Y, Koinuma D, Omata C, Ogami T, Motizuki M, Yaguchi SI, et al. A comparative analysis of Smad-responsive motifs identifies multiple regulatory inputs for TGF- $\beta$  transcriptional activation. *The Journal of biological chemistry*. 2019;294(42):15466-79.
573. Shi Y, Wang YF, Jayaraman L, Yang H, Massagué J, Pavletich NP. Crystal structure of a Smad MH1 domain bound to DNA: insights on DNA binding in TGF-beta signaling. *Cell*. 1998;94(5):585-94.

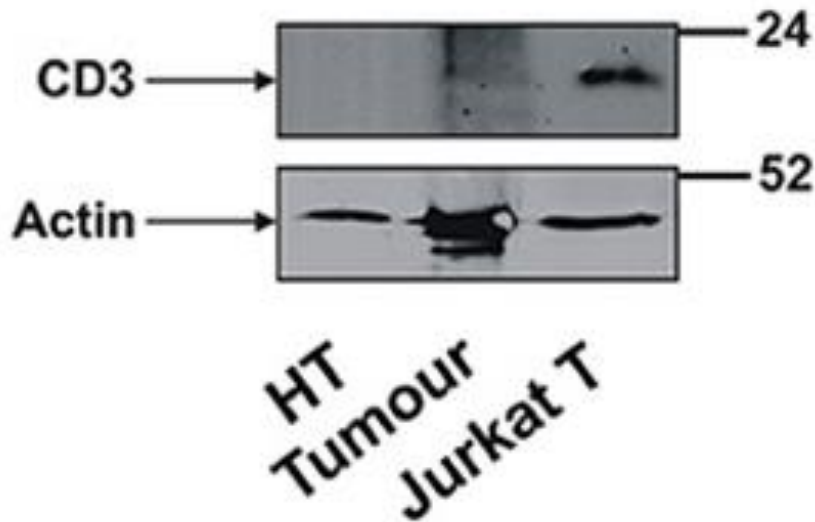
574. Martin-Malpartida P, Batet M, Kaczmarska Z, Freier R, Gomes T, Aragón E, et al. Structural basis for genome wide recognition of 5-bp GC motifs by SMAD transcription factors. *Nature communications*. 2017;8(1):2070.

## 7 APPENDIX

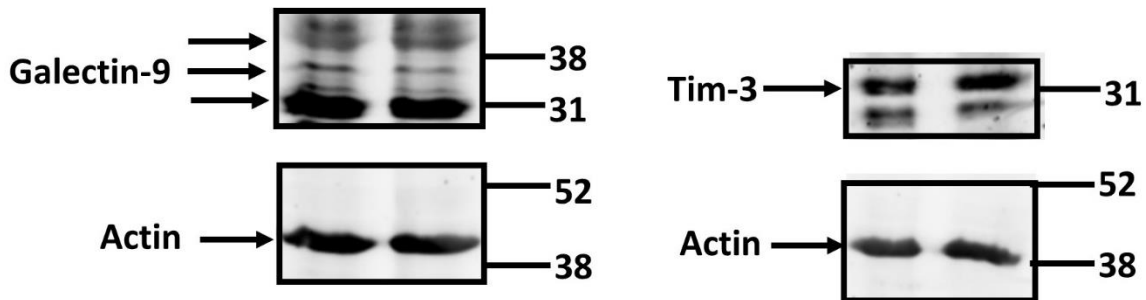
### 7.1 The FLRT3-LPHN and Galectin-9-TIM-3 Signalling Pathways – a Common Mechanism Among Different Types of Cancer to Mediate Immune Escape






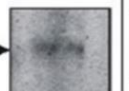
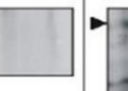




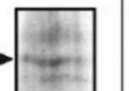



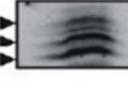
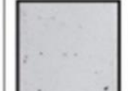
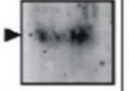




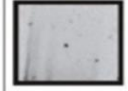

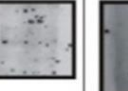


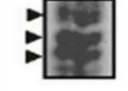



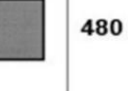

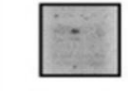
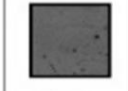



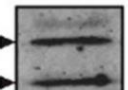
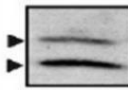
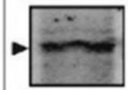

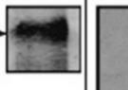
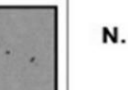

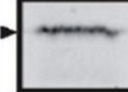




**Figure 77: Expression of galectin-9 in primary human breast tumours** (from (326)). Expression levels of galectin-9 were analysed in primary BT and HT of five patients ( $n=5$ ) by WB using 10 % PAGE. Images are from one experiment representative of five which gave similar results. Other results are shown as mean values  $\pm$  SEM. \*\*\*  $p<0.001$  vs HT (326).

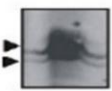
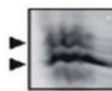

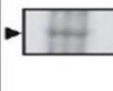

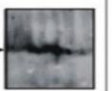
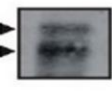
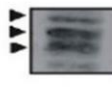



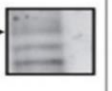
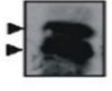
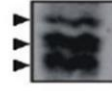



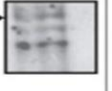

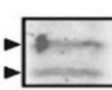

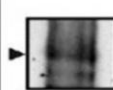
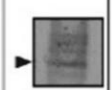


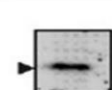


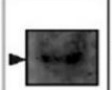

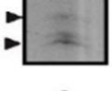

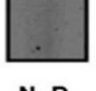
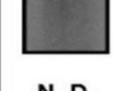

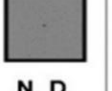
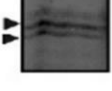
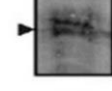

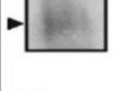





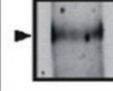

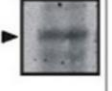


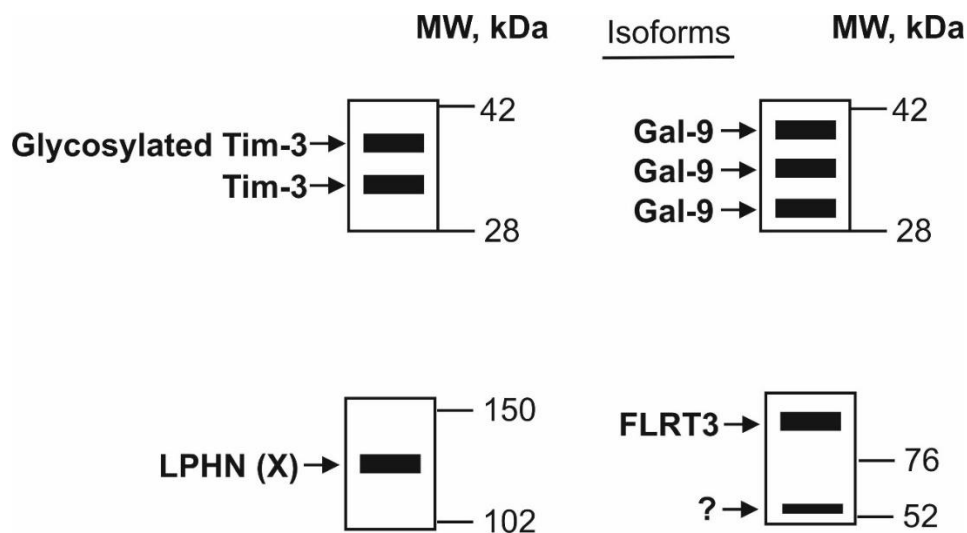
**Figure 78: CD3 is barely detectable in tumour tissue** (from (326)). The levels of CD3 (biomarker of T cells) were also measured using lysate of Jurkat T cells as a positive control. Molecular weight markers (MW) are expressed in kDa. Images are from one experiment representative of five which gave similar results. Other results are shown as mean values  $\pm$  SEM. \* $p < 0.05$ ; \*\* $p < 0.01$ , and \*\*\*when  $p < 0.001$  vs. control (326)



**Figure 79: Jurkat T cells express both Tim-3 and galectin-9 in resting conditions.** The expression of Tim-3 and galectin-9 were measured using lysate of Jurkat T cells in resting unstimulated condition. Molecular weight markers (MW) are expressed in kDa. Images are from one experiment.

TYPE OF CANCER	CELL LINE	Tim-3	Galectin-9	LPHN1	LPHN2	LPHN3	FLRT3	Galectin-9 secretion (pg/10 <sup>6</sup> cells)
BRAIN	LN401 Human glioblastoma	 +	 +	 N. D.	 +	 N. D.	 +	110 ± 24
COLORECTAL	Colo 205 Human colon adenocarcinoma type D	 +	 +	 N. D.	 +	 N. D.	 +	210 ± 36
KIDNEY	RCC-FG1 Clear cell carcinoma	 +	 +	 N. D.	 +	 N. D.	 +	<100
	RC-124 Established from non-tumour tissue of a 63-years-old man diagnosed with kidney carcinoma	 +	 +	 N. D.	 +	 N. D.	 N. D.	N. D.
Blood/bone marrow and mast cell cancer	THP-1 Acute myeloid leukaemia	 +	 +	 +	 +	 +	 N. D.	480 ± 58
	K562 Chronic myelogenous leukaemia	 +	 Traces	 N. D.	 N. D.	 N. D.	 N. D.	N. D.
	LAD2 Mast cell sarcoma	 +	 +	 +	 N. D.	 +	 N. D.	N. D.
	Primary human healthy mononuclear leukocytes	 +	 +	 N. D.	 N. D.	 N. D.	 N. D.	<100

TYPE OF CANCER	CELL LINE	Tim-3	Galectin-9	LPHN1	LPHN2	LPHN3	FLRT3	Galectin-9 secretion (pg/10 <sup>6</sup> cells)
LIVER	Hep G2 Human Hepatocellular carcinoma	 +	 +	 N. D.	 +	 Traces	 +	<100
BREAST	BC-8701 Human breast cancer	 +	 +	 N. D.	 N. D	 +	 +	N. D.
	MDA-MB-231 Human breast adenocarcinoma	 +	 +	 N. D.	 +	 N. D	 +	N. D.
PROSTATE	PC3 Prostate adenocarcinoma grade IV (cells derived from metastatic site – bone)	 +	 +	 N. D.	 +	 +	 +	N. D.
LUNG	Calu 6 Human pulmonary non-small cell carcinoma	 +	 +	 N. D.	 N.D.	 +	 +	N. D.
	BEAS-2B Human bronchial epithelium, normal	 +	 +	 N. D.	 N. D.	 N. D.	 N. D.	N. D.
SKIN	D10 Human malignant melanoma	 +	 +	 N. D.	 Traces	 N. D.	 Traces	N. D.
	HaCaT <i>In vitro</i> spontaneously transformed keratinocytes from histologically normal skin	 +	 Traces	 N. D.	 +	 N. D.	 +	N. D.



Scheme annotating WB images shown in the table.

This colour is used to indicate non-malignant human cells

**Table 2: Expression of Tim-3, galectin-9, LPHNs 1, 2 and 3 as well as FLRT3 proteins in variety of cancer cell lines detectable by WB analysis.** *Tim-3* (directly from (326): lower band represents non-glycosylated protein, upper band(s), protein with differential levels of glycosylation; **galectin-9**: multiple bands represent different isoforms of the same protein; **FLRT3** – detectable between 80 and 95 kDa (upper band where applicable or the only visible band); another band (lower band; possibly extracellular domain) often appears at around 60 most likely reflecting levels of glycosylation in the first two cases and proteolytic processing in the third. Traces – detectable expression which requires loading of >100 µg protein per well (326).



## 7.2 Human TGF- $\beta$ 1 Promoter Region and AP-1, HIF-1 and Smad3 Binding Sites

TGF- $\beta$ 1 is under transcriptional and translational regulation. Characterization of the human TGF- $\beta$ 1 promoter region have identified several possible regulators, among these are AP-1, HIF-1 and Smad3.

AP-1 complex binds to a palindromic DNA motif (5'-TGA G/C TCA-3') (502), although "it tolerates single nucleotide substitutions and binds to variants with affinities in the physiologically relevant micromolar-submicromolar range" (567). We identified two possible AP-1 binding sites using the sequences (TGTCTCA and TGACTCT) reported by Kim et al. (568).

HIF-1 complex binds the core sequence of 5'-A/G CGTG-3' (569, 570). We identified 2 possible HIF-1 binding sites

Studies analysing Smad3 recognition motif has identified 3 possible candidates, 1) the Smad binding elements (SBE) which forms the 8 bp palindromic sequence (5'-GTCTAGAC-3') (571), and 2) the CAGA motifs (5'-AGCCAGACA-3' or 5'-TGTCTGGCT-3') and/or CAGA-like motifs(572). However, "structural analysis indicated that the MH1 domains of Smad3 interact with the major groove of a 4-bp sequence within the motif through a protruding  $\beta$ -hairpin structure" (572, 573). This 4-bp sequence is also known as the Smad box (GTCT/AGAC), which is the minimal binding sequence for Smad3 MH1. Smad3 bind to this with the same affinity as SBE,  $K_d=1.18 \times 10^{-7}M$  (573). 3) The third motif is a 5-bp GC-rich motif (5'-GGC(GC)|(CG)-3') (574). Taken all these possibilities, we identified 14 possible Smad3 binding sites before the transcriptional start site.

[https://www.genecopoeia.com/product/search/view\\_seq\\_promoter.php?cid=&type=promoter&prod\\_id=HPRM30605](https://www.genecopoeia.com/product/search/view_seq_promoter.php?cid=&type=promoter&prod_id=HPRM30605)

>HPRM30605 NM\_000660:name=TGFB1;Entrez\_ID=7040;Genome=hg38;chr19:-:41355373-41353733;TSS=41353933;Upstream=1440,Downstream=200;Length=1641;

```
TGGGCTGCCCTGACATGGGGTCATGGAGGAGGATAACACAGAGAGGAAATTCAGCAGAGG
TCTGATTAGAAGGGCCTTGAATGTTGAAGAGGTTGGACTTTATACTGAGGGCACTGGGGA
GCTATGGAAGGATCCTTAGCAGGGGAGTAACATGGATTTGGAAAGATCACTTTGGCTGCT
GTGTGGGGATAGATAAGACGGTGGGAGCCTAGAAAGGAGGCTGGGTTGGAAACTCTGGGA
CAGAAACCCAGAGAGGAAAAGACTGGGCCTGGGCTCCAGTGAGTATCAGGGAGTGGGG
AATCAGCAGGAETCTGGTCCCCACCCATCCCTCCCTTCCCTCTCTCTCCTTTCCTGCAG
GCTGGCCCCGGCTCCATTTCCAGGTGTGGTCCCAGGACAGCTTTGGCCGCTGCCAGCTTG
CAGGCTATGGATTTTGCCATGTGCCAGTAGCCCGGCACCCACAGCTGGCCTGCCCCA
CGTGCGGGCCCCCTGGGCAGTTGGCGAGAACAGTTGGCACGGGCTTTCGTGGGTGGTGGGC
CGCAGCTGCTGCATGGGGACACCATCTACAGTGGGGCCGCTATCGCCTGCACACAG
CTGCTGGTGGCACCCTGCACCTGGAGATCGGCCTGCTGCTCCGCAACTTCGACCCGCTACG
CGTGAGTGCTGAGGGACTCTGCCTCCAACGTCACCACCATCCACACCCCGGACACCCA
GTGATGGGGGAGGATGGCACAGTGGTCAAGAGCACAGACTCTAGAGACTGTTCAGAGCTGA
CCCCAGCTAAGGCATGGCACCGCTTCTGTCCCTTTCTAGGACCTCGGGGTCCCTCTGGGCC
CAGTTTCCCTATCTGTAAATTTGGGGACAGTAAATGTATGGGGTGCAGGGTGTGAGTGA
CAGGAGGCTGCTTAGCCACATGGGAGGTGCTCAGTAAAGGAGAGCAATTCTTACAGGTGT
CTGCCTCCTGACCTTCCATCCTTCAGGTGTCTGTGCCCCCTCCTCCCCTGACACCC
TCCGGAGGCCCCCATGTTGACAGACTCTCTCTCCTACCTTGTTTCCCAGCTTGACTCTC
CTTCCGTTCTGGGTCCCCCTCCTCTGGTCCGGTCCCTGTCTCATCCCCCGGATTAAG
CCTTCTCCGCTGGTCTCTTTCTCTGGTGACCCACACCCGCCCGCAAAGCCACAGCGCAT
CTGGATCACCCGCTTTGGTGGCGCTTGGCCGAGGAGGACACCCTGTTTGGGGGGCG
GAGCCGGGGTGGCCGCCCTTTCCCCAGGGCTGAAGGGACCCCCCTCGGAGCCCGCCC
ACGCGAGATGAGGACGGTGGCCAGCCCCCATGCCCTCCCCCTGGGGGGCCCCCGC
TCCCGCCCCGTGCGCTTCTGGGTGGGGGGGGGCTTCAAACCCCCCTGCCGACCC
AGCCGGTCCCCGCCGCCGCCCTTCGCGCCCTGGGCCATCTCCTCCCACCTCCCTCC
GCGGAGCAGCAGACAGCGAGGGCCCCGGGGGGGGGACCCCCGTCCGGGGC
ACCCCCCGGCTCTGAGCCGCCCGGGGGGGCCCTCGGCCCGGAGCGGAGGAAGGAGTC
GCCGAGGAGCAGCCTGAGGCC
```

**Figure 80: AP-1, HIF-1 and Smad3 binding sites in the TGF- $\beta$ 1 promoter region.** Using AP-1 consensus sequence TGTCTCA = grey and TGACTCT = cyan. Two possible AP-1 binding site was identified. Using HIF-1 consensus sequence (A/G)CGTG = red, 2 possible binding sites was identified. Smad3 has can bind to several motifs, including the Smad box consensus sequence GTCT=green and AGAC =yellow, CAGA motifs AGCCAGACA =red text, and 5 bp GC-rich motif GGCGC=blue and GGCCG=pink. Using these sequences 14 possible Smad3 binding sites were identified in the TGF- $\beta$  promoter. T=red marks transcription start site.

### 7.3 LGALS9 Promoter Region and Smad3 Response Element

As mentioned Smad3 is able to bind to several motifs of which the most characteristic is the 4 bp Smad box (GTCT/AGAC). But it has also been reported to bind to CAGA motifs (5'-AGCCAGACA-3' or 5'-TGTCTGGCT-3') and a 5 bp GC-rich motif GGC(GC)|(CG). In Figure 81, we try to identify possible Smad3 binding sites and found 9 possible Smad3 binding sites in the galectin-9 promoter region.

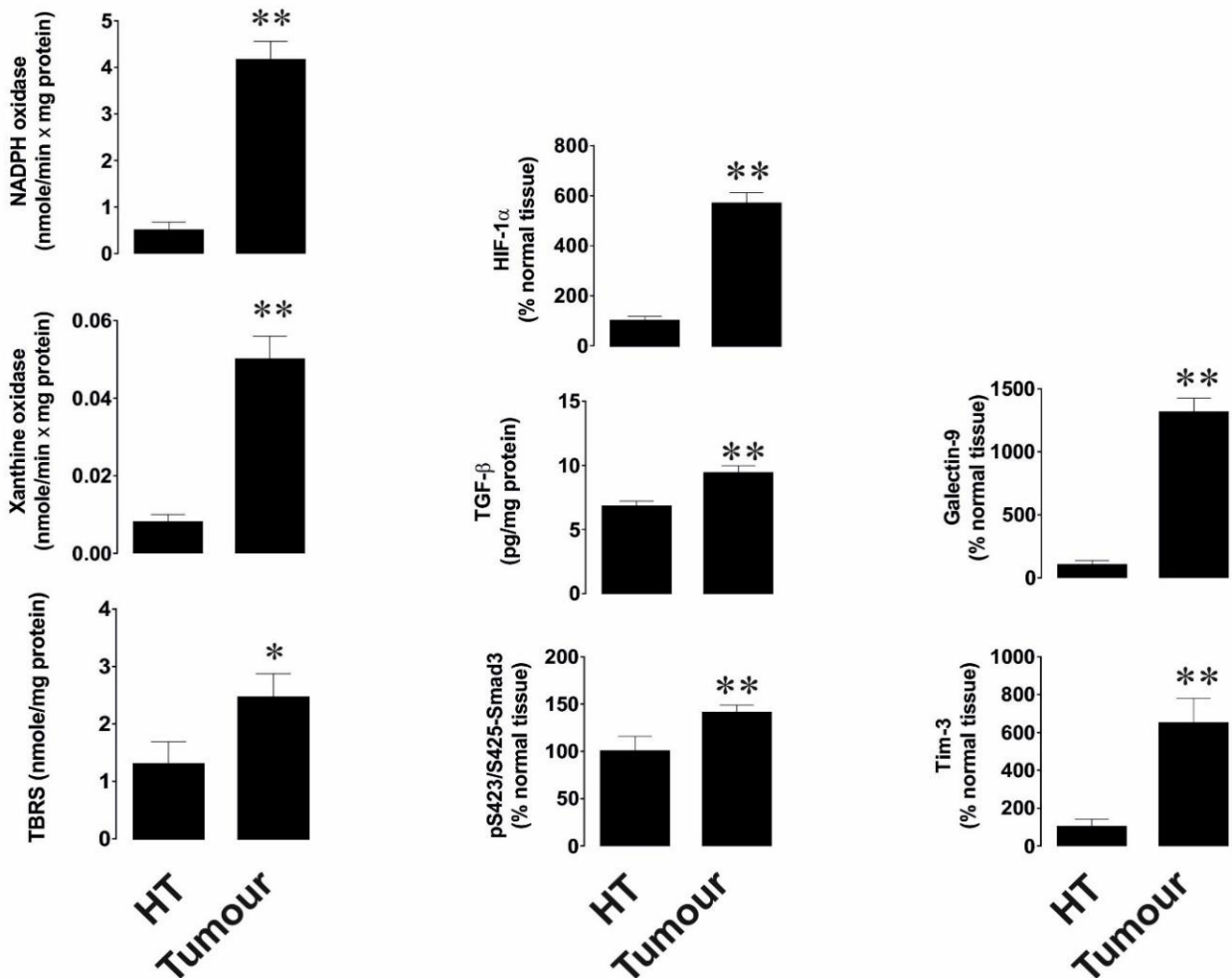
[https://www.genecopoeia.com/product/search/view\\_seq\\_promoter.php?cid=&type=promoter&prod\\_id=HPRM44237](https://www.genecopoeia.com/product/search/view_seq_promoter.php?cid=&type=promoter&prod_id=HPRM44237)

>HPRM44237 NM\_002308:name=LGALS9;Entrez\_ID=3965;Genome=hg38;chr17+:27629917-27631256;TSS=27631148;Upstream=1231,Downstream=108;Length=1340;

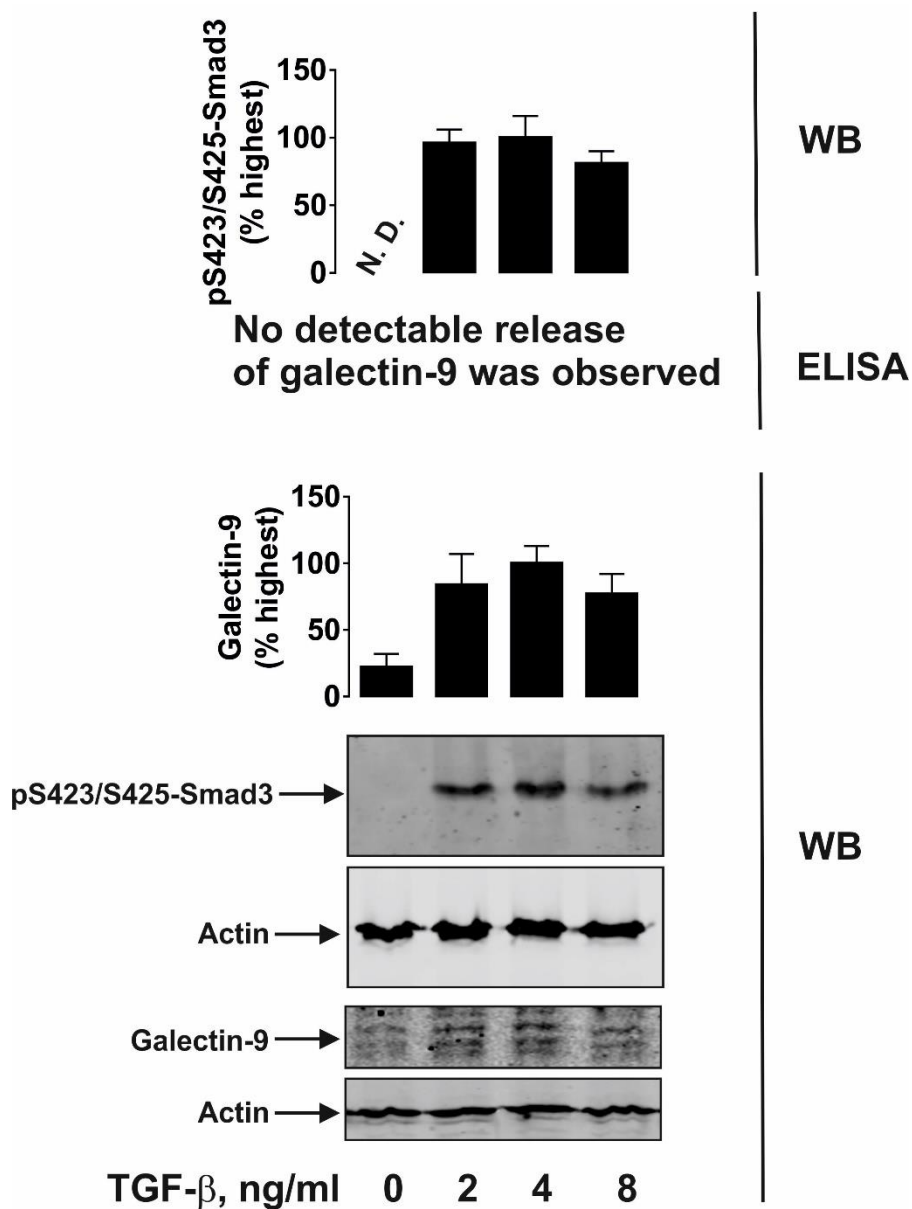
```
AGCCACCACGCCCTGCCCATTTTTCTAAGTTGGATTATTTTACACTCCA GTCT GCTGTGA
ATGAGAGTTCAGTTGTTGCGTATCGCAATCAATTTGTGATTGCCTACAAATGATGTGCC
GTGATGAAATTGTCCCTGGTGTCCGAGAGGATCGCAAAGAATTTCCCTTCCTTCTCTCC
TTTCTGCTCCCCTTGTACT GTCT ACTCCTTAAACTGGTACTTGATCCAGGAACATAATGG
GGATGGACAGTGCAGATGGCACACATGGCCTCA GTCT ATTGGAGCATCTCAAAGGAATTA
GTCT GCAAATTC TAGTGCATCTAGGTGGAGCACAGGAAGGAAGAGAGGTGC AGAC TCACG
TATGGCCCTGGGGCACCTGCCATCCTCTCGCACCCGTACAGCCCTTACCTGCCAGCACTT
ACCCTACCAGCTTGAGTTC TGGGCCCTTCTCACCAGCACATCGCTGGGACCTGGTTCGACT
TCAGGTAAGTTTATTTTCATGGCTCCCTCCCCACGACCTGCACATGCCATATGTTCCCTC
CCAGCCCCATGTCACCTTGAAATGTTCTATCATGTCCA AGACTTCTCTCCTCATCCTAAAG
TGCAGAAAATAAGGATGGAGAAGAGAAGGAGAATCAAGAGAGATTTCATTGAGAGG
GAGGATCAGAAGCTCCTGGGCACCCCATACTGTAGAATAAAAAATATTCATTATGGTGTTC
TTCTTGCAAAATATTCCTCTACATAATTATGTTTTTACATGAATAATATAAATTTAAA
CAGGAGAAATACTTTTTGAAGA GTCT GAGAATCTTCATAAAGTTCAGGCGGCCACGAATT
AGCTGTGTGACCTGGGGCATGCCCTT AGACTCTGAGCCTCAGCTTCTCTGTATGTAATA
TGGGTTGAAGCCGCCCTTCCCCACAAGCACCCCTGTGCACAGGCAATGCCAGCCCCATTA
TTTTCTGGACTCCGTGGCCAAGCATGCTTAGGACACACAGCCACATACTTCTGGGCAGTG
TCATCTGGCAACTTGCTGTCATGTCAGTGTGGTCAAGCATTGT AGACTCTATGAACCAA
ATATGCTTCAGGCTTGGGTTGAGCACAGGAGAGGGAGGGAGGAAAGGTCACCTGGGGCTGG
GAGTGCCTACTTCCCTCTGTGAGTGTCACCCCAGTCCACCCAGTACCATAACCTTTCTCTC
TCTGGACCCACTTCCTTTTGCTGCCGGCTCC TCCCCATTGAATAACAGCCAAGTTGCTTT
GGTTTTCTATTTCTTTGTTAAGTCGTTCCCTCTACAAAGGACTTCTTAGTGGGTGTGAAAG
GCAGCGGTGGCCACAGAGGC
```

**Figure 81: Smad3 binding sites in the LGALS9 promoter region.** Using the Smad box consensus sequence GTCT=green and AGAC =yellow. There were no 5-bp GC-rich sequence found in LGALS9 promoter. We found 9 possible Smad3 binding sites upstream of T. T=red marks transcription start site.

## 7.4 Transforming Growth Factor Beta Type 1 (TGF- $\beta$ ) and Hypoxia-inducible Factor 1 (HIF-1) Transcription Complex as Master Regulators of the Immunosuppressive Protein Galectin-9 Expression in Human Cancer



**Figure 82:** Values presented in Figure 51 normalised against total protein loaded for WB data and per 1 mg of total tissue protein for enzyme activity and TBRS assays (from (419)). Data are shown as mean values  $\pm$  SEM of five independent experiments. \* -  $p < 0.05$  and \*\* -  $p < 0.01$  vs non-transformed peripheral tissue abbreviated as HT (healthy tissue) (419).

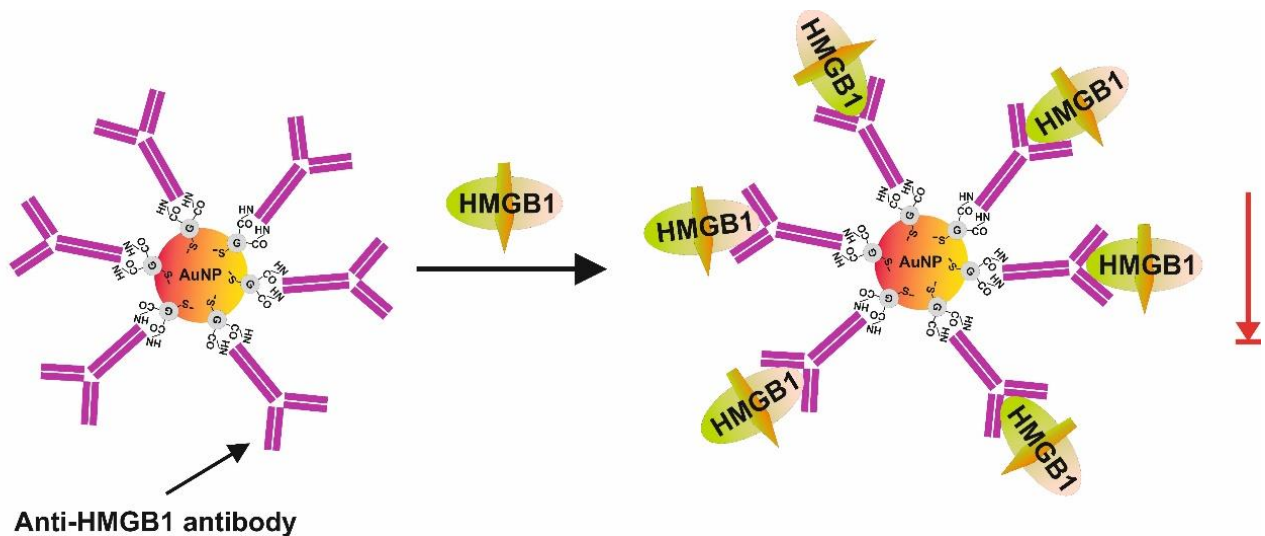


**Figure 83: TGF- $\beta$  induces galectin-9 expression in K562 human cancer cells** (from (419)). K562 human chronic myeloid leukaemia cells were exposed for 24 h to 2, 4 or 8 ng/mL TGF- $\beta$  followed by detection of phospho-S423/S425-Smad3 and galectin-9 expression by WB. Galectin-9 release was analysed by ELISA. Images are from one experiment representative of three, which gave similar results. Data are shown as mean values  $\pm$  SEM of three independent experiments (419).

## 7.5 HMGB1 Derived from Dying Tumour Cells Can Promote Immune Escape by Upregulating Galectin-9 in TLR4 Expressing Cancer Cells

<b>Acute myeloid leukaemia subtypes – based on The French-American-British (FAB) classification of AML</b>	
<b>FAB subtype</b>	<b>Name</b>
M0	Undifferentiated acute myeloblastic leukaemia
M1	Acute myeloblastic leukaemia with minimal maturation
M2	Acute myeloblastic leukaemia with maturation
M3	Acute promyelocytic leukaemia (APL)
M4	Acute myelomonocytic leukaemia
M4 eos	Acute myelomonocytic leukaemia with eosinophilia
M5	Acute monocytic leukaemia
M6	Acute erythroid leukaemia
M7	Acute megakaryoblastic leukaemia

**Table 3: The French-American-British (FAB) classification of Acute myeloid leukaemia (AML) (536).** French, American, and British leukaemia experts have divided AML into subtypes, M0 through M7, based on the type of cell the leukaemia develops from and how mature the cells are. The classification is largely based on how the leukaemia cancer cells looked under the microscope after routine staining. Subtypes M0 through M5 all start in immature forms of white blood cells. M6 AML starts in very immature forms of red blood cells, while M7 AML starts in immature forms of cells that make platelets.



**Figure 84: How nanoconjugate can be used to deplete HMGB1 (or TGF- $\beta$ ) from the medium.** Gold nanoparticles of the average size  $27.8 \pm 0.1$  nm have space to be coated with 6 anti-HMGB1 (or anti-TGF- $\beta$ ) antibodies which captures and deplete HMGB1 (or TGF- $\beta$ ) from the medium.

## 7.6 Buffers, Gel-solutions and Antibodies for Western Blot

### 7.6.1 Prepare Buffers

#### *10% SDS (30 mL) – storage at RT*

- 3 g
- Up to 30 ml ddH<sub>2</sub>O

#### *2x Sample buffer (10 mL) – storage at RT*

- 1.25 ml upper Tris buffer →62.5 mM
- 2 mL 10% SDS →2% SDS
- 2.5 ml Glycerol →25%
- 10.0 mg Bromophenol Blue →0.1%
- 3.75 mL ddH<sub>2</sub>O
  - Transfer 500 µL SB to Eppendorf and add a very small amount DTT (powder) just before use. (DTT can be com inactive in solution, therefore it is add just before use).

#### *4x sample buffer (10 mL) – storage at RT*

- 2.5 mL upper Tris buffer →125 mM
- 4 mL 10% SDS→ 4%
- 5 mL Glycerol→50%
- 10.0 mg Bromophenol Blue→0.1%
  - Transfer 500 µL SB to Eppendorf and add a very small amount DTT (powder) just before use. (DTT can be com inactive in solution, therefore it is add just before use).

#### *Lower Tris buffer (1.5M Tris-HCl pH 8.8) – storage at 4°C*

- 181.5 g Trisbase
- Up to 1 L ddH<sub>2</sub>O
- Adjust pH to 8.8

#### *Upper Tris buffer (0.5M Tris-HCl pH 6.8) – storage at 4°C*

- 60.5 g Trisbase
- Up to 1 L ddH<sub>2</sub>O
- Adjust pH to 6.8

#### *10x Running buffer (pH 8.3) (1L) – storage at 4°C*

- 30.3 g Trisbase
- 144 g Glycine
- Up to 1 L of ddH<sub>2</sub>O
- Mix and check pH (should be 8.3 – do not adjust→remake if not right)

#### *1x Running buffer (1L) – storage at 4°C*

- 100 mL 10x Running buffer

- 900 mL ddH<sub>2</sub>O

*1x Transfer buffer (20% MeOH) pH 8.3) (1L) – storage 4 month at 4°C*

- 3.03 g Trisbase
- 14.4 g Glycine
- 800 mL ddH<sub>2</sub>O
- Mix and check pH (should be 8.3 – do not adjust → remake if not right)
- 200 mL MeOH

*10x TBS (9% NaCl, 100 mM Tris-HCL, pH 7.4) (1L) – storage at 4°C*

- 12.11 g Trisbase
- 90 g NaCl
- Up to 1 L of ddH<sub>2</sub>O
- Mix and adjust pH to 7.4

*1x TBST (0.2% Tween20 and pH 7.4) (1L) – storage at 4°C*

- 100 mL 10x TBS
- 900 mL of ddH<sub>2</sub>O
- 2 mL of Tween20 →
- the main purpose of using Tween-20 is to prevent non-specific binding of the antibody, here we use slightly more to help ab bind more efficiently

*Stripping buffer – harsh*

- 20mL 10% SDS
- 12.5 mL upper tris-buffer
- 67.5 mL dH<sub>2</sub>O
- 400 mg DTT or 800 µL β-mercaptoethanol

## 7.6.2 Gel Solutions

Gel type	Separation gel					Stacking gel	
	5%	7.5%	10%	12%	15%	Gel%	4%
H <sub>2</sub> O	61.5 mL	55.25 mL	49 mL	44 mL	36.5 mL	H <sub>2</sub> O	64 mL
1.5M Tris-HCL (pH 8.8)	25 mL	25 mL	25 mL	25 mL	25 mL	0.5M Tris-HCL (pH 6.8)	25 mL
40% Acrylamid/Bis-acrylamide	12.5 mL	18.75 mL	25 mL	30 mL	37.5 mL	40% Acrylamid/Bis-acrylamide	10 mL
10% SDS	1 mL	1 mL	1 mL	1 mL	1 mL	10% SDS	1 mL
Total	100 mL	100 mL	100 mL	100	100 mL	Total	100 mL
Gel solution	10 mL					Gel solution	5 mL
10% APS	125 µL					10% APS	100 µL
TEMED	25 µL					TEMED	20 µL



### 7.6.3 Antibody List

1 <sup>st</sup> ab	Name	Cat#	Manufacture	Source	Concentration	
					Recommended	Used
Galectin-9	Anti-galectin 9 antibody (1mg/mL)	ab69630	Abcam	Rabbit Polyclonal IgG	1:500-1:1000	1:1000 – 1:1250
Tim-3	Anti-Tim-3 (3 mg/mL)		Luka Switzerland	Mouse Monoclonal		1:1000 - 1:1250
FLRT3	FLRT3 antibody (A-3) (200 µg/mL)	Sc-514482	Santa Cruz	Mouse Monoclonal IgG1	1:100-1:1000	1:500
LPHN2				Rabbit		1:500
TLR4	Toll-like receptor 4 (0.5 mg/mL)	Ab22048	Abcam	Mouse Monoclonal IgG2b		1:1000
TLR2	Toll-like receptor 2 (0.1 mg/mL)	Ab9100	Abcam	Mouse Monoclonal IgG2a	1:50	1:600
RAGE	Receptor for advance glycation endproducts (1 mg/mL)	Ab3611	Abcam	Rabbit Polyclonal IgG	1 µg/mL → 1:1000	1:1000
p-Smad3	Recombinant Anti-Smad3 (phospho S423 + S425) antibody [EP823Y] (0.576-0.591 mg/mL)	Ab52903	Abcam	Rabbit Monoclonal IgG	1:2000	1:1250 – 1:6667
p-ATF-2	Phospho ATF-2 (Thr69/71)	9225	Cell signaling	Rabbit Polyclonal	1:1000	1:1000 – 1:1250
Total ATF-2	Anti-ATF-2 antibody	Ab47476	Abcam	Rabbit Polyclonal IgG	1:500-1:1000	1:1000 – 1:1250
HIF-1a	Anti-HIF-1	Ab1	Abcam	Mouse	5 µg/mL	1µL

	alpha antibody [H1alpha67] (1mg/mL)			Monoclonal IgG2b		
b-actin	Anti-Actin antibody [ACTN05 (C4)]	ab3280	Abcam	Mouse Monoclonal IgG1		1:2000
b-actin (new started used on the 28/11/2017)	Anti-Actin antibody [EPR16769] (0.648mg/mL)	ab179467	Abcam	Rabbit Monoclonal IgG	1:5000	1:2000 - 1:2500
b-actin (new started used on the 20/08/2019)	Beta Actin Antibody	66009-1-Ig	Proteintech	Mouse Monoclonal IgG2b	1:5000 – 1:50.000	1:10.000
<b>2<sup>nd</sup> ab</b>	<b>Name</b>	<b>Cat#</b>	<b>Manufacture</b>	<b>Source</b>	<b>Concentration</b>	
					<b>Recommended</b>	<b>Used</b>
Red anti-mouse	IRDye 680RD Goat anti-mouse	926-68070	Li-cor	Goat	1:15000 1:5000-1:25000	1:2000
Green anti-mouse	IRDye 800CW Goat anti-mouse	926-32210	Li-cor	Goat	1:15000 1:5000-1:25000	1:1000 – 1:2000
Red anti-rabbit	IRDye 680RD Goat anti-rabbit	926-68071	Li-cor	Goat	1:15000 1:5000-1:25000	1:2000
Green anti-rabbit	IRDye 800CW Goat anti-rabbit	926-32211	Li-cor	Goat	1:15000 1:5000-1:25000	1:1000 – 1:2000

## 7.7 List of Publications

- 1) Yasinska et al. *Frontiers immunology* (2019) “The Tim-3-Galectin-9 Pathway and Its Regulatory Mechanisms in Human Breast Cancer”
  
- 2) Selnø et al. *Aging-US* (2020) “Transforming growth factor beta type 1 (TGF- $\beta$ ) and hypoxia-inducible factor 1 (HIF-1) transcription complex as master regulators of the immunosuppressive protein galectin-9 expression in human cancer and embryonic cells”